

# Analysis of Marine Ecology Monitoring Plan Data - Robin Rigg Offshore Wind Farm

Operational Year Four Technical Report  
– Ornithological Monitoring



09 October 2015  
E.ON Climate & Renewables

Dr Emily Nelson - Ornithologist  
Dr Gillian Vallejo - Ecological Modeller  
Dr Sarah Canning - Marine Mammal Ecologist  
Deborah Kerr - Ecological Modeller  
Dr Fiona Caryl – Ecological Modeller  
Dr Ross McGregor - Senior Ornithologist  
Victoria Rutherford - Marine Ecologist  
Dr Jane Lancaster - Principal Offshore Ecologist

1065167

## Document history

Author	Dr Emily Nelson, Dr Gillian Vallejo, Dr Sarah Canning, Deborah Kerr, Dr Fiona Caryl, Dr Ross McGregor, Victoria Rutherford & Dr Jane Lancaster	26 August 2014
Checked	Dr Ross McGregor & Dr Jane Lancaster	24 September 2014
Approved	Dr Jane Lancaster	04 December 2014

### Client Details

Contact	Tim Morgan
Client Name	E.ON Climate & Renewables

Issue	Date	Revision Details
A	04 December 2014	First issue to client
B	20 March 2015	Second issue to client
C	26 August 2015	Third issue to client
D	09 October 2015	Final issue to client



# Contents

Executive summary	1
1. Introduction	2
1.1. Site Description	2
1.2. Ecological Monitoring at Robin Rigg	6
1.2.1. Regulatory Framework	6
1.2.2. Natural Power's Role	6
1.2.3. Survey Regime	6
1.2.4. Reporting	8
2. Ornithological Monitoring	9
2.1. Introduction	9
2.1.1. Predicted Impacts	9
2.1.2. Solway Firth Bird Populations	11
2.2. Survey Methods	20
2.2.1. Overview	20
2.2.2. Data Collection	21
2.3. Analytical Methods	23
2.3.1. Overview	23
2.3.2. Data Collation	23
2.3.3. Data Processing	24
2.3.4. Data Analysis	25
2.4. Results	31
2.4.1. Scaup	31
2.4.2. Common scoter	45
2.4.3. Red-throated diver	61
2.4.4. Manx shearwater	79
2.4.5. Cormorant	96
2.4.6. Gannet	113
2.4.7. Razorbill	132
2.4.8. Guillemot	153
2.4.9. Kittiwake	177
2.4.10. Great black-backed gull	201
2.4.11. Herring gull	224
2.4.12. Comparison of collection methods for birds in flight	246
2.5. Discussion	247
2.5.1. Species accounts	247
2.5.2. Modelling approach	250
2.6. Conclusions	251
2.7. References	252
Appendices	256
A. Details of Survey regime	256
B. Analytical Methods	257

## Executive summary

Robin Rigg Offshore Wind Farm (OWF) in the Solway Firth is operated by E.ON Climate & Renewables (E.ON) and was the first commercial OWF in Scottish waters. The site is comprised of 60 three megawatt Vestas turbines and an offshore sub-station. Construction of the OWF and its associated cabling began in December 2007 and the site became fully commercially operational in April 2010.

In accordance with the consent from Scottish Ministers under Section 36 of the Electricity Act 1989, a Marine Environment Monitoring Programme (MEMP) was developed to record any changes to the local physical and ecological environment as a result of the construction and operation of the wind farm. This included monitoring requirements for a number of ecological parameters, including benthos, non-migratory and electro-sensitive fish, birds and marine mammals and covered pre construction, construction and operational phases of the wind farm.

In accordance with the MEMP no benthic, electro-sensitive fish or marine mammal surveys were undertaken in Operational Year four, therefore this report covers bird surveys and the associated analysis only. The results of the analysis for benthic, non-migratory fish, electro-sensitive fish and marine mammals, can be found in previous operational year reports.

This report presents analysis performed on bird data collected before construction (during the baseline and pre-construction years), during construction and during the first four years of operation. The data has been examined in order to assess the impact of the OWF on the Solway ecosystem and validate the predictions made in the Environmental Statement.

All surveys consisted of boat-based visual surveys comprising ten transects conducted monthly or bimonthly, depending on phase. All data were collated and verified by Natural Power's ornithological experts. The analytical methods have been determined by the data available to Natural Power, collected as part of the MEMP before, during and after construction.

This report summarises the results of the ornithological surveys carried out from the pre-construction phase to the fourth year of operation for 11 key bird species. Data analysis was undertaken using the R package 'MRSea' developed by the Centre for Research into Ecological and Environmental Modelling (CREEM). This method was commissioned by Marine Scotland to facilitate the modelling of offshore line transect data. To our knowledge, this is the first time that this method has been employed outside of CREEM. Little evidence was found for declines in bird abundance and distribution that were directly attributable to wind farm. There was weak evidence of wind farm avoidance during the construction phase for common scoter, although predicted abundance and distribution returned to pre-construction levels during operation. Cormorants were shown to be attracted to the wind farm, with birds resting on the handrails of the turbine transition pieces in between foraging bouts. There was limited evidence of a decline in cormorant site usage during operational year four. Predicted gannet abundance declined throughout development and operation, which is in contrast to national population trends. Very small densities for some species, such as red-throated diver, may have masked changes in abundance and distribution. Confidence intervals surrounding abundance and density estimates for some species (including razorbill and kittiwake) were large, showing that there was a high degree of uncertainty in the predictions. Whilst for some species modelling was not attempted due to the small number of initial observations, other models would not converge due to outliers in the data or zero-inflation. Seabird numbers are known to fluctuate greatly at any given location so the probability of detecting consistent directional change in seabird abundance and distribution is small. Few birds were recorded flying at rotor swept height, suggesting that overall collision risks are small. Although great black-backed gulls and herring gulls appear to be flying more often at rotor height during operation, it is likely that this is an artefact of more accurate observer recording. This demonstrates the importance of employing a consistent methodology throughout monitoring.

# 1. Introduction

Robin Rigg Offshore Wind Farm (OWF) is E.ON Climate & Renewables' (E.ON) third UK OWF and the first commercial OWF in Scottish waters. The site is comprised of 60, three megawatt Vestas turbines and an offshore sub-station. Turbines began full commercial operation/generation in April 2010.

In accordance with the consent from Scottish Ministers under Section 36 of the Electricity Act 1989, a Marine Environment Monitoring Programme (MEMP) was developed in conjunction with the Robin Rigg Management Group (RRMG)<sup>1</sup> prior to construction. The purpose of the MEMP was to record any changes to the local physical and ecological environment as a result of the construction of the wind farm through a survey regime. This included monitoring requirements for a number of ecological parameters, including benthos, non-migratory and electro-sensitive fish, birds and marine mammals and covered pre-construction, construction and operational phases of the wind farm.

This report represents analysis performed on bird data only, collected before construction, during construction and during the first four years of operation. In accordance with the MEMP, no benthic, electro-sensitive fish or marine mammal surveys were undertaken in operational year four; this report covers bird surveys and associated analysis only. The results of the analysis for benthic, non-migratory fish, electro-sensitive fish and marine mammals can be found in previous operational year reports (Walls *et al.*, 2013a, 2013b and 2013c).

The bird data analysed in this report were collected during baseline monitoring for the environmental impact assessment (EIA), during the pre-construction and construction phases, and post-construction during the first four years of operation. These data form a basis from which to assess any impacts on birds from the construction and operational phases of Robin Rigg OWF. The MEMP requirements for the other ecological surveys (benthic, non-migratory fish, electro-sensitive fish, and marine mammals) have been negated over time and are therefore not included in this report.

## 1.1. Site Description

The Robin Rigg OWF is situated within the central part of the Solway Firth, immediately to the north of the English/Scottish border which roughly bisects the firth (Figures 1.1 and 1.2). The centre of the turbine layout lies some 11 km from the Dumfries and Galloway coastline within Scotland and 13.5 km from the Cumbrian coastline in England. The nearest towns are Dalbeattie in Scotland, 21 km to the north-northwest, and Maryport in England, 14 km to the south-east.

---

<sup>1</sup> The RRMG is comprised of Marine Scotland, Scottish Natural Heritage, Natural England, the Royal Society for the Protection of Birds, Galloway Fisheries Trust, Scottish Environment Protection Agency, Environment Agency, the Scottish Government's Energy Consents Unit and E.ON.



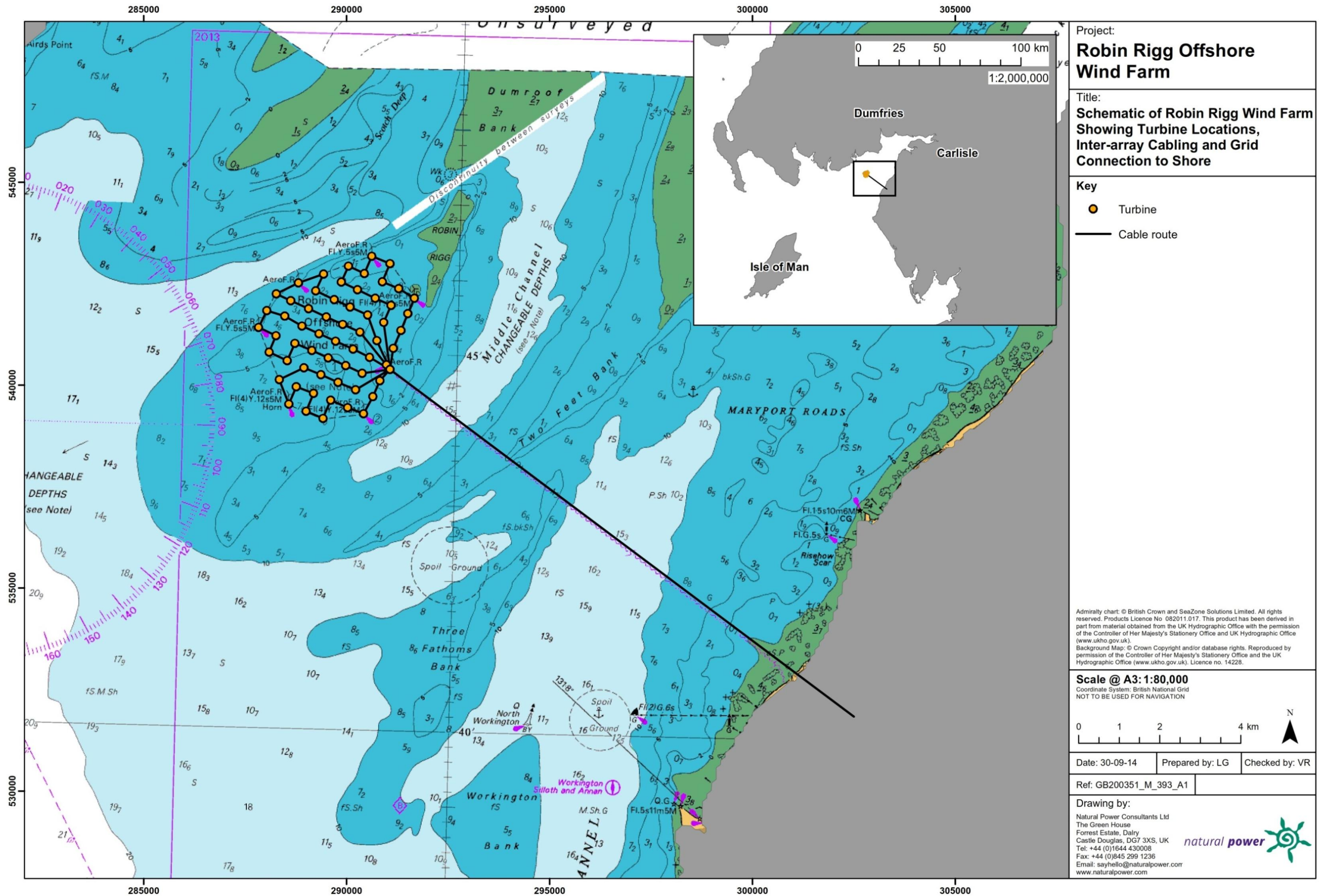


Figure 1.1: Schematic of Robin Rigg OWF showing turbine locations (yellow dots), inter-array cabling and grid connection to shore (black lines).





**Figure 1.2: Robin Rigg OWF during the construction phase.**

The turbines are connected in four loops, each containing 15 turbines, by 33 kV submarine cables with an embedded fibre optic link (Figure 1.1). There are 64 inter-array power cables installed between the wind turbine generators of the wind farm. The eight ends of these array cable loops are received by the two offshore substations. The array cables have two different cross-sections, varying with location; 150 mm<sup>2</sup> conductors are used close to the end points and 300 mm<sup>2</sup> conductors are used in the middle of the loop and close to the offshore sub-station.

The wind farm is connected via an offshore sub-station using two export cables which operate at 132 kV. These cables come ashore near Seaton, Cumbria and continue for approximately 2 km inland to an onshore substation. There are two submarine high voltage AC power cables connecting the offshore substation to the onshore network. These 132 kV XLPe insulated 300 mm<sup>2</sup> Cu submarine composite export cables contain three-phase power cable and one fibre optic element with double wire armour and single wire armour throughout the remainder of the route.

The installation of turbine foundations occurred between December 2007 and February 2009, with a gap in construction between February and August 2008 (Figure 1.3).

Cables were installed from July 2008 into early 2010 (Figure 1.4) and two different methods were used; a “lay and bury” technique and also a “surface lay and later bury” technique. The two export cables were laid in May and September 2009. The last turbine was installed during August 2009 and the first turbine operated briefly in August 2009 with main commissioning commencing in September 2009 and completed in April 2010 (Figure 1.4). A variety of ports were used during construction including Belfast, Mostyn, Newcastle, Workington, Whitehaven and Barrow.

Installation of the turbines commenced in November 2009. These activities involved the use of large jack-up barges. Turbine foundations are a monopile design, with a transition piece which provides boat fendering, access ladders and cable conduits. The monopile and transition piece are connected with a grouted joint. The turbine towers are 80 m high and each of the three blades, 44 m long. Turbines are positioned approximately 500 m apart. Turbine commissioning began in August 2009 and was completed in April 2010 (Figure 1.4).

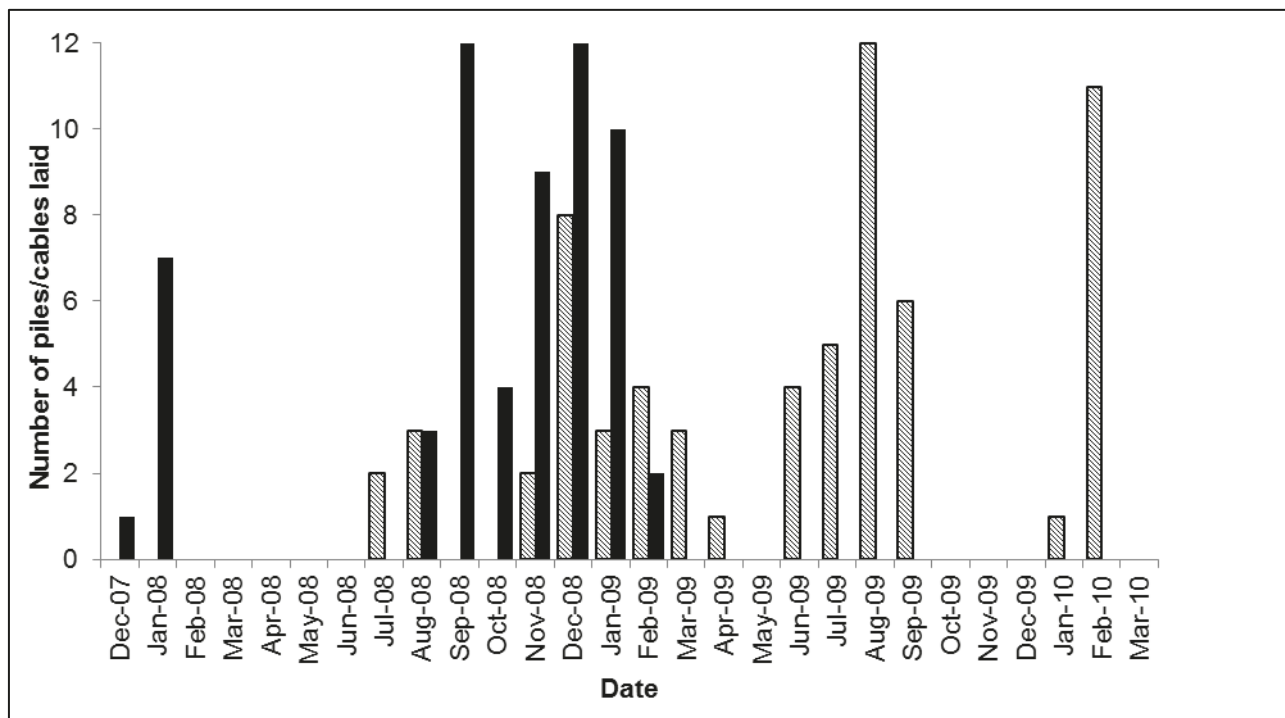


Figure 1.3: Number of foundations piled (black) and cables buried (hatched) each month during construction.

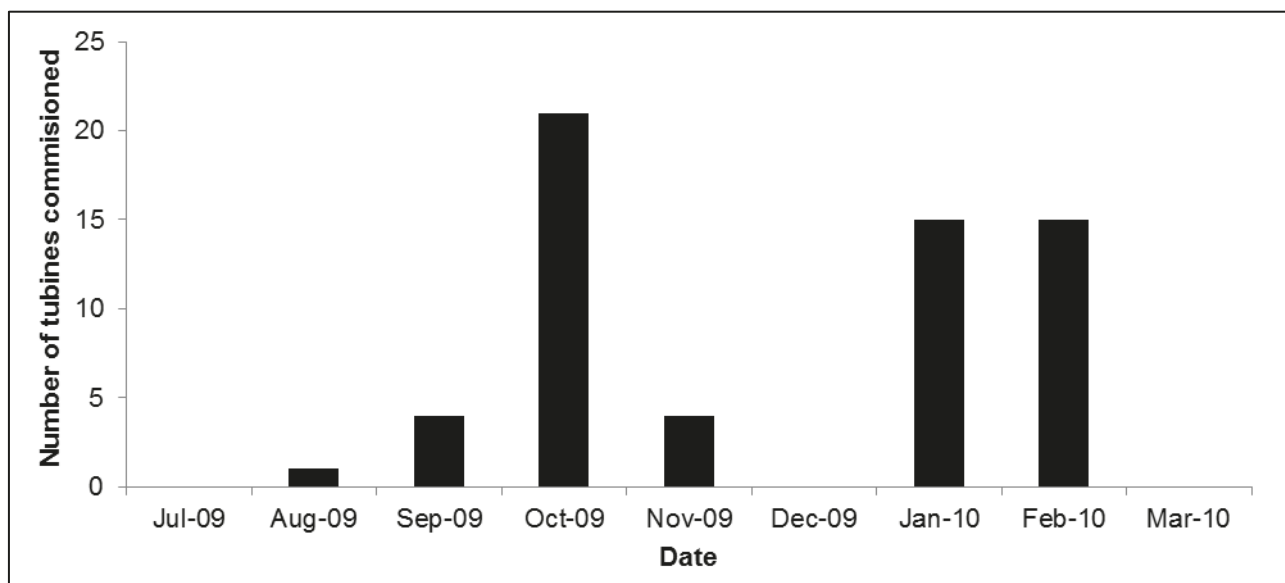


Figure 1.4: Number of turbines commissioned each month.

In March 2011, the 132 kV export cables were sold by E.ON Climate & Renewables to a private transmission company (Transmission Capital Ltd) under the government's new OFTO regime. E.ON Climate & Renewables has been retained by the OFTO as their Operations and Maintenance contractor, including management of the environmental monitoring aspects of the export cable.

## 1.2. Ecological Monitoring at Robin Rigg

### 1.2.1. Regulatory Framework

An Environmental Statement was submitted in June 2002 to the Scottish Executive Energy Division under Section 36 of the Electricity Act (Scotland) 1989; a Private Bill for the Scottish Parliament; the Scottish Executive - Transport Division under Section 34 of the Coastal Protection Act 1949 and the Scottish Executive – Rural Affairs Department under the Food and Environment Protection Act 1985; and in accordance with the statutory procedures set out in The Environmental Assessment (Scotland) Regulations 1988 and the Environmental Impact Assessment (Scotland) Regulations 1999, in support of an application for an OWF at Robin Rigg in the Solway Firth.

Section 36 and FEPA consent for the scheme was granted by the Scottish Executive in March 2003. Prior to the construction of the Robin Rigg Wind Farm, the MEMP was developed in conjunction with the RRMG covering the pre-construction, construction and post construction stages of development. The remit of the MEMP was to record any changes to the physical and ecological environment that may be caused by the construction and operation of the wind farm, complying with condition 6.4 of Section 36 Consent conditions. The programme concentrated on areas where there was uncertainty on the effects of the wind farm and where those effects may cause potential impacts on the marine ecology. This included sub-tidal benthic habitats, intertidal habitats, non-migratory and electro-sensitive fish, migratory fish, birds and marine mammals.

### 1.2.2. Natural Power's Role

Natural Power Consultants (Natural Power) were lead EIA consultant and coordinated ecological surveys at Robin Rigg during the establishment of the baseline in 2001 and 2002. After consent was granted Natural Power were employed by E.ON to coordinate ecological surveys relating to birds, marine mammals, benthos, non-migratory fish, electro-sensitive fish and intertidal habitats. The monitoring of migratory fish was undertaken by Galloway Fisheries Trust. It should be noted that although Natural Power monitored intertidal habitats these results are excluded from this report as these occurred in the English waters.

Natural Power were also contracted by E.ON to undertake detailed analysis of the data collected in order to assess any potential impacts the construction and operational of the site and its transmission assets may have had on benthic, fish (including electro-sensitive species), birds and marine mammals. All data collected on these receptors during the baseline, pre-construction, construction and operational phases of the Robin Rigg Wind Farm was analysed.

### 1.2.3. Survey Regime

A summary of the survey programme coordinated and undertaken by Natural Power is provided in Table 1.1 (full details in Appendix A), with brief descriptions of the surveys undertaken and their results provided below.

**Table 1.1: Summary of MEMP frequency of survey requirements.**

Survey Receptor	Baseline	Pre-Construction	Construction	Operational
Benthos	Single survey (2001)	Single survey (2007)	Four surveys (2008-2009)	Two surveys (2010, 2011)
Non-migratory fish	10 monthly surveys (2001-2002)	No surveys	10 surveys (2008-2010)	Seven surveys (2010-2013)
Electro-sensitive fish	No surveys	Two surveys (2007)	Four surveys (2008-2009)	Four surveys (2010-2011)
Marine mammals	No surveys	11 surveys (2004-2005, 2007)	50 surveys (2008-2010)	24 surveys (2010-2012)
Birds	30 surveys (May 2001-Dec 2002)	12 surveys (2003-2004, 2007)	50 surveys (2008-2010)	60 surveys (2010-2015)

## Benthic Surveys

Baseline data was collected as part of the ES at 100 grab sampling stations in and around the propose site (80 within the development area and 20 sites beyond) and eight sites along the cable. Bi-annual surveys took place at 17 stations (six within the site, three reference stations and at eight stations along the cable route) throughout the pre-construction and construction phase. During operational year annual surveys were carried out at the same 17 stations for the first two years of operation. No significant difference in species composition that could be attributed to the wind farm or cable route was found and the difference between years was attributed to natural cyclic fluctuations in the highly dynamic environment of the Solway Firth. It was therefore agreed by the RRMG that in line with the MEMP, no further benthic surveys would be required beyond the two years post construction.

## Fish Surveys

**Non-migratory fish surveys:** Baseline data was collected as part of the ES process via monthly epibenthic beam trawls at 31 sampling stations in and around the proposed development. Data was also collected at these sites during the construction phase and for the first three years of operation, but at a reduced frequency with varied depending on MEMP specifications dependant on construction phase (see Table 1.1). Although variations were found between years in species composition and catch rate, none of this could be attributed to the wind farm or cable route and were instead attributed to variations in recruitment over time. It was therefore agreed by the RRMG that in line with the MEMP, no further non-migratory fish surveys were required beyond the three years post construction.

**Electro-sensitive fish surveys:** In accordance with the MEMP electro-sensitive fish surveys were carried out via epibenthic beam trawls along the cable route at eight sampling stations throughout the preconstruction, construction and operational periods. In agreement with the MEMP, surveys were no longer deemed necessary after two years of operational data due to no significance differences found in samples between the survey periods. Overall very few electro-sensitive species were found in any survey period, hence statistics could not be performed, however no difference in the species composition of catch that could be attributed to the wind farm or cable route was found.

## Bird Surveys

Baseline data was collected as part of the ES process via monthly or bimonthly boat surveys covering the area in and around the proposed development (Table 1.1). In accordance with the MEMP, monthly surveys were conducted prior to construction, with the frequency increasing to bi-monthly surveys for the duration of the construction phase. Monthly surveys have taken place monthly for the first four years of operational and will continue throughout year five. The results of the analysis of all data up to year five are presented in this report.



## Marine Mammal Surveys

No survey data were collected for marine mammals as part of the ES process; however baseline boat based surveys were conducted monthly between January 2004 and March 2005. Construction phase surveys were undertaken simultaneously with bird surveys (hence twice per month). Monthly surveys were carried out during the first two years of operation at the same as the bird surveys. In accordance with the MEMP no further surveys took place after operational year two. Although no separate Marine Mammal surveys have taken place in Operational Year 4, their presence was noted throughout the bird surveys.

### 1.2.4. Reporting

This report presents analysis undertaken on bird data collected before construction (during the baseline and pre-construction years), during construction and during the first four years of operation to assess the impact of the OWF on Solway bird populations. Full details of methods, results, and discussion are found in Chapter 2.

## 2. Ornithological Monitoring

### 2.1. Introduction

Boat-based surveys have been undertaken since 2001 to gather data on bird diversity, abundance and distribution in and around Robin Rigg OWF. These data allow examination of potential impacts caused by wind farm construction and operation in accordance with the consent from Scottish Ministers under Section 36 of the Electricity Act 1989 and the MEMP.

To date, evidence has been found of little change in bird abundance and distribution attributable to Robin Rigg OWF (Walls *et al.*, 2013a, 2013b and 2013c). However, the effects of on birds remain poorly understood (Garthe & Hüppop, 2004; Furness *et al.*, 2013). Given the long operational lifespans of offshore wind farms, it is prudent that boat-based surveys continue and data analysis is undertaken to determine the effects of construction and operation on birds. This report summarises bird data collected at Robin Rigg OWF, up to and including the fourth year of operation.

#### 2.1.1. Predicted Impacts

Potential impacts of the Robin Rigg OWF on birds were assessed in the Offshore Environmental Statement (ES) which was submitted in 2002 (Natural Power, 2002). These impacts are outlined below.

##### 2.1.1.1. Habitat loss

The direct loss of habitat through the construction of turbine foundations and cabling was considered to be relatively small, such that no statistically significant impacts were predicted on bird prey species.

##### 2.1.1.2. Collision risk

A collision risk assessment was undertaken for two species present in nationally important numbers in the Solway Firth: common scoter and red-throated diver. Further assessment was undertaken for waterfowl designated at the Upper Solway Flats and Marshes SPA and for other migrant land birds and seabirds recorded during baseline surveys. For the majority of these key species, the magnitude of collision risk was negligible with an increase of less than 1% on baseline mortality rates (Table 2.1). Red-throated diver was the only species to exceed this, with a predicted increase of 22.8% on the baseline mortality rate. Whilst the predicted worst case collision mortality for red-throated divers was relatively low (3.3 birds per year), the increase in baseline mortality was thought to result from a combination of the species being long-lived and the small population size within the study area. Such high mortality was thought to be highly unrealistic since field data suggested that 98% of birds observed flew below rotor height. Overall collision risks predicted for the Robin Rigg OWF are detailed in Table 2.2. None of these were deemed statistically significant.

**Table 2.1: Worst case collision risk predictions for key species at Robin Rigg OWF, as outlined in the ES.**

Species	Predicted annual collision with wind farm	Annual mortality rate	Collision mortality as % of overall annual mortality
Common scoter	3.4	23.0%	0.3%
Red-throated diver	3.3	10.0%	22.8%
Oystercatcher	10.9	7.0%	0.4%
Barnacle goose	11.0	10.0%	0.5%

**Table 2.2: Summary of collision risks at Robin Rigg OWF, as outlined in the ES.**

Species	Sensitivity of local population	Magnitude of effect	Significance	Significant impact?
Common scoter	High	Negligible	Very low	No
Red-throated diver	High	Low	Low	No
Migrant waterfowl	Very high	Negligible	Low	No
Other seabirds	Medium	Low/negligible	Low/very low	No
Migrant land birds	Low	Negligible	Very low	No

### 2.1.1.3. Disturbance

Disturbance was predicted to be greatest during the construction period but with the potential to continue into operation. No significant disturbance effects were predicted, with regionally important numbers of birds affected at most. Displacement zones of 3 km and 5 km would be needed to affect nationally important numbers of common scoters and red-throated divers, respectively. This scale of disturbance was predicted to be unlikely given the maximum displacement distance recorded at an existing wind farm (at the time of submission) was 800 m (Pedersen & Poulsen, 1991).

A summary of species sensitivities in and around Robin Rigg OWF is presented in Table 2.3. The magnitude of impact is that which would arise if birds were displaced from a zone of 1 km around the OWF.

**Table 2.3: Summary of disturbance assessment at Robin Rigg OWF, as outlined in the ES.**

Species	Sensitivity of local population	Magnitude of effect	Significance	Significant impact?
Scaup	High	Low	Low	No
Common scoter	High	Low	Low	No
Red-throated diver	Medium	Negligible	Very low	No
Manx shearwater	Medium	Negligible	Very low	No
Storm petrel	Medium	Negligible	Very low	No
Gannet	Medium	Low	Low	No
Cormorant	Medium	Low	Low	No
Razorbill	Medium	Low	Low	No
Guillemot	Medium	Low	Low	No
Kittiwake	Medium	Low	Low	No
Other seabirds	Low	Low	Very low	No

## 2.1.2. Solway Firth Bird Populations

### 2.1.2.4. Designated sites

The Solway Firth is an important habitat for a wide range of bird species, with several areas within the Firth protected under national and international law, including:

- Protected areas established under national legislation such as Sites of Special Scientific Interest (SSSI) and National Nature Reserves (NNR);
- Protected areas established under European Union (EU) Directives such as the Natura 2000 network; and
- Protected areas established under international agreements such as Ramsar sites.

Table 2.4 details the protected sites which are located within the Solway Firth.

Table 2.4: Protected sites for birds within the Solway Firth.

Site name	Designation	Distance from Robin Rigg OWF (km)	Qualifying features
Upper Solway Flats and Marshes	Ramsar	6.4	<b>Non-breeding:</b> pink-footed goose, barnacle goose, pintail, scaup, oystercatcher, curlew, bar-tailed godwit and knot.
Upper Solway Flats and Marshes	SPA	6.4	<b>Non-breeding:</b> whooper swan, pink-footed goose, barnacle goose, shelduck, mallard, pintail, scaup, goldeneye, cormorant, great crested grebe, oystercatcher, golden plover, grey plover, lapwing, ringed plover, curlew, bar-tailed godwit, knot, dunlin, redshank. <b>Passage:</b> ringed plover.
Upper Solway Flats and Marshes	SSSI	6.4	<b>Non-breeding:</b> barnacle goose, shelduck, pintail, scaup, oystercatcher, golden plover, ringed plover, curlew, bar-tailed godwit, knot, sanderling, dunlin and redshank. <b>Breeding bird assemblage<sup>2</sup>.</b>
Abbey Burn Foot to Balcary Point	SSSI	8.5	<b>Breeding:</b> cormorant, fulmar, kittiwake, guillemot and razorbill.
Borgue Coast	SSSI	22	<b>Breeding:</b> common gull and great black-backed gull.
St Bees Head	SSSI	23	<b>Breeding:</b> fulmar, shag, puffin, black guillemot, razorbill, guillemot, kittiwake and herring gull.
Cree Estuary	SSSI	40	<b>Non-breeding:</b> pink-footed goose
Scare Rocks	SSSI	62	<b>Breeding:</b> gannet, shag and guillemot.
Loch of Inch and Torrs Warren	Ramsar	69	<b>Non-breeding:</b> Greenland white-fronted goose.
Loch of Inch and Torrs Warren	SPA	69	<b>Non-breeding:</b> Greenland white-fronted goose and hen harrier.
Torrs Warren to Luce Sands	SSSI	69	<b>Non-breeding:</b> hen harrier
Mull of Galloway	SSSI	73	<b>Breeding:</b> fulmar, razorbill and kittiwake.
Ailsa Craig	SPA	100	<b>Breeding:</b> gannet, lesser black-backed gull, guillemot, kittiwake and herring gull.

<sup>2</sup> Localities that support an especially good range of bird species characteristic of that habitat, or semi-natural habitats where at least 70 breeding species have been recorded in recent years. Taken from 'guidelines for the selection of biological SSSIs' (<http://jncc.defra.gov.uk/page-2303#download>).

### 2.1.2.5. Key species

A number of bird species listed as qualifying features for these sites were recorded in nationally important numbers in the Solway Firth during baseline surveys and were identified as key species in the ES. These key species are: scaup, common scoter, red-throated diver, Manx shearwater, cormorant, gannet, guillemot and kittiwake. These species are therefore also the focus of this report, in addition to herring gull, great-black-backed gull and razorbill which have been recorded in relatively large abundance during subsequent boat-based surveys of the Robin Rigg OWF. Accounts for each of these key species, listed according to the British List (BOU, 2013), are below.

#### Scaup (*Aythya marila*)

Scaup are present in the UK largely during the winter, with the winter population in Britain estimated at 5,200 birds (Musgrove *et al.*, 2011). Compared to previous estimates, numbers of scaup in the Solway Firth appear to have declined (Kershaw & Cranswick, 2003). The majority of individuals arrive from their breeding grounds in late October and leave again in February. Limited tagging data suggest that birds recorded in the UK disperse to a wide range of sites in north-west Europe, with ringing data showing strong links between wintering birds in the UK and breeding populations in Iceland (Wernham *et al.*, 2002).

During the winter, scaup congregate in sheltered sea lochs and firths, brackish coastal lagoons and freshwater lochs close to the coast (Forrester *et al.*, 2007). Scaup are usually active at night making regular feeding flights to the sea in the evening and returning at dawn (Nilsson, 1970). While individuals are able to switch foraging sites according to prey availability, they are limited to shallow waters of less than 10 m in depth in order to access their mollusc prey (Jones & Drobney, 1986).

Scaup are listed on Schedule I of the Wildlife and Countryside Act, Annex II of the Birds Directive and are red-listed in Birds of Conservation Concern (Eaton *et al.*, 2009). They are also listed as a UK Biodiversity Action Plan (BAP) priority species. Scaup are known to be sensitive to human disturbance, diving or hiding when low-flying aircraft approach (Austin *et al.*, 2000) or when vessels pass within 400 m of them (Platteeuw & Beekman, 1994). However, they are unlikely to be risk of collision with turbine blades since the majority of birds fly below the rotor swept height (Cook *et al.*, 2012).

#### Common scoter (*Melanitta nigra*)

Common scoters breed on inland water bodies such as moorland lochs and wooded islets. The majority breed in Scandinavia and Russia with approximately 52 breeding pairs present in Britain (Musgrove *et al.*, 2013). The UK breeding distribution is concentrated in western Northern Ireland, western Scotland and the extreme north of mainland Scotland (Forrester *et al.*, 2007).

Whilst some individuals spend the winter close to their breeding grounds, others migrate to transitional sites to moult. Moult occurs after breeding between June and October, rendering the birds flightless for 3-4 weeks. In the UK, moulting flocks are present between June and September with up to 30,000 birds migrating to UK waters from Scandinavia and Russia to moult, before departing for their wintering grounds (Wernham *et al.*, 2002).

Although small wintering populations occur widely around the coastlines of Britain, the majority occur in a small number of large congregations, with the UK wintering population estimated at approximately 100,000 individuals (Musgrove *et al.*, 2011). Wintering individuals arrive in September with the majority thought to originate from transitional moulting sites in the Baltic (Cabot, 2009). They feed predominantly on the blue mussel *Mytilus edulis*, but are known to predate upon cockles, clams, small fish and plant material.

Common scoters are listed on Annex II of the Birds Directive, Schedule I of the Wildlife and Countryside Act, the Birds of Conservation Concern red list (Eaton *et al.*, 2009) and are a UK BAP priority species. Common scoters are listed as a qualifying feature for 10 SPAs in the UK, with two of these sites situated on the west coast. The Rinn of Islay SPA is designated for 13% of the national common scoter breeding population and the Ribble and Alt Estuaries SPA is designated for 2% of the national wintering population (Stroud *et al.*, 2001). In addition to these sites, there are two marine SPAs designated for common scoters on the west coast of Britain. The Bae

Caerfyrddin/Carmarthen Bay and Liverpool Bay/Bae Lerpwl SPAs were designated in 2003 and 2010 respectively for wintering aggregations of common scoter.

Large number of common scoters are known to occur in the Solway Firth but largely in the spring and autumn, presumably en route to and from wintering areas further south (Musgrove *et al.*, 2011). Data collected during baseline surveys for the Robin Rigg OWF support these findings with peak numbers occurring in May/June and August/September (Natural Power, 2002).

Common scoters are considered highly sensitive to habitat loss and disturbance resulting from OWF construction and operation (Garthe & Hüppop, 2004; Schwemmer *et al.*, 2011; Furness *et al.*, 2013). However, collision risk is predicted to be small since 99% of common scoters fly below the rotor swept area, close to the sea surface (Cook *et al.*, 2012).

### Red-throated diver (*Gavia stellata*)

Red-throated divers breed around shallow pools on moors and bogs, travelling to the coast to feed. Approximately 1,300 pairs breed in the UK and these are concentrated in the north and west of Scotland (Musgrove *et al.*, 2013). In the winter, UK numbers swell with more than 17,000 red-throated divers found in shallow, sandy bays around the UK coastline (O'Brien *et al.*, 2008; Musgrove *et al.*, 2011). The largest aggregation occurs off south-east England with other notable concentrations off Wales in Cardigan Bay and Liverpool Bay.

The red-throated diver is listed on Annex I of the Birds Directive, Schedule I of the Wildlife and Countryside Act and the Birds of Conservation Concern amber list (Eaton *et al.*, 2009). A total of 12 SPAs have been designated for red-throated divers including ten for breeding birds. An additional two marine SPAs, the Outer Thames Estuary and Liverpool Bay/Bae Lerpwl, were designated in 2010 for large aggregations of overwintering red-throated divers.

Baseline surveys for Robin Rigg OWF found regionally important numbers of red-throated divers within the Solway Firth, with numbers peaking in December (Natural Power, 2002). Individuals were scattered throughout the firth but showed a preference for shallow waters between 5 and 10 m in depth.

As for common scoters, red-throated divers are considered highly sensitive to habitat loss and disturbance and are known to show strong avoidance of vessels and wind turbines (Garthe & Hüppop, 2004; Schwemmer *et al.*, 2011; Furness *et al.*, 2013). Data collected at 19 constructed offshore wind farms showed that approximately 2% of red-throated divers flew at rotor swept height (Cook *et al.*, 2012), indicating that potential impacts from collision are small.

### Manx shearwater (*Puffinus puffinus*)

More than 300,000 pairs of Manx shearwater breed in Britain and Ireland, representing over 80% of the world population (Mitchell *et al.*, 2004; Musgrove *et al.*, 2013). Approximately 38% of British and Irish Manx shearwaters breed in Scotland, with 95% of these breeding on the island of Rum (Mitchell *et al.*, 2004). The nearest breeding colonies to the Solway Firth are situated on the island of Sanda off Argyll, the Calf of Man, and the Copeland Islands off Northern Ireland (Mitchell *et al.*, 2004).

Manx shearwaters are highly pelagic, only returning to land to breed in late March (Forrester *et al.*, 2007). Nests are situated in burrows on flat or sloping land close to the sea, which they return to under the cover of darkness. During foraging trips, individuals have been shown to travel over large distances from the breeding colony. Indeed, GPS tracking of individuals breeding on Skomer, Wales, has recorded foraging trips of up to 330 km (Guilford *et al.*, 2008). Elsewhere, foraging ranges of between 160 km and 260 km have been recorded (Mitchell *et al.* 2004; Thaxter *et al.*, 2012). Individuals feed at the sea-surface, either plunge-diving from a height of 1-2 m, or surface-diving. Prey items include small fish species such as herring and sprat, and occasionally squid (Snow & Perrins, 1998). From July, birds depart their breeding colonies to winter off the coast of South America (Guilford *et al.*, 2009; Freeman *et al.*, 2013).

Manx shearwaters are listed on the Birds of Conservation Concern amber list (Eaton *et al.*, 2009) and as a regularly occurring migratory species under the Birds Directive. Five SPAs have been designated for breeding Manx shearwaters in the UK: St Kilda SPA, Rum SPA, Skomer, Skokholm and Middleholm SPA, Glannau



Aberdaron and Ynys Enlli/Aberdaron Coast and Bardsey Island SPA, and the Copeland Islands SPA (designated in 2009).

As expected, baseline surveys for Robin Rigg OWF recorded Manx shearwaters in the summer months only, with no birds recorded after August. Individuals were predominantly distributed over deeper waters in the south and west of the Solway Firth (Natural Power, 2002).

Potential collision risks from operating wind turbines are small for Manx shearwaters as the majority of birds fly close to the sea surface. Indeed, data collected from 10 offshore wind farms found that less than 1% flew within the rotor swept area (Cook *et al.*, 2012). Furthermore, Manx shearwaters are not considered to be particularly sensitive to disturbance and habitat loss arising from construction and operation of offshore wind farms since they are capable of foraging across large areas (Garthe & Hüppop, 2004; Furness *et al.*, 2013).

### Gannet (*Morus bassanus*)

The last complete census of gannets breeding in Britain and Ireland was undertaken in 2003/2004 when an estimated 261,000 pairs were counted (Wanless *et al.*, 2005). This figure is likely to have risen over the last decade since there has been a consistent 2% per annum rise in the world population of gannets (Wanless *et al.*, 2005). The majority of these individuals breed in Scotland (c. 70%) with colonies at Ailsa Craig and Scare Rocks (Table 2.4) in proximity to the Solway Firth. An estimated 27,130 pairs of gannets breed on Ailsa Craig with an additional 2,394 pairs breeding on Scare Rocks (Wanless *et al.*, 2005).

In Scotland, gannets first visit breeding colonies in January with breeding beginning in April. Eggs are typically laid between April and mid-July and fledging occurs between August and November (Forrester *et al.*, 2007). Post-breeding, gannets disperse southwards to wintering grounds off Iberia and west Africa (Wernham *et al.*, 2002; Kubetzki *et al.*, 2009). Small numbers of juveniles from the Bass Rock have been recorded dispersing north and west around the Scottish coast before heading south (Wernham *et al.*, 2002; Kubetzki *et al.*, 2009). Relatively small numbers of gannets have been observed in the Solway Firth post-breeding (Kober *et al.*, 2010).

Gannets are plunge divers, feeding primarily on pelagic fish species such as mackerel, herring and sandeels. However, birds also feed extensively on fishery discards and show attraction to vessels as a consequence (Votier *et al.*, 2013; Bodey *et al.*, 2014).

Satellite telemetry studies of gannets breeding on the Bass Rock off the east coast of Scotland have shown considerable variation in foraging behaviour with maximum foraging distances of up to 540 km (Hamer *et al.*, 2007). At the Hermaness colony in Shetland, foraging ranges of between 32 km and 128 km were recorded for three individuals (Garthe *et al.*, 1999). Gannets breeding on Grassholm, Wales, are capable of travelling up to 475 km away from the breeding colony to forage (Patrick *et al.*, 2013), whilst individuals breeding on Great Saltee, Ireland, had a maximum foraging range of 240 km (Hamer *et al.*, 2000). Whilst these large foraging distances show that gannets breeding at a number of colonies are capable of foraging within the Solway Firth, recent research has shown that breeding gannets from different colonies forage in mutually exclusive territories, indicating that gannets recorded in the Solway Firth during the breeding season most likely originate from Ailsa Craig and Scare Rocks (Wakefield *et al.*, 2013).

Most gannets recorded during baseline surveys undertaken for the Robin Rigg OWF ES were observed during the summer months, with occasional sightings between October and March. Records were distributed throughout the Solway Firth, with an absence of sightings in shallow waters to the north-west (Natural Power, 2002).

Gannets are listed as a regularly occurring migratory species under the Birds Directive and are amber-listed in Birds of Conservation Concern (Eaton *et al.*, 2009). Gannets are considered to be at risk of collision with offshore wind turbines. Indeed, data collected from 27 offshore wind farms found that 10% of gannets were flying at heights that put them at risk of colliding with turbine blades (Cook *et al.*, 2012). However, gannets are unlikely to be impacted by displacement and habitat loss as wind farms are very small relative to their large foraging ranges during the breeding season (Garthe & Hüppop, 2004; Furness *et al.*, 2013).



### Cormorant (*Phalacrocorax carbo*)

The UK breeding population of cormorants has been estimated at 9,000 breeding pairs, with coastal colonies concentrated in Scotland, south-west and north-east England (Mitchell *et al.*, 2004; Musgrove *et al.*, 2013). Inland-breeding birds nest in trees at large waterbodies, mostly within central and eastern England (Newson *et al.*, 2013). At sea, cormorants are restricted to coastal habitats year-round and are most frequently recorded in areas of less than 10 m in depth (Gremillet *et al.*, 2003). The breeding season can vary significantly between years with pairs nesting at different times within the same colony (Brown & Grice, 2005). Individuals can therefore be present at breeding colonies from mid-March to mid-September. Most foraging trips during the breeding season are confined to within 10 km of the colony (Gremillet, 1997), although birds can forage up to 35 km from the colony (Thaxter *et al.*, 2012). Cormorants tend to be solitary feeders but may form larger foraging flocks at sea, where they predate largely on bottom-dwelling fish species such as sculpins, gobies and flatfish, in addition to crustaceans and molluscs (Leopold *et al.*, 1998; Gremillet *et al.*, 2003).

Outside of the breeding season, numbers increase to an estimated 41,000 individuals as birds from the continent migrate into the UK for the winter (Musgrove *et al.*, 2011, 2013). Cormorants which have bred in the UK move to coastal waters in the vicinity of their breeding colony, whilst others may travel much further to inland water bodies or as far away as the Mediterranean Sea (Wernham *et al.*, 2002).

Two cormorant breeding colonies are monitored within the Solway Firth: Balcary Point and Port O' Warren. Between 1999 and 2000, these colonies held approximately 95 and 126 breeding pairs, respectively (Mitchell *et al.*, 2004). During baseline surveys for the Robin Rigg OWF ES the largest numbers of cormorants were recorded during the summer months, predominantly in the north-western part of the Solway Firth (Natural Power, 2002).

Cormorants are listed as a regularly occurring migratory species under the Birds Directive and are green-listed Birds of Conservation Concern (Eaton *et al.*, 2009). Cormorants may be at risk of habitat loss and disturbance from offshore wind farms (Furness *et al.*, 2013) but collision risk has been shown to vary between sites (Cook *et al.*, 2012). Studies have shown that cormorants have a relatively low mean flight height of c. 8 m within a relatively wide range (1-150 m; Walls *et al.*, 2004; Parnell *et al.*, 2005; Petersen *et al.*, 2006).

### Razorbill (*Alca torda*)

Razorbills are one of the most abundant seabird species in the UK with an estimated 187,100 breeding individuals present during the last national census, representing 20% of the world population (Mitchell *et al.*, 2004). The species mainly breeds around the rocky coasts of the Britain and Ireland on small ledges or in cracks on cliffs, with approximately 64% breeding in Scotland. Razorbills are usually associated with colonies of other seabirds, with breeding pairs scattered among large concentrations of guillemots and kittiwakes. Razorbills are listed as qualifying features at the SSSIs located between Abbey Burn Foot and Balcary Point, St Bees Head and the Mull of Galloway which are located between 8.5 and 73 km from the Robin Rigg OWF (Table 2.4).

Egg-laying usually begins in late April, peaking in mid-May. During chick-rearing, razorbills have been shown to have a mean maximum foraging range of  $48.5 \pm 35.0$  km (Thaxter *et al.*, 2012). Despite having shorter foraging trips than guillemots, GPS-tracking studies from the Isle of May, Scotland, have demonstrated that razorbills utilise approximately twice as much foraging area compared to guillemots (2,201 km<sup>2</sup> versus 1,094 km<sup>2</sup>; Thaxter *et al.*, 2010). Chicks fledge in July when they are partly grown and incapable of flight. As with guillemots, chicks are accompanied by the male parent as they complete their growth whilst dispersing rapidly offshore. Between August and October, adult razorbills undergo a full moult and are flightless during this time. Once the moult is complete, the majority of razorbills move gradually south with some birds dispersing as far as the western Mediterranean and the coasts of north-west Africa (Wernham *et al.*, 2002).

JNCC analysis of European Seabirds at Sea (ESAS) data has shown that relatively small densities of razorbills are present in and around the Solway Firth throughout the year (Kober *et al.*, 2010). Baseline surveys for the Robin Rigg OWF showed that razorbills were less abundant in the Solway Firth than guillemots, peaking during the breeding season and again during the late autumn (Natural Power, 2002). Razorbill distribution was more even than guillemots, although few razorbills were recorded in the shallow waters to the north of the survey area (Natural Power, 2002).

Razorbills are listed under the Birds Directive as a regularly occurring migratory species and are amber listed in Birds of Conservation Concern (Eaton *et al.*, 2009). As for guillemots, potential collision risks from operating wind turbines are small for razorbills; data collected from 19 offshore wind farms found that less than 0.5% flew within the rotor swept area (Cook *et al.*, 2012). However, razorbills may be sensitive to disturbance and habitat loss arising from construction and operation of offshore wind farms (Garthe & Hüppop, 2004; Schwemmer *et al.*, 2011; Furness *et al.*, 2013).

### Guillemot (*Uria aalge*)

An estimated 1,416,300 breeding guillemots were present in the UK during the last national census, representing 12% of the world population (Mitchell *et al.*, 2004). Breeding colonies are situated around the coasts of the UK where there is suitable cliff habitat, with approximately 75% of individuals breeding in Scotland (Mitchell *et al.*, 2004). Guillemots are listed as qualifying features at the SSSIs located between Abbey Burn Foot and Balcary Point, St Bees Head and Scare Rocks which are located between 8.5 and 62 km from the Robin Rigg OWF (Table 2.4).

Guillemots spend much of the year at-sea, only coming to land to breed between May and August. During the breeding season, guillemots forage by pursuit diving in both benthic and pelagic environments, feeding on small, lipid-rich fish species including sprats and sandeels (Anderson *et al.*, 2014). Breeding guillemots have been shown to have a mean maximum foraging range of  $84.2 \pm 50.1$  km based on 46 individual studies (Thaxter *et al.*, 2012). GPS-tracking studies on the Isle of May, Scotland, have shown that guillemot foraging trips vary by sex. The average maximum foraging distance from the colony was  $14.4 \pm 6.6$  for males and  $7.9 \pm 5.3$  km for females (based on 11 and 8 foraging trips, respectively; Thaxter *et al.*, 2010). Post-fledging, chicks are flightless for 8-10 weeks, dispersing offshore accompanied by the male parent. Many adult birds remain within a few hundred km of the breeding colony throughout the winter, with some visiting nesting ledges in late autumn/winter following the main moult which renders them flightless (Harris & Wanless, 1990; Wernham *et al.*, 2002).

Baseline surveys for the Robin Rigg OWF recorded a peak in guillemot numbers during the spring and early summer, with numbers declining from July onwards as birds dispersed further offshore, post-breeding (Natural Power, 2002). Guillemots were observed throughout the survey area with concentrations in the south-west, in relatively deep water close to the breeding colony at St Bees Head (Natural Power, 2002). Density surface maps produced by the JNCC using ESAS data show a similar annual distribution, which the largest densities in the Solway Firth recorded in post-fledging as birds move offshore (Kober *et al.*, 2010).

Guillemots are amber-listed in Birds of Conservation Concern (Eaton *et al.*, 2009) and as a regularly occurring migratory species under the Birds Directive. Potential collision risks from operating wind turbines are small for guillemots as the majority of birds fly close to the sea surface. Indeed, data collected from 23 offshore wind farms found that less than 0.05% flew within the rotor swept area (Cook *et al.*, 2012). However, guillemots may be sensitive to disturbance and habitat loss arising from construction and operation of offshore wind farms (Garthe & Hüppop, 2004; Furness *et al.*, 2013).

### Kittiwake (*Rissa tridactyla*)

The last complete census of kittiwakes in Britain and Ireland estimated a breeding population of 380,000 pairs (Mitchell *et al.*, 2004), with the largest concentrations recorded in Scotland. However this may be an overestimate since many kittiwake colonies have seen declines over the last decade (Chivers *et al.*, 2013; JNCC, 2014). Indeed, the UK kittiwake population has decreased by 40% since the 1960s (JNCC, 2014).

In Scotland, kittiwakes return to breeding colonies in late February/March with eggs typically laid in May. During this time, adult kittiwakes have been shown to forage up to 120 km from the breeding colony, with a mean maximum foraging range of  $60 \pm 23$  km (Thaxter *et al.*, 2012). Kittiwakes feed at the sea surface, preying upon small fish species such as sandeels and sprats through shallow splash dives (Snow & Perrins, 1998). Kittiwakes are also known to take discards from fishing trawlers (Erikstad *et al.*, 1988; Bicknell *et al.*, 2013). Fledging occurs in July/August with both adults and juveniles spending the winter in the North Sea, Irish Sea and Atlantic (Bogdanova *et al.*, 2011).

Baseline surveys of the Solway Firth for the Robin Rigg ES showed that the largest numbers of kittiwakes occurred during the spring and summer, with numbers falling during the winter as birds move offshore (Natural Power, 2002). This is consistent with ESAS data (Kober *et al.*, 2010).

Kittiwakes are amber-listed in Birds of Conservation Concern (Eaton *et al.*, 2009) and are listed as a regularly occurring migratory species under the Birds Directive. Kittiwakes are not predicted to be highly sensitive to disturbance and habitat loss arising through construction and operation of offshore wind farms but are at risk from collisions with turbine blades (Garthe & Hüppop, 2004; Furness *et al.*, 2013). Data collected at 26 OWF sites showed that 16% of kittiwakes flew at rotor swept height (Cook *et al.*, 2012).

### Great black-backed gull (*Larus marinus*)

Approximately 17,000 pairs of great black-backed gulls were estimated to be breeding in the UK during the last national census (Mitchell *et al.*, 2004; Musgrove *et al.*, 2013) and the global population is considered to be increasing (BirdLife International, 2014). Breeding great black-backed gulls in the UK nest almost exclusively in coastal habitats and are concentrated along the western coasts of Britain and Ireland and in the Scottish Northern Isles (Mitchell *et al.*, 2004). Numbers increase during the winter to approximately 77,000 individuals as birds migrate into the UK from Norway and Russia (Banks *et al.*, 2007).

Great black-backed gulls are listed as regularly occurring migratory species under the Birds Directive and are amber-listed in Birds of Conservation Concern (Eaton *et al.*, 2009).

Breeding begins in March/April with egg-laying occurring between late April and late June (Snow & Perrins, 1998). The breeding population is thought to be largely sedentary and movements from breeding sites are usually over relatively small distances (Furness & Tasker, 2000; Banks *et al.*, 2007), often in response to feeding opportunities. Indeed, as with other large gull species, the at-sea distribution of great-black-backed gulls may be influenced by the presence of fishing trawlers since the species is known to forage on discards (Garthe, 1997; Bicknell *et al.*, 2013). Chicks fledge after seven or eight weeks but are attended by adults for up to six months (Snow & Perrins, 1998). During the winter period, great black-backed gulls have been shown to have a more pelagic distribution than other large gull species (Snow & Perrins, 1998; Wernham *et al.*, 2002).

Small densities of great black-backed gulls were recorded in the Solway Firth during JNCC ESAS surveys, with the largest densities recorded between August and October (Kober *et al.*, 2010). Similar results were found during baseline surveys (Natural Power, 2002). As with other large gull species, great black-backed gulls are not predicted to be highly sensitive to disturbance and habitat loss arising through construction and operation of offshore wind farms but are at risk from collisions with turbine blades (Garthe & Hüppop, 2004; Furness *et al.*, 2013). Data collected at 19 OWF sites showed that 33% of herring gulls flew at rotor swept height (Cook *et al.*, 2012).

### Herring gull (*Larus argentatus*)

The breeding population of herring gulls in Britain and Ireland is estimated at 140,000 pairs with an additional 7,100 pairs on the Isle of Man (Mitchell *et al.*, 2004; Musgrove *et al.*, 2013). At the time of the last national census, around 14% of the population nested on buildings compared with natural habitats (Mitchell *et al.*, 2004). The abundant food supply in urban areas provided by street litter and refuse bins, combined with safe nesting sites has most likely led to further increases of urban nesting herring gulls, although the current number is not known. However, despite the increase in urban nesting gulls, the total herring gull population has declined by more than 50% since the mid-1980s (JNCC, 2014).

Egg-laying begins in late April, peaking in mid-May (Forrester *et al.*, 2007). For coastal breeding herring gulls, foraging ranges are likely to be influenced by the spatial distribution of fishing vessels (Garthe, 1997; Bicknell *et al.*, 2013). The maximum foraging distance recorded for herring gulls is 92 km with a mean maximum foraging range of  $61 \pm 44$  km (Thaxter *et al.*, 2012). Herring gulls are opportunistic, omnivorous feeders and the diet of adults differs considerably to that of chicks which largely comprises fish and meat (Snow & Perrins, 1998).

Chicks fledge in July/August with some adults and juveniles remaining on feeding grounds close to the nest site year-round whilst others migrate as far as the Mediterranean (Forrester *et al.*, 2007). A large proportion of birds

breeding in northern Scotland move south to central Scotland, north-east England and continental Europe (Monaghan *et al.*, 1985). Herring gull numbers in the UK swell during the winter as birds arrive from breeding colonies in Iceland and Scandinavia (Wernham *et al.*, 2002).

Baseline surveys of the Solway Firth for the Robin Rigg OWF have shown small densities of birds in the area, particularly in inshore areas (Natural Power, 2002), which is supported by ESAS data (Kober *et al.*, 2010). Herring gulls are listed as a regularly occurring migratory species under the Birds Directive and are red-listed in Birds of Conservation Concern (Eaton *et al.*, 2009). They are also a UK BAP priority species. Herring gulls are not predicted to be highly sensitive to disturbance and habitat loss arising through construction and operation of offshore wind farms but are at risk from collisions with turbine blades (Garthe & Hüppop, 2004; Furness *et al.*, 2013). Data collected at 20 OWF sites showed that 28% of herring gulls flew at rotor swept height (Cook *et al.*, 2012).

## 2.2. Survey Methods

### 2.2.1. Overview

Ecology Consulting Ltd carried out boat-based baseline surveys across the Robin Rigg OWF from 2001 to inform the Environmental Impact Assessment (EIA). To meet the requirements of the MEMP, Ecology Consulting Ltd continued boat-based surveying until 2012, after which surveys were conducted by Natural Power. Table 2.5 shows the timing of boat-based ornithological surveys undertaken across Robin Rigg OWF. The survey schedule is described below:

#### EIA baseline surveys

- Boat-based surveys were undertaken twice per month between May 2001 and April 2002 (with the exception of May and October 2001 when only one survey was completed).
- Monthly baseline boat-based surveys continued to December 2002, but only data up to and including April 2002 were included in the EIA.
- Surveying was undertaken along ten transects across the Robin Rigg OWF, approximately 18 km in length spaced 2 km apart.

#### MEMP monitoring surveys

- Pre-construction surveys were undertaken once per month in April and May 2003 and between January and September 2004. An additional two surveys were carried out in July 2007, prior to construction commencing.
- Construction phase surveys began in January 2008 and continued twice per month until the end of construction in February 2010. Surveys were completed during all months in this period, with the exception of November 2009.
- Post-construction surveys have been undertaken once per month since March 2010 and will continue until March 2015 to meet the requirements of the MEMP.

**Table 2.5: Timing of boat-based ornithological surveys at Robin Rigg OWF. Numbers refer to the number of surveys undertaken each month. Light grey = EIA baseline surveys (N.B only data collected up to and including April 2002 were included in the EIA); light purple = pre-construction surveys; dark grey = construction surveys; dark lilac = post-construction surveys.**

	2001	2002	2003	2004	2005	2006	2007	2008	2009	2010	2011	2012	2013	2014
Jan		2		1				2	2	2	1	1	1	1
Feb		2		1				2	2	2	1	1	1	1
Mar		2		1				2	2	1	1	1	1	
Apr		2	1	1				2	2	1	1	1	1	
May	1	1	1	1				2	2	1	1	1	1	
Jun	2	1		1				2	2	1	1	1	1	
Jul	2	1		1			2	2	2	1	1	1	1	
Aug	2	1		1				2	2	1	1	1	1	
Sep	2	1		1				2	2	1	1	1	1	
Oct	1	1						2	2	1	1	1	1	
Nov	2	1						2		1	1	1	1	
Dec	2	1						2	2	1	1	1	1	

## 2.2.2. Data Collection

The data collection methods used at Robin Rigg OWF differ slightly from the standard protocols commonly used today for offshore surveys (Camphuysen *et al.*, 2004; MacLean *et al.*, 2009). Although a standardised method for collecting seabird data from boats was first proposed in 1984 (Tasker *et al.*, 1984), a standardised method for collecting seabird data at OWF developments was not produced until 2004 (Camphuysen *et al.*, 2004), three years after surveys began at Robin Rigg OWF.

In order to ensure that a comparable dataset was collected across development phases, the survey method employed during EIA baseline surveys has been followed throughout the study. Consistency in data collection is important for statistical comparison of bird abundance and distribution across development phases.

During each boat-based survey, the vessel travelled along a total of ten transects each approximately 18 km in length and spaced 2 km apart (Figure 2.1). This separation distance was chosen to ensure that a good sample of the study area was covered for each key species, whilst minimising the likelihood that birds may be displaced from one transect into an adjacent one, and therefore double-counted. Since access to shallow parts of the survey area are restricted at low tide, tidal conditions have dictated whether surveys are undertaken in a single day or across two days.

Key components of the method are as follows:

- Bird detection is undertaken by naked eye, but binoculars are used to confirm identity and to occasionally look ahead for easily flushed species such as divers and seaducks;
- Birds are recorded as either in flight or on the sea by two observers working simultaneously on either side of the vessel; each observes a 90° angle ahead and to the side of the vessel;
- For each observation, time is recorded to the nearest minute. The time piece used for recording sightings is matched to the hand-held GPS used for recording survey tracks to allow the precise position of each observation to be determined;
- The survey is based on a line transect method with a strip width of 300 m;
- The 300 m transect is sub-divided into the following five bands into which all birds on the water are allocated: 0-50 m (A), 50-100 m (B), 100-200 m (C), 200-300 m (D), 300+ m (E). Distances are perpendicular to the survey vessel. Only birds within 300 m (bands A-D) are considered to be 'in transect'; and
- Additional data are collected for each bird (where possible) including: age, plumage type and behaviour.

At the onset of operational year three, additional data collection methods were employed alongside existing methods in order to collect data in a manner that is consistent with current best practice (Camphuysen *et al.*, 2004; MacLean *et al.*, 2009). One surveyor continues to collect data using existing methods on one side of the vessel, whilst the second surveyor collects data according to best practice ESAS methods.

All birds on the sea surface are recorded in the same way. However, birds in flight are recorded differently under the ESAS method. Whilst flight heights are recorded using the same height bands under both methods, the distance of flying birds from the vessel is not recorded under the ESAS method. The primary difference is that the ESAS method utilises 'snap-shots' to record flying birds whilst the existing method does not. 'Snap-shots' involve recording the number, height and behaviour of flying birds every one minute or 300 m, within a 300 (m)<sup>2</sup> block which extends perpendicular and to the front of the vessel. Previous comparison of the differences in the number of flying birds recorded using the two methods has shown that fewer birds are recorded using the 'snap-shot' method (Walls *et al.*, 2013a, 2013b and 2013c). This is examined in Section 2.4.12.



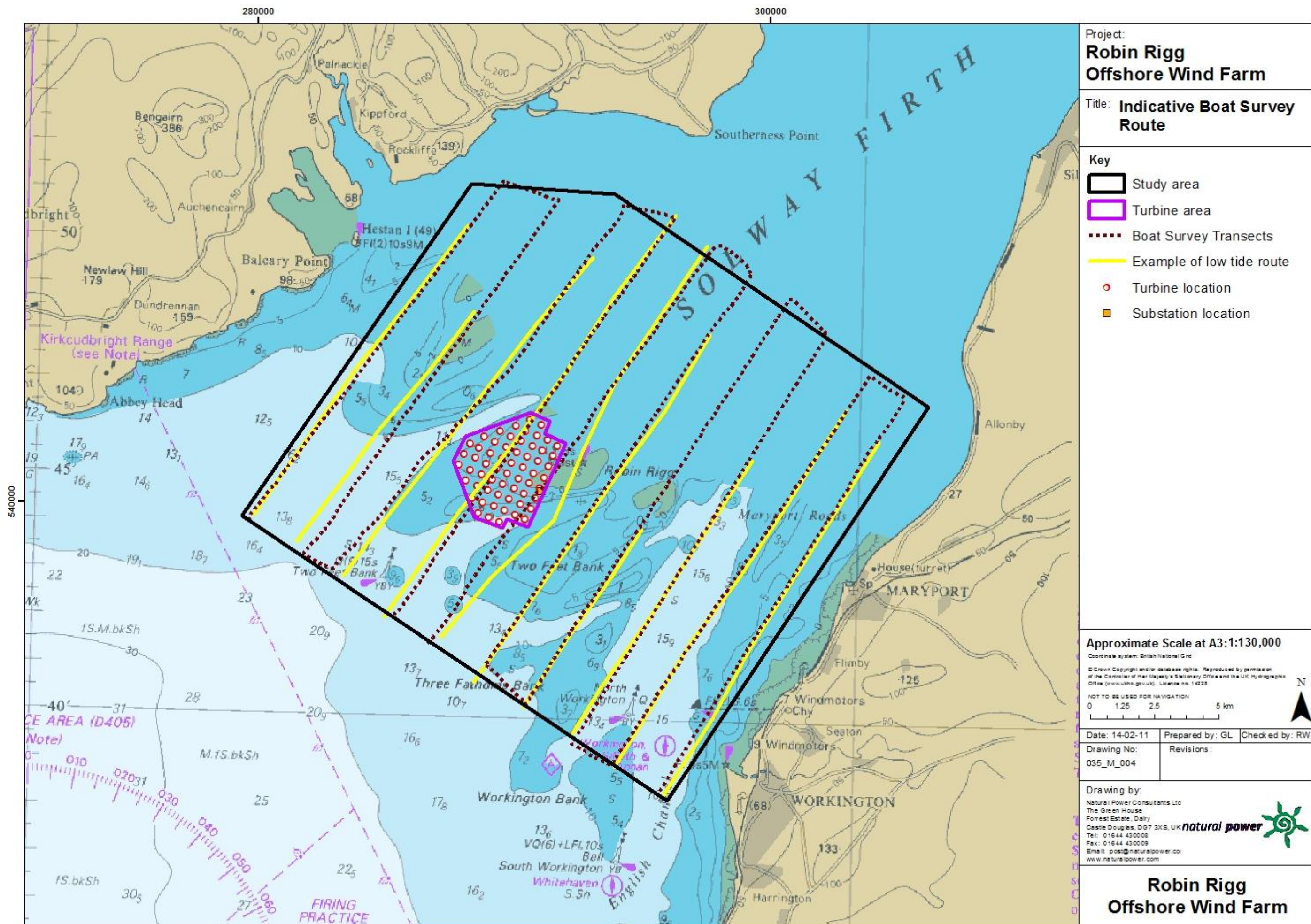


Figure 2.1: Sample survey route followed for ornithological surveys at Robin Rigg OWF between 2001 and 2014.



A number of vessels have been used throughout surveying, with viewing platforms ranging from 3.5-4.5 m above sea level (Table 2.6). Although slightly below the recommended 5 m (Camphuysen *et al.*, 2004; MacLean *et al.*, 2009), it was considered that these vessels provided suitable viewing platforms with without restricting the areas that could be surveyed; larger vessels with higher viewing platforms are unable to navigate the sandbanks that run through the Solway Firth, thus reducing the potential survey area.

**Table 2.6: Vessels used during ornithological surveys at Robin Rigg OWF between 2001 and 2014, including viewing platform height (in metres) above sea level.**

Vessel name	Viewing platform height (m)	Number of survey days
Solway Protector	4.5	101
Tiger	4.5	18
Catch Me II	4.5	2
Talisman of Wight	3.5	8
Pilgrim	4	5
Maid Good	4.5	78

## 2.3. Analytical Methods

### 2.3.1. Overview

The analytical methodology has been determined by the data available to Natural Power, collected as part of the MEMP before, during and after construction of the Robin Rigg OWF. Data analysis has focussed on 11 key species: scaup, common scoter, red-throated diver, Manx shearwater, cormorant, gannet, razorbill, guillemot, kittiwake, great-black-backed gull and herring gull, as outlined in Section 2.2.2.5.

The approach to analysis has been developed after reviewing the requirements of the MEMP, the Food and Environment Protection Act (FEPA) licence and a Centre for Environment, Fisheries and Aquaculture Science (CEFAS) review of OWF monitoring associated with FEPA licence conditions (Walker & Judd, 2010).

As part of this process, consultation with Marine Scotland, Scottish Natural Heritage (SNH) and Natural England identified key questions for specific focus. Data analysis was tailored to the predictions made in the ES (Natural Power, 2002) and addresses the FEPA licence conditions. The analysis has also focussed on key questions raised by the RRMG and on addressing uncertainties outlined in the MEMP.

Specific key questions for data analysis identified by E.ON and the RRMG relate to:

- Comparing observed patterns with predicted impacts/sensitivities from the ES;
- Changes in patterns of abundance and distribution relating to the wind farm; and
- Disturbance/displacement of specific species.

The Natural Power Ecology and Hydrology Department have undertaken all of the ornithological data analyses presented here. Questions have been investigated as fully as possible within the limits imposed by the survey programme and methods, and the rigour and consistency of the data collected. The analyses presented here provide an update to previous analyses by incorporating data collected during operational year four (Walls *et al.*, 2013a, 2013b and 2013c).

### 2.3.2. Data Collation

All data, including that collected by Ecology Consulting Ltd, were collated and verified by Natural Power. Throughout this procedure, data were visually inspected and any concerns referred back to the surveyors so that any issues with the dataset could be resolved. All data were stored and managed using Microsoft Excel.



### 2.3.3. Data Processing

Data collected prior to October 2001 were removed from the dataset as data collected during this period were grouped in 10-minute blocks and so precise positions could not be extracted.

GPS tracks from each survey were obtained and imported into ArcGIS v10. Each individual survey transect was divided into survey blocks of  $600 \text{ (m)}^2$  (Figure 2.2). The width of each block was determined by transect width (300m to either side of the survey vessel) and the same length was chosen to ensure that the resolution of spatial covariates was the same on both axes i.e. covariates are averaged across each block; if block width is smaller than block length then average covariate values will have less variation (higher resolution) along the width axis than the length axis.

Observations were assigned to survey blocks and covariates for each block were extracted including sea depth and sediment type at the midpoint of the block (data obtained from SeaZone Solutions Ltd) and distance of the block midpoint to the nearest coastline (Figure 2.3). Tidal height for each block was also obtained using data supplied by the British Oceanographic Data Centre. Percentage gravel was calculated for each sediment class (in order to allow analysis of sediment type as a continuous covariate). Although sea state data were collected during the majority of surveys, it was not possible to use this as a factor in the analysis as information on sea state was not recorded during early surveys.

### 2.3.4. Data Analysis

Analyses of ornithological data collected at Robin Rigg OWF are very complicated with issues of spatio-temporal autocorrelation and zero-inflation. In addition, different species-specific datasets have very different properties, meaning that a species by species approach was adopted. Two separate sets of analyses were undertaken for each key species:

- **Comparison between development phases** including pre-construction (baseline and pre-construction data), construction and operation (data from the first two years of operation); and
- **Comparison between operational years one to four.**

Analysis was carried out separately for birds in flight and on the water since any response to the OWF might be expected to differ depending upon behaviour. The general approach taken to data analysis is outlined below.

#### 2.3.4.1. Summary statistics

For each key species, raw observations were mapped and summary statistics were calculated to provide an initial indication of any changes in abundance or behaviour among the different development phases and operational years. The mean number of individuals and sightings observed per km of survey effort was calculated.

#### 2.3.4.2. Modelling approach

All data exploration and subsequent analysis was undertaken using R version 3.1.1 (R Core Team, 2014). The R package 'MRSea' (Scott-Hayward *et al.*, 2013) was used to analyse the ornithological data collected at Robin Rigg OWF. The MRSea package was commissioned by Marine Scotland and developed by the Centre for Research into Ecological and Environmental Modelling (CREEM) to facilitate the modelling of offshore line transect data. The package allows the implementation of Distance sampling to account for imperfect detection during surveys and makes use of a Complex Region Spatial Smoother (CReSS; Scott-Hayward *et al.*, 2014) which is implemented through Spatially Adaptive Smoothing Algorithms (SALSA: Walker *et al.*, 2011) within a Generalised Estimating Equation (GEE; Hardin & Hilbe, 2002) framework to assess animal abundance and distribution. The advantages of this approach are that:

- Drop-off in detectability with distance from the observer can be accounted for;
- Non-linear relationships among covariates and response variables can be modelled flexibly using SALSA; and
- Spatio-temporal autocorrelation and over-dispersion can be accounted for using GEEs with fewer assumptions than are made using other modelling techniques.

However, unlike previous analyses undertaken by Natural Power (Walls *et al.*, 2013a, 2013b and 2013c), the MRSea approach does not account for the underlying causes of zero-inflation within the data. Zero-inflated data can violate the distributional assumptions of any analysis, leading to invalid scientific inference and computational difficulties (Tu, 2002). Zero-inflation may also cause over-dispersion of the data, although over-dispersion can occur independently in any dataset.



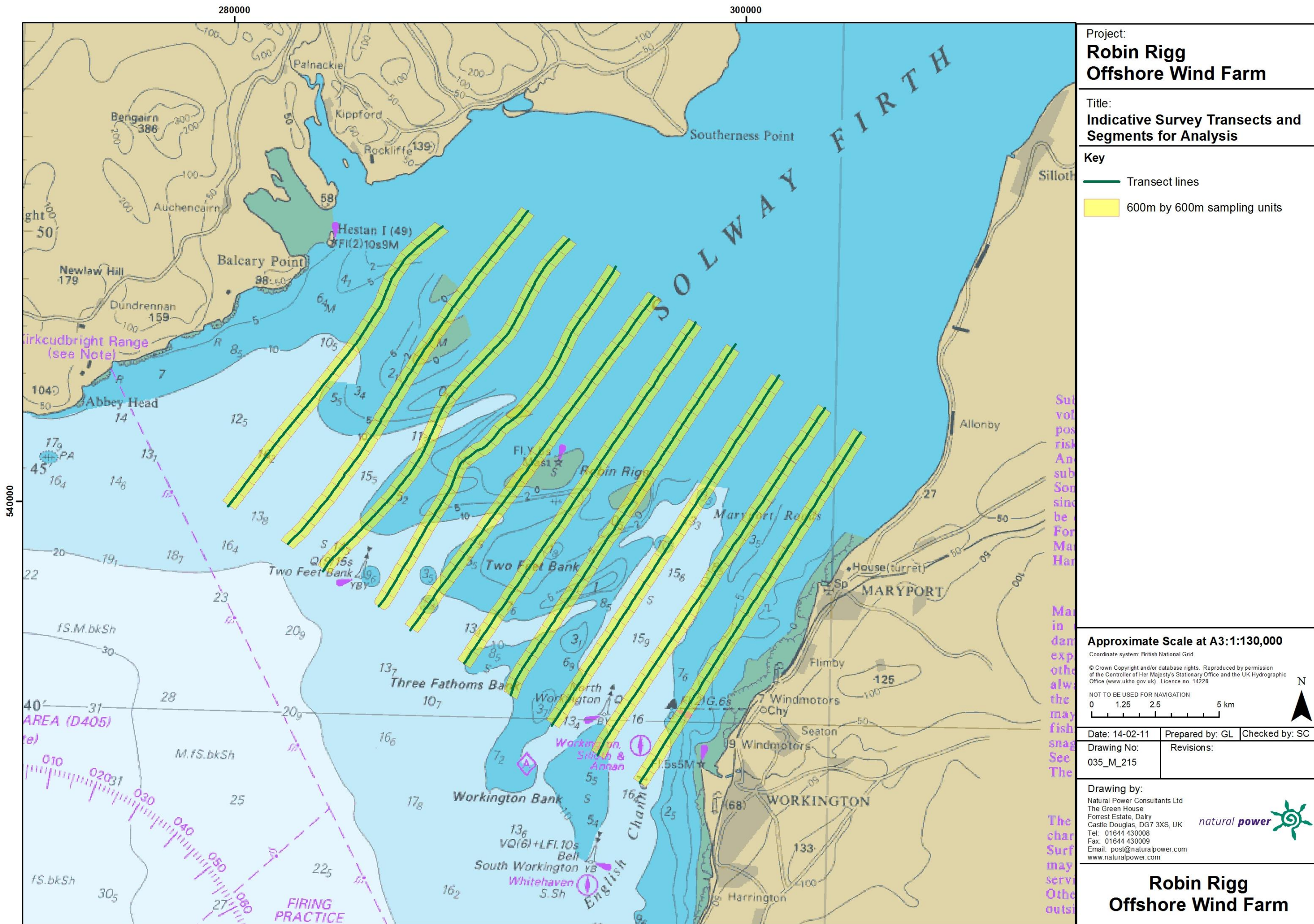


Figure 2.2: Example of 600 (m)<sup>2</sup> survey segments applied to survey transects.



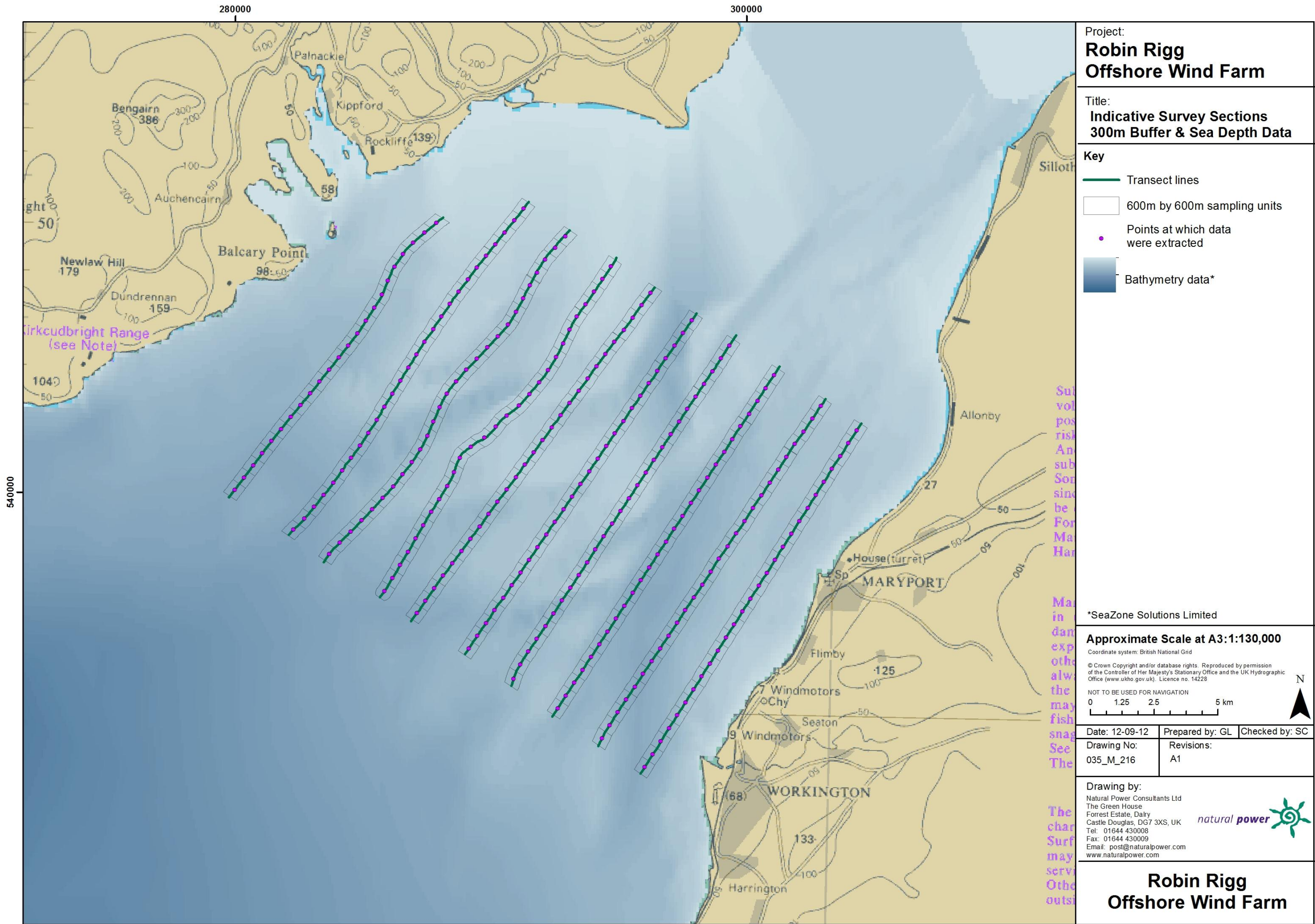


Figure 2.3: Example of sea depth data extracted for each 600 (m)<sup>2</sup> survey block.

## Data exploration

Data exploration followed the protocol outlined by Zuur *et al.* (2009), which involves asking the following questions:

- Are there outliers in the explanatory variables?
- Is there even coverage of the explanatory variables?
- Is there collinearity among explanatory variables?
- Are there potential outliers in the response variable?
- Is the response variable zero-inflated?

A summary of the variables considered for inclusion in the models is provided in Table 2.7. The response variable and all covariates were assessed to ensure even data coverage and to check for potential outliers. Collinearity among covariates was investigated and all collinear variables except tide height were excluded<sup>3</sup>. This is an important step since the inclusion of collinear variables in a model inflates probability (p)-values. This can lead to unstable models in which important relationships in the data are masked. Variables selected for inclusion in the models following this step are highlighted in bold in Table 2.7. Full details of the data exploration process can be found in Appendix B. Any dataset with >99% zero observations was not analysed.

**Table 2.7: Variables considered for inclusion in modelling of bird abundance and distribution at Robin Rigg OWF. Variables selected for inclusion in the models are highlighted in bold.**

Variable	Variable type
<b>Number of birds</b>	<b>Discrete response</b>
<b>Latitude</b>	<b>Continuous variable</b>
<b>Longitude</b>	<b>Continuous variable</b>
Sea depth	Continuous variable
<b>Tide height</b>	<b>Continuous variable</b>
Distance to nearest coast	Continuous variable
Time of day (GMT)	Continuous variable
<b>Month</b>	<b>Factor variable</b>
Sediment type	Factor variable
<b>Operation year</b>	<b>Factor variable</b>
Survey number	Factor variable
Transect number	Factor variable

## Incorporation of Distance sampling techniques

For birds on sea, Distance sampling techniques were employed to account for imperfect detection. Distance sampling cannot be undertaken for birds in flight as it is not possible to accurately allocate flying birds to distance bands as many move too quickly.

Distance sampling operates on the principle that randomly distributed animals become more difficult to detect with increasing distance from the observer (Buckland *et al.*, 2001). As a result, an increasing proportion of animals that are present will go undetected with distance. To account for this decline in detectability, a detection function is

---

<sup>3</sup> Since the bathymetry of the Solway Firth is highly dynamic with shifting sandbanks, sea depth calculated in ArcGIS is likely to be inaccurate. Therefore, tide height was retained as a proxy to give an indication of variation in sea depth. Tide height has not previously been used in previous analyses of the Robin Rigg ornithological dataset (Walls *et al.*, 2013a, 2013b and 2013c).

fitted to the data. This function allows the estimation of the proportion of individuals within a surveyed area that go undetected, enabling adjustment of observed counts.

Several detection functions were considered for modelling the drop-off in detectability for each species of interest. The most appropriate function was selected by minimising the Akaike Information Criterion (AIC), a relative measure that allows comparison of nested models based on a trade-off between the goodness-of-fit of the model to the data and the complexity of the model. Covariates considered likely to affect detectability were sea state, group size (in discrete bands), observer and vessel. Goodness-of-fit of the selected detection functions was assessed using QQ plots. Full details of the detection function selection process can be found in Appendix B.

### 2.3.4.3. Modelling outputs

#### Distribution and abundance

Where possible, the initial model constructed for each key species included 'month' and 'development phase/operational year' as factor variables. 'Tidal height' was included as a continuous covariate and was modelled using a one dimensional smooth. 'Latitude' and 'longitude', also included as continuous covariates, were modelled using a two-dimensional smooth to account for unmeasured spatial variables. To allow the modelled effect of spatial location to vary depending upon the development phase or operational year, an interaction term was included between the spatial smooth and the development phase/operational year. This allowed changes in the distribution of birds over time to be investigated.

By fitting GEE models with a panel variable any non-independence within the residuals due to autocorrelation and over-dispersion was accounted for in model estimates and confidence intervals. A conjugate variable made up from 'transect' and 'survey' was used as a panel variable, allowing residuals within surveys for each transect to be correlated, but residuals from different transects or different surveys within the same transect were considered independent. Uncertainty within modelling stages, i.e. fitting a detection function (where applicable) and the spatial modelling process itself, was accounted for by refitting both stages to resampled data during 250 non-parametric bootstrap iterations. Parameter estimates were taken as the median estimate of the resulting distribution of 250 estimates, while 95 % percentiles were used as confidence intervals. If 95 % confidence intervals excluded zero they were considered to be statistically significant.

#### Model validation

The effectiveness of modelling the smooths was determined using cumulative residual plots. Covariate relationships were assessed using partial residual plots. Partial residual plots show the relationship between a given independent variable (e.g. phase) and the response variable (e.g. abundance) given that other independent variables are also included in the model. An estimate of effect size (e.g. abundance) with uncertainty (confidence levels) is compared to a reference represented as straight line at zero. To assess the fit of the final model, the following plots were used:

- observed versus fitted values (indication of data fit);
- fitted values versus residuals (indication of the correct mean-variance relationship assumed under the model);
- cumulative residuals (assessment of systematic over- or under-prediction);
- runs sequence (assessment of correlation in model residuals);
- COVRATIO and PRESS statistics (to assess how the model might change if individual survey blocks are removed); and
- raw residuals (to determine if certain parts of the survey area are over- or under-predicted).

#### Predictions

Once a model was selected, predictions were made using the model outputs. All predictions were made for the month of peak abundance. Where possible, abundance and density estimates were calculated for the Robin Rigg OWF site, the entire survey area and within circular buffer zones at different distances from the site. These estimates were then used to determine the proportion of birds predicted to be using the Robin Rigg OWF across development phases and operational years.



### Collision risk

Available flight height data for each key species were grouped into six bands: 0-5 m, 6-25 m, 26-34 m, 35-125 m, 126-200 m and >200 m. These bands were chosen to reflect the known rotor height of the turbines used at Robin Rigg OWF (35-125 m), bird behaviour and data collection practicalities. For key species flying at rotor height, the proportion of birds in each band for each development phase or operational year was calculated and compared using chi-squared tests. To aid this analysis and interpretation, all data in height bands above and below the rotor height band were combined into single upper and lower bands (i.e. 0-34 m, 35-125 m and >126 m).

## 2.4. Results

### 2.4.1. Scaup

#### 2.4.1.1. Across three development phases

##### 2.4.1.1.1. Summary statistics

Numbers of individual scaup remained relatively similar during pre-construction and construction phases with larger numbers recorded on the sea compared to those in flight (Table 2.8). The data suggest an increase during the operational phase, although this may be an artefact of data collection. Anecdotal evidence from surveys has shown that scaup are typically observed in the distance when flushed from the sea surface by the approaching survey vessel.

Relatively few sightings of scaup were recorded during any phase of the development (Table 2.8). The majority of sightings occurred during the winter months (November to March). The small number of sightings for this species prevents further abundance modelling from being undertaken.

**Table 2.8: Number of scaup recorded per block during each development phase per km survey effort (all data).**

	Pre-construction		Construction		Operation years 1-2	
	On sea	In flight	On sea	In flight	On sea	In flight
<b>Total number individuals</b>	362	46	351	0	1,883	200
<b>Total number sightings</b>	5	6	4	0	7	4
<b>Number individuals/km</b>	0.10	0.01	0.05	0	0.49	0.05
	Total		Total		Total	
<b>Total number individuals</b>	408		351		2,083	
<b>Total number sightings</b>	11		4		11	
<b>Number individuals/km</b>	0.11		0.05		0.54	

Data were filtered as described in the methodology (Section 2.4.4). The percentage of analysis blocks without observations was calculated to ensure there were sufficient data to perform the analysis (Table 2.9). Since >99% of analysis blocks for both birds on sea and in flight contained zero observations, further abundance modelling of scaup across the three development phases was not undertaken.

**Table 2.9: Percentage of scaup analysis blocks without observations across the three development phases: pre-construction, construction and operational years one and two.**

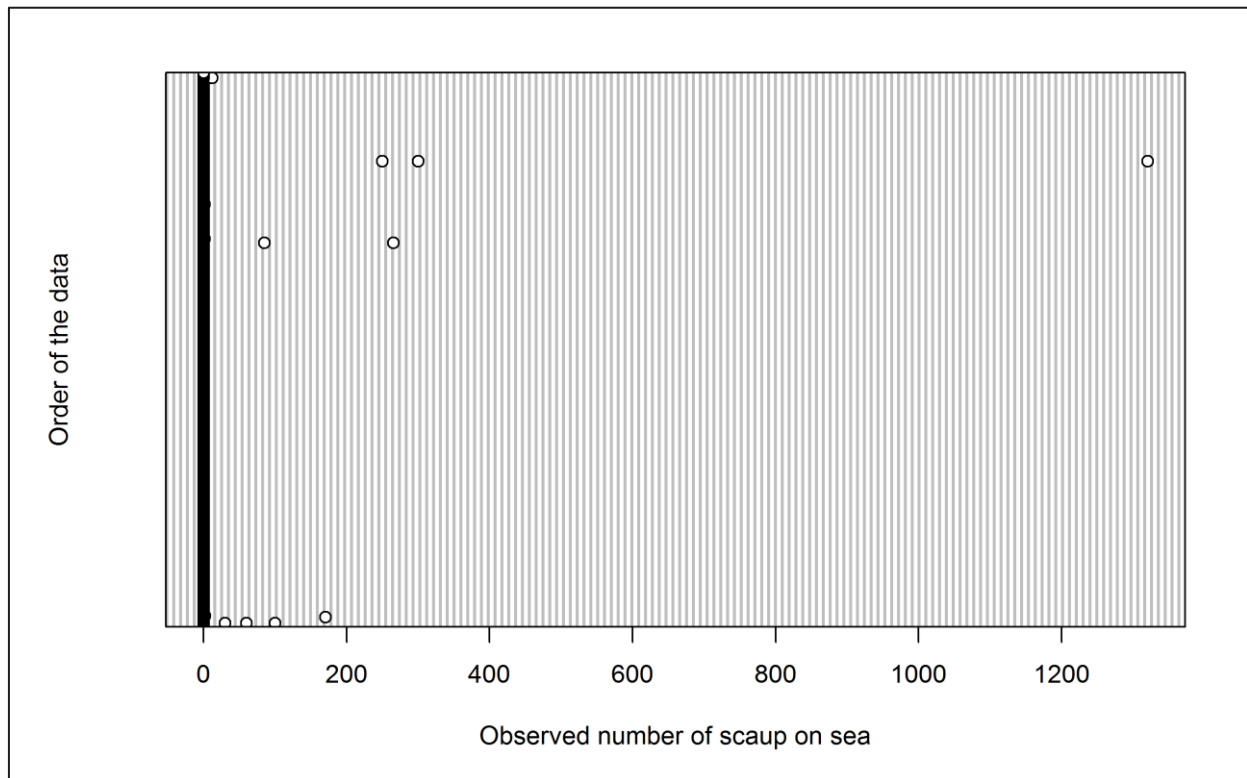
	On sea	In flight
<b>Percentage zero blocks</b>	99.9%	99.9%



## 2.4.1.1.2. Density

### 2.4.1.1.2.1. On sea

Group size for scaup recorded on the sea ranged from single individuals up to 1,320 birds (Figure 2.4). Mean density of scaup indicates that an increase during the operational phase (Figure 2.5). However, since further modelling was not undertaken, the significance of this increase cannot be tested. Figure 2.6 shows that the majority of scaup on the sea were recorded during the winter months between November and January.



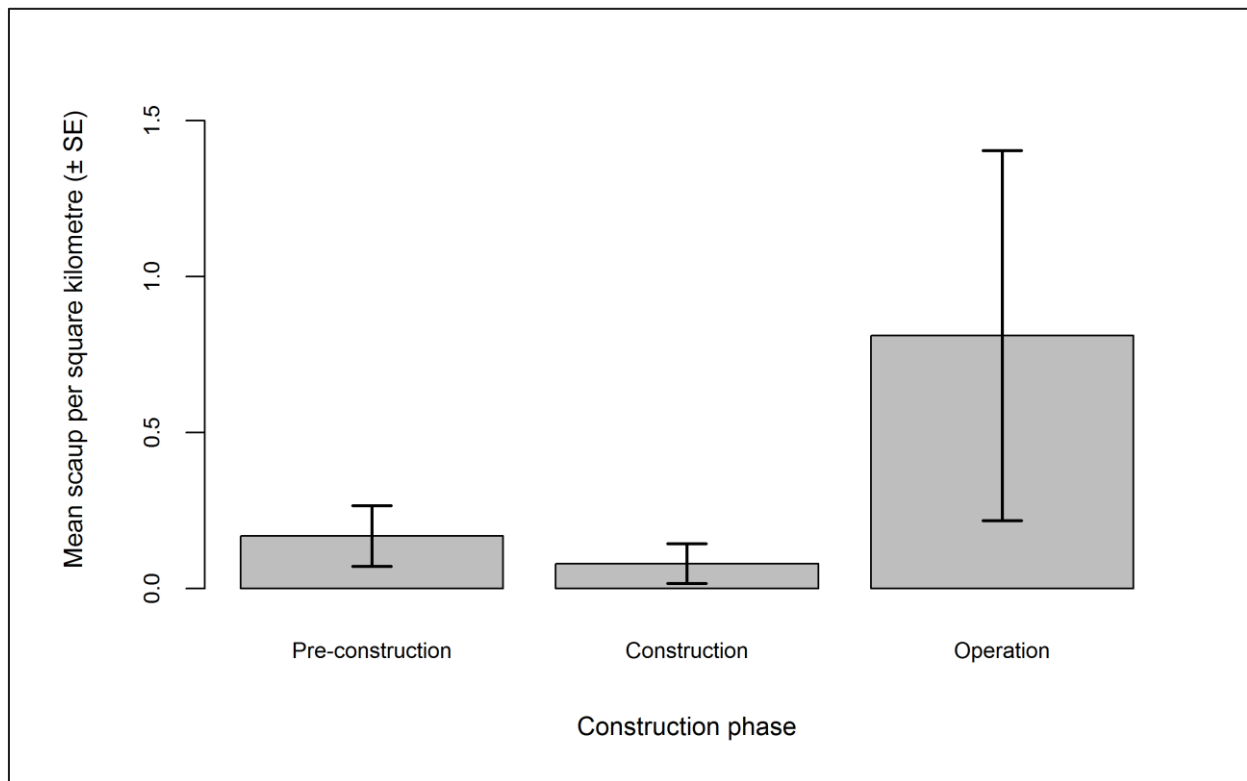


Figure 2.5: Mean density ( $\pm$  se) of scaup recorded on the sea during each development phase: pre-construction, construction and operational years one and two.

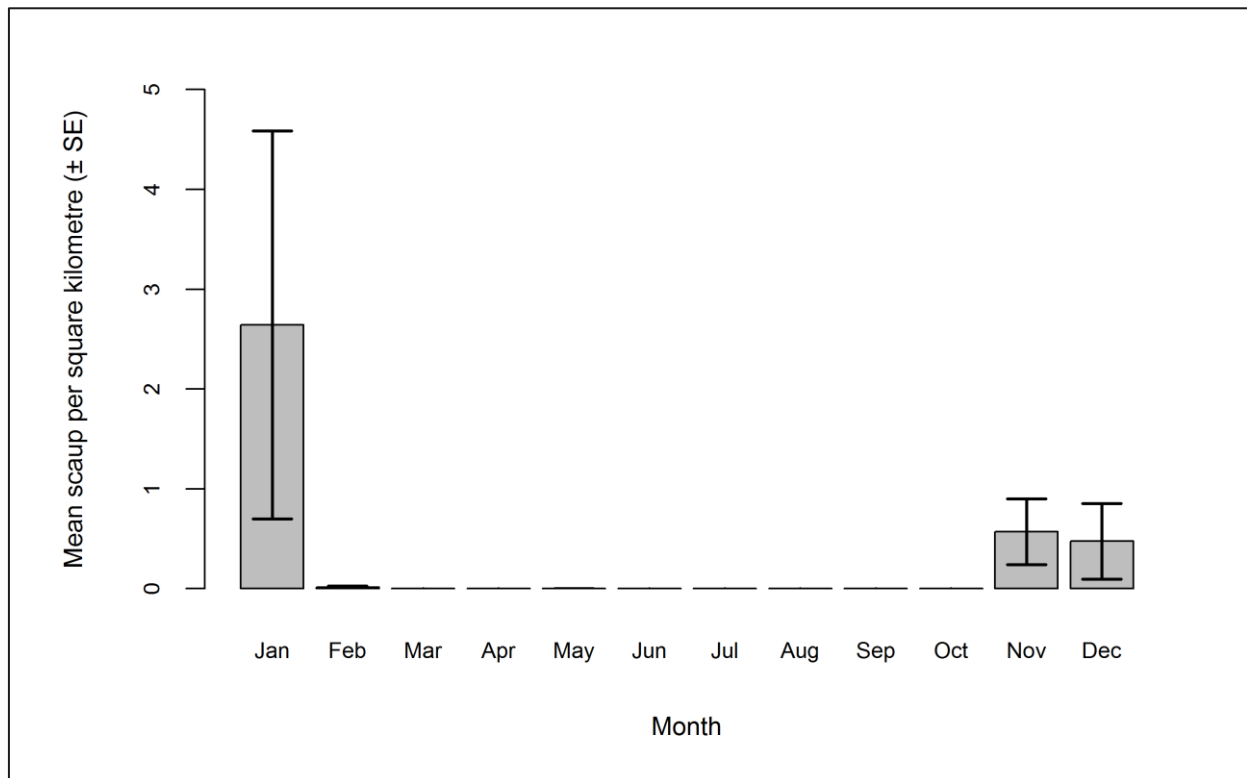


Figure 2.6: Mean density ( $\pm$  se) of scaup recorded on the sea during each month across the three development phases: pre-construction, construction and operational years one and two.

#### 2.4.1.1.2.2. In flight

Group size for scaup recorded on the sea ranged from single individuals up to 100 birds (Figure 2.7). As for scaup recorded on the sea, there is an indication that the number of scaup in flight increased during the operational phase (Figure 2.8). However, since further modelling was not undertaken, the significance of this increase cannot be tested. Figure 2.9 shows that the majority of scaup in flight were recorded during the winter months, although slightly later than scaup on the sea (January to March).

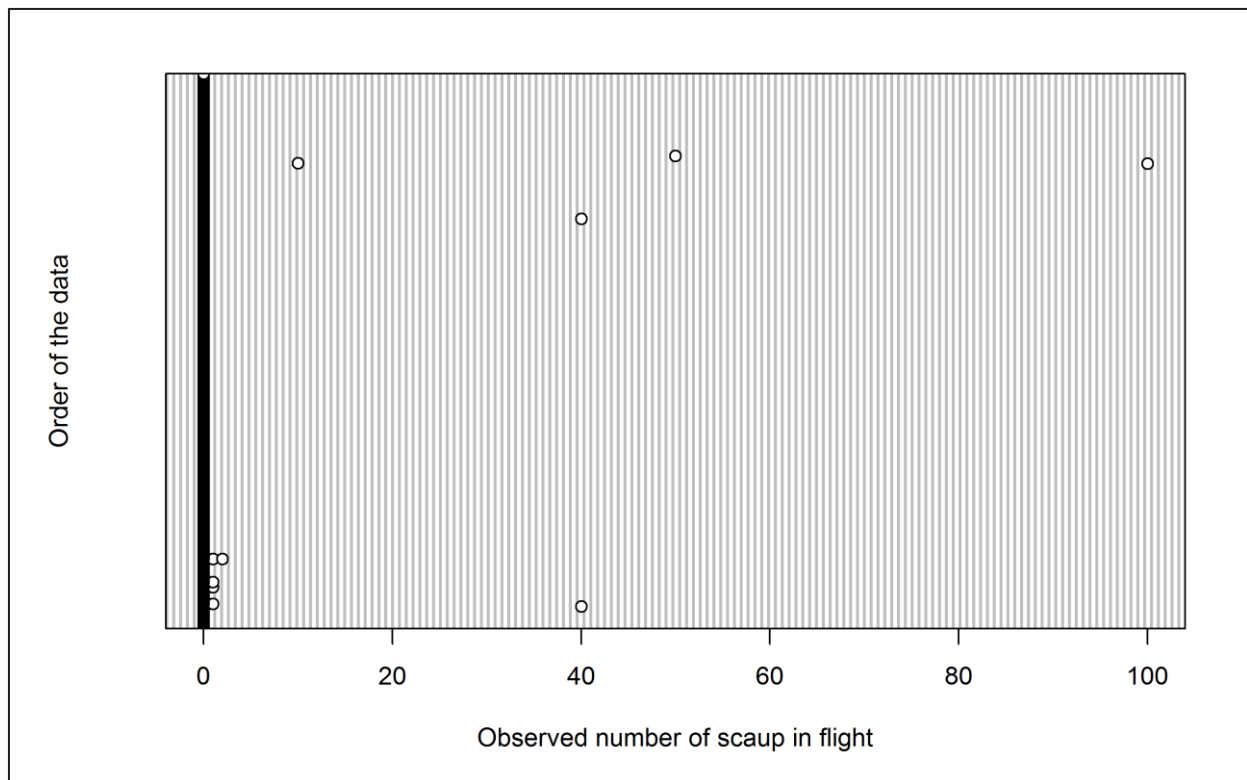


Figure 2.7: Dot plot of the number of scaup observed in flight per analysis block across the three development phases: pre-construction, construction and operational years one and two.



Figure 2.8: Mean density ( $\pm$  se) of scaup recorded in flight during each development phase: pre-construction, construction and operational years one and two.

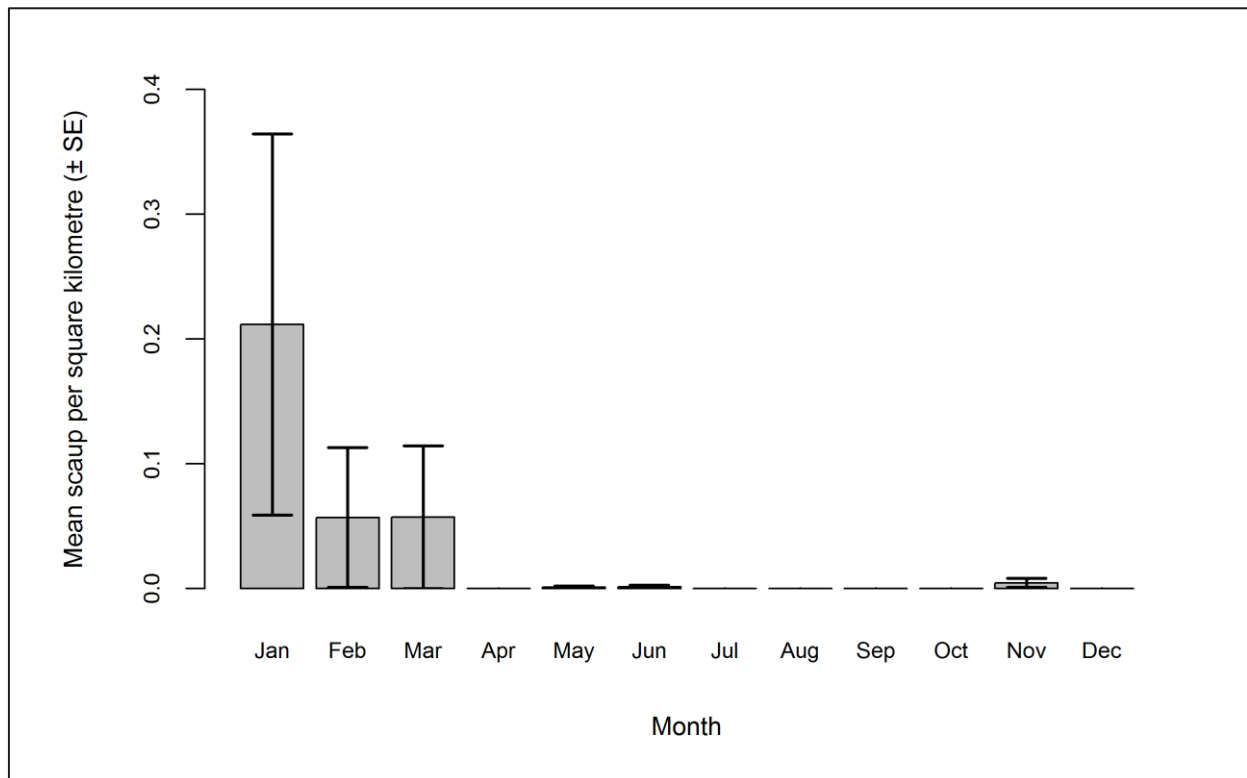


Figure 2.9: Mean density ( $\pm$  se) of scaup recorded in flight during each month across the three development phases: pre-construction, construction and operational years one and two.

### 2.4.1.1.3. Collision risk

The percentage of scaup recorded in different height bands are illustrated in Table 2.10 and Figure 2.10 below. No birds were observed flying at rotor swept height and therefore a chi-squared was not undertaken. Scaup are not considered at risk from collision with turbine blades as they generally fly close to the water's surface, as was found with birds observed at Robin Rigg OWF (Table 2.10).

**Table 2.10:** Percentage of scaup recorded in different flight height bands across the three development phases: pre-construction, construction and operational years one and two. Shaded column indicates percentage at rotor swept height (flight height band 4).

Phase	Flight height band					
	1 (0–5 m)	2 (6–25 m)	3 (26–34 m)	4 (35–125 m)	5 (126–200 m)	6 (>200 m)
Pre-construction	95.65	4.35	0.00	0.00	0.00	0.00
Construction	0.00	0.00	0.00	0.00	0.00	0.00
Operation	100	0.00	0.00	0.00	0.00	0.00

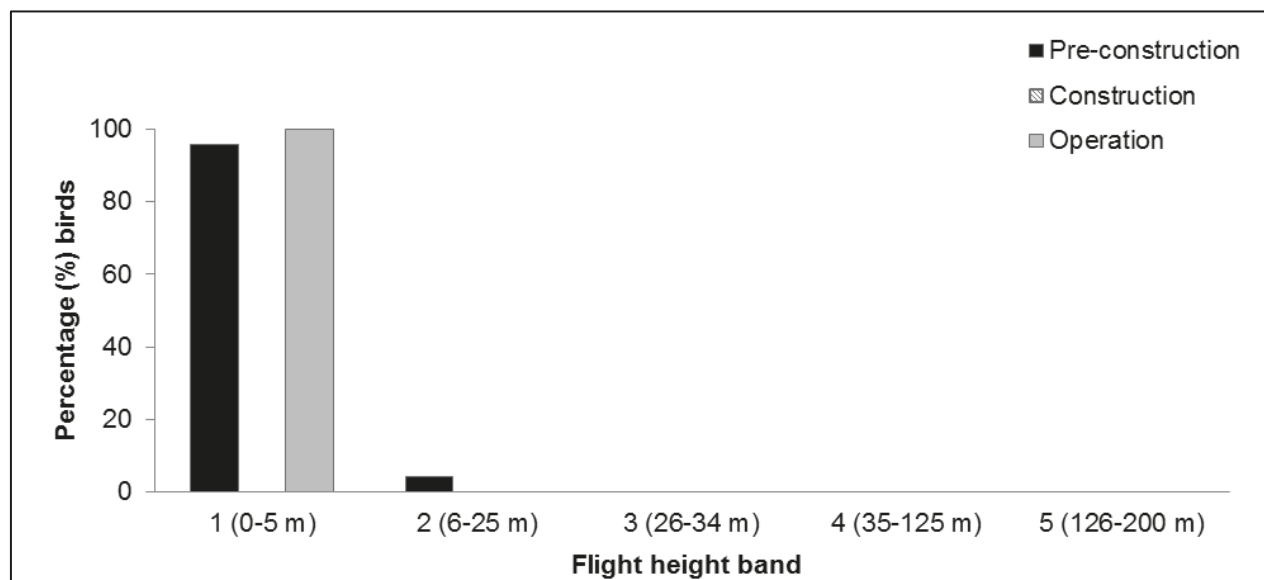


**Figure 2.10:** Percentage of scaup recorded in different flight height bands across the three development phases: pre-construction, construction and operational years one and two.



## 2.4.1.2. Across operational years

### 2.4.1.2.1. Summary statistics

Numbers of individual scaup were largest in operational year one before reducing to a single sighting of 12 individuals in operational year two. Numbers had increased again by the following year and remained relatively similar during operational years three and four, with larger numbers recorded on the sea than in flight throughout operational monitoring (Table 2.11).

Relatively few sightings of scaup were recorded during any operational year (Table 2.11). All sightings occurred during the winter months (November-January). The small number of sightings for this species prevents further abundance modelling from being undertaken.

**Table 2.11: Number of scaup recorded per block during each operational year per km survey effort (all data).**

	Operational year 1		Operational year 2		Operational year 3		Operational year 4	
	On sea	In flight	On sea	In flight	On sea	In flight	On sea	In flight
<b>Total number individuals</b>	1,871	200	12	0	1,865	35	1,100	2
<b>Total number sightings</b>	6	4	1	0	4	2	2	1
<b>Number individuals/km</b>	1.03	0.11	0.01	0	0.86	0.02	0.50	<0.01
	Total		Total		Total		Total	
<b>Total number individuals</b>	2,071		12		1,900		1,102	
<b>Total number sightings</b>	10		1		6		3	
<b>Number individuals/km</b>	1.14		0.01		0.88		0.50	

Data were filtered as described in the methodology (Section 2.4.4). The percentage of segments without observations was calculated to ensure there were sufficient data to perform the analysis (Table 2.12). Since >99% of blocks for both scaup on sea and in flight contained zero observations, further abundance modelling of scaup across the three development phases was not undertaken.

**Table 2.12: Percentage of scaup analysis blocks without observations across operational years one to four.**

	On sea	In flight
<b>Percentage zero blocks</b>	99.9%	99.9%

## 2.4.1.2.2. Density

### 2.4.1.2.2.3. On sea

Group size for scaup recorded on the sea ranged from single individuals up to 1,300 birds (Figure 2.11). There is an indication that the number of scaup decreased during operational years two and four (Figure 2.12). However, since further modelling was not undertaken, the significance of this increase cannot be tested. Figure 2.13 shows that the majority of scaup on the sea were recorded during the winter months from December through to March.

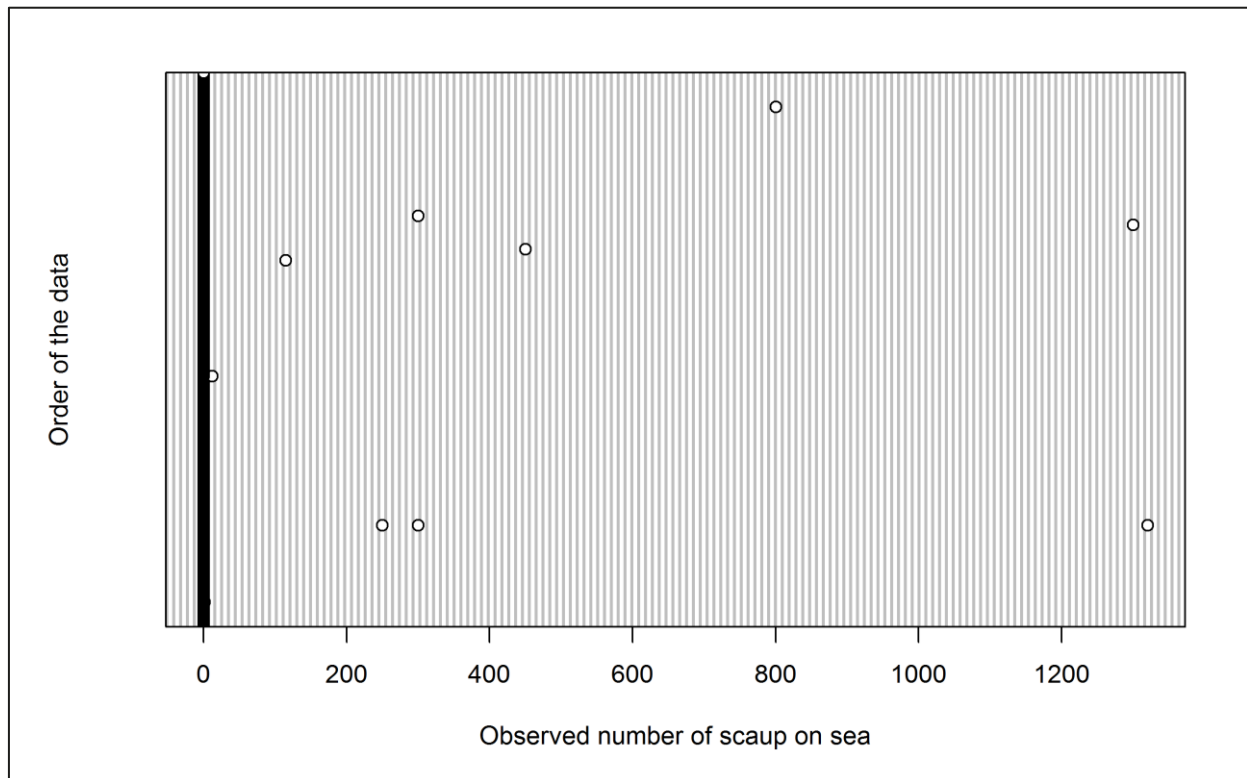


Figure 2.11: Dot plot of the number of scaup observed on sea per analysis block across operational years one to four.

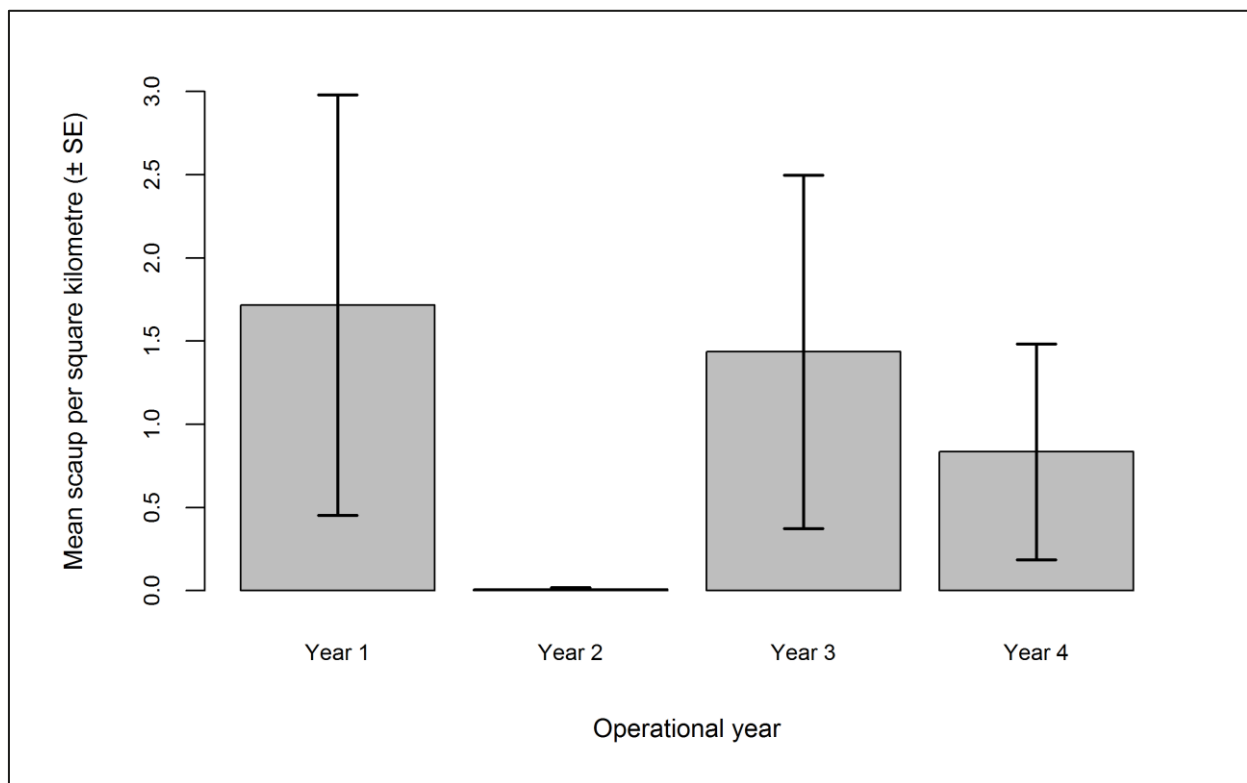


Figure 2.12: Mean density ( $\pm$  se) of scaup recorded on the sea across operational years one to four.

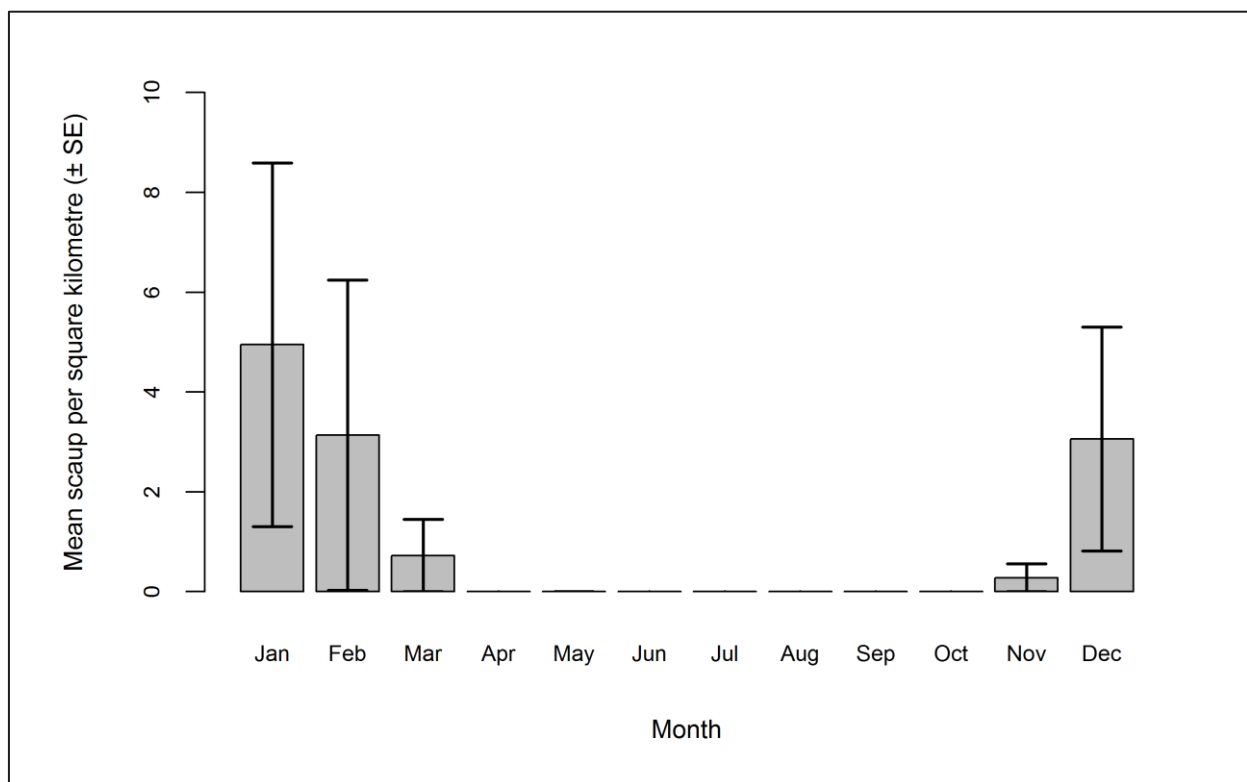


Figure 2.13: Mean density ( $\pm$  se) of scaup recorded on the sea during each month across operational years one to four.

#### 2.4.1.2.2.4. In flight

Group size for scaup recorded on the sea ranged from single individuals up to 100 birds (Figure 2.14). Mean density of scaup in flight indicates that relatively few were recorded during any phase of the development (Figure 2.15). No scaup in flight were recorded in operational year two and very small densities were recorded in operational year four. Figure 2.16 shows that the majority of scaup in flight were recorded during the winter months between November and March.

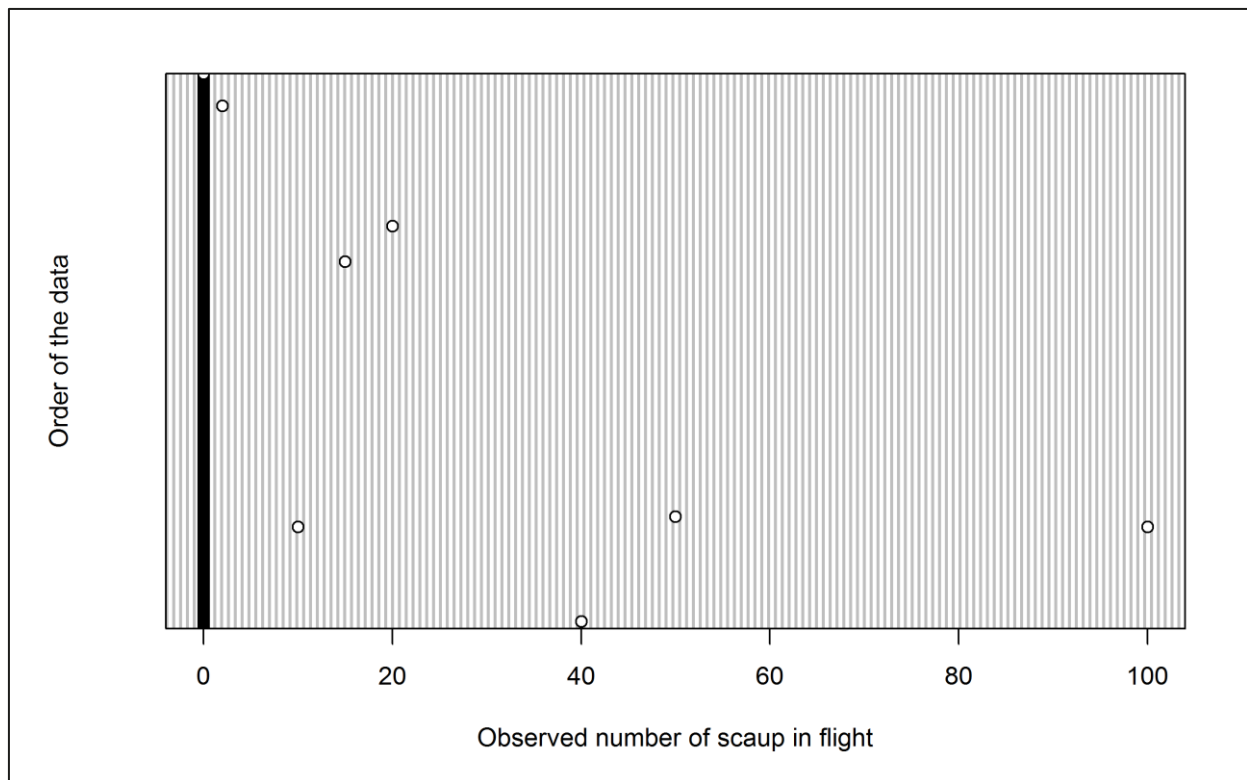


Figure 2.14: Dot plot of the number of scaup observed in flight per analysis block across operational years one to four.

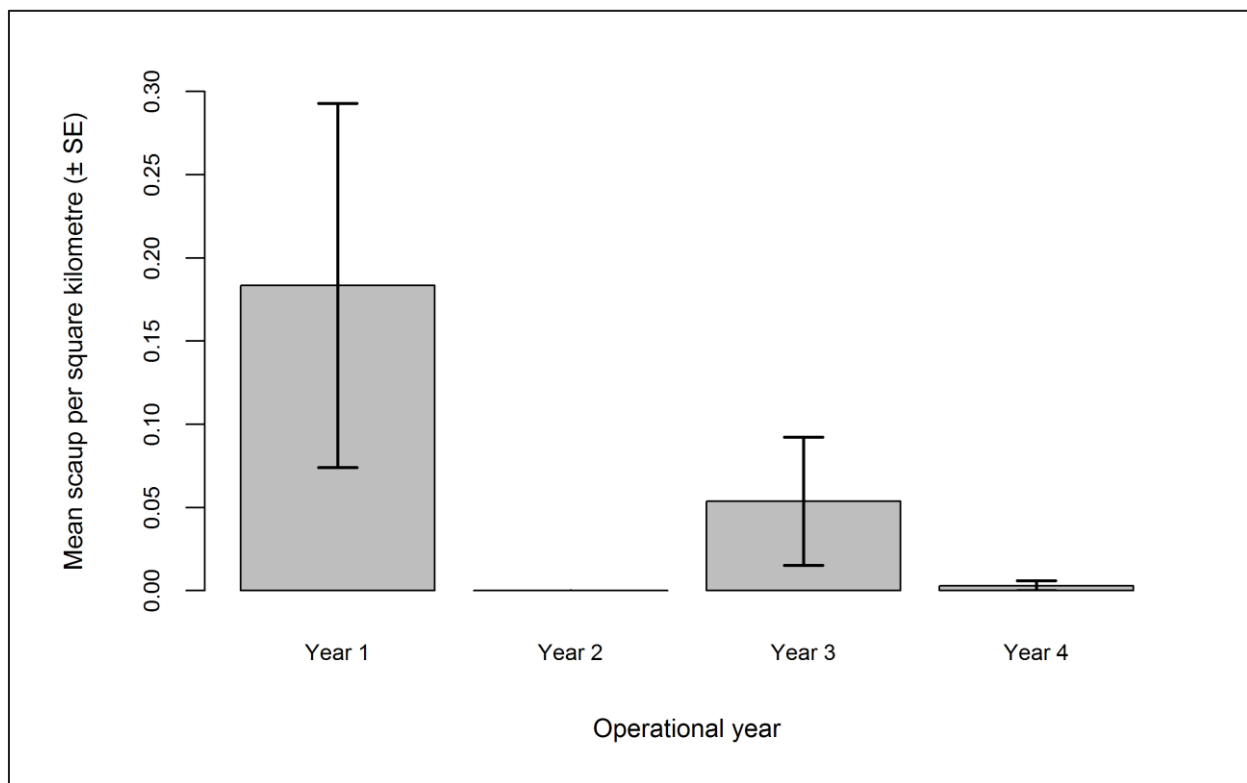


Figure 2.15: Mean density ( $\pm$  se) of scaup recorded in flight across operational years one to four.

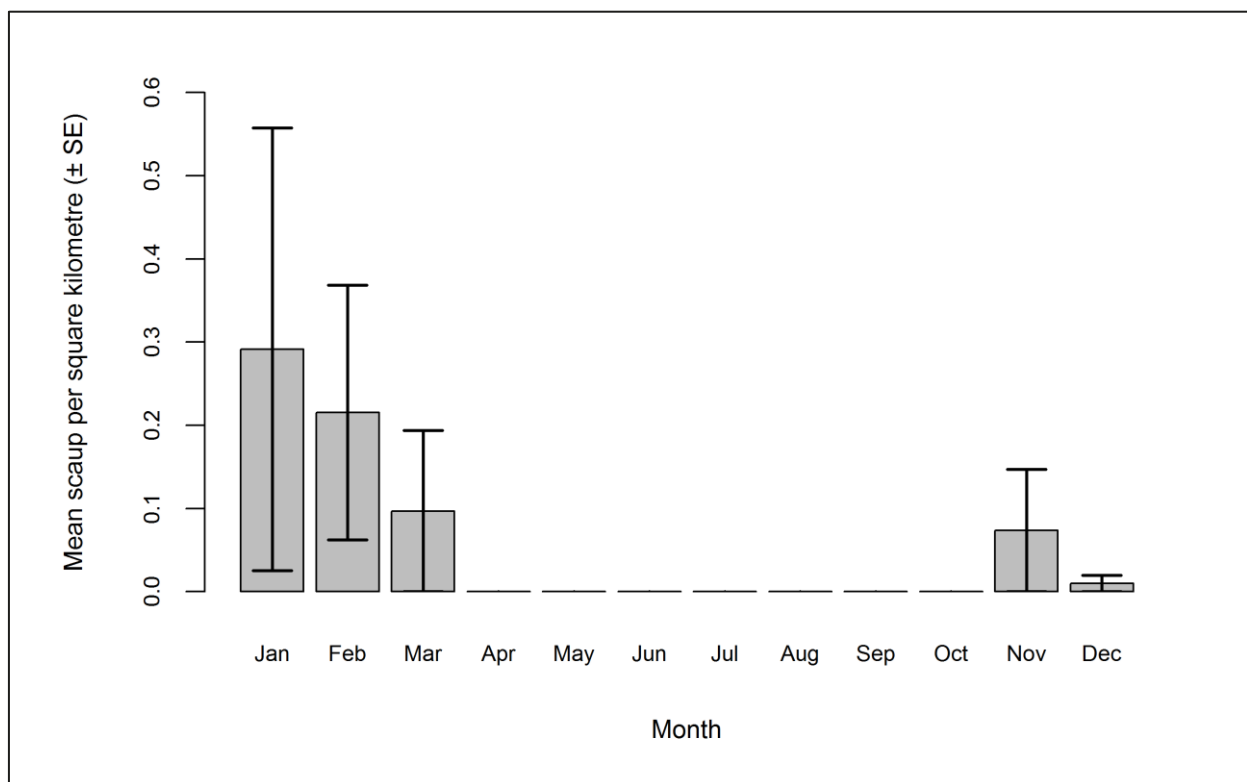


Figure 2.16: Mean density ( $\pm$  se) of scaup recorded in flight during each month across operational years one to four.



### 2.4.1.2.3. Collision risk

The percentage of scaup recorded in different height bands is shown in Table 2.13 and Figure 2.17 below. No birds were observed flying at rotor swept height. As such, a chi-squared test was not undertaken. Scaup are not considered at risk from collision with turbine blades as they generally fly close to the water's surface, as was found with birds observed at Robin Rigg (Table 2.13).

**Table 2.13: Percentage of scaup recorded in different flight height bands across operational years one to four. Shaded column indicates percentage at rotor swept height (flight height band 4).**

Operational year	Flight height band					
	1 (0–5 m)	2 (6–25 m)	3 (26–34 m)	4 (35–125 m)	5 (126–200 m)	6 (>200 m)
1	100.00	0.00	0.00	0.00	0.00	0.00
2	0.00	0.00	0.00	0.00	0.00	0.00
3	59.46	40.54	0.00	0.00	0.00	0.00
4	0.00	100.00	0.00	0.00	0.00	0.00

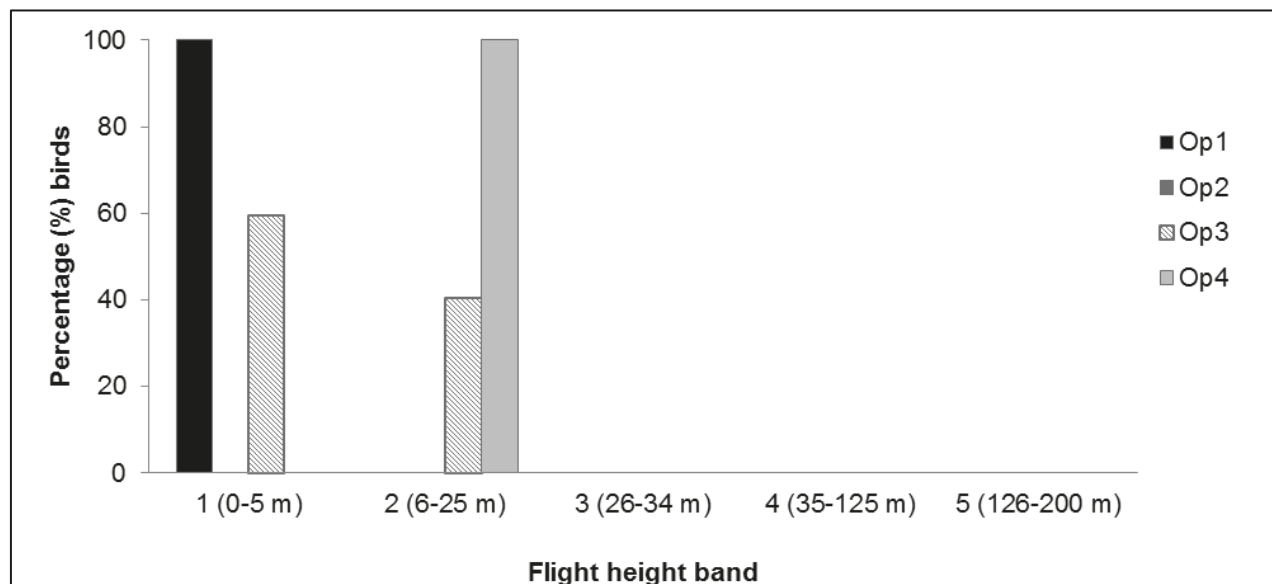


**Figure 2.17: Percentage of scaup recorded in different flight height bands across operational years one to four.**

#### 2.4.1.3. Distribution

Since abundance modelling of scaup was not possible, Figure 2.18 shows the distribution of raw scaup observations during pre-construction, construction and operational monitoring. Both flying and sitting birds are represented. Since relatively small numbers of scaup sightings were recorded during operational monitoring (Table 2.11), data from all four operational years are presented in Figure 2.18:C. Figure 2.18 shows that scaup were recorded in close proximity to the Robin Rigg OWF during pre-construction surveys, with the majority of birds recorded in the northern corner of the survey area during construction and operation. Larger numbers of scaup were recorded during operation in comparison to construction.

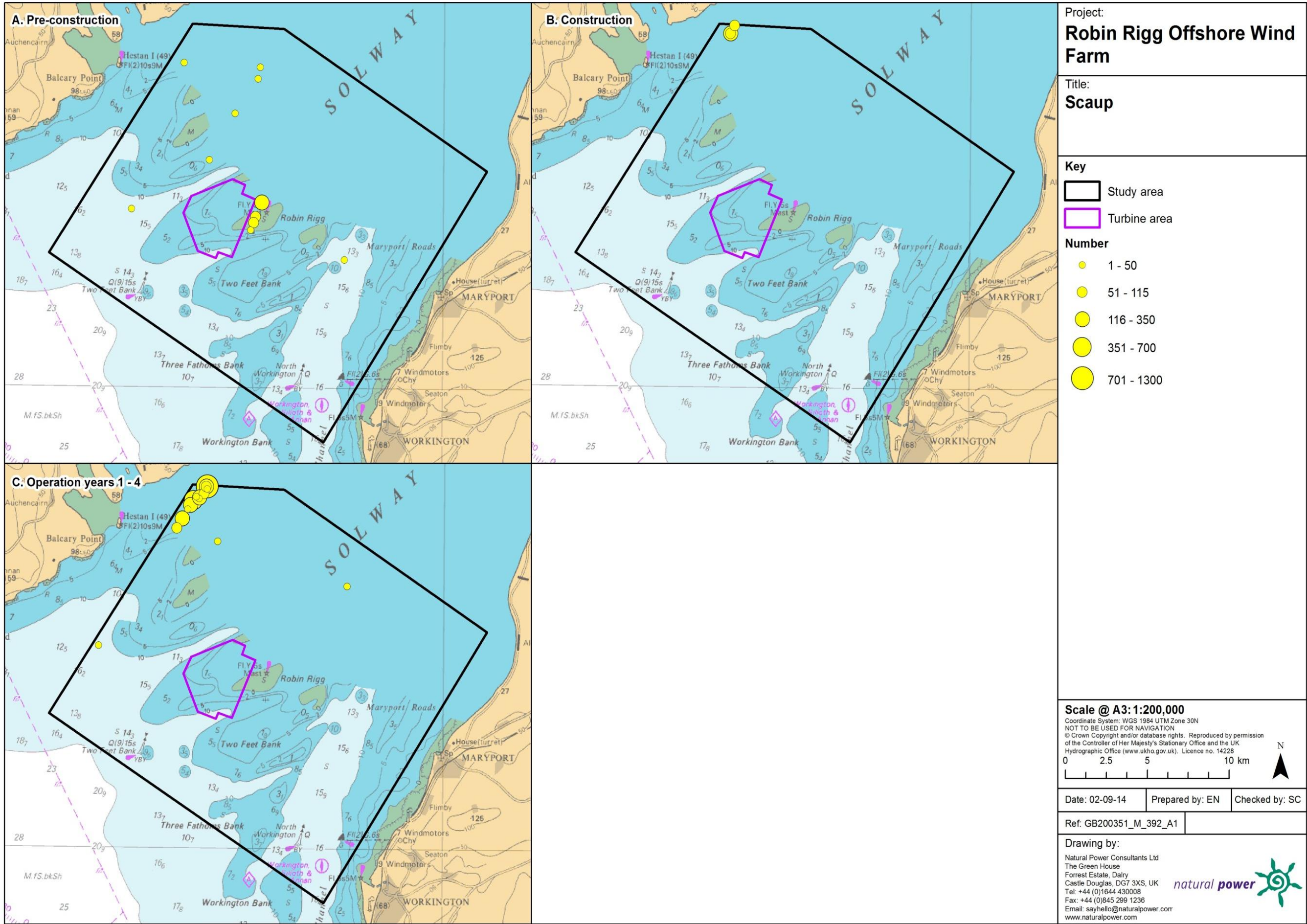


Figure 2.18: Location of raw scaup observations during a) pre-construction, b) construction and c) operational monitoring. Both flying and sitting birds are represented. Circle size is proportional to the number of scaup sighted.

## 2.4.2. Common scoter

### 2.4.2.1. Across three development phases

#### 2.4.2.1.4. Summary statistics

The number of common scoter sightings was highest during construction, although the number of individuals observed per km of survey effort was highest during the first two years of operation phase (Table 2.14). Numbers of common scoters recorded on the sea surface were larger than those recorded in flight throughout the three development phases (Table 2.14).

**Table 2.14: Number of common scoters recorded per block during each development phase per km survey effort (all data).**

	Pre-construction		Construction		Operation years 1-2	
	On sea	In flight	On sea	In flight	On sea	In flight
<b>Total number individuals</b>	58,312	12,045	69,182	18,277	52,952	4,827
<b>Total number sightings</b>	358	325	1,100	800	734	366
<b>Number individuals/km</b>	16.36	3.38	9.51	2.51	13.70	1.25
	Total		Total		Total	
<b>Total number individuals</b>	70,357		87,459		57,779	
<b>Total number sightings</b>	683		1,900		1,100	
<b>Number individuals/km</b>	19.74		12.02		14.94	

Data were filtered as described in the methods (Section 2.4.4). The percentage of analysis blocks without observations was calculated to ensure there were sufficient data to perform the analysis (Table 2.15). Data were also checked to ensure observations were recorded in all months of the year.

**Table 2.15: Percentage of common scoter analysis blocks without observations across the three development phases: pre-construction, construction and operational years one and two.**

	On sea	In flight
<b>Percentage zero blocks</b>	96.0%	97.4%



### 2.4.2.1.5. Density and distribution

#### 2.4.2.1.5.5. On sea

Initial data exploration highlighted several outliers that may influence the modelling process (Figure 2.19). The model was attempted with and without these large groups but in both cases the model would not converge. It may be possible to repeat the model using a binomial distribution to predict presence/absence rather than abundance. However, at the time of analysis the MRSea package was unable to accommodate binomial distributions. Therefore, further modelling work could not be undertaken and raw data are presented instead.

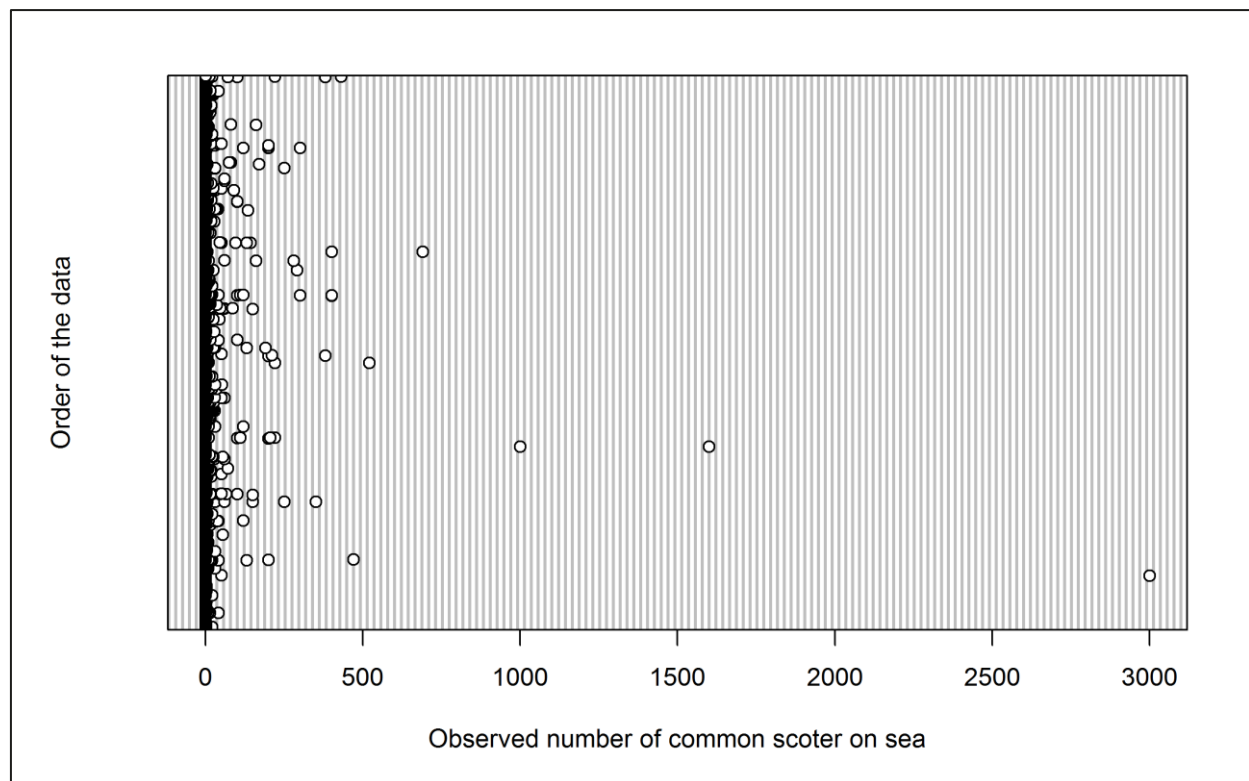


**Figure 2.19: Dot plot of the number of common scoters observed on sea per analysis block across the three development phases: pre-construction, construction and operational years one and two.**

Group size for common scoter recorded on the sea ranged from single individuals up to 3,000 birds. Mean density of common scoter (following data filtering; Section 2.4.4) indicates little change across development phases (Figure 2.20). However, since further modelling was not undertaken, the significance of any differences could not be tested. Figure 2.21 shows that the majority of common scoters on the sea were recorded between May and July.



Figure 2.20: Mean density ( $\pm$  se) of common scoter recorded on the sea during each development phase: pre-construction, construction and operational years one and two.

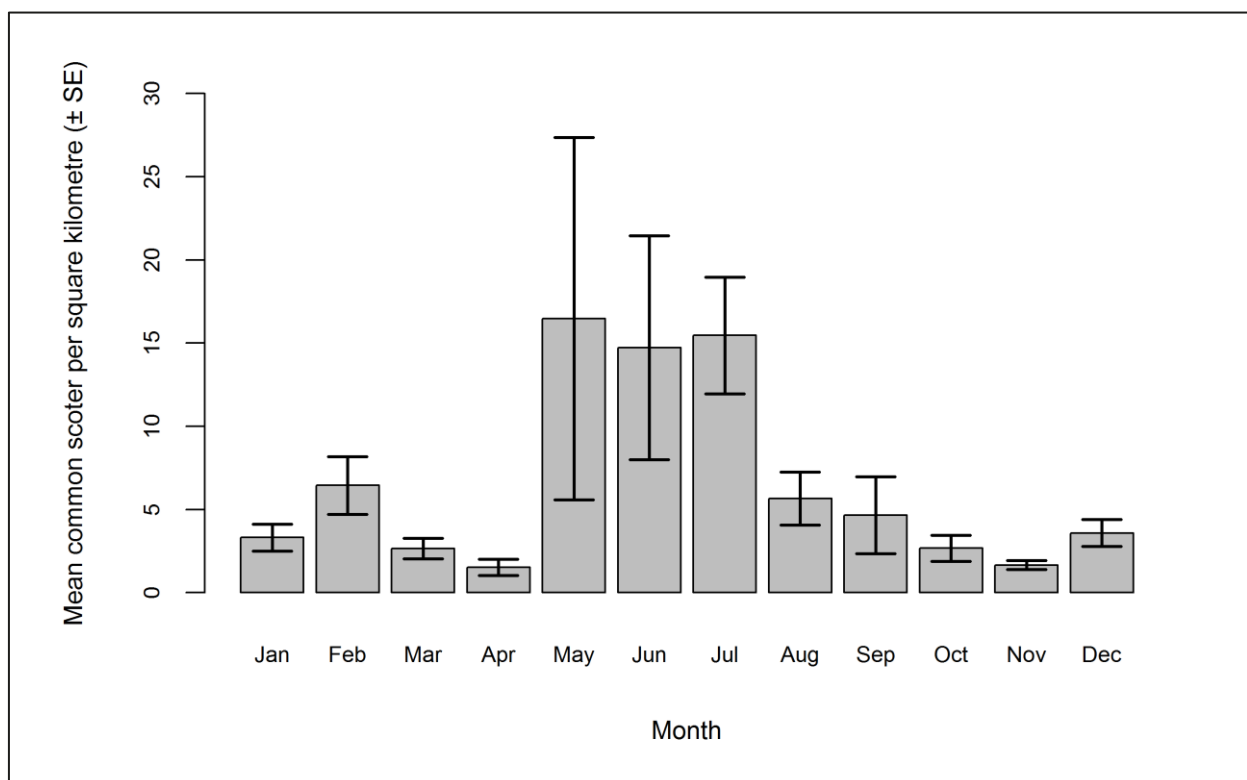
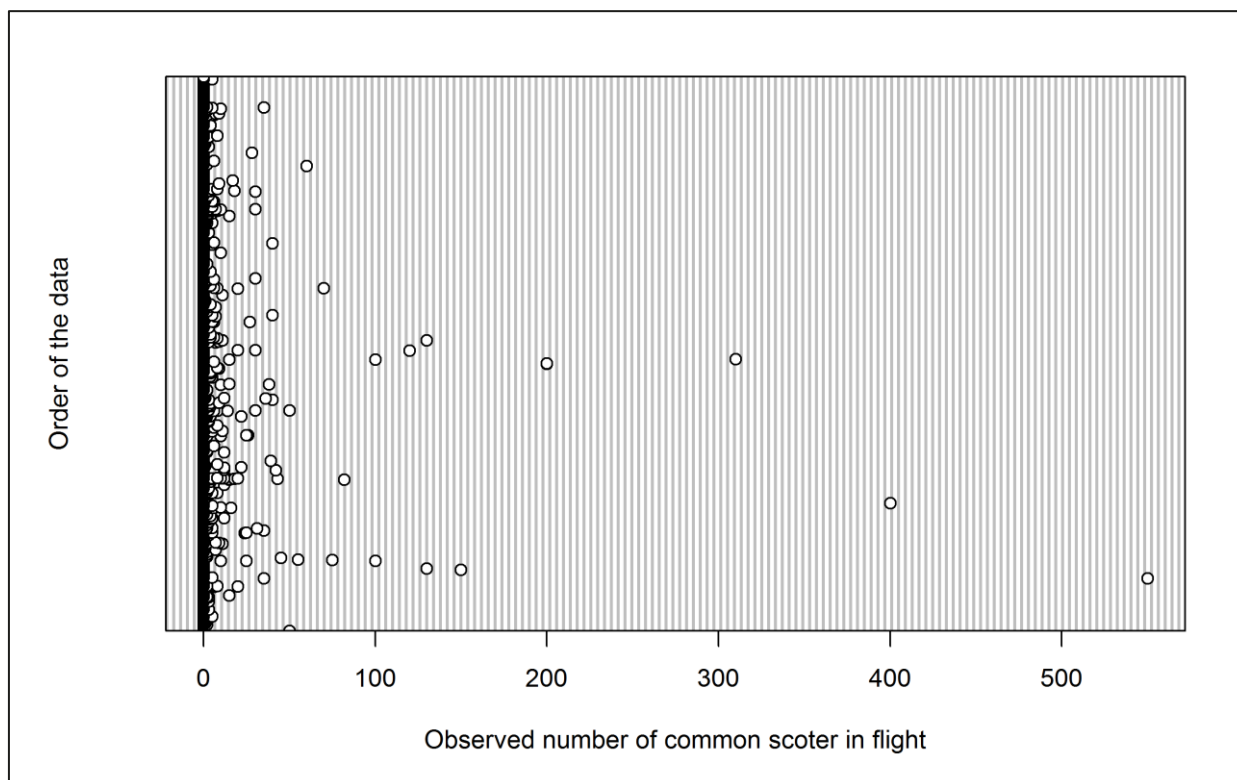


Figure 2.21: Mean density ( $\pm$  se) of common scoter recorded on the sea during each month across the three development phases: pre-construction, construction and operational years one and two.

### 2.4.2.1.5.6. In flight

Initial data exploration highlighted several outliers that may influence the modelling process (Figure 2.22). Since common scoter typically aggregate in large groups, the model was run with and without the five largest groups and the outputs compared.



**Figure 2.22:** Dot plot of the number of common scoters observed in flight per analysis block across the three development phases: pre-construction, construction and operational years one and two.

The initial GEE predicted that month, phase, tide height and location all have a statistically significant influence on common scoter abundance within the survey area (Table 2.16). Specifically, larger numbers were observed during the pre-construction phase (Figure 2.23), and during the months of May and June (Figure 2.24). The interaction between location and phase was statistically significant.

P-values for phase and location remained the statistically significant after removing the outliers. However, tide height and month were no longer significant (data not shown). The interaction between location and phase was also no longer statistically significant after the removal of the largest group sizes ( $p = 0.161$ ). As density surfaces for both models were similar, outputs from the model including the large group sizes are presented here.

Since June was the month of peak activity, abundance estimates were predicted for this month.

**Table 2.16:** Final model outputs for common scoters in flight across the three development phases: pre-construction, construction and operational years one and two.

Term	Marginal p-value
Month	0.0188
Phase	0.0037
Tide height	0.0021
Location (X,Y)	<0.0001
Interaction (location: phase)	<0.0001

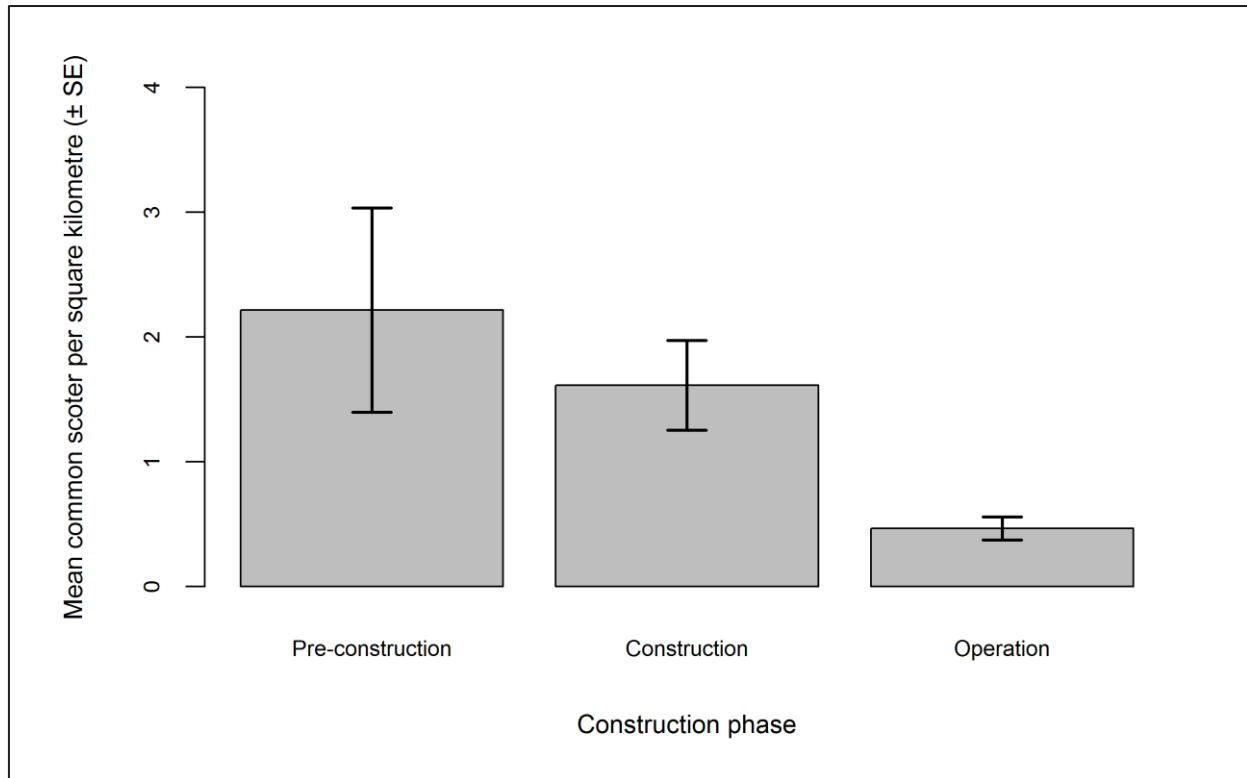


Figure 2.23: Mean density ( $\pm$  se) of common scoters recorded in flight during each development phase: pre-construction, construction and operational years one and two.

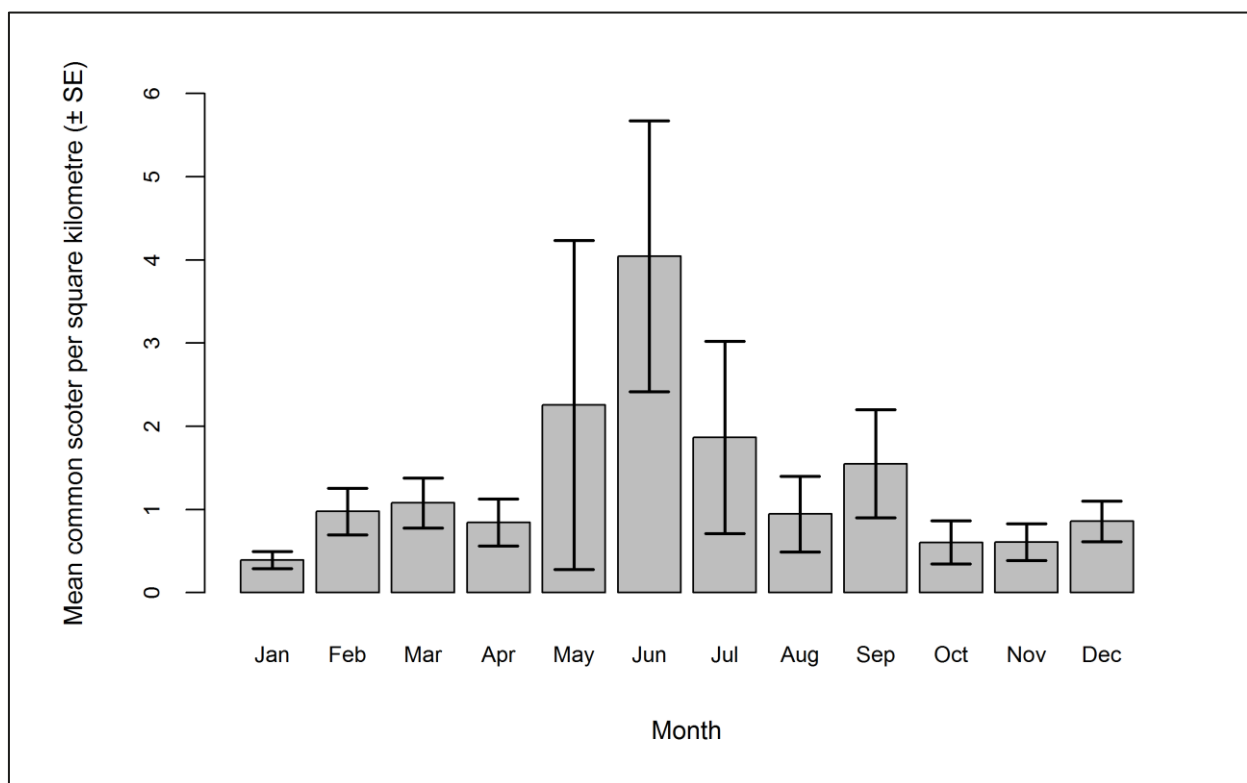


Figure 2.24: Mean density ( $\pm$  se) of common scoters recorded in flight during each month across the three development phases: pre-construction, construction and operational years one and two.

The abundance and densities for the month of June (by site, buffer and total survey area) are presented in Table 2.17. The largest total abundance of common scoters during June was predicted for the pre-construction phase, with abundance falling during construction before increasing again during operation. Whilst the largest proportion of common scoters within the Robin Rigg OWF itself was predicted to occur during the construction phase, it should be noted that the site represents 3.5% of the total survey area so the numbers involved are very small (Table 2.17).

**Table 2.17: Abundance and density of common scoters in flight during the three development phases: pre-construction, construction and operational years one and two. Values in parentheses represent upper and lower 95% confidence intervals.**

Phase	Abundance			Density			
	Site	Buffer	Total	Site	Buffer	Total	% within site
<b>Pre-construction</b>	6 (1-45)	1,372 (250-8,604)	1,378 (251-8,649)	0.48 (0.07-3.49)	3.94 (0.72-24.74)	3.82 (0.69-23.97)	0.45
<b>Construction</b>	14 (2-112)	583 (96-3,870)	597 (98-3,981)	1.05 (0.14-8.62)	1.68 (0.28-11.13)	1.65 (0.27-11.04)	2.28
<b>Operation</b>	2 (0-60)	784 (70-14,867)	786 (70-14,927)	0.15 (0.01-4.60)	2.25 (0.20-42.74)	2.18 (0.19-41.37)	0.25

The density surface maps show that common scoters in flight were widely distributed in the northern half of the survey area during pre-construction surveys, with a significant decline in density to the north-east of the Robin Rigg OWF during construction (Figure 2.25). Common scoter density increased significantly in the north-western corner of the survey area during operation, close to the northern coast of the Solway Firth, with further significant increases seen to south-east of the OWF during this phase (Figure 2.25).



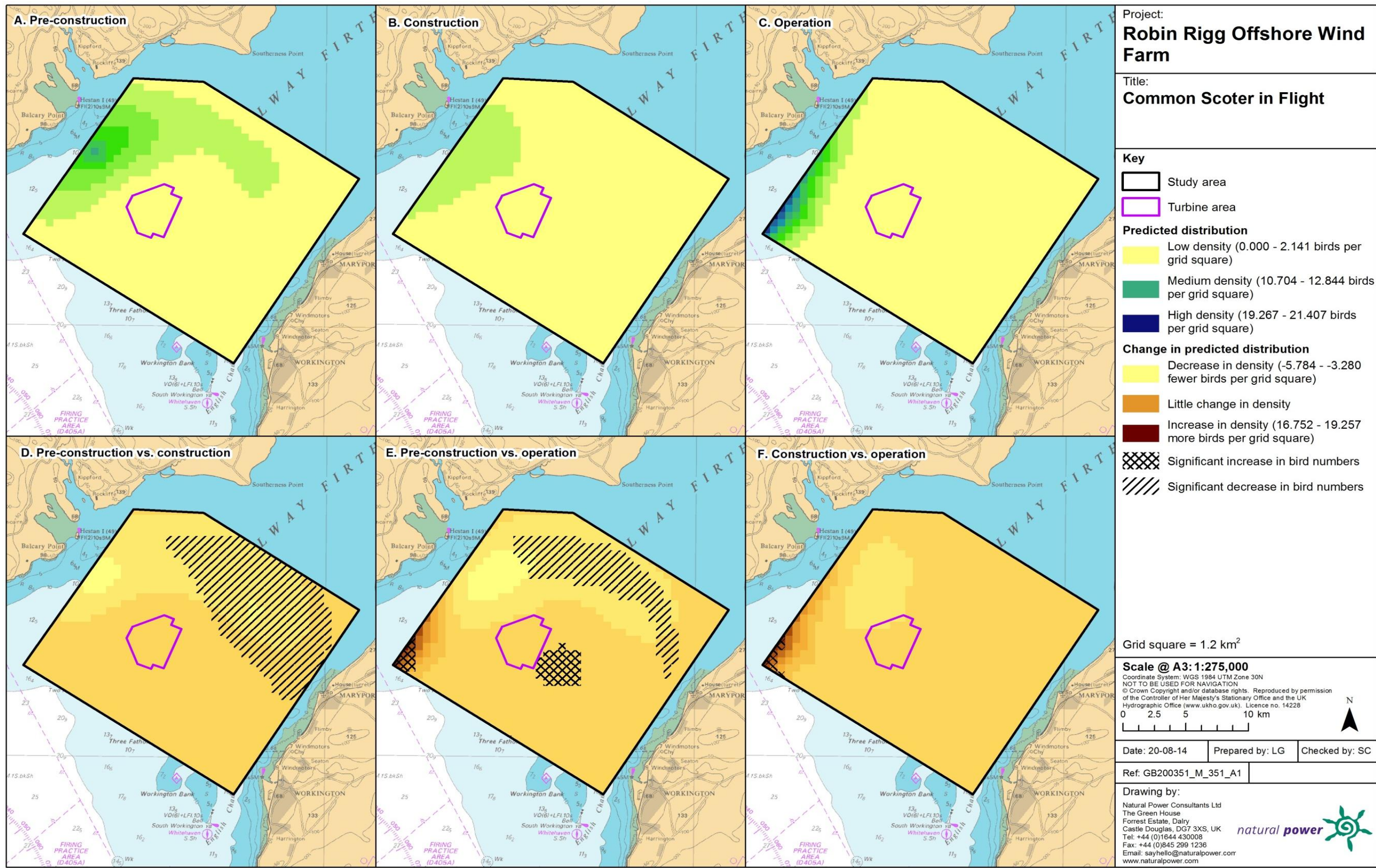


Figure 2.25: Predicted density of common scoters in flight during a) pre-construction, b) construction and c) operational monitoring. Changes in predicted density between d) pre-construction and construction, e) pre-construction and operation and f) construction and operation are also shown. Significant differences are marked with diagonal shading.



#### 2.4.2.1.6. Collision risk

The percentage of common scoter recorded across the three development phases in different height bands relative to rotor height are shown in Table 2.18 and Figure 2.26. As would be expected for this species, the majority (>99%) of common scoters were observed flying at less than 25 m in height during all phases. As the majority of observations occurred below rotor swept height, a chi-squared test was not undertaken.

**Table 2.18: Percentage of common scoter recorded in different flight height bands across the three development phases: pre-construction, construction and operational years one and two. Shaded column indicates percentage at rotor swept height (flight height band 4).**

Phase	Flight height band					
	1 (0–5 m)	2 (6–25 m)	3 (26–34 m)	4 (35–125 m)	5 (126–200 m)	6 (>200 m)
Pre-construction	60.61	39.39	0.00	0.00	0.00	0.00
Construction	62.61	36.83	0.05	0.50	0.00	0.00
Operation	70.83	29.02	0.08	0.06	0.00	0.00

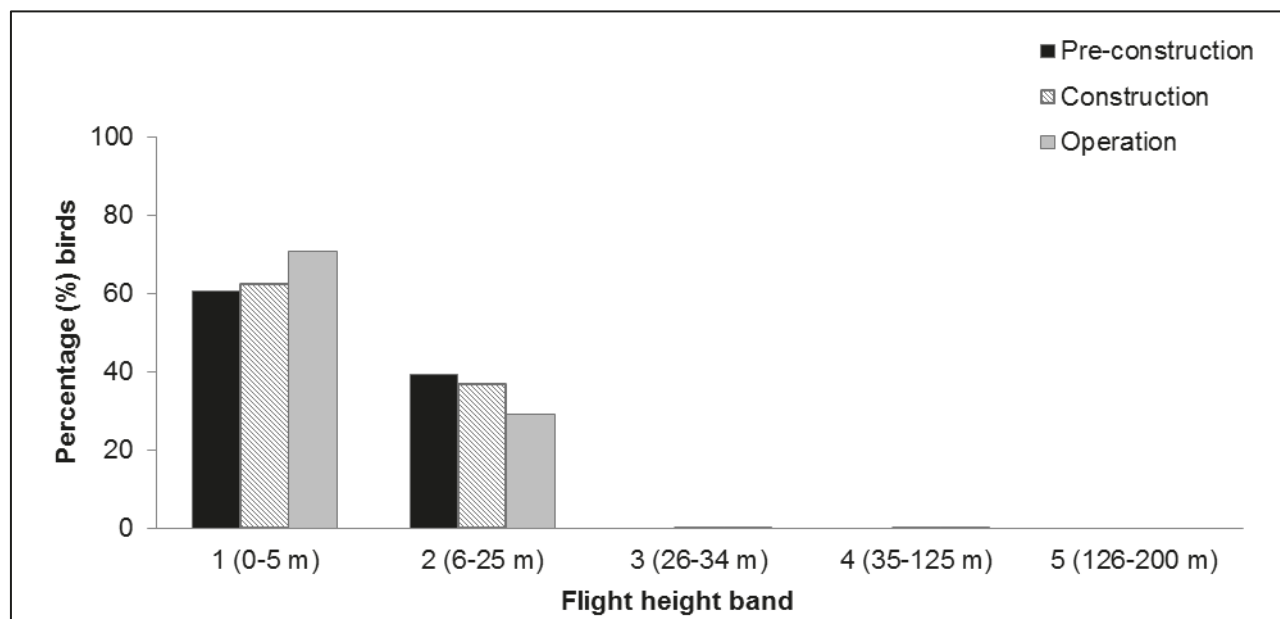


**Figure 2.26: Percentage of common scoter recorded in different flight height bands during the three development phases: pre-construction, construction and operational years one and two.**

## 2.4.2.2. Across operational years

### 2.4.2.2.1. Summary statistics

The number of flying common scoter sightings appears to have increased through the four operational years, as have the number of individuals observed per km of survey effort (Table 2.19). Numbers of common scoters recorded on the sea surface were larger than those recorded in flight throughout the four operational years (Table 2.19).

**Table 2.19: Number of common scoter recorded per block during each operational year per km survey effort (all data).**

	Operational year 1		Operational year 2		Operational year 3		Operational year 4	
	On sea	In flight	On sea	In flight	On sea	In flight	On sea	In flight
<b>Total number individuals</b>	18,571	2,538	34,381	2,289	41,082	8,605	54,155	13,439
<b>Total number sightings</b>	296	207	438	159	693	509	1,190	580
<b>Number individuals/km</b>	10.23	1.40	16.77	1.12	18.98	3.97	24.67	6.21
	Total		Total		Total		Total	
<b>Total number individuals</b>	21,109		36,670		49,687		67,594	
<b>Total number sightings</b>	503		597		1,202		1,770	
<b>Number individuals/km</b>	11.62		17.89		22.95		30.79	

Data were filtered as described in the methodology (Section 2.4.4). The percentage of analysis blocks without observations was calculated to ensure there were sufficient data to perform the analysis (Table 2.20). Data were also checked to ensure observations were recorded in all months of the year.

**Table 2.20: Percentage of common scoter analysis blocks without observations across operational years one to four. Zero inflation prior to removal of effort is presented in parentheses.**

	On sea	In flight
<b>Percentage zero blocks</b>	(92.7%) 92.70%	97.9%

## 2.4.2.2.2. Density

### 2.4.2.2.2.1. On sea

Initial data exploration highlighted outliers that may influence the modelling process (Figure 2.27). The model was attempted with these large groups but would not converge. Upon inspection of influential datum, analysis block 299 was considered to adversely affect the model as it contained a single outlier (an observation of 4,024 Distance adjusted individuals). However, even when this outlier was removed, the model produced extremely large confidence intervals. Therefore, raw data are presented here.

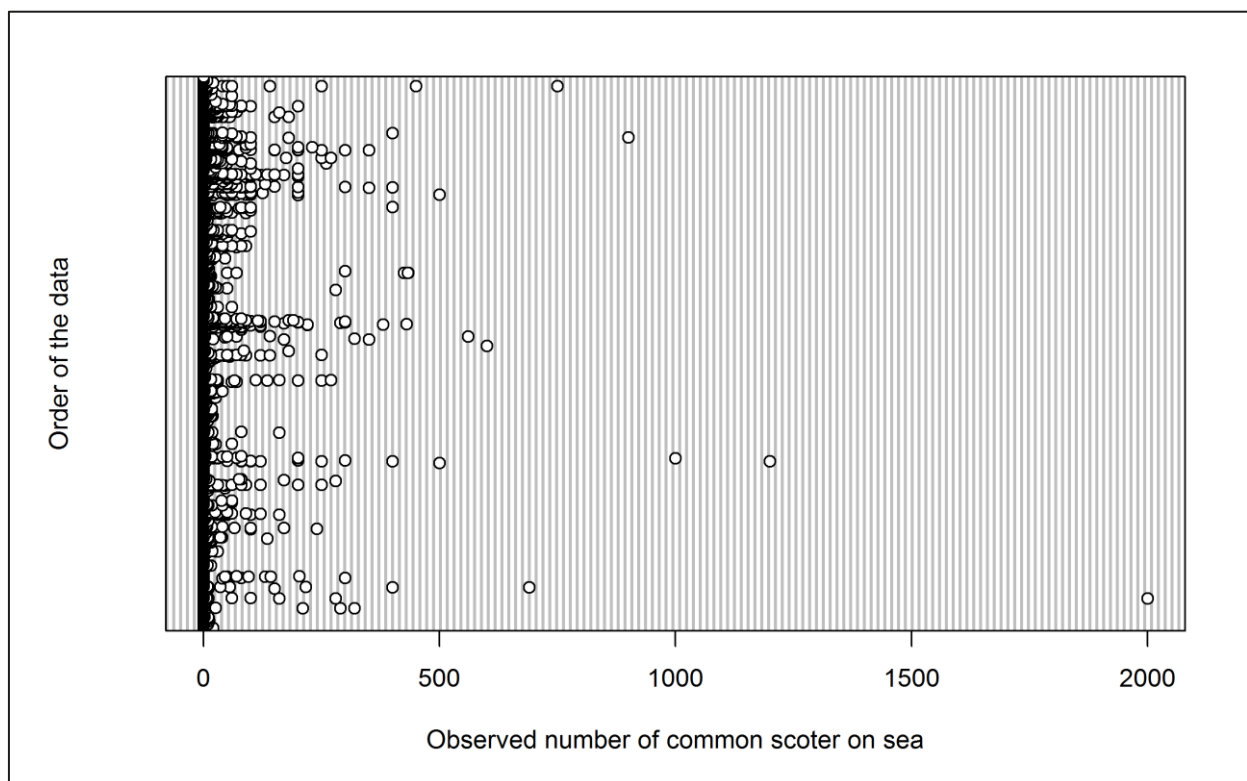


**Figure 2.27:** Dot plot of the number of common scoters observed on sea per analysis block across operational years one to four.

Group size for raw common scoter observations ranged from single individuals up to 2,000 birds (increasing to 2-4,024 individuals after Distance adjustment). Mean density of common scoter indicates an increase across operational years (Figure 2.28). However, since further modelling was not undertaken, the significance of any differences could not be tested. Figure 2.29 shows that the majority of common scoters on the sea were recorded in June and July during operational years.

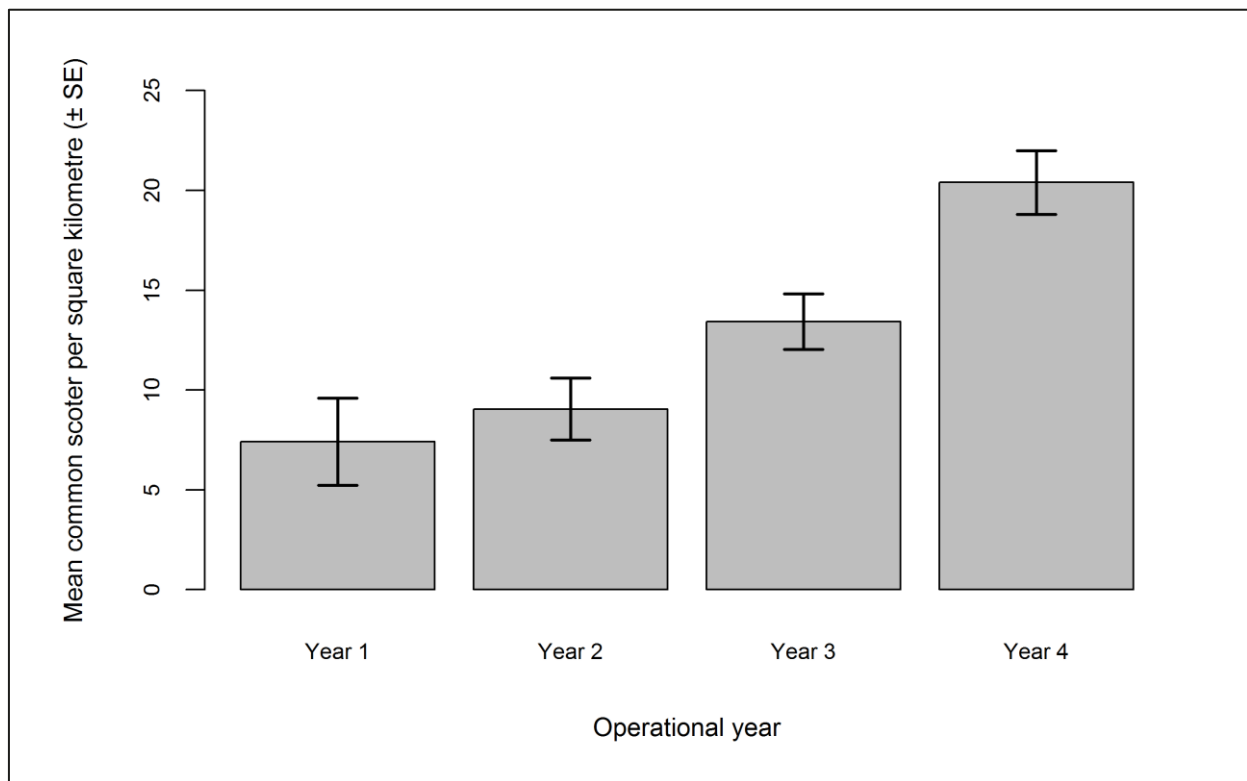


Figure 2.28: Mean density (± se) of common scoter recorded on the sea across operational years one to four.

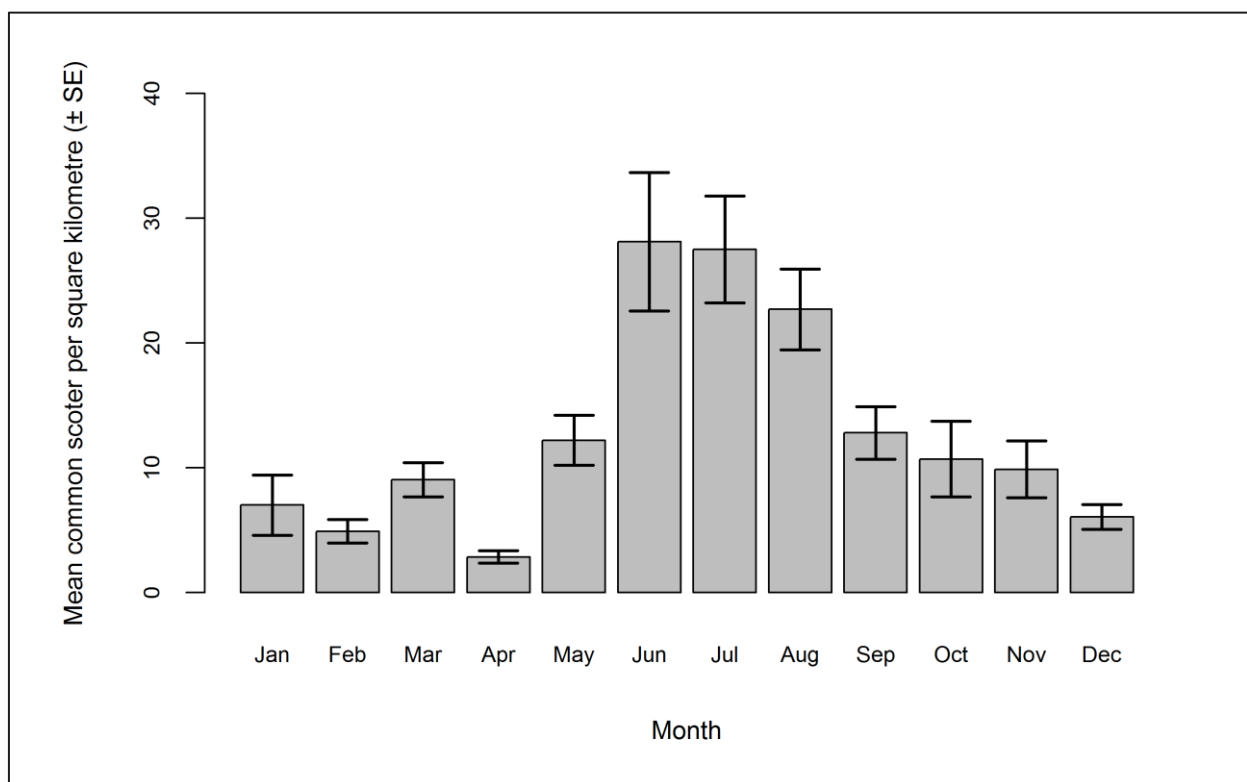


Figure 2.29: Mean density (± se) of common scoter recorded on the sea during each month across operational years one to four.



#### 2.4.2.2.2. In flight

Initial data exploration highlighted several outliers that may influence the modelling process (Figure 2.30). The model was attempted with and without these large groups but in both cases the model would not converge. Instead, a model which used the number of sightings within a segment rather than the number of individuals was attempted. However the majority of segments contained only a single observation.

It may be possible to repeat the model using a binomial distribution to predict presence/absence rather than abundance estimates. However, at the time of analysis the MRSea package was unable to accommodate binomial distributions. Therefore, further modelling work could not be undertaken and raw data are presented instead.

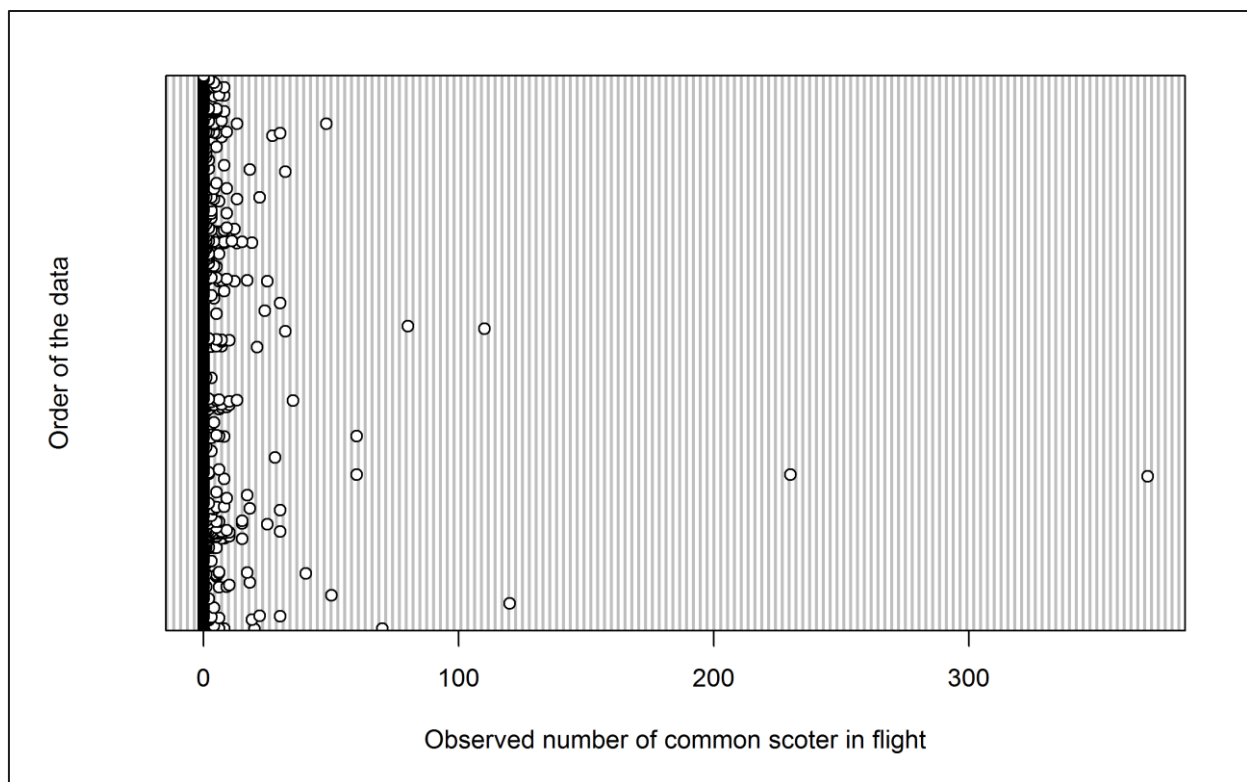


**Figure 2.30:** Dot plot of the number of common scoters observed in flight per analysis block across operational years one to four.

Group size for raw common scoter observations ranged from single individuals up to 370 birds. Mean density of flying common scoter indicates an increase across operational years, with a slight decrease during operational year four (Figure 2.31). However, since further abundance modelling was not undertaken, the significance of any differences could not be tested. Figure 2.32 shows that the majority of common scoters in flight were recorded during the months of May and June, slightly earlier than for birds on the sea.

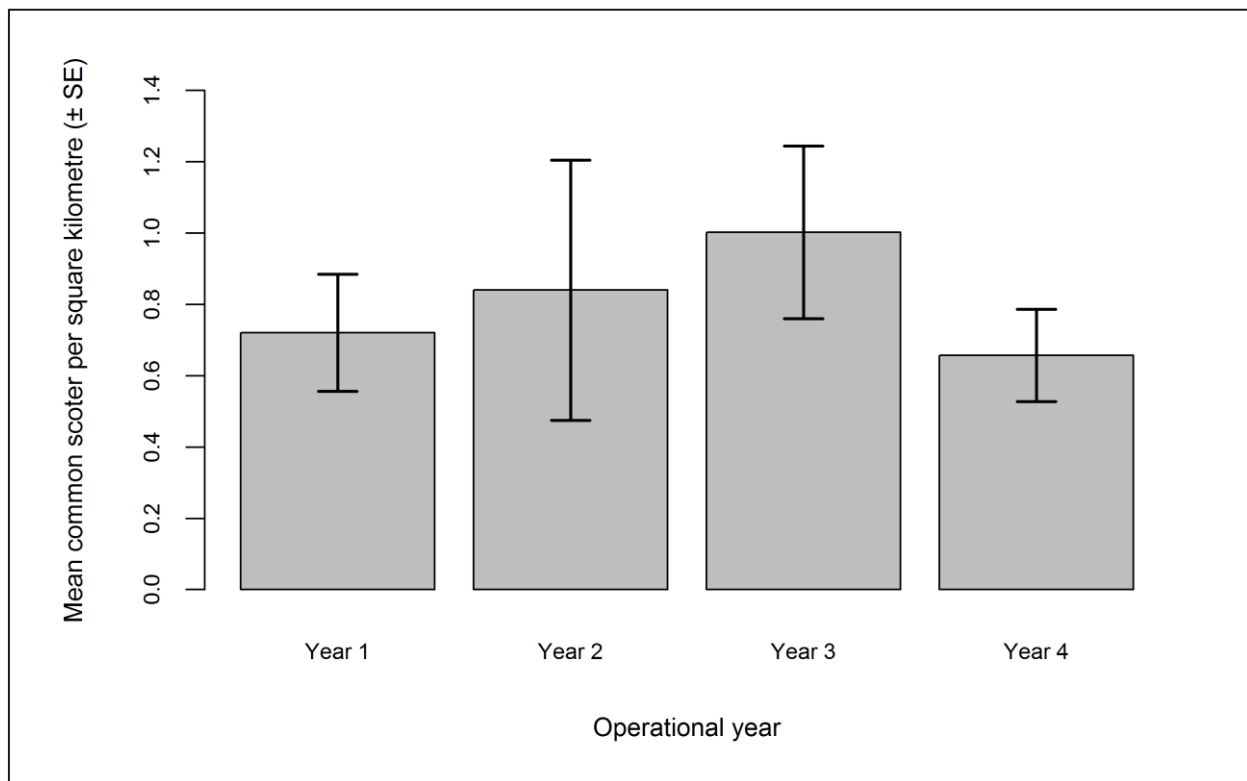


Figure 2.31: Mean density ( $\pm$  se) of common scoter recorded in flight across operational years one to four.

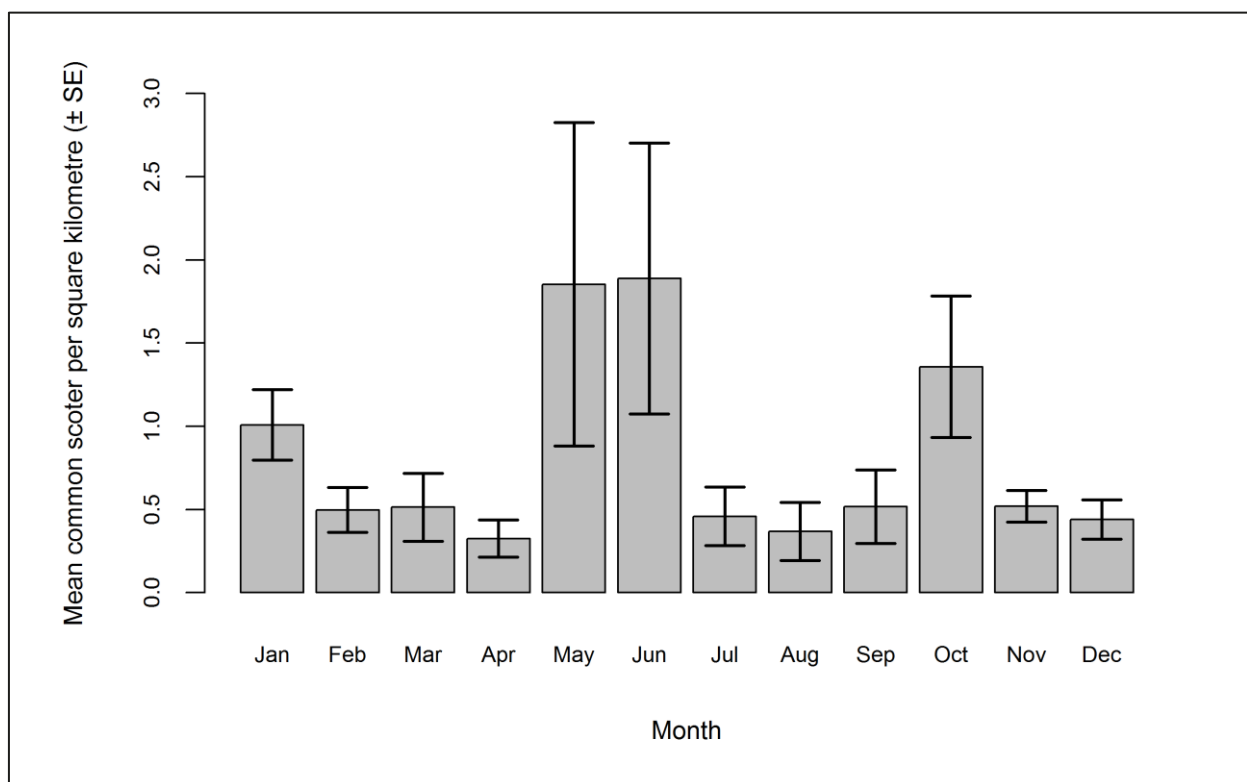


Figure 2.32: Mean density ( $\pm$  se) of common scoter recorded in flight during each month across operational years one to four.

#### 2.4.2.2.3. Distribution

Since abundance modelling of common scoter was not possible for comparison between operational years, Figure 2.33 shows the distribution of raw common scoter observations during this monitoring period. Both flying and sitting birds are represented. The largest densities of both flying and sitting common scoters were recorded across the northern half of the survey area, with birds distributed in inshore waters off the northern coast of the Solway Firth. Distribution appears to have changed little across the four operational years, although there is an indication of an increase in the number of sightings in the south of the survey area (Figure 2.33).



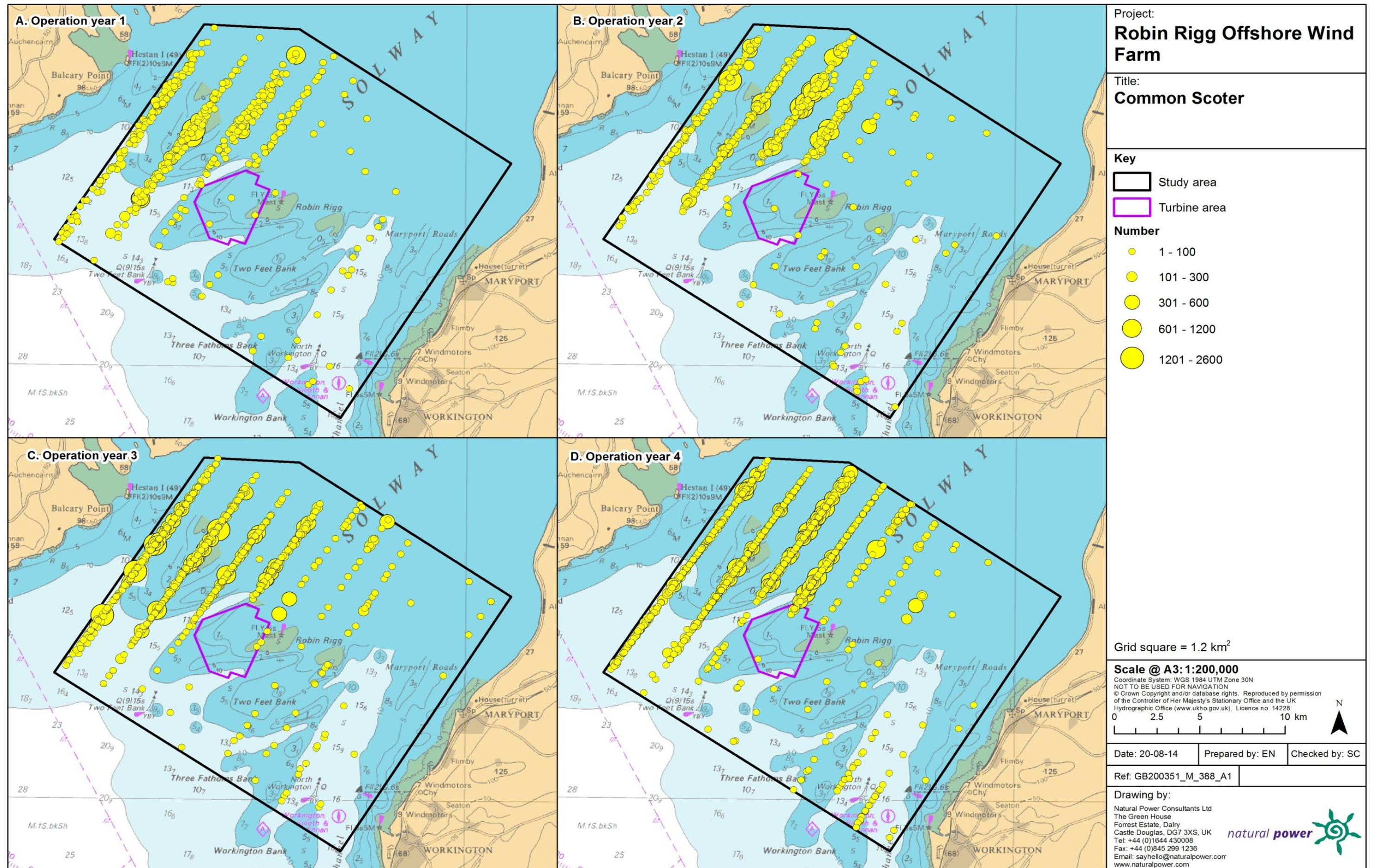


Figure 2.33: Location of raw common scoter observations during a) pre-construction, b) construction and c) operational monitoring. Both flying and sitting birds are represented. Circle size is proportional to the number of common scoters sighted.



#### 2.4.2.2.4. Collision risk

The percentage of common scoter recorded across the four operational years in different height bands relative to rotor swept height are shown in Table 2.21 and Figure 2.34. As would be expected for this species, the majority (>90%) of common scoters were observed flying at less than 25 m in height across all operational years. As such, a chi-squared test was not undertaken.

**Table 2.21: Percentage of common scoter recorded in different flight height bands across operational years one to four. Shaded column indicates percentage at rotor swept height (flight band 4).**

Operational year	Flight height band					
	1 (0–5 m)	2 (6–25 m)	3 (26–34 m)	4 (35–125 m)	5 (126–200 m)	6 (>200 m)
1	60.48	39.24	0.16	0.12	0.00	0.00
2	82.31	17.69	0.00	0.00	0.00	0.00
3	52.78	43.60	3.57	0.04	0.00	0.00
4	68.71	25.92	4.38	0.99	0.00	0.00

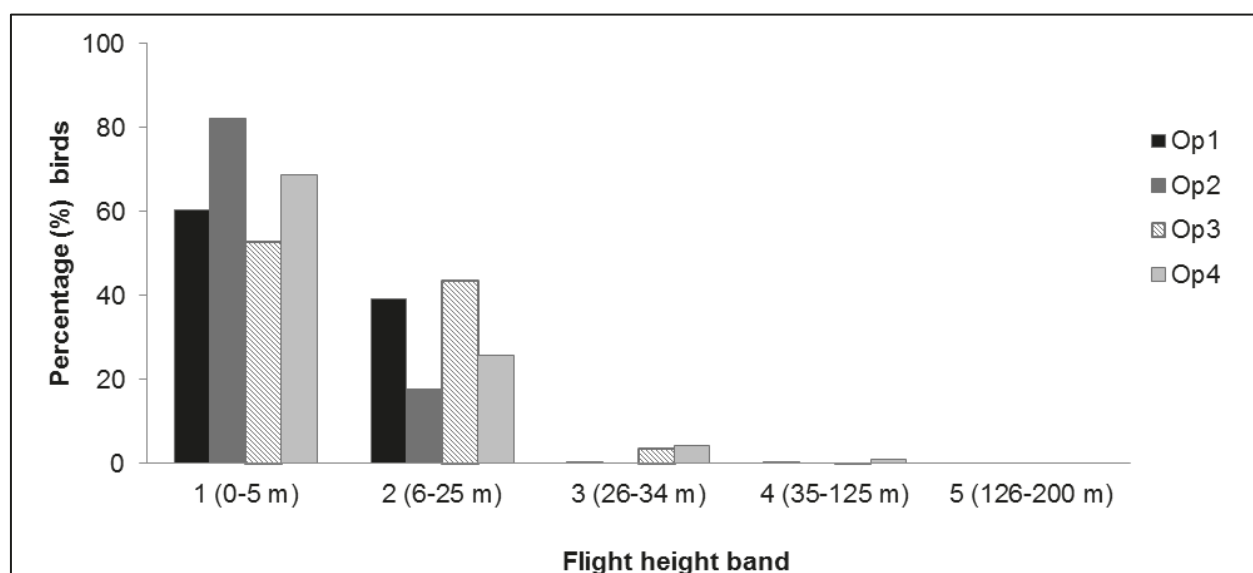


**Figure 2.34: Percentage of common scoter recorded in different flight height bands across operational years one to four.**



### 2.4.3. Red-throated diver

#### 2.4.3.3. Across three development phases

##### 2.4.3.3.5. Summary statistics

The number of red-throated diver sightings has remained relatively similar during the pre-construction and construction phases, with an increase during operation (Table 2.22). Numbers of red-throated divers recorded on the sea surface and in flight were comparable throughout the three development phases (Table 2.22).

**Table 2.22: Number of red-throated divers recorded per block during each development phase per km survey effort (all data).**

	Pre-construction		Construction		Operation years 1-2	
	On sea	In flight	On sea	In flight	On sea	In flight
<b>Total number individuals</b>	370	161	301	237	529	433
<b>Total number sightings</b>	(152)	(87)	(198)	(177)	(207)	(257)
<b>Number individuals/km</b>	0.10	0.05	0.04	0.03	0.14	0.11
	Total		Total		Total	
<b>Total number individuals</b>	531		538		962	
<b>Total number sightings</b>	(239)		(375)		(464)	
<b>Number individuals/km</b>	0.15		0.07		0.25	

Data were filtered as described in the methods (Section 2.4.4). The percentage of analysis blocks without observations was calculated to ensure there were sufficient data to perform the analysis (Table 2.23). Data were also checked to ensure observations were recorded in all months of the year.

**Table 2.23: Percentage of red-throated diver analysis blocks without observations across the three development phases: pre-construction, construction and operational years one and two. Zero inflation prior to removal of effort is presented in parentheses.**

	On sea	In flight
<b>Percentage zero blocks</b>	98.6%	(99.3%) 99.0%

### 2.4.3.3.6. Density

#### 2.4.3.3.6.1. On sea

Initial data exploration highlighted several outliers that may influence the modelling process (Figure 2.35). The model was attempted with and without these large groups but in both cases the model would not converge. It may be possible to repeat the model using a binomial distribution to predict presence/absence rather than abundance. However, at the time of analysis the MRSea package was unable to accommodate binomial distributions. Therefore, further modelling work could not be undertaken and raw data are presented instead.

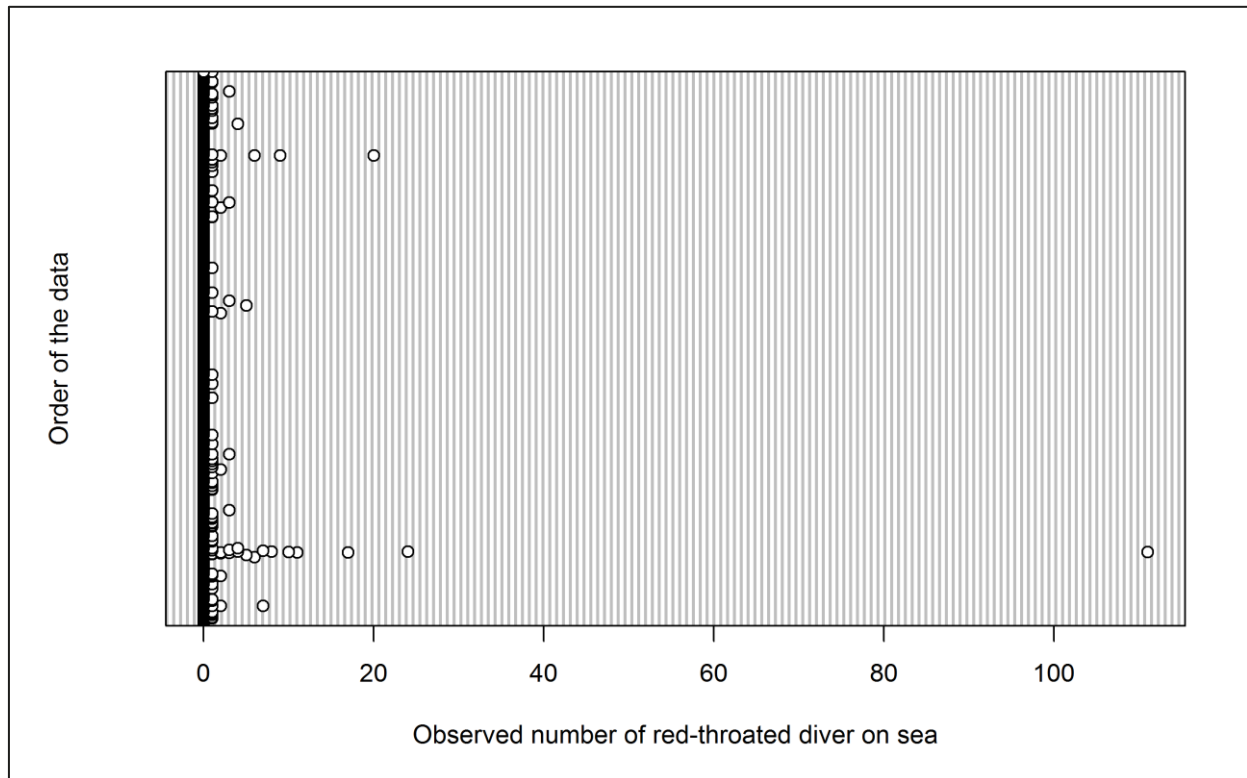


Figure 2.35: Dot plot of the number of red-throated divers observed on sea per analysis block across the three development phases: pre-construction, construction and operational years one and two.

Group size for red-throated divers recorded on the sea ranged from single individuals up to 110 birds. Mean density of red-throated diver indicates a decrease between pre-construction and construction phases, with a slight increase during operation (Figure 2.36). However, since further modelling was not undertaken, the significance of any differences could not be tested. Figure 2.37 shows that the majority of red-throated divers on the sea across the three development phases were recorded in September.

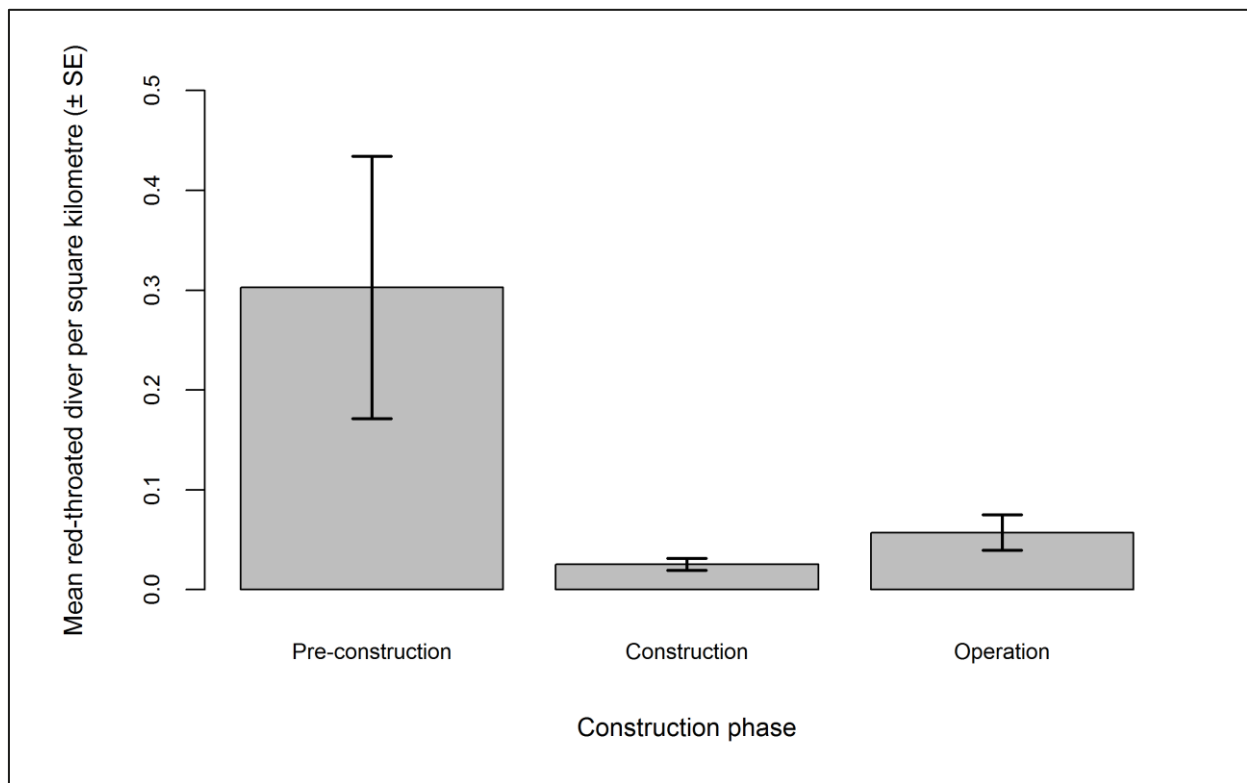


Figure 2.36: Mean density ( $\pm$  se) of red-throated divers recorded on the sea across the three development phases: pre-construction, construction and operational years one and two.

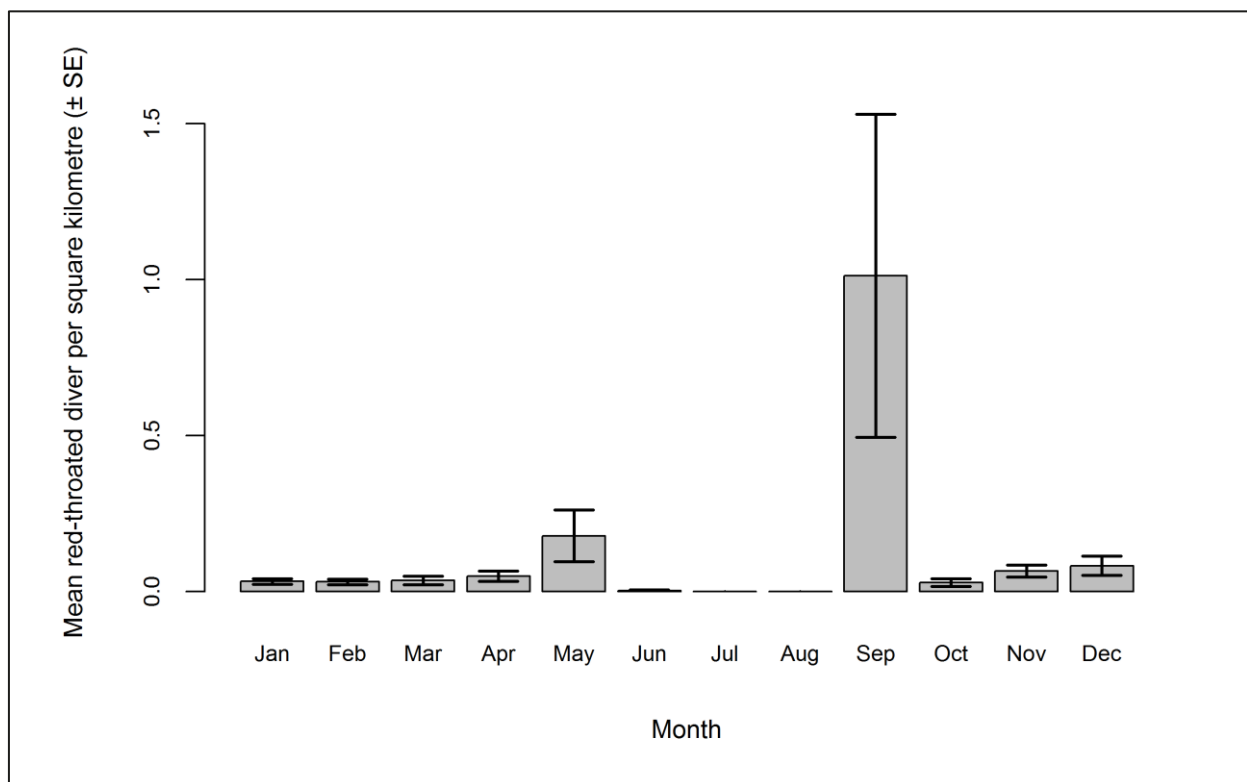


Figure 2.37: Mean density ( $\pm$  se) of red-throated divers recorded on the sea during each month across the three development phases: pre-construction, construction and operational years one and two.

#### 2.4.3.3.6.2. In flight

Initial data exploration highlighted that >99% of analysis blocks for red-throated divers in flight during the three development phases contained zero observations (Figure 2.38). Since red-throated divers are not present in the Solway Firth during the summer months, data was removed for June to August in order to reduce the number of zero observations. However, even after removal of these months, 99% of analysis blocks still contained zero observations (Table 2.23). Therefore, further abundance modelling of red-throated divers in flight across the three development phases was not undertaken and raw data are presented.

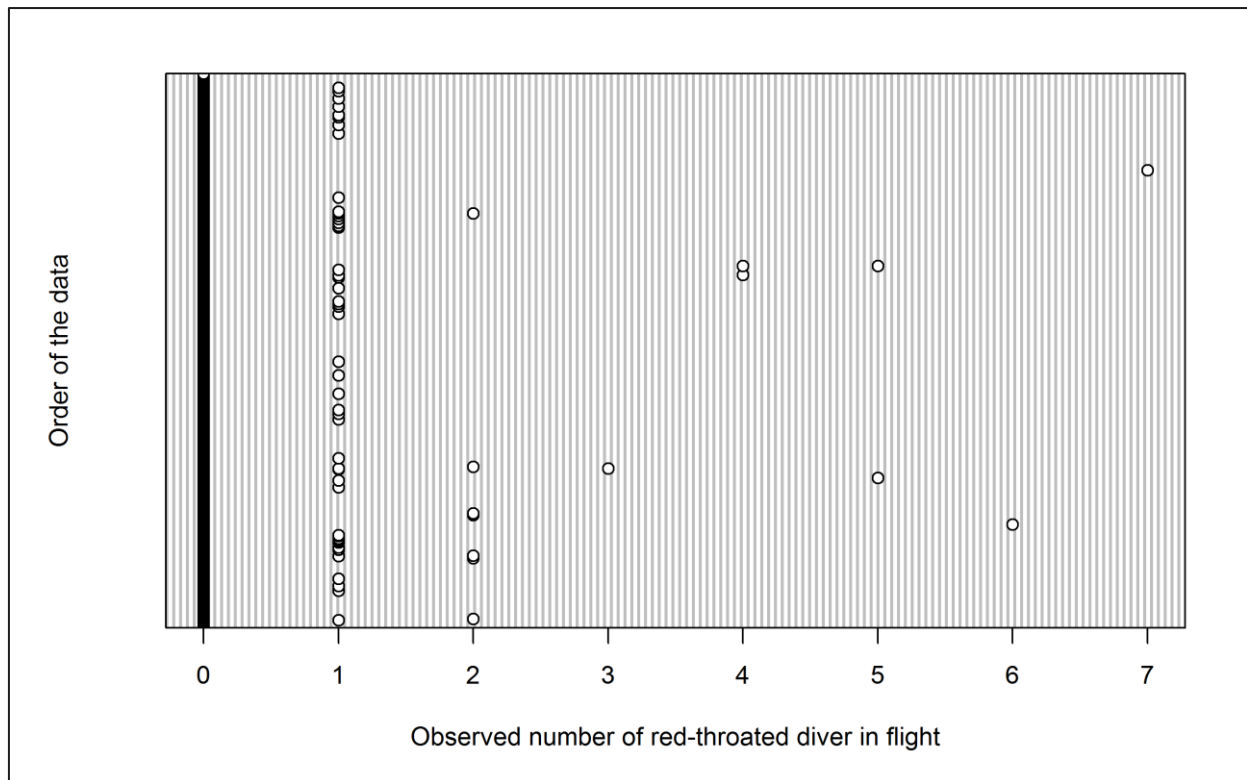


Figure 2.38: Dot plot of the number of red-throated divers observed in flight per analysis block across the three development phases: pre-construction, construction and operational years one and two.

Most observations were of single birds with seven being the maximum group size (Figure 2.38). Mean density of red-throated divers indicates a decrease in the numbers of birds recorded in flight between the pre-construction and construction phases, with an increase during the operational phase (Figure 2.39). However, since further modelling was not undertaken, the significance of any differences could not be tested. Figure 2.40 shows that the majority of red-throated divers were recorded in May, with no birds recorded during the summer months of June, July and August.

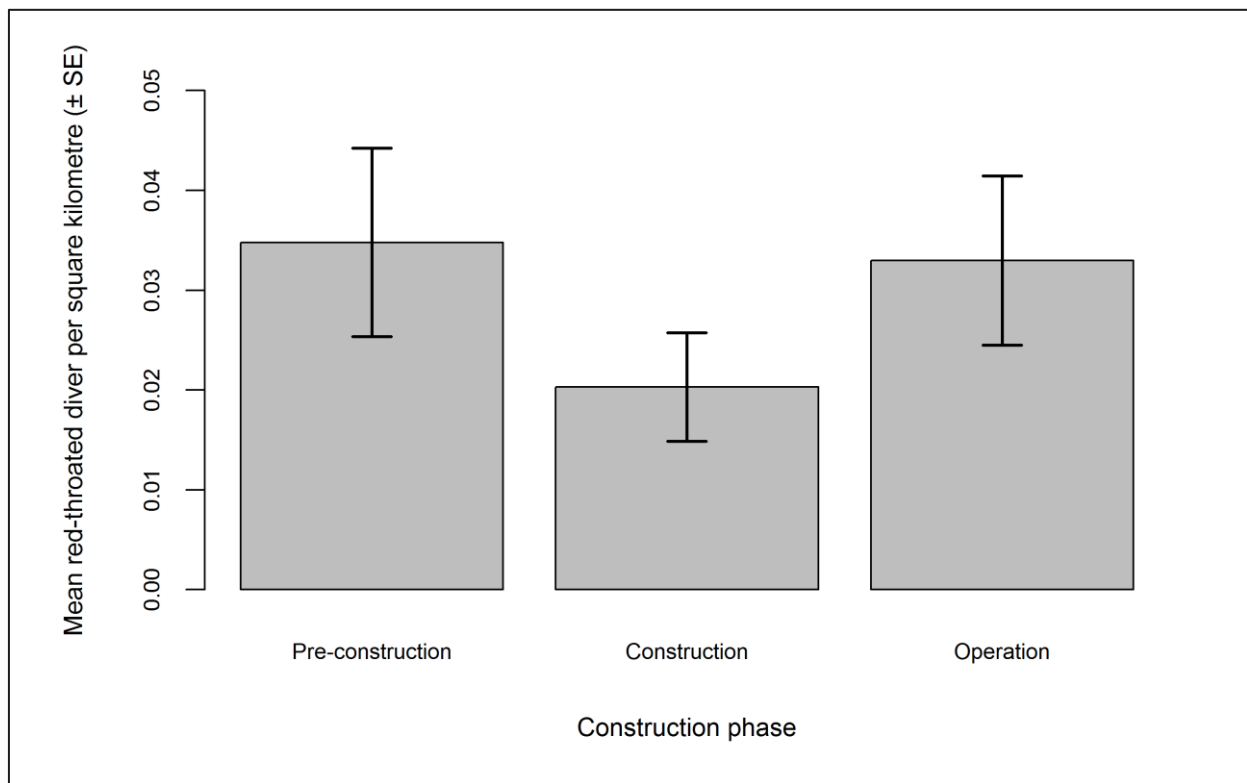


Figure 2.39: Mean density ( $\pm$  se) of red-throated divers recorded in flight across the three development phases: pre-construction, construction and operational years one and two.

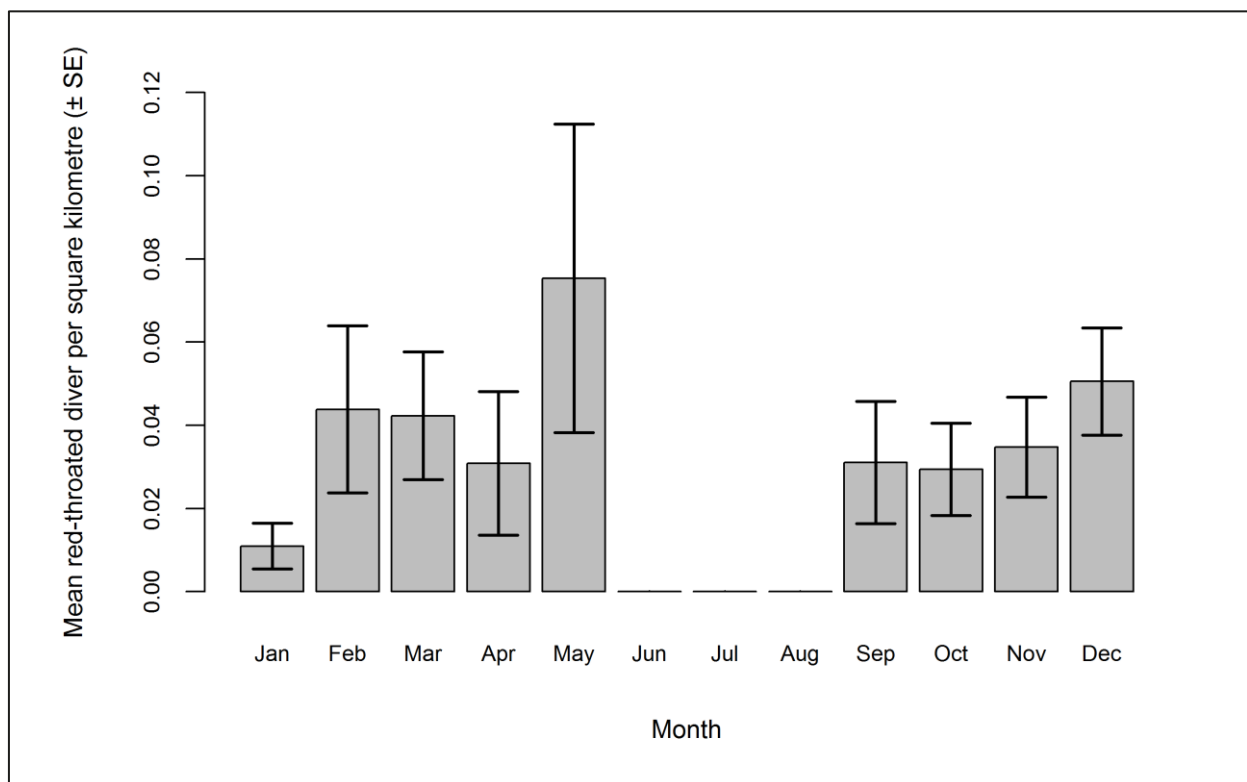


Figure 2.40: Mean density ( $\pm$  se) of red-throated divers recorded in flight during each month across the three development phases: pre-construction, construction and operational years one and two.



#### 2.4.3.3.7. Distribution

Since abundance modelling of common scoter across the three phase comparison was not possible, Figure 2.41 shows the distribution of raw common scoter observations during pre-construction, construction and operational monitoring. Both flying and sitting birds are represented. Relatively low numbers of red-throated divers were recorded across the survey area during all three phases, with larger numbers recorded in inshore waters Figure 2.41. There is an indication of a slight increase in numbers across the three phases, with larger groups of birds recorded during operation in comparison to previous phases Figure 2.41.

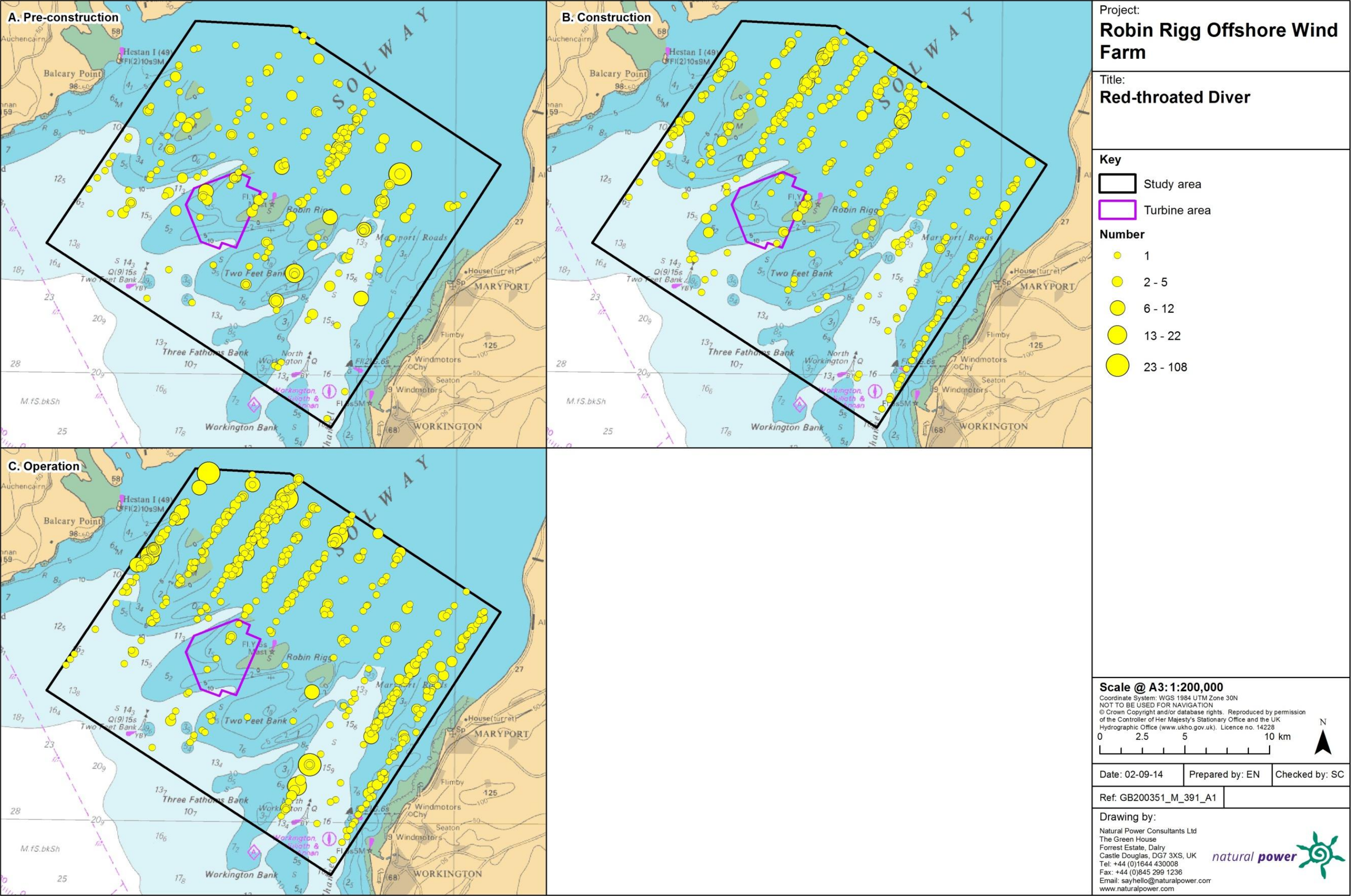


Figure 2.41: Location of raw red-throated diver observations during a) pre-construction, b) construction and c) operational monitoring. Both flying and sitting birds are represented. Circle size is proportional to the number of red-throated divers sighted.



#### 2.4.3.3.8. Collision risk

The percentage of red-throated divers recorded during the three development phases in different height bands relative to rotor swept height are shown in Table 2.24 and Figure 2.42. Since only a small percentage (<3%) were observed flying at rotor swept height, a chi-squared test was not undertaken.

**Table 2.24:** Percentage of red-throated divers recorded in different flight height bands across the three development phases: pre-construction, construction and operational years one and two. Shaded column indicates percentage at rotor swept height (flight band 4).

Phase	Flight height band					
	1 (0–5 m)	2 (6–25 m)	3 (26–34 m)	4 (35–125 m)	5 (126–200 m)	6 (>200 m)
Pre-construction	80.75	19.25	0.00	0.00	0.00	0.00
Construction	62.45	31.65	3.38	2.53	0.00	0.00
Operation	50.35	38.34	9.47	1.85	0.00	0.00

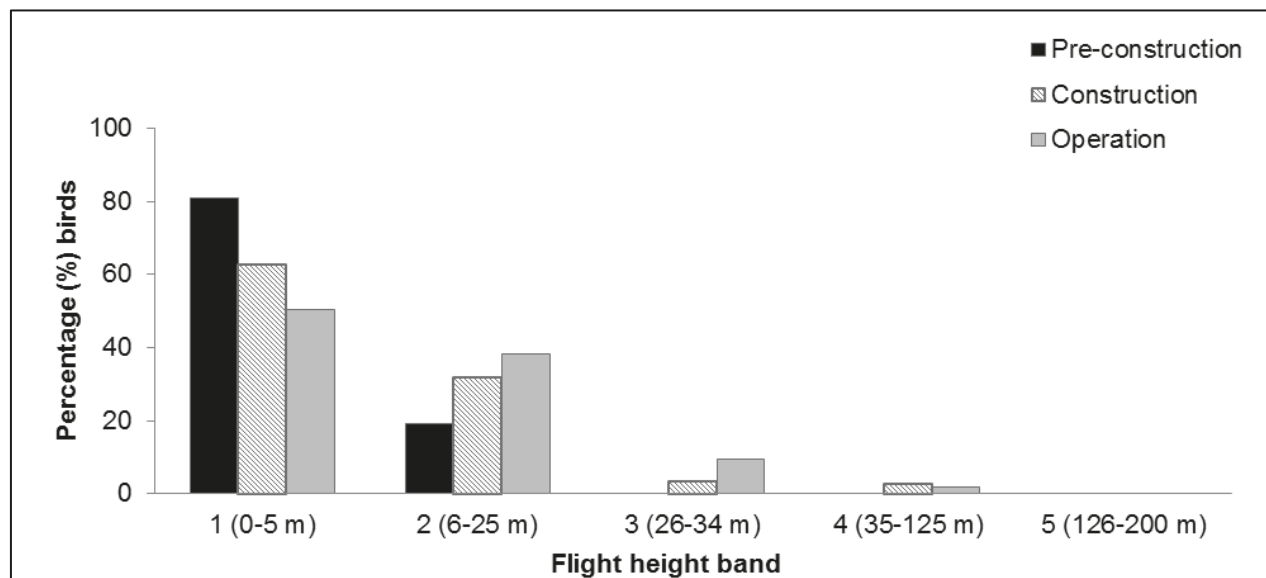


**Figure 2.42:** Percentage of red-throated divers recorded in different flight height bands across the three development phases: pre-construction, construction and operational years one and two.

## 2.4.3.4. Across operational years

### 2.4.3.4.9. Summary statistics

The number of red-throated diver sightings has remained relatively similar during operational years one to three, with a small decrease in operational year four (Table 2.25). Slightly larger numbers of red-throated divers were recorded on the sea than in flight, with the exception of operational year four (Table 2.25). Average group size does not appear to have changed between operational years (Table 2.25).

**Table 2.25: Number of red-throated divers recorded per block during each operational year per km survey effort (all data).**

	Operational year 1		Operational year 2		Operational year 3		Operational year 4	
	On sea	In flight	On sea	In flight	On sea	In flight	On sea	In flight
<b>Total number individuals</b>	288	225	241	208	293	283	166	230
<b>Total number sightings</b>	78	116	129	141	166	193	121	165
<b>Number individuals/km</b>	0.16	0.12	0.12	0.10	0.14	0.13	0.08	0.11
	Total		Total		Total		Total	
<b>Total number individuals</b>	513		449		576		396	
<b>Total number sightings</b>	194		270		359		286	
<b>Number individuals/km</b>	0.28		0.22		0.27		0.18	

Data were filtered as described in the methodology (Section 2.4.4). The percentage of segments without observations was calculated to ensure there were sufficient data to perform the analysis (Table 2.26). Data were also checked to ensure observations were recorded in all months of the year.

**Table 2.26: Percentage of red-throated diver analysis blocks without observations across operational years one to four. Zero inflation prior to removal of effort is presented in parentheses.**

	On sea	In flight
<b>Percentage zero blocks</b>	(97.6%) 97.1%	99.1%

#### 2.4.3.4.10. Density and distribution

##### 2.4.3.4.10.1. On sea

A half-normal detection function with sea state as a covariate was found to be the best fitting model. Figure 2.43 shows the selected detection curve for red-throated divers.

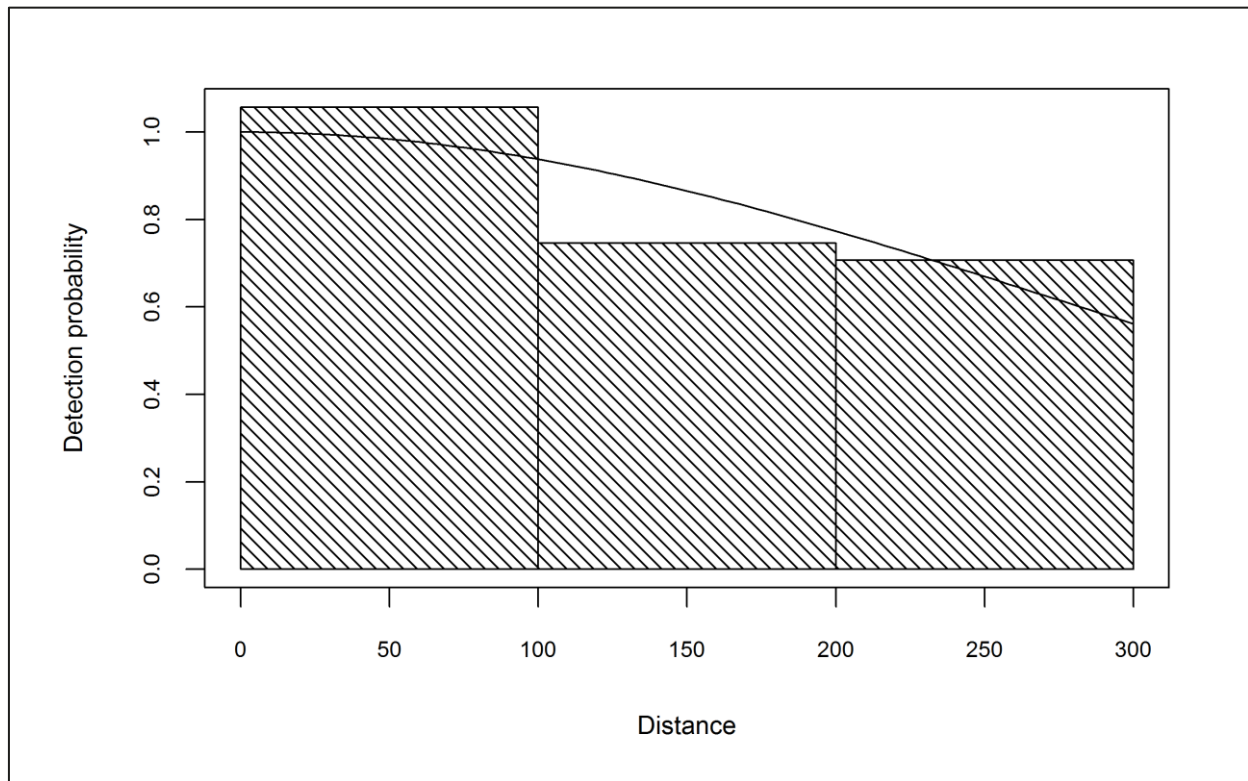


Figure 2.43: Detection curve used to adjust red-throated diver on sea counts for imperfect detection across operational years one to four.

Initial data exploration of adjusted red-throated diver numbers indicated that there were no outlying observations (Figure 2.44).



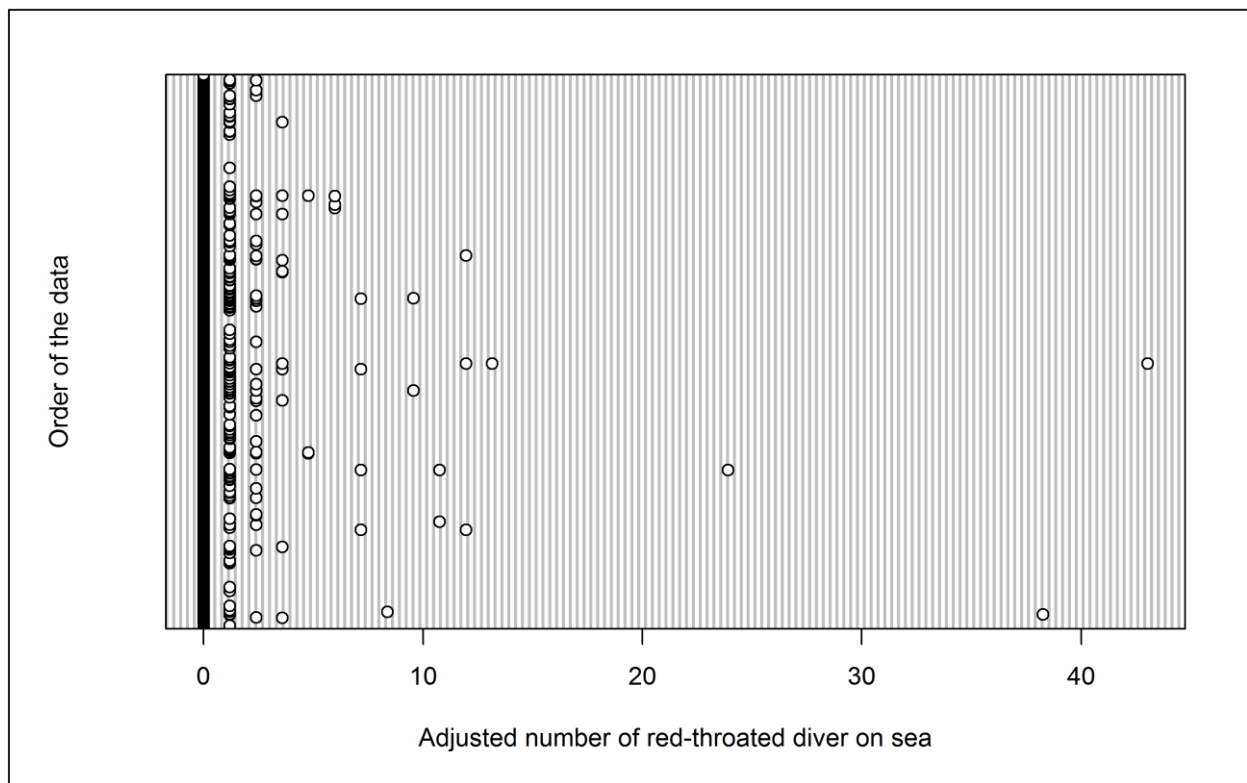


Figure 2.44: Dot plot of the number of red-throated divers observed on sea per analysis block across operational years one to four.

The GEE predicted that month, location and the interaction between the two all had a statistically significant influence of red-throated diver abundance within the survey area (Table 2.27). Operational year had no statistically significant effect on red-throated diver abundance and density (Figure 2.45). Significantly smaller numbers of red-throated divers were recorded in June (Figure 2.46). Red-throated diver abundance and density did not differ significantly across the remaining months, although there was a non-significant peak in spring (March and April; Figure 2.46). Model predictions were therefore made for March.

Table 2.27: Final model outputs for red-throated divers on the sea across operational years one to four.

Term	Marginal p-value
Month	0.0007
Phase	0.3142
Tide height	0.0491
Location (X,Y)	<0.0001
Interaction (location: phase)	0.0046

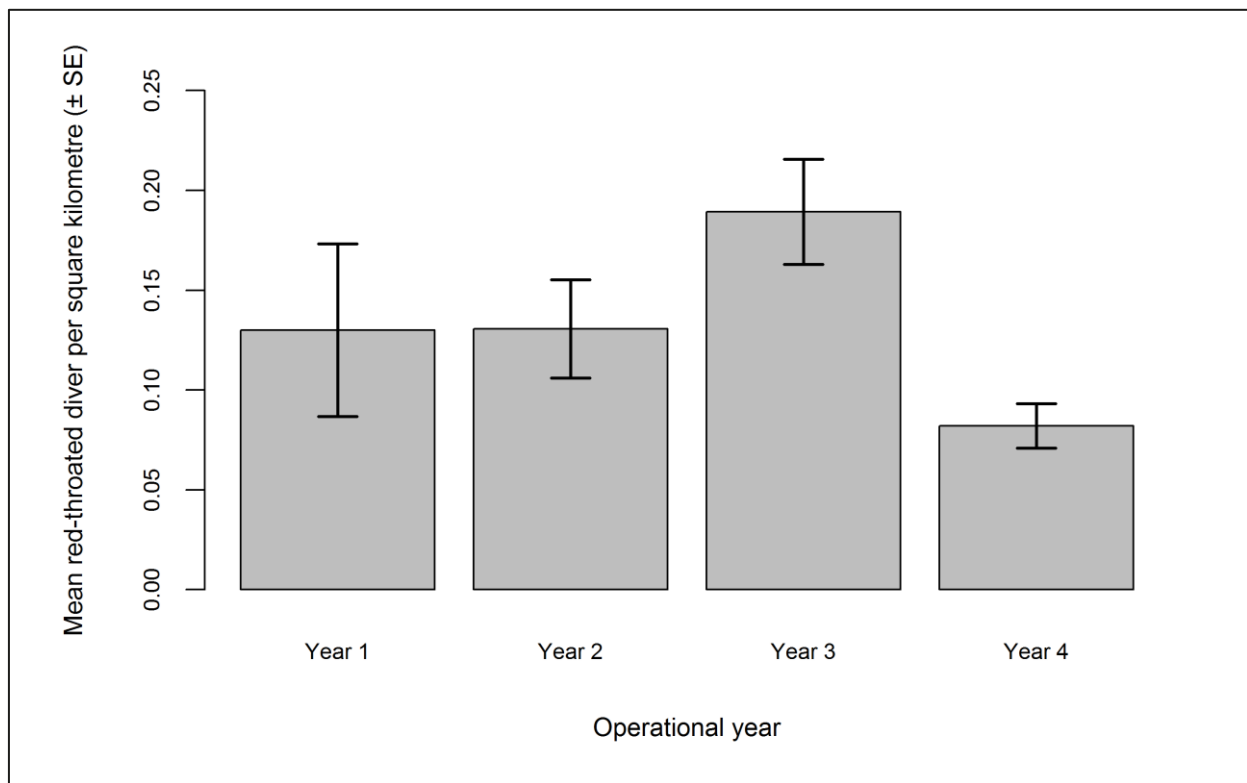


Figure 2.45: Mean density (± se) of red-throated divers recorded on the sea across operational years one to four.

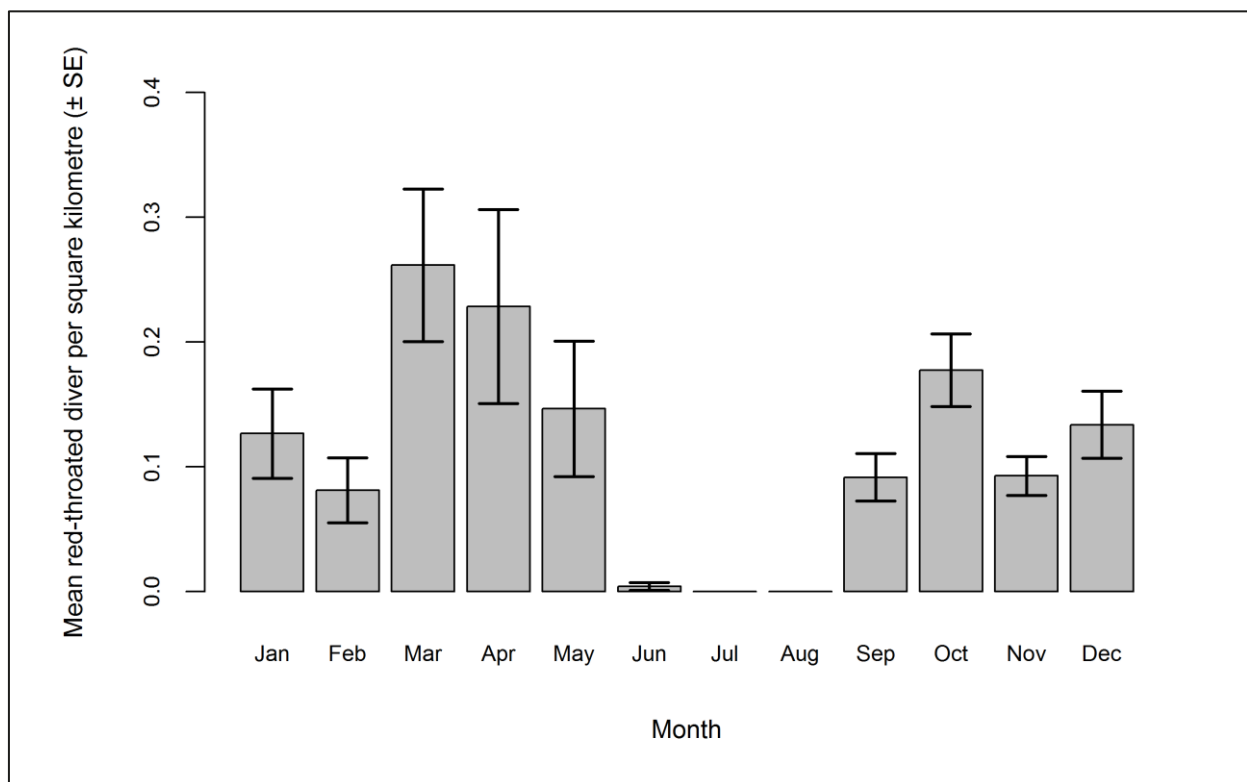


Figure 2.46: Mean density (± se) of red-throated divers recorded on the sea across operational years one to four.

The abundance and densities (by site, buffer and total survey area) are presented in Table 2.28. There is little change in abundance and density during successive operational years. In comparison to other species recorded within the Robin Rigg OWF and wider survey area, relatively few red-throated divers were recorded during all operational years. The lowest percentage of individuals recorded within the Robin Rigg OWF itself occurred during operational year one, with a slight increase during subsequent operational years (Table 2.28).

**Table 2.28: Abundance and density of red-throated divers on the sea across operational years one to four. Values in parentheses represent upper and lower 95% confidence intervals.**

Operational year	Abundance			Density			% within site
	Site	Buffer	Total	Site	Buffer	Total	
<b>1</b>	0 (0-2)	39 (2-555)	39 (2-557)	0.01 (0-0.19)	0.11 (0.01-1.60)	0.11 (0.01-1.54)	0.26
<b>2</b>	1 (0-2)	29 (5-171)	30 (5-174)	0.04 (0.01-0.19)	0.08 (0.01-0.49)	0.08 (0.01-0.48)	1.80
<b>3</b>	0 (0-4)	48 (7-309)	48 (7-313)	0.04 (0-0.28)	0.14 (0.02-0.89)	0.13 (0.02-0.87)	1.03
<b>4</b>	0 (0-1)	15 (2-85)	15 (2-86)	0.01 (0-0.08)	0.04 (0-0.24)	0.04 (0-0.24)	1.11

The density surface maps show that relatively small densities of red-throated divers were predicted to occur across all four operational years (Figure 2.47), consistent with the densities shown in Table 2.28. As such, there were few significant differences observed in red-throated diver density between operational years (Figure 2.47). A small area of significant decline was predicted in year four close to the Cumbrian coastline Figure 2.48. This is likely to reflect the larger densities recorded operational years one and three in comparison to years two and four.

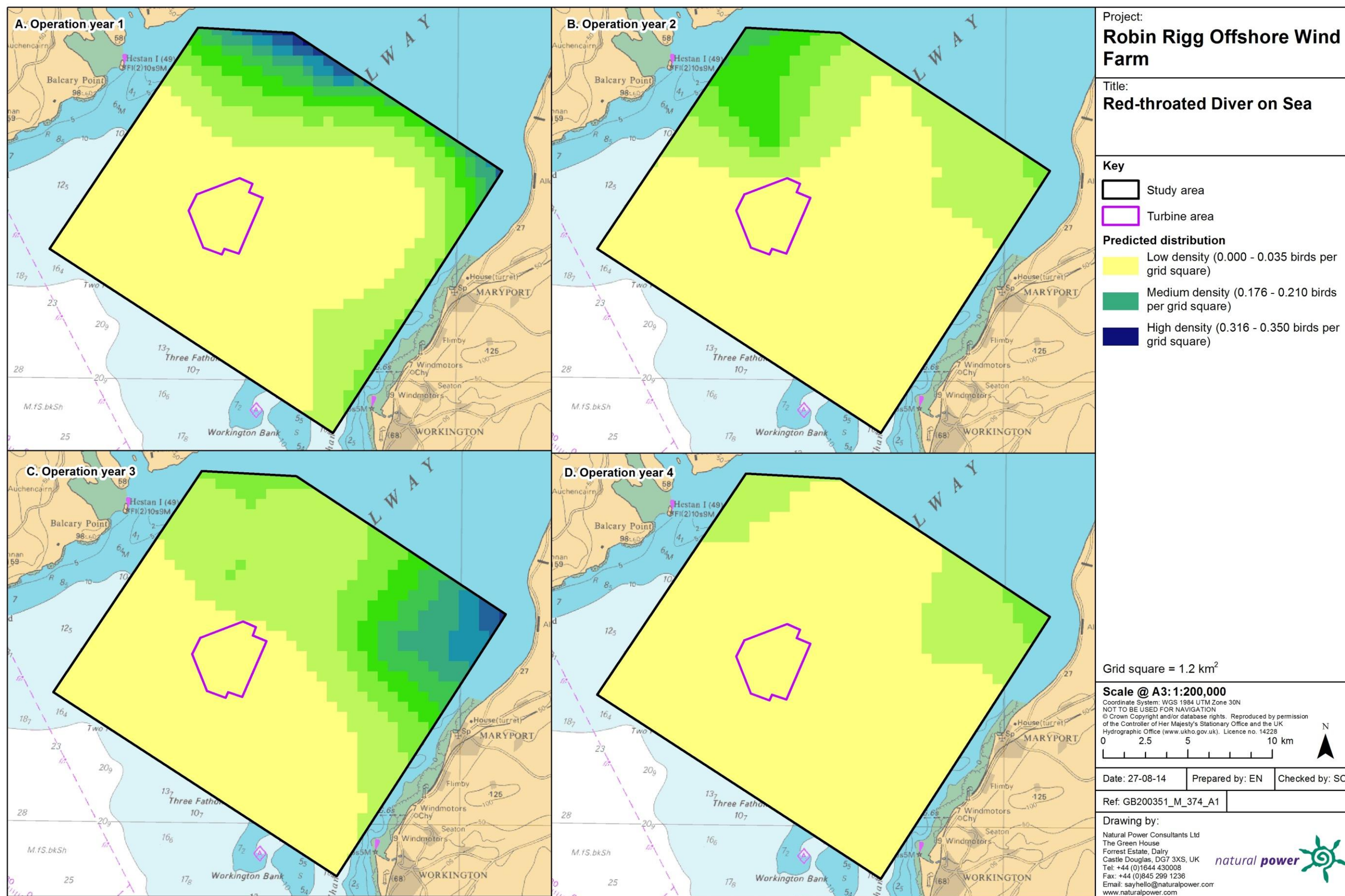


**Figure 2.47: Predicted density of red-throated divers on the sea during a) operational year one, b) operational year two, c) operational year three and d) operational year four.**



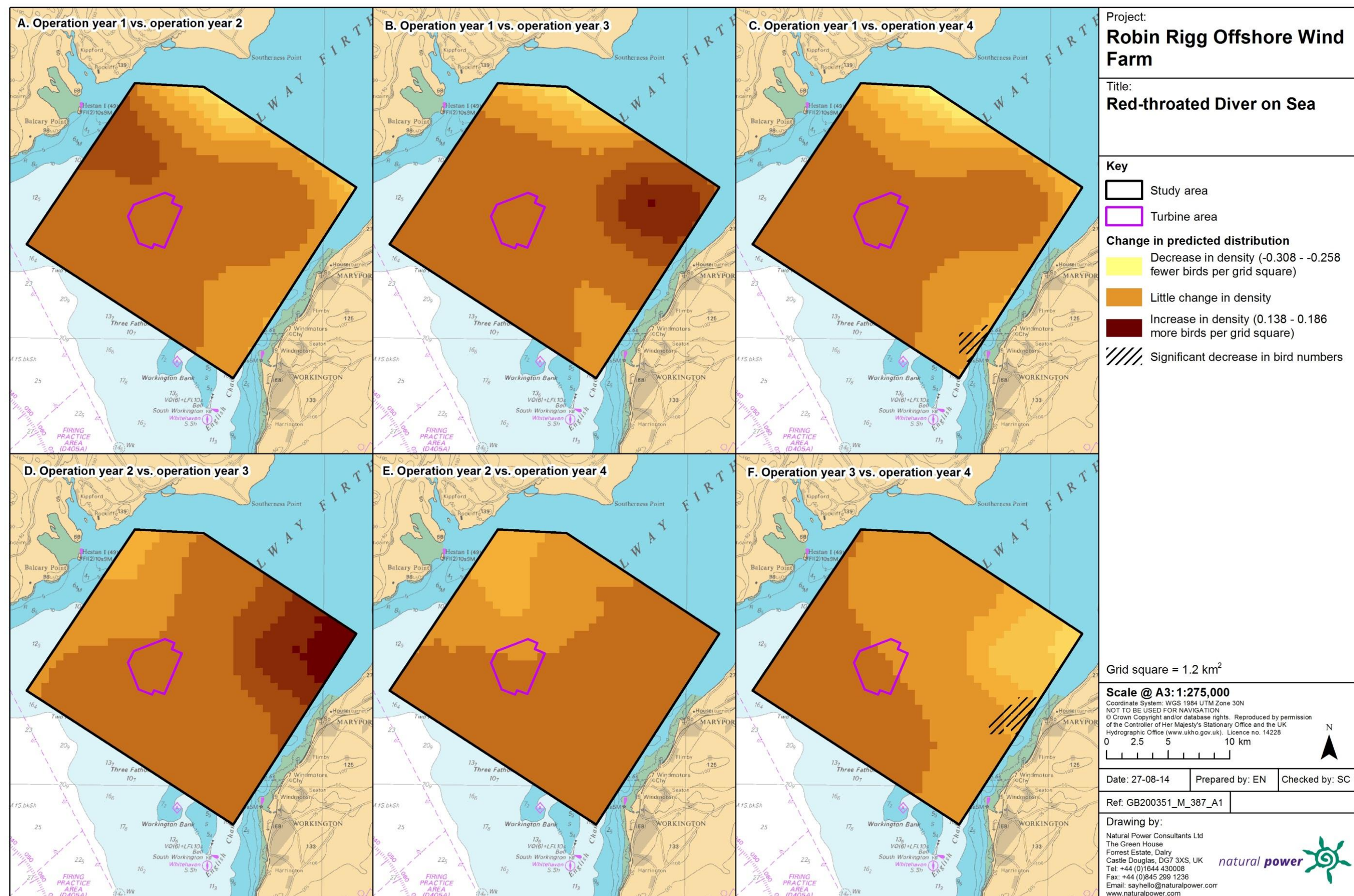


**Figure 2.48: Differences in predicted sitting red-throated diver density between operational years one to four. Significant differences are marked with diagonal shading.**



#### 2.4.3.4.10.2. In flight

Initial data exploration highlighted that >99% of analysis blocks for red-throated divers in flight during the four operational years contained zero observations (Figure 2.49). Since red-throated divers are not present in the Solway Firth during the summer months, data was removed for June to August in order to reduce the number of zero observations. However, even after removal of these months, 99% of analysis blocks still contained zero observations (Table 2.23). Therefore, further modelling of red-throated divers in flight across the three development phases was not undertaken and raw data are presented.

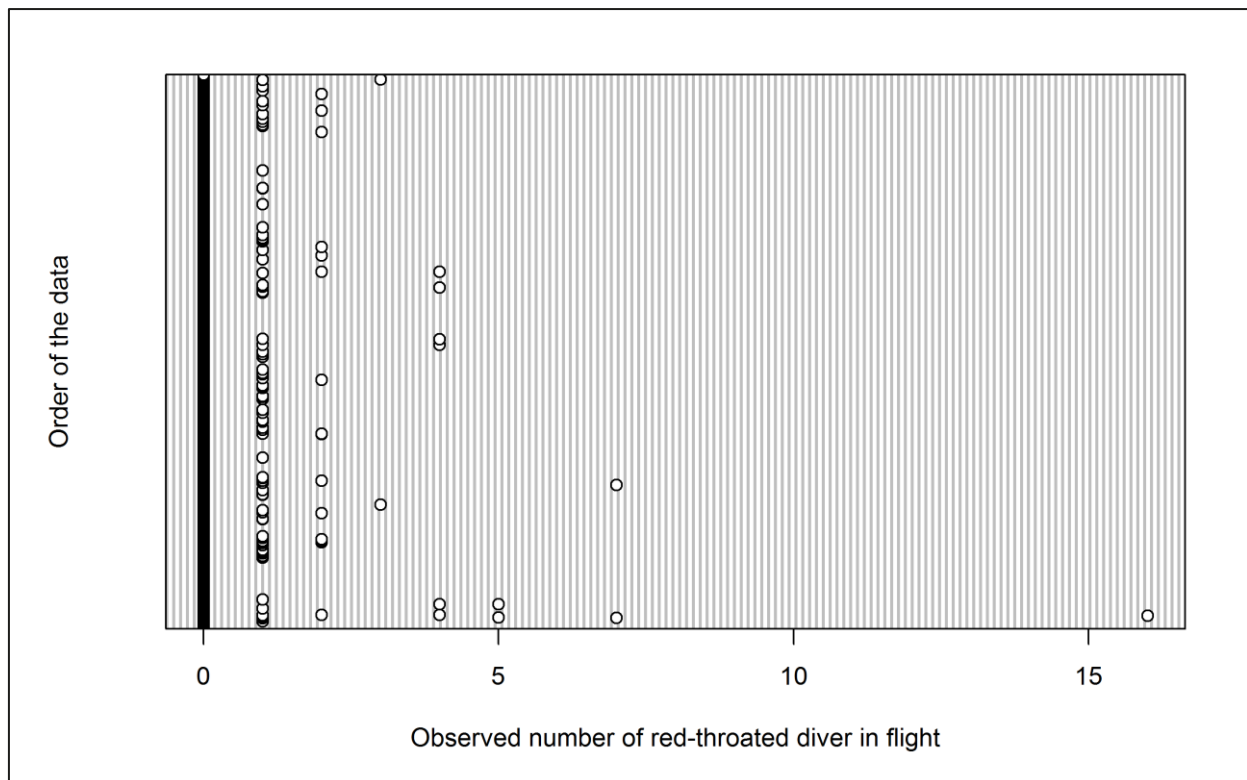


Figure 2.49: Dot plot of the number of red-throated divers observed in flight per analysis block across operational years one to four.

Most observations were of single birds with 16 being the maximum group size (Figure 2.49). Mean density of red-throated divers was largest during operational one, with a possible decline across subsequent operational years (Figure 2.50). However, since further abundance modelling was not undertaken, the significance of any differences could not be tested. Figure 2.51 shows that the majority of red-throated divers were recorded in April and May.

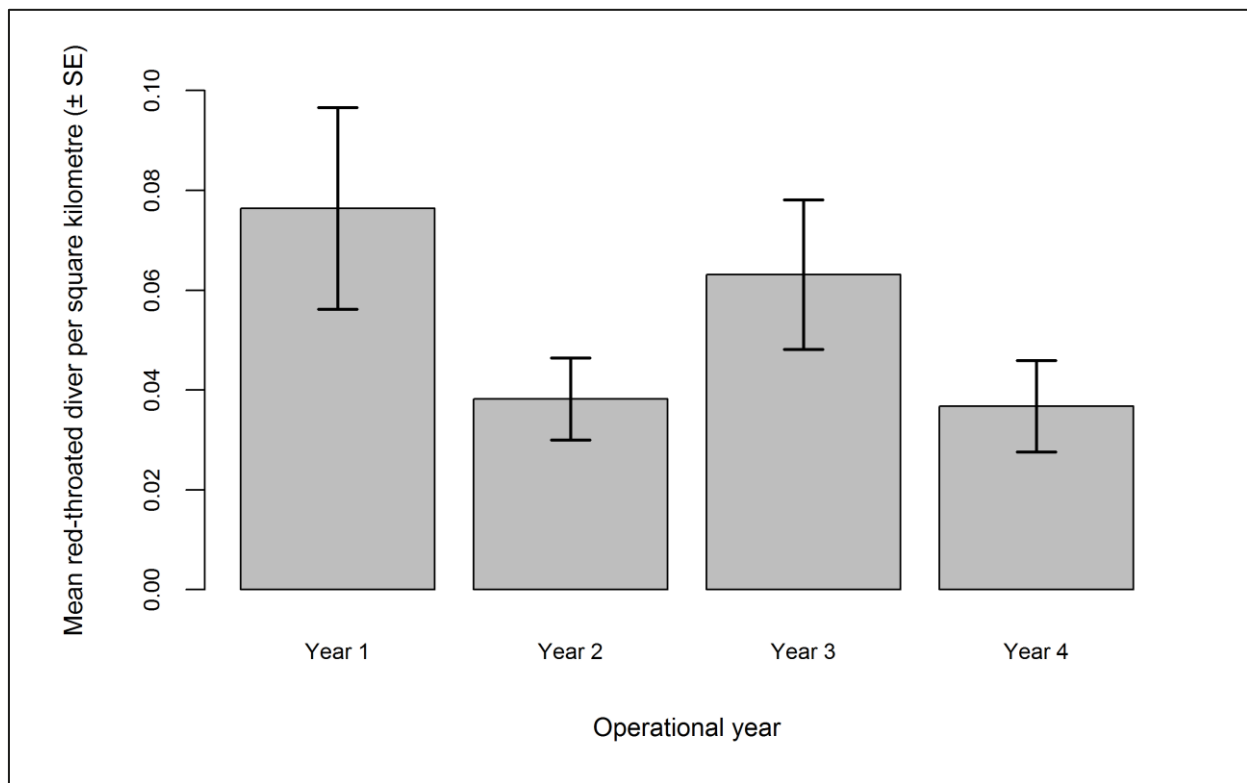


Figure 2.50: Mean density ( $\pm$  se) of red-throated divers recorded in flight across operational years one to four.

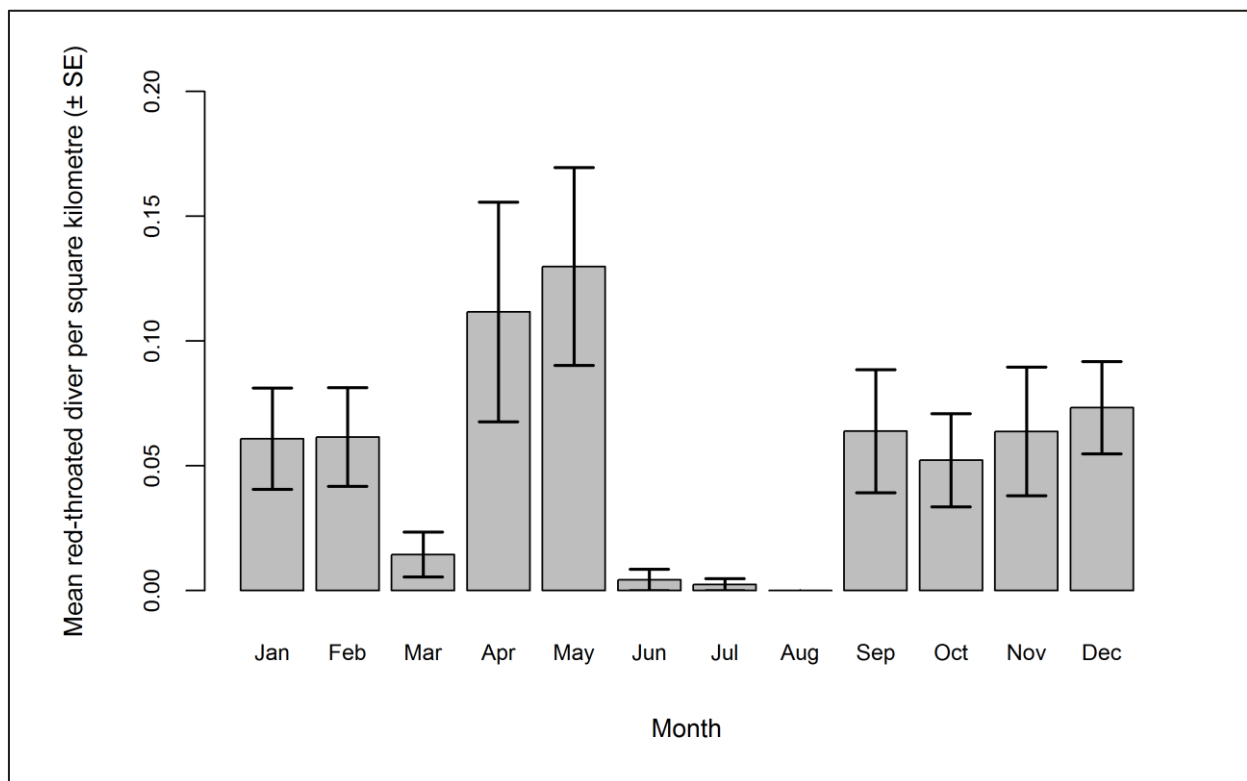


Figure 2.51: Mean density ( $\pm$  se) of red-throated divers recorded in flight during each month across operational years one to four.

#### 2.4.3.4.11. Collision risk

The percentage of red-throated divers recorded during the four operational years in different height bands relative to rotor swept height can be found in Table 2.29 and Figure 2.52. Since only a small percentage (<5%) were observed flying at rotor swept height across all operational years, a chi-squared test was not undertaken.

**Table 2.29: Percentage of red-throated divers recorded in different flight height bands across operational years one to four. Shaded column indicates percentage at rotor swept height (flight band 4).**

Operational year	Flight height band					
	1 (0–5 m)	2 (6–25 m)	3 (26–34 m)	4 (35–125 m)	5 (126–200 m)	6 (>200 m)
1	44.00	38.67	15.11	2.22	0.00	0.00
2	57.21	37.98	3.37	1.44	0.00	0.00
3	42.76	36.34	16.15	4.75	0.00	0.00
4	62.17	30.87	5.22	1.74	0.00	0.00

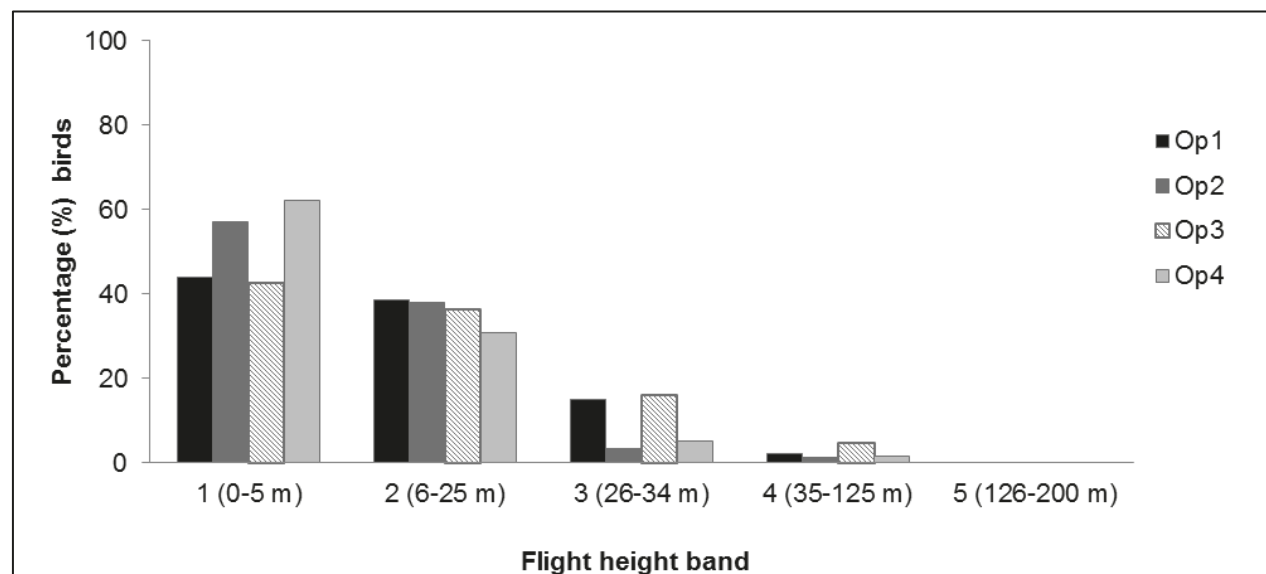


**Figure 2.52: Percentage of red-throated divers recorded in different flight height bands across operational years one to four.**

## 2.4.4. Manx shearwater

### 2.4.4.5. Across three development phases

#### 2.4.4.5.12. Summary statistics

Manx shearwaters were seen in relatively small numbers across the three development phases, with the number of individuals seen per km of survey effort reducing during the first two years of operation (Table 2.30). Similar numbers of individuals were observed in both flight and on the sea during the operational phase whereas the majority (94%) of individuals were recorded in flight during pre-construction (Table 2.30).

**Table 2.30: Number of Manx shearwater recorded per block during each development phase per km survey effort (all data).**

	Pre-construction		Construction		Operation years 1-2	
	On sea	In flight	On sea	In flight	On sea	In flight
<b>Total number individuals</b>	99	1,469	1,021	664	302	249
<b>Total number sightings</b>	17	124	101	208	62	117
<b>Number individuals/km</b>	0.03	0.41	0.14	0.09	0.08	0.06
	Total		Total		Total	
<b>Total number individuals</b>	1,568		1,685		551	
<b>Total number sightings</b>	141		309		179	
<b>Number individuals/km</b>	0.44		0.23		0.14	

Data were filtered as described in the methods (Section 2.4.4). The percentage of segments without observations was calculated to ensure there were sufficient data to perform the analysis (Table 2.31). Data were also checked to ensure observations were recorded in all months of the year. Manx shearwaters were only recorded during the months of April to August. As such, all other effort was removed from the analysis.

**Table 2.31: Percentage of Manx shearwater analysis blocks without observations across the three development phases: pre-construction, construction and operational years one and two. Zero inflation prior to removal of effort is presented in parentheses.**

	On sea	In flight
<b>Percentage zero blocks</b>	98.8%	(98.8%) 96.9%

### 2.4.4.5.13. Density and distribution

#### 2.4.4.5.13.1. On sea

Initial data exploration highlighted that nearly 99% of analysis blocks for Manx shearwaters on the sea contained zero observations (Figure 2.53). Since no birds were recorded between September and March, further removal of data was not possible. Therefore, further abundance modelling of Manx shearwaters across the three development phases was not undertaken and raw data are presented.

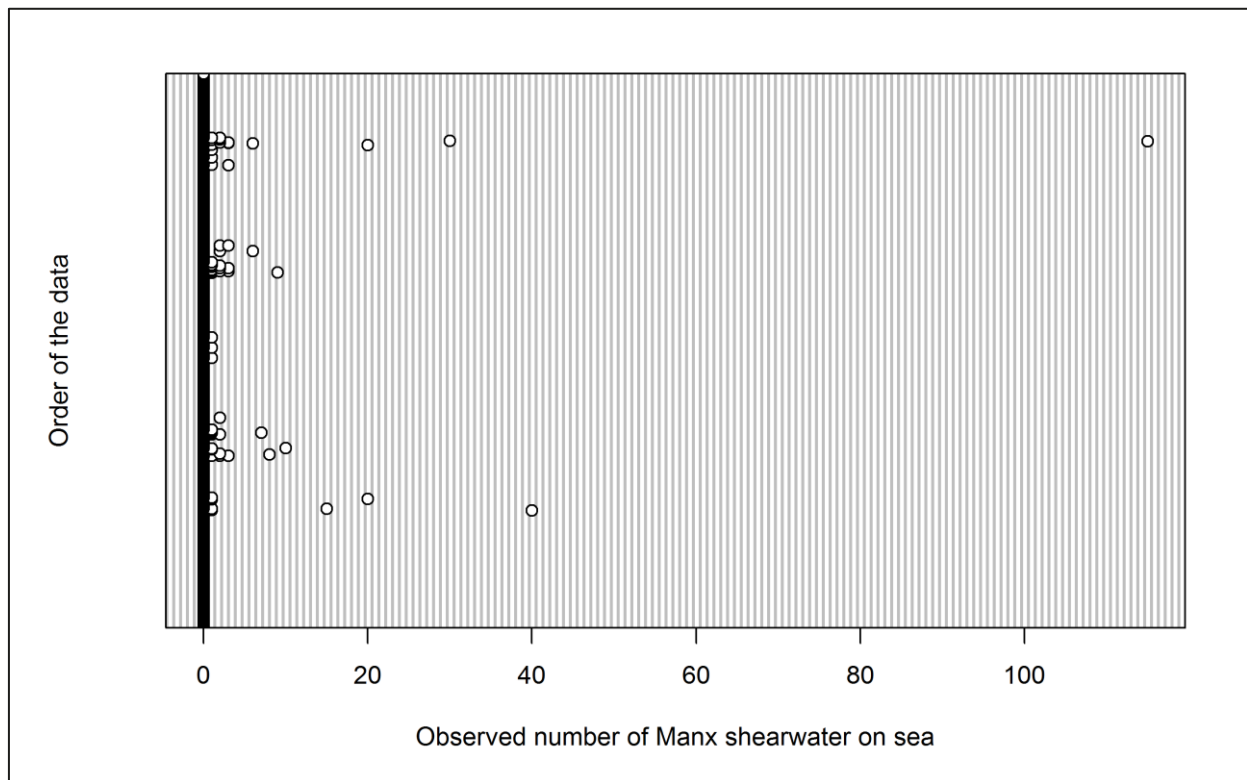


**Figure 2.53:** Dot plot of the number of Manx shearwaters observed on sea per analysis block across the three development phases: pre-construction, construction and operational years one and two.

Group size for Manx shearwaters recorded on the sea ranged from single individuals up to 120 birds. Mean density of Manx shearwaters on the sea indicates a decrease during the construction phase, with an increase during operation (Figure 2.54). However, since further abundance modelling was not undertaken, the significance of any differences could not be tested. Figure 2.55 shows that Manx shearwaters on the sea were only present during the summer months of April to August, peaking in July.



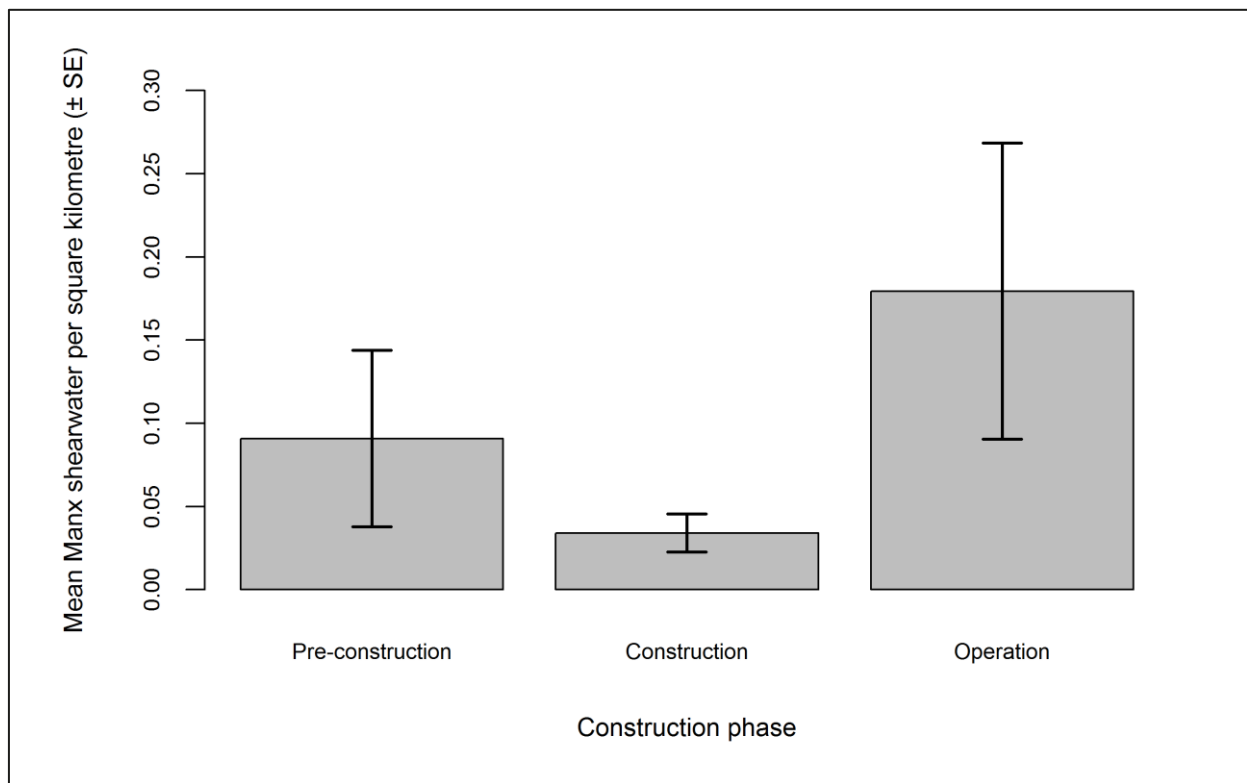


Figure 2.54: Mean density ( $\pm$  se) of Manx shearwaters recorded on the sea during each development phase: pre-construction, construction and operational years one and two.

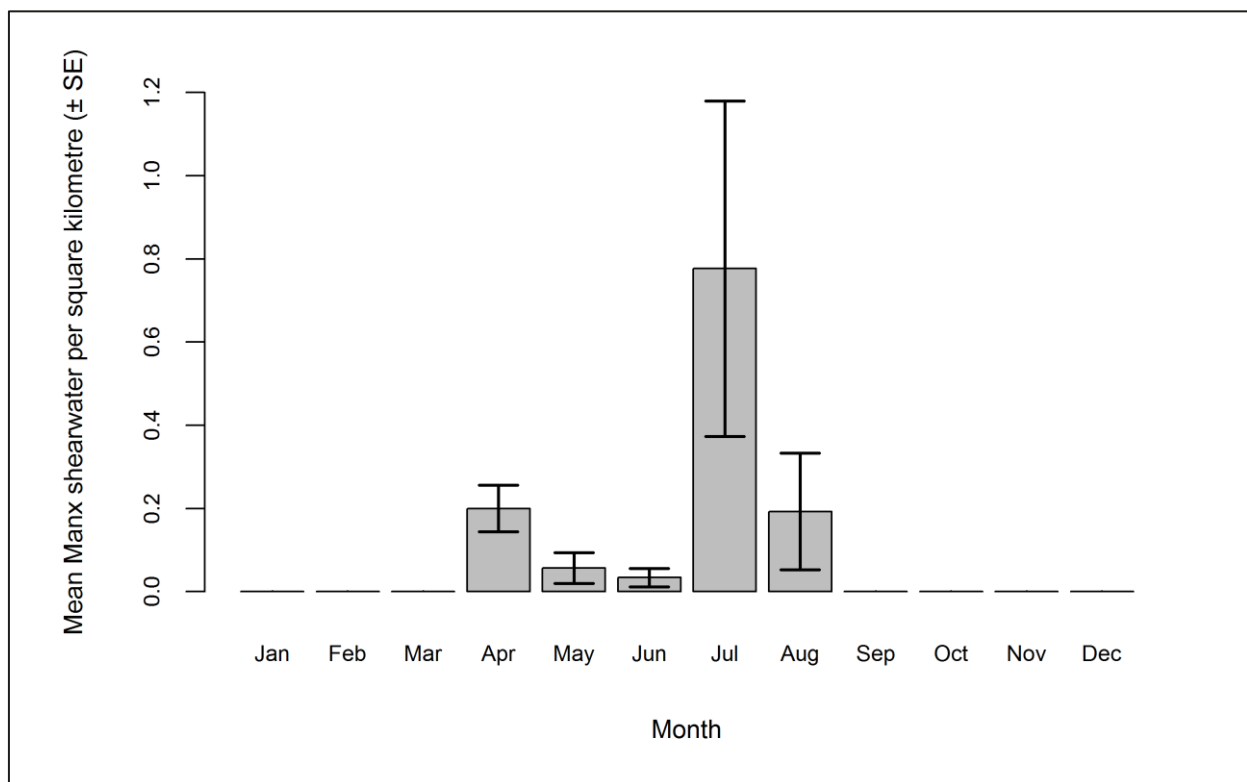
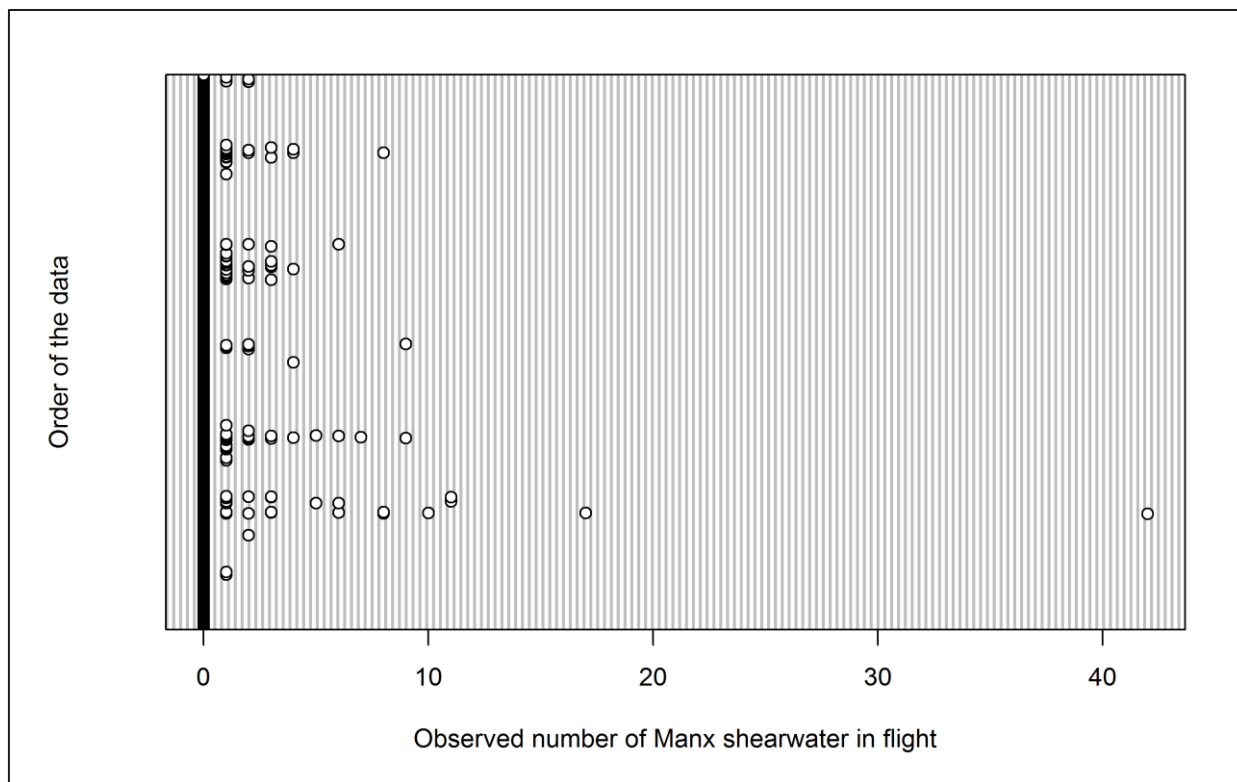


Figure 2.55: Mean density ( $\pm$  se) of Manx shearwaters recorded on the sea during each month across the three development phases: pre-construction, construction and operational years one and two.

### 2.4.4.5.13.2. In flight

Initial data exploration highlighted a single outlier (an analysis block containing 42 birds recorded in August 2004; Figure 2.56). Modelling was undertaken with and without this datum and the outputs compared.



**Figure 2.56:** Dot plot of the number of Manx shearwaters observed in flight per analysis block across the three development phases: pre-construction, construction and operational years one and two.

The GEE predicted that month, phase and location all have a statistically significant influence on Manx shearwater abundance within the survey area (Table 2.32). Specifically, larger numbers were observed during the pre-construction phase (Table 2.32), and during the months of July and August (Table 2.32). Since July was the month of peak activity, model predictions were made for this month.

P-values remained the same after removing the outlier for all variables except phase, which was no longer statistically significant (data not shown). In both models, the interaction between phase and location was statistically significant. Density surfaces for both models were also very similar; therefore outputs from the model including the outlier are presented here.

**Table 2.32:** Final model outputs for Manx shearwaters in flight across the three development phases: pre-construction, construction and operational years one and two.

Term	Marginal p-value
Month	0.0052
Phase	0.0100
Tide height	0.2410
Location (X,Y)	<0.0001
Interaction (location: phase)	<0.0001



Figure 2.57: Mean density ( $\pm$  se) of Manx shearwaters recorded in flight across the three development phases: pre-construction, construction and operational years one and two.

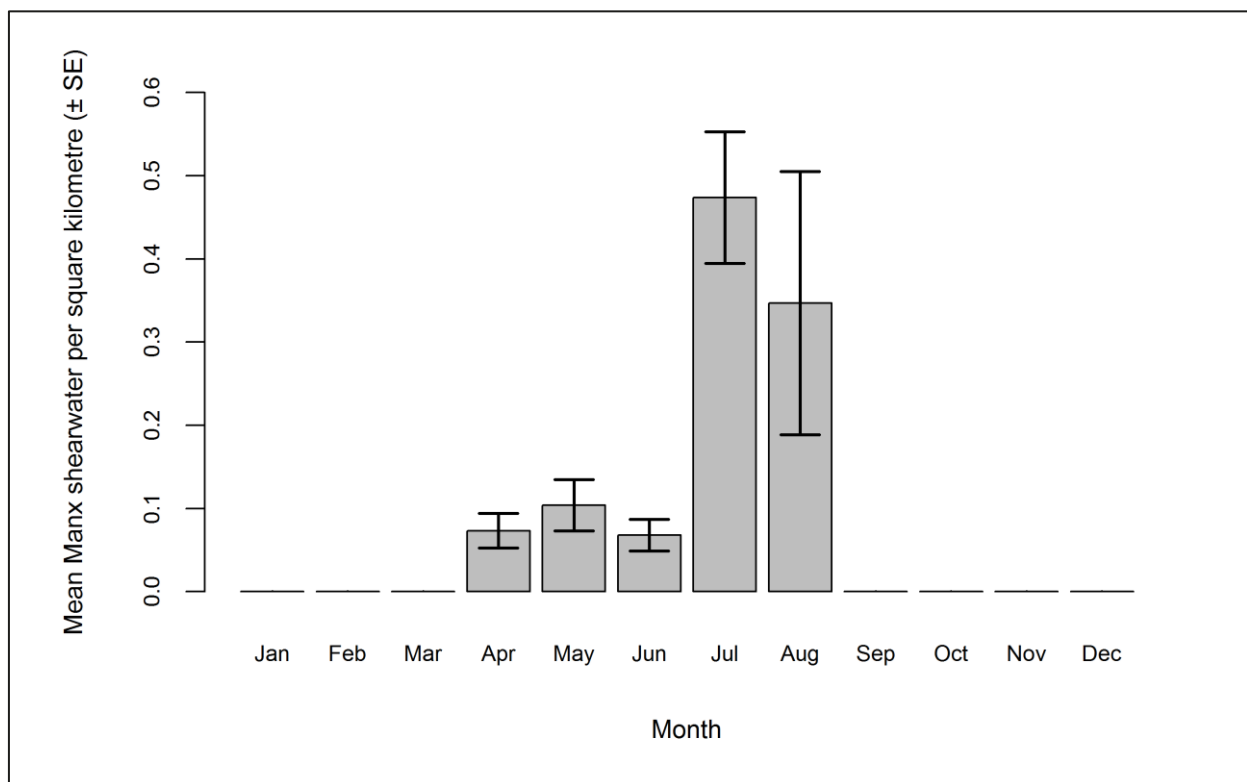


Figure 2.58: Mean density ( $\pm$  se) of Manx shearwaters recorded in flight during each month across the three development phases: pre-construction, construction and operational years one and two.

The abundance and densities (by site, buffer and total survey area) are presented in Table 2.33. Overall Manx shearwater abundance was largest during the construction and operation periods, although the proportion of birds within the Robin Rigg OWF itself was largest during the pre-construction phase (Table 2.33).

**Table 2.33: Abundance and density of Manx shearwaters in flight during the three development phases. Values in parentheses represent upper and lower 95% confidence intervals.**

Phase	Abundance			Density			% within site
	Site	Buffer	Total	Site	Buffer	Total	
<b>Pre-construction</b>	5 (1-12)	113 (33-266)	118 (34-278)	0.38 (0.09-0.93)	0.32 (0.09-0.76)	0.33 (0.09-0.77)	4.13
<b>Construction</b>	7 (1-18)	193 (53-495)	199 (54-513)	0.51 (0.11-1.41)	0.55 (0.15-1.42)	0.55 (0.15-1.42)	3.31
<b>Operation</b>	1 (0-5)	178 (32-648)	178 (32-653)	0.06 (0-0.42)	0.51 (0.09-1.86)	0.49 (0.09-1.81)	0.44

As shown in Table 2.33, relatively small densities of Manx shearwaters were recorded across the survey area during subsequent development phases (Figure 2.59). Manx shearwaters were predicted to occur in the west of the survey area during pre-construction surveys, showing a statistically significant shift to the south during construction (Figure 2.59). A further shift in distribution was seen between construction and operation, with birds declining in the south and significantly increasing in the north, close to the northern coast of the Solway Firth (Figure 2.59).



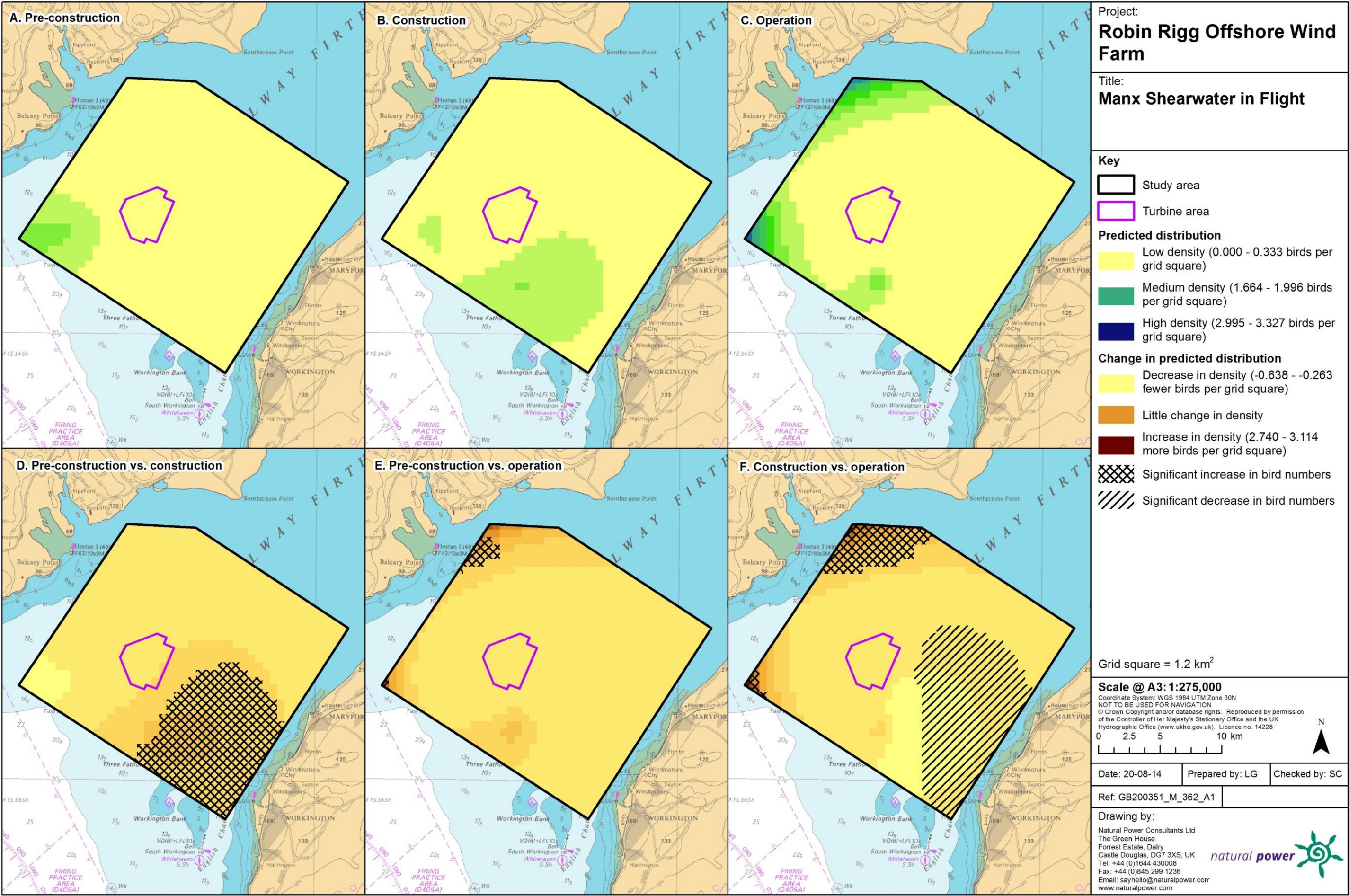


Figure 2.59: Predicted density of Manx shearwaters in flight during a) pre-construction, b) construction and c) operational monitoring. Changes in predicted density between d) pre-construction and construction, e) pre-construction and operation and f) construction and operation are also shown. Significant differences are marked with diagonal shading.



#### 2.4.4.5.14. Collision risk

The percentage of Manx shearwaters recorded during the three development phases in different height bands relative to rotor swept height are shown in Table 2.34 and Figure 2.60. Whilst all birds were recorded flying close to the sea surface during pre-construction, approximately 20% of Manx shearwaters recorded during the construction phase were in the second height band (6-25 m). This number dropped during the operational phase with two Manx shearwaters recorded at 6-25 m (Table 2.34). A chi-squared test was not undertaken as no flights were observed at rotor swept height.

**Table 2.34: Percentage of Manx shearwaters recorded in different flight height bands across the three development phases: pre-construction, construction and operational years one and two. Shaded column indicates percentage at rotor swept height (flight band 4).**

Phase	Flight height band					
	1 (0–5 m)	2 (6–25 m)	3 (26–34 m)	4 (35–125 m)	5 (126–200 m)	6 (>200 m)
Pre-construction	100.00	0.00	0.00	0.00	0.00	0.00
Construction	81.78	18.22	0.00	0.00	0.00	0.00
Operation	99.20	0.80	0.00	0.00	0.00	0.00

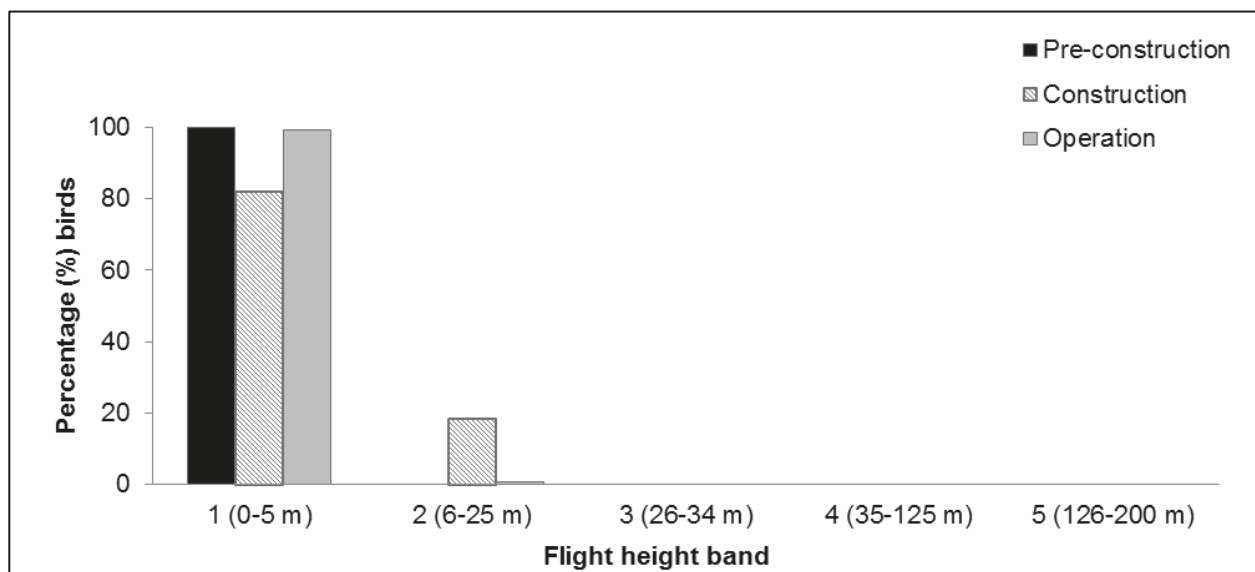


**Figure 2.60: Percentage of Manx shearwaters recorded in different flight height bands across the three development phases: pre-construction, construction and operational years one and two.**

## 2.4.4.6. Across operational years

### 2.4.4.6.15. Summary statistics

Manx shearwaters were seen in relatively small numbers across the four operational years, with the number of individuals seen per km of survey effort largest during operational year four (Table 2.35). Larger groups of Manx shearwaters were recorded on the sea surface during this year (Table 2.35).

**Table 2.35: Number of Manx shearwater recorded per block during each operational year per km survey effort (all data).**

	Operational year 1		Operational year 2		Operational year 3		Operational year 4	
	On sea	In flight	On sea	In flight	On sea	In flight	On sea	In flight
<b>Total number individuals</b>	57	103	245	146	76	100	459	262
<b>Total number sightings</b>	27	59	35	58	21	29	59	112
<b>Number individuals/km</b>	0.03	0.06	0.12	0.07	0.04	0.05	0.21	0.12
	Total		Total		Total		Total	
<b>Total number individuals</b>	160		391		176		721	
<b>Total number sightings</b>	86		93		50		171	
<b>Number individuals/km</b>	0.09		0.19		0.08		0.33	

Data were filtered as described in the methodology (Section 2.4.4). The percentage of segments without observations was calculated to ensure there were sufficient data to perform the analysis (Table 2.36). Data were also checked to ensure observations were recorded in all months of the year. Manx shearwaters were only recorded during the months of April to August. Subsequently, all other effort was removed from the analysis.

**Table 2.36: Percentage of Manx shearwater analysis blocks without observations across operational years one to four. Zero inflation prior to removal of effort is presented in parentheses.**

	On sea	In flight
<b>Percentage zero blocks</b>	99.0%	(99.1%) 98.1%

#### 2.4.4.6.16. Density and distribution

##### 2.4.4.6.16.1. On sea

Initial data exploration highlighted that nearly 99% of analysis blocks for Manx shearwaters on the sea contained zero observations (Figure 2.61). Since no birds were recorded between September and March, further removal of effort was not possible. Therefore, further modelling of Manx shearwaters across the four operational years was not undertaken and raw data are presented.

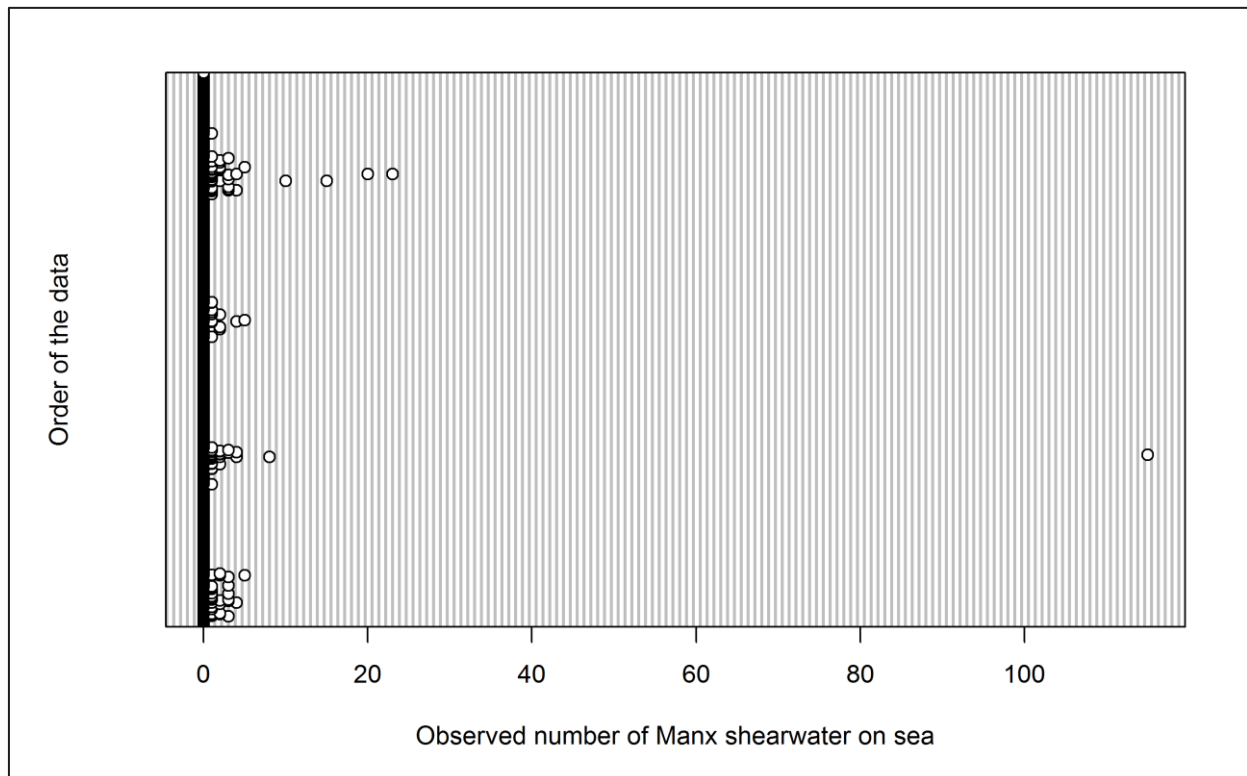


**Figure 2.61: Dot plot of the number of Manx shearwaters observed on sea per analysis block across operational years one to four.**

Group size for Manx shearwaters recorded on the sea ranged from single individuals up to 120 birds. Mean density of Manx shearwaters on the sea was largest during operational years two and four (Figure 2.62). However, since further modelling was not undertaken, the significance of any differences could not be tested. Figure 2.63 shows that Manx shearwaters on the sea were only present during the summer months, peaking in July.

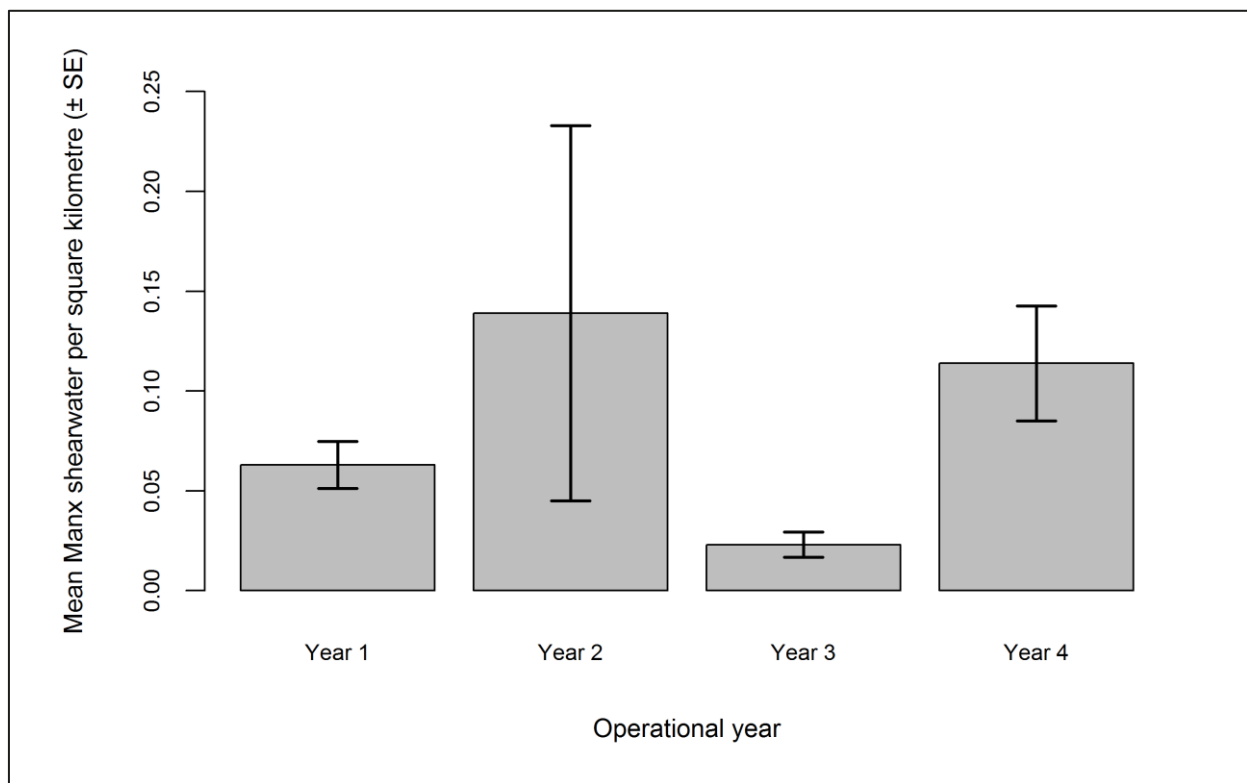


Figure 2.62: Mean density ( $\pm$  se) of Manx shearwaters recorded on the sea across operational years one to four.

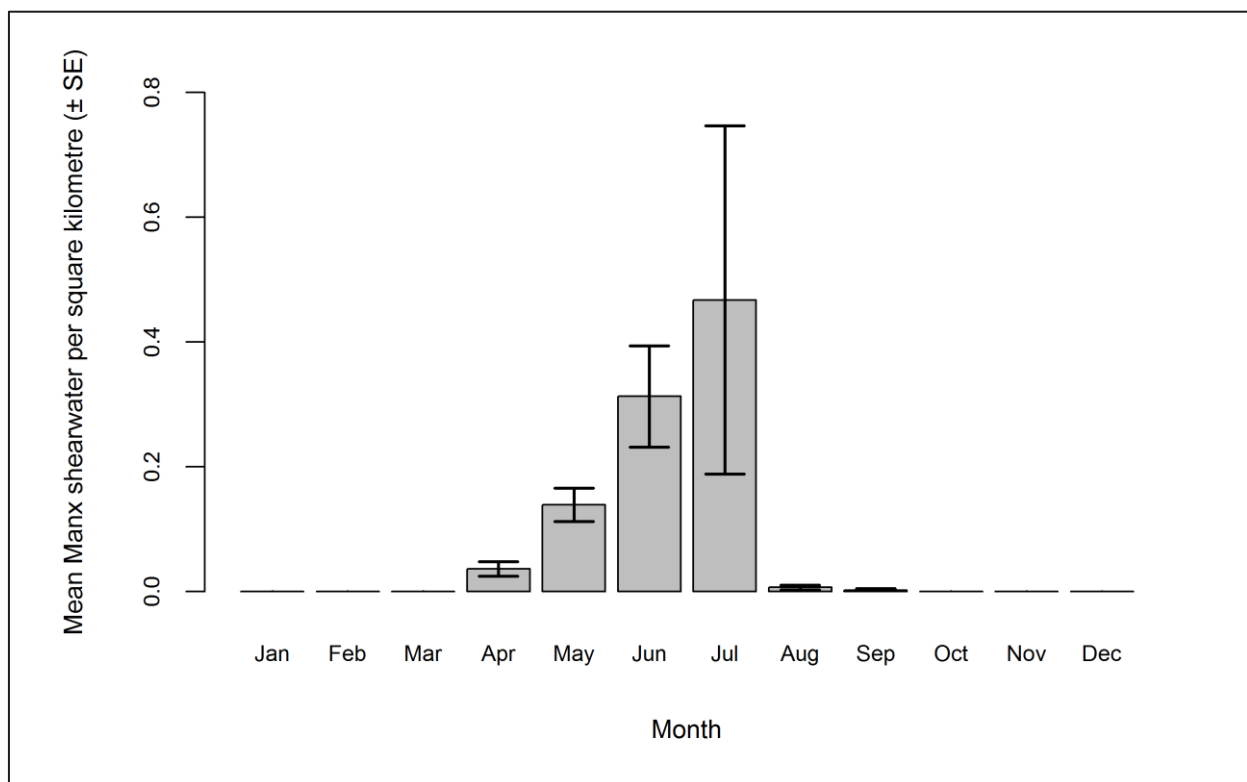


Figure 2.63: Mean density ( $\pm$  se) of Manx shearwaters recorded on the sea during each month across operational years one to four.

#### 2.4.4.6.16.2. In flight

Initial data exploration highlighted a single outlier (an analysis block containing 27 birds recorded in June 2013; Figure 2.64). Modelling was undertaken with and without this datum and the outputs compared.

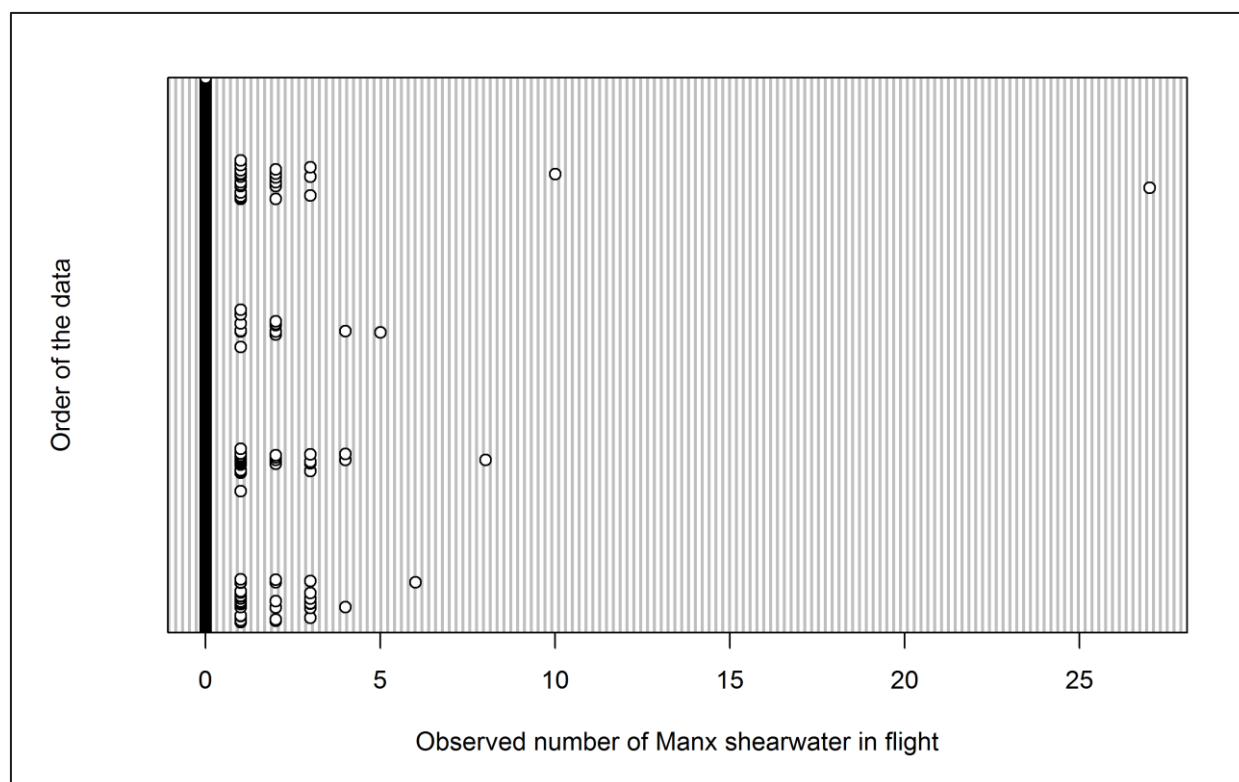


Figure 2.64: Dot plot of the number of Manx shearwaters observed in flight per analysis block across operational years one to four.

The initial model including the outlier did not converge correctly. Therefore, the outputs from the model excluding the outlier are presented. The GEE predicted that month and location have a statistically significant influence on Manx shearwater abundance within the survey area (Table 2.37). Specifically, larger numbers of flying Manx shearwaters were predicted during the months of June and July (Figure 2.66). Although not statistically significant, higher numbers of flying Manx shearwaters were predicted during operational year four in comparison to the other operational years (Figure 2.65). The interaction between operational year (phase) and location was statistically significant. Since June was the month of peak activity, model predictions were made for this month.

Table 2.37: Final model outputs for Manx shearwaters in flight across operational years one to four.

Term	Marginal p-value
Month	0.0001
Phase	0.8268
Tide height	0.4776
Location (X,Y)	0.0002
Interaction (location: phase)	<0.0001



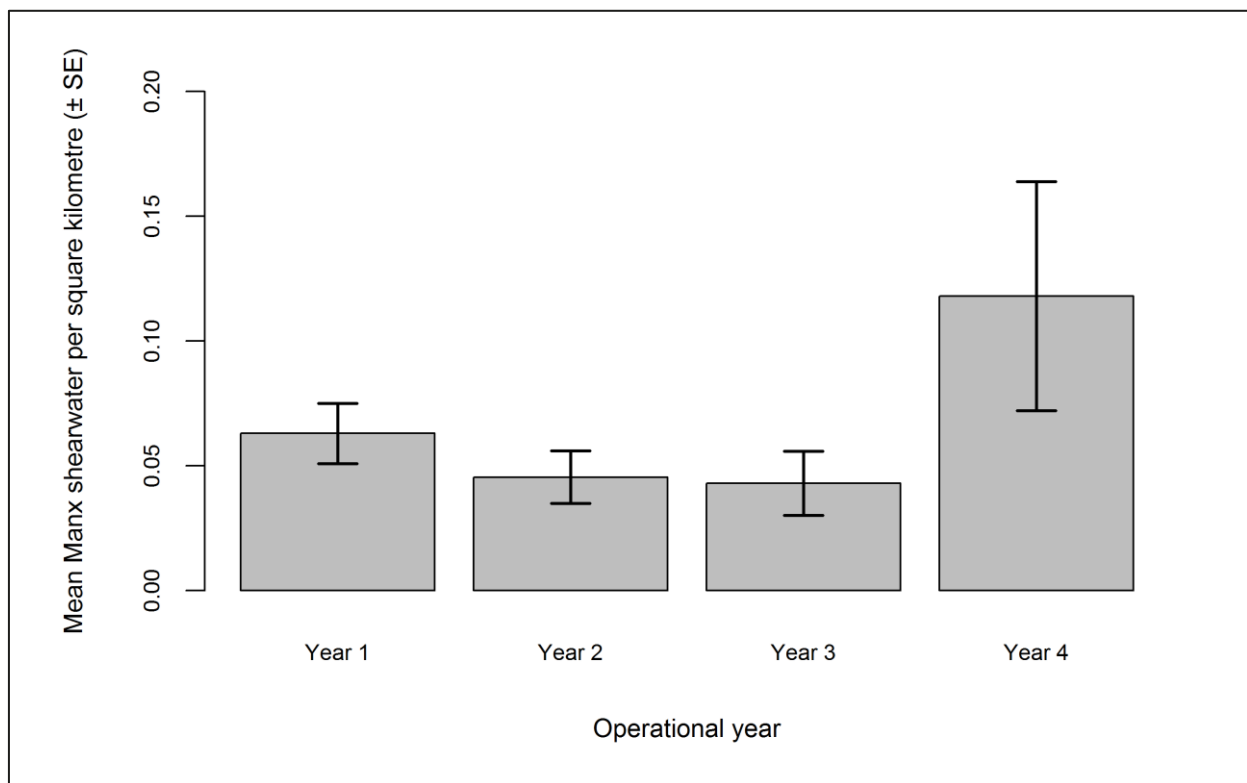


Figure 2.65: Mean density ( $\pm$  se) of Manx shearwaters recorded in flight across operational years one to four.

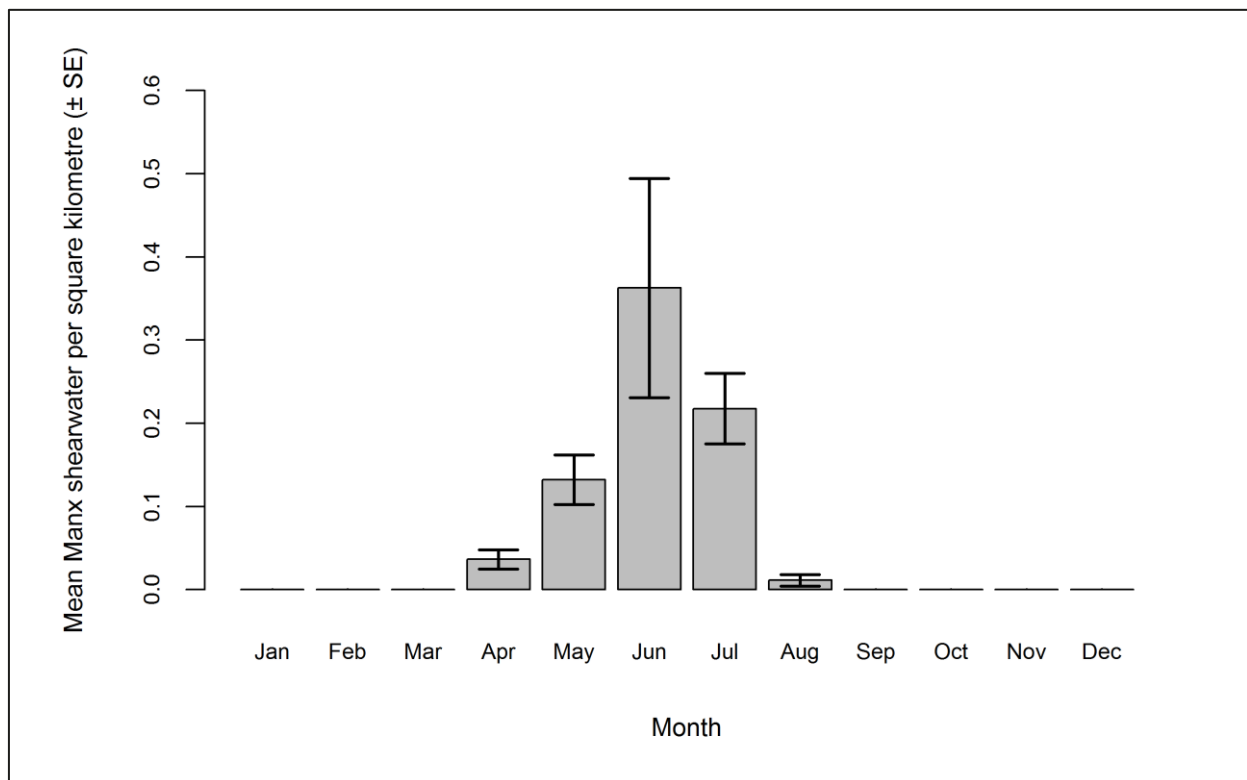


Figure 2.66: Mean density ( $\pm$  se) of Manx shearwaters recorded in flight across operational years one to four.


The abundance and densities (by site, buffer and total survey area) are presented in Table 2.38. The lowest total abundance is predicted for operational year two. However, the overall trend appears to be an increase in the number of flying Manx shearwaters, both across the survey area and within the Robin Rigg OWF site itself (Table 2.38).


**Table 2.38: Abundance and density of Manx shearwaters in flight across operational years one to four. Values in parentheses represent upper and lower 95% confidence intervals.**

Operational year	Abundance			Density			% within site
	Site	Buffer	Total	Site	Buffer	Total	
<b>1</b>	6 (1-26)	96 (18-534)	102 (19-560)	0.44 (0.09-2.02)	0.28 (0.05-1.54)	0.28 (0.05-1.55)	5.63
<b>2</b>	2 (0-17)	44 (7-324)	46 (7-341)	0.15 (0.02-1.34)	0.13 (0.02-0.93)	0.13 (0.02-0.95)	4.22
<b>3</b>	22 (2-233)	224 (23-2,349)	245 (25-2,582)	1.66 (0.12-18.00)	0.64 (0.07-6.75)	0.68 (0.07-7.16)	8.78
<b>4</b>	52 (4-703)	330 (34-3,661)	382 (38-4,364)	4.04 (0.28-54.33)	0.95 (0.10-10.52)	1.06 (0.10-12.10)	13.67


As shown in Table 2.38, predicted densities of Manx shearwaters increased during subsequent operational years, with the largest densities predicted in operational years three and four (Figure 2.67). Indeed, a statistically significant increase in Manx shearwater density was predicted to occur between operational years one and four in the centre of the survey area (Figure 2.68).


**Key**


 Study area



 Turbine area

**Predicted distribution**

 Low density (0.000 - 0.071 birds per grid square)

 Medium density (0.926 - 1.334 birds per grid square)

 High density (6.938 - 11.641 birds per grid square)

<p><b>Grid square = 1.2m<sup>2</sup></b></p>		
<p><b>Scale @ A3: 1:200,000</b></p> <p>Coordinate System: WGS 1984 UTM Zone 30N              NOT TO BE USED FOR NAVIGATION              © Crown Copyright and/or database rights. Reproduced by permission              of the Controller of Her Majesty's Stationary Office and the UK              Hydrographic Office (www.ukho.gov.uk). Licence no. 14228</p>		
<p>0      2.5      5      10 km</p> 		<p>N</p> 
Date: 27-08-14	Prepared by: EN	Checked by: SC
Ref: GB200351_M_372_A1		

93



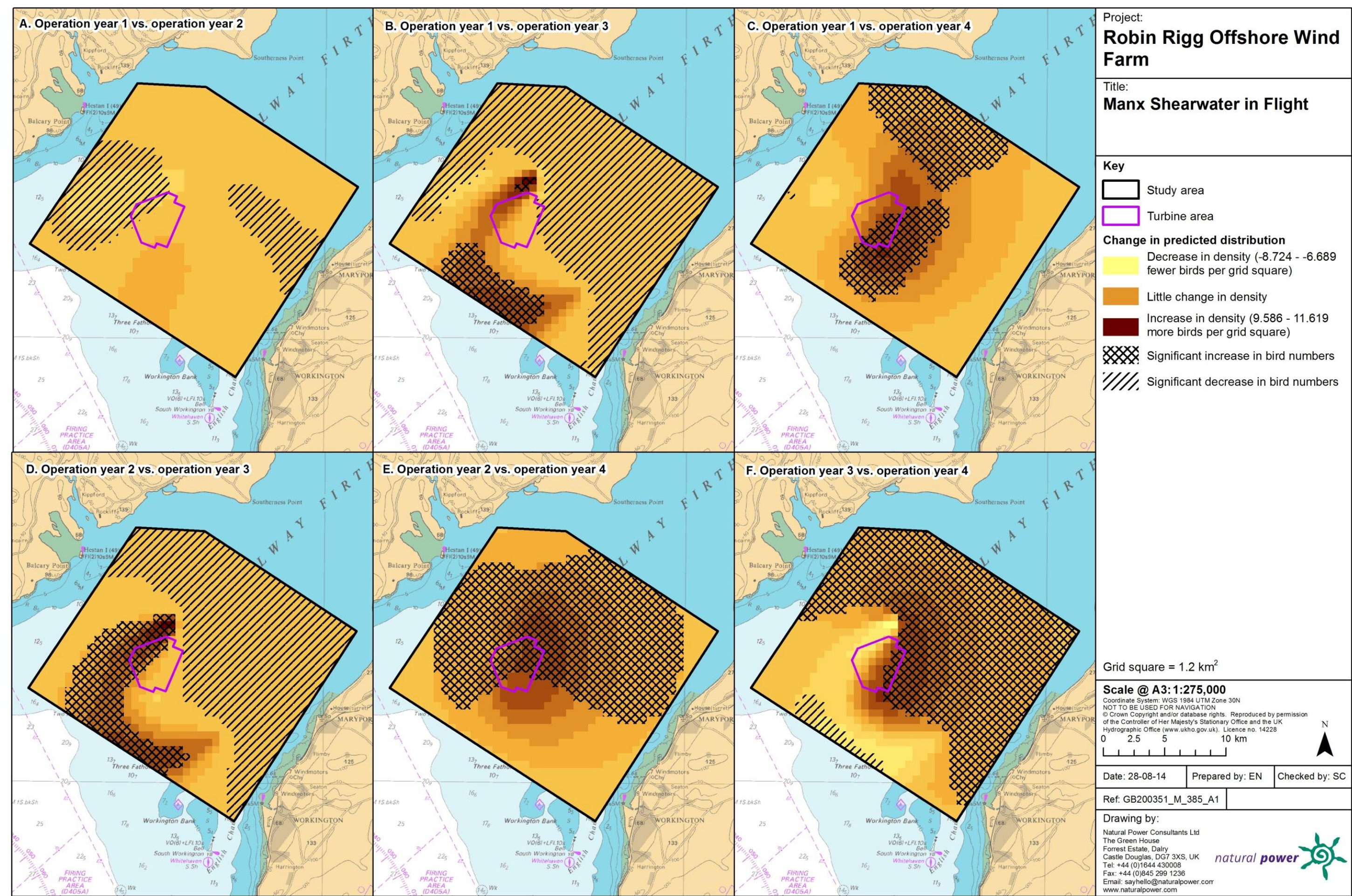


Figure 2.68: Differences in predicted flying Manx shearwater density between operational years. Significant differences are marked with diagonal shading.



#### 2.4.4.6.17. Collision risk

The percentage of Manx shearwaters recorded during the four operational years in different height bands relative to rotor swept height are shown in Table 2.39 and Figure 2.69. Whilst all Manx shearwaters were recorded flying close to the sea surface in operational years two and three, individuals were recorded in higher flight bands during the first and fourth operational years. Indeed, small numbers of Manx shearwaters were recorded up to and including rotor swept height during operational year four (Table 2.39). However, since birds were only recorded at rotor swept height during operational year four, a chi-squared test was not undertaken.

**Table 2.39: Percentage of Manx shearwaters recorded in different flight height bands across operational years one to four. Shaded column indicates percentage at rotor swept height (flight band 4).**

Operational year	Flight height band					
	1 (0–5 m)	2 (6–25 m)	3 (26–34 m)	4 (35–125 m)	5 (126–200 m)	6 (>200 m)
1	98.06	1.94	0.00	0.00	0.00	0.00
2	100.00	0.00	0.00	0.00	0.00	0.00
3	100.00	0.00	0.00	0.00	0.00	0.00
4	84.35	8.78	3.82	3.05	0.00	0.00

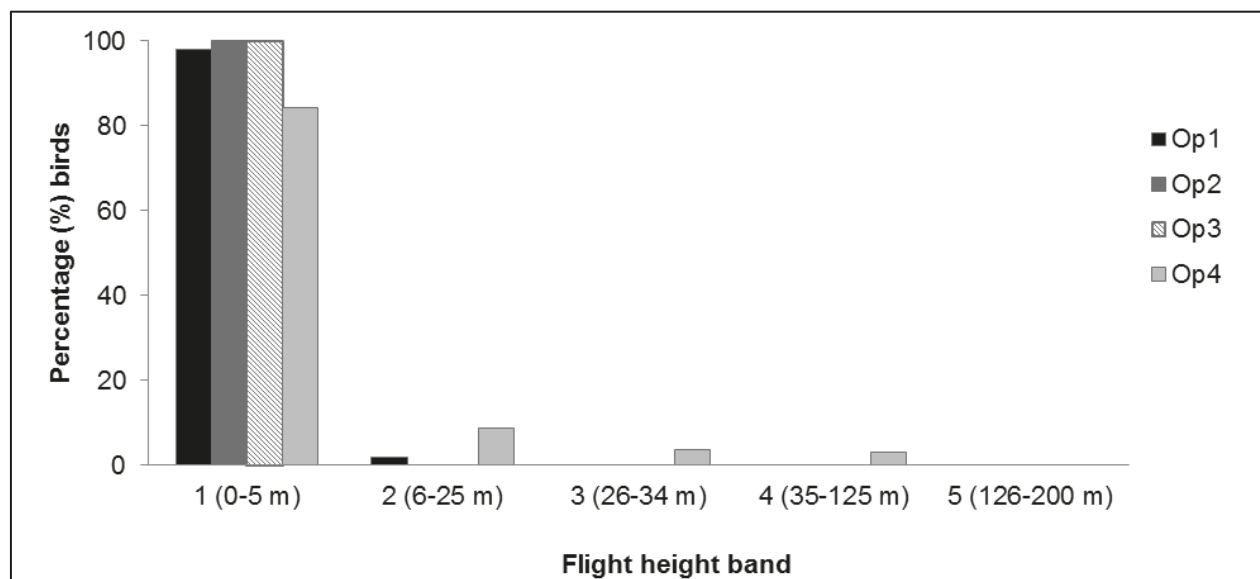


**Figure 2.69: Percentage of Manx shearwaters recorded in different flight height bands across operational years one to four.**



## 2.4.5. Cormorant

### 2.4.5.7. Across three development phases

#### 2.4.5.7.18. Summary statistics

Cormorants increased in number during the three development years (Table 2.40). More cormorants were observed during the winter months during and after construction of the wind farm. Approximately 40% of cormorants recorded during pre-construction surveys were in flight. This increased to 50% during the construction phase, before reducing back to 40% after construction (Table 2.40).

**Table 2.40: Number of cormorants recorded per block during each development phase per km survey effort (all data).**

	Pre-construction		Construction		Operation years 1-2	
	On sea	In flight	On sea	In flight	On sea	In flight
<b>Total number individuals</b>	260	191	1,659	1,636	1,053	1,191
<b>Total number sightings</b>	141	151	380	591	263	492
<b>Number individuals/km</b>	0.07	0.05	0.23	0.22	0.27	0.31
	Total		Total		Total	
<b>Total number individuals</b>	451		3,295		2,244	
<b>Total number sightings</b>	292		971		755	
<b>Number individuals/km</b>	0.13		0.45		0.58	

Data were filtered as described in the methods (Section 2.4.4). The percentage of segments without observations was calculated to ensure there were sufficient data to perform the analysis (Table 2.41). Data were also checked to ensure observations were recorded in all months of the year.

**Table 2.41: Percentage of cormorant analysis blocks without observations across the three development phases: pre-construction, construction and operational years one and two.**

	On sea	In flight
<b>Percentage zero blocks</b>	97.8%	97.6%

### 2.4.5.7.19. Density and distribution

#### 2.4.5.7.19.1. On sea

Initial data exploration highlighted several outliers that may influence the modelling process (Figure 2.70). The model was attempted with and without these large groups but in both cases the model would not converge. It may be possible to repeat the model using a binomial distribution to predict presence/absence rather than abundance. However, at the time of analysis the MRSea package was unable to accommodate binomial distributions. Therefore, further modelling work could not be undertaken and raw data are presented instead.

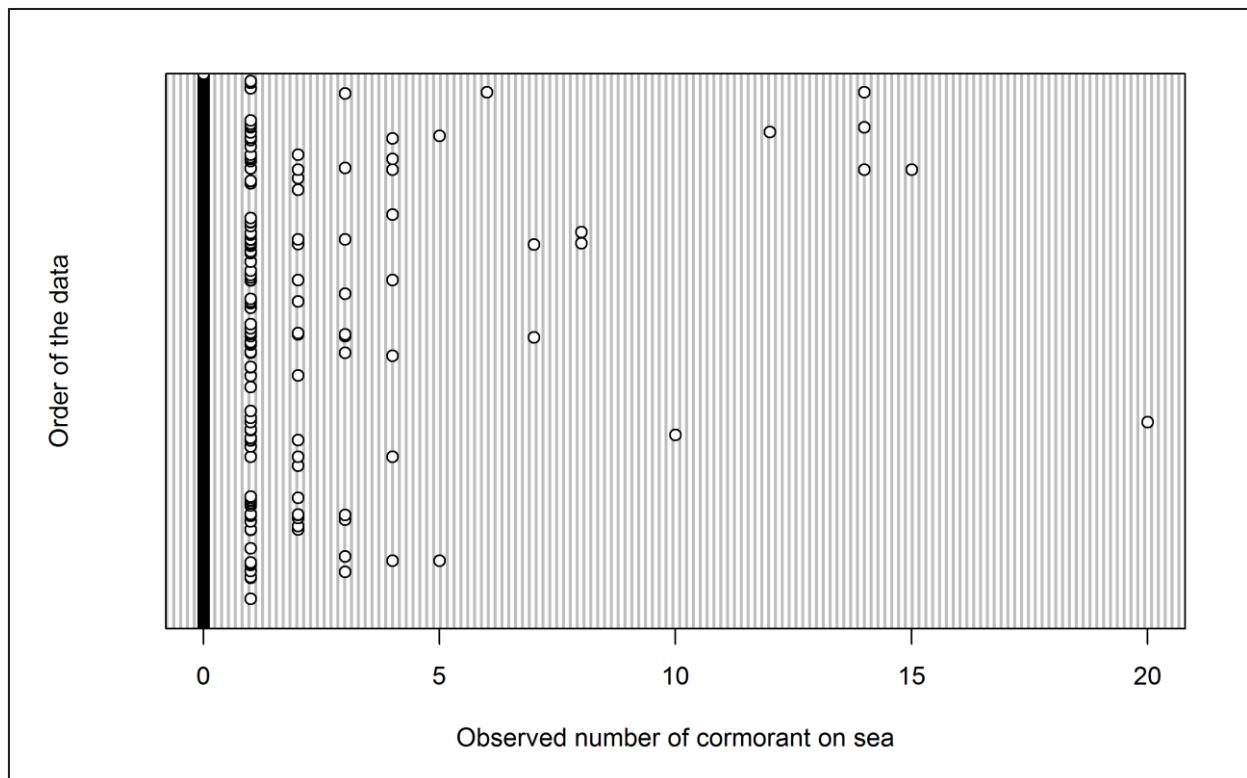


**Figure 2.70:** Dot plot of the number of cormorants observed on sea per analysis block across the three development phases: pre-construction, construction and operational years one and two.

Group size for cormorants recorded on the sea ranged from single individuals up to 20 birds. Mean density of cormorants indicates an increase during the operational phase in comparison to the other development phases (Figure 2.71). However, since further abundance modelling was not undertaken, the significance of any differences could not be tested. Figure 2.72 shows that the majority of cormorants on the sea across the three development phases were recorded in the summer months of July and August.

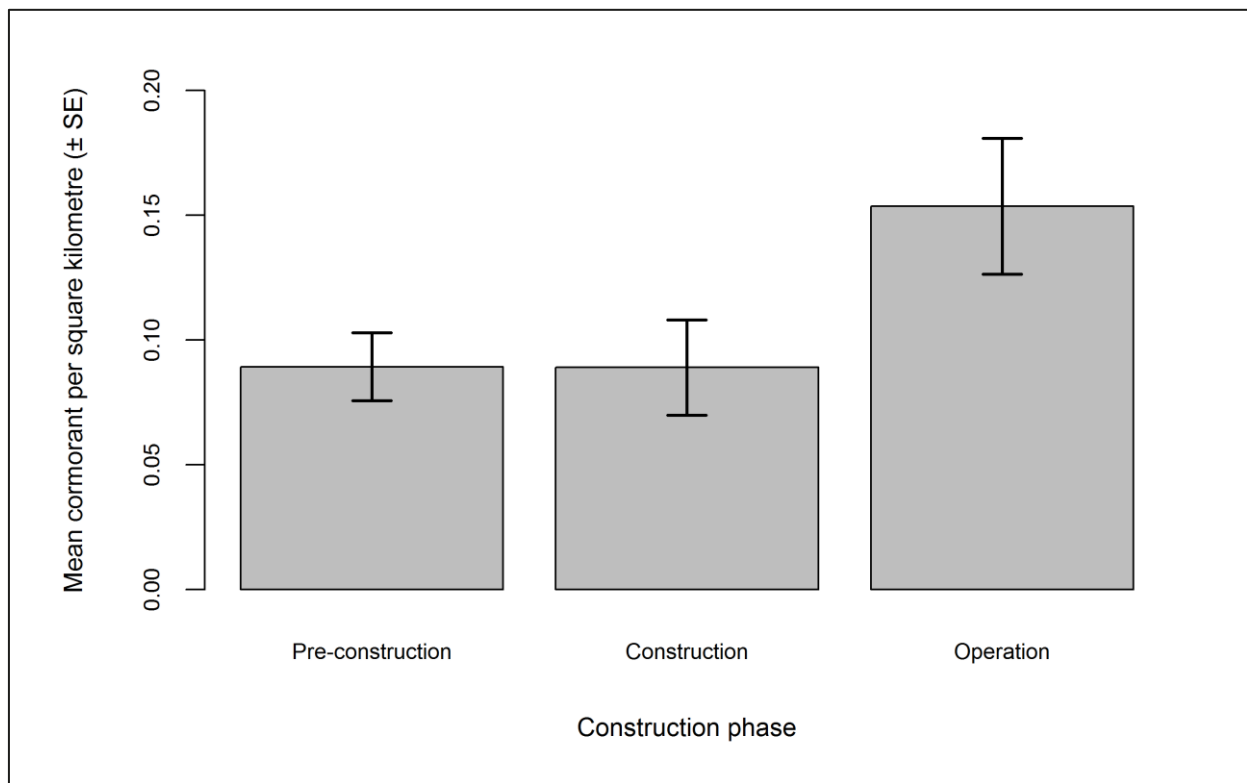


Figure 2.71: Mean density ( $\pm$  se) of cormorants recorded on the sea across the three development phases: pre-construction, construction and operational years one and two.

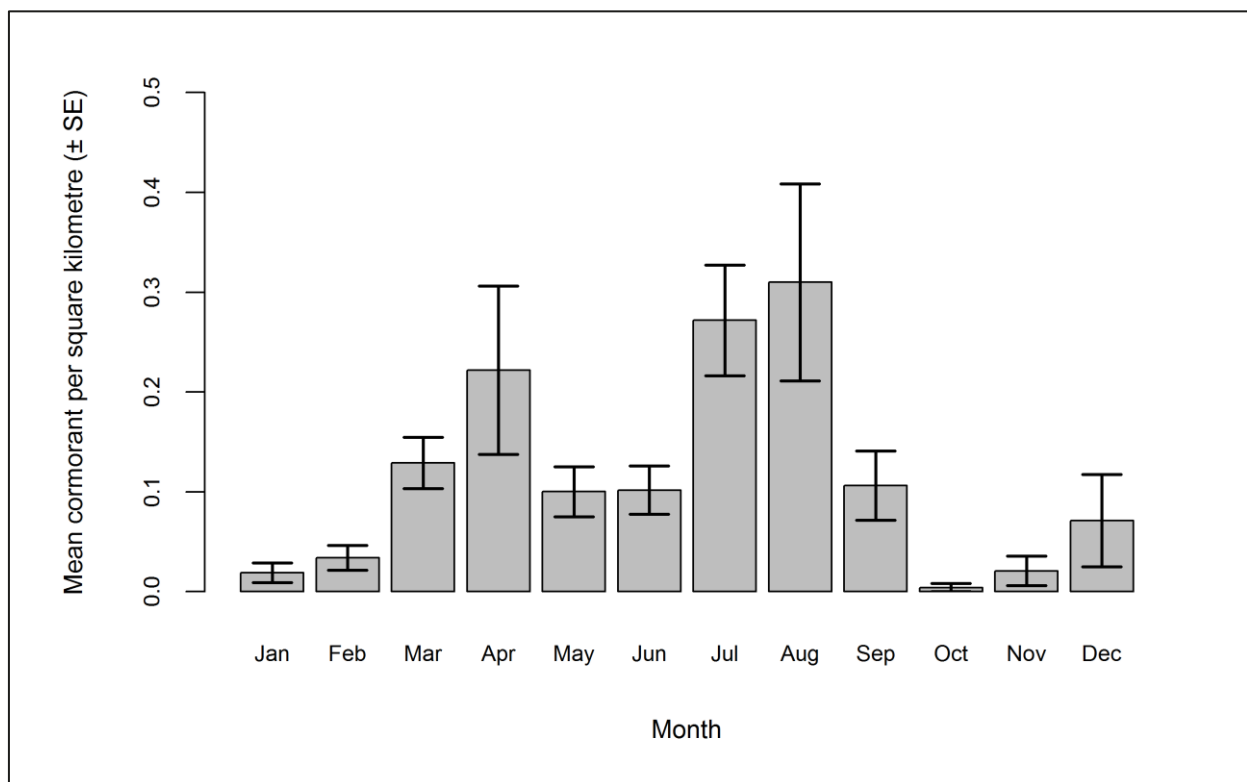


Figure 2.72: Mean density ( $\pm$  se) of cormorants recorded on the sea during each month across the three development phases: pre-construction, construction and operational years one and two.

### 2.4.5.7.19.2. In flight

Initial data exploration highlighted several outliers that may influence the modelling process (Figure 2.73). As a result the model was run with and without these data and the outputs compared.

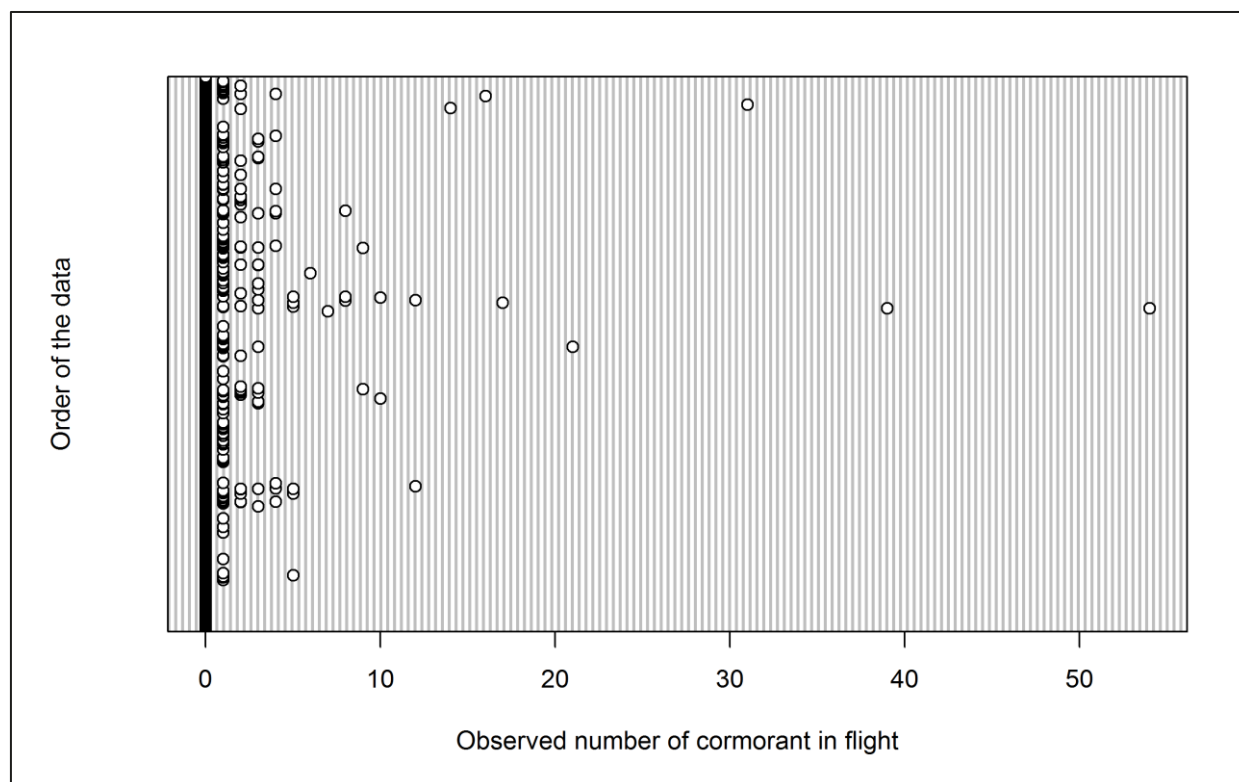


Figure 2.73: Dot plot of the number of cormorants observed in flight per analysis block across the three development phases: pre-construction, construction and operational years one and two.

The GEE predicted that all variables have a statistically significant influence on cormorant abundance within the survey area (Table 2.42). All p-values remained statistically significant after removing the outliers (data not shown) except the interaction between location and phase ( $p = 0.118$ ). Density surfaces for the models run with and without outliers were very similar. Therefore outputs from the model including the outliers are presented.

Larger mean densities were observed during the construction phase (Figure 2.74), and during the winter months of December and January (Figure 2.75). Since December was the month of peak activity, model predictions were made for this month.

Table 2.42: Final model outputs for cormorants in flight across the three development phases: pre-construction, construction and operational years one and two.

Term	Marginal p-value
Month	<0.0001
Phase	<0.0001
Tide height	0.0084
Location (X,Y)	<0.0001
Interaction (location: phase)	0.0004



Figure 2.74: Mean density ( $\pm$  se) of cormorants recorded in flight across the three development phases: pre-construction, construction and operational years one and two.

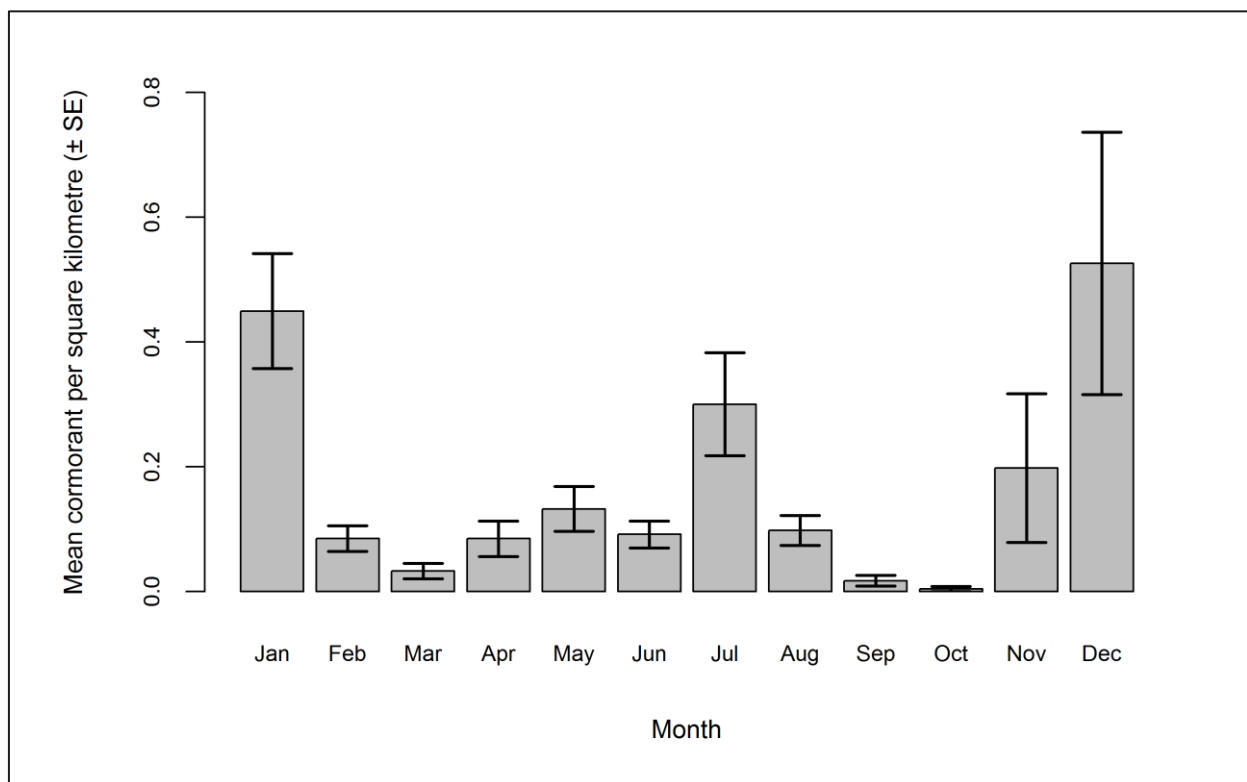


Figure 2.75: Mean density ( $\pm$  se) of cormorants recorded in flight during each month across the three development phases: pre-construction, construction and operational years one and two.



Abundance and density estimates for December (by site, buffer and total survey area) are presented in Table 2.43. In contrast to the mean density estimates (Figure 2.74), model predictions based upon median bootstrap estimates showed that total cormorant abundance was largest during the operational phase. However, the largest proportion of cormorants predicted within Robin Rigg OWF itself occurred during the construction phase, consistent with mean densities (Table 2.43).

**Table 2.43: Abundance and density of cormorants in flight across the three development phases: pre-construction, construction and operational years one and two. Values in parentheses represent upper and lower 95% confidence intervals.**

Phase	Abundance			Density			% within site
	Site	Buffer	Total	Site	Buffer	Total	
<b>Pre-construction</b>	0 (0-3)	24 (5-131)	24 (5-133)	0.01 (0-0.19)	0.07 (0.01-0.38)	0.07 (0.01-0.37)	0.65
<b>Construction</b>	8 (2-50)	194 (49-1,040)	202 (50-1,090)	0.59 (0.12-3.83)	0.56 (0.14-2.99)	0.56 (0.14-3.02)	3.77
<b>Operation</b>	7 (1-29)	360 (99-1,519)	367 (101-1,549)	0.53 (0.11-2.28)	1.04 (0.29-4.37)	1.02 (0.28-4.29)	1.87

Relatively small densities of cormorants in flight were predicted across the survey area during the pre-construction phase, with a statistically significant increase in density across subsequent phases (Figure 2.76). During construction, the largest cormorant densities were recorded in inshore waters to the east of Robin Rigg OWF (Figure 2.76). A distributional shift was predicted to occur between construction and operation, with the largest cormorant densities predicted to occur to the north of Robin Rigg OWF, close to the coast of Dumfries and Galloway (Figure 2.76).



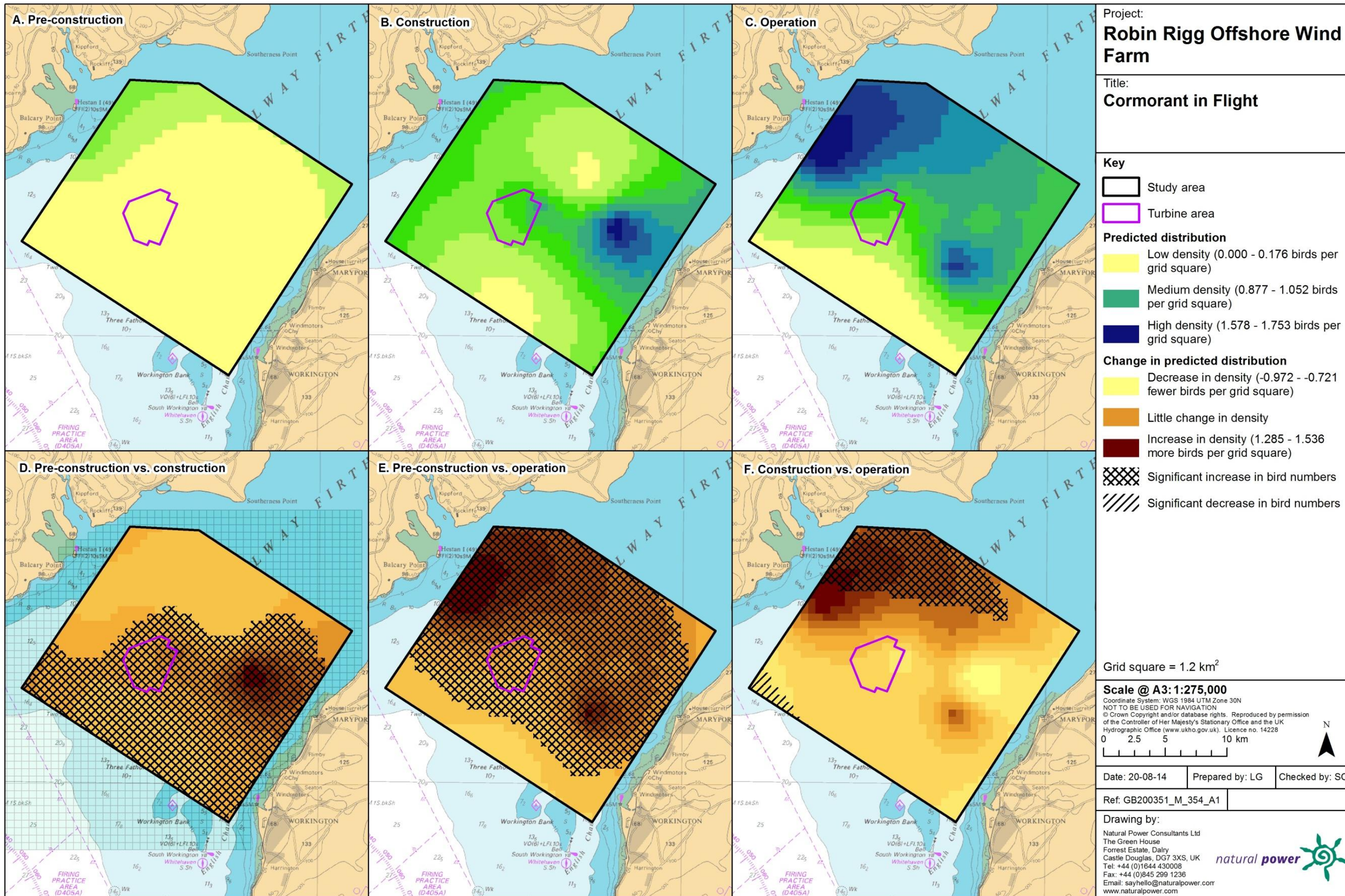


Figure 2.76: Predicted density of cormorants in flight during a) pre-construction, b) construction and c) operational monitoring. Changes in predicted density between d) pre-construction and construction, e) pre-construction and operation and f) construction and operation are also shown. Significant differences are marked with diagonal shading.



### 2.4.5.7.20. Collision risk

The percentage of cormorants recorded during the three development phases in different height bands relative to rotor swept height are shown in Table 2.44 and Figure 2.77. Since a relatively small percentage (<3%) of cormorants were recorded at rotor swept height, this species is not considered to be at risk from collision and a chi-squared test was not undertaken.

**Table 2.44:** Percentage of cormorants recorded in different flight height bands across the three development phases: pre-construction, construction and operational years one and two. Shaded column indicates percentage at rotor swept height (flight band 4).

Phase	Flight height band					
	1 (0–5 m)	2 (6–25 m)	3 (26–34 m)	4 (35–125 m)	5 (126–200 m)	6 (>200 m)
Pre-construction	74.87	24.61	0.52	0.00	0.00	0.00
Construction	67.24	30.43	1.35	0.98	0.00	0.00
Operation	68.01	23.43	5.63	2.94	0.00	0.00

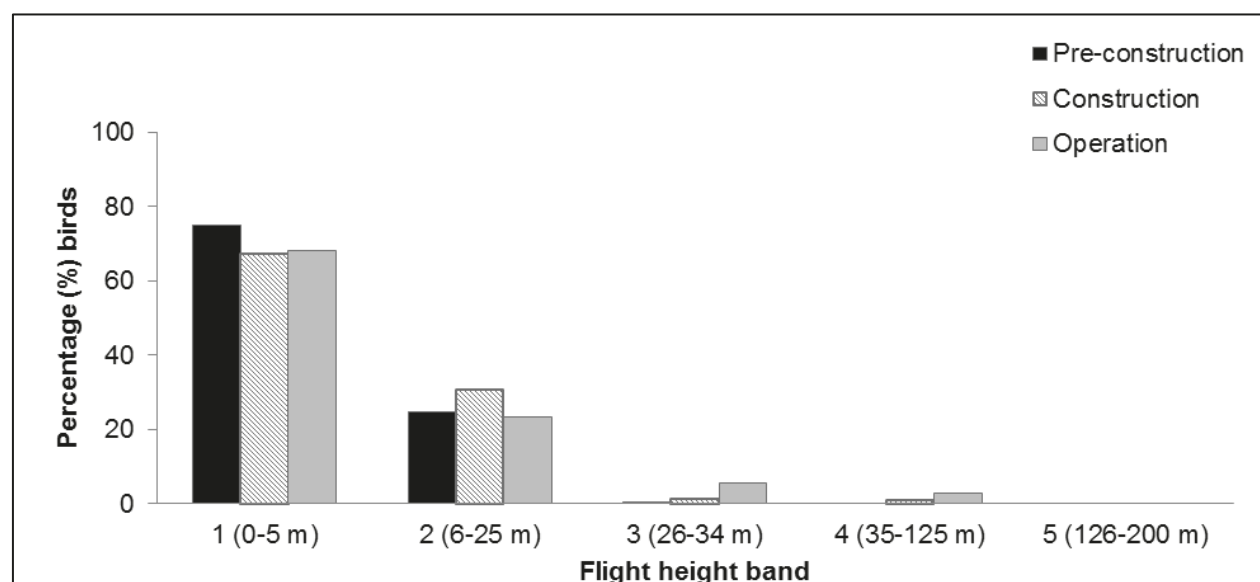


**Figure 2.77:** Percentage of cormorants recorded in different flight height bands across the three development phases: pre-construction, construction and operational years one and two.

## 2.4.5.8. Across operational years

### 2.4.5.8.21. Summary statistics

Cormorants numbers were similar during operational years one to three, but increased greatly in operational year four with nearly three times as many birds present (Table 2.45). This increase was largely due to an increase in the average group size of cormorants on the sea (c.17 birds per group in operational year four compared to c. 5 birds per group in operational year three; Table 2.45).

**Table 2.45: Number of cormorant recorded per block during each operational year per km survey effort (all data).**

	Operational year 1		Operational year 2		Operational year 3		Operational year 4	
	On sea	In flight	On sea	In flight	On sea	In flight	On sea	In flight
<b>Total number individuals</b>	525	694	528	497	856	590	2,830	1,390
<b>Total number sightings</b>	130	291	133	201	187	287	171	392
<b>Number individuals/km</b>	0.29	0.38	0.26	0.24	0.40	0.27	1.29	0.64
	Total		Total		Total		Total	
<b>Total number individuals</b>	1,219		1,025		1,446		4,220	
<b>Total number sightings</b>	421		334		474		563	
<b>Number individuals/km</b>	0.67		0.50		0.67		1.92	

Data were filtered as described in the methodology (Section 2.4.4). The percentage of segments without observations was calculated to ensure there were sufficient data to perform the analysis (Table 2.46). Data were also checked to ensure observations were recorded in all months of the year.

**Table 2.46: Percentage of cormorant analysis blocks without observations across operational years one to four. Zero inflation prior to removal of effort is presented in parentheses.**

	On sea	In flight
<b>Percentage zero blocks</b>	(97.5%) 97.0%	97.3%

## 2.4.5.8.22. Density and distribution

### 2.4.5.8.22.1. On sea

It was not possible to model a detection function on cormorant data for operational years. Initial data exploration highlighted two outliers of 550 and 950 birds recorded in February 2014. These observations which were both contained in analysis block 28 (Figure 2.78). Block 28 was therefore removed from the analysis but the model would not converge. It may be possible to repeat the model using a binomial distribution to predict presence/absence rather than abundance. However, at the time of analysis the MRSea package was unable to accommodate binomial distributions. Therefore, further modelling work could not be undertaken and raw data are presented instead.

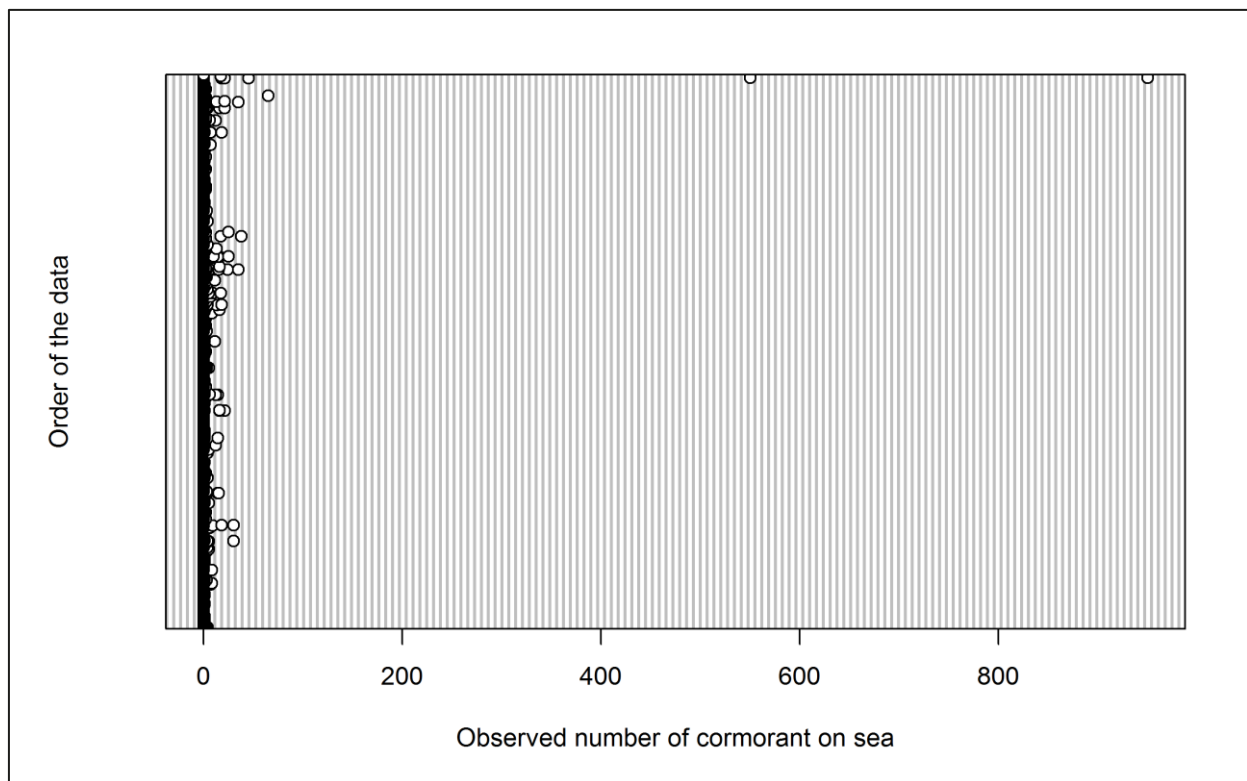


**Figure 2.78:** Dot plot of the number of cormorants observed on sea per analysis block across operational years one to four.

Mean density of cormorants on the sea shows a large increase during operational year four (Figure 2.79). However, since further abundance modelling was not undertaken, the significance of any differences could not be tested. Figure 2.80 shows that the majority of cormorants on the sea during operation were recorded in the winter months, with a peak in numbers during February.



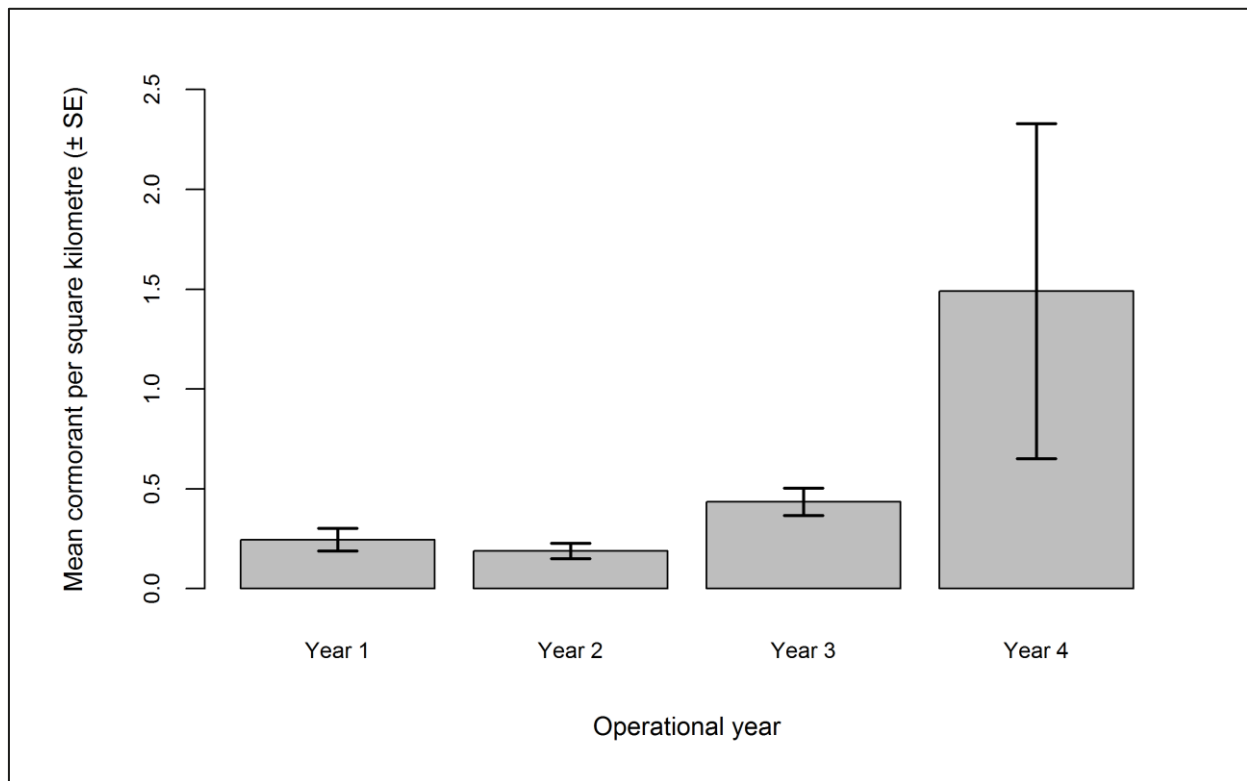


Figure 2.79: Mean density ( $\pm$  se) of cormorants recorded on the sea across operational years one to four.

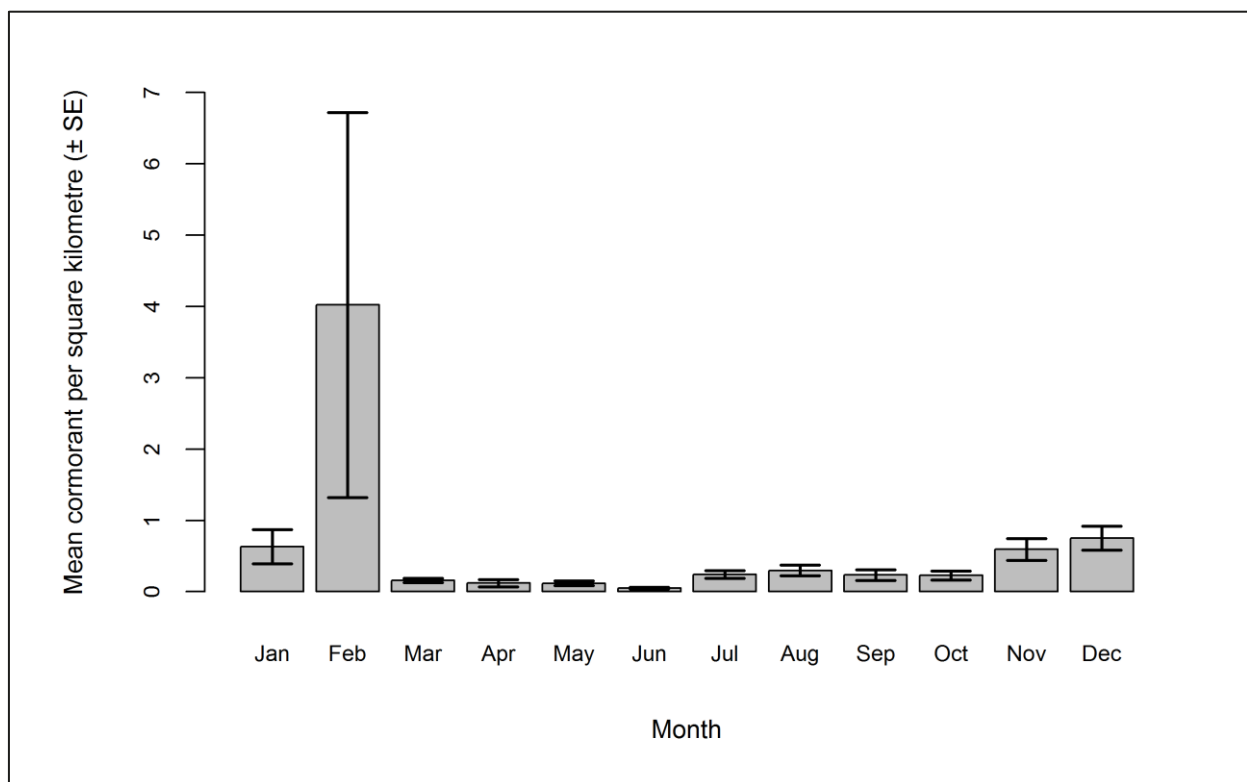


Figure 2.80: Mean density ( $\pm$  se) of cormorants recorded on the sea during each month across operational years one to four.

#### 2.4.5.8.22.2. In flight

Initial data exploration highlighted a group of 55 birds that may influence the modelling process (Figure 2.81). As a result the model was run with and without this datum and the outputs compared.

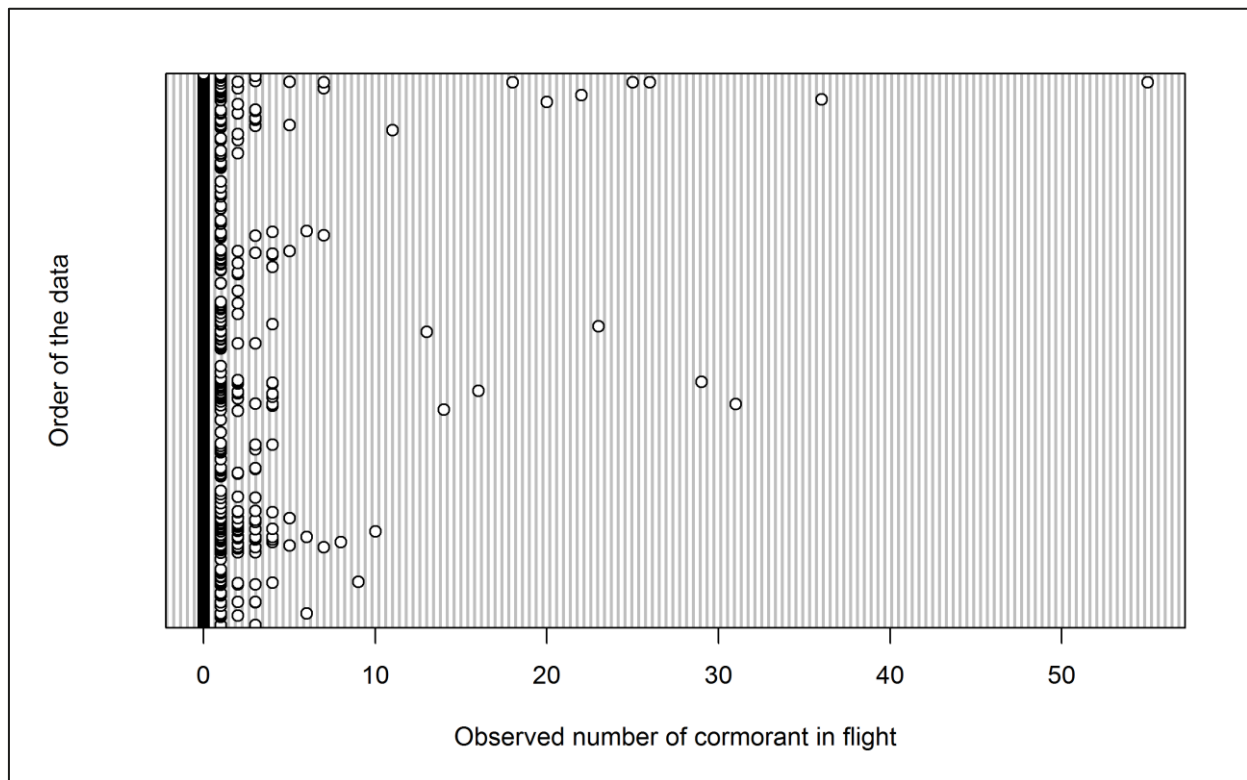


Figure 2.81: Dot plot of the number of cormorants observed in flight per analysis block across operational years one to four.

The GEE predicted that month and location have a statistically significant influence on cormorant abundance within the survey area (Table 2.47). Although operational year was not statistically significant on its own, a significant interaction was predicted between location and operational year (phase). Removal of the outlier from the model did not change the statistically significant of any of these variables. Specifically, larger numbers were predicted during the operational year four (Figure 2.82) and during February (Figure 2.83). Since February was the month of peak activity, abundance estimates was predicted for this month.

Table 2.47: Final model outputs for cormorants in flight across operational years one to four.

Term	Marginal p-value
Month	<0.0001
Phase	0.1271
Tide height	0.1335
Location (X,Y)	<0.0001
Interaction (location: phase)	<0.0001

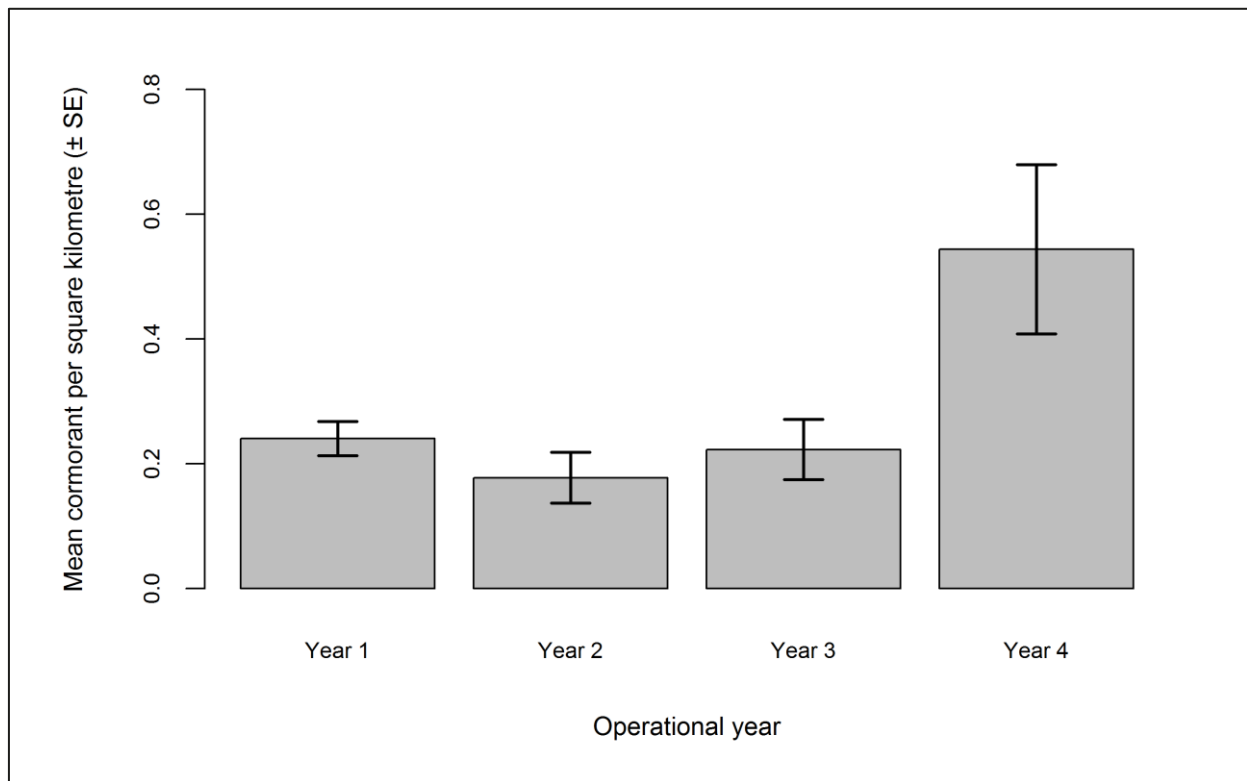


Figure 2.82: Mean density ( $\pm$  se) of cormorants recorded in flight across operational years one to four.

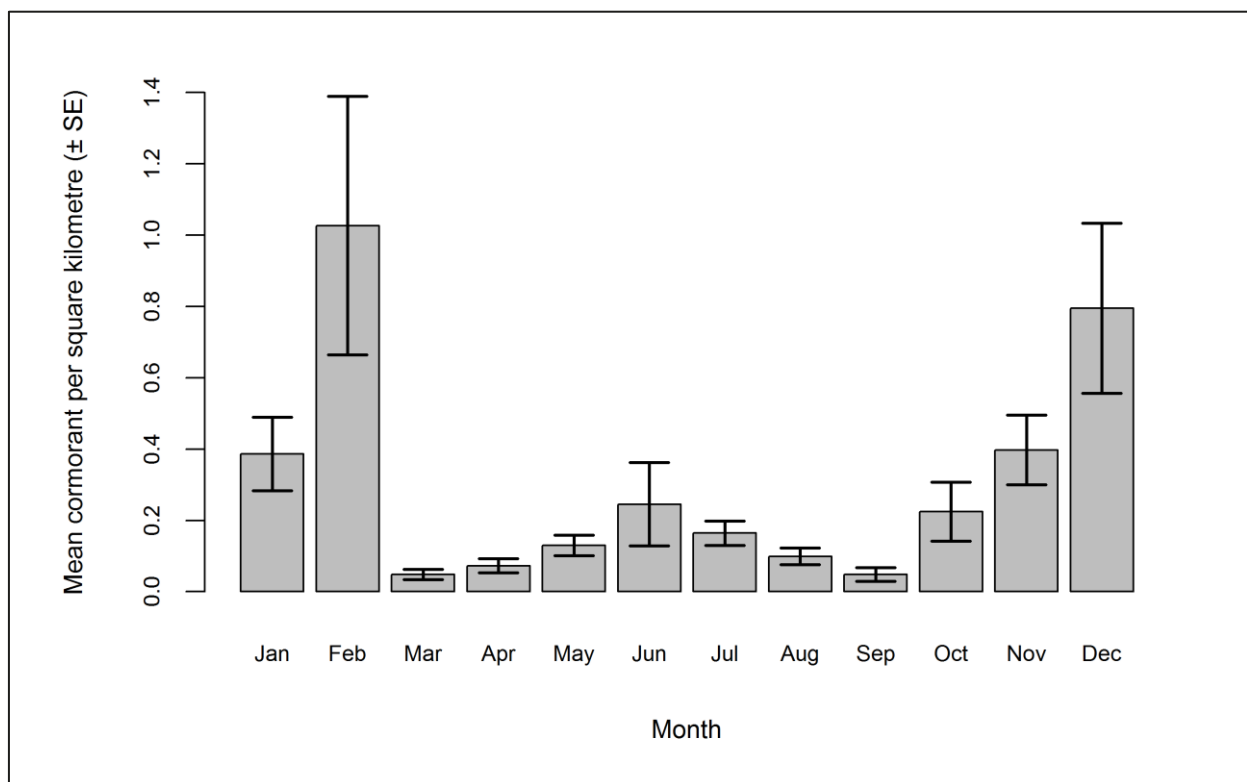


Figure 2.83: Mean density ( $\pm$  se) of cormorants recorded in flight during each month across operational years one to four.

The abundance and densities (by site, buffer and total survey area) are presented in Table 2.48. In contrast to mean density estimates (Figure 2.82), model predictions based upon median bootstrap estimates showed that the largest total abundance of cormorants was predicted for operational year one with a decline in predicted abundance across subsequent operational years. However, the proportion of cormorants within the Robin Rigg OWF itself remained similar across operational years (Table 2.48).

**Table 2.48: Abundance and density of cormorants in flight across operational years one to four. Values in parentheses represent upper and lower 95% confidence intervals.**

Operational years	Abundance			Density			% within site
	Site	Buffer	Total	Site	Buffer	Total	
<b>1</b>	16 (4-62)	564 (153-2,026)	580 (157-2,088)	1.26 (0.32-4.83)	1.62 (0.44-5.82)	1.61 (0.44-5.79)	2.82
<b>2</b>	5 (1-18)	181 (42-773)	186 (43-791)	0.36 (0.08-1.39)	0.52 (0.12-2.22)	0.51 (0.12-2.19)	2.50
<b>3</b>	6 (1-28)	248 (48-1,354)	254 (49-1,382)	0.46 (0.09-2.20)	0.71 (0.14-3.89)	0.70 (0.14-3.83)	2.35
<b>4</b>	7 (2-29)	233 (46-1,319)	240 (48-1,348)	0.54 (0.13-2.23)	0.67 (0.13-3.79)	0.67 (0.13-3.74)	2.92

As shown in Table 2.48, the largest densities of flying cormorants were predicted to occur during operational year one with a concentration predicted to the north of Robin Rigg OWF, close to the northern coast of the Solway Firth (Figure 2.84). This concentration declined significantly in subsequent operational years with similar, relatively small densities recorded during operational years two to four (Figure 2.85).



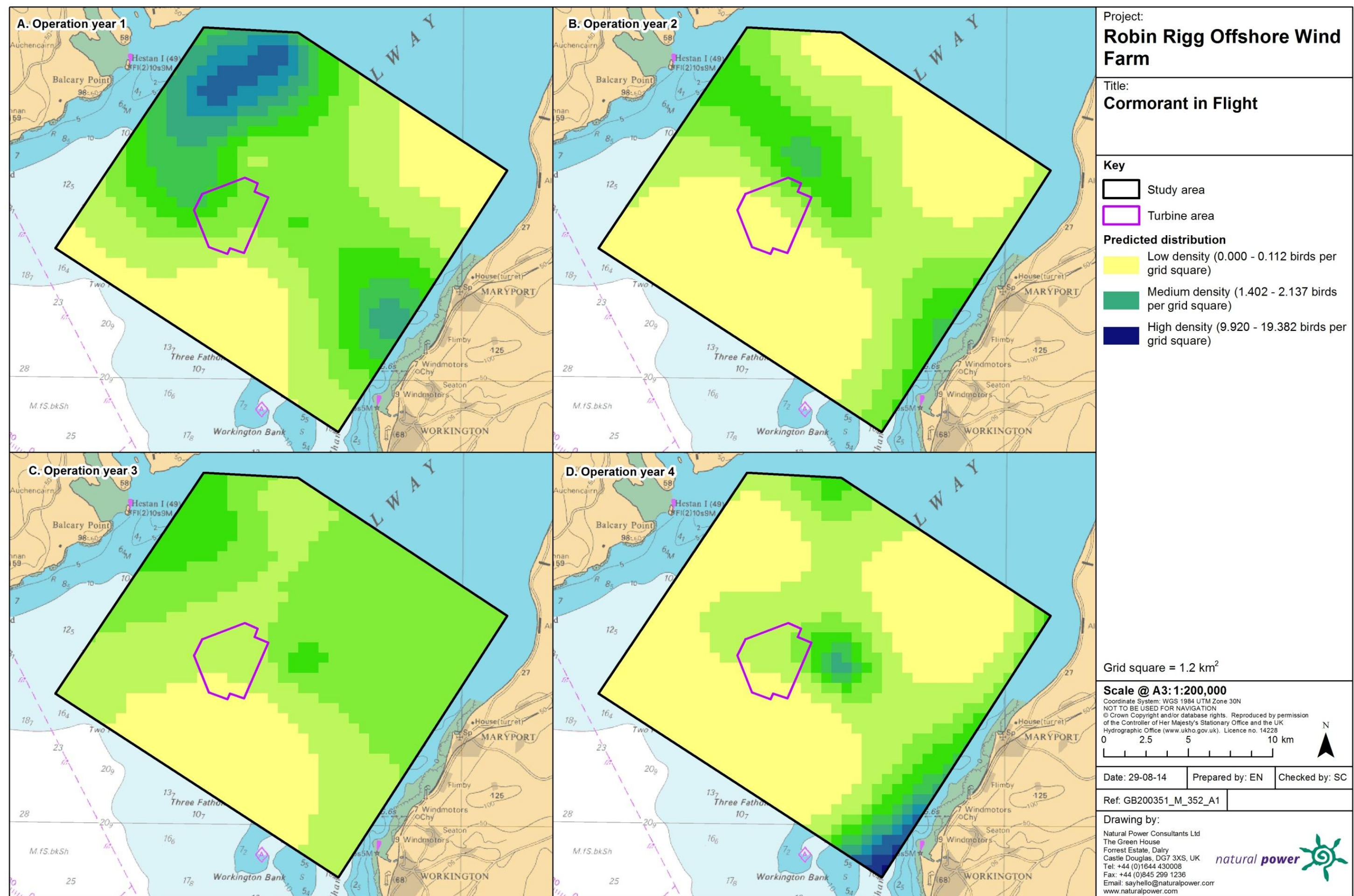


Figure 2.84: Predicted density of cormorants in flight during a) operational year one, b) operational year two, c) operational year three and d) operational year four.



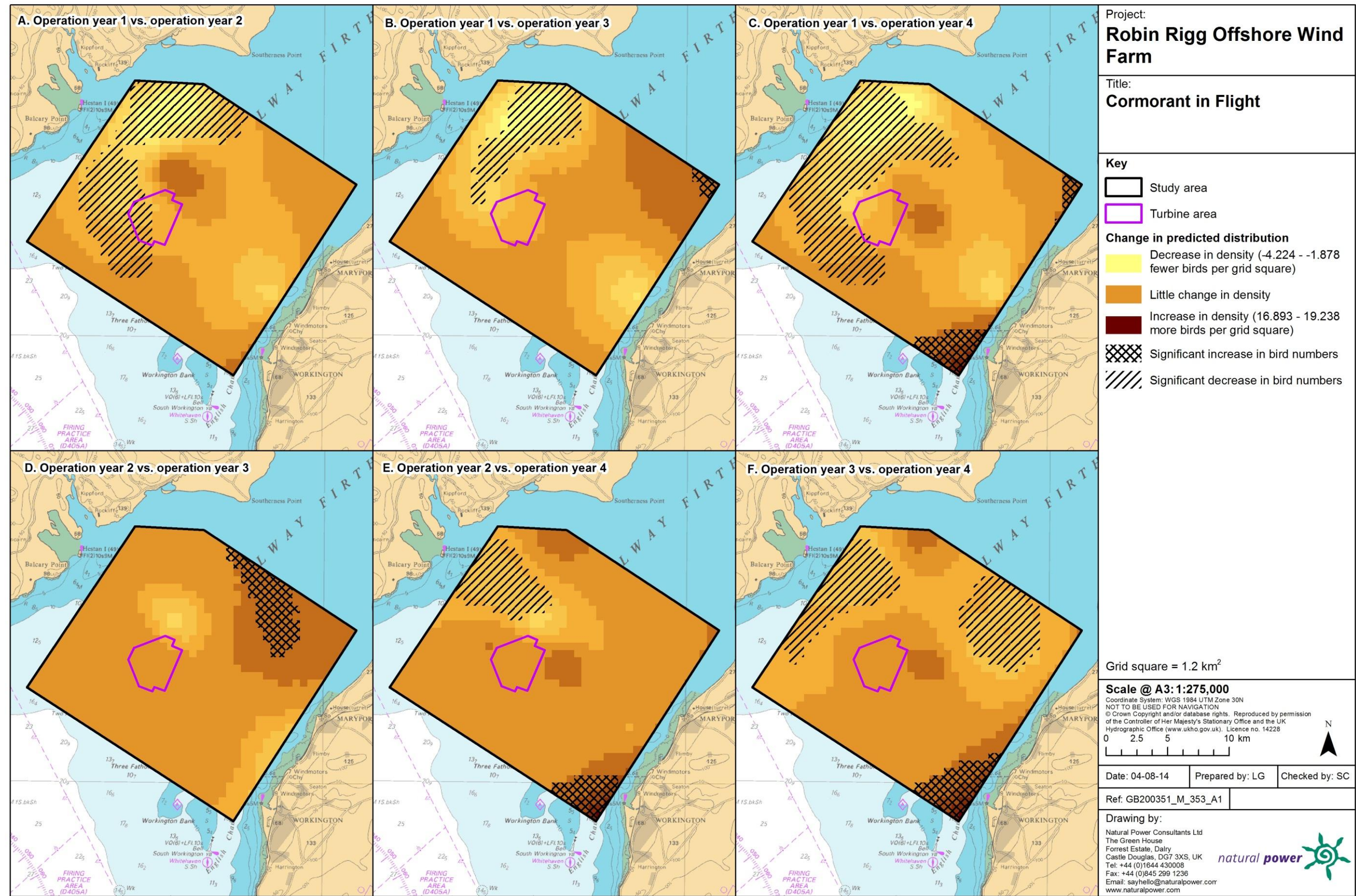


Figure 2.85: Differences in predicted flying cormorant density between operational years. Significant differences are marked with diagonal shading.



### 2.4.5.8.23. Collision risk

The percentage of cormorants recorded during the four operational years in different height bands relative to rotor swept height are shown in Table 2.49 and Figure 2.86. Data were combined for chi-squared analysis and a significant difference was found between flight bands ( $\chi^2 = 289$ ,  $df = 3$ ,  $p < 0.001$ ). Fewer cormorants than expected were observed flying at rotor swept height during operational years one to three; conversely, more cormorants were observed flying at rotor swept height during operational year four.

**Table 2.49: Percentage of cormorants recorded in different flight height bands across operational years one to four. Shaded column indicates percentage at rotor swept height (flight band 4).**

Operational year	Flight height band					
	1 (0–5 m)	2 (6–25 m)	3 (26–34 m)	4 (35–125 m)	5 (126–200 m)	6 (>200 m)
1	65.27	21.90	8.79	4.03	0.00	0.00
2	71.83	25.55	1.21	1.41	0.00	0.00
3	85.04	12.14	1.35	1.48	0.00	0.00
4	47.70	19.06	16.98	16.26	0.00	0.00

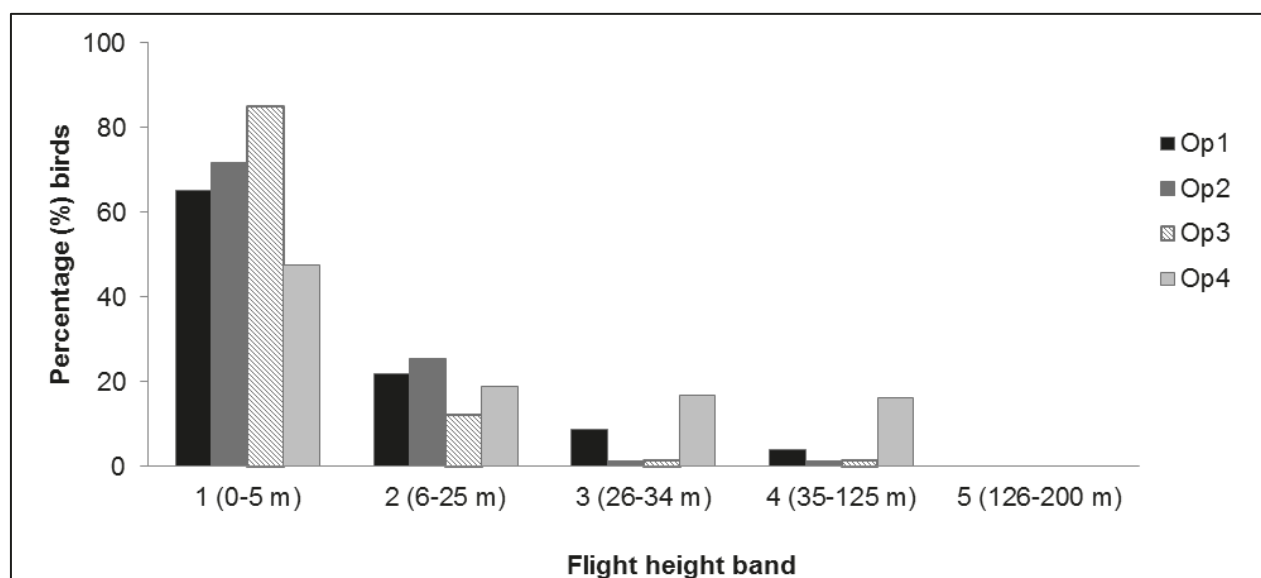


**Figure 2.86: Percentage of cormorants recorded in different flight height bands across operational years one to four.**

## 2.4.6. Gannet

### 2.4.6.9. Across three development phases

#### 2.4.6.9.24. Summary statistics

While the number of gannets on the sea recorded per km of effort appears to have remained relatively similar throughout the three development phases, the number recorded in flight decreased slightly during construction and the first two years of operation (Table 2.50). Overall, gannet numbers were largest during the construction phase (Table 2.50).

**Table 2.50: Number of gannets recorded per block during each development phase per km survey effort (all data).**

	Pre-construction		Construction		Operation years 1-2	
	On sea	In flight	On sea	In flight	On sea	In flight
<b>Total number individuals</b>	124	352	246	599	114	294
<b>Total number sightings</b>	77	235	152	431	86	216
<b>Number individuals/km</b>	0.03	0.10	0.03	0.08	0.03	0.08
	Total		Total		Total	
<b>Total number individuals</b>	476		845		408	
<b>Total number sightings</b>	312		583		302	
<b>Number individuals/km</b>	0.13		0.12		0.11	

Data were filtered as described in the methods (Section 2.4.4). The percentage of segments without observations was calculated to ensure there were sufficient data to perform the analysis (Table 2.51). Data were also checked to ensure observations were recorded in all months of the year.

**Table 2.51: Percentage of gannet analysis blocks without observations across the three development phases: pre-construction, construction and operational years one and two. Zero inflation prior to removal of effort is presented in parentheses.**

	On sea	In flight
<b>Percentage zero blocks</b>	99.0%	(98.3%) 95.6%

## 2.4.6.9.25. Density and distribution

### 2.4.6.9.25.1. On sea

Initial data exploration highlighted that 99% of analysis blocks for gannets on the sea contained zero observations (Figure 2.87). Since no birds were recorded between November and February, further removal of effort data was not possible. Therefore, further abundance modelling of gannets on the sea across the three development phases was not undertaken and raw data are presented.

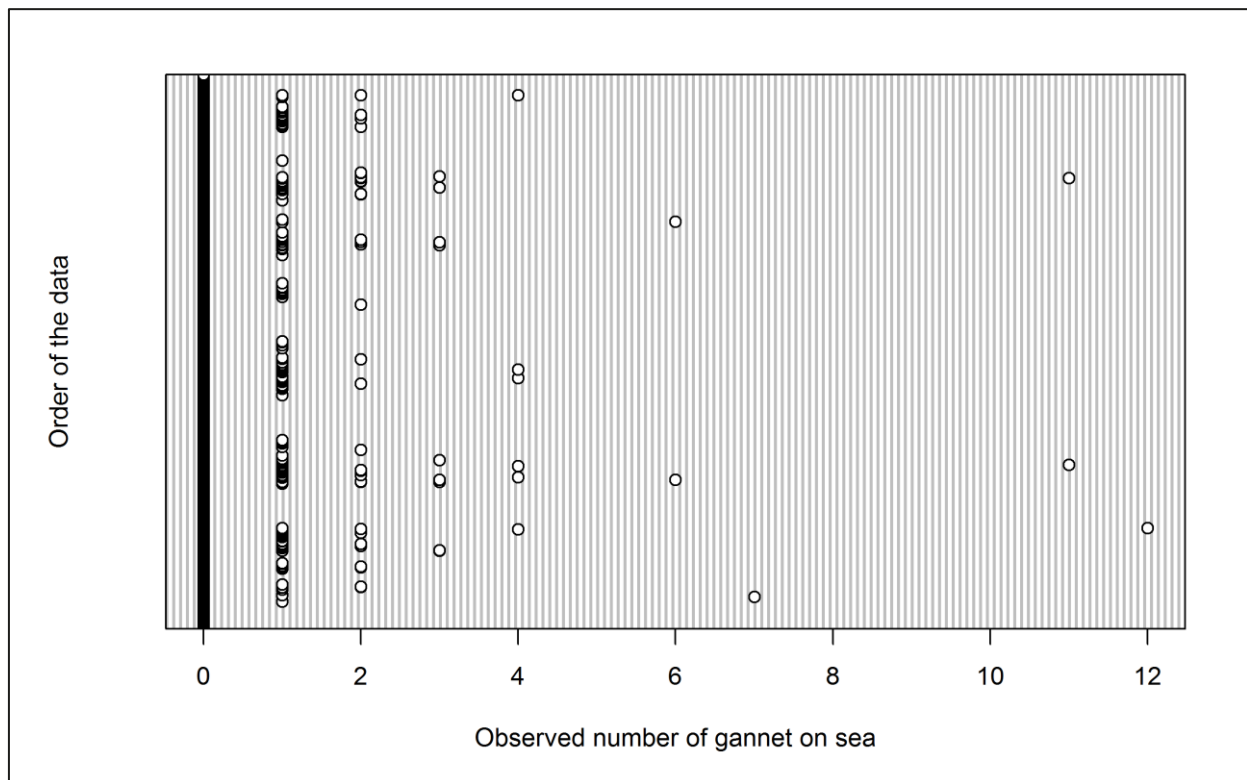


Figure 2.87: Dot plot of the number of gannets observed on sea per analysis block across the three development phases: pre-construction, construction and operational years one and two.

Group size for gannets recorded on the sea ranged from single individuals up to 12 birds (Figure 2.87). Mean density of gannets on the sea remained similar across development phases (Figure 2.88). Figure 2.89 shows that the majority of gannets on the sea across the three development phases were recorded during the months of April and October, peaking in July.



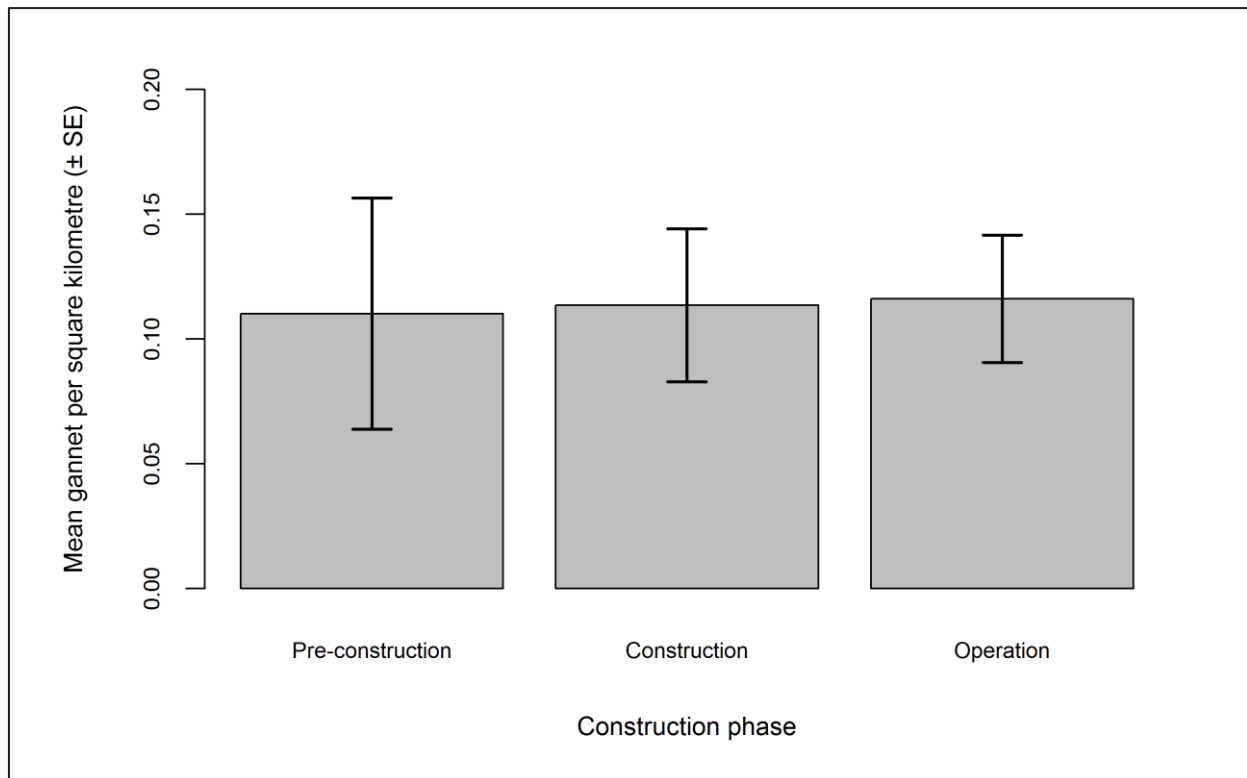


Figure 2.88: Mean density (± se) of gannets recorded on the sea across the three development phases: pre-construction, construction and operational years one and two.

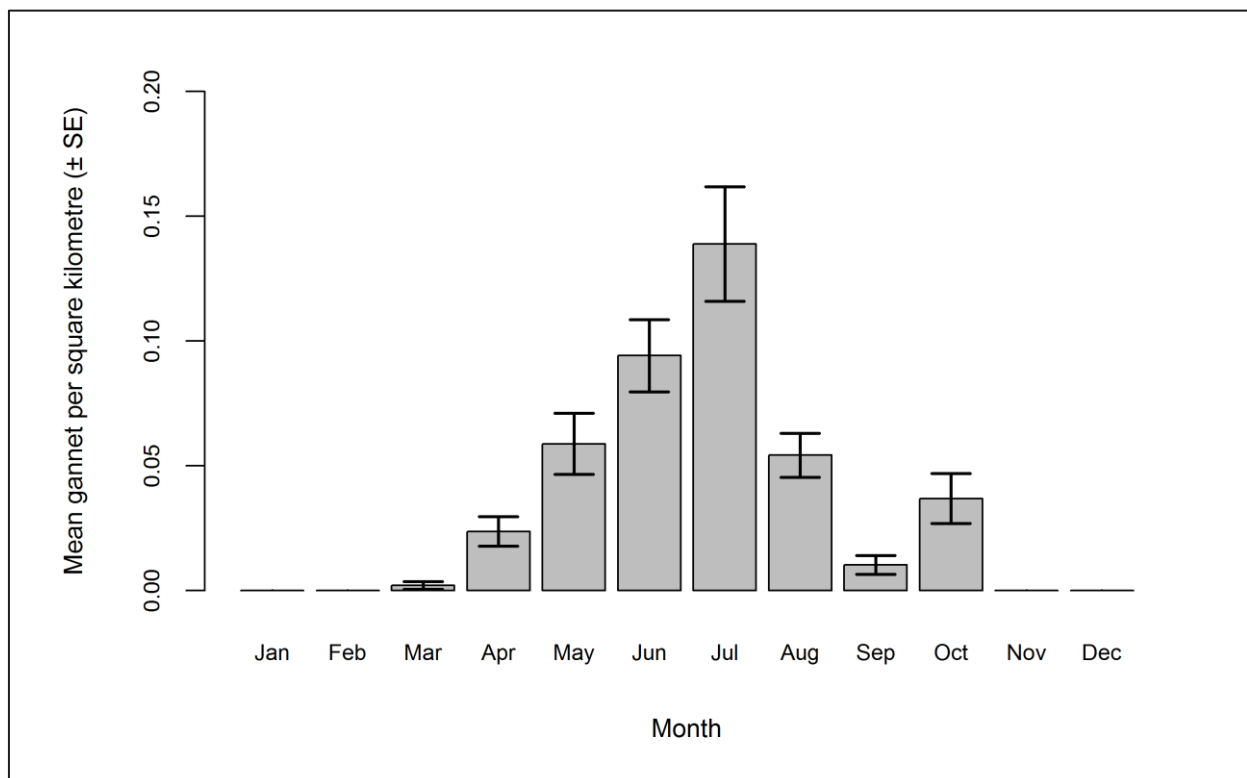


Figure 2.89: Mean density (± se) of gannets recorded on the sea during each month across the three development phases: pre-construction, construction and operational years one and two.

#### 2.4.6.9.25.2. In flight

Initial data exploration highlighted that gannets were not observed in all months of the year (Table 2.52). The model requires a response variable for all factor levels. As such, months without observations were removed prior to analysis. Initially, only survey effort collected in January and December was removed but the model would not converge. Therefore, the final dataset contained data collected between May and August.

**Table 2.52: Number of gannets available for analysis each month across the three development phases: pre-construction, construction and operational years one and two. Months highlighted in bold were used in the analysis.**

Month	Pre-Construction	Construction	Operation	Total
January	0	0	0	0
February	1	0	0	1
March	4	0	1	5
April	6	0	1	7
<b>May</b>	<b>4</b>	<b>23</b>	<b>14</b>	<b>41</b>
<b>June</b>	<b>2</b>	<b>30</b>	<b>14</b>	<b>46</b>
<b>July</b>	<b>45</b>	<b>32</b>	<b>47</b>	<b>124</b>
<b>August</b>	<b>6</b>	<b>4</b>	<b>8</b>	<b>18</b>
September	0	0	1	1
October	0	1	10	11
November	0	0	1	1
December	0	0	0	0

Data exploration of the final dataset highlighted two outliers (30 birds recorded in July 2007 and 15 in July 2010) that may have influenced the modelling process (Figure 2.90). These outliers may be a result of multiple sightings within the same analysis block. The model was run with and without these data and the outputs compared.

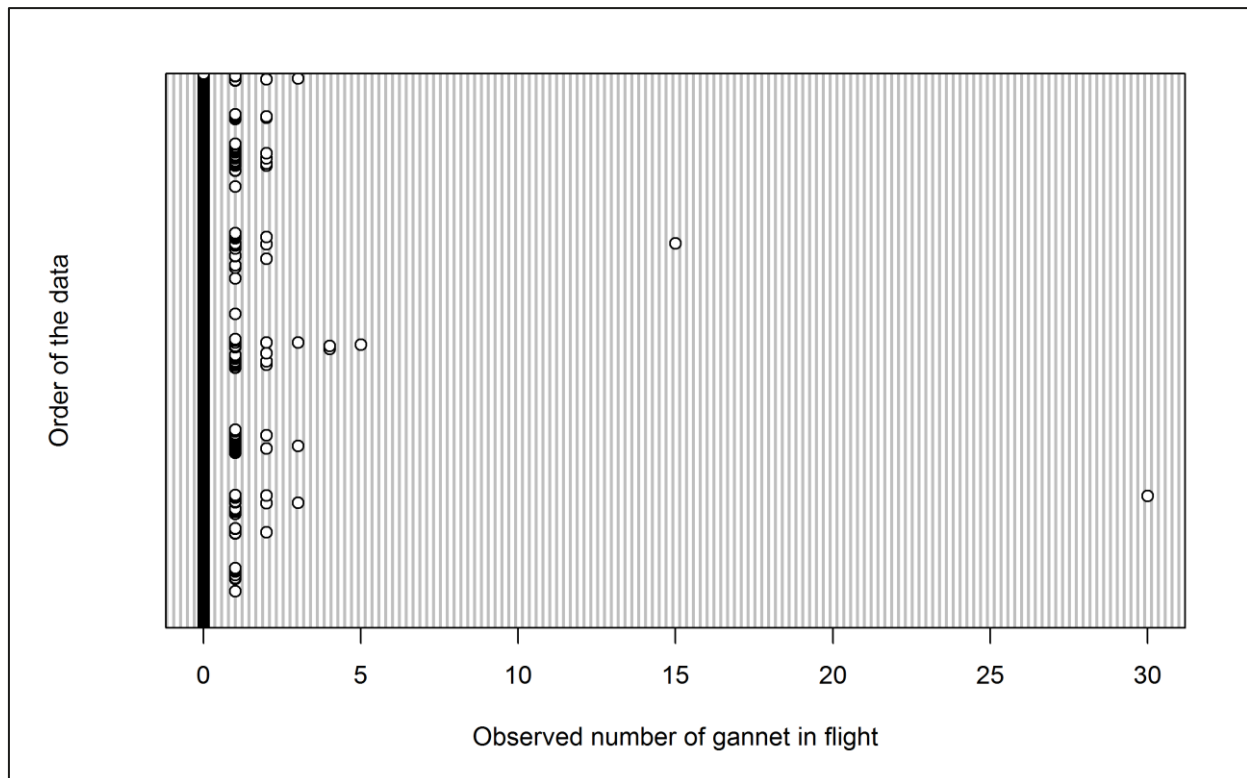


Figure 2.90: Dot plot of the number of gannets observed in flight per analysis block across the three development phases: pre-construction, construction and operational years one and two.

The initial GEE predicted that month and tide both have a statistically significant influence on gannet abundance within the survey area (Table 2.53). After removal of the two outliers, location was also statistically significant ( $p = 0.0005$ ). In both models, the interaction between phase and location was statistically significant.

Specifically, significantly smaller numbers of gannets were recorded in flight during the operational phase (Figure 2.91), and significantly high numbers were recorded during the month of July (Figure 2.92). Since July was the month of peak activity, model predictions were made for this month.

Table 2.53: Final model outputs for gannets in flight across the three development phases: pre-construction, construction and operational years one and two.

Term	Marginal p-value
Month	<0.0001
Phase	0.0443
Tide height	0.0018
Location (X,Y)	0.1977
Interaction (location: phase)	0.0026

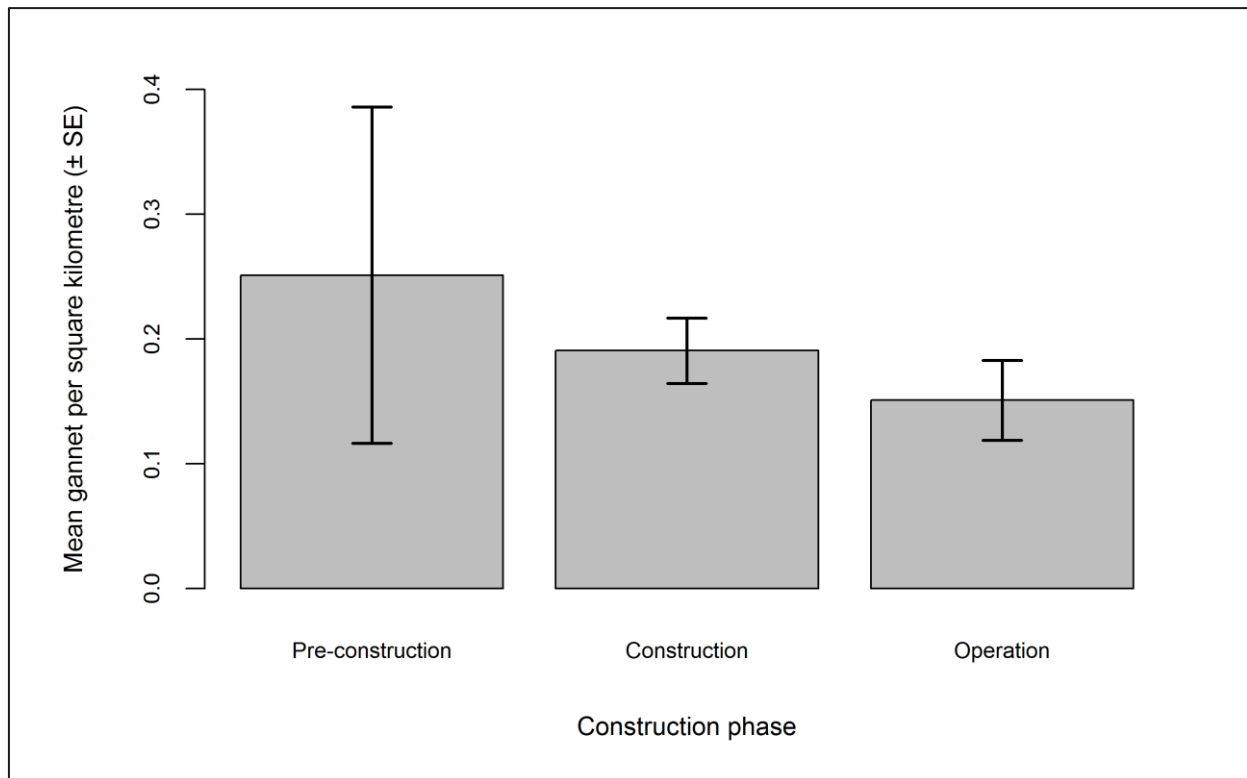


Figure 2.91: Mean density ( $\pm$  se) of gannets recorded in flight across the three development phases: pre-construction, construction and operational years one and two.

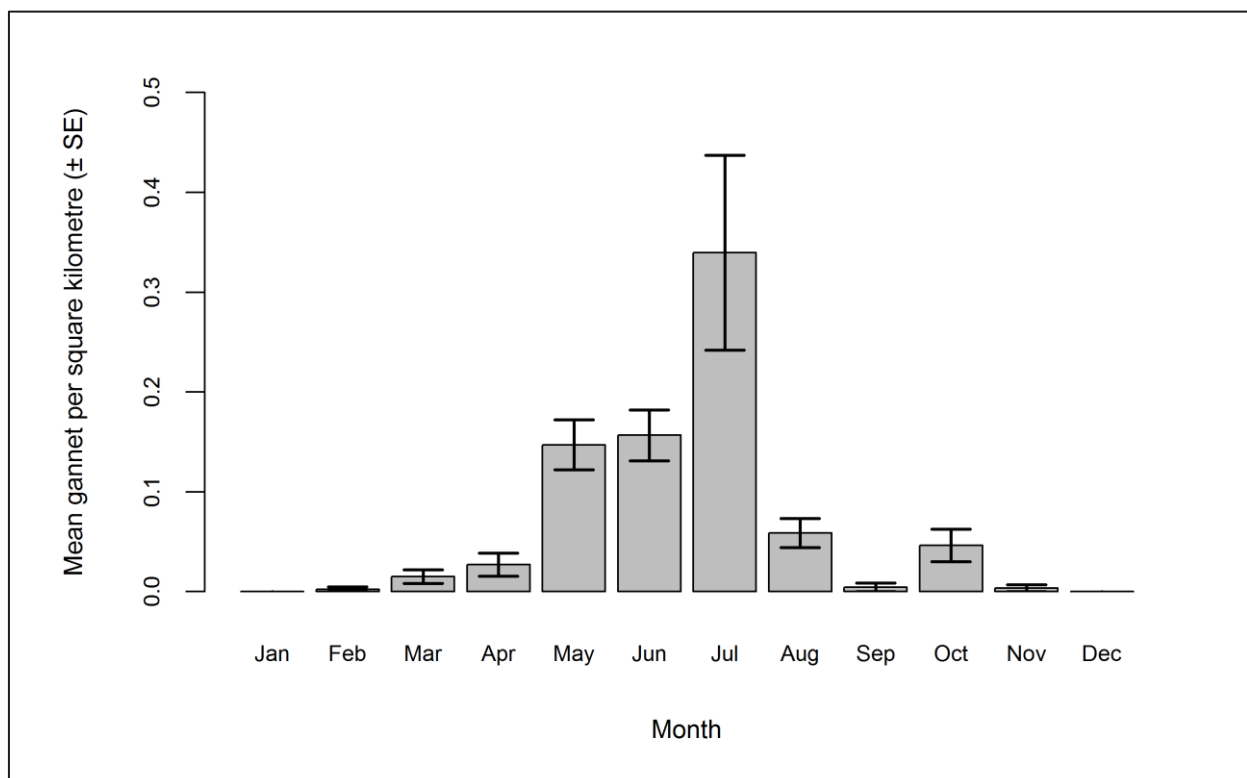


Figure 2.92: Mean density ( $\pm$  se) of gannets recorded in flight during each month across the three development phases: pre-construction, construction and operational years one and two.



Predicted gannet abundance and density estimates (by site, buffer and total survey area) are presented in Table 2.54. The smallest total abundance was predicted for the operational phase; however, the smallest proportion of gannets within the Robin Rigg OWF itself was predicted for the construction phase (Table 2.54).

**Table 2.54: Abundance and density of gannets in flight across the three development phases: pre-construction, construction and operational years one and two. Values in parentheses represent upper and lower 95% confidence intervals.**

Phase	Abundance			Density			% within site
	Site	Buffer	Total	Site	Buffer	Total	
<b>Pre-construction</b>	9 (1-27)	146 (32-443)	155 (34-469)	0.67 (0.11-2.08)	0.42 (0.09-1.27)	0.43 (0.09-1.30)	5.64
<b>Construction</b>	4 (1-11)	112 (46-240)	116 (47-251)	0.31 (0.08-0.88)	0.32 (0.13-0.69)	0.32 (0.13-0.70)	3.50
<b>Operation</b>	4 (1-9)	120 (32-402)	123 (33-411)	0.30 (0.10-0.70)	0.34 (0.09-1.16)	0.34 (0.09-1.14)	3.16

As seen in Table 2.54, the density surface maps show that the largest predicted gannet densities occurred during the pre-construction phase, to the south of Robin Rigg OWF (Figure 2.93). Gannet densities in this area declined significantly during the construction phase, with a small increase to the north-east of this area during operation (Figure 2.93).



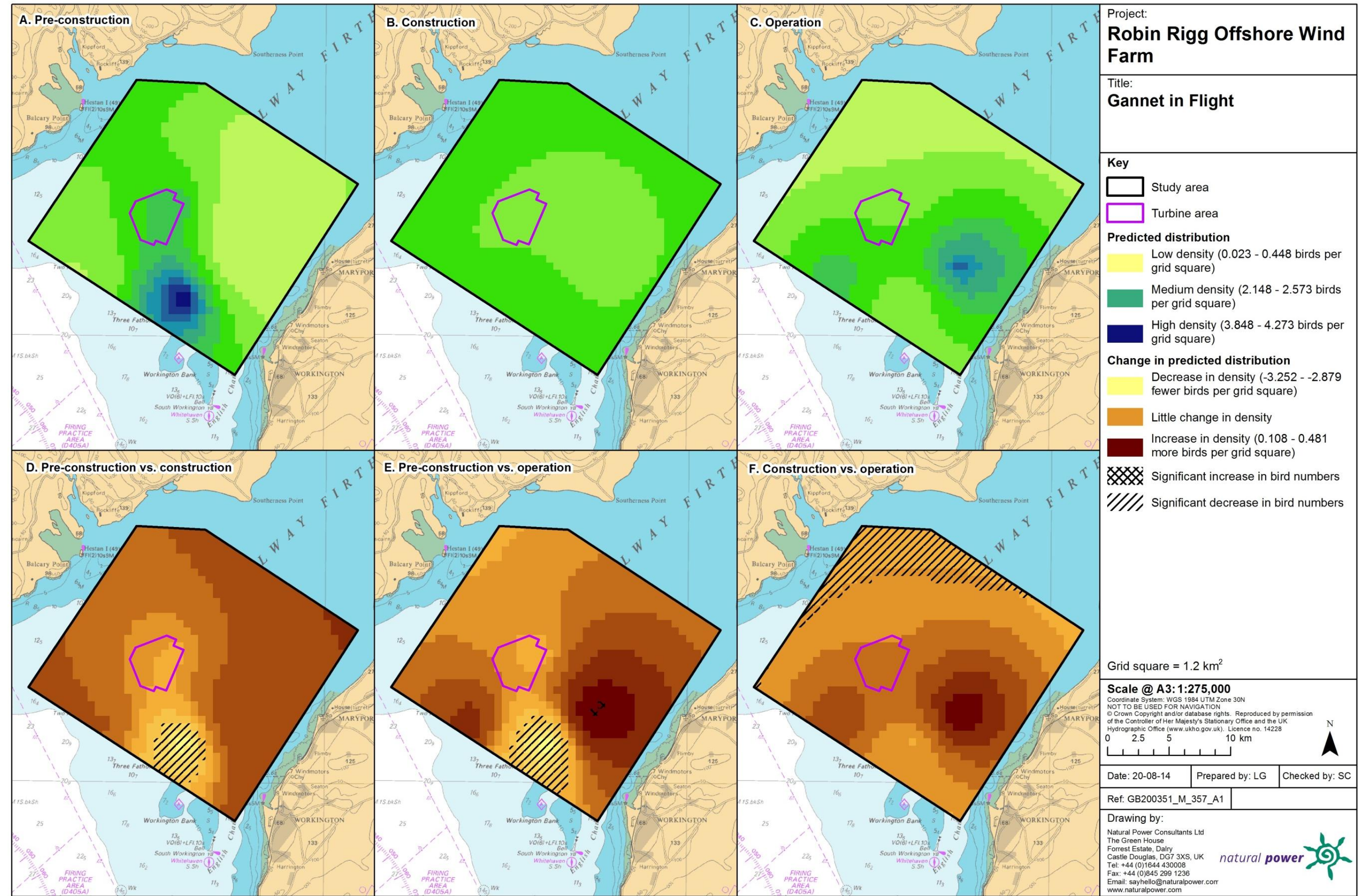


Figure 2.93: Predicted density of gannets in flight during a) pre-construction, b) construction and c) operational monitoring. Changes in predicted density between d) pre-construction and construction, e) pre-construction and operation and f) construction and operation are also shown. Significant differences are marked with diagonal shading.



### 2.4.6.9.26. Collision risk

The percentage of gannets recorded during the three development phases in different height bands relative to rotor swept height can be found in Table 2.55 and Figure 2.94. Data were combined for chi-squared analysis and a statistically significant difference was found between flight bands ( $\chi^2 = 7.32$ ,  $df = 1$ ,  $p = 0.03$ ). More gannets than expected were observed flying at rotor swept height during the construction phase. During the operational phase, observed and expected gannet numbers at rotor swept height were similar.

**Table 2.55: Percentage of gannets recorded in different flight height bands across the three development phases: pre-construction, construction and operational years one and two. Shaded column indicates percentage at rotor swept height (flight band 4).**

Phase	Flight height band					
	1 (0–5 m)	2 (6–25 m)	3 (26–34 m)	4 (35–125 m)	5 (126–200 m)	6 (>200 m)
Pre-construction	32.95	65.06	1.99	0.00	0.00	0.00
Construction	26.88	60.77	8.51	3.84	0.00	0.00
Operation	41.84	43.20	6.46	8.50	0.00	0.00

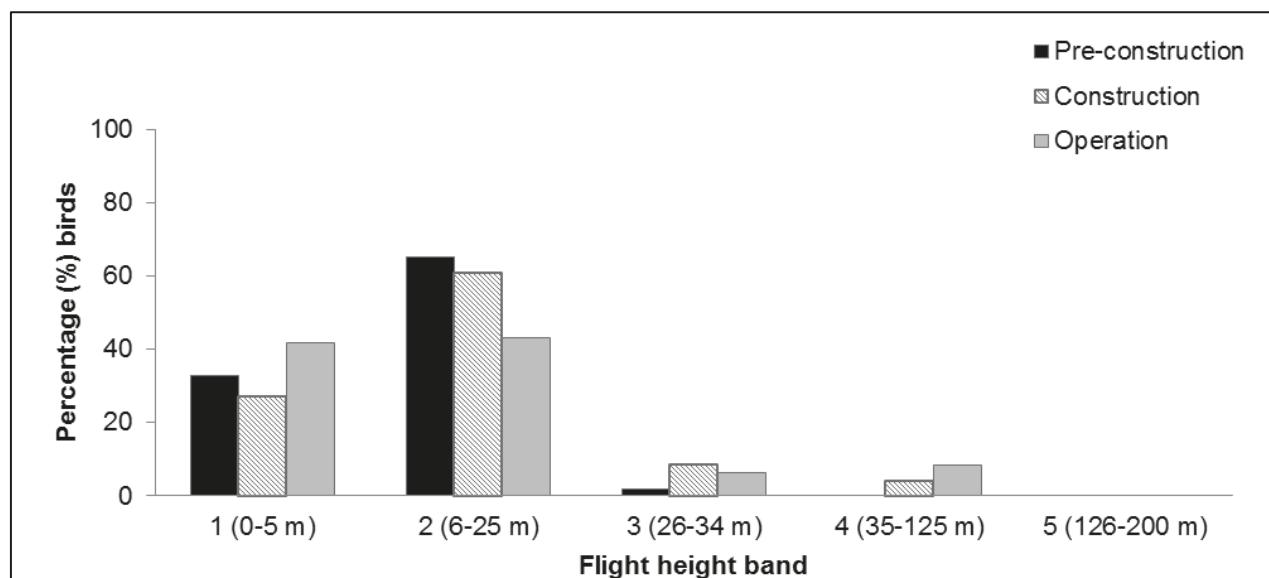


**Figure 2.94: Percentage of gannets recorded in different flight height bands across the three development phases: pre-construction, construction and operational years one and two.**

## 2.4.6.10. Across operational years

### 2.4.6.10.27. Summary statistics

Throughout operational monitoring, gannet numbers were relatively small in comparison to other species recorded (Table 2.56). Gannet numbers were similar throughout operational surveying, with the largest numbers recorded in operational year two at 0.14 individuals per km effort (Table 2.56). The majority (c. 60%) of gannets recorded were in flight throughout all operational years (Table 2.56).

**Table 2.56: Number of gannets recorded per block during each operational year per km survey effort (all data).**

	Operational year 1		Operational year 2		Operational year 3		Operational year 4	
	On sea	In flight	On sea	In flight	On sea	In flight	On sea	In flight
<b>Total number individuals</b>	19	105	95	189	77	101	55	136
<b>Total number sightings</b>	18	79	68	137	50	75	44	93
<b>Number individuals/km</b>	0.01	0.06	0.05	0.09	0.04	0.05	0.03	0.06
	Total		Total		Total		Total	
<b>Total number individuals</b>	124		284		178		191	
<b>Total number sightings</b>	97		205		125		137	
<b>Number individuals/km</b>	0.07		0.14		0.08		0.09	

Data were filtered as described in the methodology (Section 2.4.4). The percentage of segments without observations was calculated to ensure there were sufficient data to perform the analysis (Table 2.57). Data were also checked to ensure observations were recorded in all months of the year.

**Table 2.57: Percentage of gannet analysis blocks without observations across operational years one to four. Zero inflation prior to removal of effort is presented in parentheses.**

	On sea	In flight
<b>Percentage zero blocks</b>	99.1%	(98.9%) 97.7%



## 2.4.6.10.28. Density and distribution

### 2.4.6.10.28.1. On sea

Initial data exploration highlighted that 99% of analysis blocks for gannets on the sea contained zero observations (Figure 2.95). Since no birds were recorded between November and February, further removal of effort was not possible. Therefore, further abundance modelling of gannets on the sea across the four operational years was not undertaken and raw data are presented.

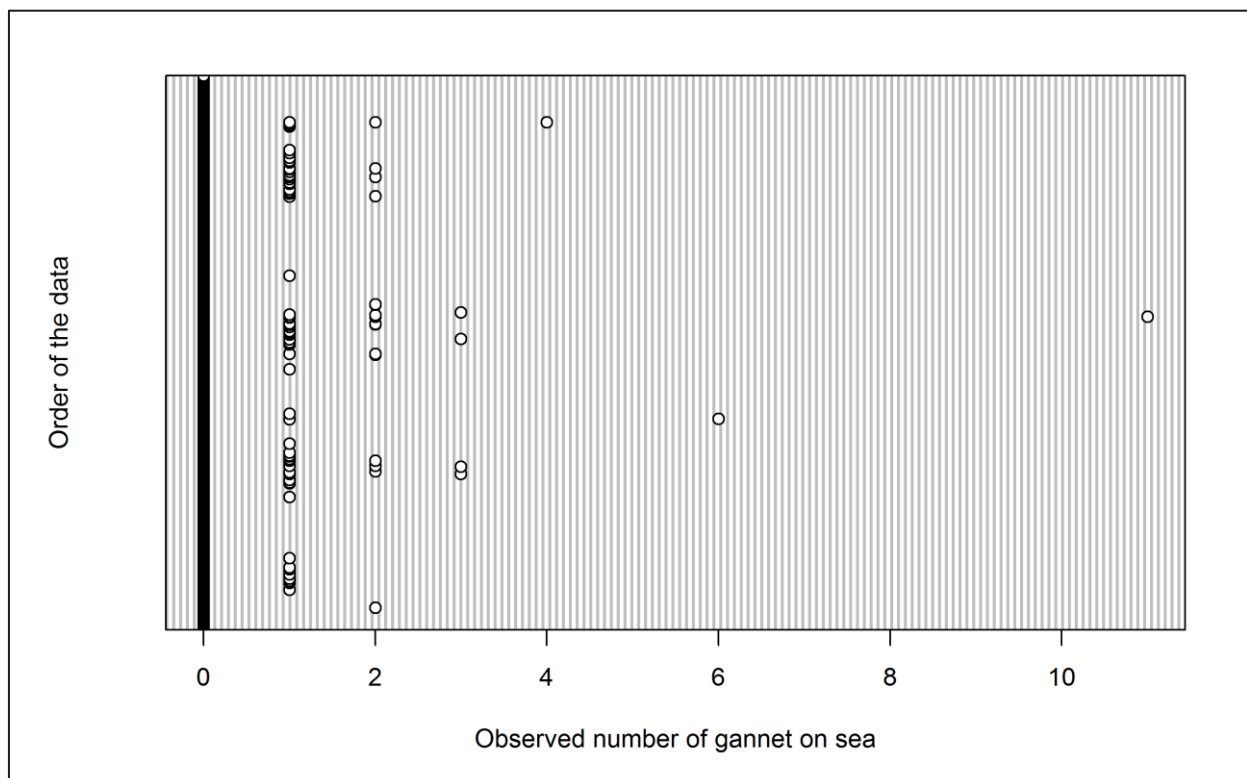


Figure 2.95: Dot plot of the number of gannets observed on sea per analysis block across operational years one to four.

Group size for gannets recorded on the sea ranged from single individuals up to 11 birds (Figure 2.95). Mean density of gannets shows little change after operational year one, with an indication of a peak during operational year three (Figure 2.96). However, since further modelling was not undertaken, the significance of any differences could not be tested. Figure 2.97 shows that gannet density increased from March to peak in July, before declining in winter.

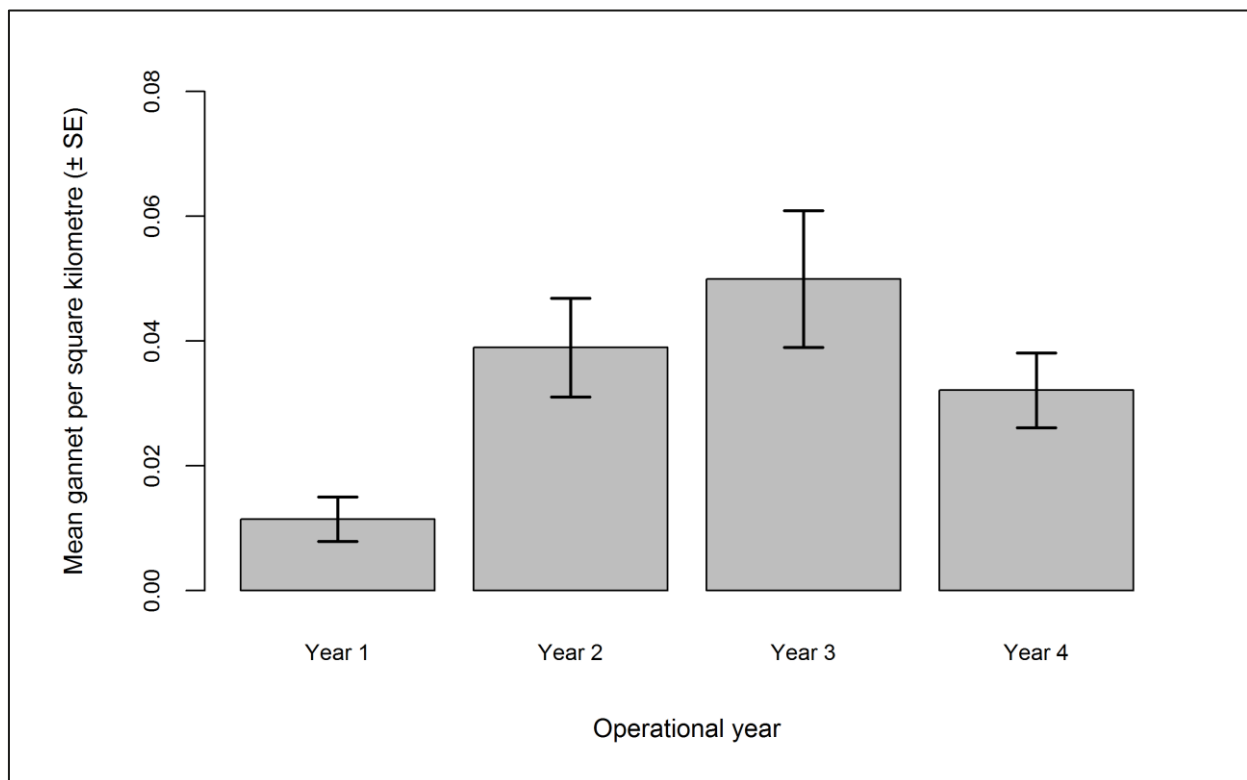


Figure 2.96: Mean density (± se) of gannets recorded on the sea across operational years one to four.

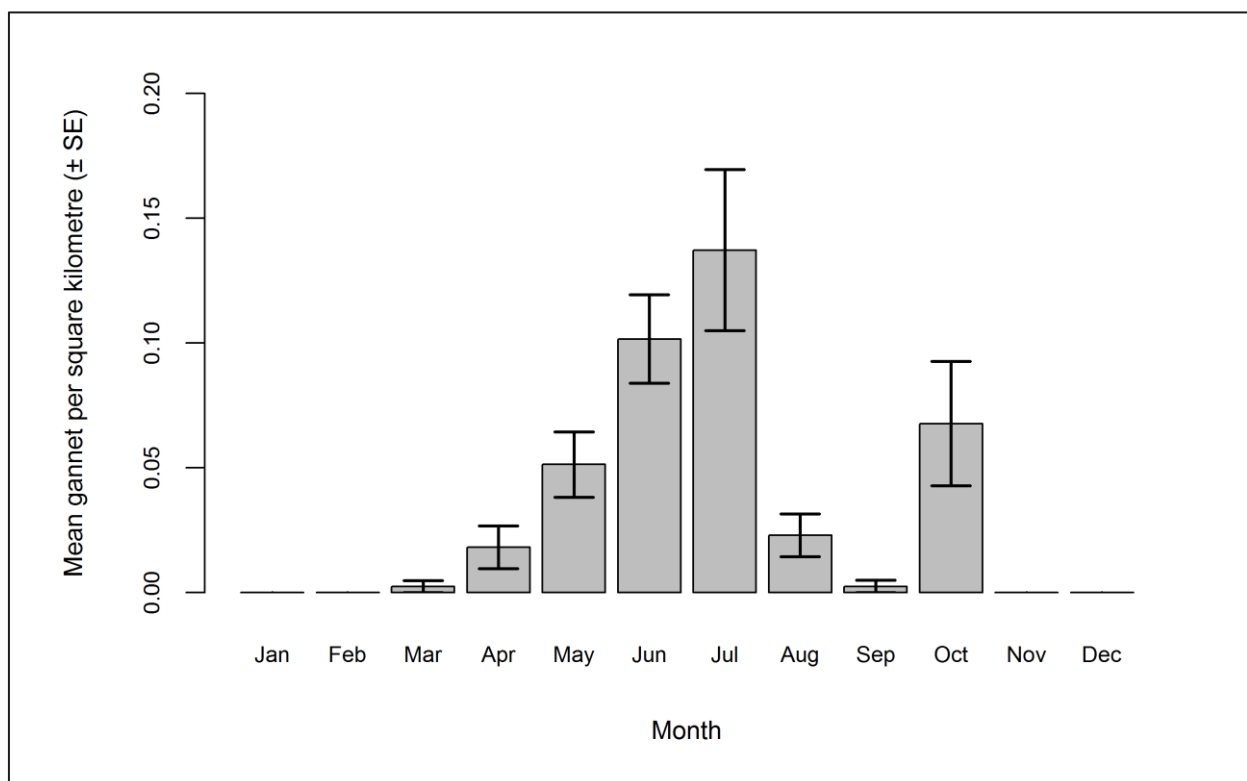


Figure 2.97: Mean density (± se) of gannets recorded on the sea during each month across operational years one to four.

### 2.4.6.10.28.2. In flight

As for data pooled across the three development phases, gannets were not observed in all months across the four operational years (Table 2.58). As a result, the final dataset only contained data collected between May and August.

**Table 2.58: Number of gannets available for analysis each month across operational years one to four. Months highlighted in bold were used in the analysis.**

Month	Operational year 1	Operational year 2	Operational year 3	Operational year 4	Total
January	0	0	0	0	0
February	0	0	0	0	0
March	0	2	0	11	13
April	3	0	1	0	4
<b>May</b>	<b>6</b>	<b>14</b>	<b>4</b>	<b>2</b>	<b>26</b>
<b>June</b>	<b>9</b>	<b>12</b>	<b>11</b>	<b>11</b>	<b>43</b>
<b>July</b>	<b>28</b>	<b>21</b>	<b>10</b>	<b>14</b>	<b>73</b>
<b>August</b>	<b>6</b>	<b>2</b>	<b>4</b>	<b>3</b>	<b>15</b>
September	2	0	2	1	5
October		18	3	14	35
November	0	2	0	1	3
December	0	0	0	0	0

Data exploration of the final dataset highlighted a single outlier (15 in July 2010) that may have influenced the modelling process (Figure 2.98). This outlier may be a result of multiple sightings within the same analysis block. The model was run with and without these data and the outputs compared.

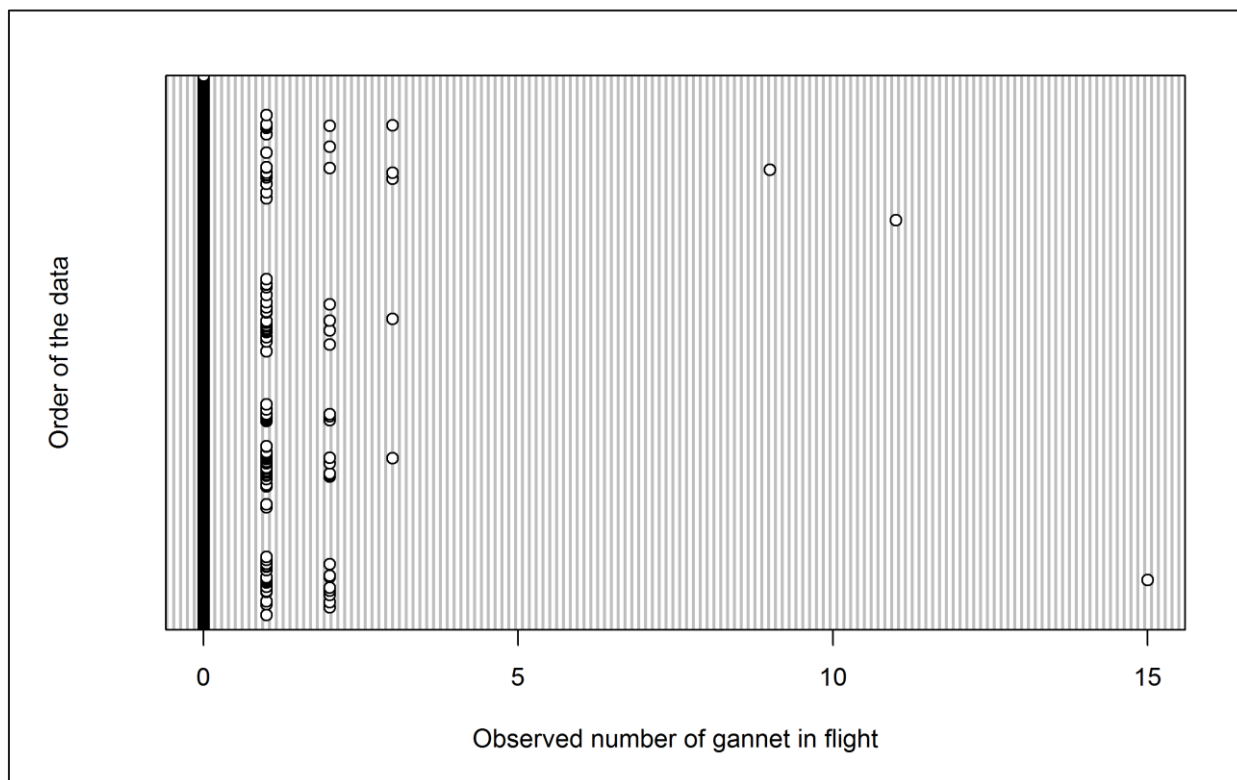


Figure 2.98: Dot plot of the number of gannets observed in flight per analysis block across operational years one to four.

The GEE predicted that month and location have a statistically significant influence on gannet abundance within the survey area (Table 2.59). Removal of the outliers resulted in tide height becoming statistically significant ( $p = 0.006$ ) and location becoming marginally non-significant ( $p = 0.051$ ). Both models predicted a statistically significant interaction between location and operational year (phase).

Operational year alone was not significant; indeed, the mean density of gannets in flight shows across operational years (Figure 2.99). Peak numbers were recorded during July (Figure 2.100), and model predictions were made for this month.

Table 2.59: Final model outputs for gannets in flight across operational years one to four.

Term	Marginal p-value
Month	0.0015
Phase	0.9804
Tide height	0.1176
Location (X,Y)	0.0110
Interaction (location: phase)	<0.0001



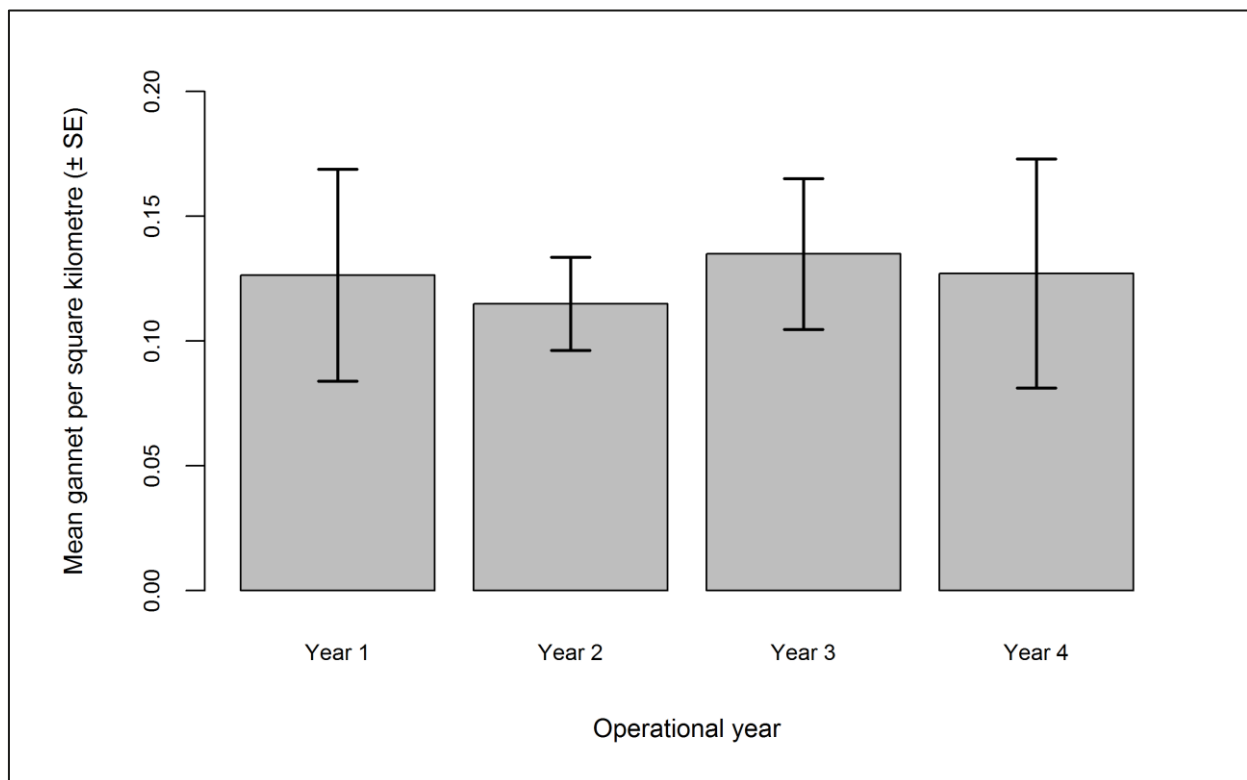


Figure 2.99: Mean density ( $\pm$  se) of gannets recorded in flight across operational years one to four.

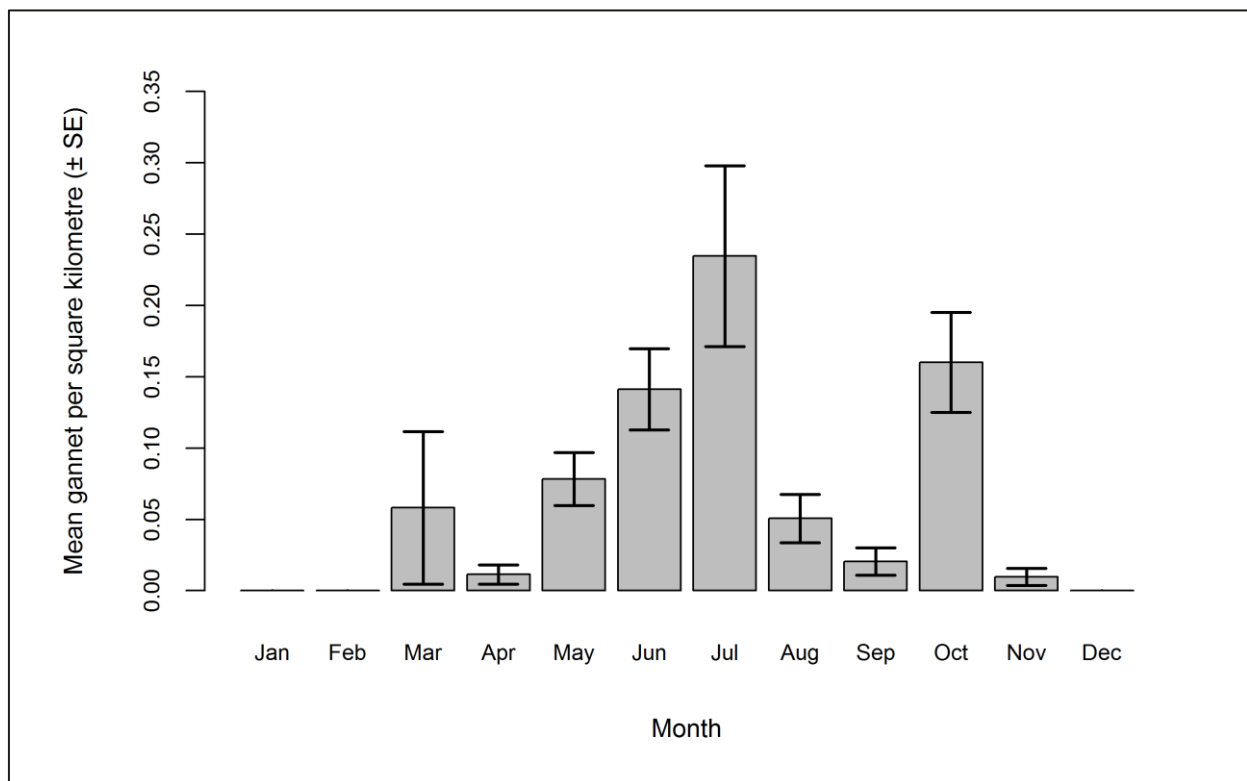


Figure 2.100: Mean density ( $\pm$  se) of gannets recorded in flight during each month across operational years one to four.

Predicted gannet abundance and density estimates (by site, buffer and total survey area) are presented in Table 2.60. The smallest total abundance was predicted for operational year four; however, this is the phase with the greatest proportion of birds within the Robin Rigg OWF itself (Table 2.60).

**Table 2.60: Abundance and density of gannets in flight across operational years one to four. Values in parentheses represent upper and lower 95% confidence intervals.**

Operational years	Abundance			Density			% within site
	Site	Buffer	Total	Site	Buffer	Total	
<b>1</b>	5 (1-16)	198 (39-628)	203 (40-644)	0.37 (0.08-1.23)	0.57 (0.11-1.81)	0.56 (0.11-1.78)	2.40
<b>2</b>	6 (2-15)	125 (37-329)	130 (38-344)	0.45 (0.13-1.54)	0.36 (0.11-0.95)	0.36 (0.11-0.95)	4.63
<b>3</b>	7 (2-20)	106 (27-335)	113 (29-355)	0.52 (0.13-1.54)	0.30 (0.08-0.96)	0.31 (0.08-0.98)	6.36
<b>4</b>	26 (1-140)	139 (15-637)	164 (15-777)	1.99 (0.05-10.79)	0.40 (0.04-1.83)	0.46 (0.04-2.15)	18.61

As shown in Table 2.60, largest gannet densities were predicted for operational year one, to the south-east of Robin Rigg OWF (Figure 2.101). Predicted gannet densities declined significantly in this area during subsequent operational years (Figure 2.102). Predicted density was similar across operational years two and three, although spatial distribution varied between years (Figure 2.101). Predicted gannet distribution was concentrated in a small area on the north-eastern edge of the OWF during operational year four with numbers declining elsewhere in the survey area (Figure 2.102).

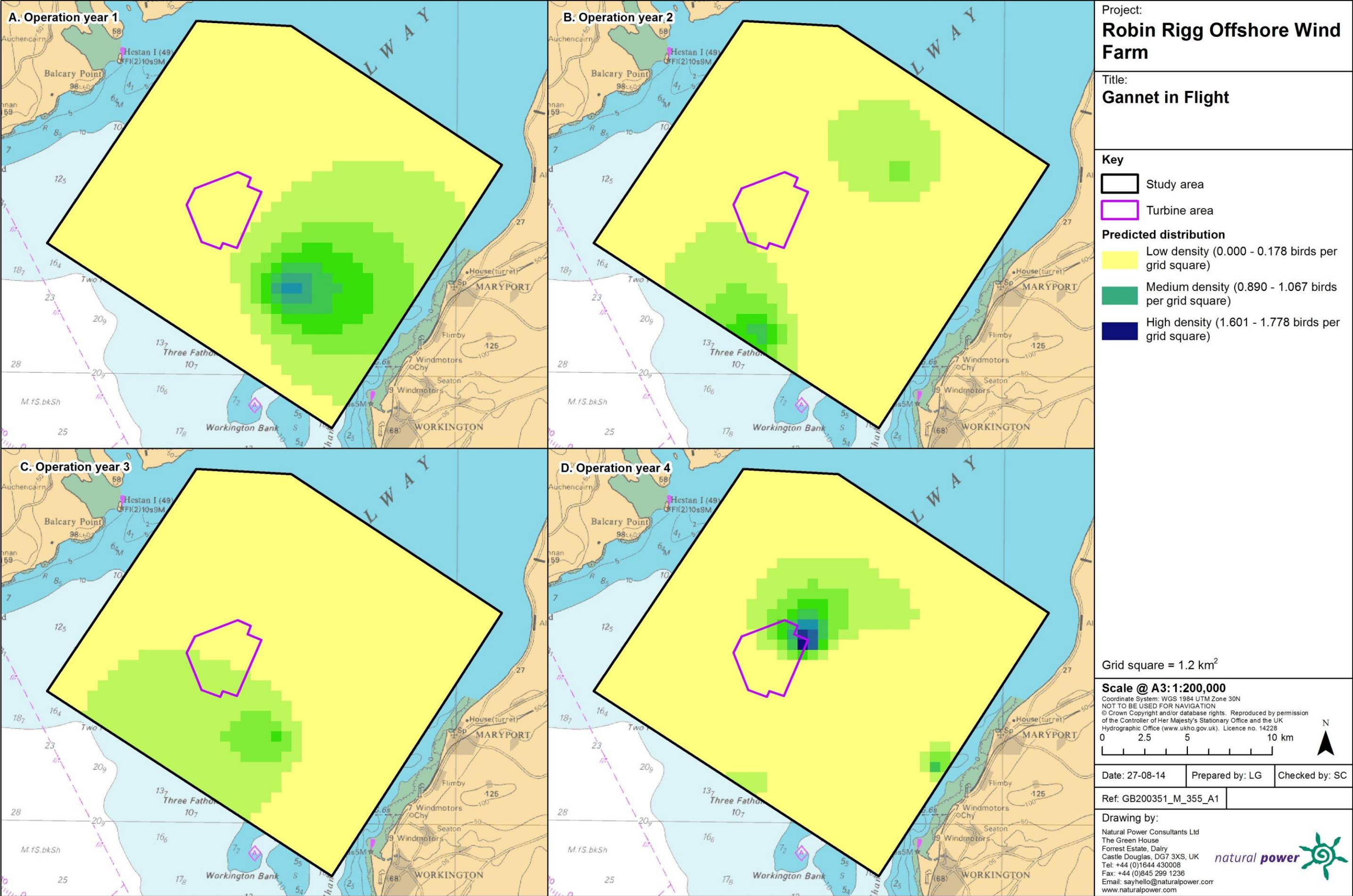


Figure 2.101: Predicted density of gannets in flight during a) operational year one, b) operational year two, c) operational year three and d) operational year four.



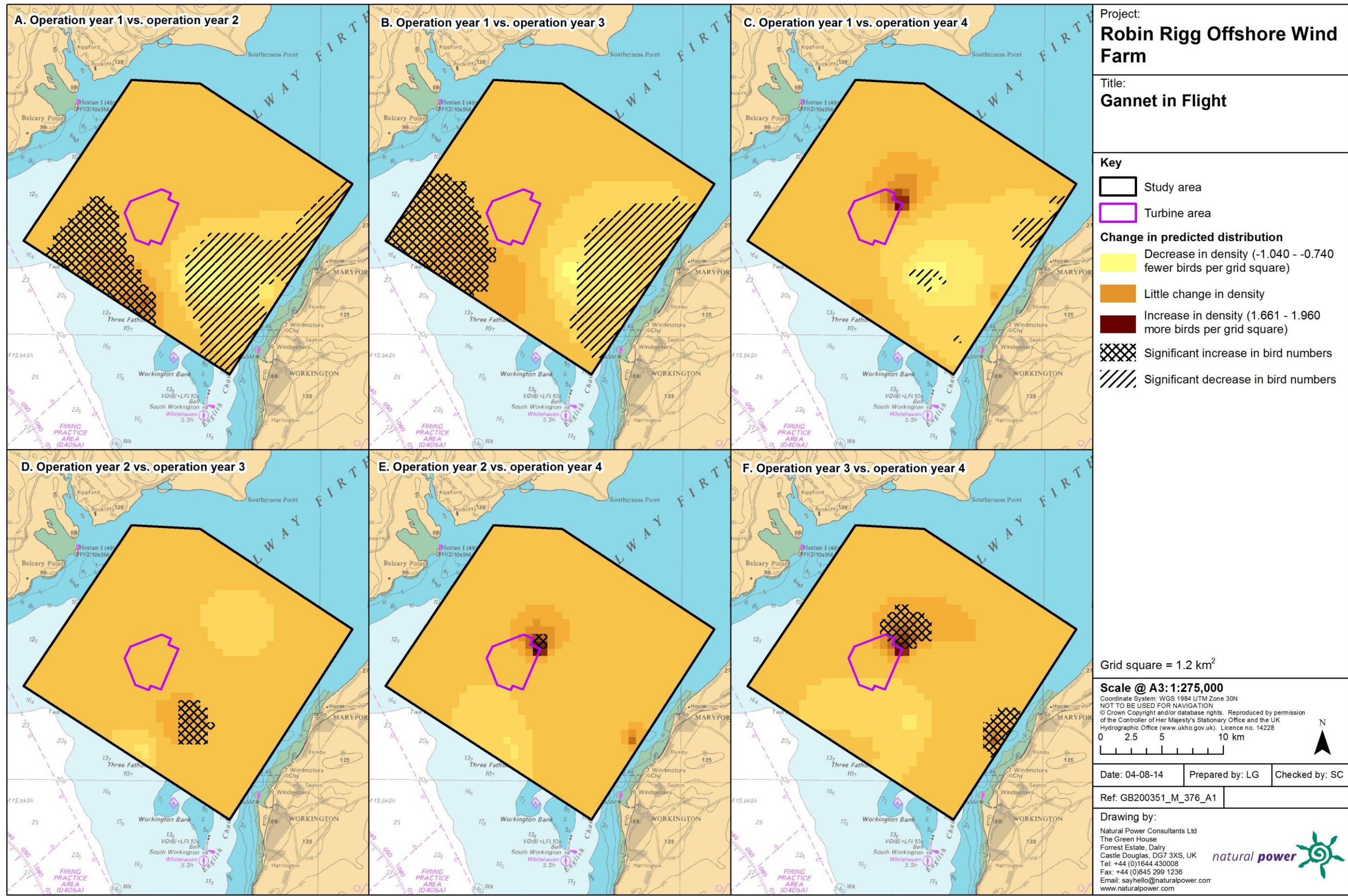


Figure 2.102: Differences in predicted flying gannet density between operational years. Significant differences are marked with diagonal shading.



### 2.4.6.10.29. Collision risk

The percentage of gannets recorded during the three development phases in different height bands relative to rotor swept height can be found in Table 2.61 and Figure 2.103. Data were combined for chi-squared analysis and a statistically significant difference was found between flight bands ( $\chi^2 = 12.49$ ,  $df = 3$ ,  $p = 0.002$ ). More gannets than expected were observed flying at rotor swept height during operational years two and three. Conversely, fewer gannets than expected were observed flying at rotor swept height during operational years one and four.

**Table 2.61: Percentage of gannets recorded in different flight height bands across operational years one to four. Shaded column indicates percentage at rotor swept height (flight band 4).**

Operational year	Flight height band					
	1 (0–5 m)	2 (6–25 m)	3 (26–34 m)	4 (35–125 m)	5 (126–200 m)	6 (>200 m)
1	31.43	60.00	5.71	2.86	0.00	0.00
2	47.62	33.86	6.88	11.64	0.00	0.00
3	26.04	51.04	10.42	12.50	0.00	0.00
4	38.97	39.71	18.38	2.94	0.00	0.00

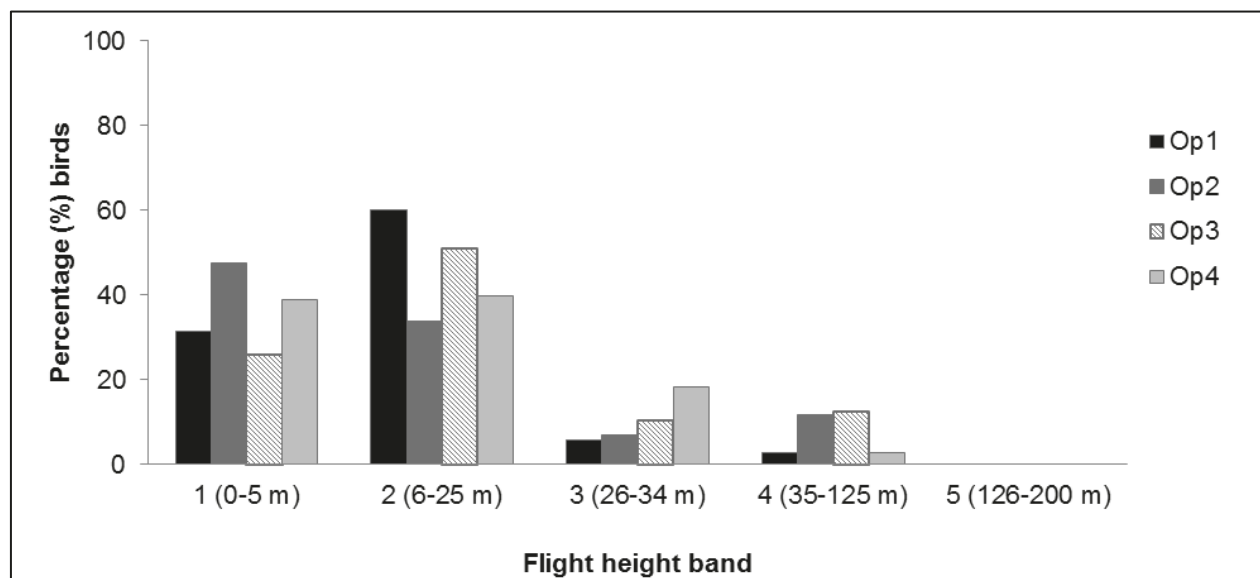


**Figure 2.103: Percentage of gannets recorded in different flight height bands across operational years one to four.**

## 2.4.7. Razorbill

### 2.4.7.11. Across three development phases

#### 2.4.7.11.30. Summary statistics

Razorbill numbers remained relatively high across all three development phases with the highest numbers recorded during the construction phase (Table 2.62). However, the highest number of individuals per km of effort was recorded during the pre-construction phase. The percentage of razorbills recorded on the sea ranged from 58% during the pre-construction phase to 91% during construction (Table 2.62).

**Table 2.62: Number of razorbill recorded per block during each development phase per km survey effort (all data).**

	Pre-construction		Construction		Operation years 1-2	
	On sea	In flight	On sea	In flight	On sea	In flight
<b>Total number individuals</b>	1,258	917	2,610	272	1,584	378
<b>Total number sightings</b>	490	189	1,080	144	1,158	177
<b>Number individuals/km</b>	0.35	0.26	0.36	0.04	0.41	0.10
	Total		Total		Total	
<b>Total number individuals</b>	2,175		2,882		1,962	
<b>Total number sightings</b>	679		1,224		1,335	
<b>Number individuals/km</b>	0.61		0.40		0.51	

Data were filtered as described in the methods (Section 2.4.4). The percentage of segments without observations was calculated to ensure there were sufficient data to perform the analysis (Table 2.63). Data were also checked to ensure observations were recorded in all months of the year.

**Table 2.63: Percentage of razorbill analysis blocks without observations across the three development phases: pre-construction, construction and operational years one and two. Zero inflation prior to removal of effort is presented in parentheses.**

	On sea	In flight
<b>Percentage zero blocks</b>	90.0%	(98.6%) 98.0%

### 2.4.7.11.31. Density and distribution

#### 2.4.7.11.31.1. On sea

A hazard-rate detection function with cluster size as a covariate was found to be the best fitting model. Figure 2.104 shows the selected detection curve for razorbills across the four operational years.

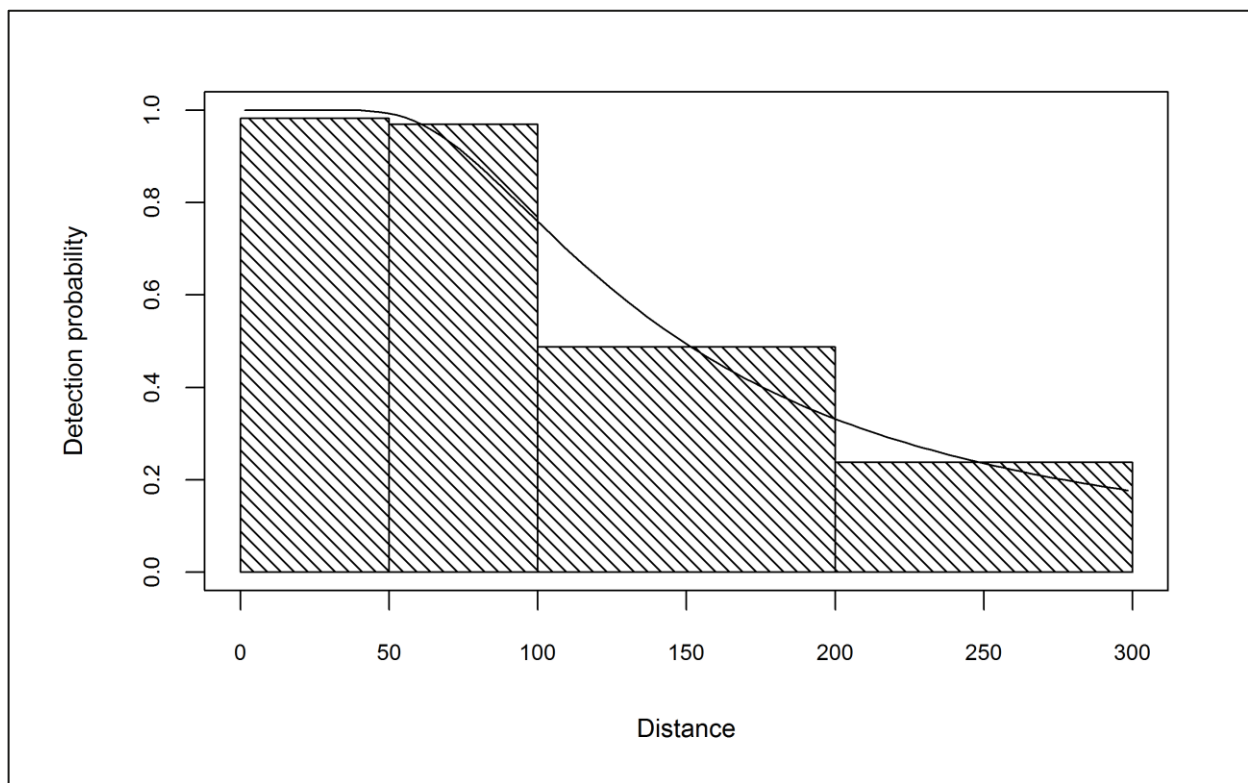


Figure 2.104: Detection curve used to adjust razorbill on sea counts for imperfect detection across the three development phases: pre-construction, construction and operational years one and two.

Initial data exploration of adjusted razorbill numbers indicated that there were no outlying observations which may influence the modelling process (Figure 2.105).

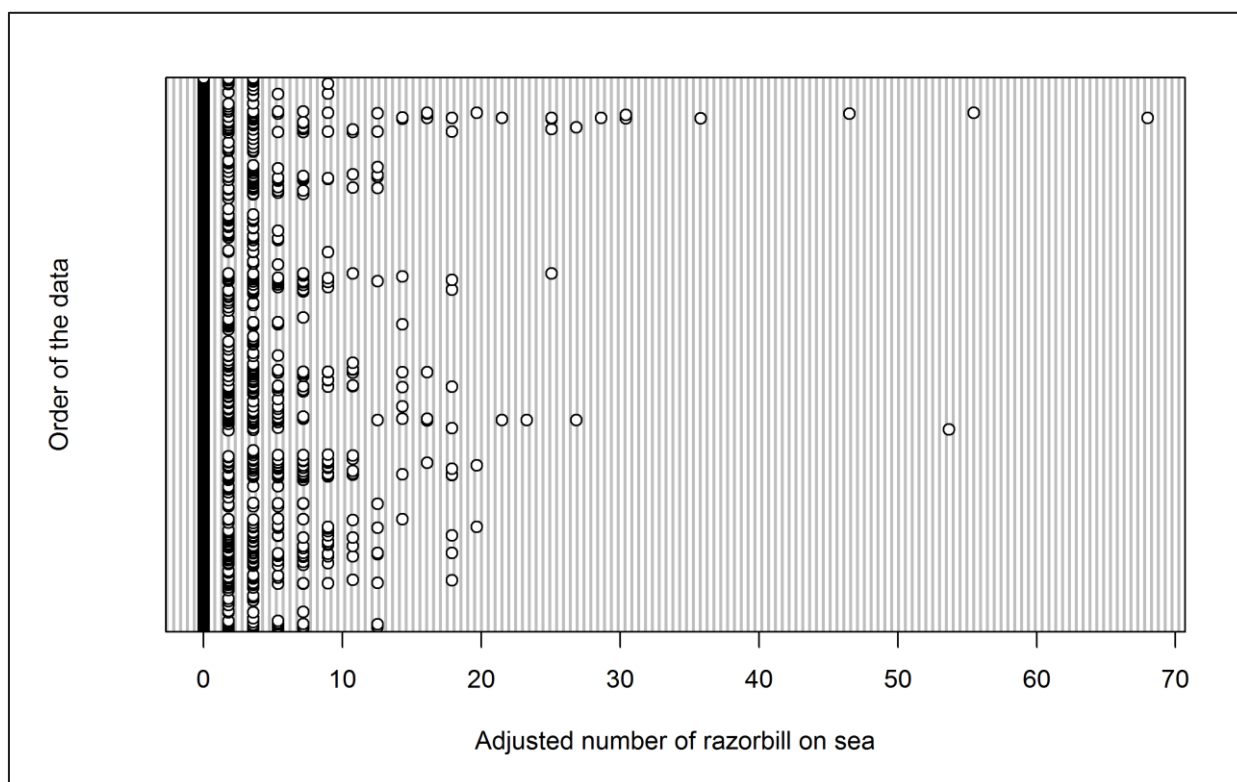


Figure 2.105: Dot plot of the number of razorbills observed on sea per analysis block across the three development phases: pre-construction, construction and operational years one and two.

The GEE predicted that month, tidal height, location, and the interaction between month and location all had a statistically significant influence on razorbill abundance across the survey area (Table 2.64). Development phase did not have a statistically significant effect (Figure 2.106). Month was statistically significant due to a large increase in birds observed during the spring (particularly during April) and autumn (particularly during November; Figure 2.107). Since April was the month of peak activity, model predictions were made for this month.

Table 2.64: Final model outputs for razorbills on the sea across the three development phases: pre-construction, construction and operational years one and two.

Term	Marginal p-value
Month	<0.0001
Phase	0.5691
Tide height	0.0001
Location (X,Y)	<0.0001
Interaction (location: phase)	0.0051





Figure 2.106: Mean density (± se) of razorbills recorded on the sea during across the three development phases: pre-construction, construction and operational years one and two.

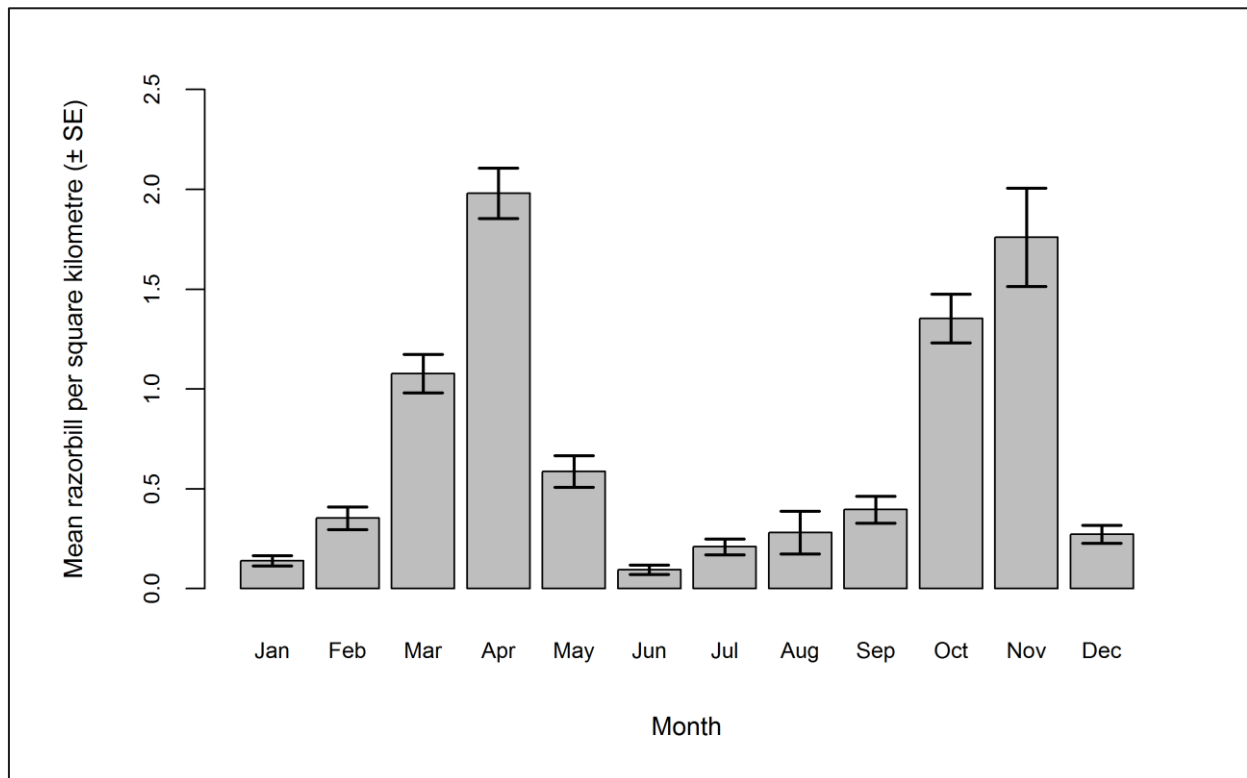


Figure 2.107: Mean density (± se) of razorbills recorded on the sea during each month across the three development phases: pre-construction, construction and operational years one and two.

Predicted razorbill abundance and densities (by site, buffer and total survey area) are presented in Table 2.65. There is an increase in the abundance and density across the three development phases, peaking during operation as is reflected in the density surface maps. The highest percentage of razorbills on the sea within Robin Rigg OWF itself was also predicted to occur during the operational phase (Table 2.65).

**Table 2.65: Abundance and density of razorbills on the sea across the three development phases: pre-construction, construction and operational years one and two. Values in parentheses represent upper and lower 95% confidence intervals.**

Phase	Abundance			Density			% within site
	Site	Buffer	Total	Site	Buffer	Total	
<b>Pre-construction</b>	6 (2-21)	168 (71-421)	174 (73-443)	0.48 (0.13-1.66)	0.48 (0.20-1.21)	0.48 (0.20-1.23)	3.54
<b>Construction</b>	17 (5-44)	267 (92-694)	284 (97-738)	1.31 (0.35-3.37)	0.77 (0.27-2.00)	0.79 (0.27-2.05)	5.96
<b>Operation</b>	36 (10-146)	443 (141-1,454)	479 (152-1,602)	2.76 (0.81-11.44)	1.27 (0.41-4.18)	1.33 (0.42-4.44)	7.45

As shown in Table 2.65, predicted razorbill density increased across the three development phases (Figure 2.108). A statistically significant increase in razorbills on the sea was predicted to occur both within the Robin Rigg OWF and to the west of the site between pre-construction and operational monitoring (Figure 2.108).



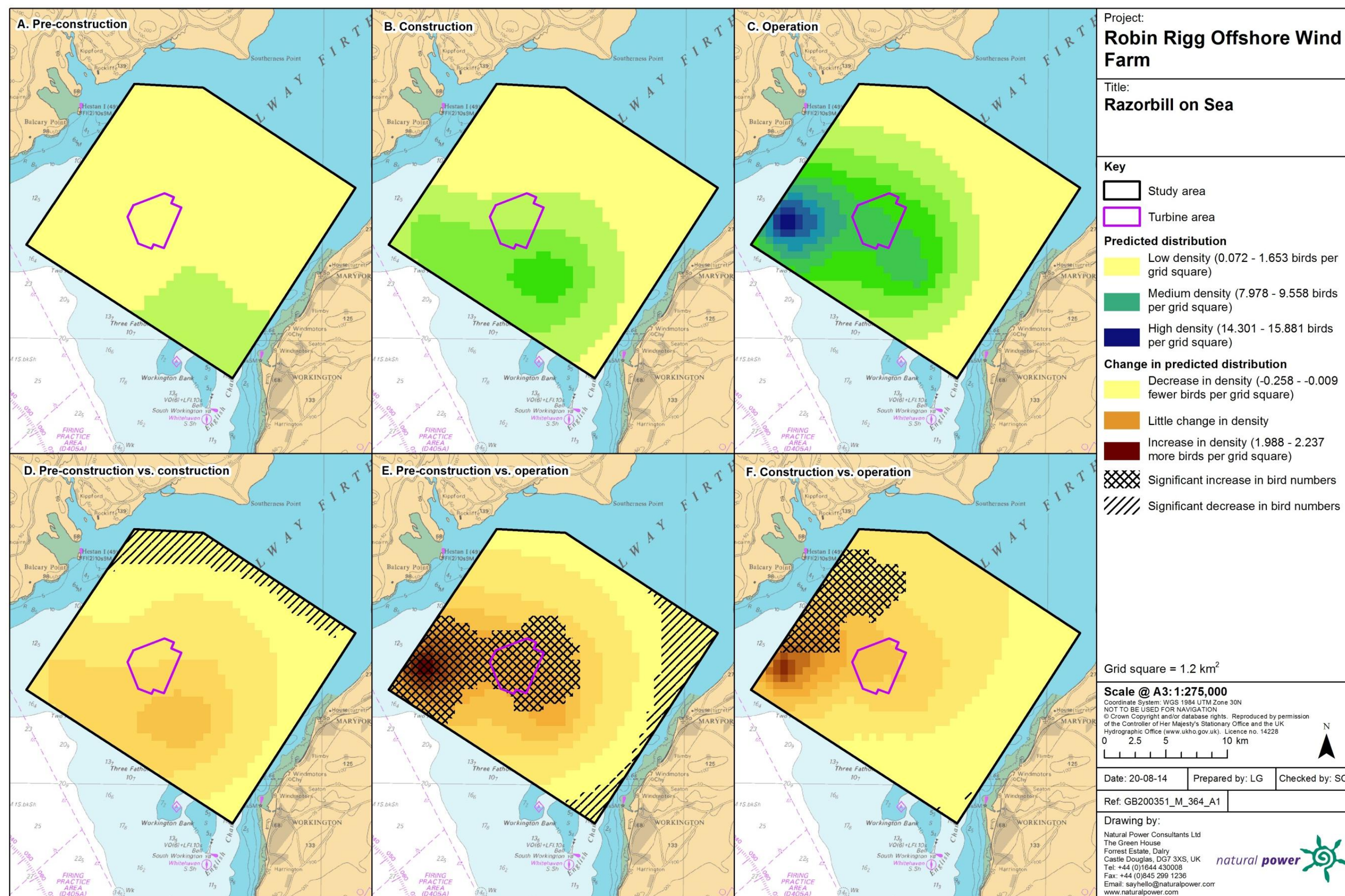


Figure 2.108: Predicted density of razorbills on the sea during a) pre-construction, b) construction and c) operational monitoring. Changes in predicted density between d) pre-construction and construction, e) pre-construction and operation and f) construction and operation are also shown. Significant differences are marked with diagonal shading.



### 2.4.7.11.31.2. In flight

Since small numbers of razorbill observations were recorded between June and September, these five months of effort were removed from the analysis. Initial data exploration of this refined dataset highlighted a single outlier (segment containing 50 razorbills recorded in November 2011) that may influence the modelling process (Figure 2.109). As a result the model was run with and without this outlier and the outputs compared.

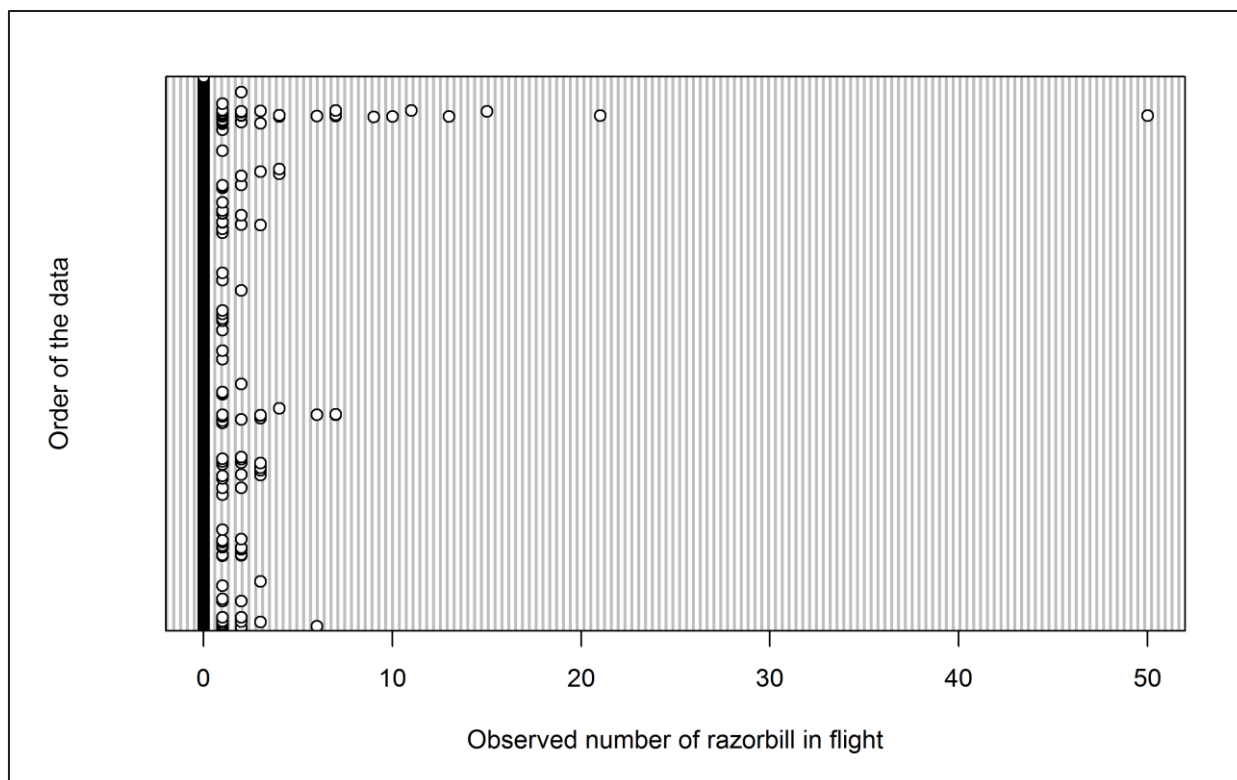


Figure 2.109: Dot plot of the number of razorbills observed in flight per analysis block across the three development phases: pre-construction, construction and operational years one and two.

The initial model including the outlier did not converge. Therefore, the outputs from the model excluding the outlier are presented. The GEE predicted that month, tide height and location have a statistically significant influence on razorbill abundance within the survey area (Table 2.66). Specifically, mean razorbill density was larger during the operational phase (Figure 2.110), and during the months of October and November (Figure 2.111). Since November was the month of peak activity, model predictions were made for this month.

Table 2.66: Final model outputs for razorbills in flight across the three development phases: pre-construction, construction and operational years one and two.

Term	Marginal p-value
Month	<0.0001
Phase	0.3436
Tide height	<0.0001
Location (X,Y)	<0.0001
Interaction (location: phase)	0.1147



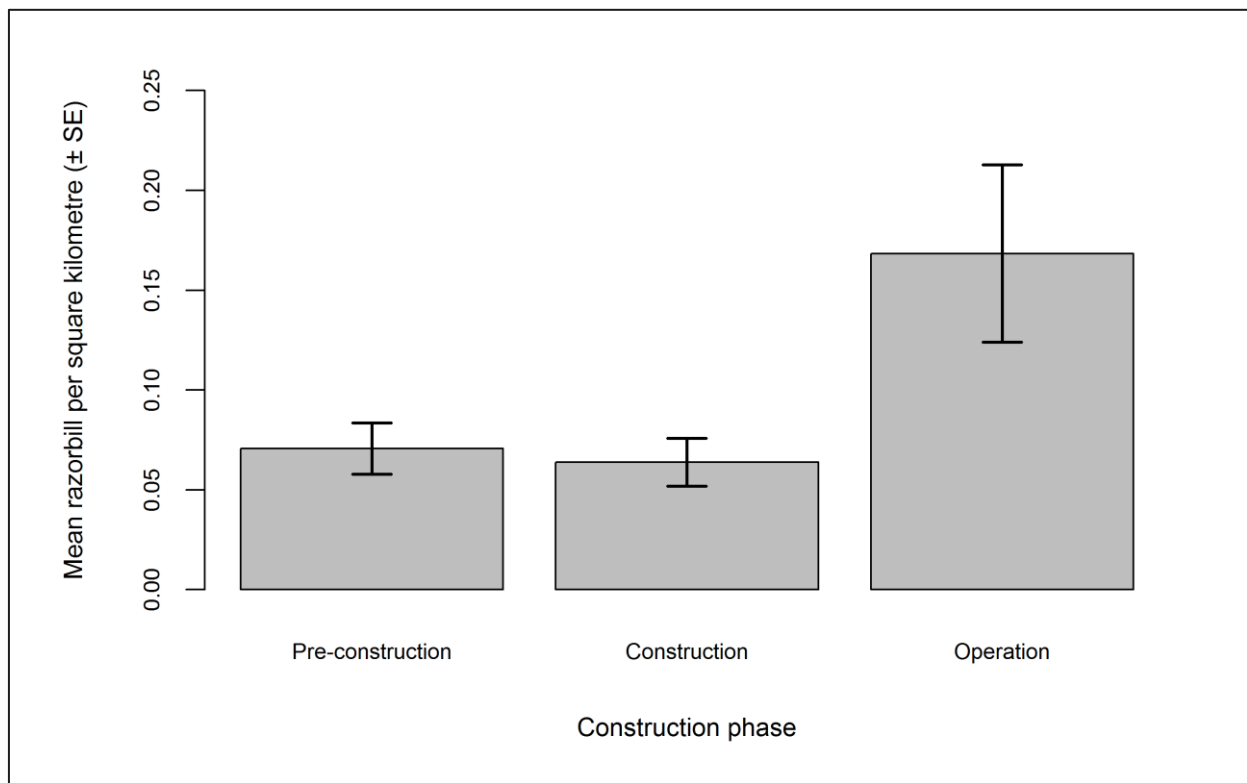


Figure 2.110: Mean density (± se) of razorbills recorded in flight across the three development phases: pre-construction, construction and operational years one and two.

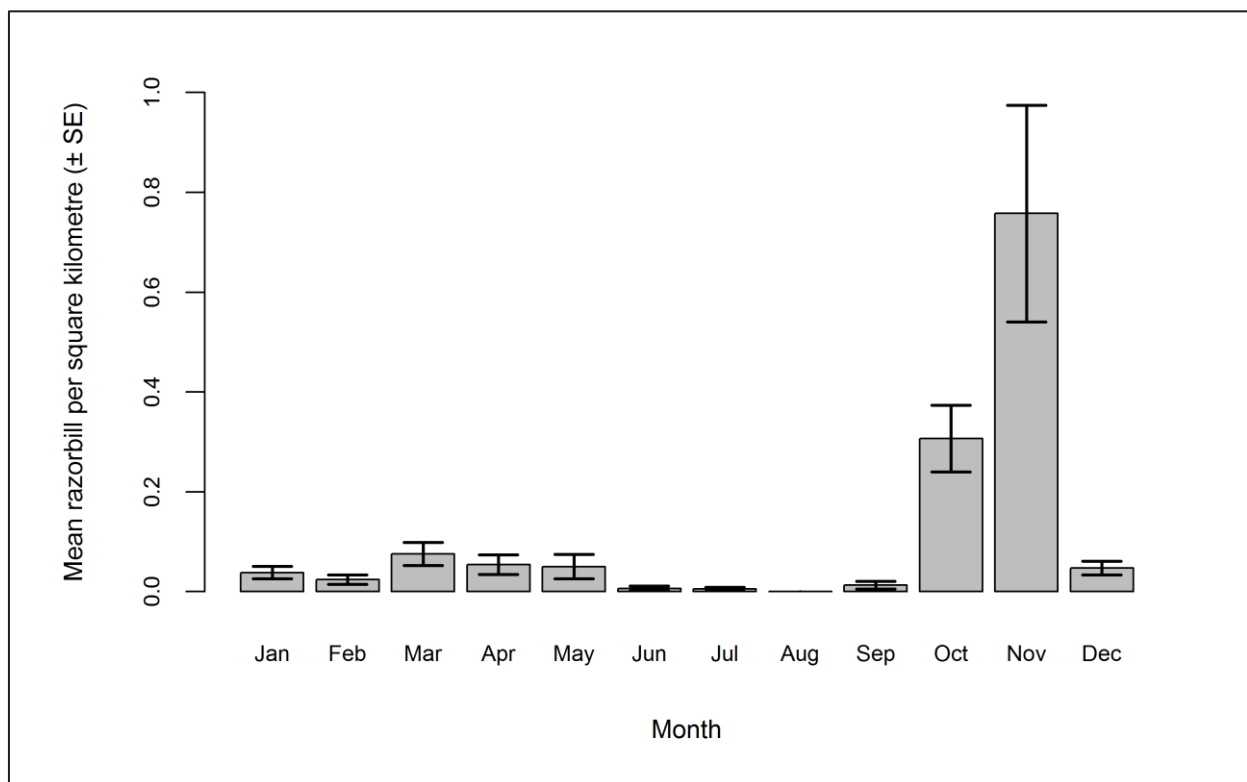


Figure 2.111: Mean density (± se) of razorbills recorded in flight during each month across the three development phases: pre-construction, construction and operational years one and two.

Predicted razorbill abundance and densities (by site, buffer and total survey area) are presented in Table 2.67. The smallest total abundance was predicted for the pre-construction phase. Conversely, this is also the phase with the greatest proportion of birds within the Robin Rigg OWF itself (Table 2.67). Predicted abundance and density increased across subsequent development phases to peak during the operational phase. However, the confidence intervals surrounding these estimates are relatively large so there is high uncertainty in these patterns.

**Table 2.67: Abundance and density of razorbills in flight across the three development phases: pre-construction, construction and operational years one and two. Values in parentheses represent upper and lower 95% confidence intervals.**

Phase	Abundance			Density			% within site
	Site	Buffer	Total	Site	Buffer	Total	
<b>Pre-construction</b>	31	532	563	2.42	1.53	1.56	5.56
	(5-200)	(109-3,873)	(114-4,073)	(0.42-15.47)	(0.31-11.13)	(0.32-1.29)	
<b>Construction</b>	61	1,944	2,005	4.71	5.59	5.56	3.04
	(5-595)	(162-20,572)	(167-21,167)	(0.37-46.01)	(0.47-59.14)	(0.46-58.67)	
<b>Operation</b>	217	5,428	5,645	16.80	15.60	15.65	3.85
	(11-5,430)	(384-143,541)	(395-148,970)	(0.88-419.71)	(1.10-412.65)	(1.10-412.90)	

As shown in Table 2.67, predicted razorbill densities increased across subsequent development phases. Razorbills were predicted in deeper waters to the west of Robin Rigg OWF during the pre-construction phase, becoming more concentrated in this area during construction (Figure 2.112). By the operational phase, statistically significant increases of razorbills were predicted to have occurred to the north-east of the OWF in more shallow waters, and to the south-west (Figure 2.112).



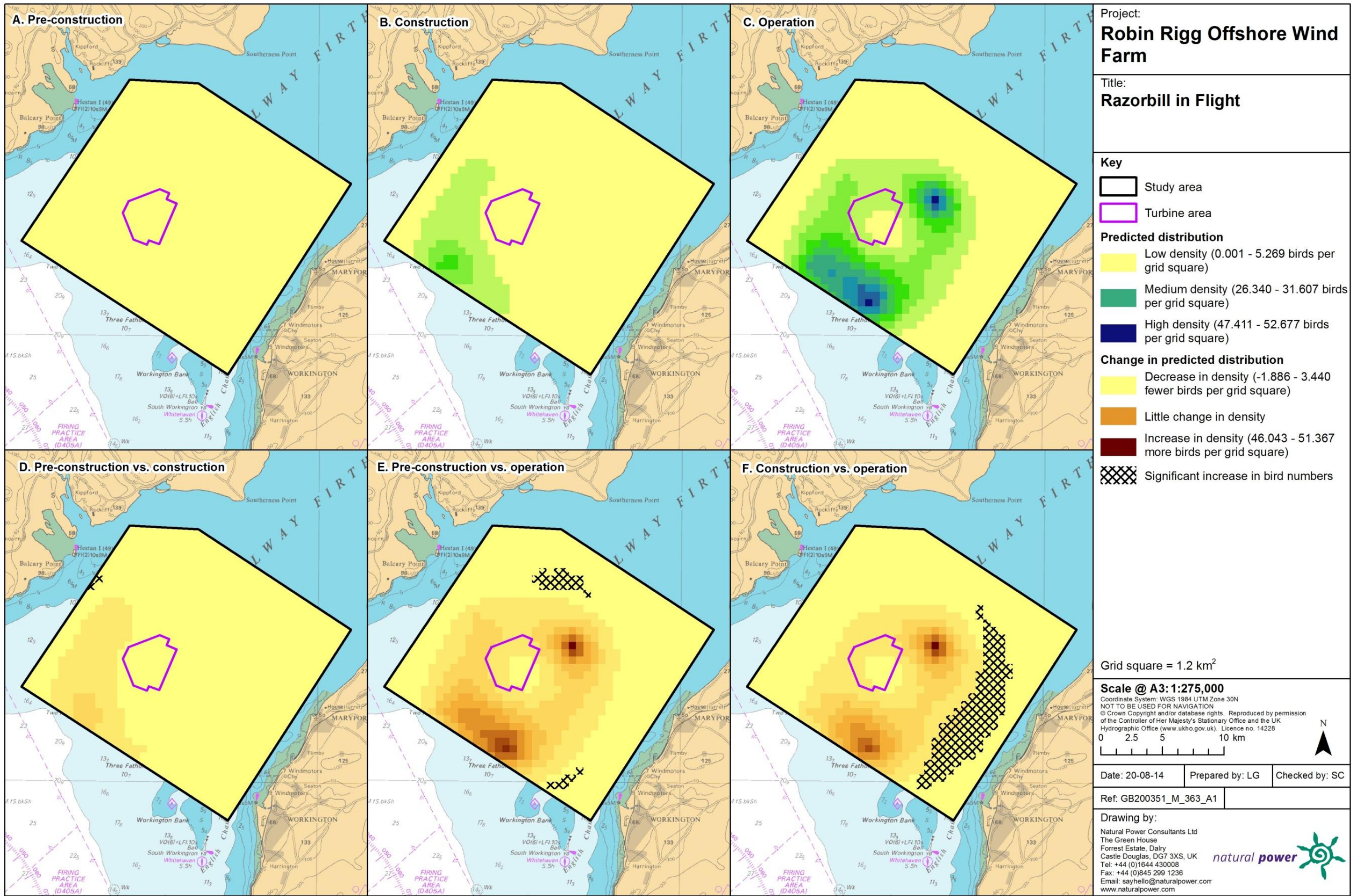


Figure 2.112: Predicted density of razorbills in flight during a) pre-construction, b) construction and c) operational monitoring. Changes in predicted density between d) pre-construction and construction, e) pre-construction and operation and f) construction and operation are also shown. Significant differences are marked with diagonal shading.



### 2.4.7.11.32. Collision risk

The percentage of razorbills recorded during the three development phases in different height bands relative to rotor swept height can be found in Table 2.68 and Figure 2.113. A chi-squared test was not undertaken since no flights were recorded at rotor swept height, indicating that razorbills are not at risk from collision at Robin Rigg OWF.

**Table 2.68:** Percentage of razorbills recorded in different flight height bands across the three development phases: pre-construction, construction and operational years one and two. Shaded column indicates percentage at rotor swept height (flight band 4).

Phase	Flight height band					
	1 (0–5 m)	2 (6–25 m)	3 (26–34 m)	4 (35–125 m)	5 (126–200 m)	6 (>200 m)
Pre-construction	99.56	0.44	0.00	0.00	0.00	0.00
Construction	96.32	3.68	0.00	0.00	0.00	0.00
Operation	94.44	5.56	0.00	0.00	0.00	0.00

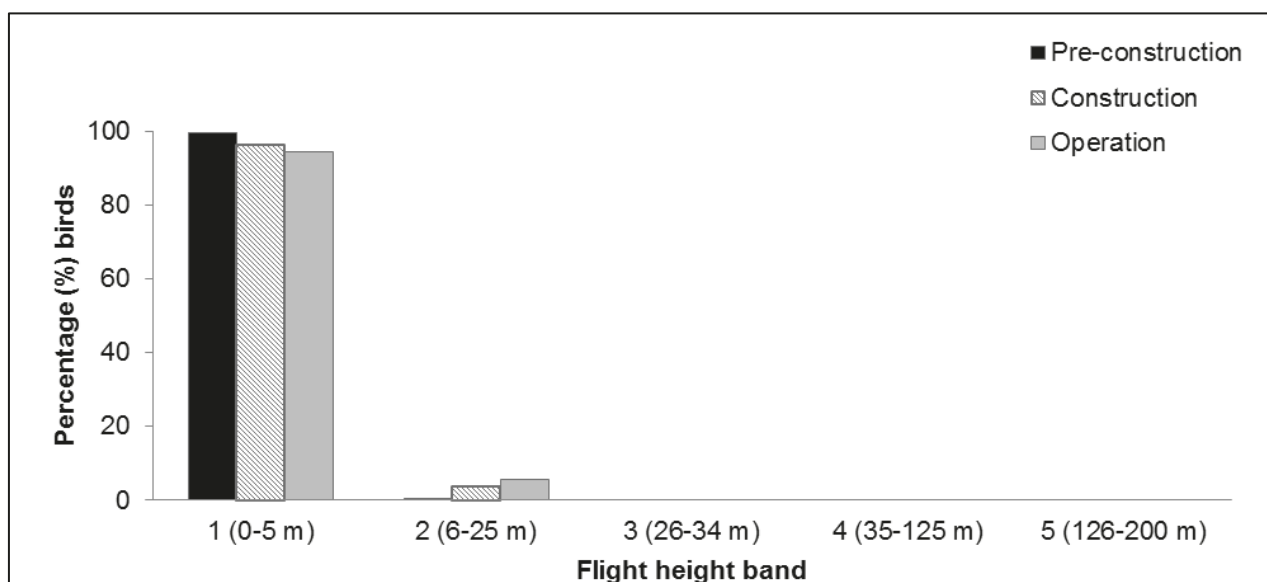


**Figure 2.113:** Percentage of razorbills recorded in different flight height bands across the three development phases: pre-construction, construction and operational years one and two.



## 2.4.7.12. Across operational years

### 2.4.7.12.33. Summary statistics

Razorbill numbers fluctuated throughout operational monitoring with larger numbers recorded in operational years two and three compared to operational years one and four (Table 2.69). However, the number of individuals recorded per km of survey effort was similar throughout operational years one to four, with an average of approximately three razorbills per observation (Table 2.69).

**Table 2.69: Number of razorbills recorded per block during each operational year per km survey effort (all data).**

	Operational year 1		Operational year 2		Operational year 3		Operational year 4	
	On sea	In flight	On sea	In flight	On sea	In flight	On sea	In flight
<b>Total number individuals</b>	568	23	1,016	355	1,161	51	595	68
<b>Total number sightings</b>	218	18	303	80	372	35	265	44
<b>Number individuals/km</b>	0.31	0.01	0.50	0.17	0.54	0.02	0.27	0.03
	Total		Total		Total		Total	
<b>Total number individuals</b>	591		1,371		1,212		663	
<b>Total number sightings</b>	236		383		407		309	
<b>Number individuals/km</b>	0.33		0.67		0.56		0.30	

Data were filtered as described in the methodology (Section 2.4.4). The percentage of segments without observations was calculated to ensure there were sufficient data to perform the analysis (Table 2.70). Data were also checked to ensure observations were recorded in all months of the year.

**Table 2.70: Percentage of razorbill analysis blocks without observations across operational years one to four. Zero inflation prior to removal of effort is presented in parentheses.**

	On sea	In flight
<b>Percentage zero blocks</b>	92.2%	(99.3%) 99.1%

#### 2.4.7.12.34. Density and distribution

##### 2.4.7.12.34.1. On sea

A hazard-rate detection function with sea state and cluster size as covariate was found to be the best fitting model for razorbills during the three development phases. Figure 2.114 shows the selected detection curve for razorbills.

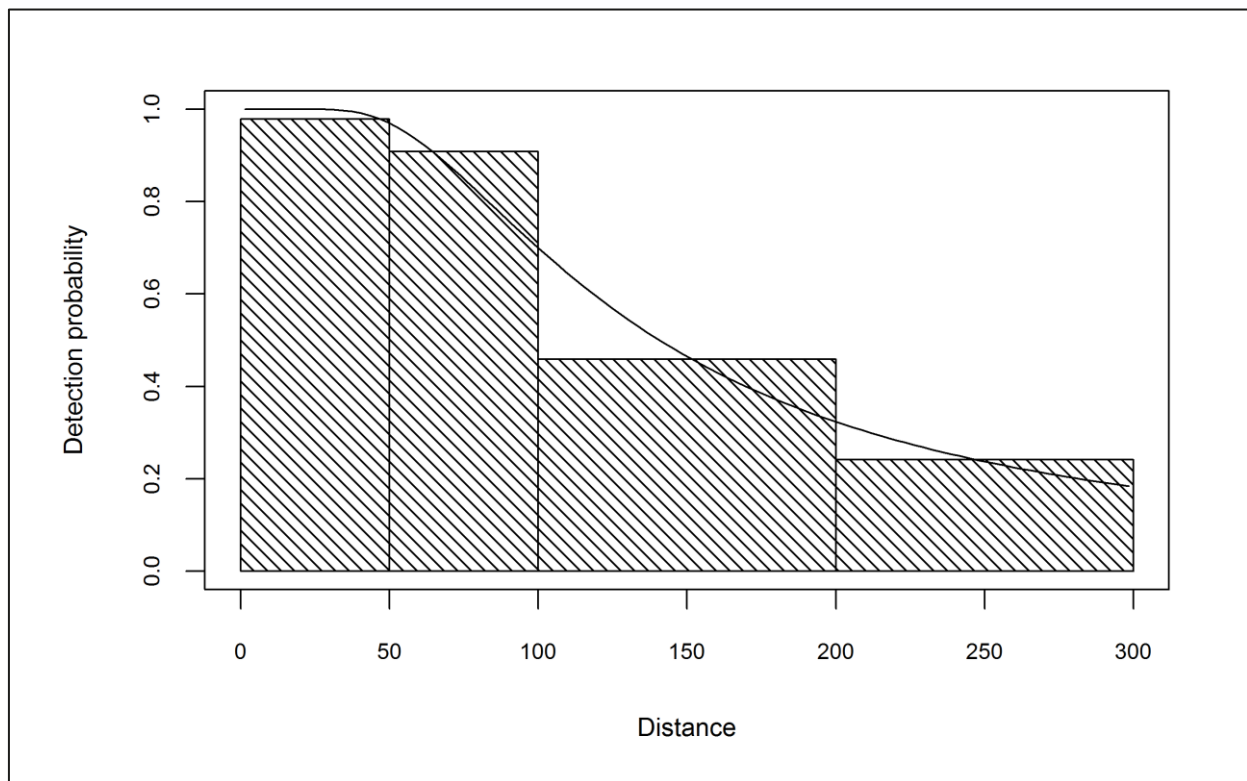


Figure 2.114: Detection curve used to adjust razorbill on sea counts for imperfect detection across operational years one to four.

Initial data exploration of adjusted razorbill numbers indicated that there were no outlying observations which may influence the modelling process (Figure 2.115).

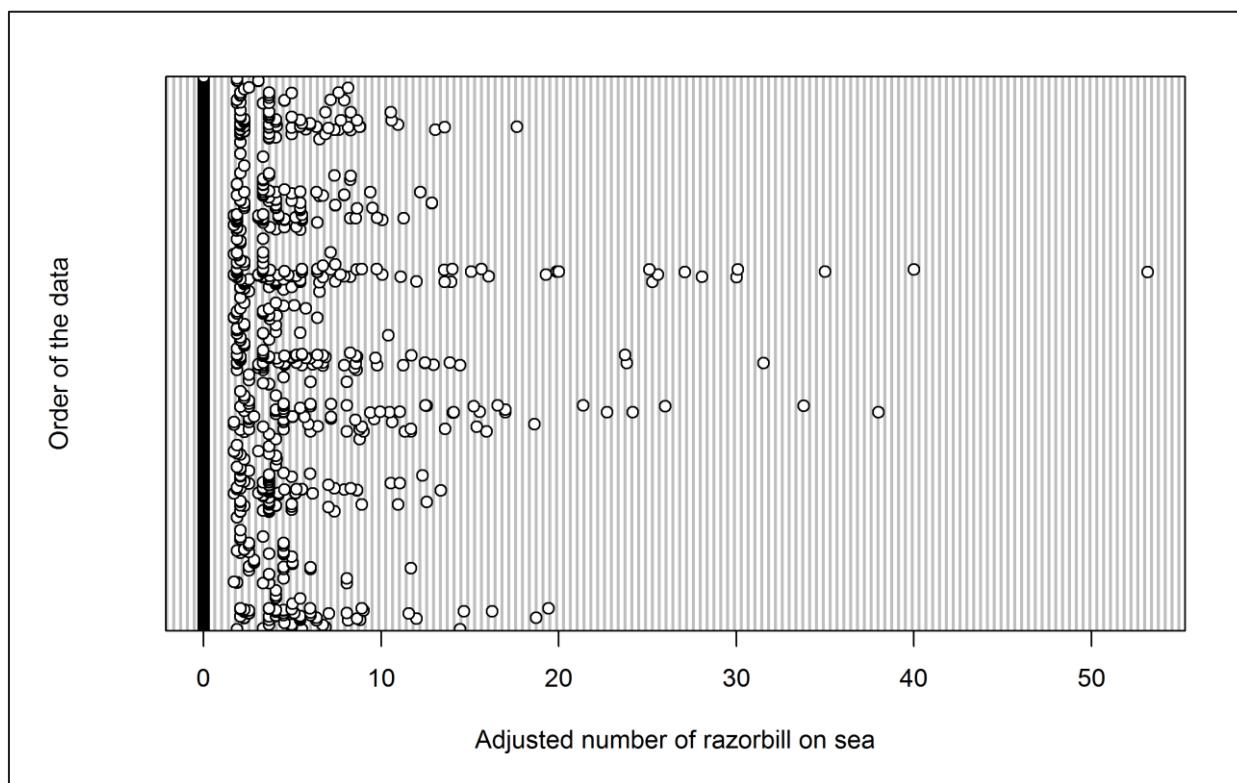


Figure 2.115: Dot plot of the number of razorbills observed on sea per analysis block across operational years one to four.

The GEE predicted that month, tidal height and location all had a statistically significant influence on razorbill abundance within the survey area (Table 2.71). Operational year had no effect of razorbill densities (Figure 2.116). The influence of month indicated statistically significant increases in spring (March and April) and autumn (October and November; Figure 2.117). Since razorbill numbers peaked in November, model predictions were made for this month.

Table 2.71: Final model outputs for razorbills on the sea across operational years one to four.

Term	Marginal p-value
Month	<0.0001
Phase	0.1178
Tide height	<0.0001
Location (X,Y)	<0.0001
Interaction (location: phase)	0.2380

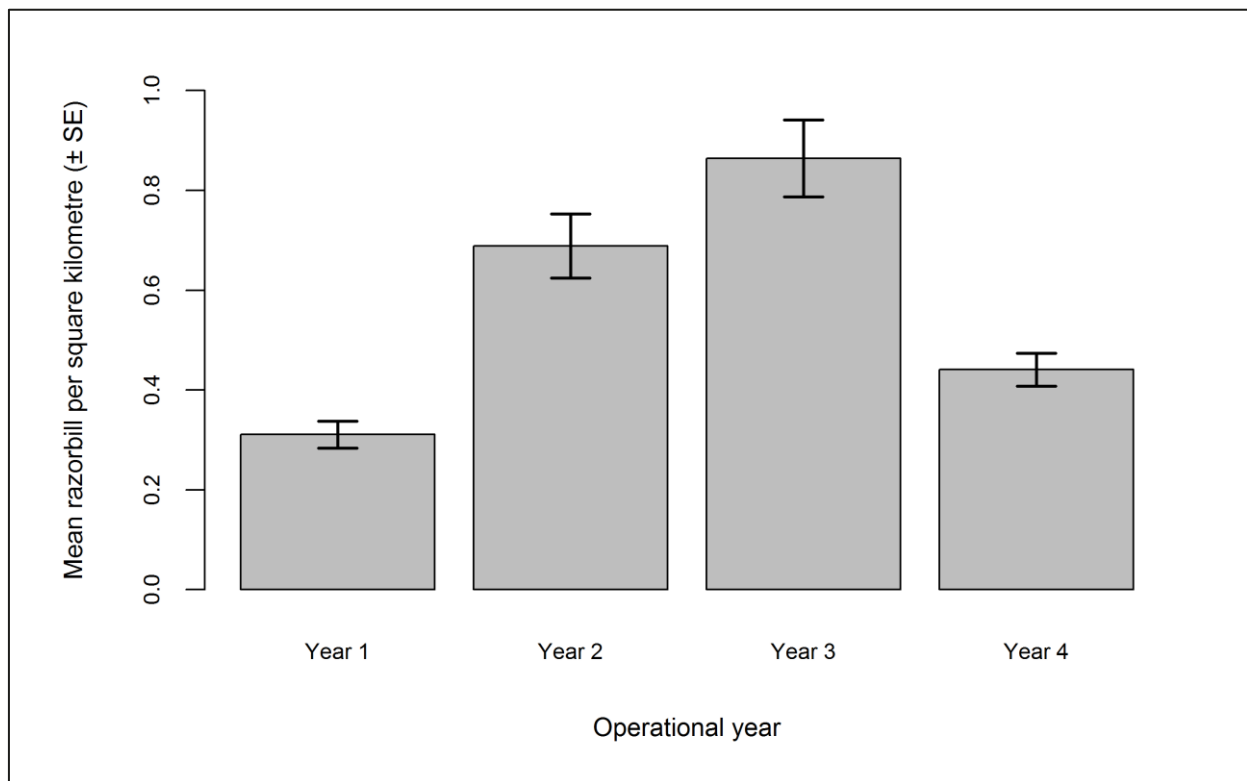


Figure 2.116: Mean density (± se) of razorbills recorded on the sea across operational years one to four.

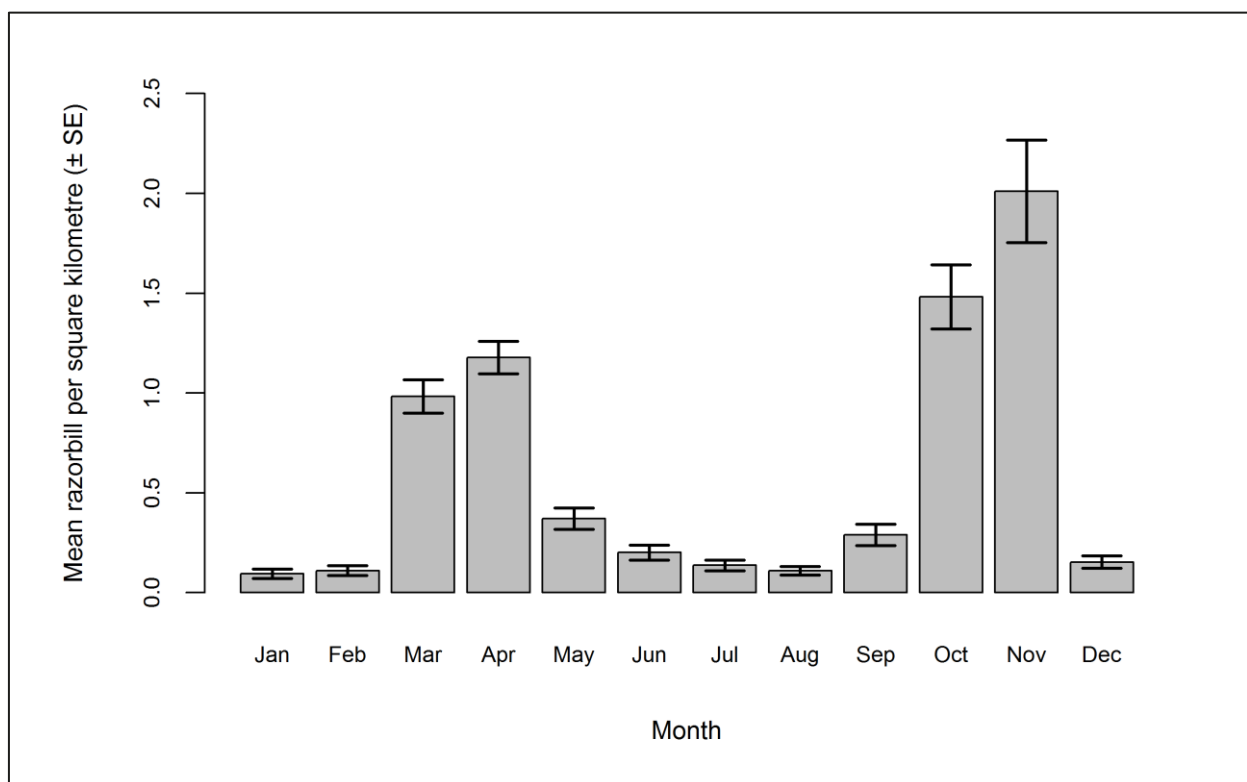


Figure 2.117: Mean density (± se) of razorbills recorded on the sea during each month across operational years one to four.



Predicted razorbill abundance and density (by site, buffer and total survey area) are presented in Table 2.72. There was little change in razorbill abundance and density during successive operational years, as is reflected in the density surface maps. The percentage of razorbills predicted to occur within Robin Rigg OWF itself was also comparable across operational years (Table 2.72).

**Table 2.72: Abundance and density of razorbills on the sea across operational years one to four. Values in parentheses represent upper and lower 95% confidence intervals.**

Operational year	Abundance			Density			% within site
	Site	Buffer	Total	Site	Buffer	Total	
<b>1</b>	6 (1-25)	94 (25-324)	100 (26-349)	0.49 (0.10-1.95)	0.27 (0.07-0.93)	0.28 (0.07-0.97)	6.29
<b>2</b>	5 (1-17)	85 (26-279)	90 (28-295)	0.39 (0.10-1.29)	0.24 (0.08-0.80)	0.25 (0.08-0.82)	5.54
<b>3</b>	4 (1-14)	91 (25-294)	94 (26-308)	0.28 (0.08-1.06)	0.26 (0.07-0.85)	0.26 (0.07-0.85)	3.91
<b>4</b>	5 (1-13)	67 (19-200)	72 (21-213)	0.35 (0.10-1.02)	0.19 (0.06-0.58)	0.20 (0.06-0.59)	6.27

There were no statistically significant changes in predicted razorbill abundance or distribution across operational years, with the exception of a significant decrease between operational years three and four towards the south of the OWF (Figure 2.118 and Figure 2.119).

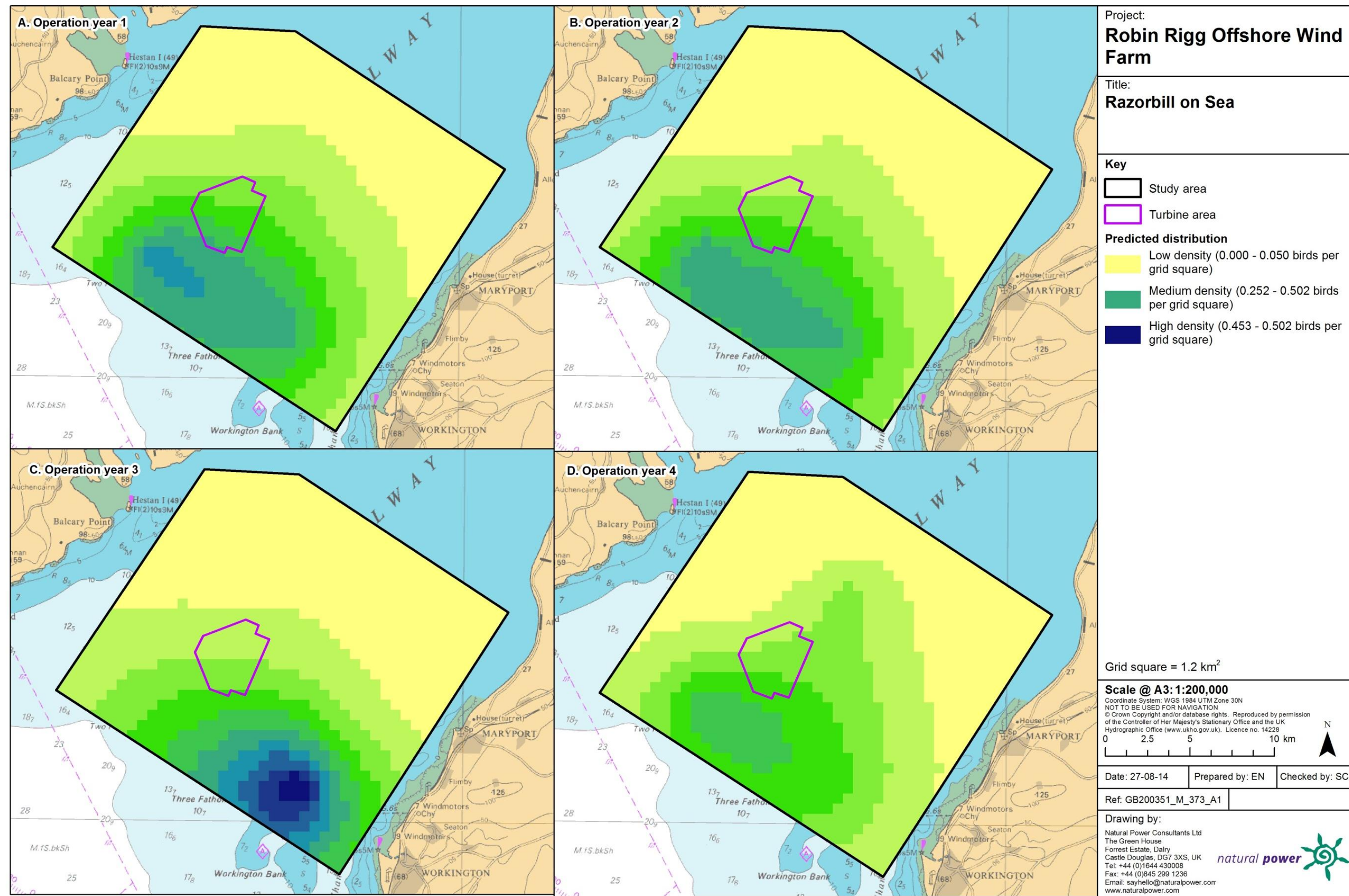


Figure 2.118: Predicted density of razorbills on the sea during a) operational year one, b) operational year two, c) operational year three and d) operational year four.



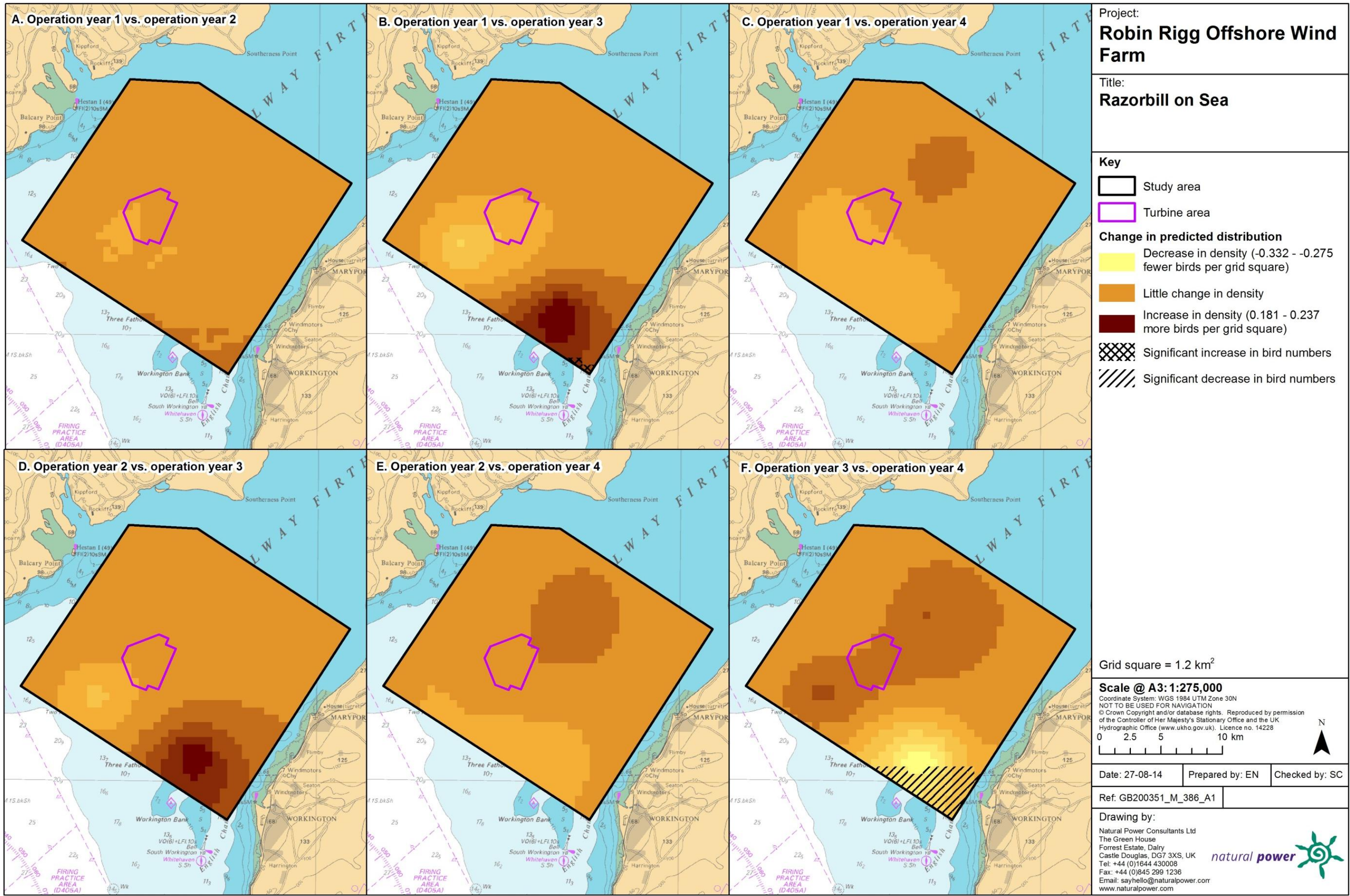
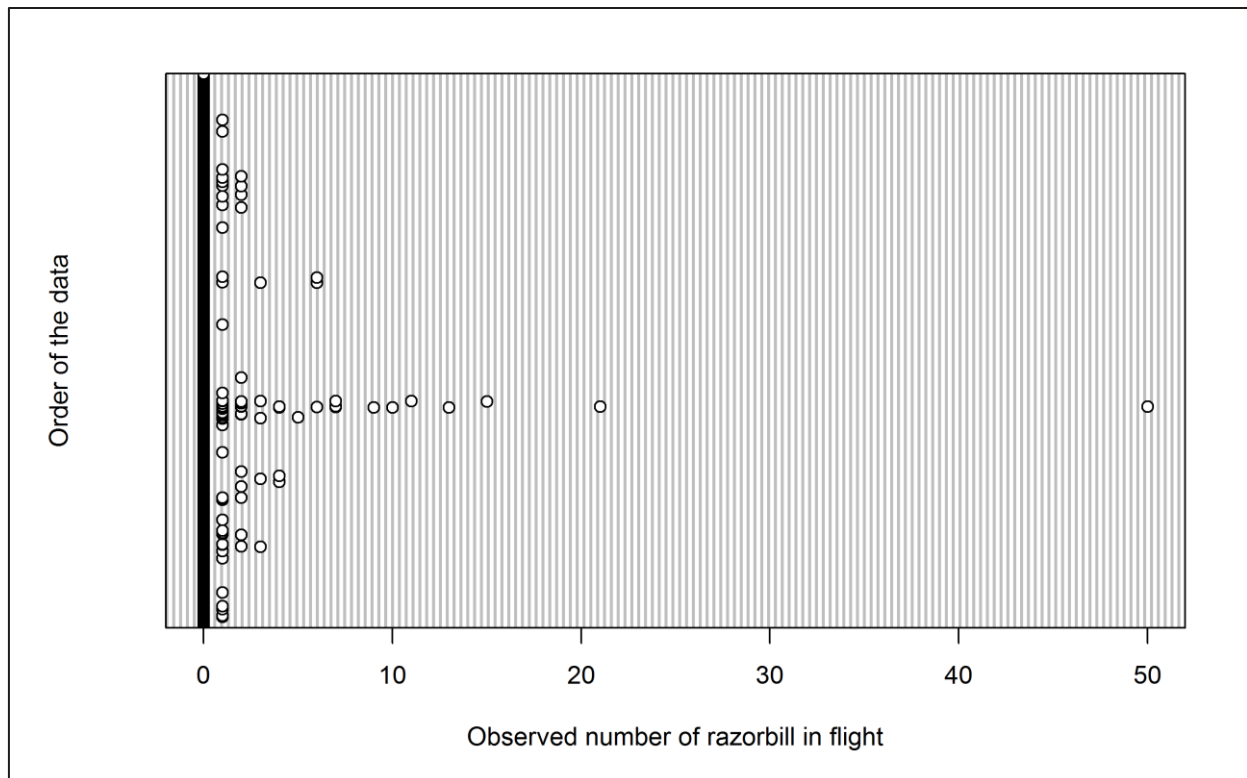


Figure 2.119: Differences in predicted sitting razorbill density between operational years. Significant differences are marked with diagonal shading.



#### 2.4.7.12.34.2. In flight

Initial data exploration highlighted that >99% of analysis blocks for razorbills in flight during the four operational years contained zero observations (Figure 2.120). Since very few flying razorbills were observed between June and September as birds moved offshore post-breeding, data was removed for these months in order to reduce the number of zero observations. However, even after removal of these months, 99.1% of analysis blocks still contained zero observations (Table 2.69). Therefore, further modelling of razorbills in flight across the four operational years was not undertaken and raw data are presented.



**Figure 2.120: Dot plot of the number of razorbills observed in flight per analysis block across operational years one to four.**

Most observations were of single birds with 50 being the maximum group size. Mean density of razorbills was largest during operational year two, with similar small densities recorded during other operational years (Figure 2.121). However, since further modelling was not undertaken, the significance of any differences could not be tested. Figure 2.122 shows an increase in flying razorbills in the autumn, peaking in November before dropping in December.



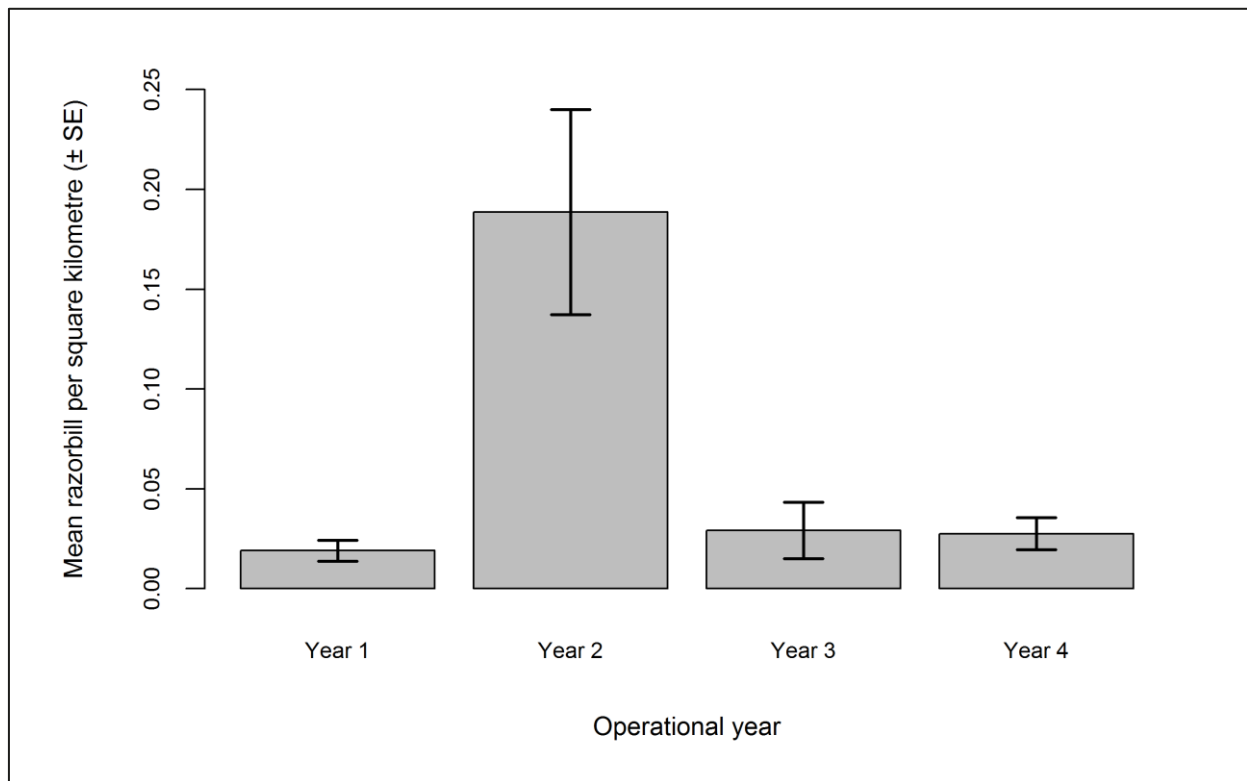


Figure 2.121: Mean density (± se) of razorbills recorded in flight across operational years one to four.

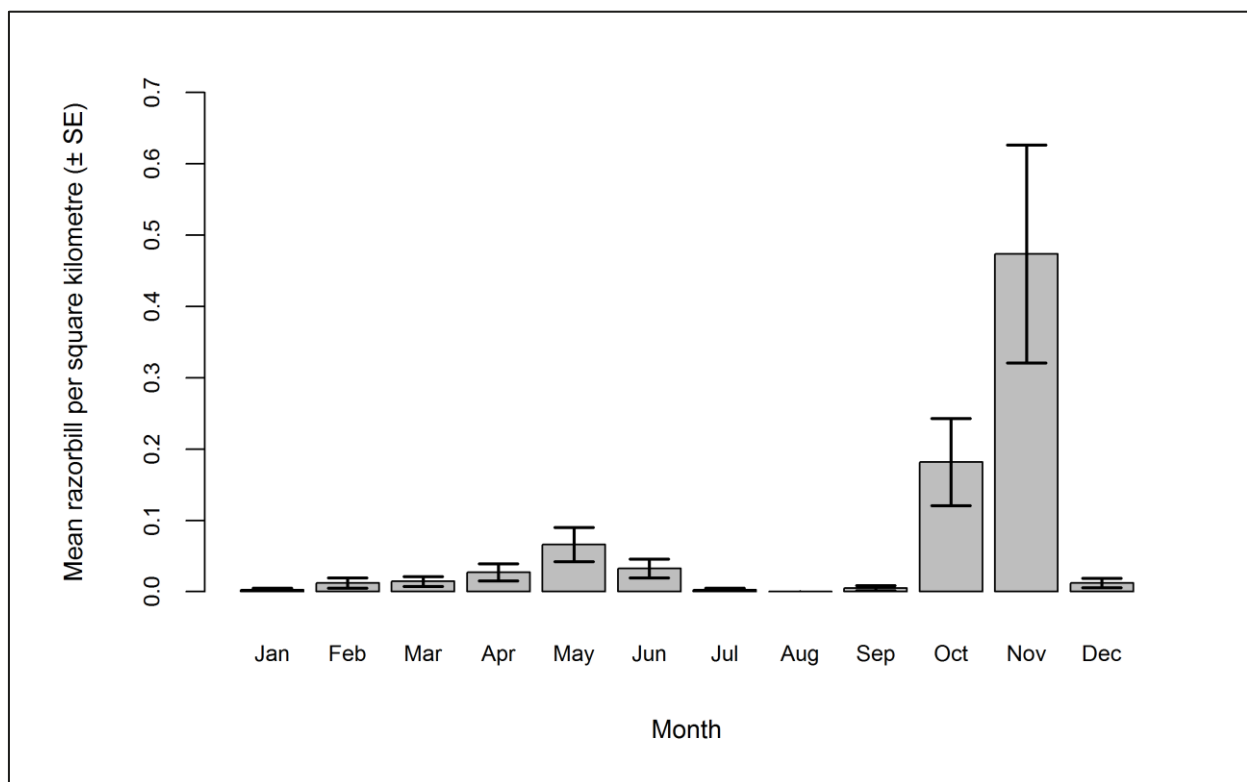


Figure 2.122: Mean density (± se) of razorbills recorded in flight during each month across operational years one to four.

### 2.4.7.12.35. Collision risk

The percentage of razorbills recorded during the four operational years in different height bands relative to rotor swept height can be found in Table 2.73 and Figure 2.123. A chi-squared test was not undertaken since no flights were recorded at rotor swept height, indicating that razorbills are not at risk from collision at Robin Rigg OWF.

**Table 2.73: Percentage of razorbills recorded in different flight height bands across operational years one to four. Shaded column indicates percentage at rotor swept height (flight band 4).**

Operational year	Flight height band					
	1 (0–5 m)	2 (6–25 m)	3 (26–34 m)	4 (35–125 m)	5 (126–200 m)	6 (>200 m)
1	100.00	0.00	0.00	0.00	0.00	0.00
2	94.08	5.92	0.00	0.00	0.00	0.00
3	98.04	1.96	0.00	0.00	0.00	0.00
4	82.35	11.76	5.88	0.00	0.00	0.00

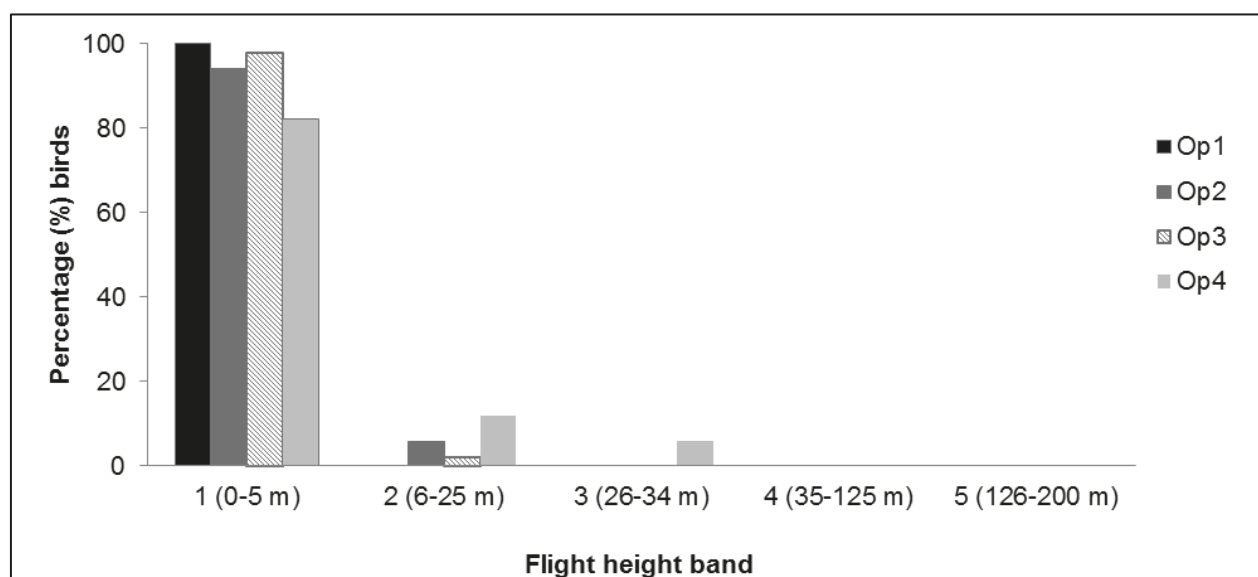


**Figure 2.123: Percentage of razorbills recorded in different flight height bands across operational years one to four.**

## 2.4.8. Guillemot

### 2.4.8.13. Across three development phases

#### 2.4.8.13.36. Summary statistics

Guillemot numbers were relatively high across the three development phases, with the largest number of individuals recorded during construction (Table 2.74). Conversely, the number of individuals recorded per km of effort was lowest during the construction phase. The majority (c. 90%) of guillemots recorded were on the sea throughout the three development phases (Table 2.74).

**Table 2.74: Number of guillemot recorded per block during each development phase per km survey effort (all data).**

	Pre-construction		Construction		Operation years 1-2	
	On sea	In flight	On sea	In flight	On sea	In flight
<b>Total number individuals</b>	3,689	334	5,107	618	3,517	462
<b>Total number sightings</b>	2,122	248	3,671	497	2,249	318
<b>Number individuals/km</b>	1.04	0.09	0.70	0.08	0.91	0.12
	Total		Total		Total	
<b>Total number individuals</b>	4,023		5,725		3,979	
<b>Total number sightings</b>	2,370		4,168		2,567	
<b>Number individuals/km</b>	1.13		0.79		1.03	

Data were filtered as described in the methods (Section 2.4.4). The percentage of segments without observations was calculated to ensure there were sufficient data to perform the analysis (Table 2.75). Data were also checked to ensure observations were recorded in all months of the year.

**Table 2.75: Percentage of guillemot analysis blocks without observations across the three development phases: pre-construction, construction and operational years one and two. Zero inflation prior to removal of effort is presented in parentheses.**

	On sea	In flight
<b>Percentage zero blocks</b>	68.3%	(96.4%) 95.9%

### 2.4.8.13.37. Density and distribution

#### 2.4.8.13.37.1. On sea

A hazard-rate detection function with cluster size as a covariate was found to be the best fitting model. Figure 2.124 shows the selected detection curve for guillemots during the three development phases.

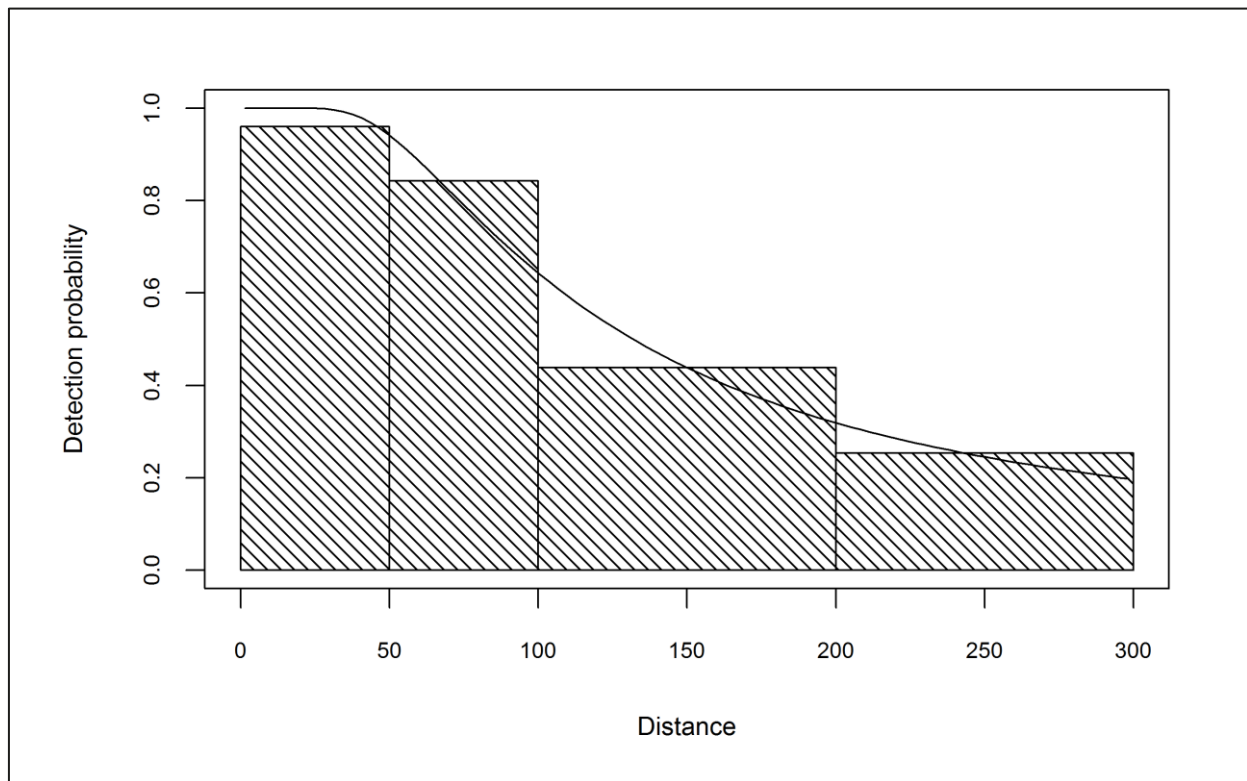


Figure 2.124: Detection curve used to adjust guillemot on sea counts for imperfect detection across the three development phases: pre-construction, construction and operational years one and two.

Initial data exploration of adjusted guillemot numbers indicated that there were no outlying observations which may influence the modelling process (Figure 2.125).



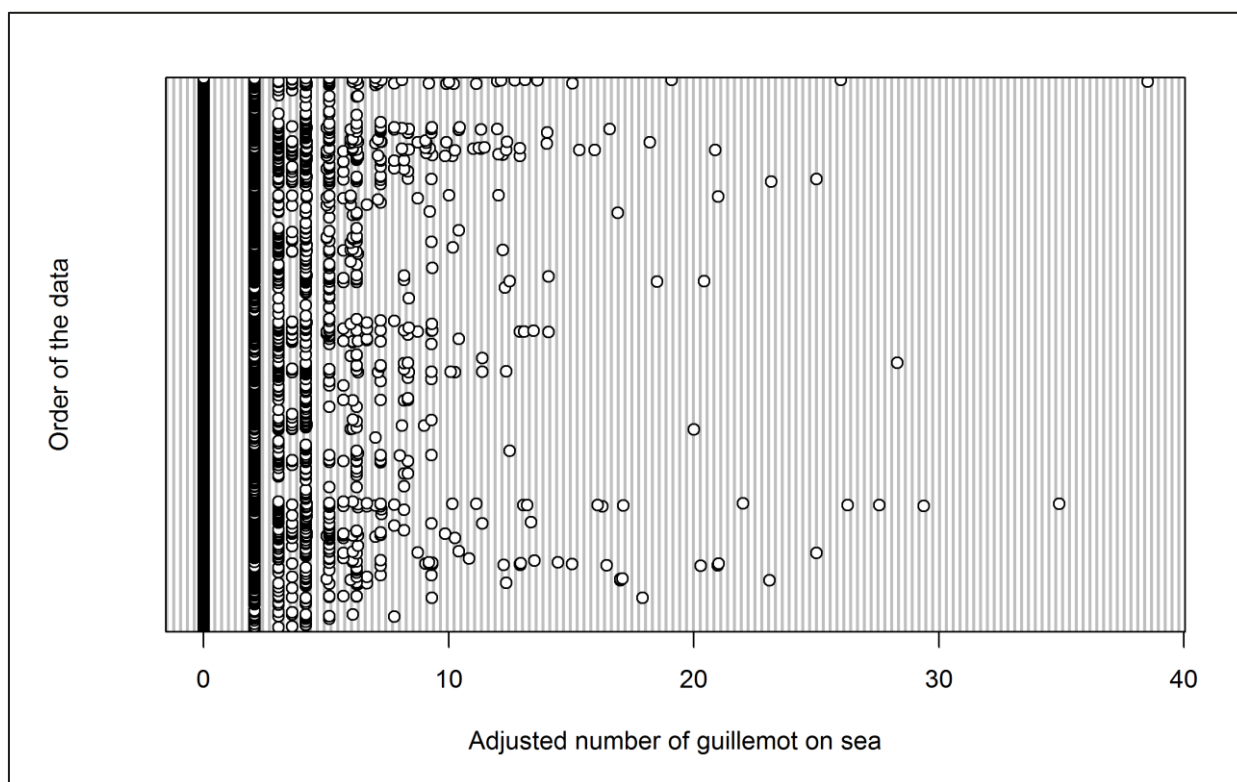


Figure 2.125: Dot plot of the number of guillemots observed on sea per analysis block across the three development phases: pre-construction, construction and operational years one and two.

The GEE predicted that month, phase, tidal height, location and the interaction between location and phase all had a statistically significant influence of guillemot abundance within the survey area (Table 2.76). Specifically, smaller numbers were observed during the construction phase (Figure 2.126), and higher numbers during the month of July (Figure 2.127). Since July was the month of peak activity, model predictions were made for this month.

Table 2.76: Final model outputs for guillemots on the sea across the three development phases: pre-construction, construction and operational years one and two.

Term	Marginal p-value
Month	<0.0001
Phase	0.0001
Tide height	0.0019
Location (X,Y)	<0.0001
Interaction (location: phase)	0.0091

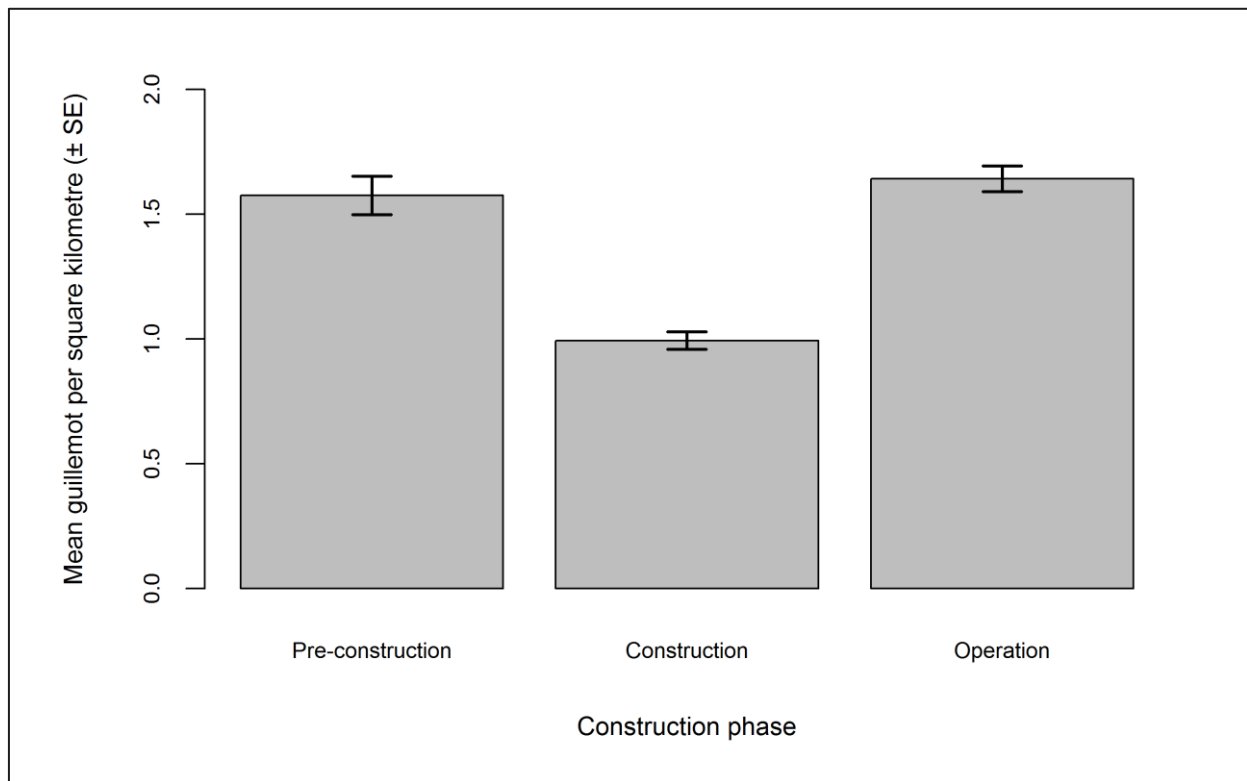


Figure 2.126: Mean density ( $\pm$  se) of guillemots recorded on the sea across the three development phases: pre-construction, construction and operational years one and two.

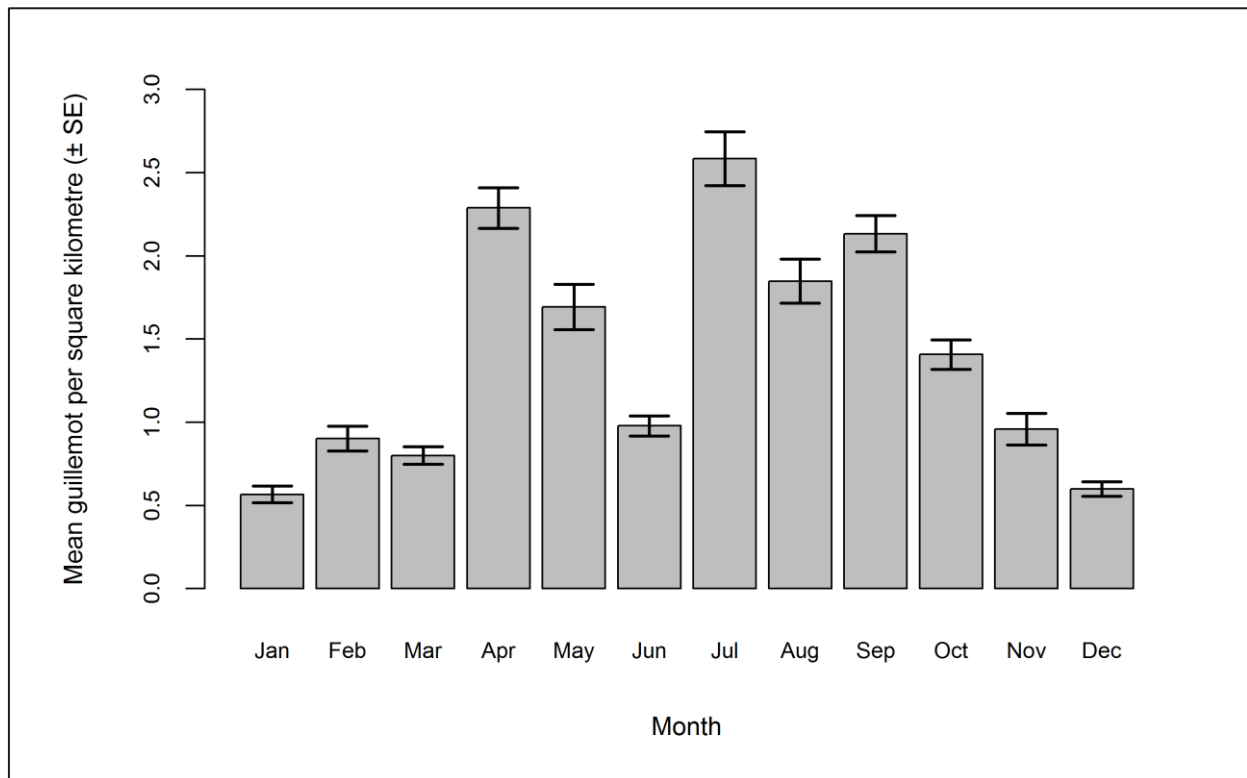


Figure 2.127: Mean density ( $\pm$  se) of guillemots recorded on the sea during each month across the three development phases: pre-construction, construction and operational years one and two.

Predicted guillemot abundance and densities (by site, buffer and total survey area) are presented in Table 2.77. Guillemot numbers increased across the three development phases, peaking during the operational phase. Larger percentages of guillemots were predicted to be using the Robin Rigg OWF itself during both the construction and operational years (Table 2.77).

**Table 2.77: Abundance and density of guillemots on the sea across the three development phases: pre-construction, construction and operational years one and two. Values in parentheses represent upper and lower 95% confidence intervals.**

Phase	Abundance			Density			% within site
	Site	Buffer	Total	Site	Buffer	Total	
<b>Pre-construction</b>	50 (24-98)	1,209 (625-2,201)	1,259 (649-2,299)	3.87 (1.82-7.59)	3.48 (1.80-6.37)	3.49 (1.80-6.37)	3.97
<b>Construction</b>	144 (75-312)	2,339 (1,334-4,182)	2,483 (1,409-4,494)	11.15 (5.76-24.10)	6.72 (3.90-12.46)	6.88 (3.90-12.46)	5.81
<b>Operation</b>	181 (85-400)	2,927 (1,456-5,879)	3,108 (1,541-6,279)	14.00 (6.60-30.94)	8.41 (4.19-16.90)	8.61 (4.27-17.40)	5.83

Significant increases in predicted guillemot densities were observed across the survey area between pre-construction and operational phases (Figure 2.128). These predicted increases were concentrated in the deep waters to the west of the survey area (Figure 2.128).



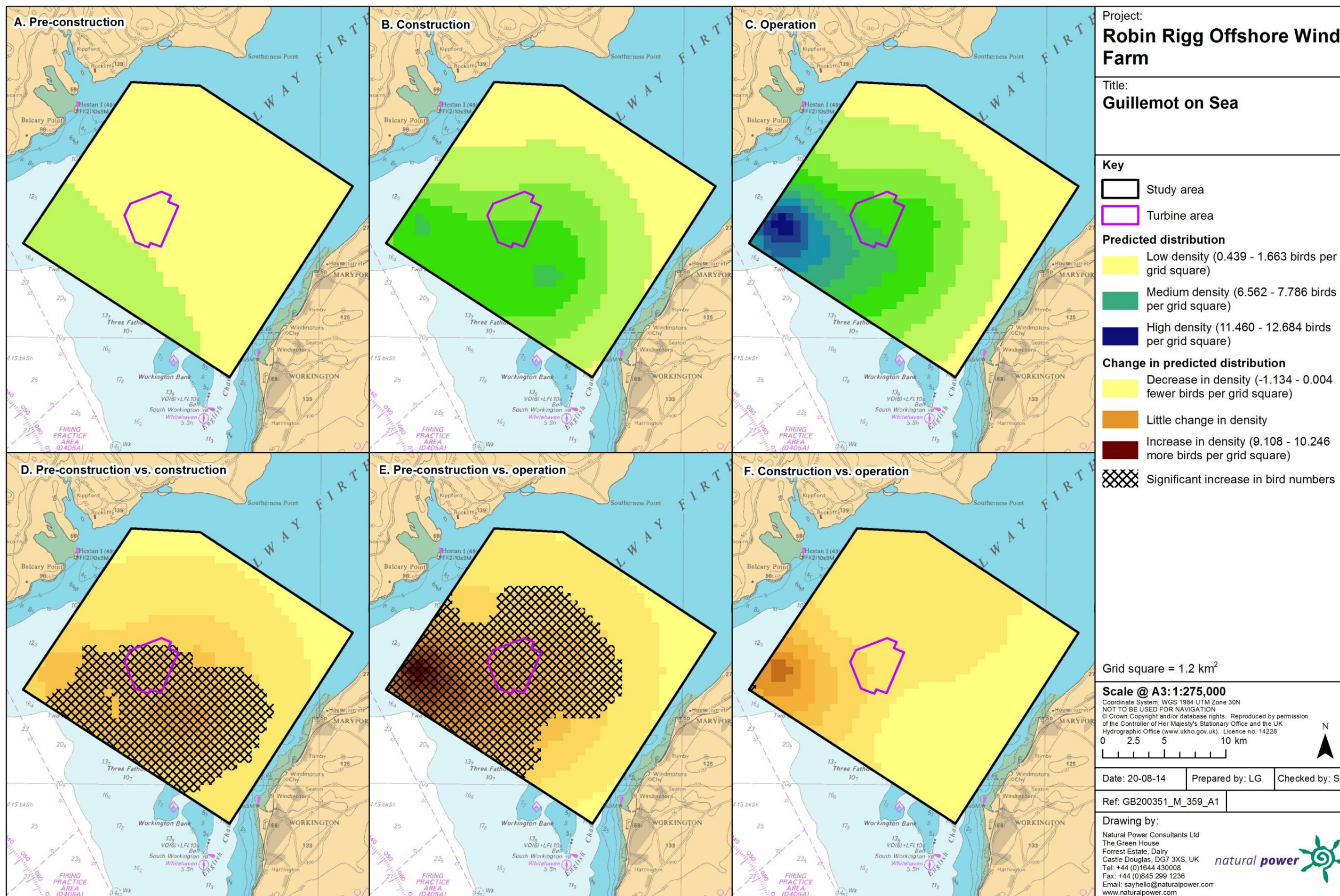


Figure 2.128: Predicted density of guillemots on the sea during a) pre-construction, b) construction and c) operational monitoring. Changes in predicted density between d) pre-construction and construction, e) pre-construction and operation and f) construction and operation are also shown. Significant differences are marked with diagonal shading.



### 2.4.8.13.37.2. In flight

Small numbers of guillemots were recorded in flight during August and September, as birds are flightless during their post-breeding moult. These two months of effort were therefore removed from the analysis. Initial data exploration of this refined dataset highlighted two outliers (segments containing 15 birds each were recorded in March 2010 and January 2011) that may influence the modelling process (Figure 2.129). As a result the model was run with and without these outliers and the outputs compared.

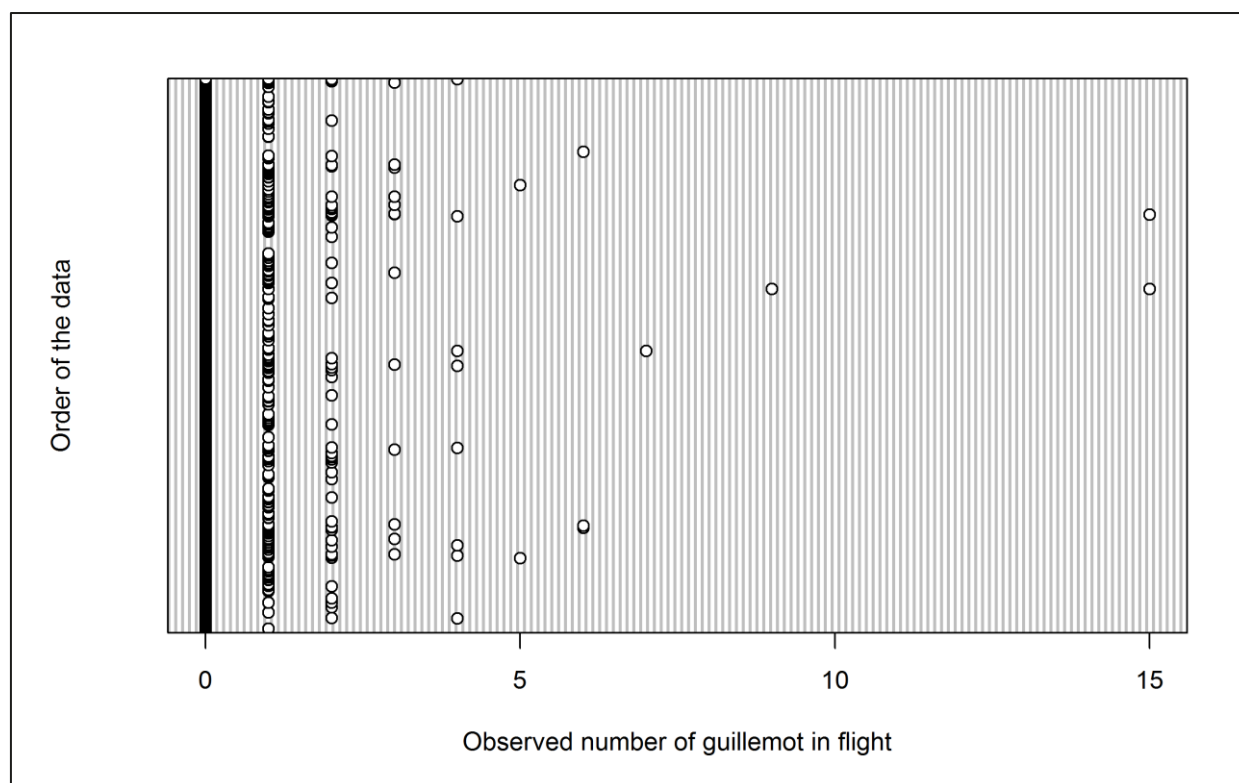


Figure 2.129: Dot plot of the number of guillemots observed in flight per analysis block across the three development phases: pre-construction, construction and operational years one and two.

P-values remained the same after removing the outliers for all variables. Density surfaces for both models were also very similar; therefore outputs from the model including the outliers are presented here.

The GEE predicted that location had a statistically significant influence on predicted flying guillemot abundance within the survey area (Table 2.78). Development phase was not statistically significant (Figure 2.130) and neither was month (Figure 2.131). Since June was the month of peak activity, model predictions were made for this month.

Table 2.78: Final model outputs for guillemots in flight across the three development phases: pre-construction, construction and operational years one and two.

Term	Marginal p-value
Month	0.0635
Phase	0.1088
Tide height	0.0511
Location (X,Y)	<0.0001
Interaction (location: phase)	0.0813



Figure 2.130: Mean density ( $\pm$  se) of guillemots recorded in flight across the three development phases: pre-construction, construction and operational years one and two.

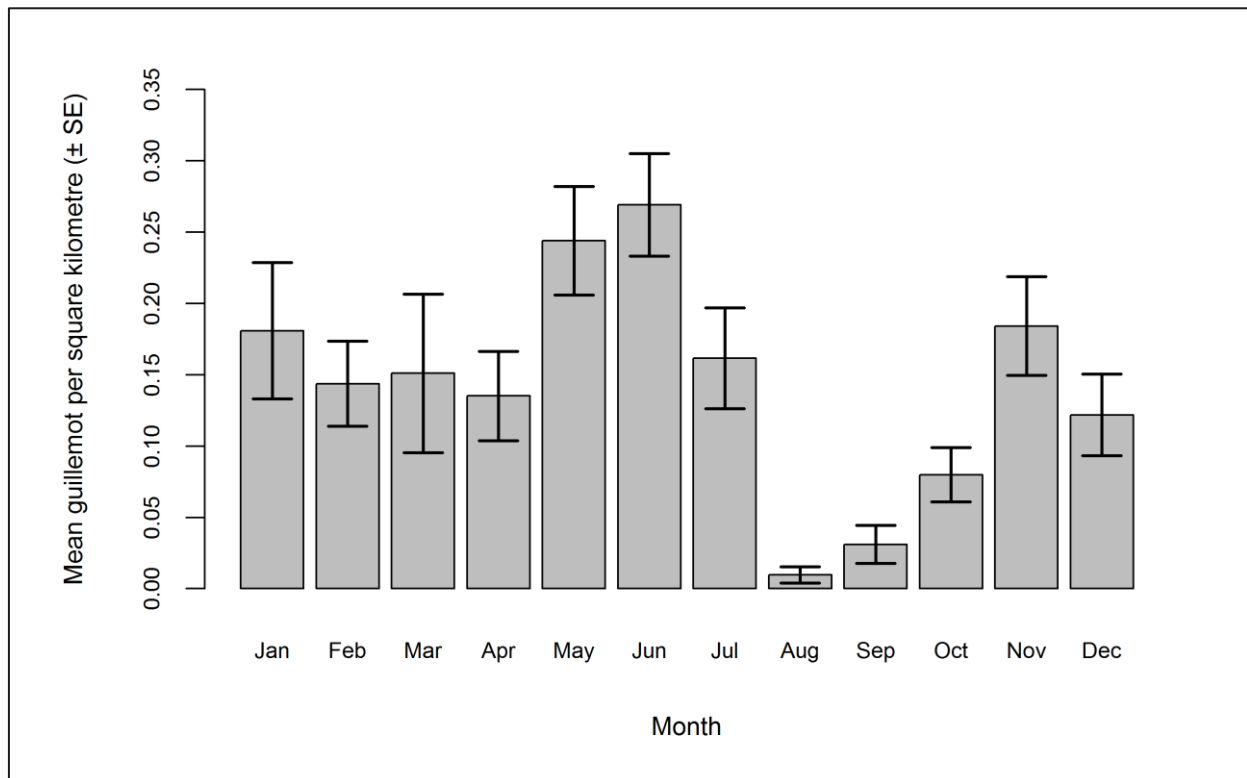


Figure 2.131: Mean density ( $\pm$  se) of guillemots recorded in flight during each month across the three development phases: pre-construction, construction and operational years one and two.

Predicted guillemot abundance and densities (by site, buffer and total survey area) are presented in Table 2.78. Total abundance and density showed an increase across the three development phases, peaking during the operational phase. This is in contrast to Figure 2.130 which shows a decrease in guillemots during construction. This is because predicted abundance and density estimates were based upon median bootstrap values, whilst Figure 2.130 present mean density. Whilst the percentage of guillemots predicted to be using the Robin Rigg OWF itself was similar throughout the three phases, the largest percentage was predicted for the operational phase (Table 2.78).

**Table 2.79: Abundance and density of guillemots in flight across the three development phases: pre-construction, construction and operational years one and two. Values in parentheses represent upper and lower 95% confidence intervals.**

Phase	Abundance			Density			% within site
	Site	Buffer	Total	Site	Buffer	Total	
<b>Pre-construction</b>	2	66	68	0.16	0.19	0.19	3.00
	(1-6)	(25-175)	(26-181)	(0.05-0.47)	(0.07-0.50)	(0.07-0.50)	
<b>Construction</b>	4	118	122	0.34	0.34	0.34	3.59
	(2-14)	(47-317)	(49-331)	(0.12-1.10)	(0.14-0.91)	(0.14-0.92)	
<b>Operation</b>	10	210	220	0.80	0.60	0.61	4.69
	(3-34)	(70-651)	(73-684)	(0.24-2.59)	(0.20-1.87)	(0.20-1.90)	

As shown in Table 2.79, the density surface maps show an increase in flying guillemot density across the three development phases (Figure 2.132). However, while statistically significant, densities were relatively small throughout (Figure 2.132). The largest concentration of guillemots was predicted to occur to the west of Robin Rigg OWF in deeper waters towards to mouth of the Solway Firth, as was predicted for guillemots on the sea (Figure 2.132).



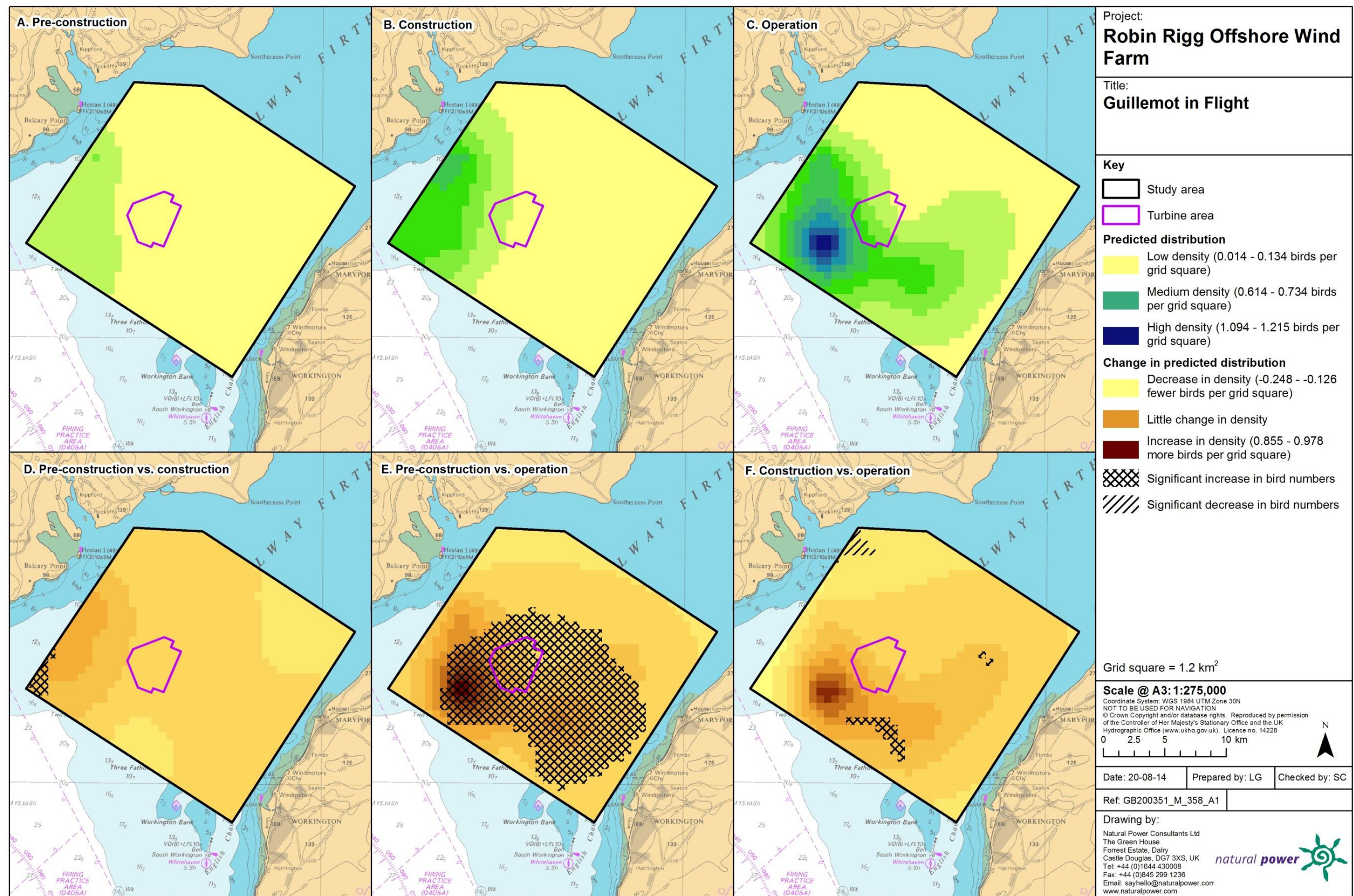


Figure 2.132: Predicted density of guillemots in flight during a) pre-construction, b) construction and c) operational monitoring. Changes in predicted density between d) pre-construction and construction, e) pre-construction and operation and f) construction and operation are also shown. Significant differences are marked with diagonal shading.



#### 2.4.8.13.38. Collision risk

The percentage of guillemots recorded during the three development phases in different height bands relative to rotor swept height can be found in Table 2.80 and Figure 2.133. A chi-squared test was not undertaken since less than 1% of guillemots were recorded at rotor swept height during operational monitoring.

**Table 2.80:** Percentage of guillemots recorded in different flight height bands across the three development phases: pre-construction, construction and operational years one and two. Shaded column indicates percentage at rotor swept height (flight band 4).

Phase	Flight height band					
	1 (0–5 m)	2 (6–25 m)	3 (26–34 m)	4 (35–125 m)	5 (126–200 m)	6 (>200 m)
Pre-construction	98.50	1.50	0.00	0.00	0.00	0.00
Construction	97.41	2.43	0.00	0.16	0.00	0.00
Operation	97.79	2.10	0.00	0.11	0.00	0.00

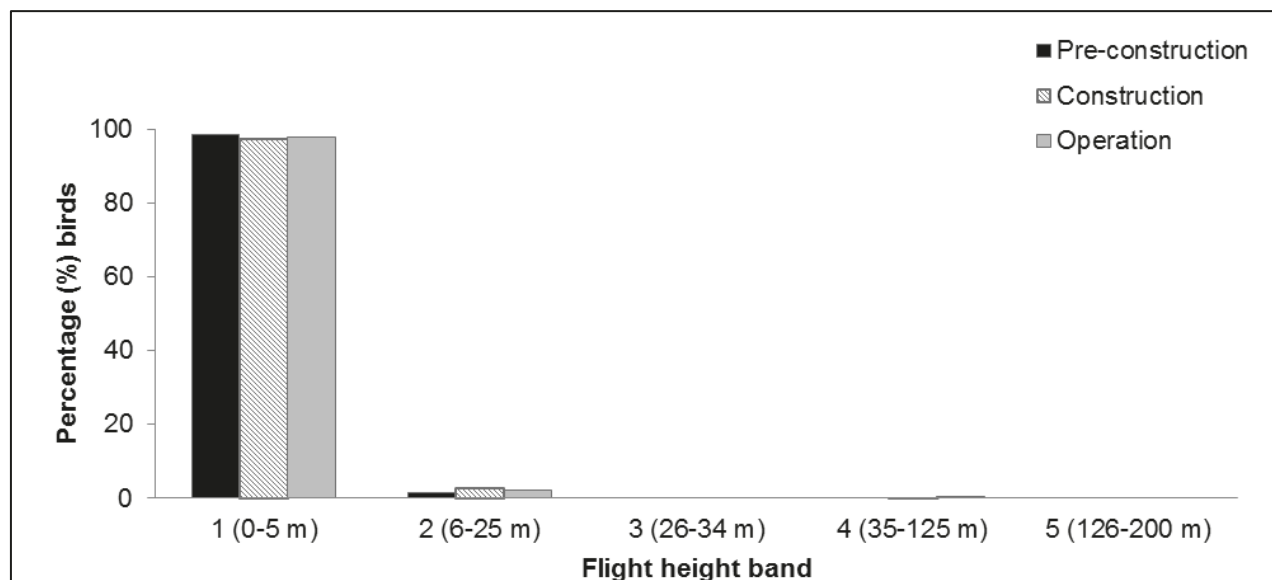


**Figure 2.133:** Percentage of guillemots recorded in different flight height bands across the three development phases: pre-construction, construction and operational years one and two.

## 2.4.8.14. Across operational years

### 2.4.8.14.39. Summary statistics

The total number of guillemots recorded during operational monitoring was similar across all four years, with the largest numbers recorded in operational years two and three, and the smallest numbers recorded in operational year four (Table 2.81). Group size was also comparable throughout operational monitoring (Table 2.81). In all years, the majority of guillemots were recorded on the sea surface (>80%; Table 2.81).

**Table 2.81: Number of guillemot recorded per block during each operational year per km survey effort (all data).**

	Operational year 1		Operational year 2		Operational year 3		Operational year 4	
	On sea	In flight	On sea	In flight	On sea	In flight	On sea	In flight
<b>Total number individuals</b>	1,481	315	2,036	147	1,866	203	1,369	111
<b>Total number sightings</b>	1,006	208	1,243	110	1,100	136	1,009	93
<b>Number individuals/km</b>	0.82	0.17	0.99	0.07	0.86	0.09	0.62	0.05
	Total		Total		Total		Total	
<b>Total number individuals</b>	1,796		2,183		2,069		1,480	
<b>Total number sightings</b>	1,214		1,353		1,236		1,102	
<b>Number individuals/km</b>	0.99		1.06		0.96		0.67	

Data were filtered as described in the methodology (Section 2.4.4). The percentage of segments without observations was calculated to ensure there were sufficient data to perform the analysis (Table 2.82). Data were also checked to ensure observations were recorded in all months of the year.

**Table 2.82: Percentage of guillemot analysis blocks without observations across operational years one to four. Zero inflation prior to removal of effort is presented in parentheses.**

	On sea	In flight
<b>Percentage zero blocks</b>	72.7%	(97.6%) 97.2%

#### 2.4.8.14.40. Density and distribution

##### 2.4.8.14.40.1. On sea

A hazard-rate detection function with cluster size as a covariate was found to be the best fitting model. Figure 2.134 shows the selected detection curve for guillemots during the four operational years.

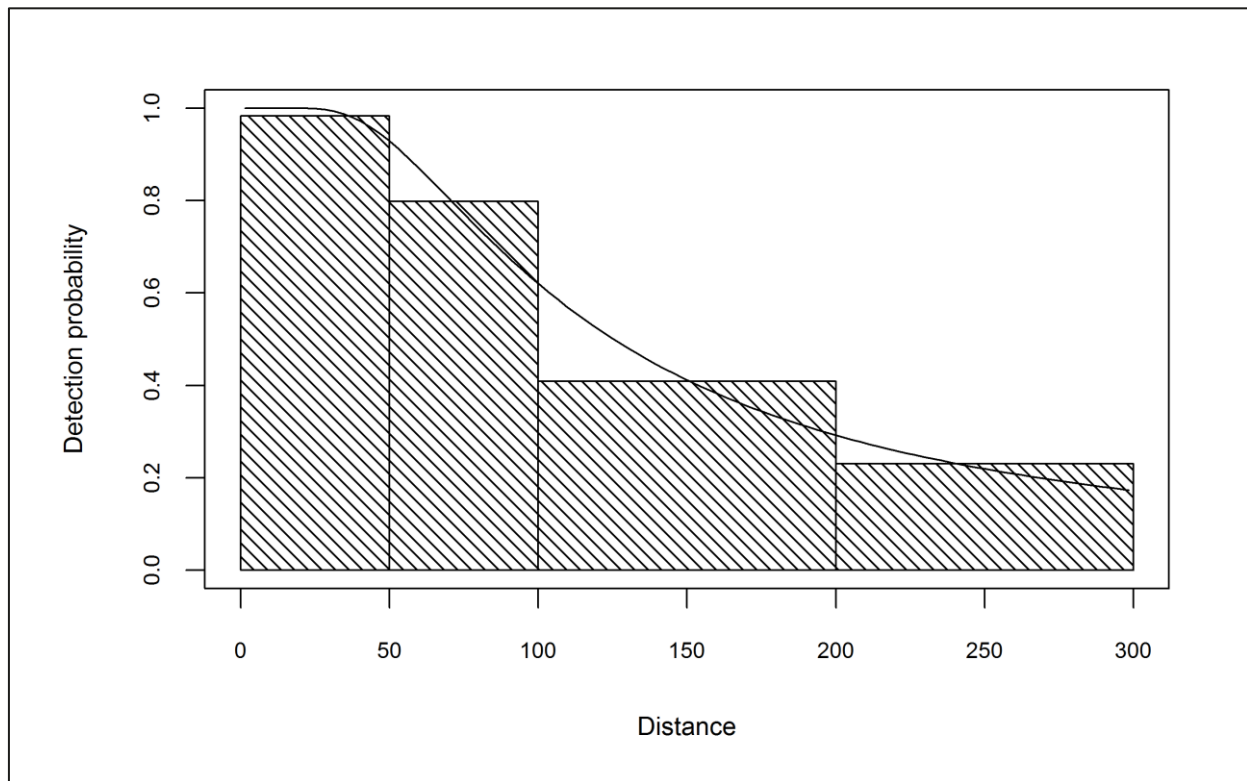


Figure 2.134: Detection curve used to adjust guillemot on sea counts for imperfect detection across operational years one to four.

Initial data exploration of adjusted guillemot numbers indicated that there were no outliers that may influence the modelling process (Figure 2.135).

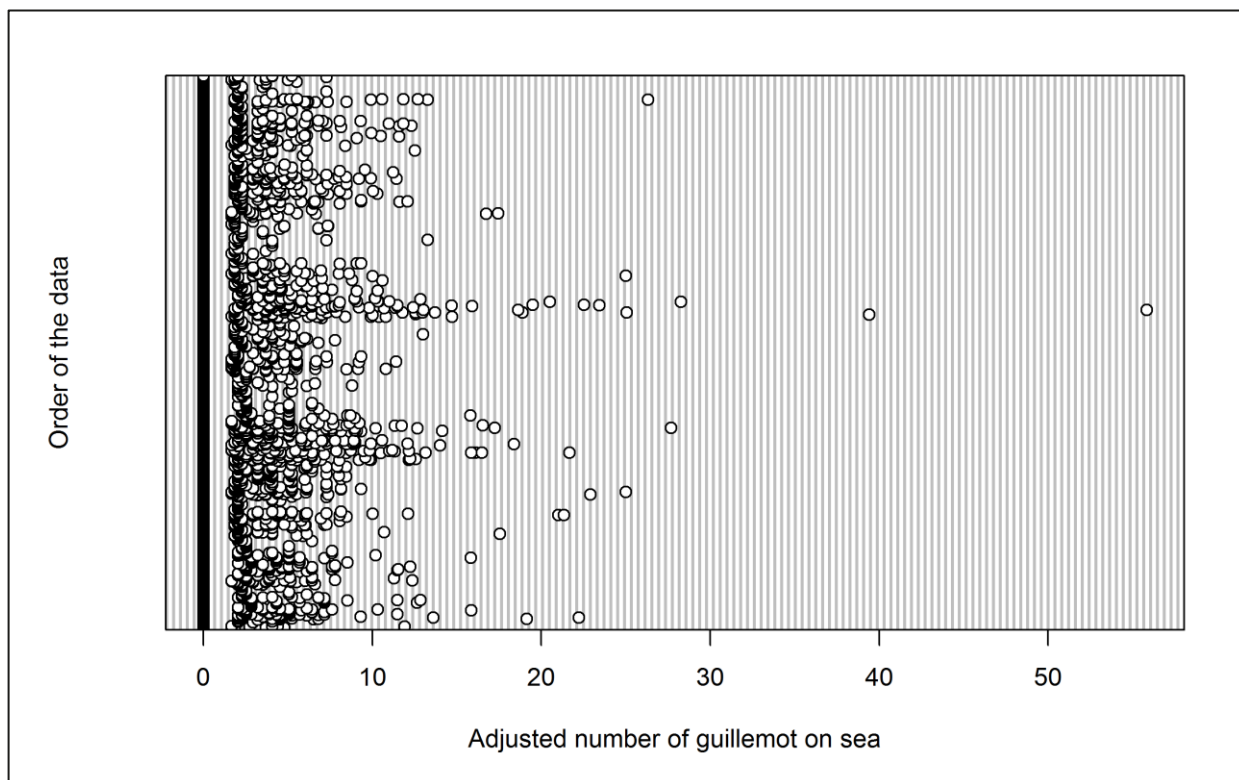


Figure 2.135: Dot plot of the number of guillemots observed on sea per analysis block across operational years one to four.

The GEE predicted that month, location, and the interaction between location and operational year all had a statistically significant influence of guillemot abundance within the survey area (Table 2.83). Specifically, mean density was larger during operational year two (Figure 2.136), and during the month of August (Figure 2.137). Since August was the month of peak activity, model predictions were made for this month.

Table 2.83: Final model outputs for guillemots on the sea across operational years one to four.

Term	Marginal p-value
Month	<0.0001
Phase	0.1238
Tide height	0.0770
Location (X,Y)	<0.0001
Interaction (location: phase)	0.0014



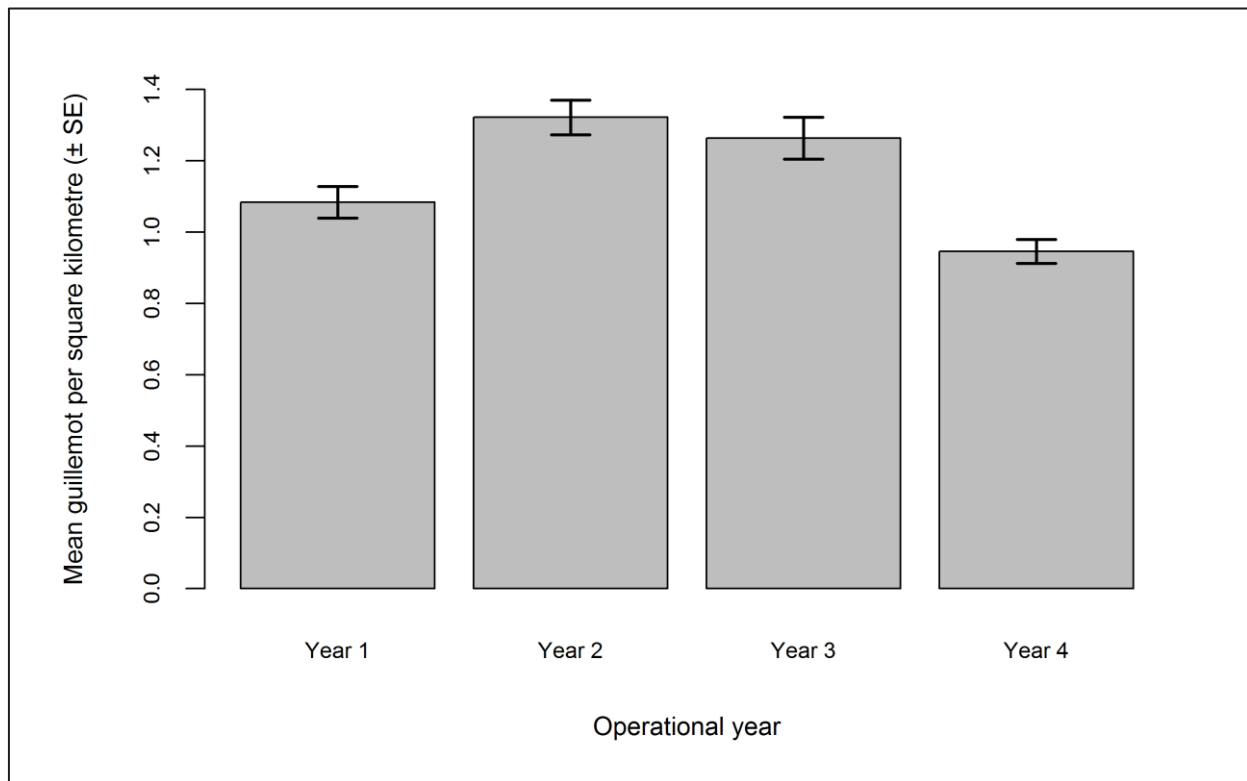


Figure 2.136: Mean density (± se) of guillemots recorded on the sea across operational years one to four.

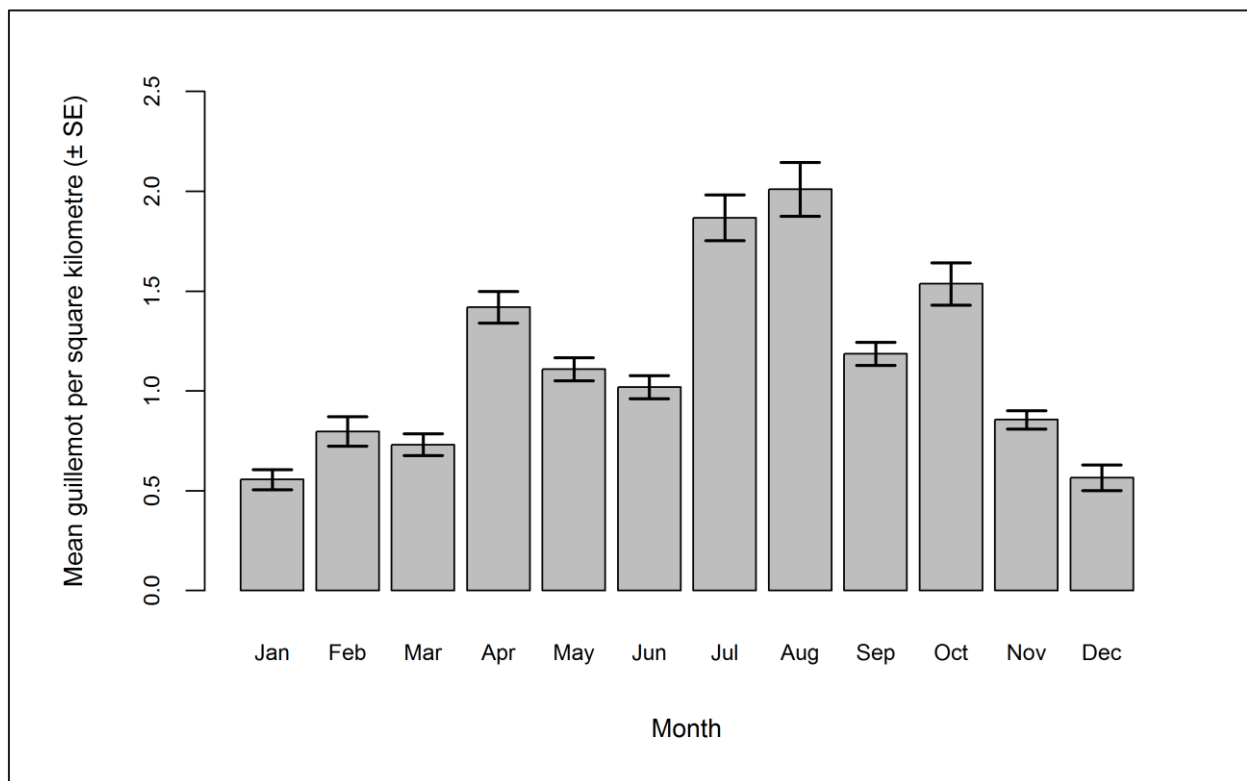


Figure 2.137: Mean density (± se) of guillemots recorded on the sea across operational years one to four.

Guillemot abundance and densities (by site, buffer and total survey area) are presented in Table 2.83. Total abundance shows a slight decrease across the four operational years, as does the percentage of guillemots using the OWF (Table 2.84).

**Table 2.84: Abundance and density of guillemots on the sea across operational years one to four. Values in parentheses represent upper and lower 95% confidence intervals.**

Operational year	Abundance			Density			% within site
	Site	Buffer	Total	Site	Buffer	Total	
<b>1</b>	45 (22-98)	908 (450-1,823)	953 (472-1,921)	3.47 (1.71-7.59)	2.61 (1.29-5.24)	2.64 (1.31-5.32)	4.71
<b>2</b>	48 (25-104)	716 (368-1,507)	764 (393-1,612)	3.71 (1.96-8.07)	2.06 (1.06-4.33)	2.12 (1.09-4.47)	6.29
<b>3</b>	44 (12-120)	700 (226-1,906)	743 (238-2,026)	3.37 (0.94-9.29)	2.01 (0.65-5.48)	2.06 (0.66-5.62)	5.86
<b>4</b>	30 (12-75)	661 (294-1,795)	691 (294-1,795)	2.32 (0.90-5.79)	1.90 (0.81-4.95)	1.91 (0.81-4.98)	4.34

The density surface maps show that predicted guillemot density was more concentrated towards the Robin Rigg OWF during operational year two. This is consistent with the percentage of guillemots using the OWF in year two (Table 2.84). During operational years three and four, predicted guillemot densities are concentrated to the south-west of the OWF, towards deeper waters in the mouth of the Solway Firth (Figure 2.138). Density within the Robin Rigg OWF site increased during operational year two and decreased over operational years three and four. None of these distributional shifts in guillemot densities were statistically significant (Figure 2.139).

169



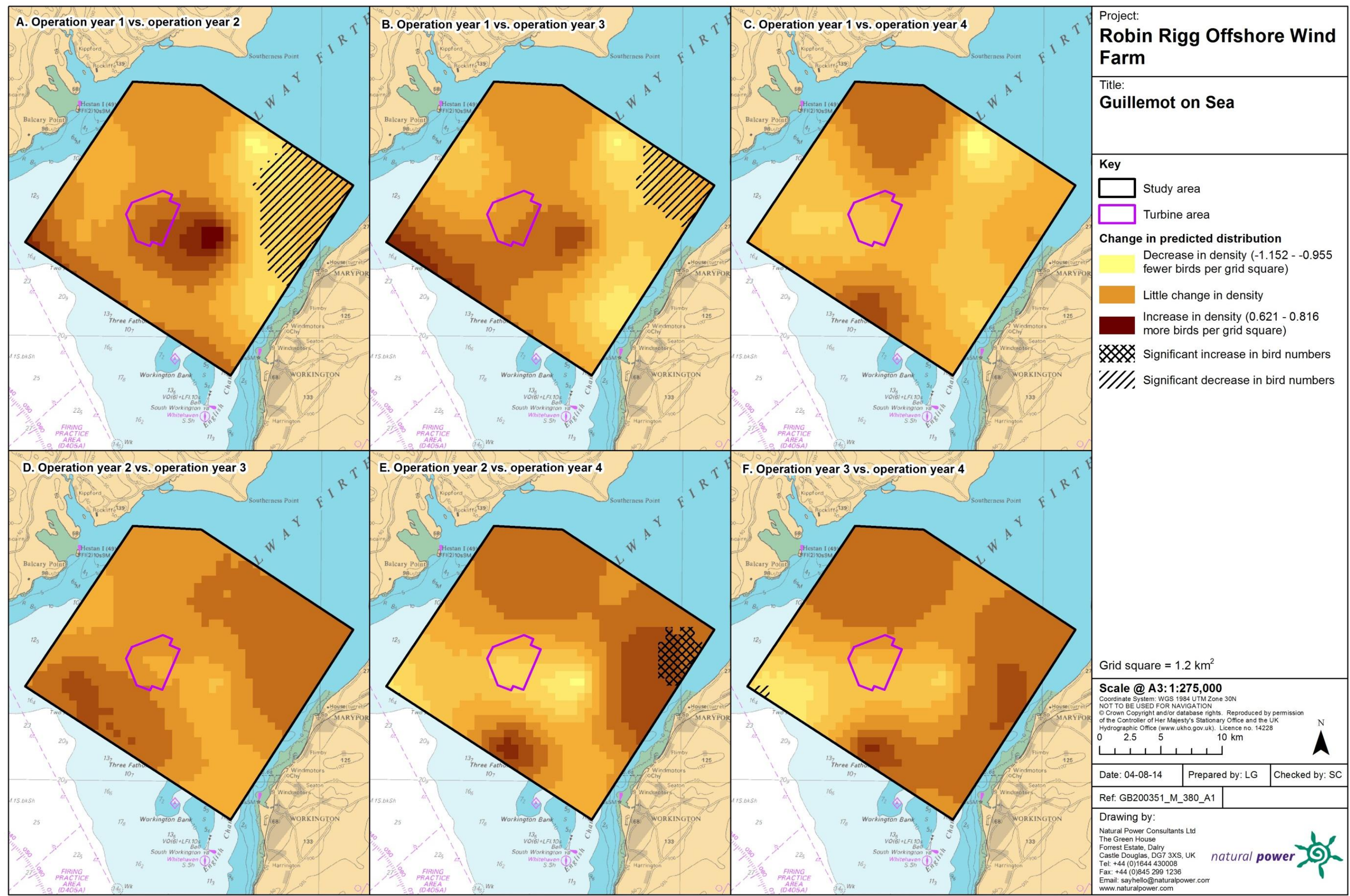


Figure 2.139: Differences in predicted sitting guillemot density between operational years. Significant differences are marked with diagonal shading.



#### 2.4.8.14.40.2. In flight

Small numbers of guillemots were recorded in flight during August and September as birds are flightless during their post-breeding moult. These two months of data were therefore removed from the analysis. Initial data exploration of the refined dataset highlighted two outliers (segments containing 15 birds each were recorded in March 2010 and January 2011) that may influence the modelling process (Figure 2.140). As a result the model was run with and without these outliers and the outputs compared.

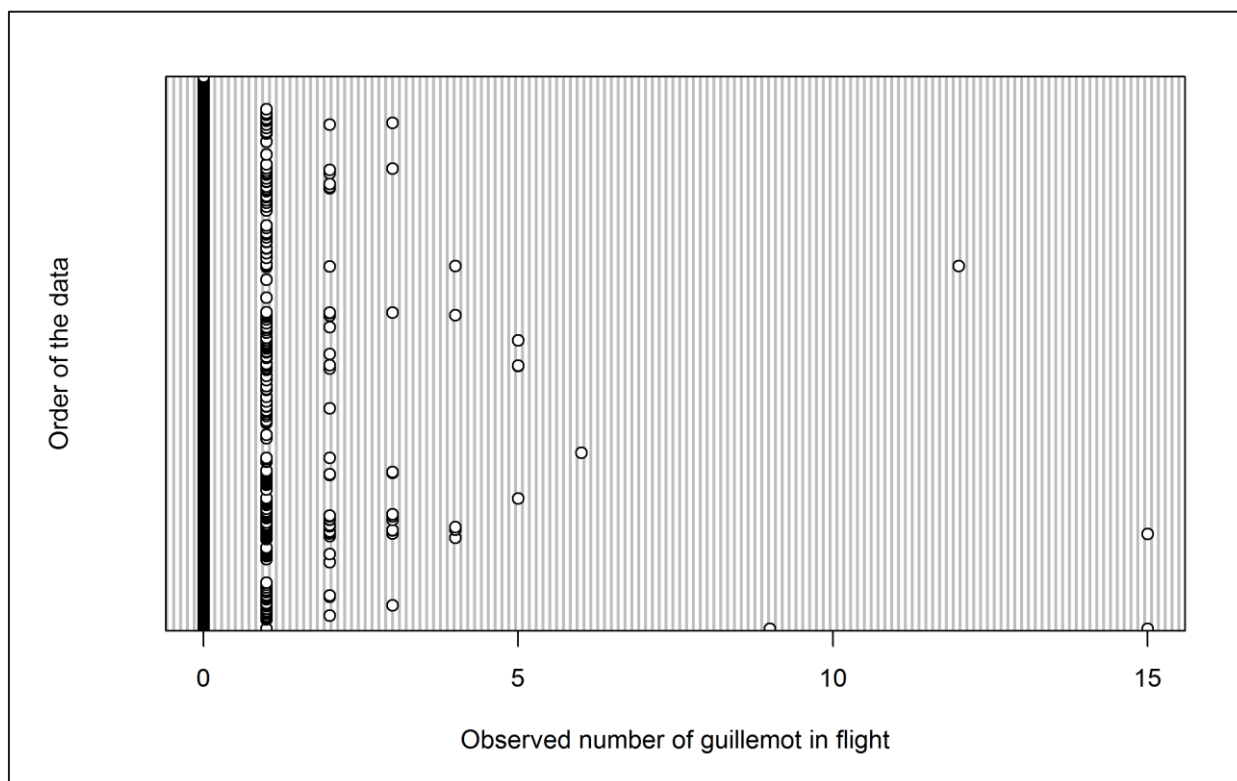


Figure 2.140: Dot plot of the number of guillemots observed in flight per analysis block across operational years one to four.

P-values remained the same after removing the outliers for all variables; therefore outputs from the model including the outliers are presented here. The GEE predicted that month, operational year, tide height and location all have a statistically significant influence on flying guillemot abundance (Table 2.85). The interaction between location and operational year (phase) was also statistically significant. Mean density was larger during operational years one and three (Figure 2.141), and was smaller during October and December (Figure 2.142).

Table 2.85: Final model outputs for guillemots in flight across operational years one to four.

Term	Marginal p-value
Month	0.0211
Phase	<0.0001
Tide height	0.0543
Location (X,Y)	<0.0001
Interaction (location: phase)	<0.0001

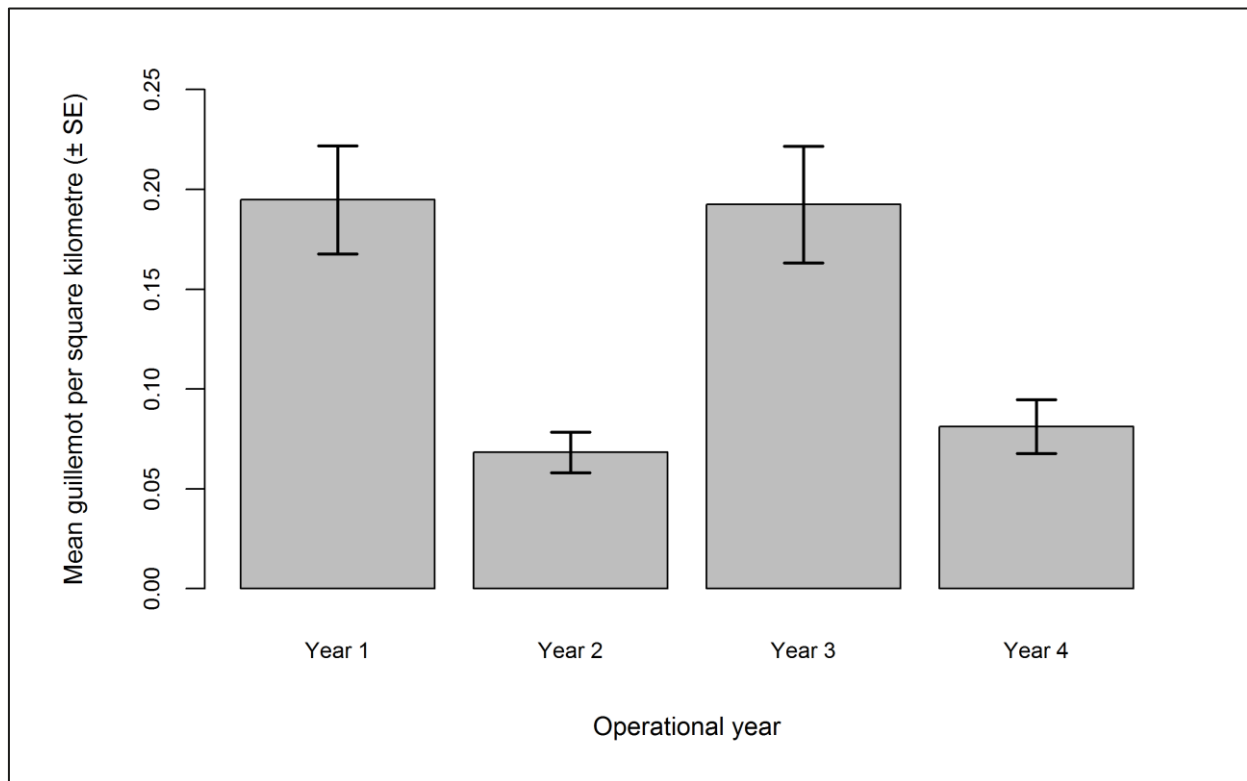


Figure 2.141: Mean density ( $\pm$  se) of guillemots recorded in flight across operational years one to four.

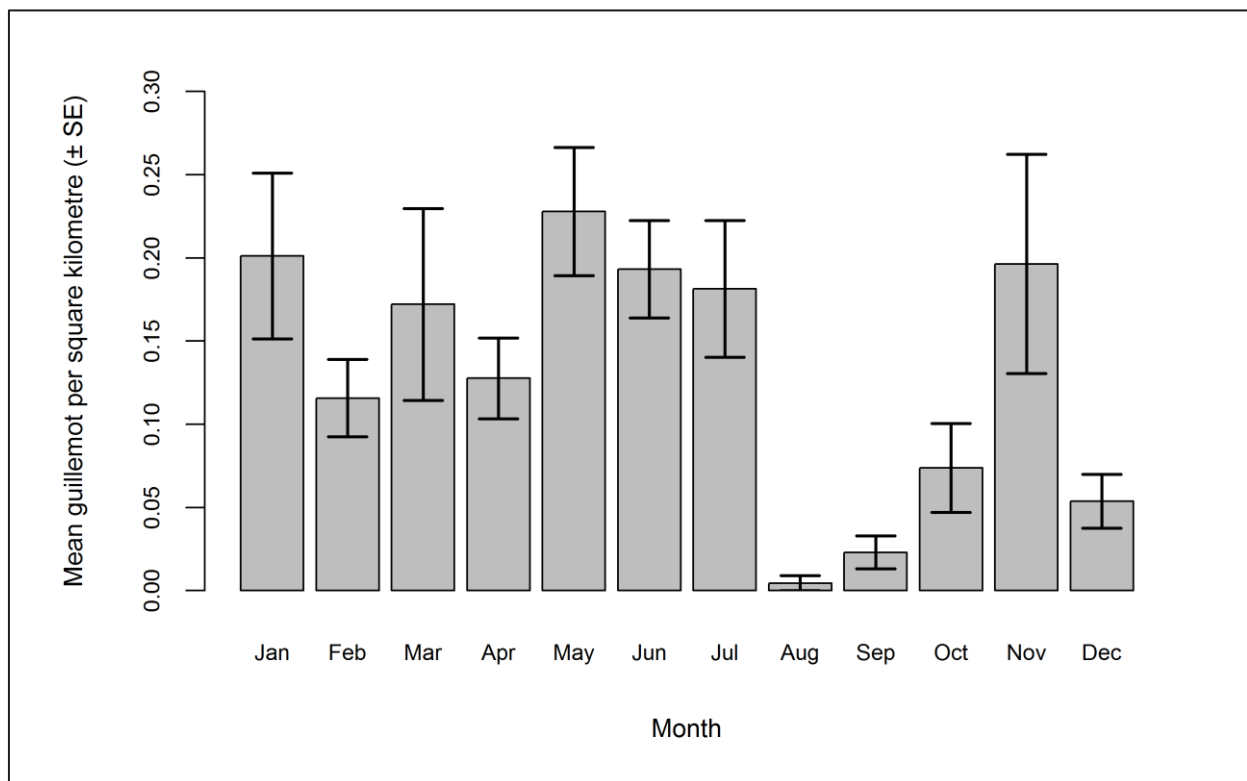


Figure 2.142: Mean density ( $\pm$  se) of guillemots recorded in flight during each month across operational years one to four.

Predicted guillemot abundance and densities (by site, buffer and total survey area) are presented in Table 2.86. Total predicted abundance across the survey area was largest during operational year three, although the largest percentage of guillemots utilising the Robin Rigg OWF were predicted to occur during operational years two and four (Table 2.86).

**Table 2.86: Abundance and density of guillemots in flight across operational years one to four. Values in parentheses represent upper and lower 95% confidence intervals.**

Operational year	Abundance			Density			% within site
	Site	Buffer	Total	Site	Buffer	Total	
<b>1</b>	4 (2-7)	131 (56-266)	135 (58-273)	0.33 (0.14-0.58)	0.38 (0.16-0.76)	0.37 (0.16-0.76)	3.13
<b>2</b>	6 (2-12)	60 (20-137)	66 (22-150)	0.47 (0.16-0.96)	0.17 (0.06-0.40)	0.18 (0.06-0.42)	9.19
<b>3</b>	8 (2-20)	229 (81-501)	238 (83-521)	0.65 (0.19-1.51)	0.66 (0.23-1.44)	0.66 (0.23-1.44)	3.56
<b>4</b>	5 (2-13)	90 (28-222)	96 (29-235)	0.42 (0.13-1.01)	0.26 (0.08-0.64)	0.27 (0.08-0.65)	5.72

The density surface maps show that predicted guillemot abundance was largest during operational year three, consistent with the results presented in Table 2.86. This statistically significant increase in comparison to operational year one, was predicted to occur in the north-west of the survey area, close to the coast of Dumfries and Galloway (Figure 2.143). A statistically significant decrease was predicted in the same area between operational years three and four (Figure 2.144).

174



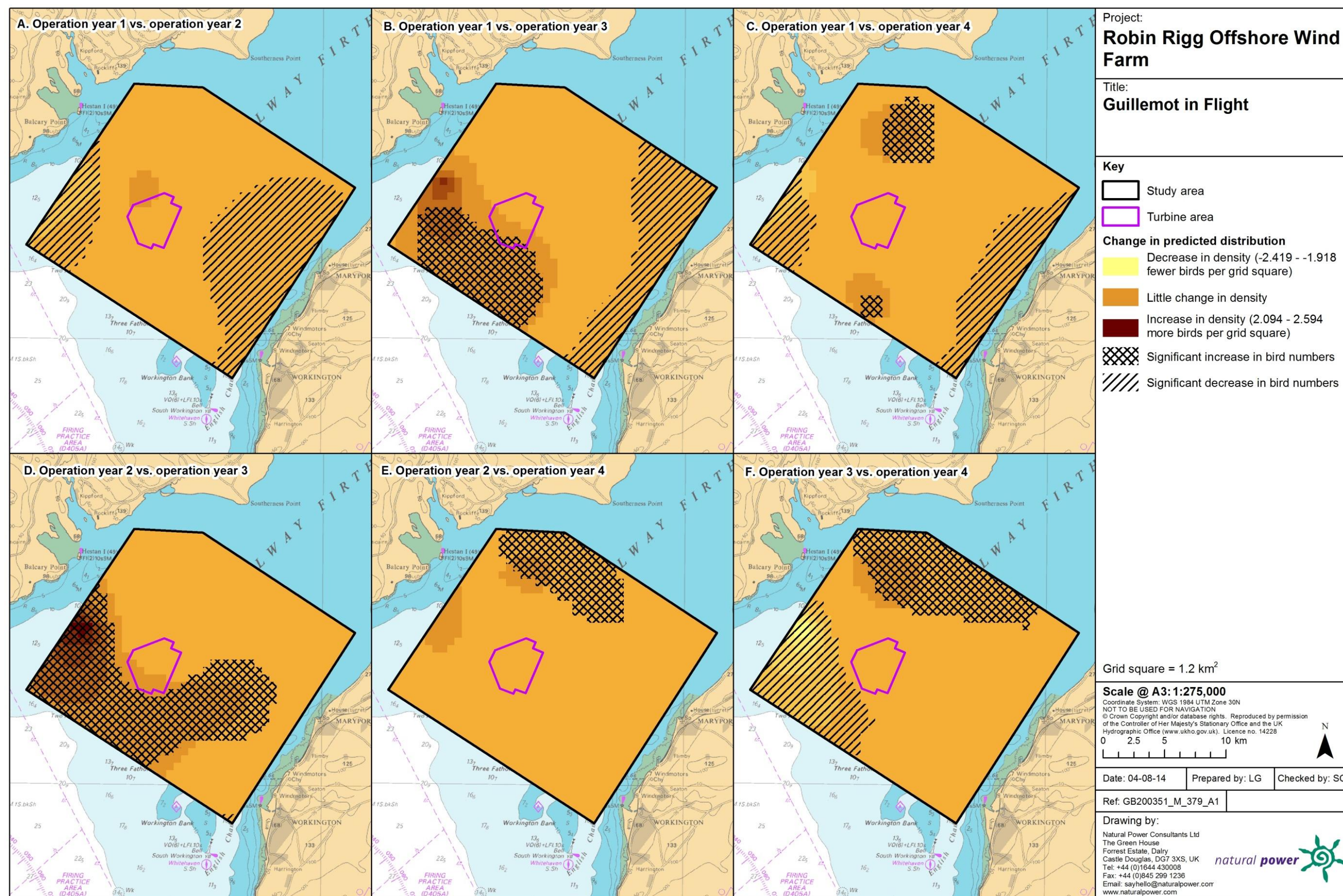


Figure 2.144: Differences in predicted flying guillemot density between operational years. Significant differences are marked with diagonal shading.



#### 2.4.8.14.41. Collision risk

The percentage of guillemots recorded during the four operational years in different height bands relative to rotor swept height can be found in Table 2.87 and Figure 2.145. A chi-squared test was not undertaken as fewer than 5% of guillemots were recorded at rotor swept height during operational monitoring, indicating that guillemots are not at risk from collision at Robin Rigg OWF.

**Table 2.87: Percentage of guillemots recorded in different flight height bands across operational years one to four. Shaded column indicates percentage at rotor swept height (flight band 4).**

Operational year	Flight height band					
	1 (0–5 m)	2 (6–25 m)	3 (26–34 m)	4 (35–125 m)	5 (126–200 m)	6 (>200 m)
1	92.38	7.30	0.32	0.00	0.00	0.00
2	99.32	0.68	0.00	0.00	0.00	0.00
3	98.08	1.92	0.00	0.00	0.00	0.00
4	68.47	17.12	10.81	3.60	0.00	0.00

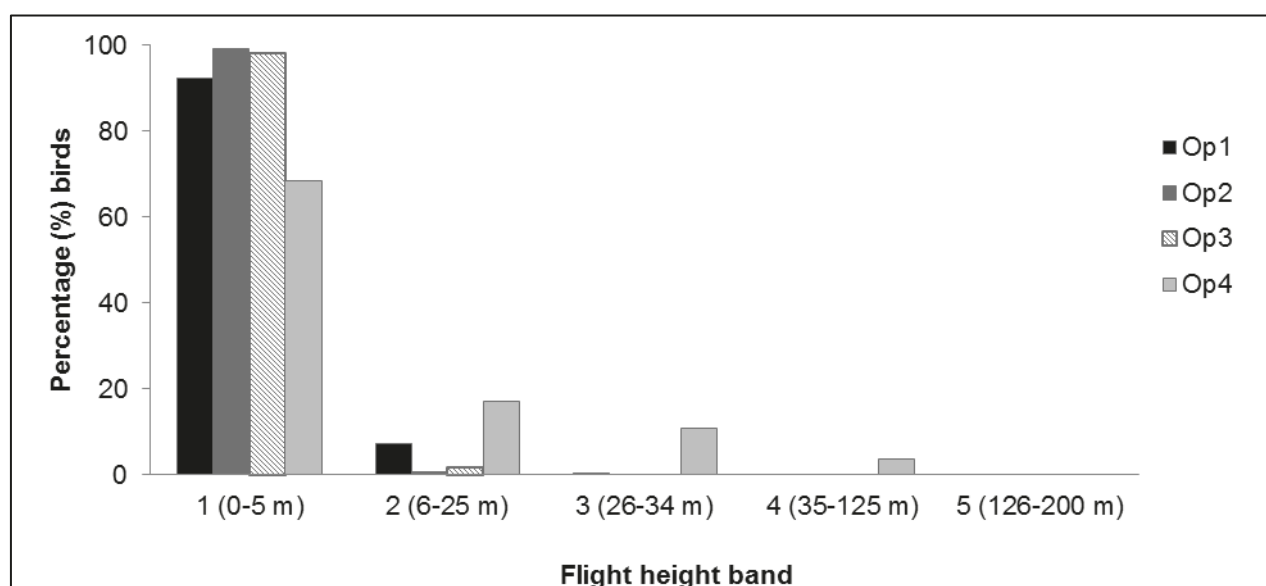


**Figure 2.145: Percentage of guillemots recorded in different flight height bands across operational years one to four.**

## 2.4.9. Kittiwake

### 2.4.9.15. Across three development phases

#### 2.4.9.15.42. Summary statistics

The total number of kittiwakes was largest during the construction phase at 1,758 individuals (Table 2.88). However, the number of kittiwakes recorded per km of survey effort was greatest during the first two years of operation (Table 2.88). Comparable numbers of kittiwakes were recorded in flight and on the sea throughout the three development phases (Table 2.88).

**Table 2.88: Number of kittiwakes recorded per block during each development phase per km survey effort (all data).**

	Pre-construction		Construction		Operation years 1-2	
	On sea	In flight	On sea	In flight	On sea	In flight
<b>Total number individuals</b>	443	472	829	929	490	358
<b>Total number sightings</b>	168	292	406	494	228	355
<b>Number individuals/km</b>	0.12	0.13	0.11	0.13	0.13	0.14
	Total		Total		Total	
<b>Total number individuals</b>	915		1,758		1,028	
<b>Total number sightings</b>	460		900		583	
<b>Number individuals/km</b>	0.26		0.24		0.27	

Data were filtered as described in the methods (Section 2.4.4). The percentage of segments without observations was calculated to ensure there were sufficient data to perform the analysis (Table 2.89). Data were also checked to ensure observations were recorded in all months of the year.

**Table 2.89: Percentage of kittiwake analysis blocks without observations across the three development phases: pre-construction, construction and operational years one and two. Zero inflation prior to removal of effort is presented in parentheses.**

	On sea	In flight
<b>Percentage zero blocks</b>	(96.4%) 96.4%	96.7%

## 2.4.9.15.43. Density and distribution

### 2.4.9.15.43.1. On sea

A hazard-rate detection function with no covariates was found to be the best fitting model. Figure 2.146 shows the selected detection curve for kittiwakes on the sea.

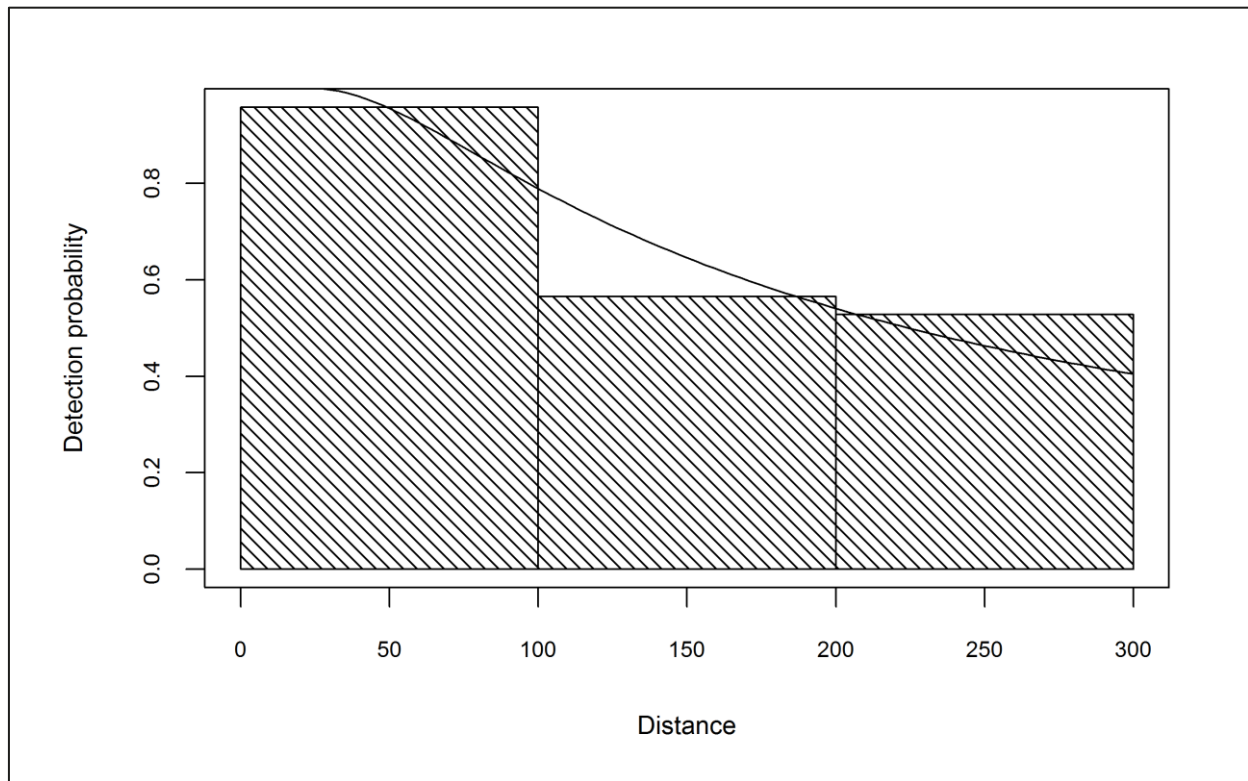


Figure 2.146: Detection curve used to adjust kittiwake on sea counts for imperfect detection across the three development phases: pre-construction, construction and operational years one and two.

Initial data exploration of adjusted kittiwake numbers indicated that there were no outlying observations (Figure 2.147). Kittiwakes were not observed during any development phase in December as individuals move offshore and out of the Solway Firth. Therefore, this month was removed from the analysis.



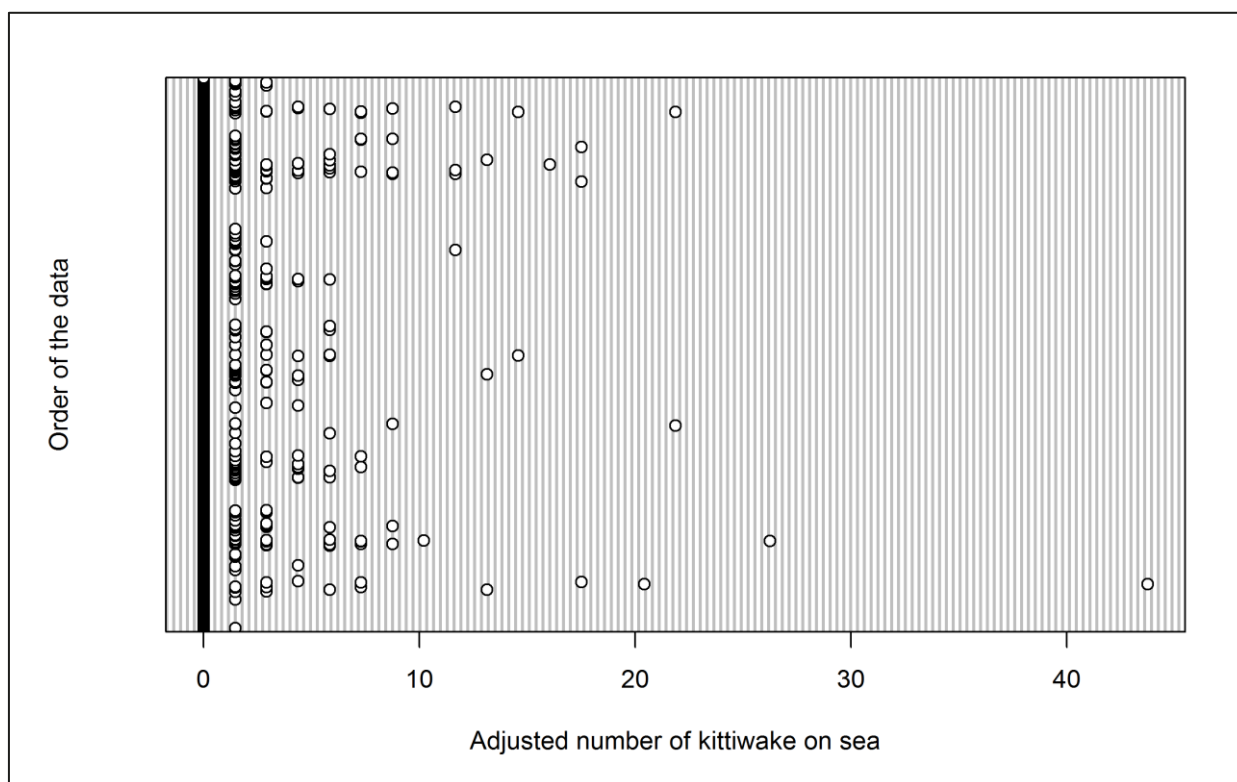


Figure 2.147: Dot plot of the number of kittiwakes observed on sea per analysis block across the three development phases: pre-construction, construction and operational years one and two.

The GEE predicted that development phase had no effect on kittiwake abundance across the survey area (Table 2.90). Although mean kittiwake densities were marginally depressed during the construction phase compared with pre-construction and operation, the effect was not statistically significant (Figure 2.148). Statistically significant effects were detected for month, location, and the interaction between the two. Since the largest mean kittiwake density occurred in April, model predictions were made for this month (Figure 2.149).

Table 2.90: Final model outputs for kittiwakes on the sea across the three development phases: pre-construction, construction and operational years one and two.

Term	Marginal p-value
Month	<0.0001
Phase	0.2293
Tide height	0.2107
Location (X,Y)	0.0246
Interaction (location: phase)	0.0197

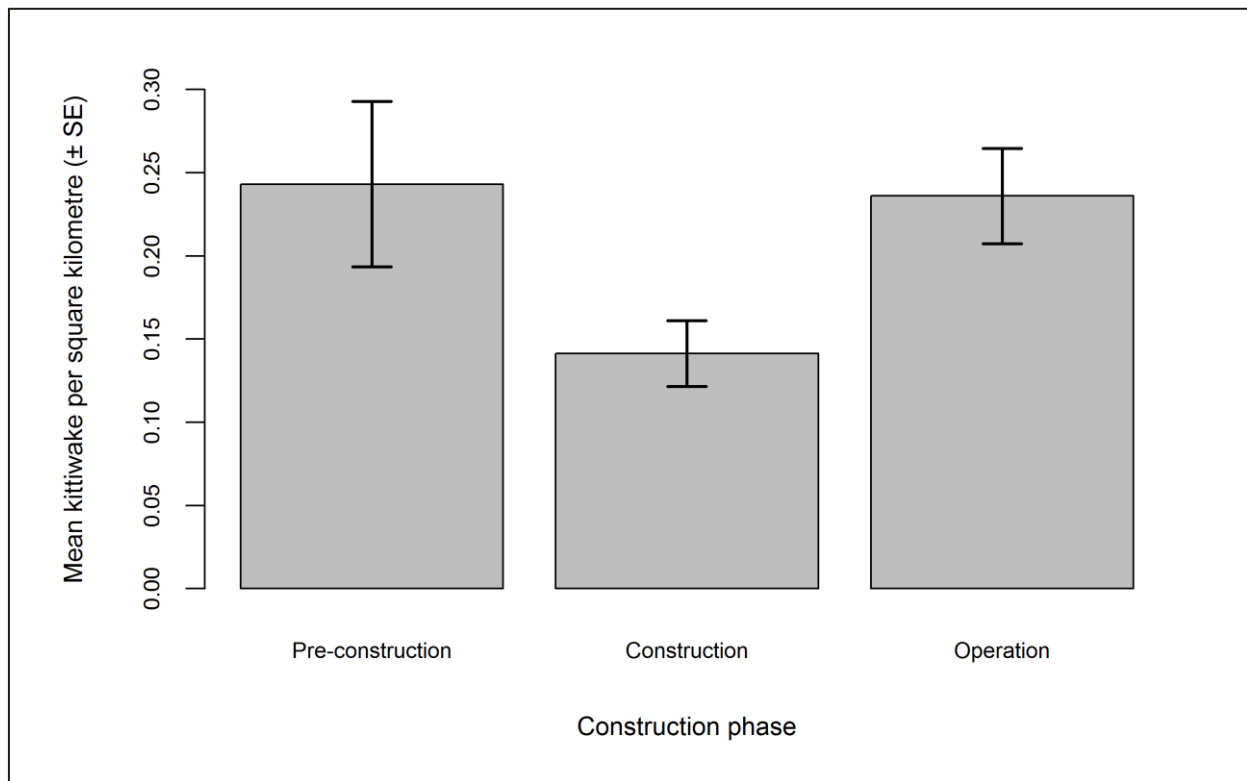


Figure 2.148: Mean density ( $\pm$  se) of kittiwakes recorded on the sea across the three development phases: pre-construction, construction and operational years one and two.

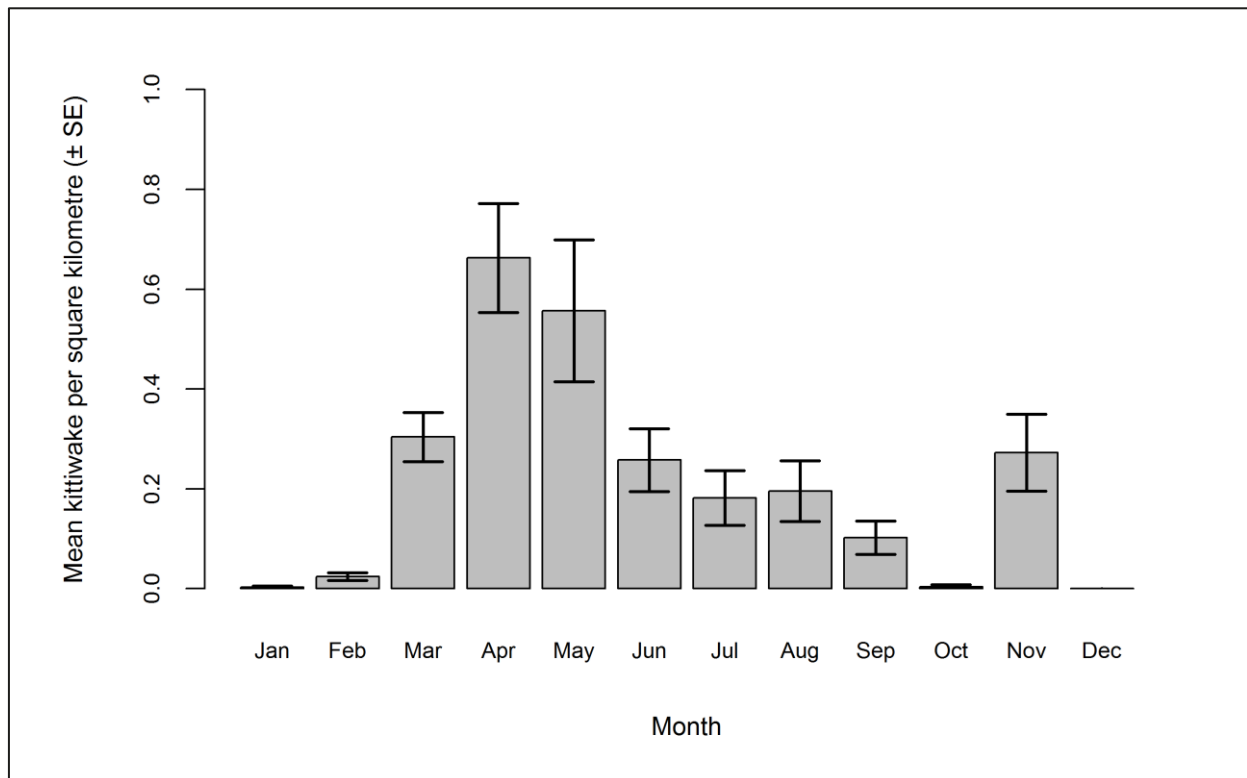


Figure 2.149: Mean density ( $\pm$  se) of kittiwakes recorded on the sea during each month across the three development phases: pre-construction, construction and operational years one and two.

Predicted kittiwake abundance and densities (by site, buffer and total survey area) are presented in Table 2.91. The smallest total abundance was predicted for the construction phase. However abundance increased during the operational phase to a level beyond that predicted for the pre-construction phase (Table 2.91). The percentage of kittiwakes predicted to occur within Robin Rigg OWF itself, was also largest during the operational phase (Table 2.91).

**Table 2.91: Abundance and density of kittiwakes on the sea across the three development phases: pre-construction, construction and operational years one and two. Values in parentheses represent upper and lower 95% confidence intervals.**

Phase	Abundance			Density			% within site
	Site	Buffer	Total	Site	Buffer	Total	
<b>Pre-construction</b>	7 (2-46)	266 (78-975)	274 (80-1,021)	0.57 (0.15-3.53)	0.77 (0.23-2.80)	0.76 (0.22-2.83)	2.69
<b>Construction</b>	5 (6-139)	173 (118-1,400)	178 (124-1,539)	0.39 (0.48-10.71)	0.50 (0.34-4.03)	0.49 (0.34-4.26)	2.87
<b>Operation</b>	39 (6-162)	413 (122-9,392)	452 (128-9,554)	3.03 (0.46-12.50)	1.19 (0.35-27.00)	1.25 (0.35-26.48)	8.67

The density surface maps show that predicted kittiwake densities on the sea were largest during the operational phase (Figure 2.150), consistent with the results presented in Table 2.91. A statistically significant increase was predicted to occur in the south-east of the survey area between pre-construction and construction phases (Figure 2.150), consistent with the increase in the percentage of birds within the site during the construction phase.



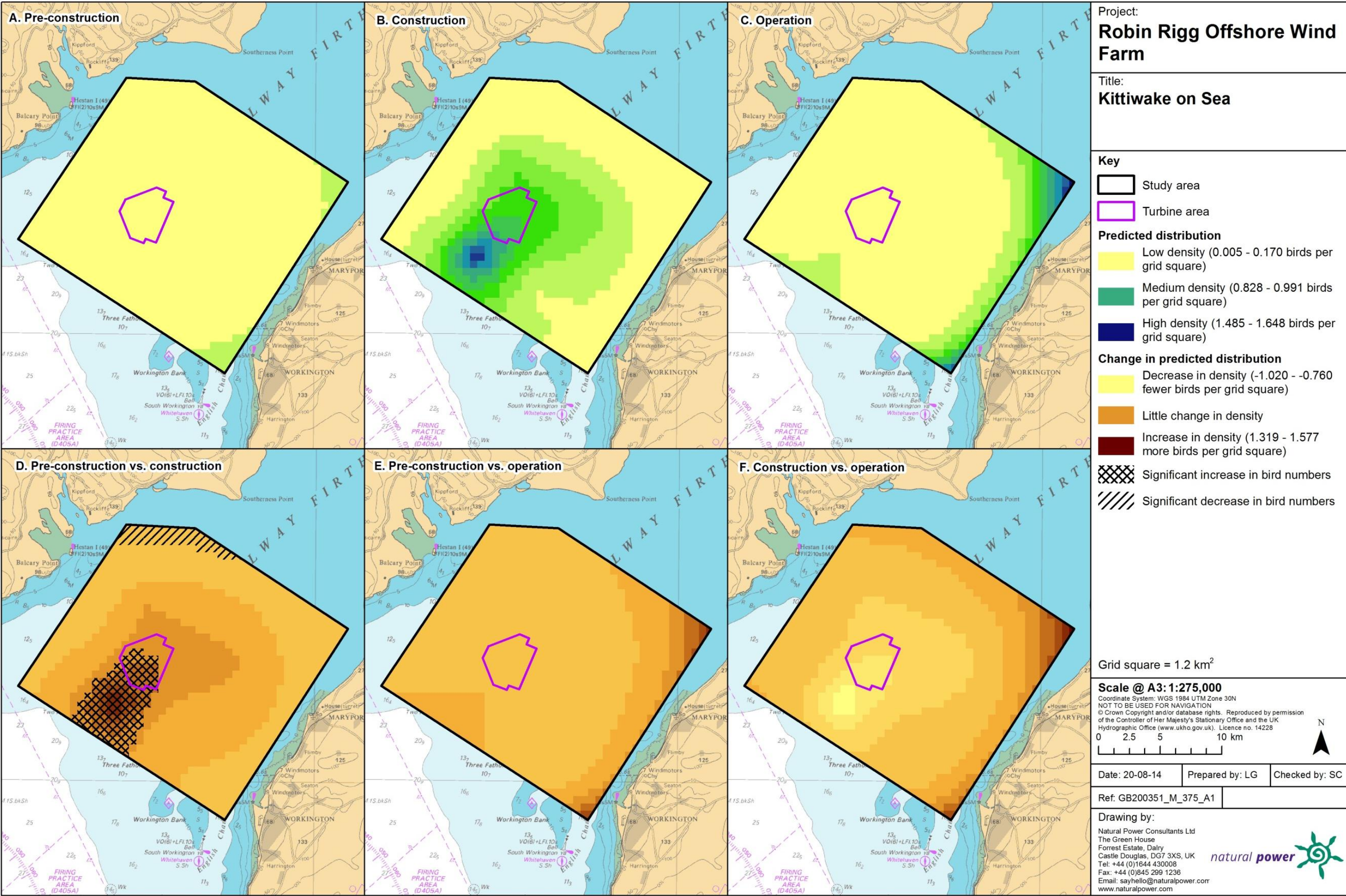


Figure 2.150: Predicted density of kittiwakes on the sea during a) pre-construction, b) construction and c) operational monitoring. Changes in predicted density between d) pre-construction and construction, e) pre-construction and operation and f) construction and operation are also shown. Significant differences are marked with diagonal shading.



### 2.4.9.15.43.2. In flight

Data exploration did not highlight any outliers that would influence the modelling process (Figure 2.151).

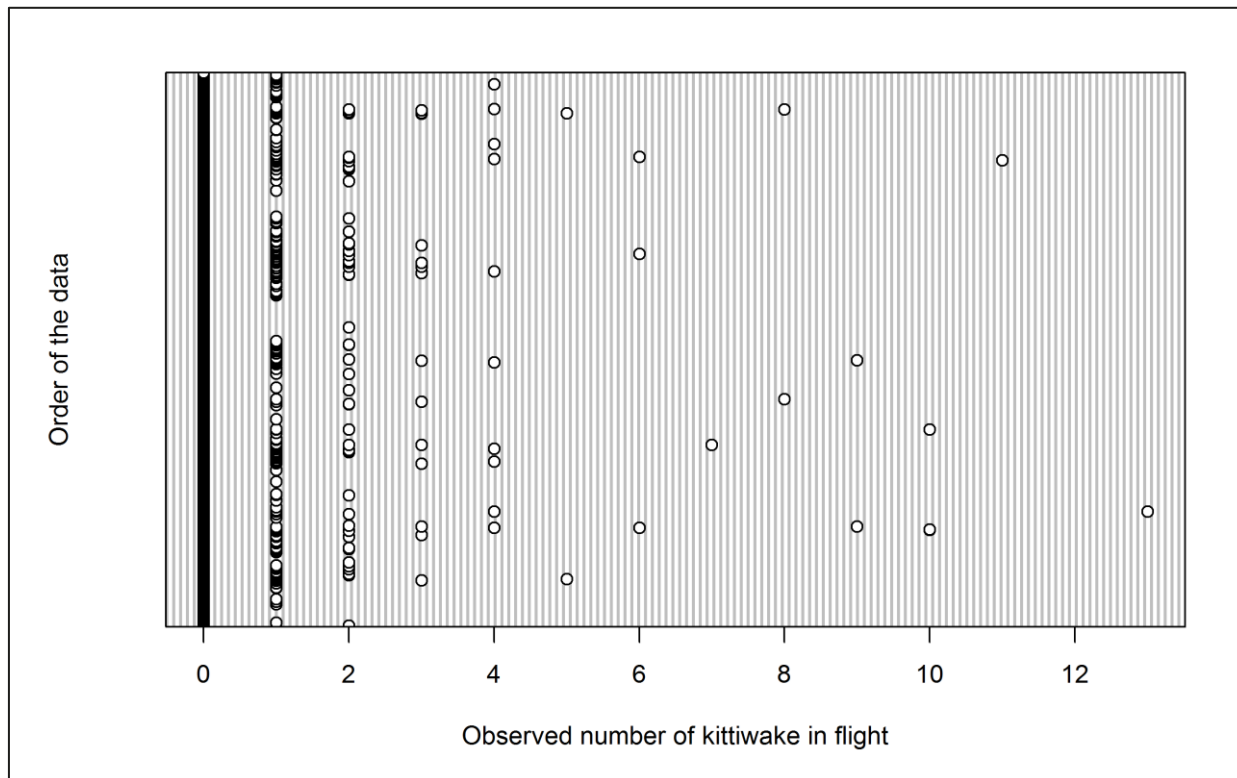


Figure 2.151: Dot plot of the number of kittiwakes observed in flight per analysis block across the three development phases: pre-construction, construction and operational years one and two.

The GEE predicted that month and tide height have a statistically significant influence on kittiwake abundance within the survey area (Table 2.92). Specifically, smaller numbers were predicted during the construction phase, (although not statistically significant; Figure 2.152) and larger numbers were predicted during the spring and summer (March-July; Figure 2.153). The interaction between phase and location was not statistically significant. Since April was the month of peak activity, model predictions were made for this month.

Table 2.92: Final model outputs for kittiwakes in flight across the three development phases: pre-construction, construction and operational years one and two.

Term	Marginal p-value
Month	<0.0001
Phase	0.4536
Tide height	0.0005
Location (X,Y)	0.0541
Interaction (location: phase)	0.0828

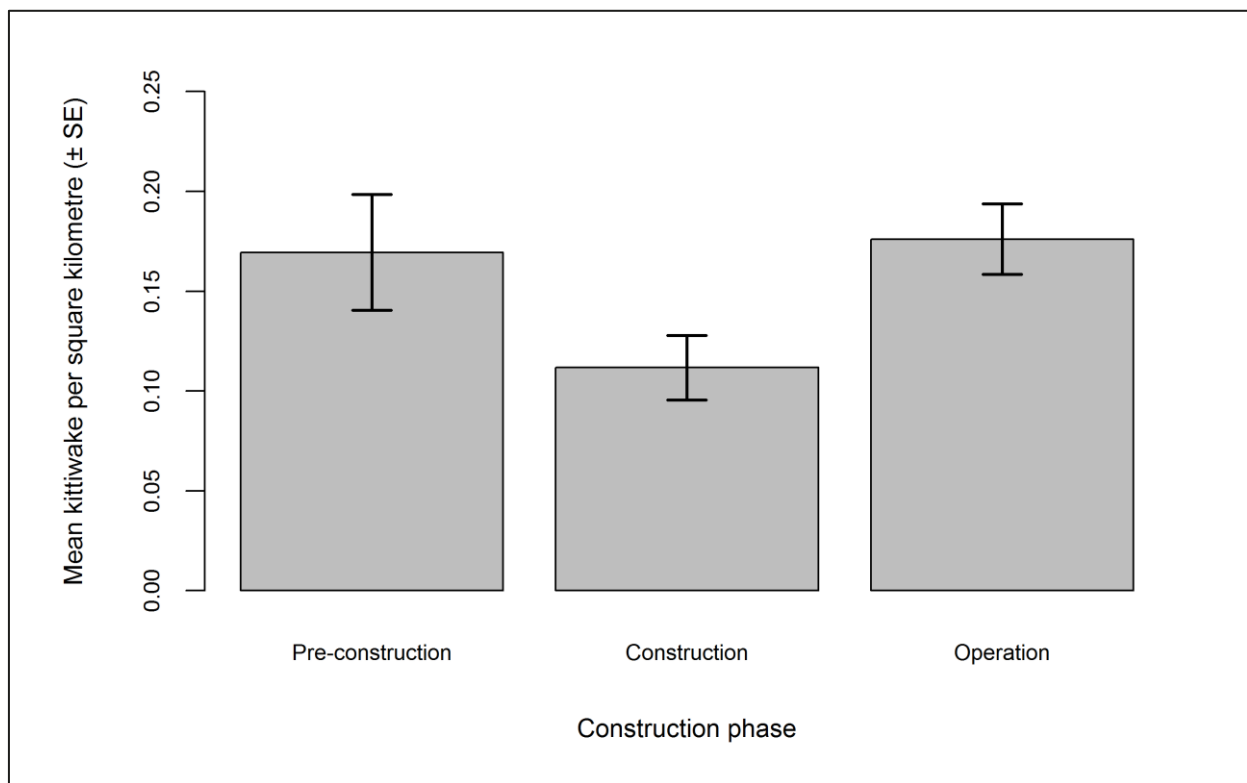


Figure 2.152: Mean density ( $\pm$  se) of kittiwakes recorded in flight across the three development phases: pre-construction, construction and operational years one and two.

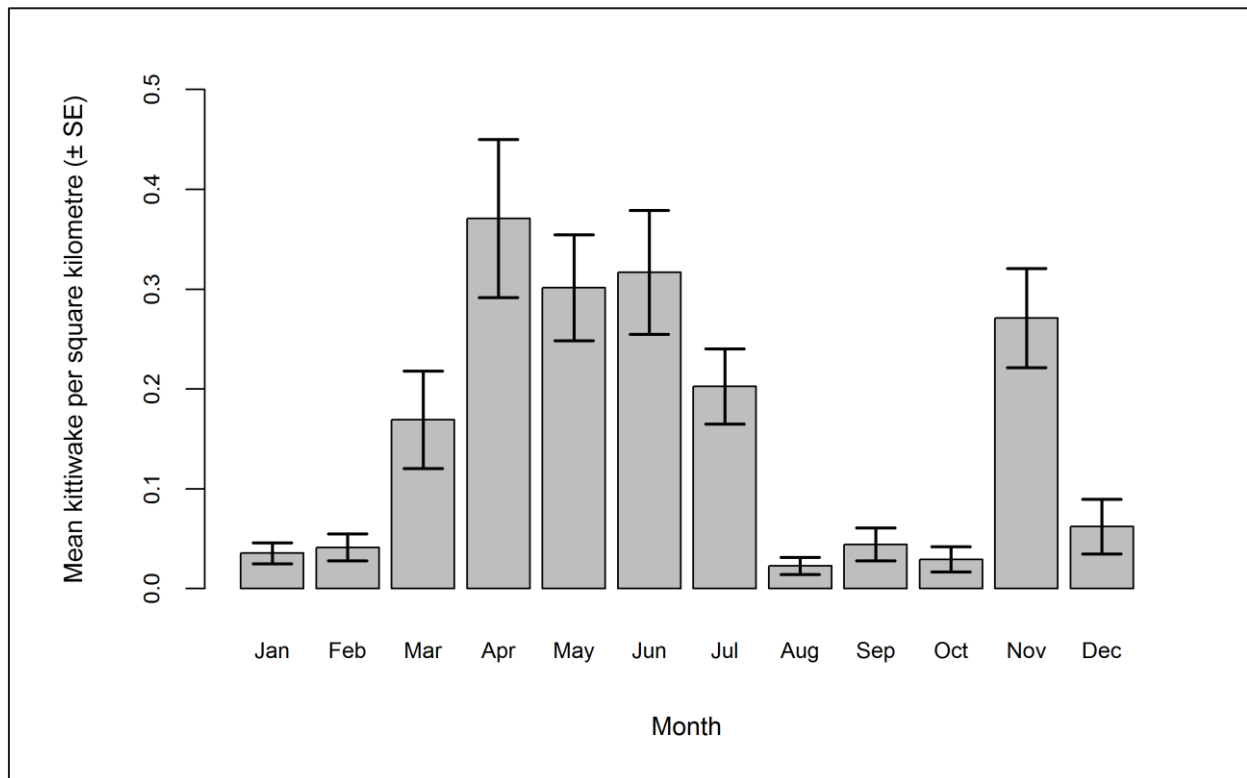


Figure 2.153: Mean density ( $\pm$  se) of kittiwakes recorded in flight across the three development phases: pre-construction, construction and operational years one and two.

Predicted kittiwake abundance and densities (by site, buffer and total survey area) are presented in Table 2.93. The proportion of kittiwakes in flight within the Robin Rigg OWF increased throughout the three development phases. However, the smallest total abundance was predicted to occur during the construction phase (Table 2.93).

**Table 2.93: Abundance and density of kittiwakes in flight across the three development phases: pre-construction, construction and operational years one and two. Values in parentheses represent upper and lower 95% confidence intervals.**

Phase	Abundance			Density			% within site
	Site	Buffer	Total	Site	Buffer	Total	
<b>Pre-construction</b>	7 (2-30)	173 (41-248)	180 (43-278)	0.54 (0.13-2.29)	0.50 (0.12-0.71)	0.50 (0.12-0.77)	3.85
<b>Construction</b>	7 (6-54)	96 (81-352)	103 (87-406)	0.53 (0.47-4.15)	0.28 (0.23-1.01)	0.29 (0.24-1.12)	6.61
<b>Operation</b>	17 (1-35)	165 (58-519)	182 (60-553)	1.28 (0.11-2.67)	0.48 (0.17-1.49)	0.50 (0.17-1.53)	9.12

The density surface maps show a statistically significant increase in predicted kittiwake density both within the Robin Rigg OWF and to the north-east of the site between pre-construction and construction phases (Figure 2.154). Predicted kittiwake distribution shifted between construction and operation, with statistically significant declines to the north of the OWF and statistically significant increase in the south of the survey area (Figure 2.154).



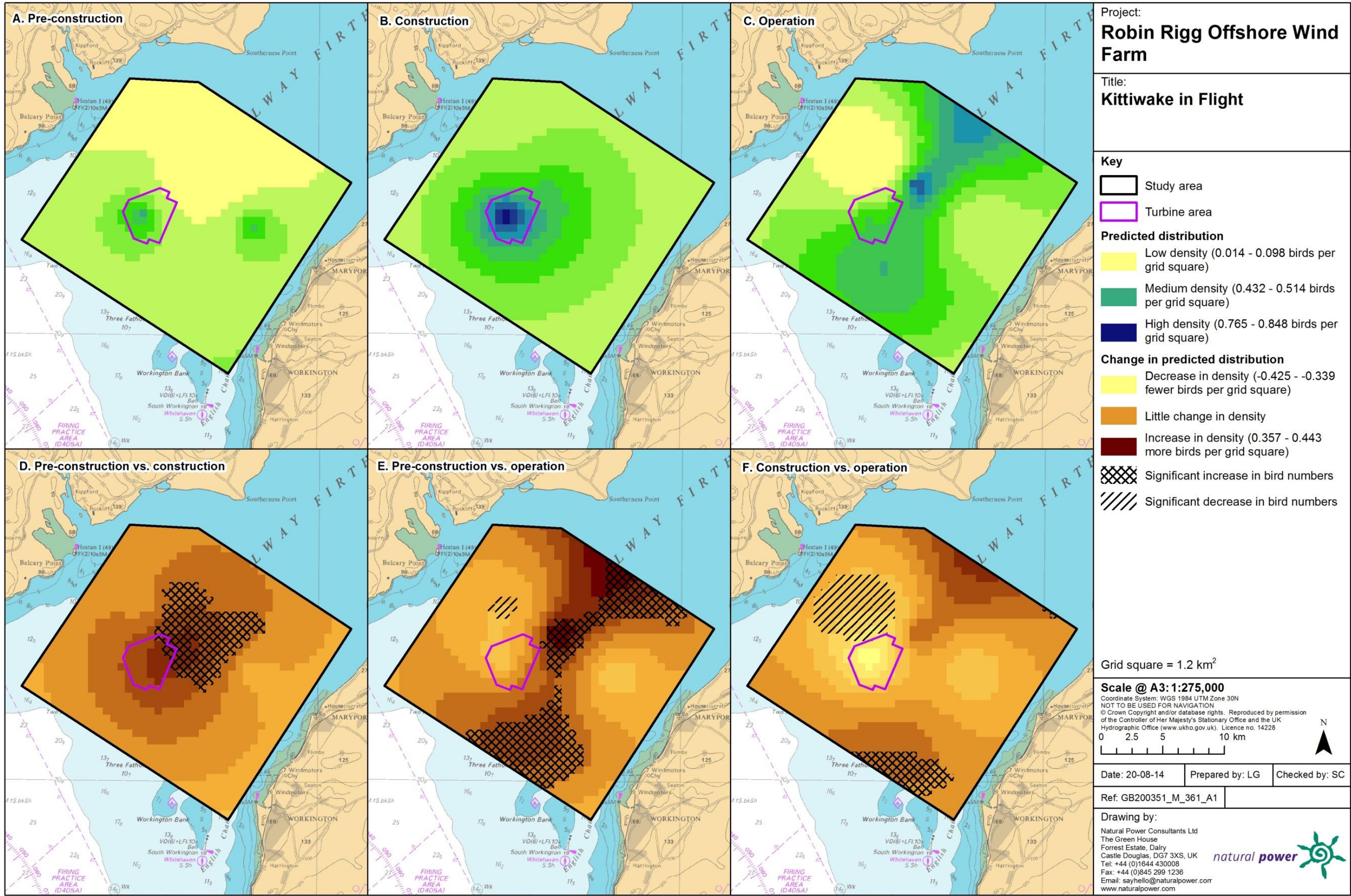


Figure 2.154: Predicted density of kittiwakes in flight during a) pre-construction, b) construction and c) operational monitoring. Changes in predicted density between d) pre-construction and construction, e) pre-construction and operation and f) construction and operation are also shown. Significant differences are marked with diagonal shading.



#### 2.4.9.15.44. Collision risk

The percentage of kittiwakes recorded during the three development phases in different height bands relative to rotor swept height can be found in Table 2.94 and Figure 2.155. Since a relatively small percentage of kittiwakes were recorded flying at rotor swept height, a chi-squared test was not undertaken.

**Table 2.94:** Percentage of kittiwakes recorded in different flight height bands across the three development phases: pre-construction, construction and operational years one and two. Shaded column indicates percentage at rotor swept height (flight band 4).

Phase	Flight height band					
	1 (0–5 m)	2 (6–25 m)	3 (26–34 m)	4 (35–125 m)	5 (126–200 m)	6 (>200 m)
<b>Pre-construction</b>	50.00	48.09	0.85	1.06	0.00	0.00
<b>Construction</b>	25.40	71.04	2.26	1.29	0.00	0.00
<b>Operation</b>	37.92	56.13	3.35	2.60	0.00	0.00

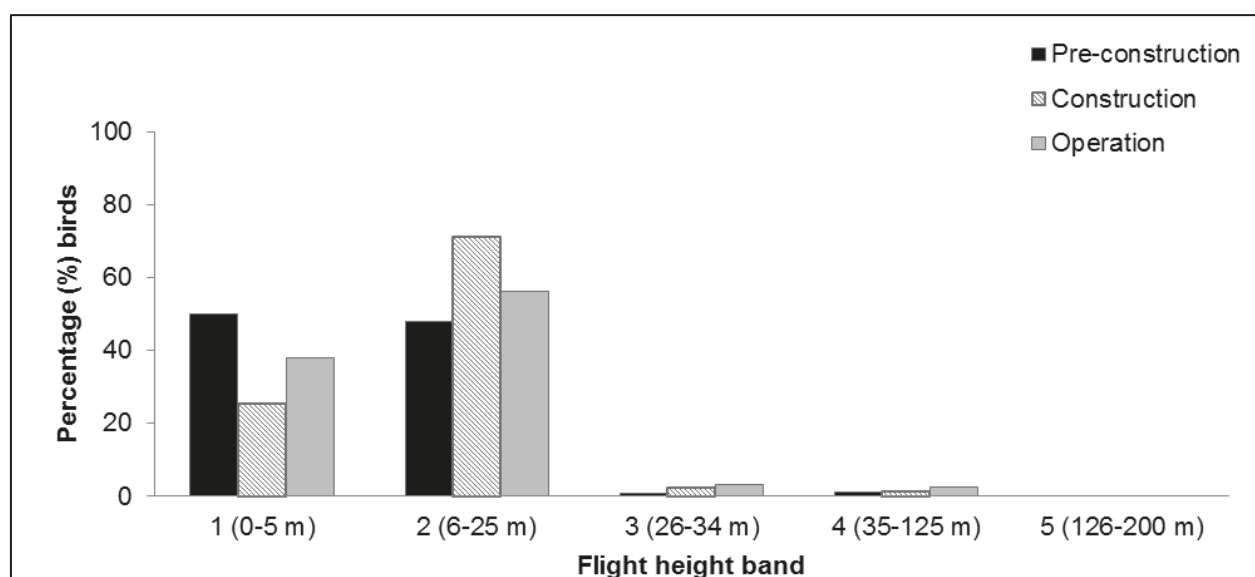


**Figure 2.155:** Percentage of kittiwakes recorded in different flight height bands across the three development phases: pre-construction, construction and operational years one and two.

## 2.4.9.16. Across operational years

### 2.4.9.16.45. Summary statistics

The total number of kittiwakes was smaller in the first operational year than in subsequent operational years (Table 2.95). The number of kittiwakes recorded per km of survey effort was largest during the second year, and similar numbers were recorded during operational years three and four (Table 2.95). Larger numbers of kittiwakes were recorded in flight than on the sea during the first operational year, but the number of kittiwakes in flight and on the sea during subsequent operational years was similar (Table 2.95).

**Table 2.95: Number of kittiwakes recorded per block during each operational year per km survey effort (all data).**

	Operational year 1		Operational year 2		Operational year 3		Operational year 4	
	On sea	In flight	On sea	In flight	On sea	In flight	On sea	In flight
<b>Total number individuals</b>	98	193	382	345	351	155	360	211
<b>Total number sightings</b>	67	142	161	213	113	113	113	173
<b>Number individuals/km</b>	0.05	0.11	0.19	0.17	0.16	0.07	0.16	0.10
	Total		Total		Total		Total	
<b>Total number individuals</b>	291		737		506		571	
<b>Total number sightings</b>	209		374		226		286	
<b>Number individuals/km</b>	0.16		0.36		0.23		0.26	

Data were filtered as described in the methodology (Section 2.4.4). The percentage of segments without observations was calculated to ensure there were sufficient data to perform the analysis (Table 2.96). Data were also checked to ensure observations were recorded in all months of the year.

**Table 2.96: Percentage of kittiwake analysis blocks without observations across operational years one to four. Zero inflation prior to removal of effort is presented in parentheses.**

	On sea	In flight
<b>Percentage zero blocks</b>	(97.2%) 96.7%	97.8%

## 2.4.9.16.46. Density and distribution

### 2.4.9.16.46.1. On sea

A hazard-rate detection function with no covariates was found to be the best fitting model. Figure 2.156 shows the selected detection curve for kittiwakes on the sea.

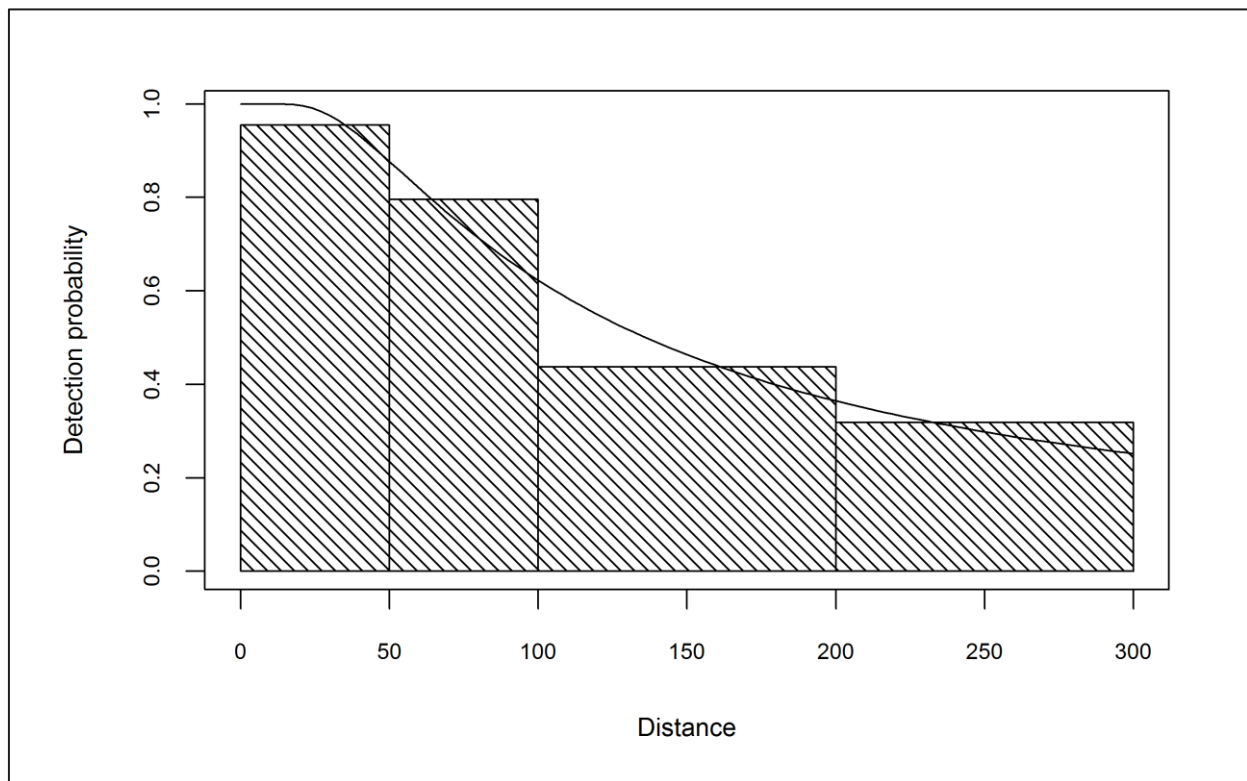


Figure 2.156: Detection curve used to adjust kittiwake on sea counts for imperfect detection across operational years one to four.

Initial data exploration of adjusted kittiwake numbers did not highlight any outliers (Figure 2.157). Kittiwakes were not observed during any development phase in December as individuals move offshore and out of the Solway Firth. Therefore, this month was removed from the analysis.

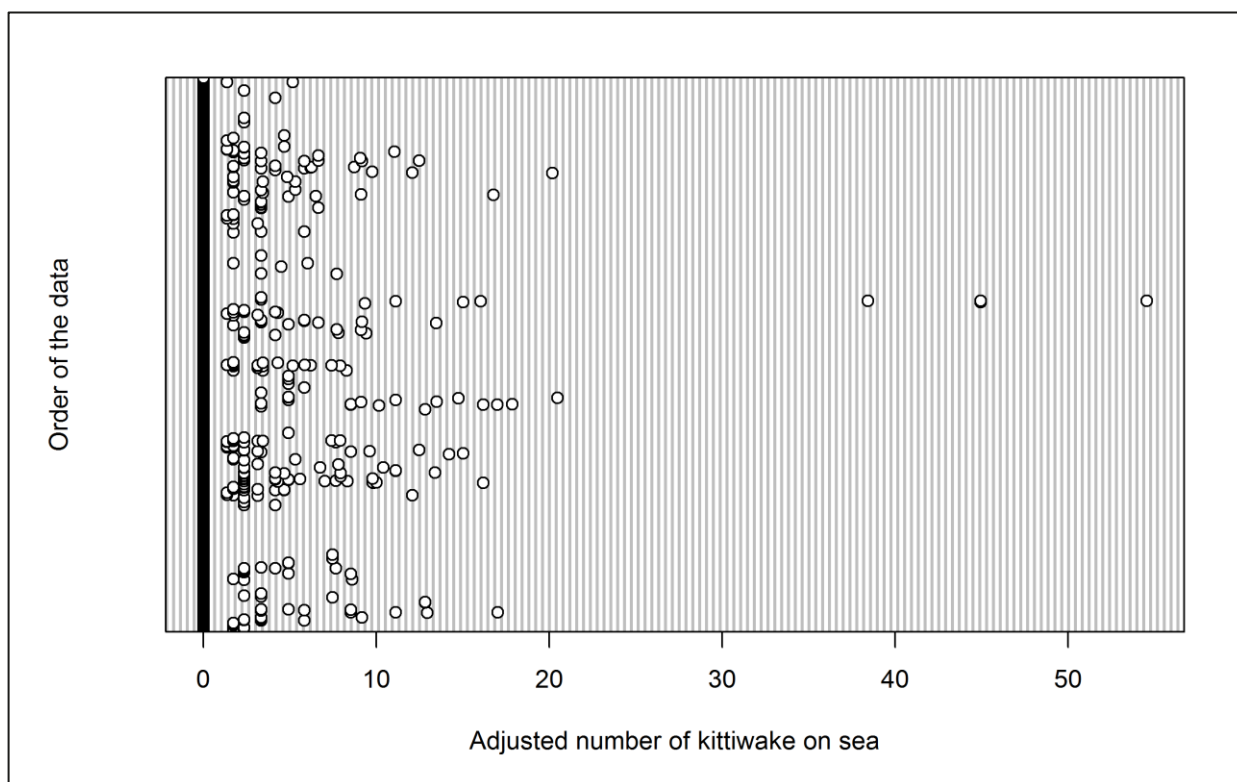


Figure 2.157: Dot plot of the number of kittiwakes observed on sea per analysis block across operational years one to four.

The GEE predicted that month, operational year, tidal height, location, and the interaction between location and operational year (phase), all had a statistically significant influence of kittiwake abundance within the survey area (Table 2.97). Specifically, mean density was significantly larger during operational years two and four (Figure 2.158). Mean kittiwake density was largest during spring and summer months with a peak in August (Figure 2.159). Model predictions were therefore made for this month.

Table 2.97: Final model outputs for kittiwakes on the sea across operational years one to four.

Term	Marginal p-value
Month	<0.0001
Phase	0.0023
Tide height	0.0211
Location (X,Y)	0.0072
Interaction (location: phase)	0.0087



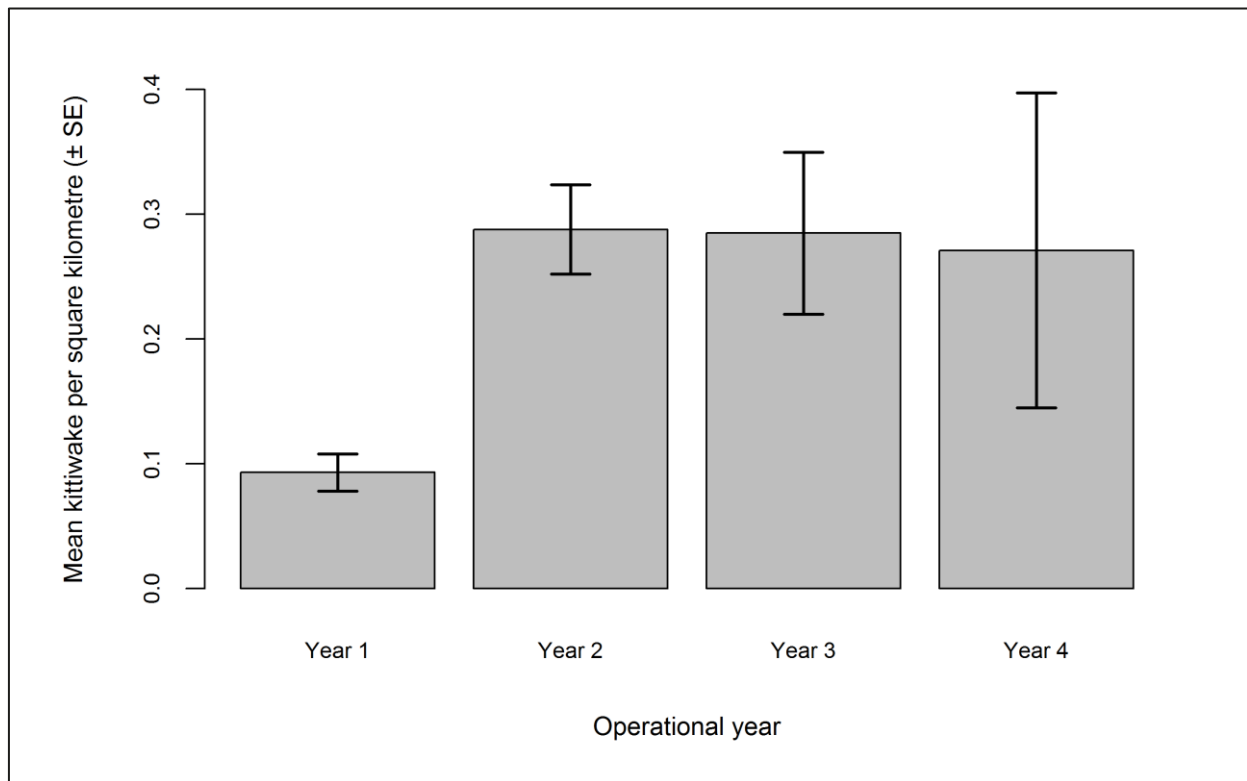


Figure 2.158: Mean density ( $\pm$  se) of kittiwakes recorded on the sea across operational years one to four.

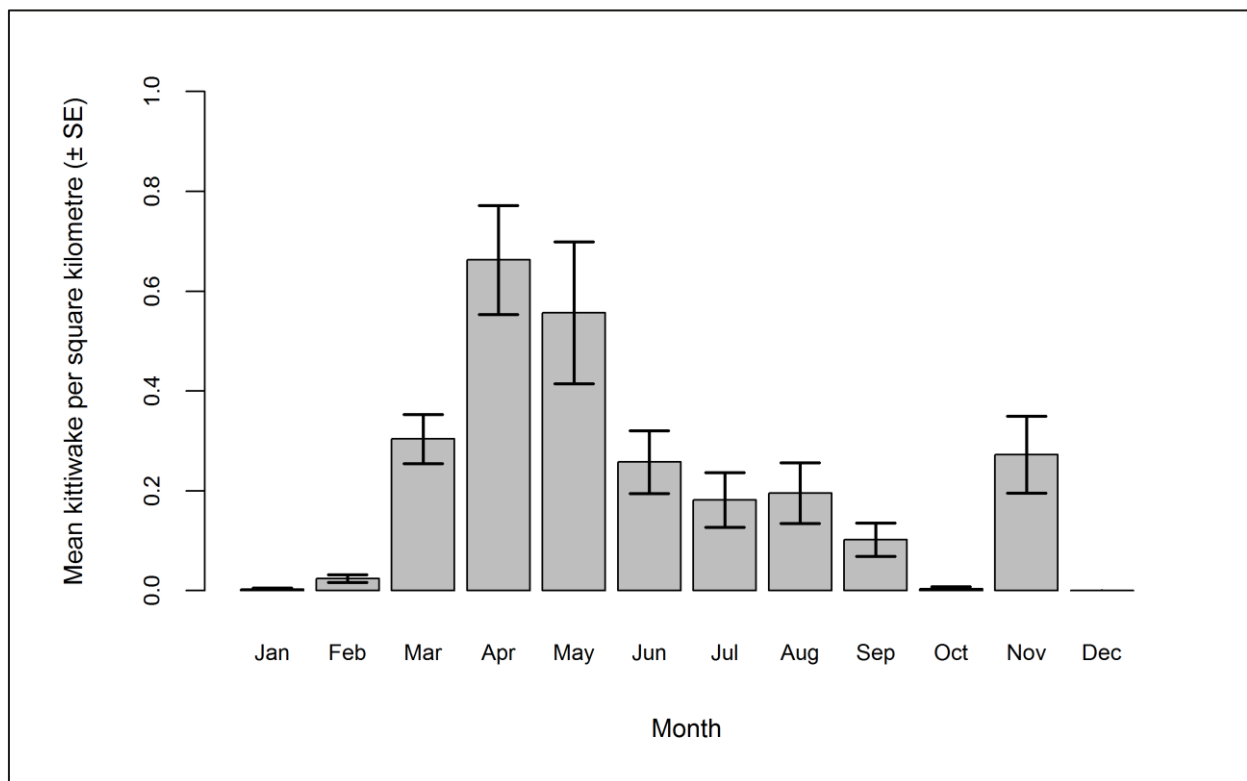


Figure 2.159: Mean density ( $\pm$  se) of kittiwakes recorded on the sea during each month across operational years one to four.

Predicted kittiwake abundance and densities by site, buffer and total survey area are presented in Table 2.98. Total kittiwake abundance and density was largest during operational year three, as was the percentage of kittiwakes predicted to occur within Robin Rigg OWF. However, it should be noted that the inclusion of an outlier in the data may have led to relatively high confidence intervals and increased uncertainty in model predictions.

**Table 2.98: Abundance and density of kittiwakes on the sea across operational years one to four. Values in parentheses represent upper and lower 95% confidence intervals.**

Operational year	Abundance			Density			% within site
	Site	Buffer	Total	Site	Buffer	Total	
<b>1</b>	2 (0-14)	61 (10-336)	63 (10-350)	0.16 (0.02-1.07)	0.18 (0.03-0.97)	0.18 (0.03-0.97)	3.26
<b>2</b>	29 (5-128)	432 (100-1,825)	461 (105-1,953)	2.25 (0.41-9.93)	1.24 (0.29-5.25)	1.28 (0.29-5.41)	6.31
<b>3</b>	169 (3-10,554)	805 (38-24,661)	974 (41-35,215)	13.10 (0.25-815.87)	2.31 (0.11-70.89)	2.70 (0.11-97.61)	17.39
<b>4</b>	29 (3-996)	314 (37-4,069)	343 (40-5,065)	2.28 (0.23-76.98)	0.90 (0.11-11.70)	0.95 (0.11-14.04)	8.59

The density surface maps show that predicted kittiwake density was largest during operational year three (Figure 2.160), consistent with the results shown in Table 2.98. Statistically significant increases in density were seen between operational years one and two, and one and three, with a statistically non-significant decline predicted between operational years three and four (Figure 2.161).

193



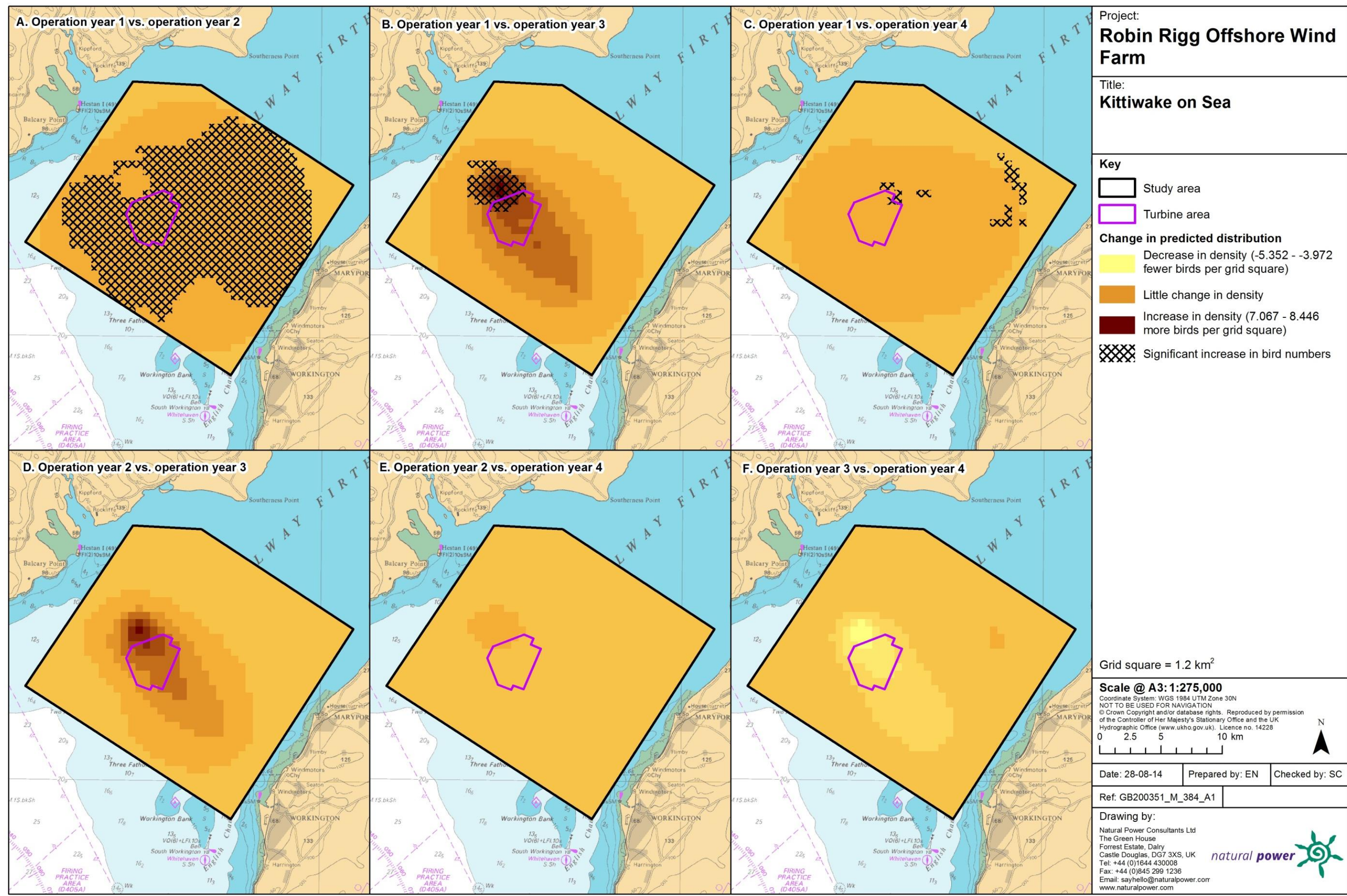


Figure 2.161: Differences in predicted sitting kittiwake density between operational years. Significant differences are marked with diagonal shading.



### 2.4.9.16.46.2. In flight

Data exploration did not highlight any outliers that would influence the modelling process (Figure 2.162).

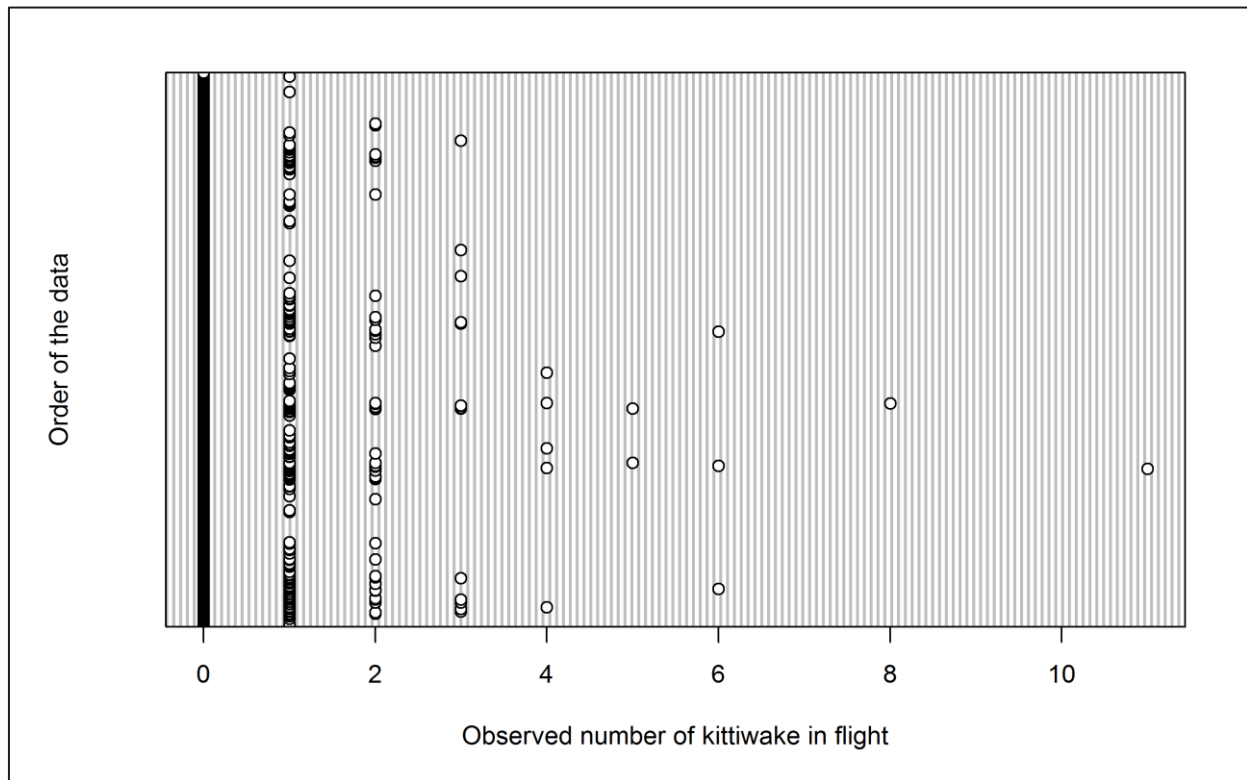


Figure 2.162: Dot plot of the number of kittiwakes observed in flight per analysis block across operational years one to four.

The GEE predicted that month, tide height and location all have a statistically significant influence on kittiwake abundance within the survey area (Table 2.99). Mean kittiwake density was comparable across operational years (Figure 2.163), although mean density was larger during the spring and summer (Figure 2.164). The interaction between operational year (phase) and location was not statistically significant. Since June was the month of peak activity, model predictions were made for this month.

Table 2.99: Final model outputs for kittiwakes in flight across operational years one to four.

Term	Marginal p-value
Month	<0.0001
Phase	0.2090
Tide height	<0.0001
Location (X,Y)	<0.0001
Interaction (location: phase)	0.2405

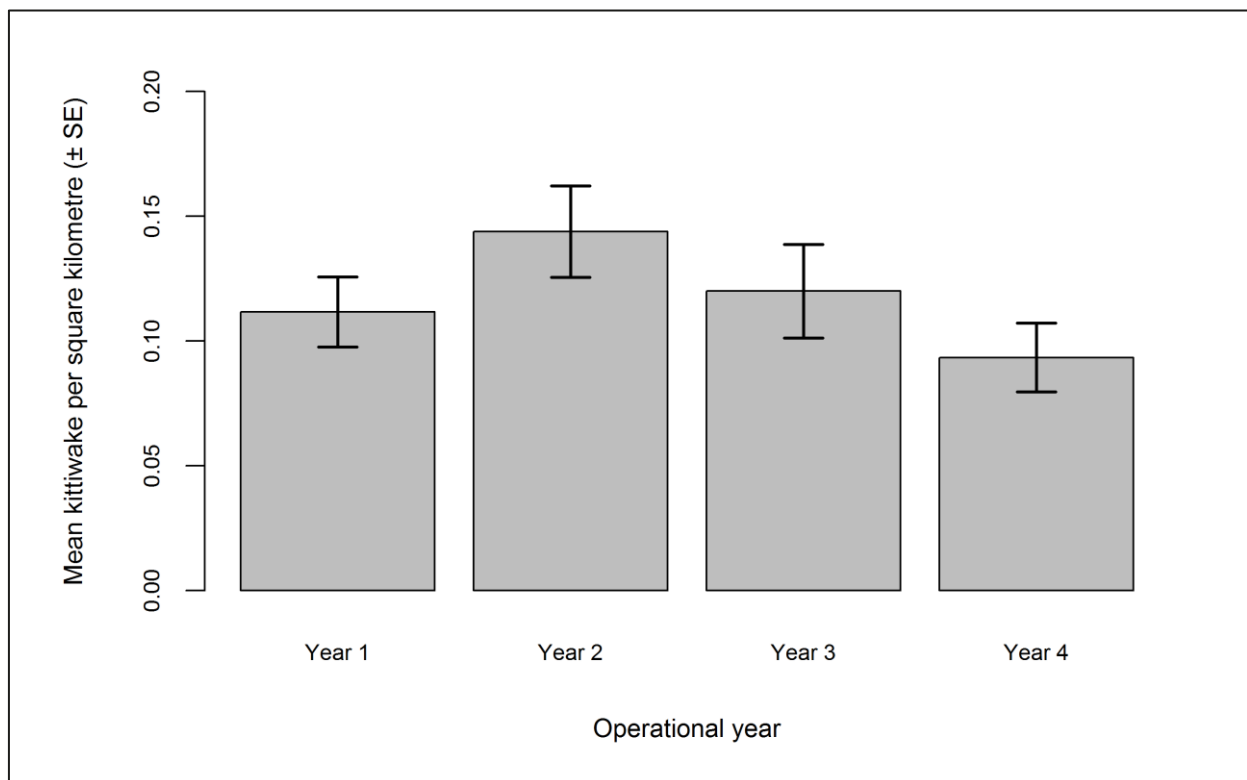


Figure 2.163: Mean density ( $\pm$  se) of kittiwakes recorded in flight across operational years one to four.

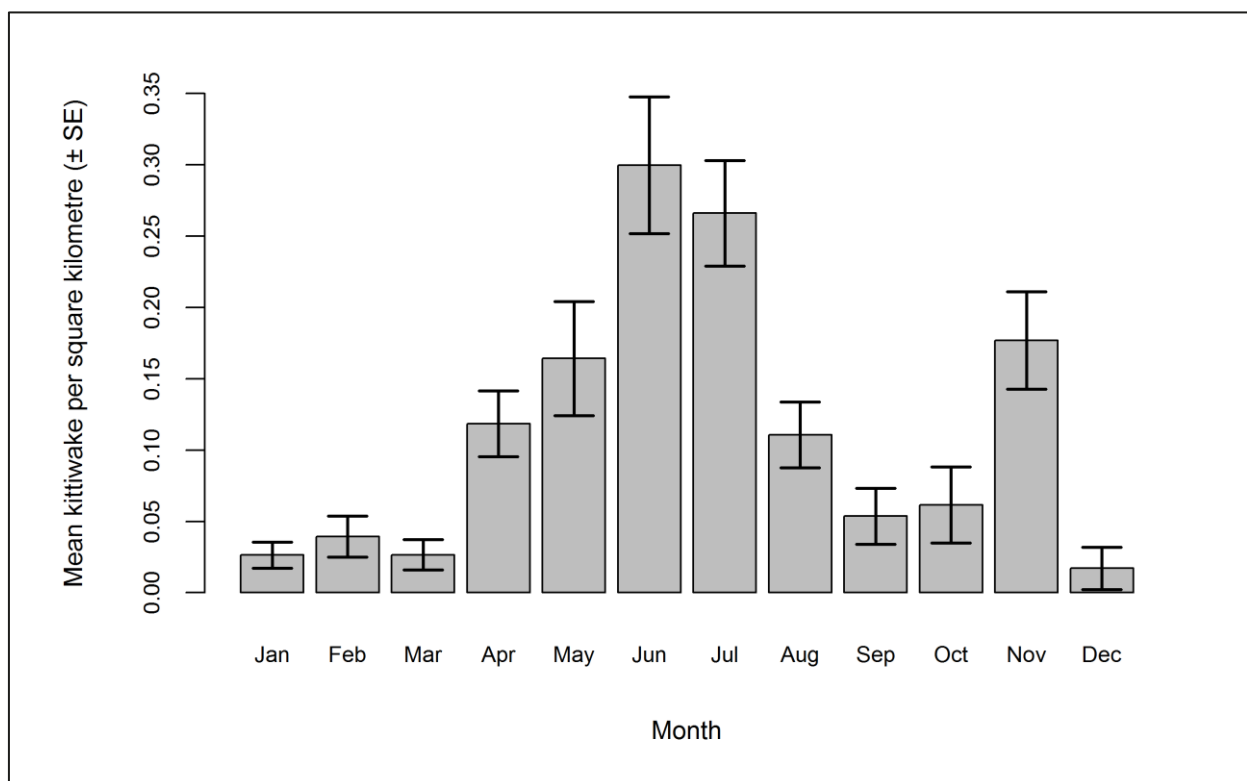


Figure 2.164: Mean density ( $\pm$  se) of kittiwakes recorded in flight during each month across operational years one to four.

Predicted kittiwake abundance and densities by site, buffer and total survey area are presented in Table 2.100. Within the Robin Rigg OWF itself, the proportion of flying kittiwakes was greatest during operational year two, as was total abundance. The smallest number of kittiwakes in flight was predicted to occur during operational year one (Table 2.100).

**Table 2.100: Abundance and density of kittiwakes in flight across operational years one to four. Values in parentheses represent upper and lower 95% confidence intervals.**

Operational year	Abundance			Density			% within site
	Site	Buffer	Total	Site	Buffer	Total	
<b>1</b>	10 (3-26)	118 (44-267)	128 (47-293)	0.80 (0.25-2.02)	0.34 (0.13-0.77)	0.36 (0.13-0.81)	8.05
<b>2</b>	56 (15-144)	361 (131-802)	416 (146-946)	4.30 (1.16-11.12)	1.04 (0.38-2.31)	1.15 (0.40-2.62)	13.35
<b>3</b>	20 (6-498)	203 (65-505)	222 (71-554)	1.53 (0.46-3.80)	0.58 (0.19-1.45)	0.62 (0.20-1.54)	8.88
<b>4</b>	40 (7-138)	289 (62-892)	329 (69-1,030)	3.12 (0.52-10.63)	0.83 (0.18-2.57)	0.91 (0.19-2.85)	12.28

The density surface maps show statistically significant increases in flying kittiwake abundance within the Robin Rigg OWF between operational year one and operational year two (Figure 2.165). This area of increased density declined during operational year three, but not significantly so (Figure 2.166). Kittiwake densities increases were seen again in operational year four although these were only statistically significant in the east of the survey area (Figure 2.165 and Figure 2.166).

198



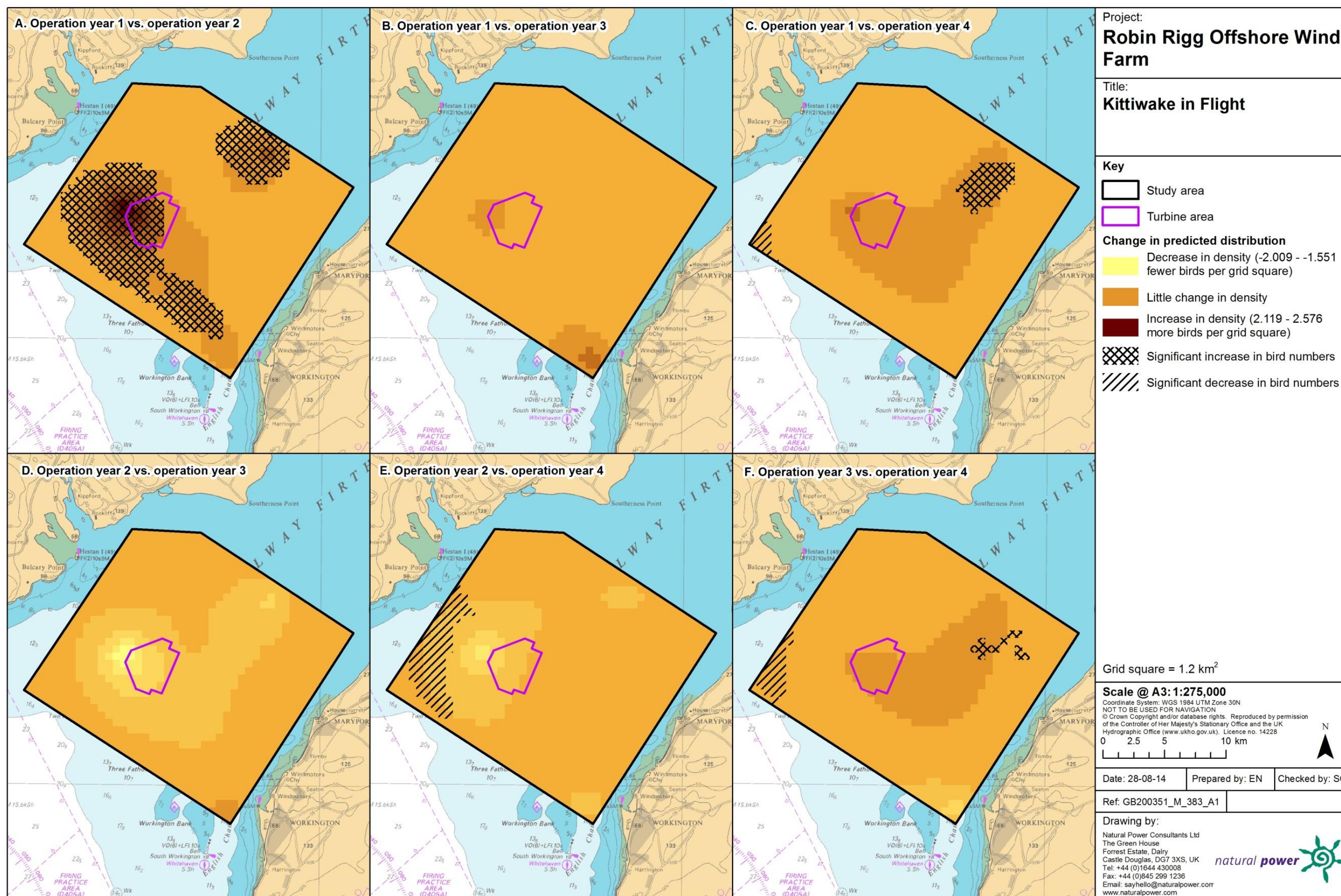


Figure 2.166: Differences in predicted flying kittiwake density between operational years. Significant differences are marked with diagonal shading.



#### 2.4.9.16.47. Collision risk

The percentage of kittiwakes recorded during the three development phases in different height bands relative to rotor swept height can be found in Table 2.101 and Figure 2.167. Since a relatively small percentage of kittiwakes were recorded flying at rotor swept height (<4%), a chi-squared test was not undertaken.

**Table 2.101: Percentage of kittiwakes recorded in different flight height bands across operational years one to four. Shaded column indicates percentage at rotor swept height (flight band 4).**

Operational year	Flight height band					
	1 (0–5 m)	2 (6–25 m)	3 (26–34 m)	4 (35–125 m)	5 (126–200 m)	6 (>200 m)
1	24.87	69.43	2.59	3.11	0.00	0.00
2	45.22	48.70	3.77	2.32	0.00	0.00
3	18.75	71.53	6.94	2.78	0.00	0.00
4	31.75	54.03	11.37	2.84	0.00	0.00

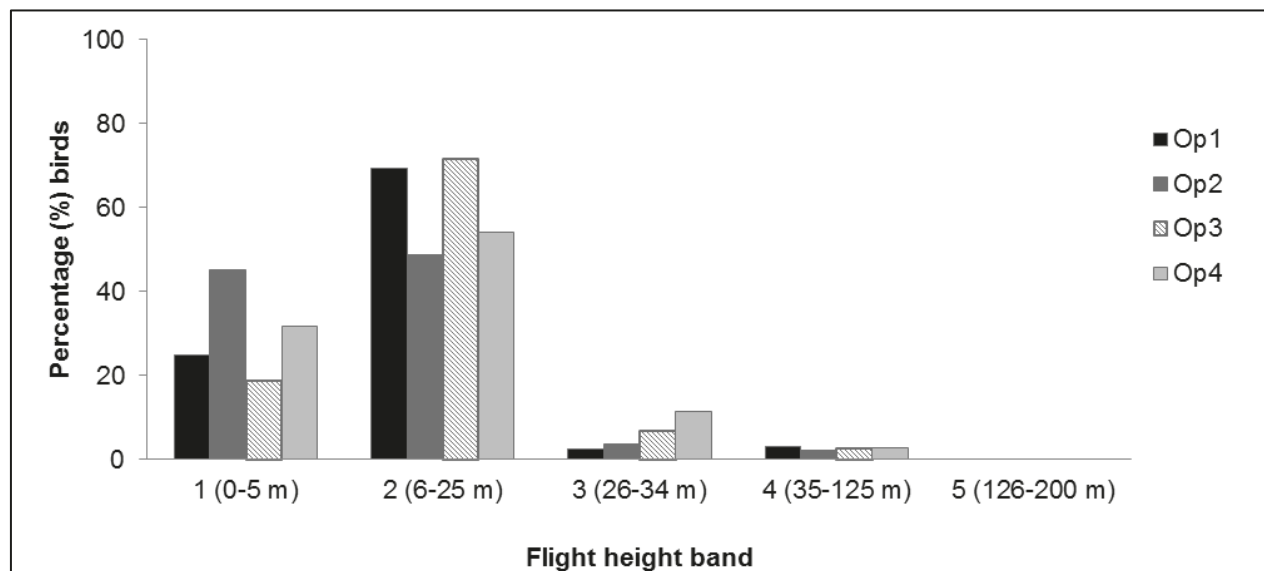


**Figure 2.167: Percentage of kittiwakes recorded in different flight height bands across operational years one to four.**

## 2.4.10. Great black-backed gull

### 2.4.10.17. Across three development phases

#### 2.4.10.17.48. Summary statistics

The total number of great black-backed gulls increased during the construction and operational phases in comparison to the pre-construction phase (Table 2.102). Whilst similar numbers of great black-backed gulls were recorded in flight and on the sea during the construction and operational phases, a larger proportion (0.67) of birds were recorded in flight during the pre-construction phase (Table 2.102).

**Table 2.102: Number of great black-backed gulls recorded per block during each development phase per km survey effort (all data).**

	Pre-construction		Construction		Operation years 1-2	
	On sea	In flight	On sea	In flight	On sea	In flight
<b>Total number individuals</b>	64	129	270	273	222	243
<b>Total number sightings</b>	41	111	154	212	122	146
<b>Number individuals/km</b>	0.02	0.04	0.04	0.04	0.06	0.06
	Total		Total		Total	
<b>Total number individuals</b>	193		534		465	
<b>Total number sightings</b>	152		366		268	
<b>Number individuals/km</b>	0.05		0.07		0.12	

Data were filtered as described in the methods (Section 2.4.4). The percentage of segments without observations was calculated to ensure there were sufficient data to perform the analysis (Table 2.103). Data were also checked to ensure observations were recorded in all months of the year.

**Table 2.103: Percentage of great black-backed gull analysis blocks without observations across the three development phases: pre-construction, construction and operational years one and two.**

	On sea	In flight
<b>Percentage zero blocks</b>	99.4%	99.0%

## 2.4.10.17.49. Density

### 2.4.10.17.49.1. On sea

Initial data exploration highlighted that >99% of analysis blocks for great black-backed gulls on the sea during the three development phases contained zero observations (Figure 2.168). When the segments were broken down by month and phase (Table 2.104), a number of combinations were highlighted as having no observations. Therefore MRSea modelling was not undertaken.

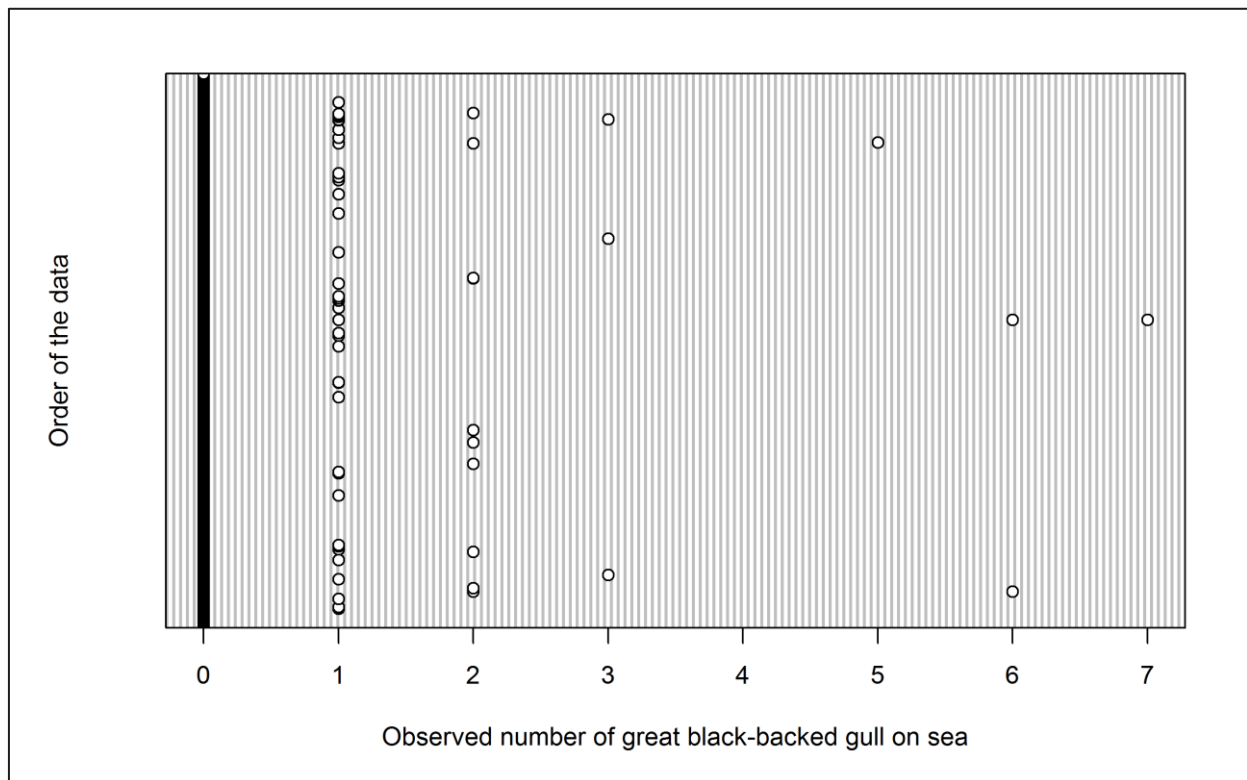


Figure 2.168: Dot plot of the number of great black-backed gulls observed on sea per analysis block across the three development phases: pre-construction, construction and operational years one and two.



**Table 2.104: Number of great black-backed gulls available for analysis each month across the three development phases: pre-construction, construction and operational years one and two.**

Month	Pre-construction	Construction	Operation	Total
Jan	5	1	1	7
Feb	4	0	10	14
Mar	2	6	1	9
Apr	0	1	0	1
May	0	0	3	3
Jun	4	1	0	5
Jul	2	13	2	17
Aug	2	1	0	3
Sep	16	5	3	24
Oct	0	5	0	5
Nov	0	2	3	5
Dec	3	0	2	5

Group size for great black-backed gulls recorded on the sea ranged from single individuals up to seven birds. Mean density of great black-backed gulls on the sea indicates little change between development phases (Figure 2.169). However, since further modelling was not undertaken, the significance of any differences could not be tested. Figure 2.170 shows that mean density of great black-backed gulls peaked in September, although density was small across all months.



Figure 2.169: Mean density (± se) of great black-backed gull recorded on the sea across the three development phases: pre-construction, construction and operational years one and two.

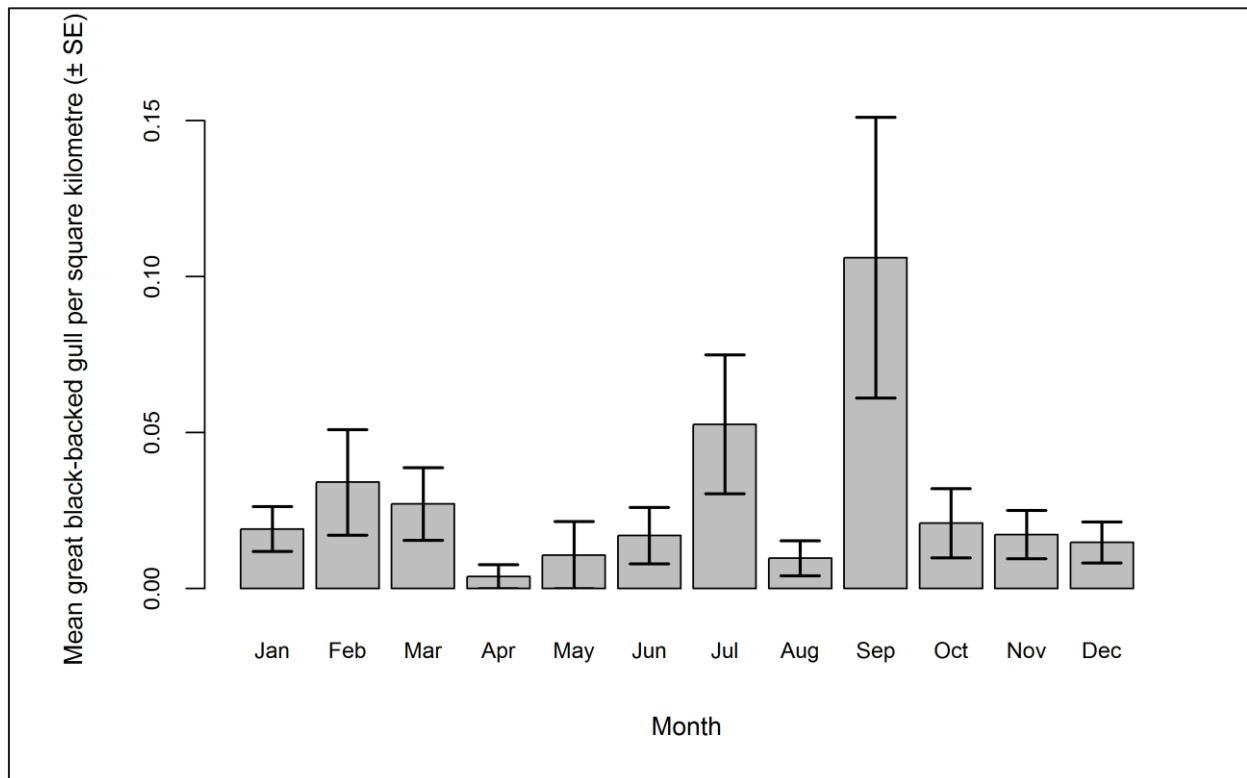


Figure 2.170: Mean density (± se) of great black-backed gull recorded on the sea during each month across the three development phases: pre-construction, construction and operational years one and two.

#### 2.4.10.17.49.2. In flight

Data exploration indicated that less than 1% of segments contained observations (Table 2.103). When the segments were broken down by month and phase (Table 2.105), a number of combinations were highlighted as having no observations. Therefore MRSea modelling was not undertaken.

**Table 2.105: Number of great black-backed gulls available for analysis each month across the three development phases: pre-construction, construction and operational years one and two.**

Month	Pre-construction	Construction	Operation	Total
Jan	2	3	1	6
Feb	6	0	13	19
Mar	5	3	9	17
Apr	6	2	0	8
May	0	4	0	4
Jun	7	2	1	10
Jul	2	11	3	16
Aug	4	2	2	8
Sep	3	5	0	8
Oct	1	5	2	8
Nov	0	0	0	0
Dec	3	5	7	15

The majority of segments contained only a single bird, with six being the maximum (Figure 2.171). Density of gulls across the three phases suggests a decrease in numbers compared to the pre-construction phase (Figure 2.172), although it is not possible to test this significance. The raw data suggest that great black-backed gulls are present in small numbers throughout the year (Figure 2.173).

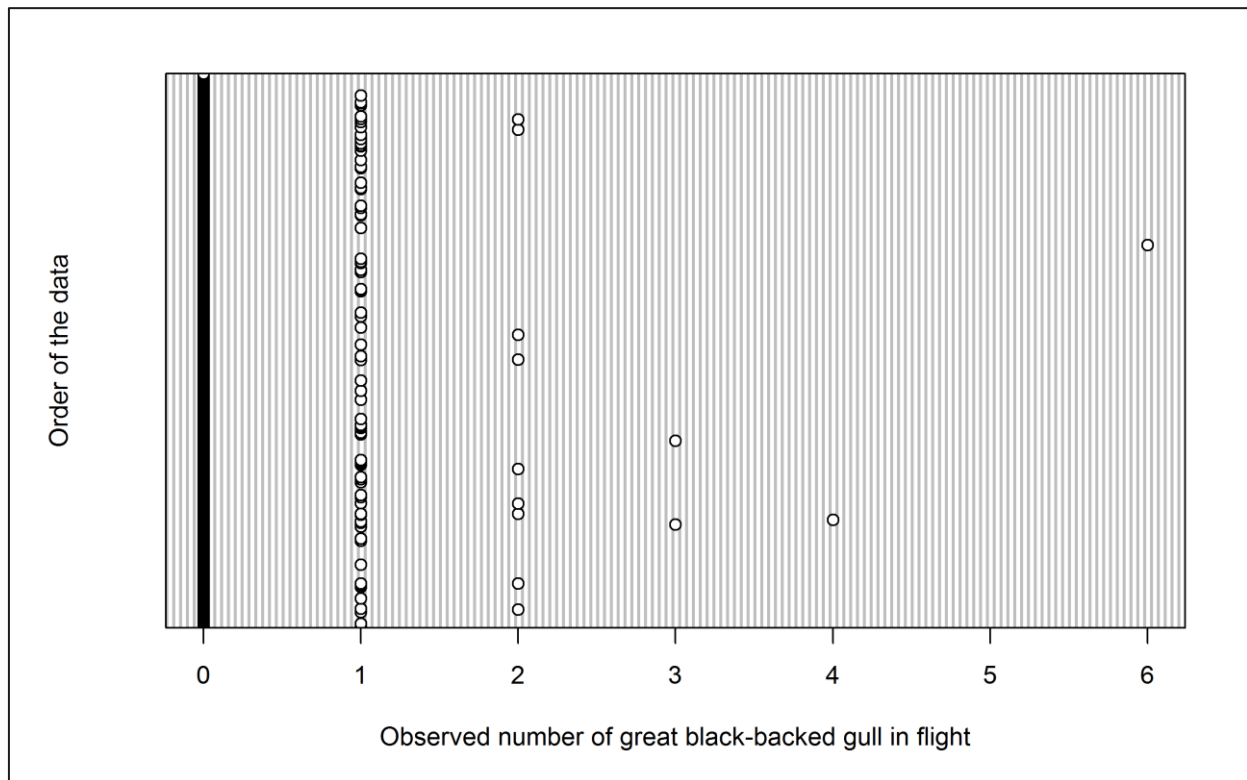


Figure 2.171: Dot plot of the number of great black-backed gulls observed in flight per analysis block across the three development phases: pre-construction, construction and operational years one and two.





Figure 2.172: Mean density (± se) of great black-backed gulls recorded in flight across the three development phases: pre-construction, construction and operational years one and two.

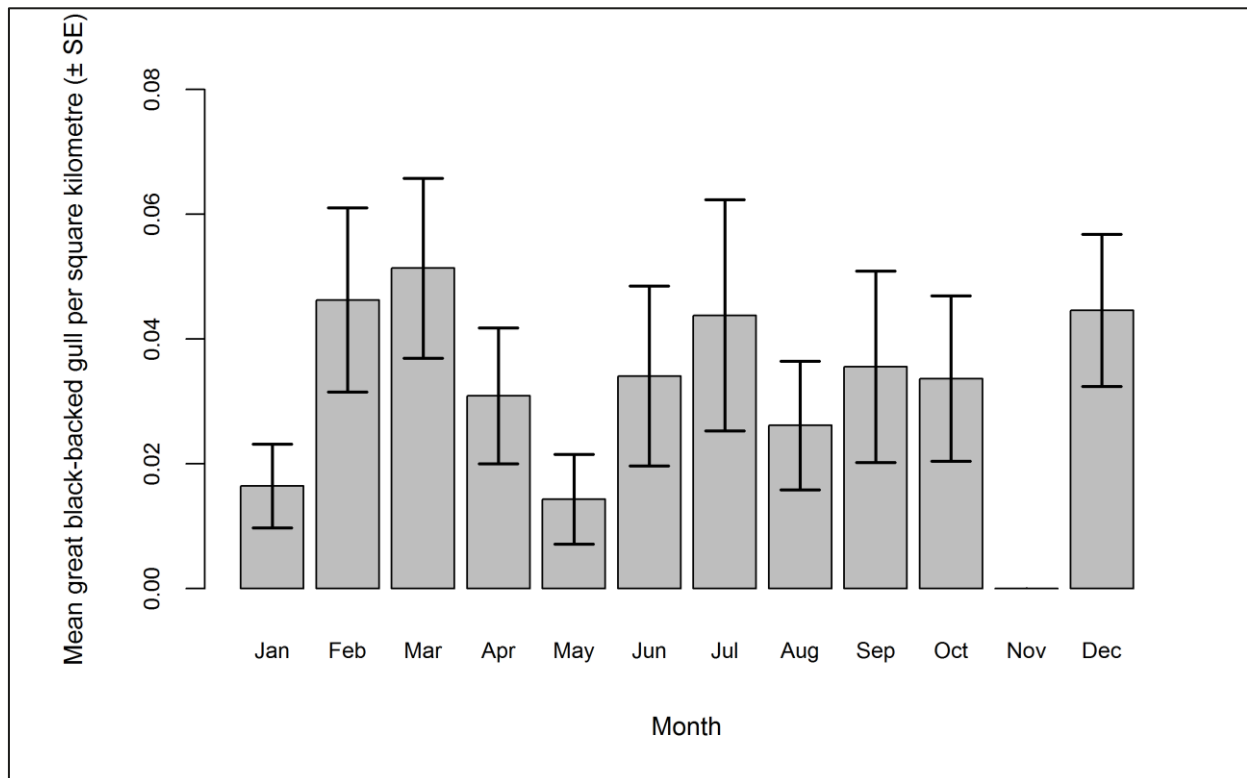


Figure 2.173: Mean density (± se) of great black-backed gulls recorded in flight during each month across the three development phases: pre-construction, construction and operational years one and two.

#### 2.4.10.17.50. Distribution

Since abundance modelling of great black-backed gull was not possible across the three development phases, Figure 2.174 shows the distribution of raw great black-backed gull observations during pre-construction, construction and operational monitoring. Both flying and sitting birds are represented. Relatively small numbers of great black-backed gull sightings were recorded during across the three development phases (Figure 2.174). Birds were more evenly distributed across the survey area during the pre-construction phase, showing a more concentrated distribution along the Cumbrian coast during construction and operation (Figure 2.174).

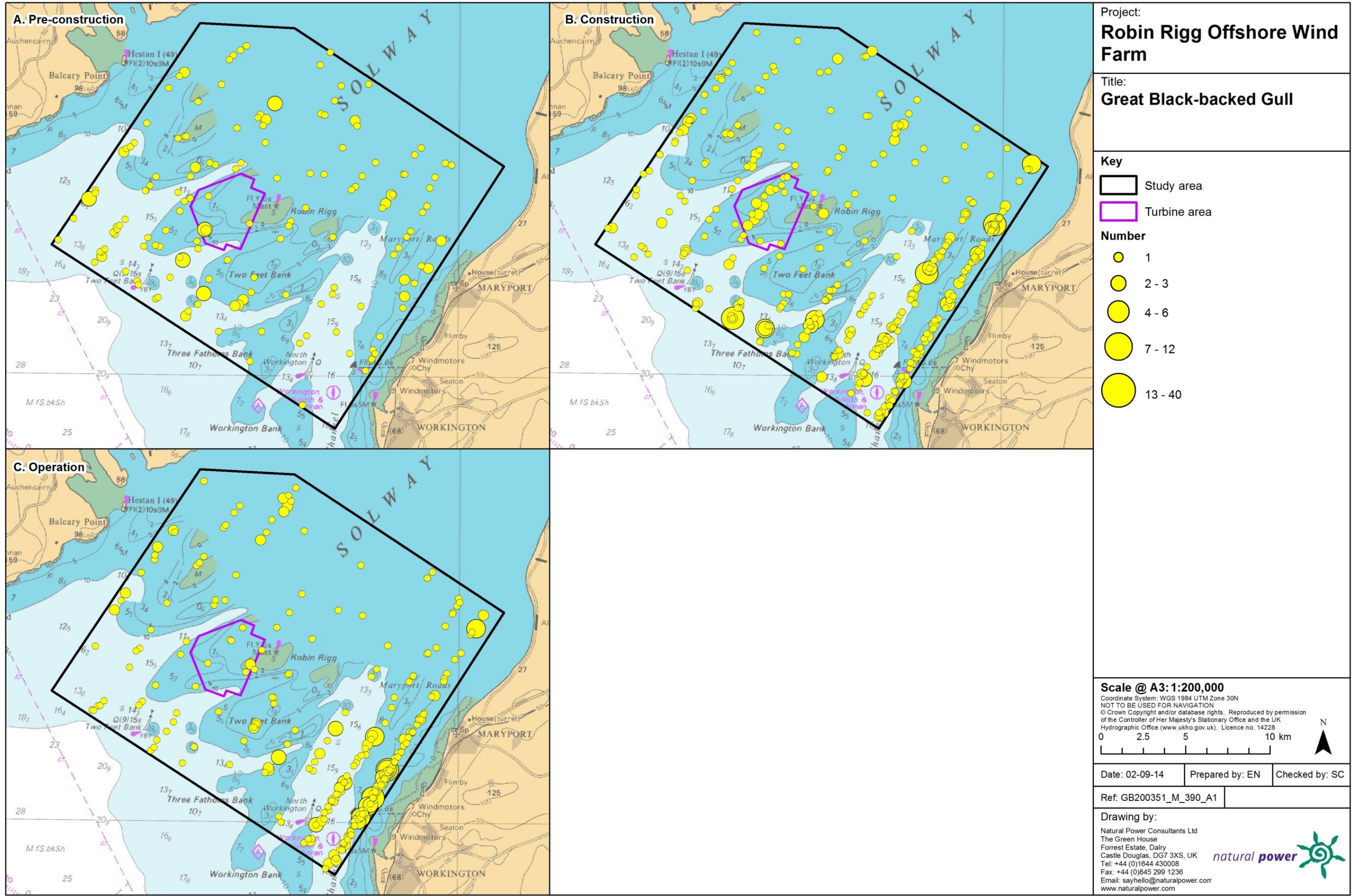


Figure 2.174: Location of raw great black-backed observations during a) pre-construction, b) construction and c) operational monitoring. Both flying and sitting birds are represented. Circle size is proportional to the number of great black-backed gulls sighted.



### 2.4.10.17.51. Collision risk

The percentage of great black-backed gulls recorded during the three development phases in different height bands relative to rotor swept height can be found in Table 2.106 and Figure 2.175. Data were combined for chi-squared analysis and a statistically significant difference was found between flight bands ( $\chi^2 = 5.98$ ,  $df = 2$ ,  $p = 0.05$ ). Fewer great black-backed gulls than expected were observed at rotor swept height during pre-construction surveys. This may be a result of great black-backed gull flight heights being underestimated since there were no turbines present in the survey area to use as a reference. Larger numbers than expected were recorded at rotor swept height during operational monitoring.

**Table 2.106: Percentage of great black-backed gulls recorded in different flight height bands across the three development phases: pre-construction, construction and operational years one and two. Shaded column indicates percentage at rotor swept height (flight band 4).**

Phase	Flight height band					
	1 (0–5 m)	2 (6–25 m)	3 (26–34 m)	4 (35–125 m)	5 (126–200 m)	6 (>200 m)
Pre-construction	25.58	61.24	7.75	5.43	0.00	0.00
Construction	12.87	58.09	16.54	12.50	0.00	0.00
Operation	12.76	60.49	13.17	13.58	0.00	0.00

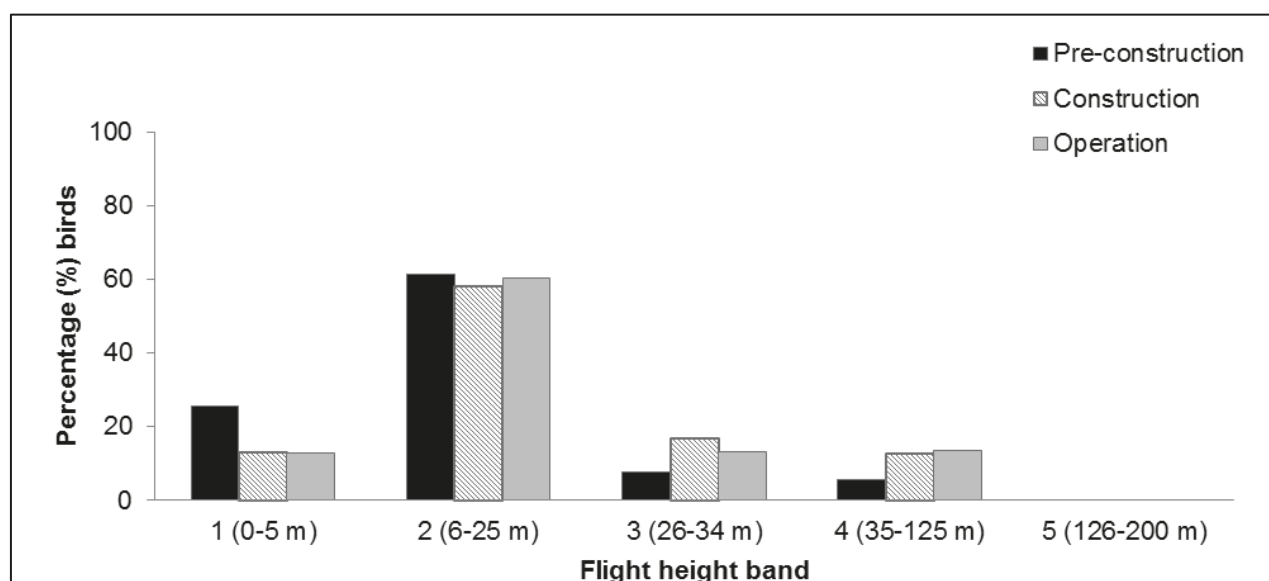


**Figure 2.175: Percentage of great black-backed gulls recorded in different flight height bands across the three development phases: pre-construction, construction and operational years one and two.**



## 2.4.10.18. Across operational years

### 2.4.10.18.52. Summary statistics

The number of great black-backed gulls recorded per km of survey effort was similar throughout operational monitoring (Table 2.107). Comparable numbers were recorded on the sea and in flight throughout operational years one to three, with a slightly larger majority (c. 60%) of great black-backed gulls recorded on the sea during operational year four (Table 2.107).

**Table 2.107: Number of great black-backed gulls recorded per block during each operational year per km survey effort (all data).**

	Operational year 1		Operational year 2		Operational year 3		Operational year 4	
	On sea	In flight	On sea	In flight	On sea	In flight	On sea	In flight
<b>Total number individuals</b>	113	105	109	138	190	141	159	96
<b>Total number sightings</b>	61	57	61	89	126	127	132	89
<b>Number individuals/km</b>	0.06	0.06	0.05	0.07	0.09	0.07	0.07	0.04
	Total		Total		Total		Total	
<b>Total number individuals</b>	218		247		331		255	
<b>Total number sightings</b>	118		150		253		221	
<b>Number individuals/km</b>	0.12		0.12		0.15		0.12	

Data were filtered as described in the methodology (Section 2.4.4). The percentage of segments without observations was calculated to ensure there were sufficient data to perform the analysis (Table 2.108). Data were also checked to ensure observations were recorded in all months of the year.

**Table 2.108: Percentage of great black-backed gull analysis blocks without observations across operational years one to four.**

	On sea	In flight
<b>Percentage zero blocks</b>	97.7%	98.9%

## 2.4.10.18.53. Density and distribution

### 2.4.10.18.53.1. On sea

A hazard-rate detection function with sea state as a covariate was found to be the best fitting model. Figure 2.176 shows the selected detection curve for great black-backed gulls.

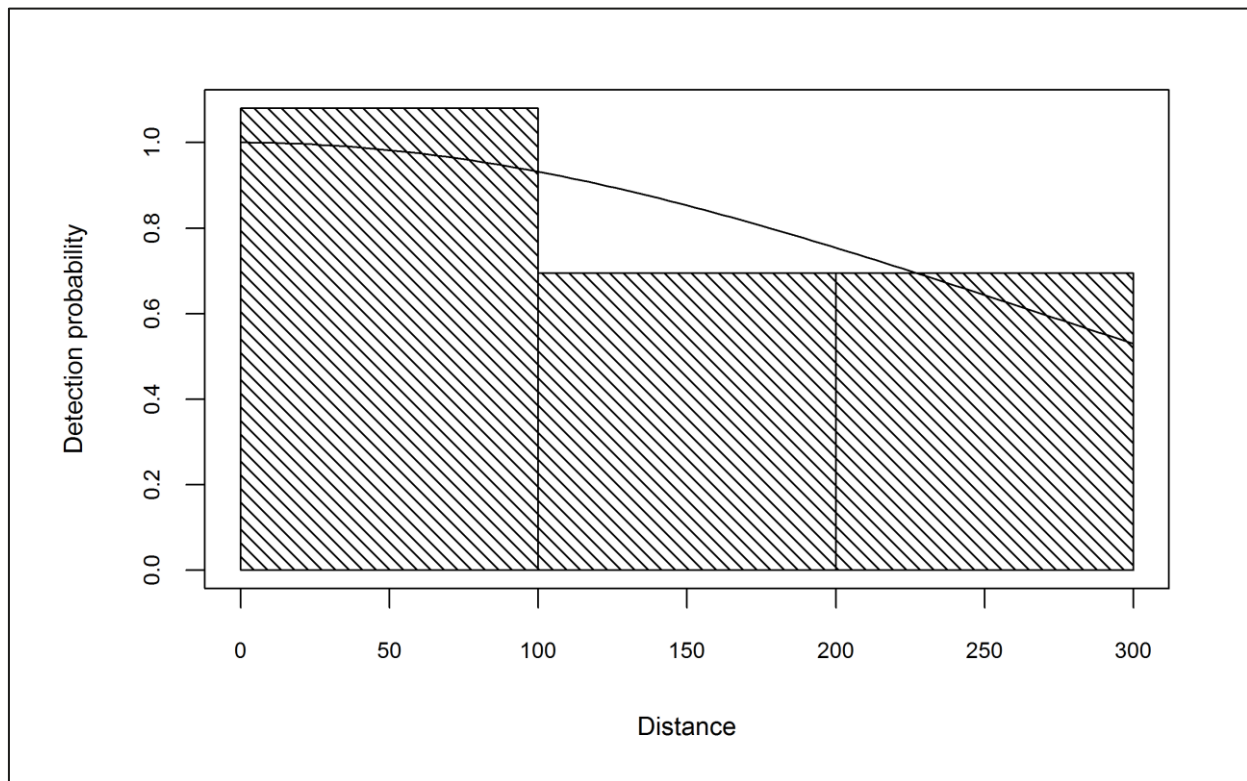


Figure 2.176: Detection curve used to adjust great black-backed gull on sea counts for imperfect detection across operational years one to four.

Initial data exploration of adjusted numbers of great black-backed gulls indicated there were no outlying observations (Figure 2.177).

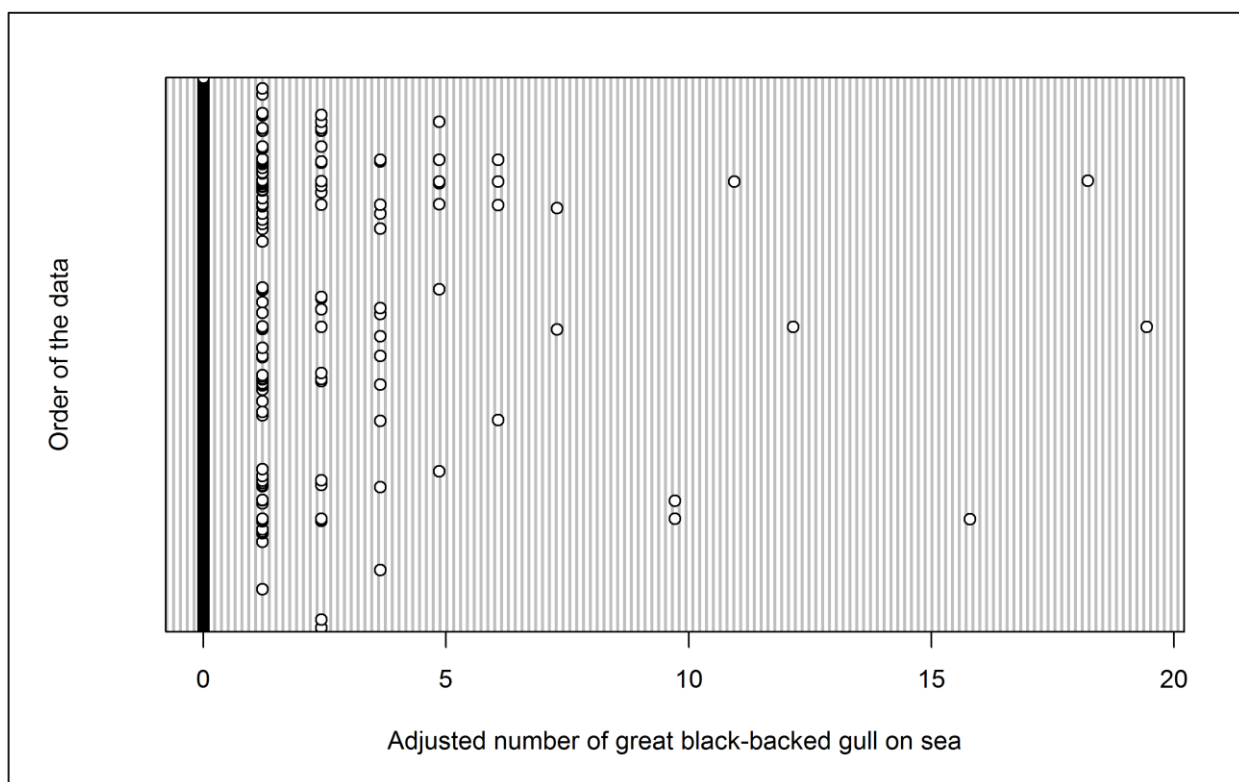


Figure 2.177: Dot plot of the number of great black-backed gulls observed on sea per analysis block across operational years one to four.

The model predicted that month, location, and the interaction location and operational year (phase) had a statistically significant influence on great black-backed gull abundance within the survey area (Table 2.109). Operational year had no effect on numbers (Figure 2.178). Although not statistically significant, great black-backed gull numbers peaked November (Figure 2.179). Model predictions were therefore made for this month.

Table 2.109: Final model outputs for great black-backed gulls on the sea across operational years one to four.

Term	Marginal p-value
Month	<0.0001
Phase	0.2326
Tide height	0.0837
Location (X,Y)	<0.0001
Interaction (location: phase)	0.0290

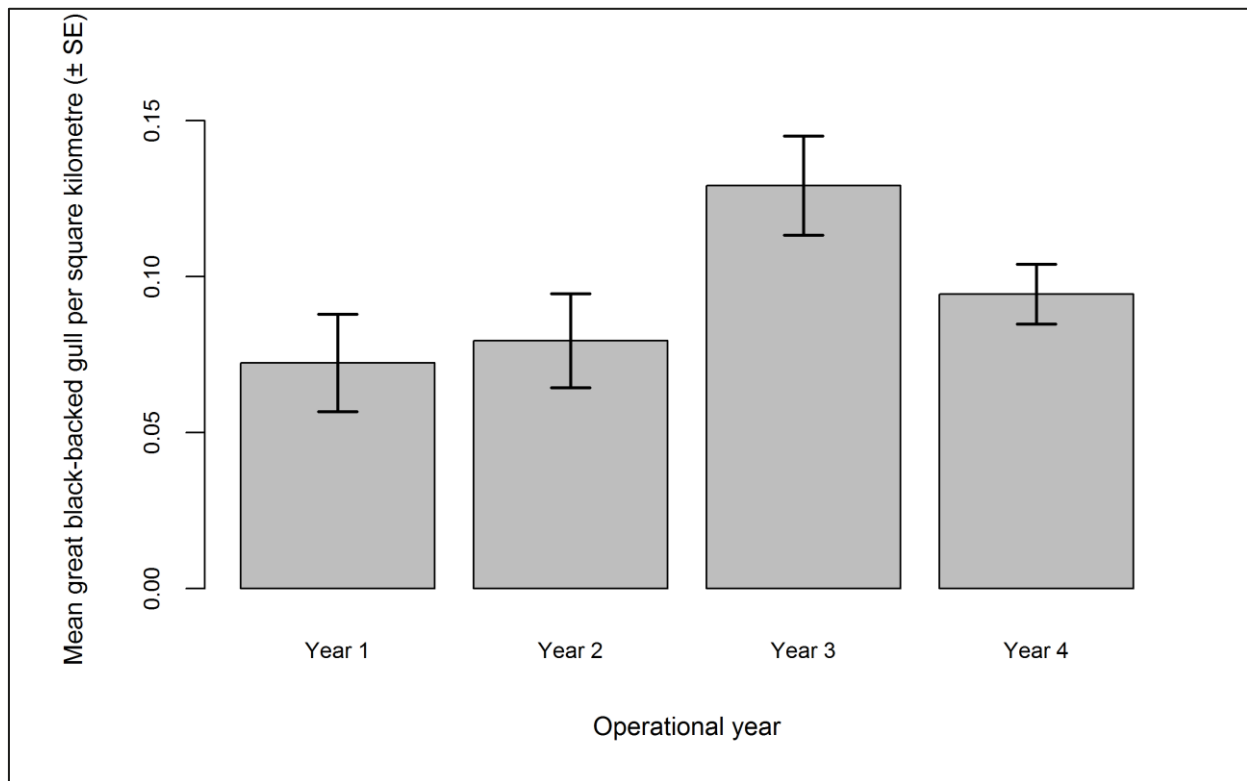


Figure 2.178: Mean density ( $\pm$  se) of great black-backed gulls recorded on the sea across operational years one to four.

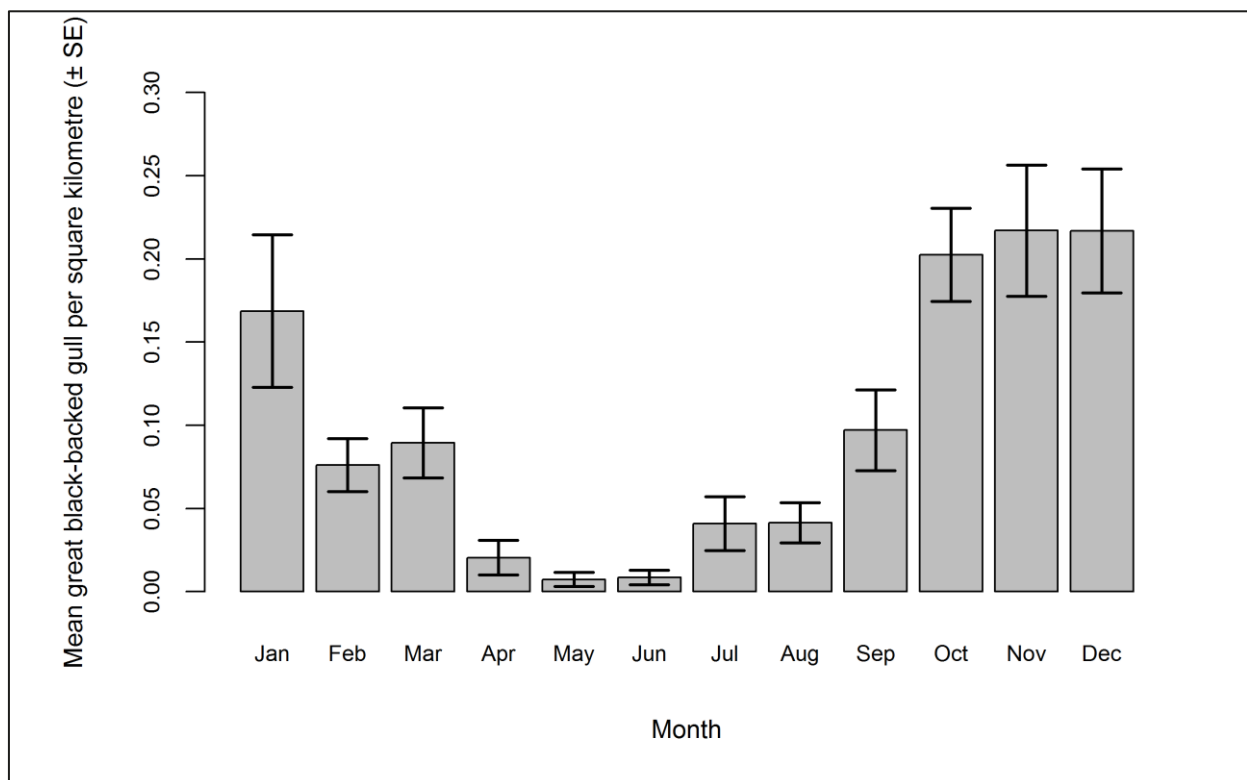


Figure 2.179: Mean density ( $\pm$  se) of great black-backed gulls recorded on the sea during each month across operational years one to four.

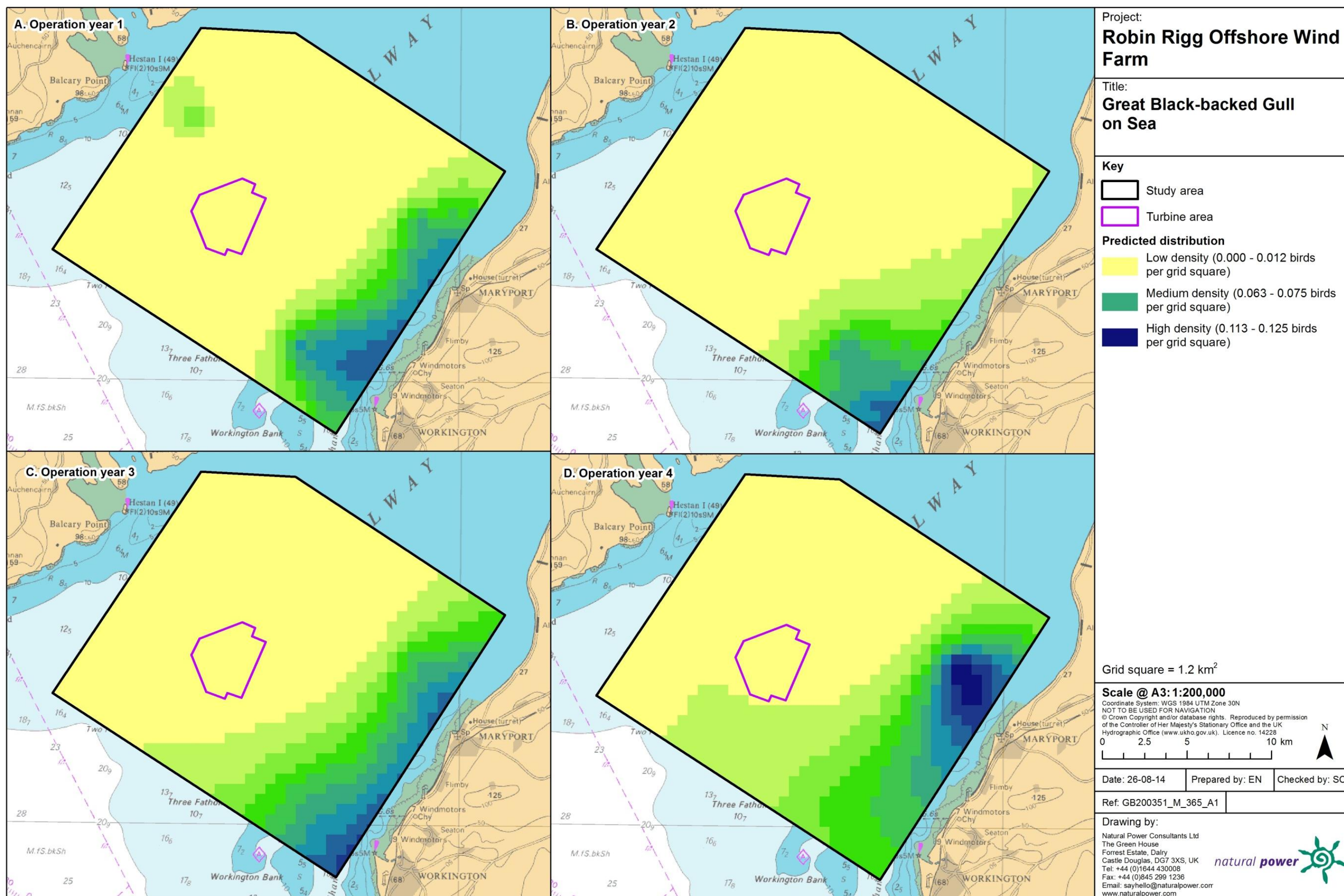


The abundance and densities by site, buffer and total survey area are presented in Table 2.110. There was little change in the abundance and density of great black-backed gulls throughout operation.

**Table 2.110: Abundance and density of great black-backed gulls on the sea across operational years one to four. Values in parentheses represent upper and lower 95% confidence intervals.**

Operational year	Abundance			Density			% within site
	Site	Buffer	Total	Site	Buffer	Total	
<b>1</b>	0	2	2	0.00	0.01	0.01	0.09
	(0-0)	(0-421)	(0-422)	(0.00-0.02)	(0.00-1.21)	(0.00-1.17)	
<b>2</b>	0	59	59	0.00	0.00	0.00	0.62
	(0-0)	(1-105)	(1-106)	(0.00-0.01)	(0.00-0.05)	(0.00-0.05)	
<b>3</b>	1	92	93	0.00	0.01	0.01	0.60
	(0-1)	(2-127)	(2-129)	(0.00-0.02)	(0.00-0.06)	(0.00-0.06)	
<b>4</b>	1	101	103	0.00	0.01	0.01	1.07
	(0-1)	(2-157)	(2-161)	(0.00-0.04)	(0.00-0.08)	(0.00-0.08)	

The density surface maps reflect that there was little change in the abundance and density of great black-backed gulls throughout operation. There was a statistically significant increase in great black-backed gull densities in a small area to the far east of the survey area between operational years two and three, and two and four (Figure 2.180 and Figure 2.181).





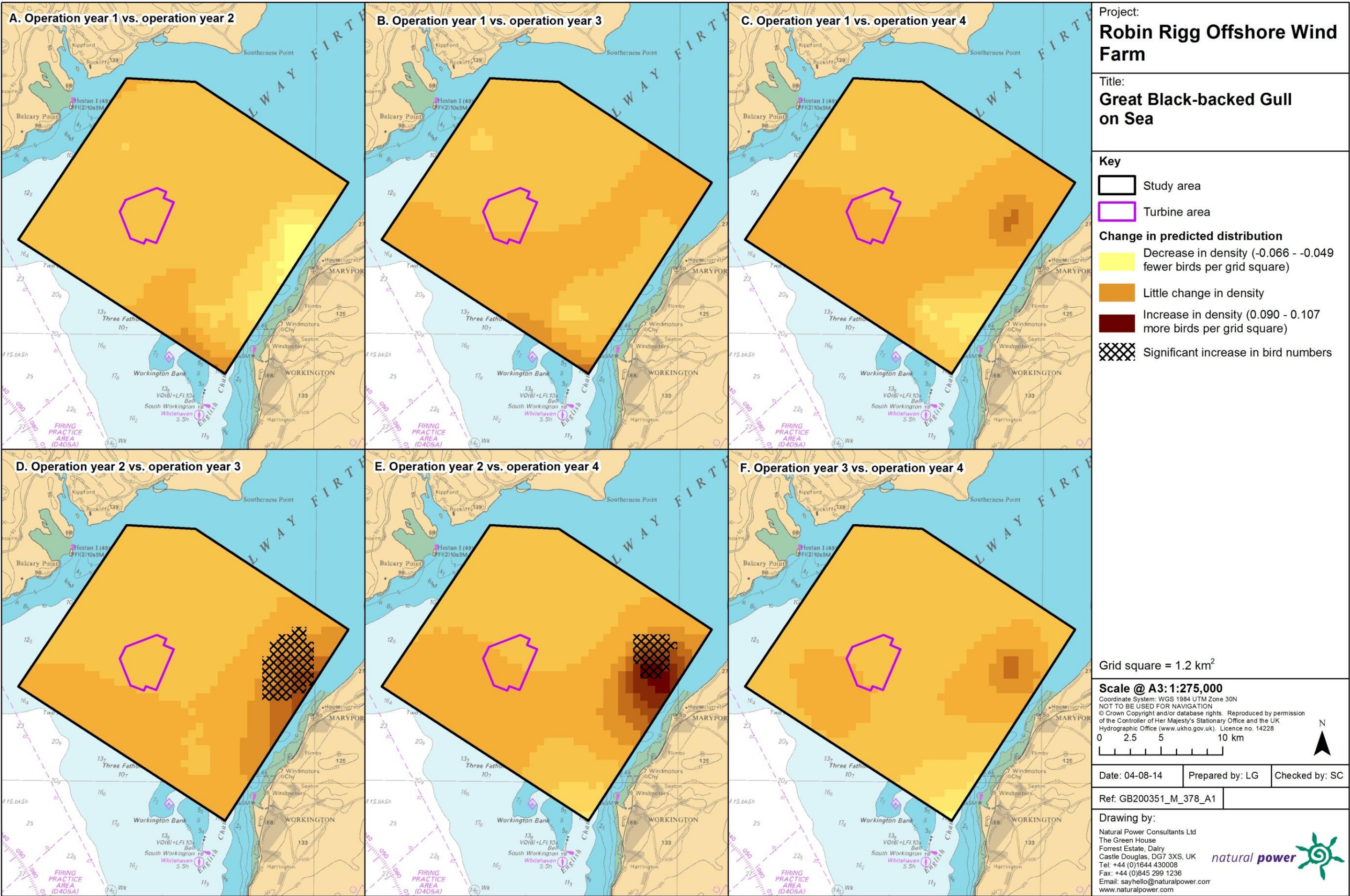


Figure 2.181: Differences in predicted sitting great black-backed gull density between operational years. Significant differences are marked with diagonal shading.



#### 2.4.10.18.53.2. In flight

Initial data exploration highlighted a possible outlier (segment containing six birds recorded in July 2010) that may influence the modelling process (Figure 2.182). However, the model was not run without this outlier as it did not appear to have a large influence.

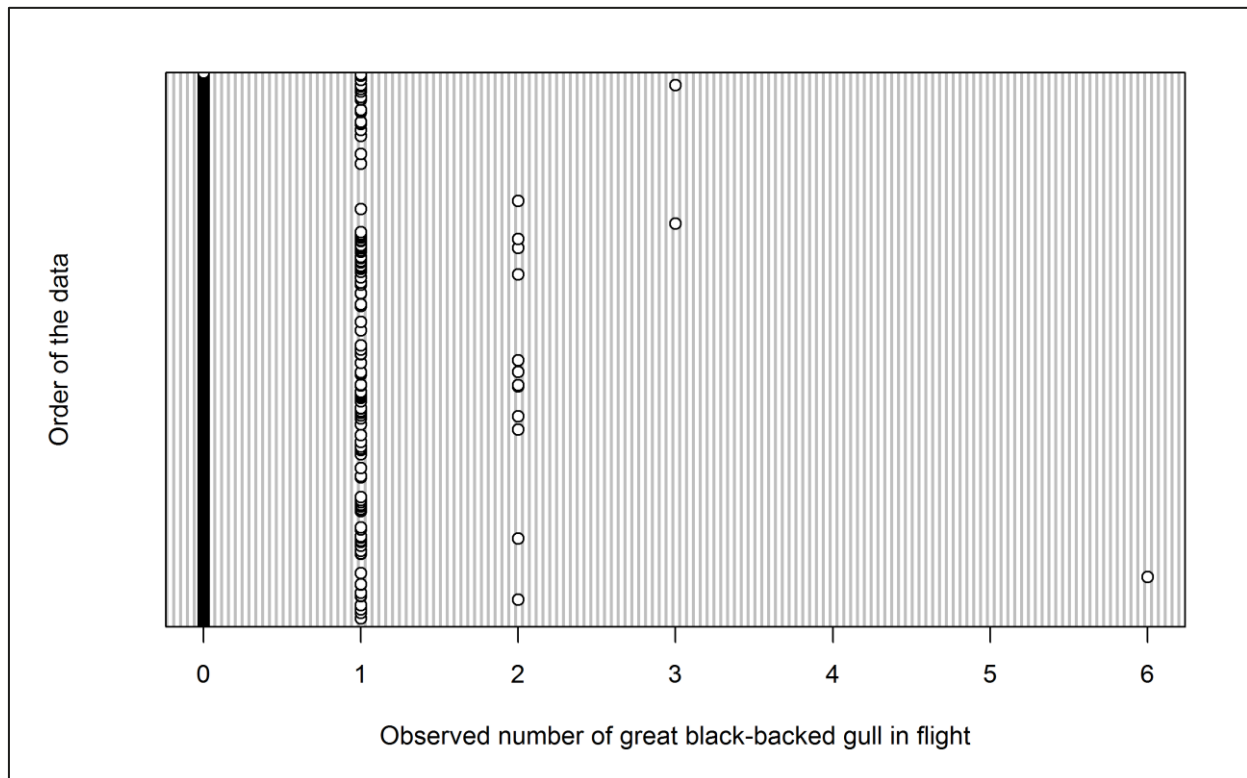


Figure 2.182: Dot plot of the number of great black-backed gulls observed in flight per analysis block across operational years one to four.

The GEE predicted that all variables had a statistically significant influence on great black-backed gull abundance within the survey area (Table 2.111). However the interaction between location and operational year was not statistically significant. Specifically, larger numbers were predicted in operational year three (Figure 2.183), and during the winter months, with peak numbers predicted for January (Figure 2.184). Since January was the month of peak activity, model predictions were made for this month.

Table 2.111: Final model outputs for great black-backed gulls in flight across operational years one to four.

Term	Marginal p-value
Month	<0.0001
Phase	0.0186
Tide height	0.0188
Location (X,Y)	<0.0001
Interaction (location: phase)	0.0854



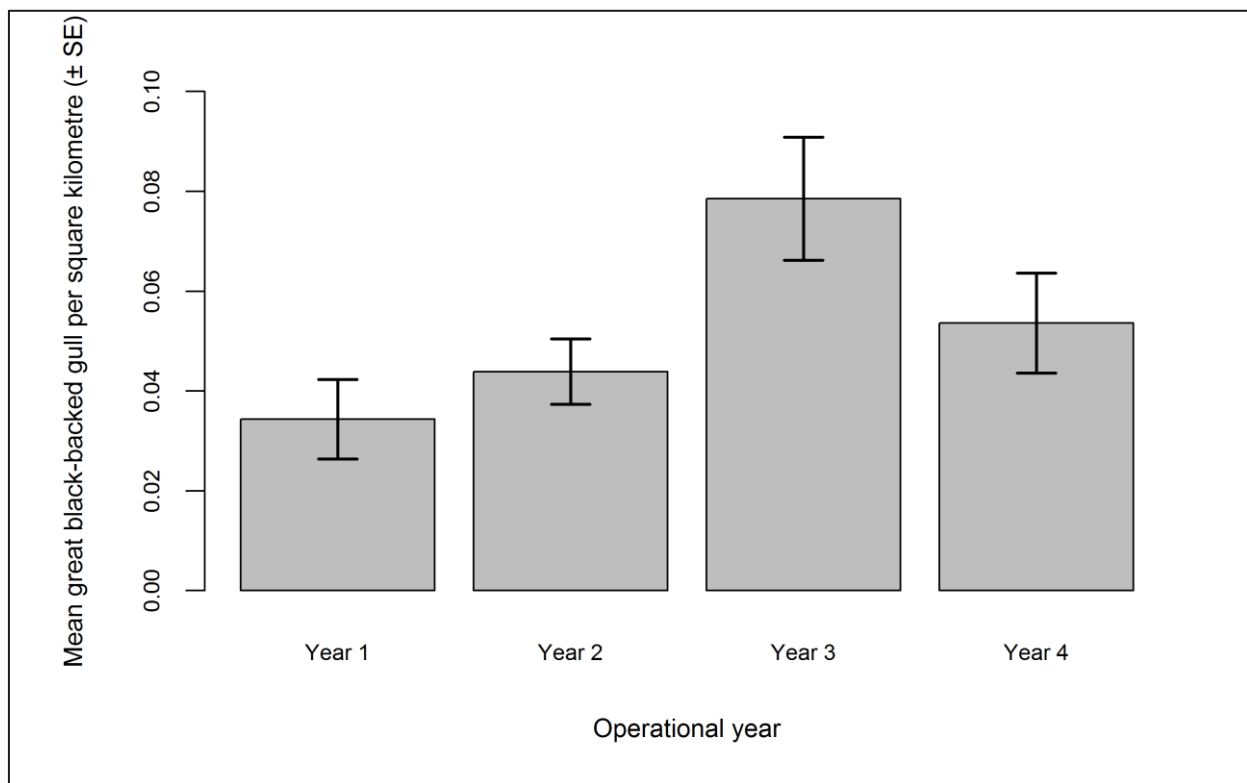


Figure 2.183: Mean density ( $\pm$  se) of great black-backed gulls recorded in flight across operational years one to four.

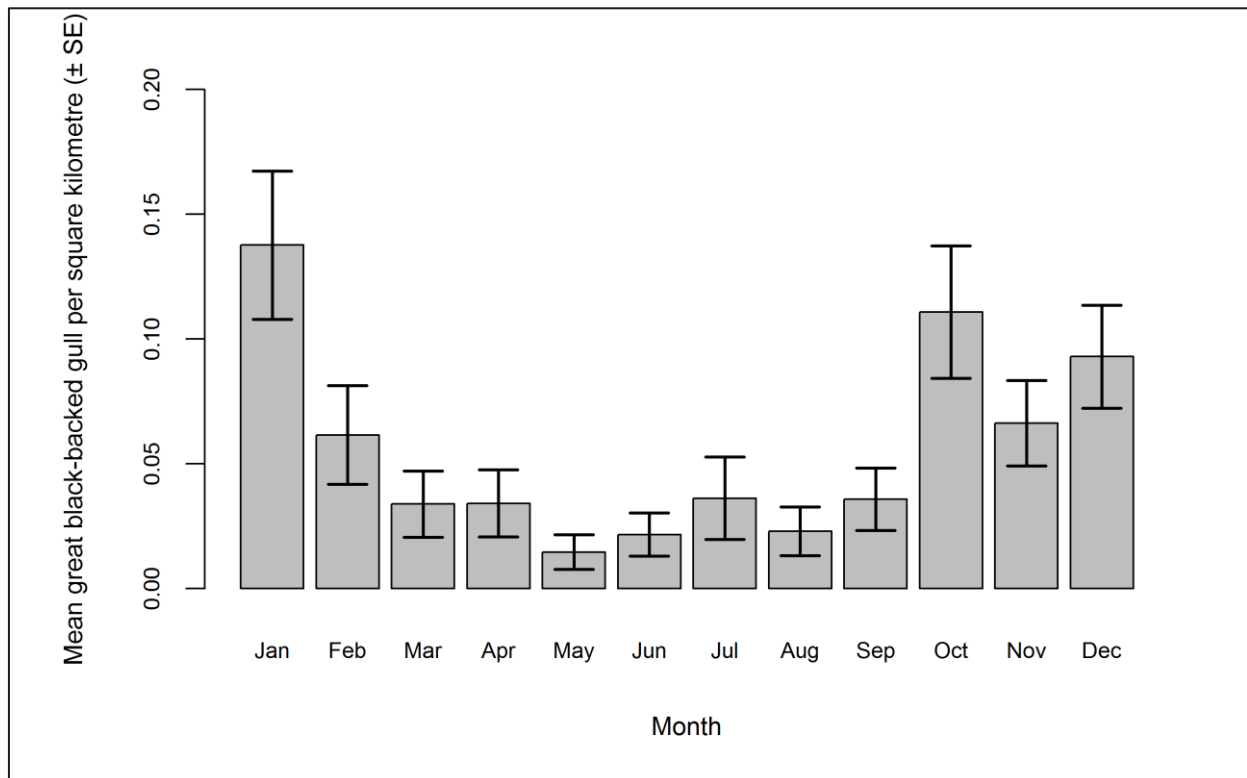


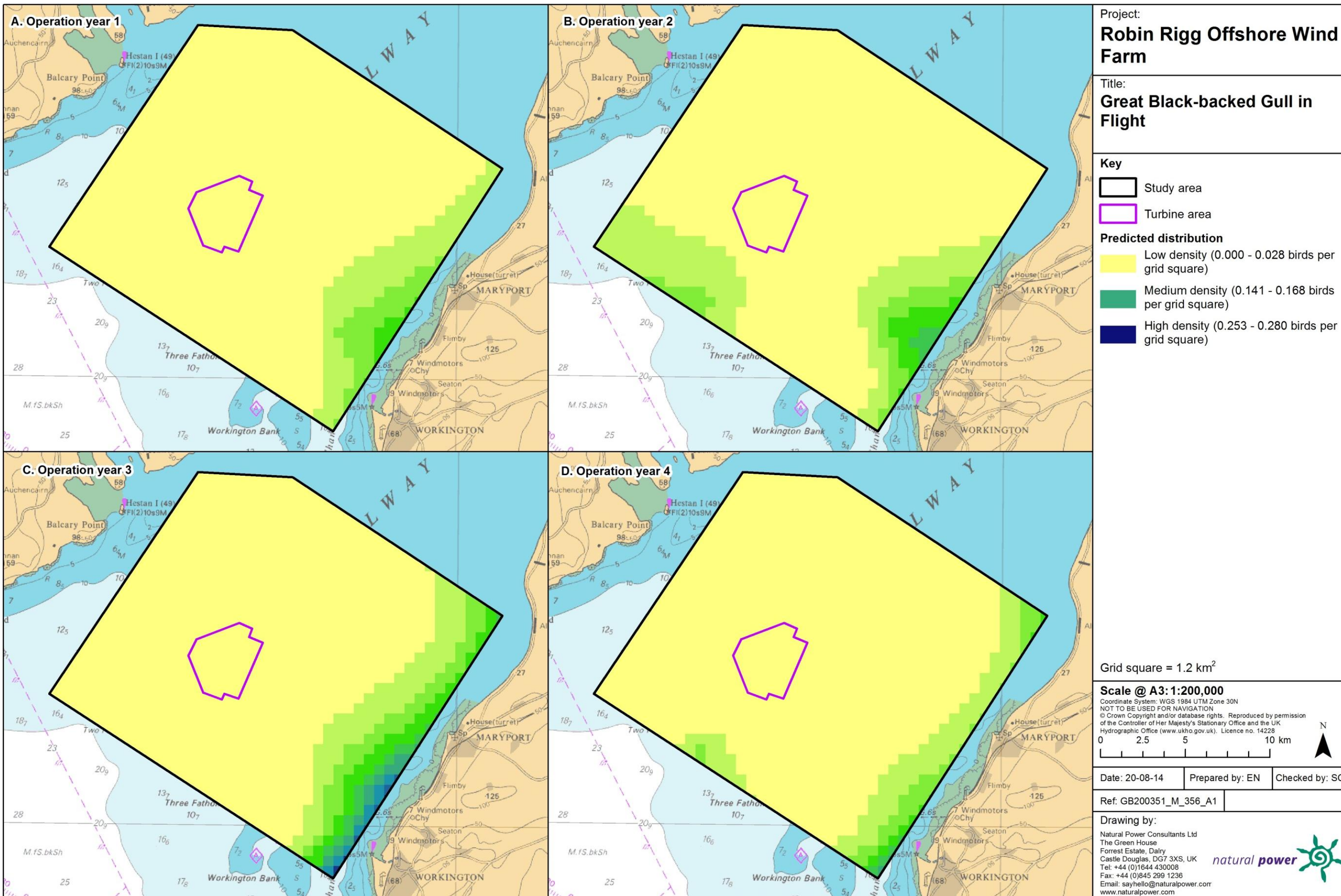
Figure 2.184: Mean density ( $\pm$  se) of great black-backed gulls recorded in flight during each month across operational years one to four.

The abundance and densities (by site, buffer and total survey area) are presented in Table 2.112. Although total abundance was greatest during operational year three, the smallest percentage of great black-backed gulls was recorded within the Robin Rigg OWF during this year (Table 2.112).

**Table 2.112: Abundance and density of great black-backed gulls in flight across operational years one to four.** Values in parentheses represent upper and lower 95% confidence intervals.

Operational year	Abundance			Density			% within site
	Site	Buffer	Total	Site	Buffer	Total	
<b>1</b>	0	14	15	0.02	0.04	0.04	1.77
	(0-1)	(4-51)	(4-53)	(0-0.11)	(0.01-0.15)	(0.01-0.15)	
<b>2</b>	1	19	20	0.05	0.06	0.06	3.06
	(0-2)	(7-57)	(7-59)	(0.01-0.19)	(0.02-0.16)	(0.02-0.16)	
<b>3</b>	0	23	23	0.02	0.07	0.06	0.88
	(0-1)	(9-64)	(9-64)	(0-0.06)	(0.02-0.18)	(0.02-0.18)	
<b>4</b>	0	12	12	0.00	0.03	0.03	0.50
	(0-0)	(3-42)	(3-42)	(0-0.02)	(0.01-0.12)	(0.01-0.12)	

The density surface maps reflect that there was little change in the abundance and density of flying great black-backed gulls throughout operation (Figure 2.185). Whilst there is a statistically significant decline in great black-backed density in the centre of the survey area between operational years two and four, densities were very small so these changes are unlikely to be biologically meaningful (Figure 2.186).





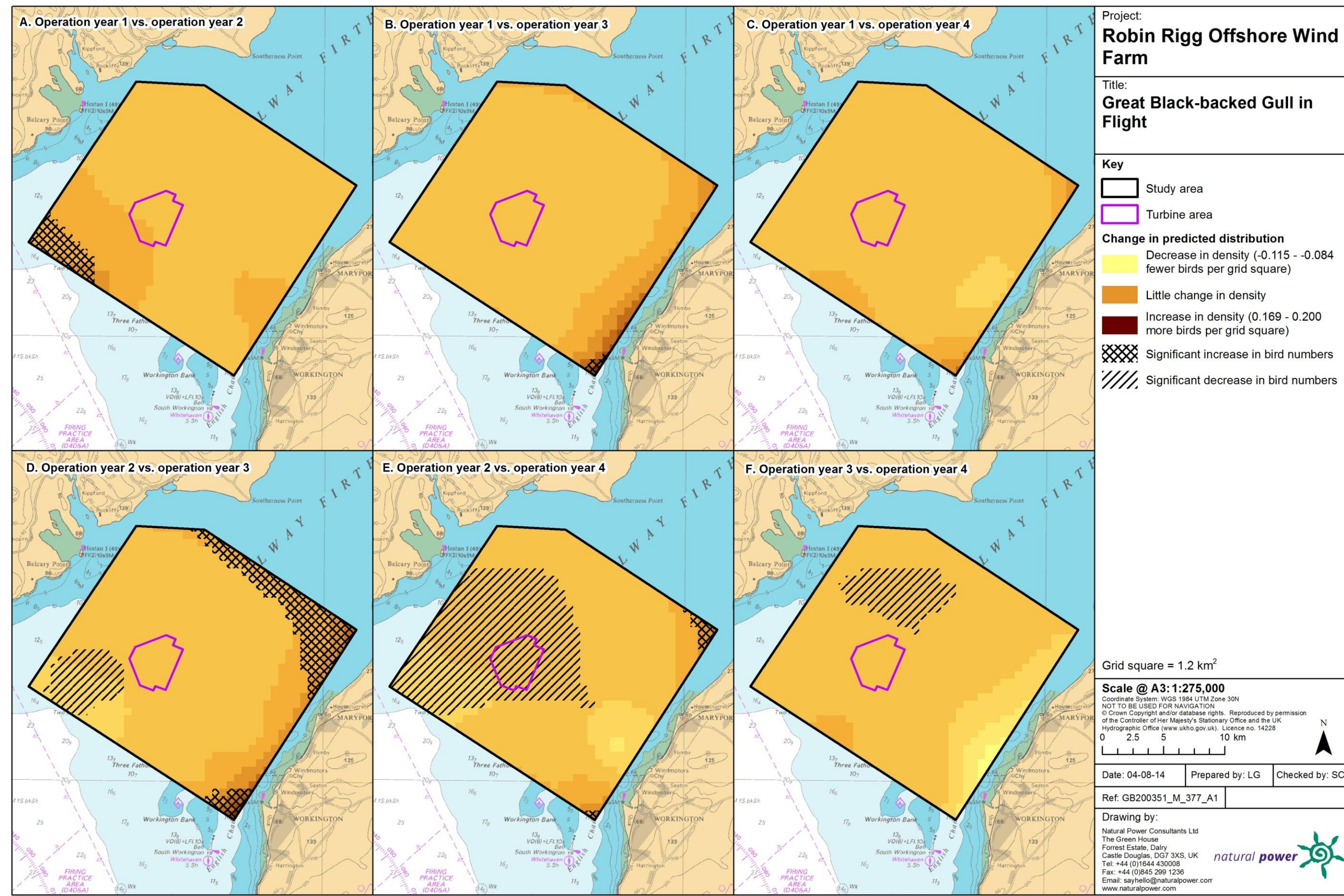


Figure 2.186: Differences in predicted flying great black-backed gull density between operational years. Significant differences are marked with diagonal shading.



#### 2.4.10.18.54. Collision risk

The percentage of great black-backed gulls recorded during the four operational years in different height bands relative to rotor swept height can be found in Table 2.113 and Figure 2.187. Data were combined for chi-squared analysis and a statistically significant difference was found between flight bands ( $\chi^2 = 12.49$ ,  $df = 3$ ,  $p = 0.002$ ). Fewer great black-backed gulls were recorded at rotor swept height than expected during operational years one and four, and more birds than expected were recorded at rotor level during operational years two and three.

**Table 2.113: Percentage of great black-backed gulls recorded in different flight height bands across operational years one to four. Shaded column indicates percentage at rotor swept height (flight band 4).**

Operational year	Flight height band					
	1 (0–5 m)	2 (6–25 m)	3 (26–34 m)	4 (35–125 m)	5 (126–200 m)	6 (>200 m)
1	16.19	60.00	11.43	12.38	0.00	0.00
2	10.14	60.87	14.49	14.49	0.00	0.00
3	20.24	27.38	22.02	29.76	0.60	0.00
4	43.75	28.13	21.88	6.25	0.00	0.00

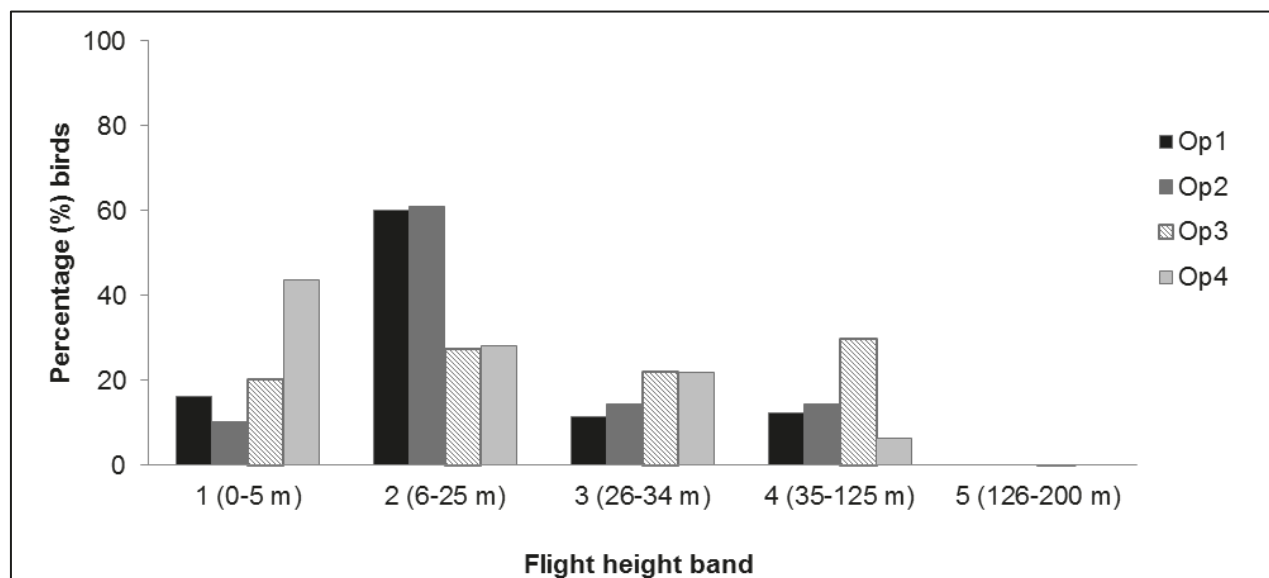


**Figure 2.187: Percentage of great black-backed gulls recorded in different flight height bands across operational years one to four.**

## 2.4.11. Herring gull

### 2.4.11.19. Across three development phases

#### 2.4.11.19.55. Summary statistics

Herring gull numbers were largest during the construction phase with the smallest numbers recorded during the first two years of operation (Table 2.114). However, the number of individuals sightings per km surveyed was smallest during the construction phase and a large proportion of birds (72%) were in flight in comparison to other development phases (Table 2.114).

**Table 2.114: Number of herring gull recorded per block during each development phase per km survey effort (all data).**

	Pre-construction		Construction		Operation years 1-2	
	On sea	In flight	On sea	In flight	On sea	In flight
<b>Total number individuals</b>	369	672	445	1,147	383	493
<b>Total number sightings</b>	60	407	127	653	101	287
<b>Number individuals/km</b>	0.10	0.19	0.06	0.16	0.10	0.13
	Total		Total		Total	
<b>Total number individuals</b>	1,041		1,592		876	
<b>Total number sightings</b>	467		780		388	
<b>Number individuals/km</b>	0.29		0.22		0.23	

Data were filtered as described in the methods (Section 2.4.4). The percentage of segments without observations was calculated to ensure there were sufficient data to perform the analysis (Table 2.115). Data were also checked to ensure observations were recorded in all months of the year.

**Table 2.115: Percentage of herring gull analysis blocks without observations across the three development phases: pre-construction, construction and operational years one and two.**

	On sea	In flight
<b>Percentage zero blocks</b>	98.8%	96.7%

## 2.4.11.19.56. Density and distribution

### 2.4.11.19.56.1. On sea

Initial data exploration highlighted that nearly 99% of analysis blocks for herring gulls on the sea during the three development phases contained zero observations (Figure 2.188). When the segments were broken down by month and phase (Table 2.115), a number of combinations were highlighted as having no observations. Therefore MRSea modelling was not undertaken.

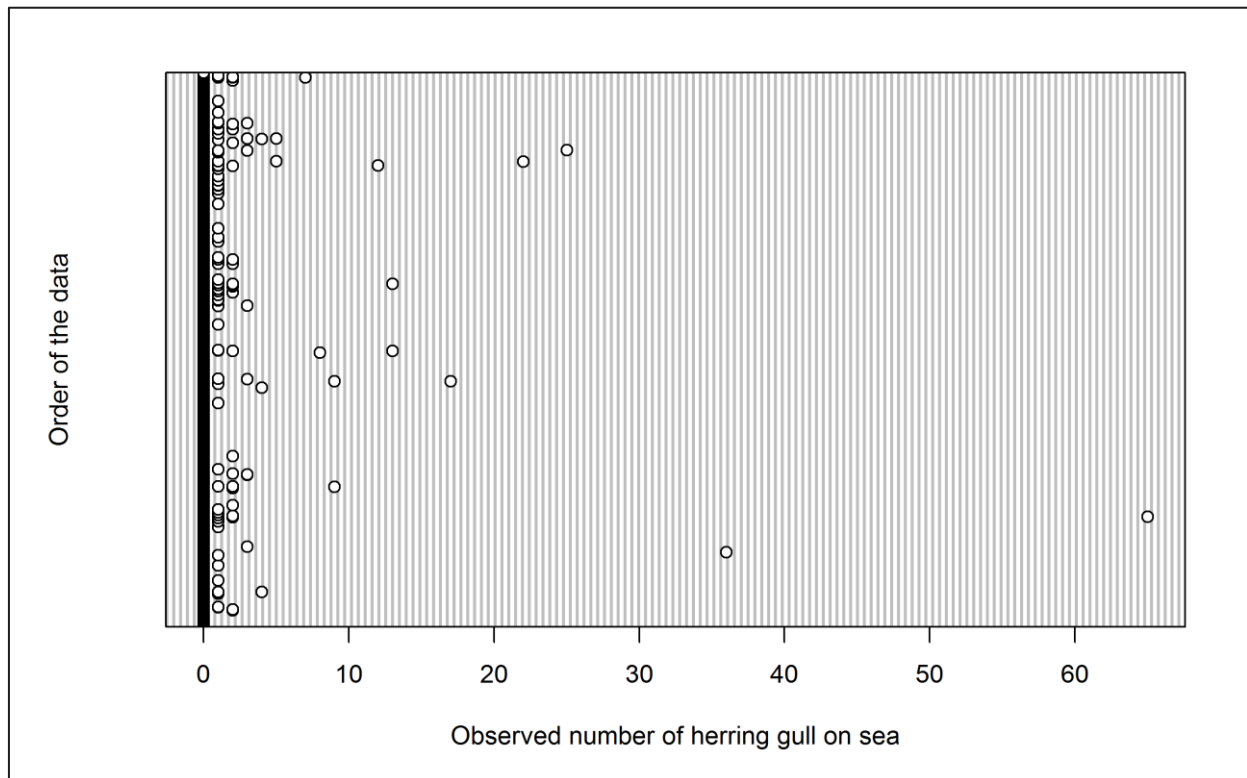


Figure 2.188: Dot plot of the number of herring gulls observed on sea per analysis block across the three development phases: pre-construction, construction and operational years one and two.

**Table 2.116: Number of herring gulls available for analysis each month across the three development phases: pre-construction, construction and operational years one and two.**

Month	Pre-construction	Construction	Operation	Total
Jan	22	1	0	23
Feb	45	1	7	53
Mar	1	38	73	112
Apr	2	2	1	5
May	0	20	0	20
Jun	25	35	1	61
Jul	0	48	0	48
Aug	0	17	3	20
Sep	1	6	37	44
Oct	0	9	0	9
Nov	1	1	3	5
Dec	4	1	6	11

Group size for herring gulls recorded on the sea ranged from single individuals up to 70 birds. Mean density of herring gulls on the sea indicates little change between development phases (Figure 2.189). However, since further modelling was not undertaken, the significance of any differences could not be tested. Figure 2.190 shows that mean density of herring gulls peaked in March.



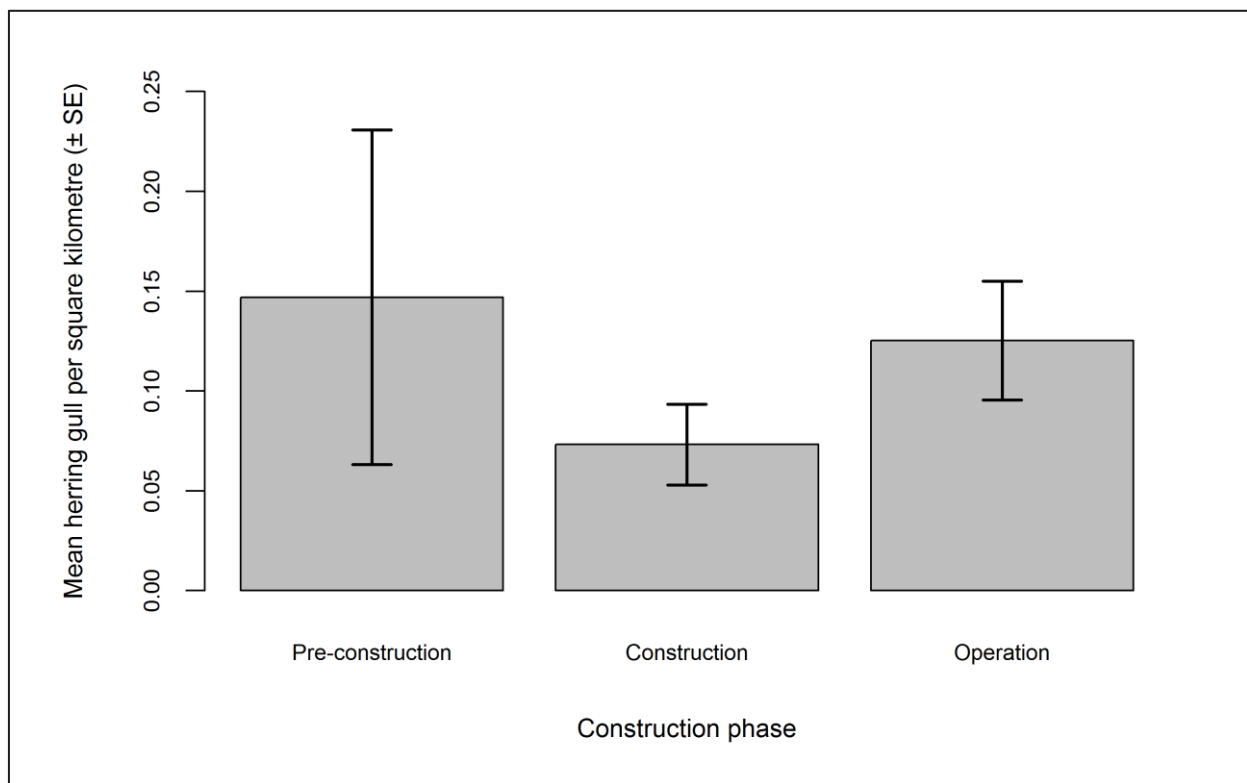


Figure 2.189: Mean density (± se) of herring gulls recorded on the sea across the three development phases: pre-construction, construction and operational years one and two.

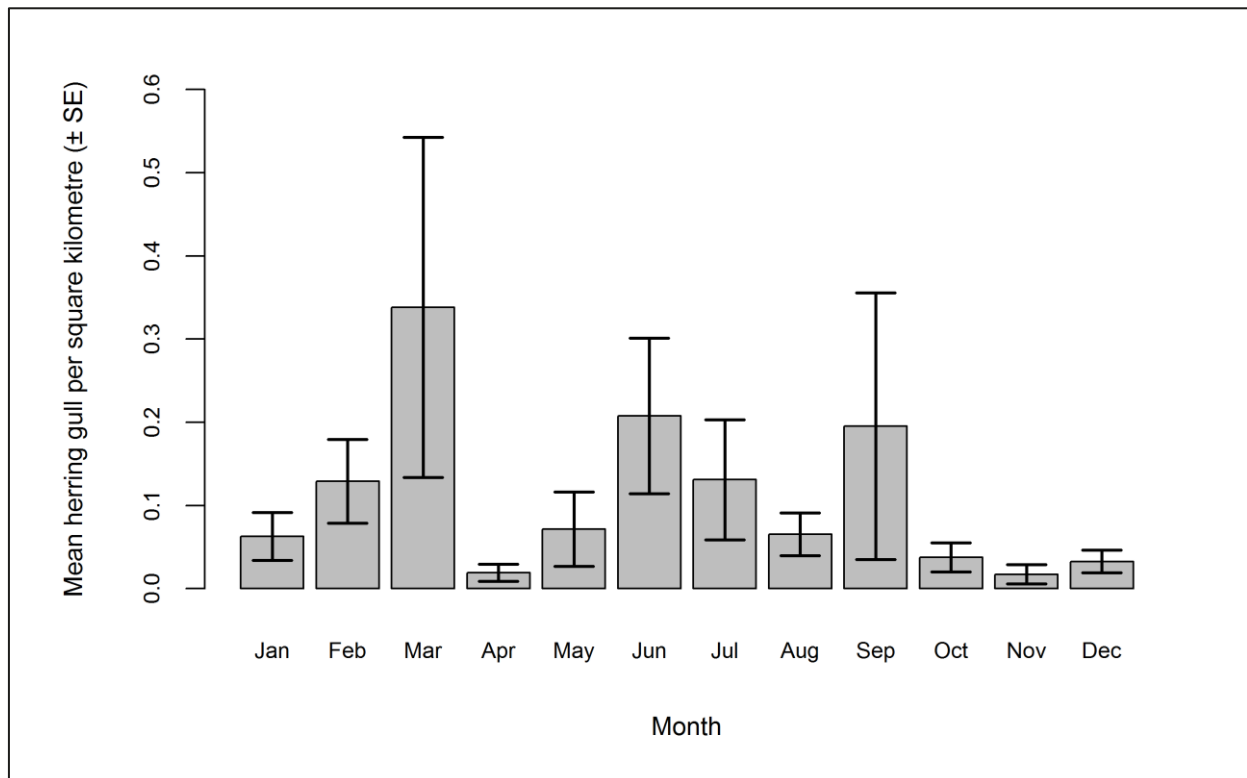


Figure 2.190: Mean density (± se) of herring gulls recorded on the sea across the three development phases: pre-construction, construction and operational years one and two.

### 2.4.11.19.56.2. In flight

Initial data exploration highlighted two outliers (a segment containing 90 birds recorded in March 2008 and a segment containing 50 birds in July 2010) that may influence the modelling process (Figure 2.191). As a result the model was run with and without these data and the outputs compared.

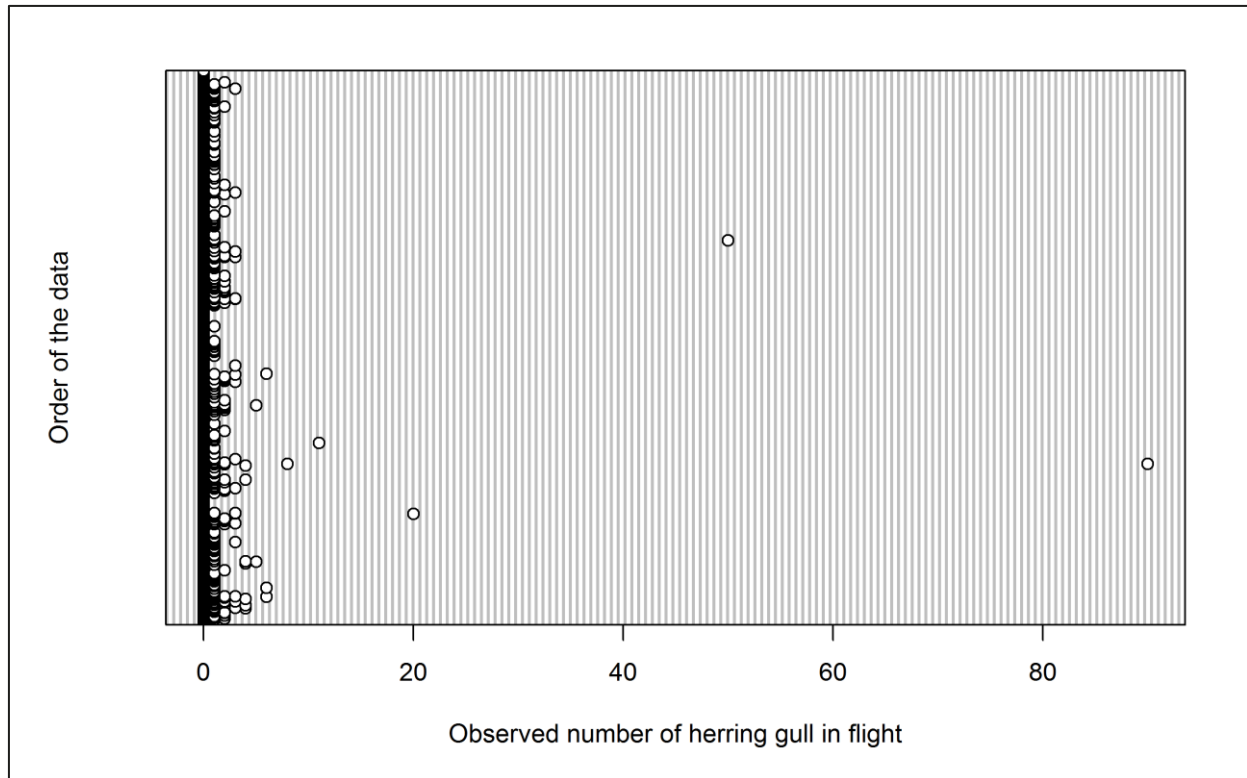


Figure 2.191: Dot plot of the number of herring gulls observed in flight per analysis block across the three development phases: pre-construction, construction and operational years one and two.

The GEE predicted that month, phase, tide height, location, and the interaction between location and phase, all have a statistically significant influence on flying herring gull abundance within the survey area (Table 2.117). Specifically, mean density was smaller during the operational phase (Figure 2.192) and largest during the month of March (Figure 2.193). Since March was the month of peak activity, model predictions were made for this month.

Table 2.117: Final model outputs for herring gulls in flight across the three development phases: pre-construction, construction and operational years one and two.

Term	Marginal p-value
Month	<0.0001
Phase	0.0094
Tide height	0.0002
Location (X,Y)	<0.0001
Interaction (location: phase)	0.0058



Figure 2.192: Mean density (± se) of herring gulls recorded in flight across the three development phases: pre-construction, construction and operational years one and two.

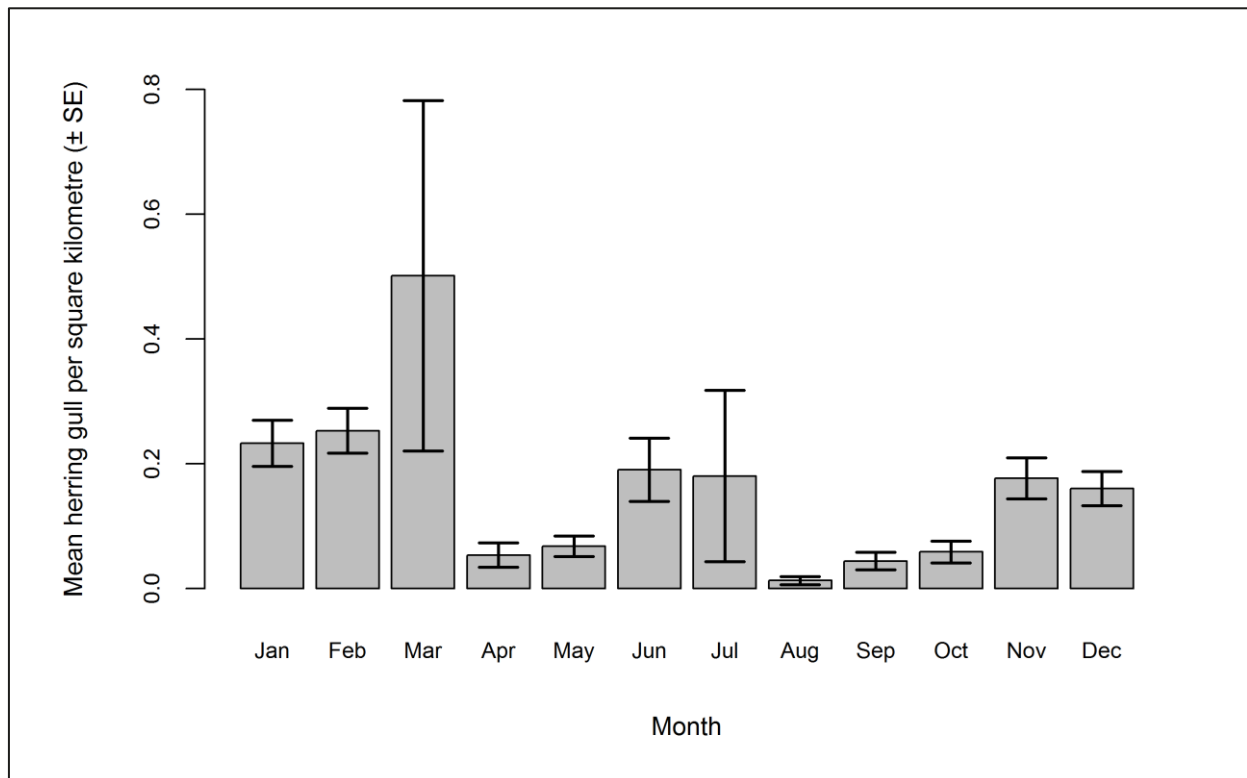


Figure 2.193: Mean density (± se) of herring gulls recorded in flight during each month across the three development phases: pre-construction, construction and operational years one and two.

Predicted herring gull abundance and densities (by site, buffer and total survey area) are presented in Table 2.118. The smallest total abundance was predicted for the construction phase, with a slight increase during operation but not to the levels seen pre-construction. However, little change was seen across development phases in the percentage of herring gulls predicted to be within the Robin Rigg OWF itself (Table 2.118).

**Table 2.118: Abundance and density of herring gulls in flight across the three development phases: pre-construction, construction and operational years one and two. Values in parentheses represent upper and lower 95% confidence intervals.**

Phase	Abundance			Density			% within site
	Site	Buffer	Total	Site	Buffer	Total	
<b>Pre-construction</b>	6 (1-39)	237 (39-1,594)	244 (40-1,633)	0.49 (0.07-3.05)	0.68 (0.11-4.53)	0.68 (0.11-4.53)	2.60
<b>Construction</b>	2 (0-13)	64 (9-733)	66 (9-746)	0.12 (0.02-1.00)	0.18 (0.03-2.07)	0.18 (0.03-2.07)	2.46
<b>Operation</b>	3 (0-19)	104 (14-1,081)	107 (15-1,100)	0.21 (0.03-1.46)	0.30 (0.04-3.11)	0.30 (0.04-3.05)	2.55

The density surface maps show a statistically significant decline in herring gull density across the survey area between the pre-construction and construction phases, with a relatively small area of significant increase seen post-construction (Figure 2.194).



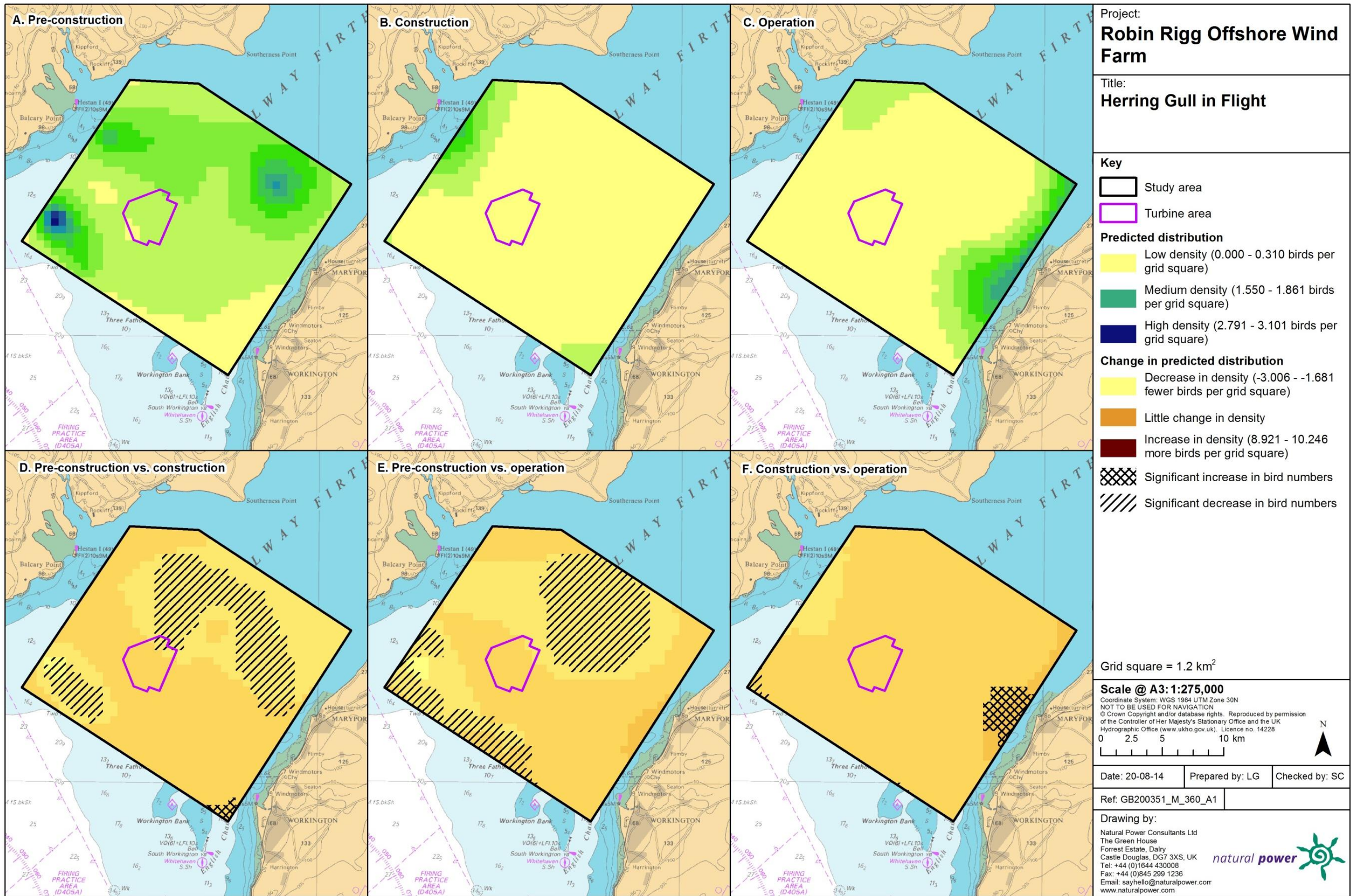


Figure 2.194: Predicted density of herring gulls in flight during a) pre-construction, b) construction and c) operational monitoring. Changes in predicted density between d) pre-construction and construction, e) pre-construction and operation and f) construction and operation are also shown. Significant differences are marked with diagonal shading.



### 2.4.11.19.57. Collision risk

The percentage of herring gulls recorded during the three development phases in different height bands relative to rotor swept height can be found in Table 2.119 and Figure 2.195. Data were combined for chi-squared analysis and a statistically significant difference was found between flight bands ( $\chi^2 = 139.58$ ,  $df = 2$ ,  $p = <0.001$ ). Fewer herring gulls than expected were observed at rotor swept height during pre-construction surveys. This may be a result of herring gull flight heights being underestimated since there were no turbines present in the survey area to use as a reference. Larger numbers than expected were recorded at rotor swept height during operational monitoring.

**Table 2.119: Percentage of herring gulls recorded in different flight height bands across the three development phases: pre-construction, construction and operational years one and two. Shaded column indicates percentage at rotor swept height (flight band 4).**

Phase	Flight height band					
	1 (0–5 m)	2 (6–25 m)	3 (26–34 m)	4 (35–125 m)	5 (126–200 m)	6 (>200 m)
Pre-construction	21.28	74.11	4.02	0.60	0.00	0.00
Construction	16.04	68.89	10.43	4.65	0.00	0.00
Operation	18.26	43.81	21.10	16.84	0.00	0.00

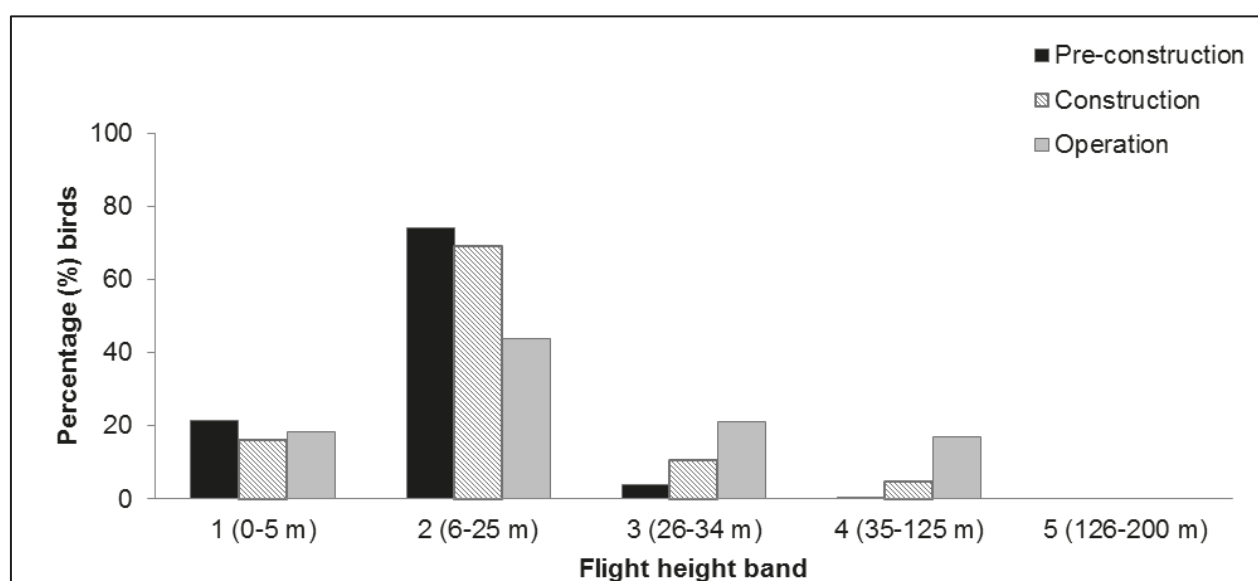


**Figure 2.195: Percentage of herring gulls recorded in different flight height bands across the three development phases: pre-construction, construction and operational years one and two.**

## 2.4.11.20. Across operational years

### 2.4.11.20.58. Summary statistics

The total number of herring gulls recorded during operational monitoring was similar across survey years, although larger numbers were recorded per km of survey effort during operational year three (Table 2.120). A larger percentage c. 60% of herring gulls recorded on the sea surface during this year in comparison to other operational years (Table 2.120). A larger percentage (75%) of herring gulls were recorded in flight during operational year one, similar to the increase in flying birds noted during the construction phase (Table 2.120).

**Table 2.120: Number of herring gulls recorded per block during each operational year per km survey effort (all data).**

	Operational year 1		Operational year 2		Operational year 3		Operational year 4	
	On sea	In flight	On sea	In flight	On sea	In flight	On sea	In flight
<b>Total number individuals</b>	93	275	290	218	714	502	256	218
<b>Total number sightings</b>	41	150	60	137	186	242	134	182
<b>Number individuals/km</b>	0.05	0.15	0.14	0.11	0.33	0.23	0.12	0.10
	Total		Total		Total		Total	
<b>Total number individuals</b>	368		508		1,216		474	
<b>Total number sightings</b>	191		197		428		316	
<b>Number individuals/km</b>	0.20		0.25		0.56		0.22	

Data were filtered as described in the methodology (Section 2.4.4). The percentage of segments without observations was calculated to ensure there were sufficient data to perform the analysis (Table 2.121). Data were also checked to ensure observations were recorded in all months of the year.

**Table 2.121: Percentage of herring gull analysis blocks without observations across operational years one to four.**

	On sea	In flight
<b>Percentage zero blocks</b>	97.3%	97.4%

## 2.4.11.20.59. Density and distribution

### 2.4.11.20.59.1. On sea

A half-normal detection function with sea state as a covariate was found to be the best fitting model for herring gulls on the sea during the four operational years. Figure 2.196 shows the selected detection curve for herring gulls.

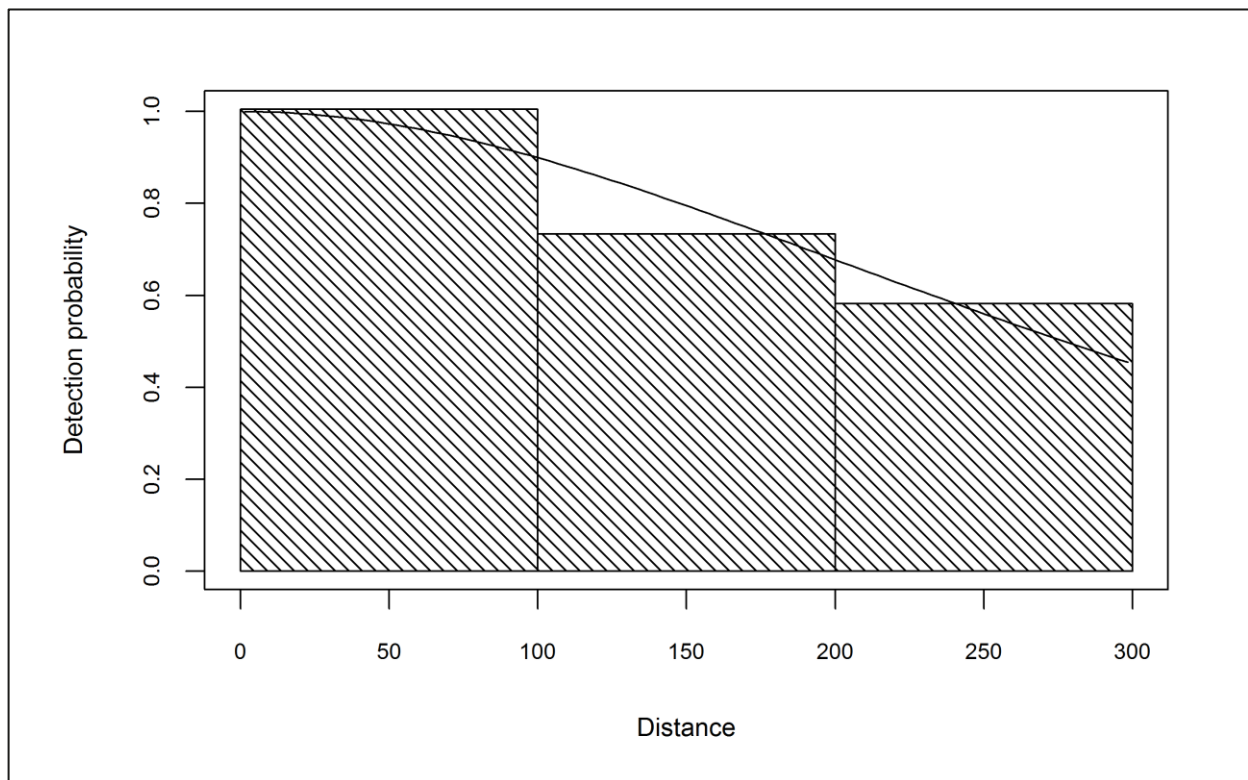


Figure 2.196: Detection curve used to adjust herring gull on sea counts for imperfect detection across operational years one to four.

Initial data exploration of adjusted herring gull numbers highlighted a single outlier (segment containing 82 birds recorded in November 2012) that may influence the modelling process (Figure 2.197). As a result the model was run with and without this outlier and the outputs compared.



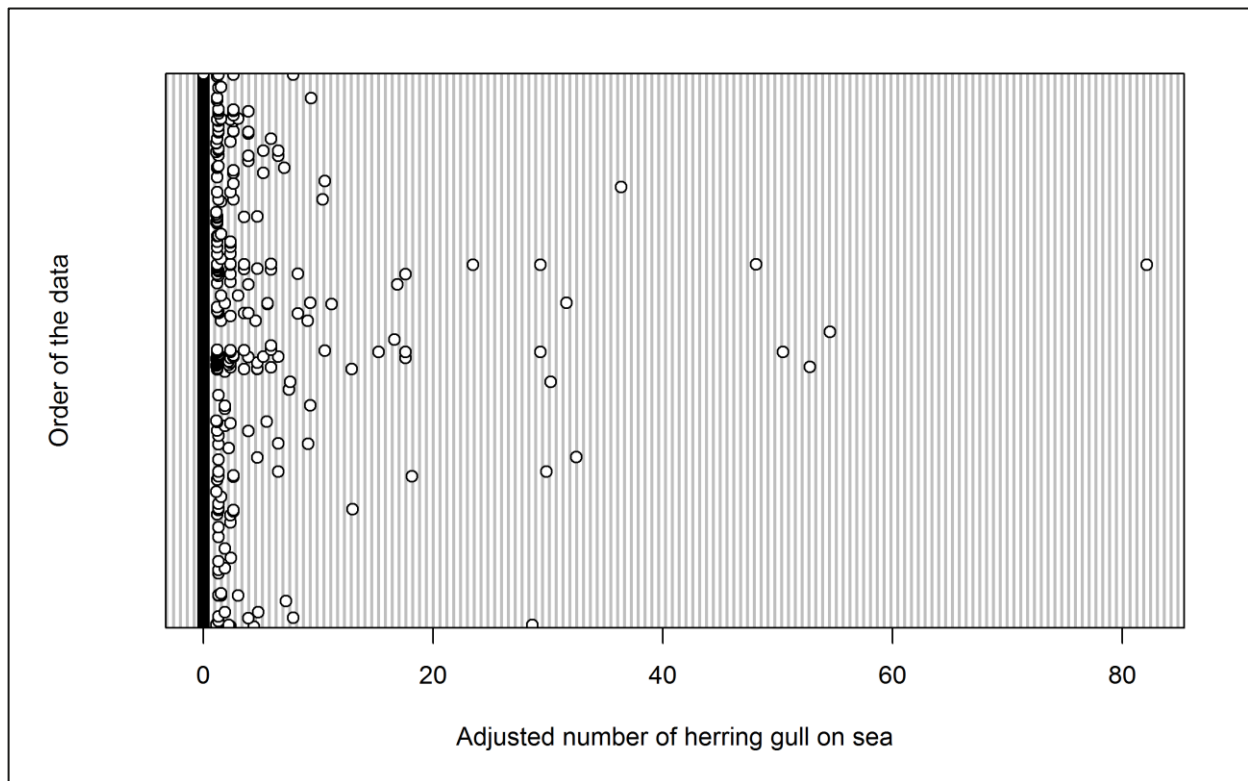


Figure 2.197: Dot plot of the number of herring gulls observed on sea per analysis block across operational years one to four.

The model excluding the outlier would not converge. Therefore, results are presented for the model including the outlier. The GEE predicted that operational year, location, and the interaction of the two all have a statistically significant influence on herring gull abundance within the survey area (Table 2.122). Specifically, larger numbers were observed during operational year three (Figure 2.198). Although not statistically significant, larger numbers of herring gulls on the sea were observed in November (Figure 2.199), and therefore model predictions were made for this month.

Table 2.122: Final model outputs for herring gulls on the sea across operational years one to four.

Term	Marginal p-value
Month	0.1189
Phase	<0.0001
Tide height	0.2201
Location (X,Y)	<0.0001
Interaction (location: phase)	0.0080

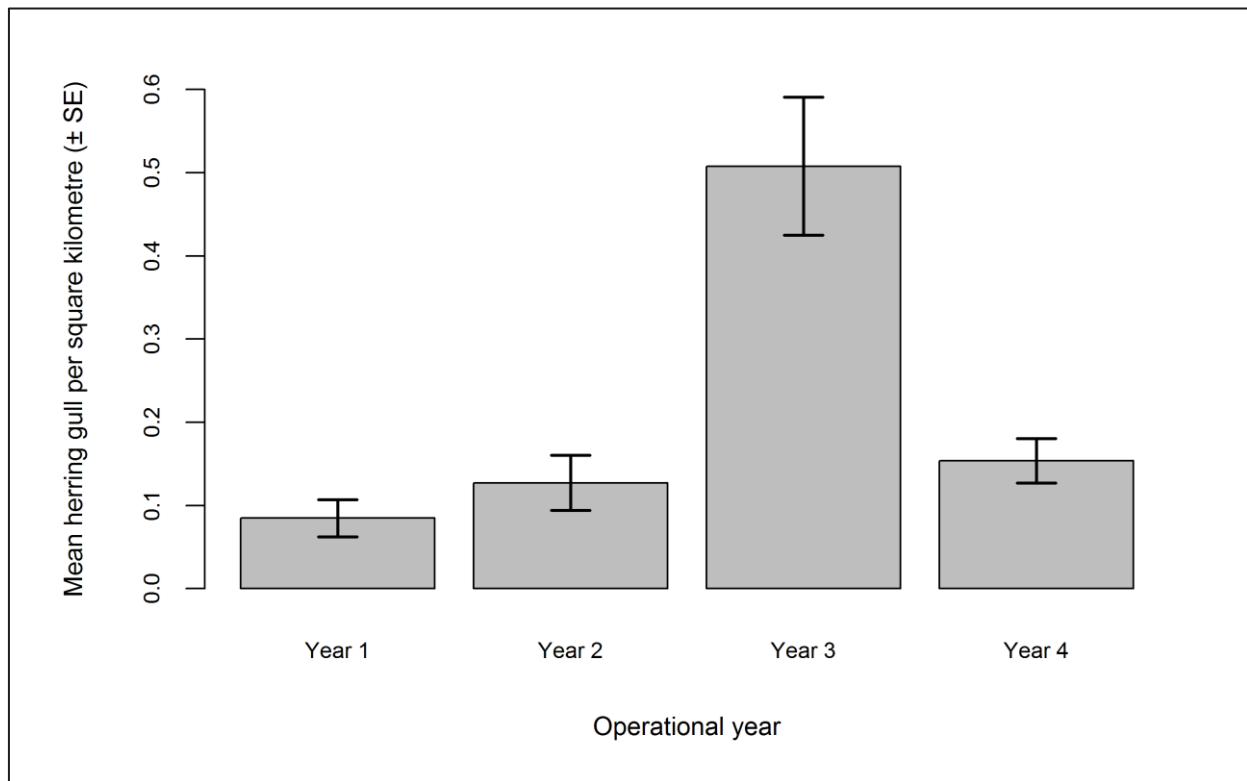


Figure 2.198: Mean density ( $\pm$  se) of herring gulls recorded on the sea across operational years one to four.

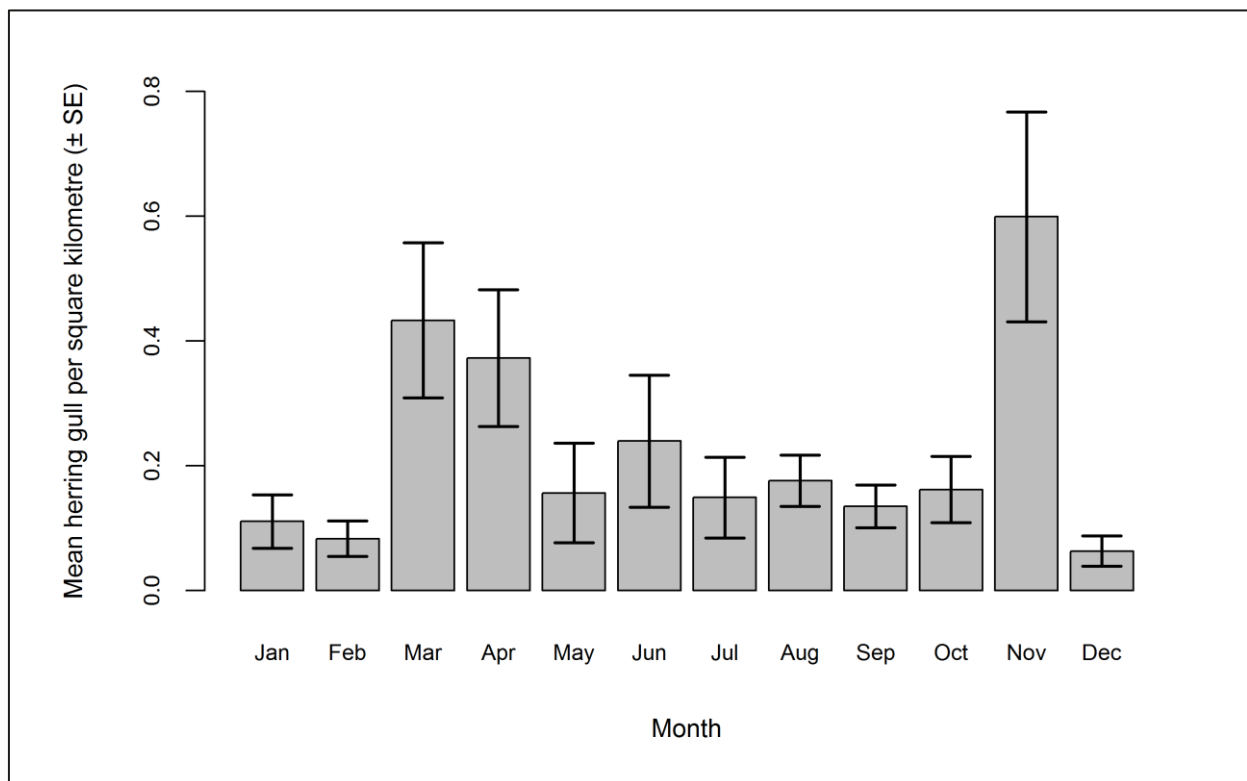


Figure 2.199: Mean density ( $\pm$  se) of herring gulls recorded on the sea during each month across operational years one to four.

The abundance and densities (by site, buffer and total survey area) are presented in Table 2.123. The smallest total abundance was predicted for operational year one. However, both abundance and density increase during successive operational years (Table 2.123). It should be noted that the inclusion of an outlier in the data may have led to relatively large confidence intervals and increased uncertainty in model predictions.

**Table 2.123: Abundance and density of herring gulls on the sea across operational years one to four. Values in parentheses represent upper and lower 95% confidence intervals.**

Operational year	Abundance			Density			% within site
	Site	Buffer	Total	Site	Buffer	Total	
<b>1</b>	1 (0-16)	32 (1-540)	33 (1-556)	0.05 (0-1.25)	0.09 (0-1.55)	0.09 (0-1.54)	1.80
<b>2</b>	16 (0-1,699)	222 (9-9,549)	238 (9-11,248)	1.23 (0.03-131.35)	0.64 (0.02-27.45)	0.66 (0.03-31.18)	6.69
<b>3</b>	23 (4-478)	558 (44-5,796)	581 (47-6,274)	1.77 (0.27-36.91)	1.60 (0.13-16.66)	1.61 (0.13-17.39)	3.95
<b>4</b>	27 (2-566)	350 (28-4,639)	378 (30-5,204)	2.12 (0.14-43.72)	1.01 (0.08-13.34)	1.05 (0.08-14.42)	7.26

The increase in abundance of herring gulls on sea during successive operational years is reflected in the density surface maps (Figure 2.200). A statistically significant increase in herring gull densities across the survey area was predicted between operational years one and three, and operational years one and four (Figure 2.201). It should be noted that an outlier in the data may have influenced the density surfaces; as such, these maps should be interpreted with this in mind.

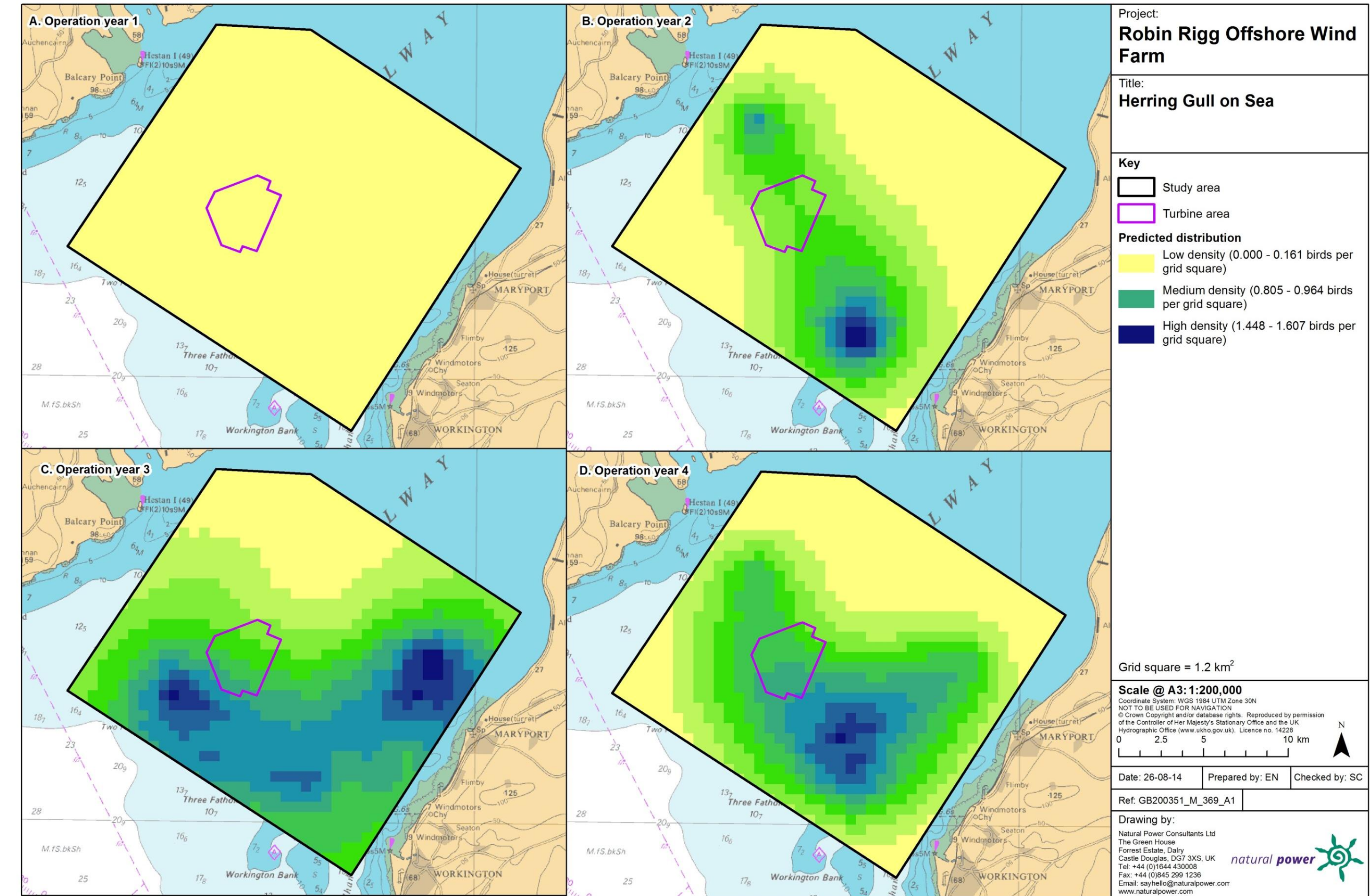


**Figure 2.200:** Predicted density of herring gulls on the sea during a) operational year one, b) operational year two, c) operational year three and d) operational year four.



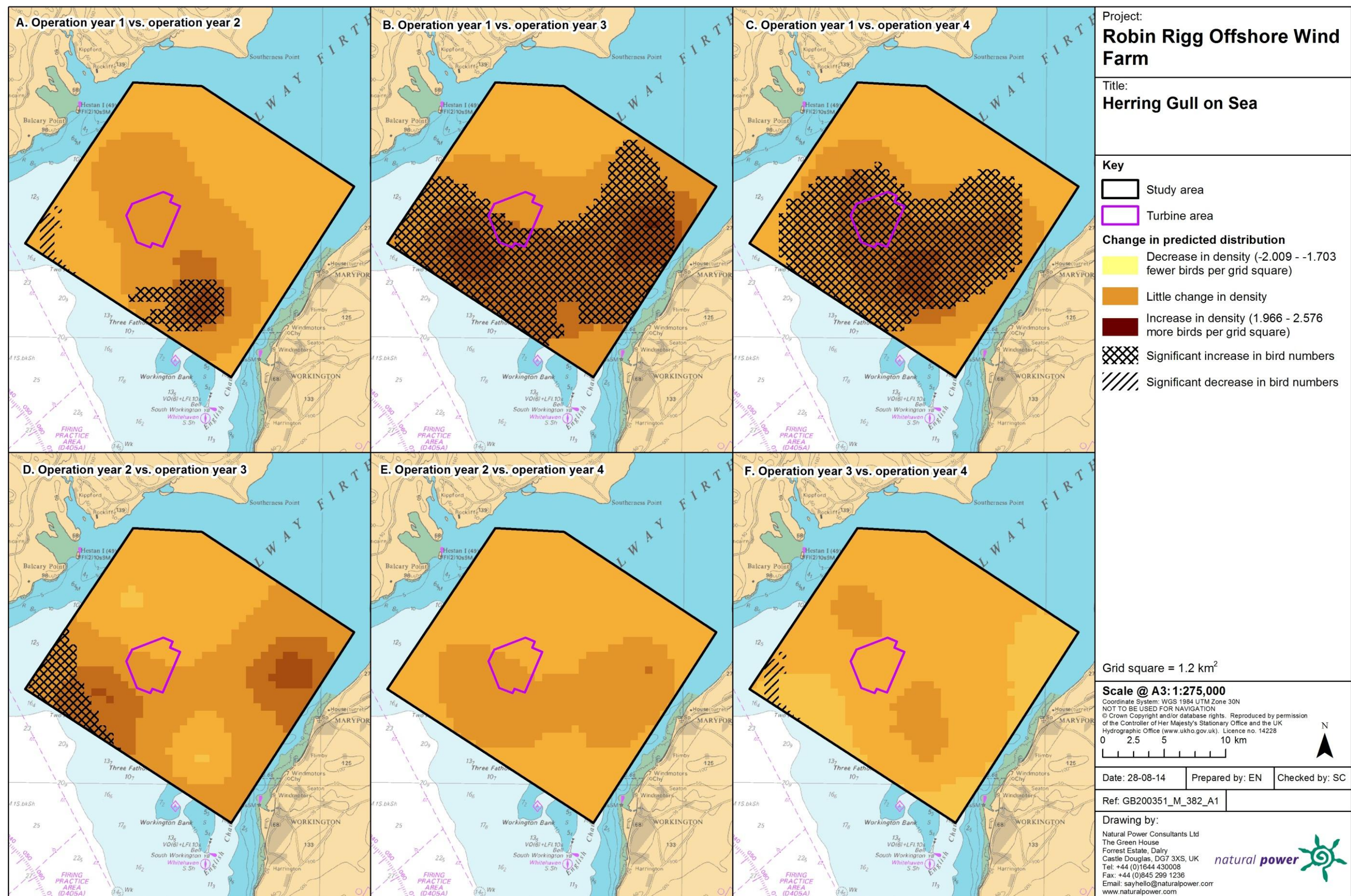


Figure 2.201: Differences in predicted sitting herring gull density between operational years. Significant differences are marked with diagonal shading.



### 2.4.11.20.59.2. In flight

Initial data exploration of herring gull data indicated there were no outlying observations (Figure 2.202).

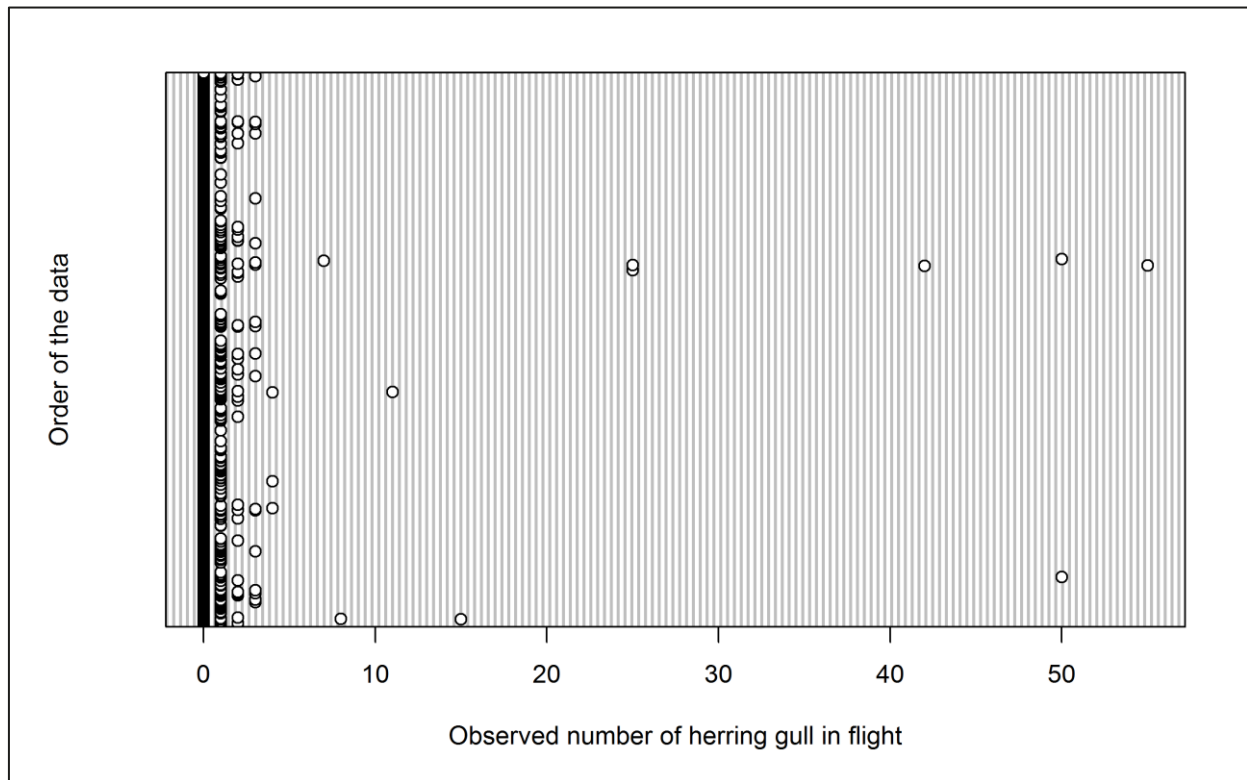


Figure 2.202: Dot plot of the number of herring gulls observed in flight per analysis block across operational years one to four.

The GEE predicted that month, operational year, tide height, location, and the interaction between location and operational year (phase), all have a statistically significant influence on flying herring gull abundance within the survey area (Table 2.124). Specifically, mean herring gull density was largest during operational year three (Figure 2.203), and during November (Figure 2.204). Since November was the month of peak activity, model predictions were made for this month.

Table 2.124: Final model outputs for herring gulls in flight across operational years one to four.

Term	Marginal p-value
Month	<0.0001
Phase	<0.0001
Tide height	0.0122
Location (X,Y)	<0.0001
Interaction (location: phase)	0.0021

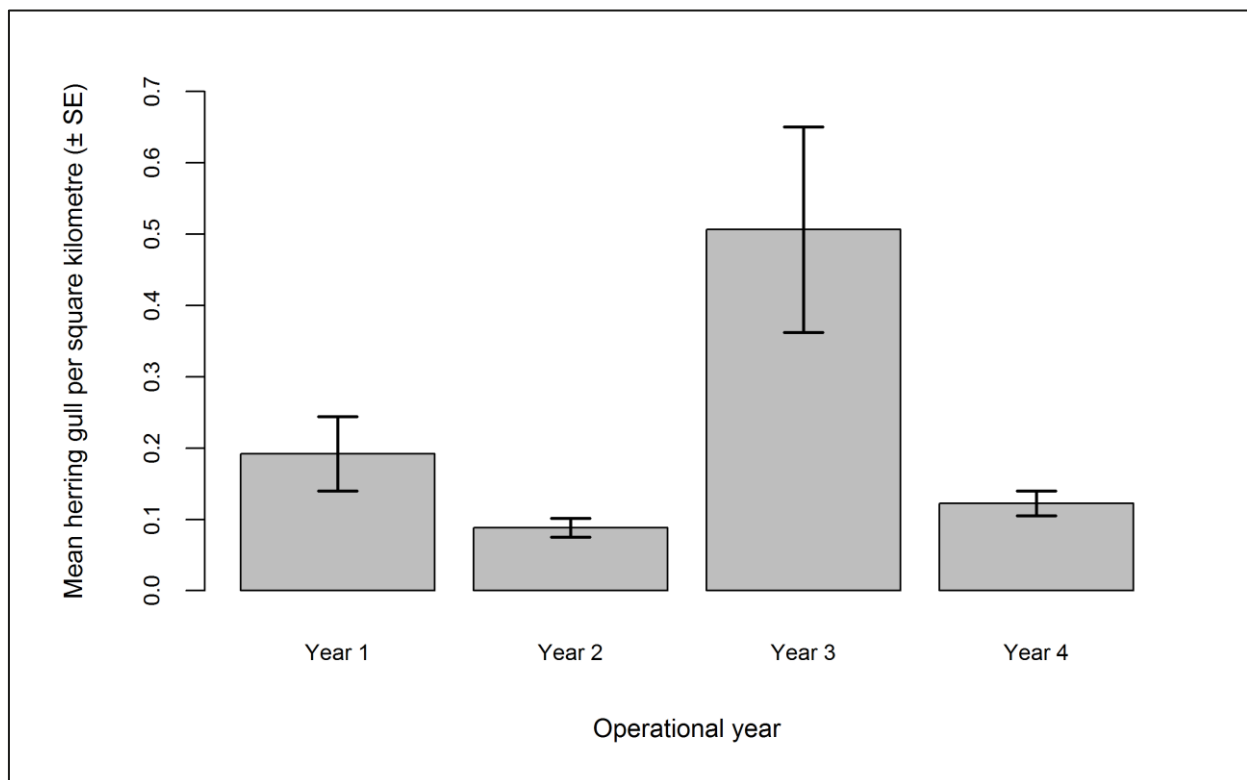


Figure 2.203: Mean density (± se) of herring gulls recorded in flight across operational years one to four.

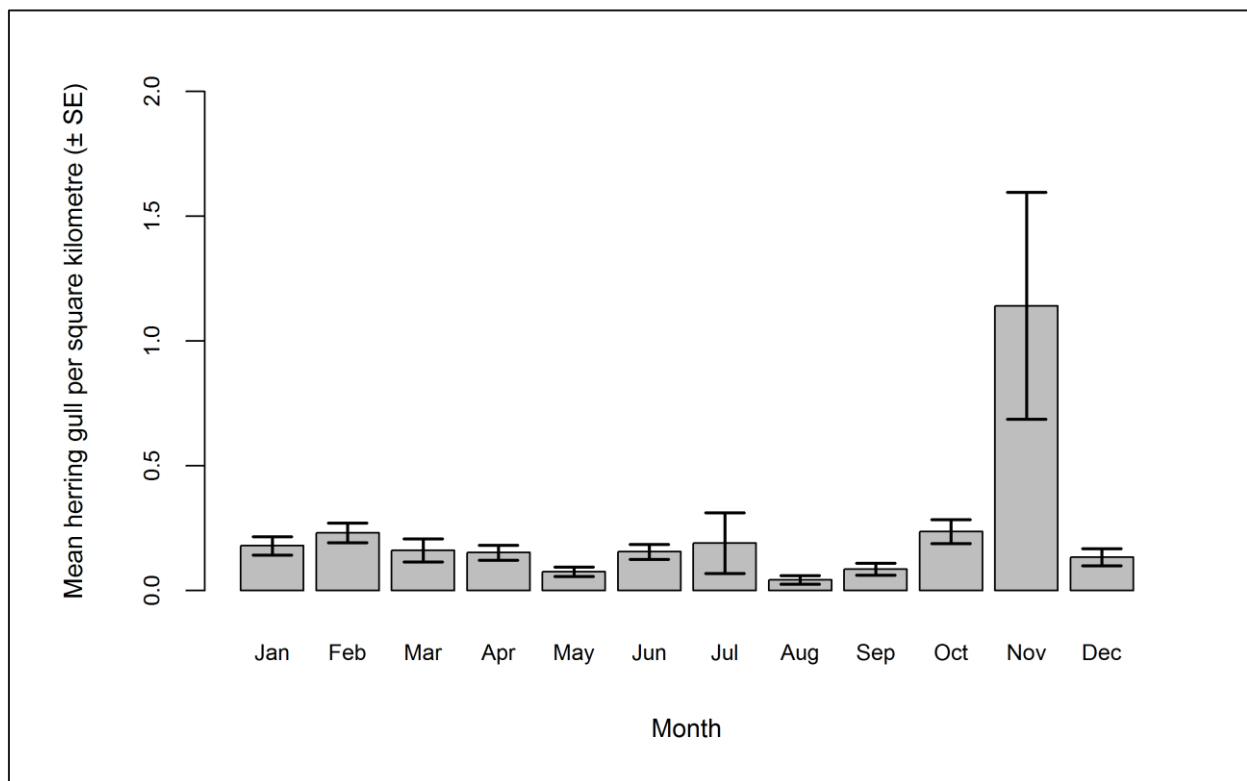


Figure 2.204: Mean density (± se) of herring gulls recorded in flight during each month across operational years one to four.

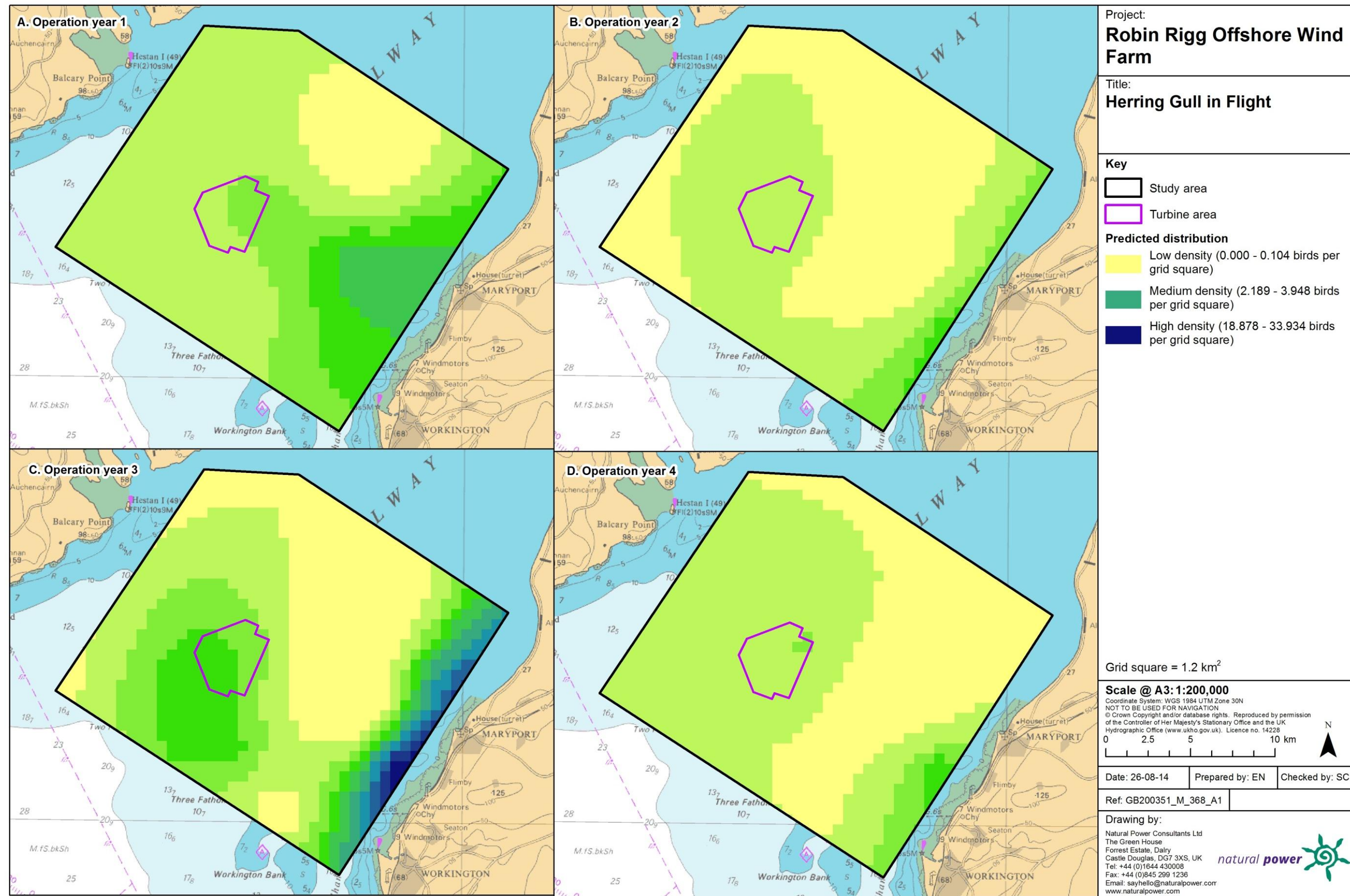
Predicted herring gull abundance and densities (by site, buffer and total survey area) are presented in Table 2.125. Total abundance across the survey area was largest during operational year three; however, this is the year with the smallest proportion of birds flying within the Robin Rigg OWF itself (Table 2.125).

**Table 2.125: Abundance and density of herring gulls in flight across operational years one to four. Values in parentheses represent upper and lower 95% confidence intervals.**

Operational year	Abundance			Density			% within site
	Site	Buffer	Total	Site	Buffer	Total	
<b>1</b>	12	333	345	0.90	0.96	0.96	3.39
	(4-34)	(84-1,348)	(88-1,382)	(0.29-2.60)	(0.24-3.83)	(0.24-3.83)	
<b>2</b>	8	121	129	0.35	0.35	0.36	6.18
	(3-26)	(42-387)	(45-413)	(0.12-1.11)	(0.12-1.11)	(0.12-1.15)	
<b>3</b>	24	814	838	2.34	2.34	2.32	2.86
	(6-101)	(184-4,321)	(191-4,422)	(0.53-12.42)	(0.53-12.42)	(0.53-12.26)	
<b>4</b>	9	129	138	0.37	0.37	0.38	6.62
	(2-45)	(42-438)	(44-484)	(0.12-1.26)	(0.12-1.26)	(0.12-1.34)	

The density surface maps show that herring gull density was concentrated to the west of the Robin Rigg OWF, and along the Cumbrian coastline during operational year three (Figure 2.205). Densities in these areas during operational year three increased significantly from operational year one, but had declined by operational year four, (Figure 2.206).







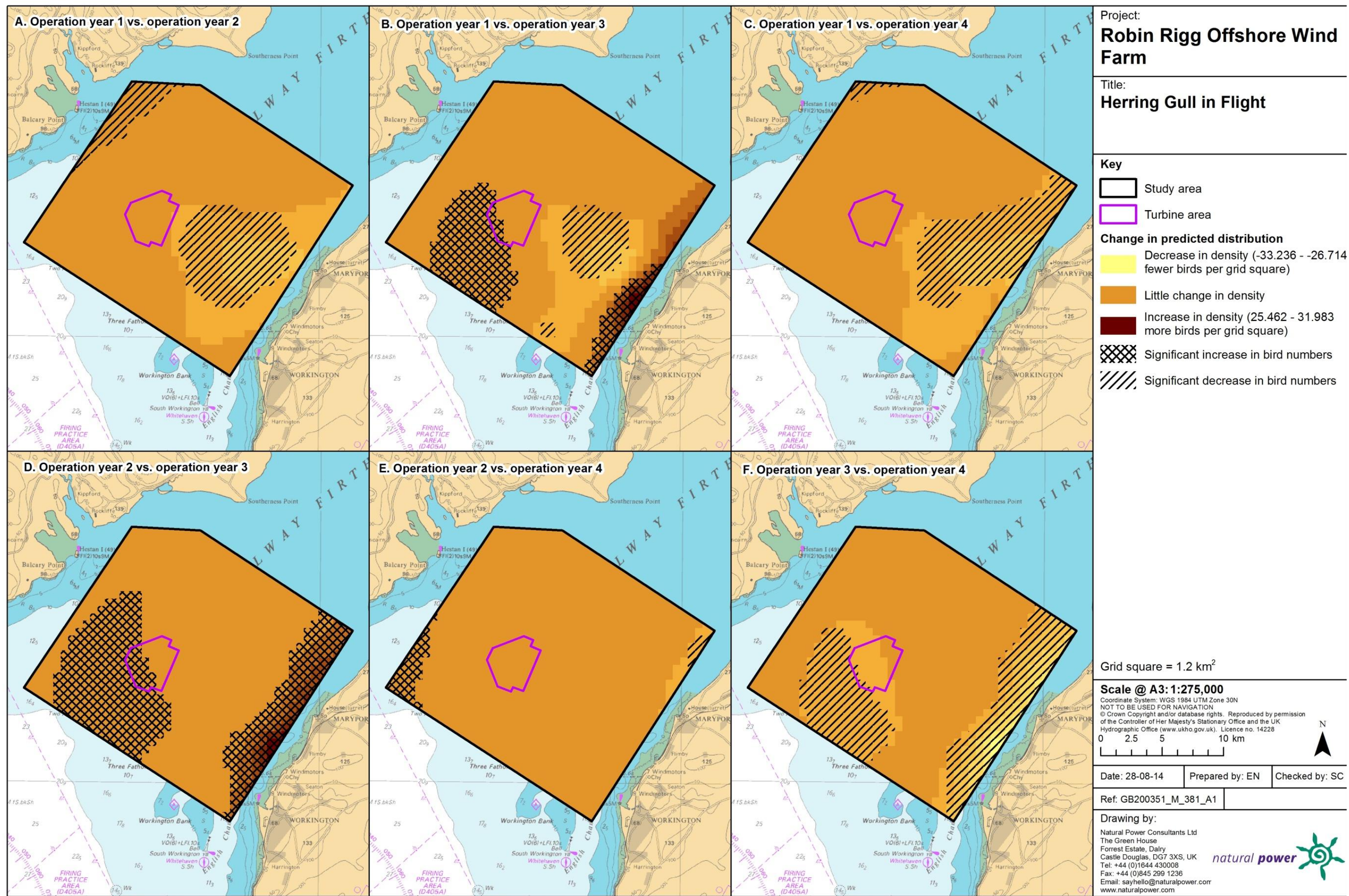


Figure 2.206: Differences in predicted flying herring gull density between operational years. Significant differences are marked with diagonal shading.



### 2.4.11.20.60. Collision risk

The percentage of herring gulls recorded during the four operational years in different height bands relative to rotor swept height can be found in Table 2.126 and Figure 2.207. Data were combined for chi-squared analysis and a statistically significant difference was found between flight bands ( $\chi^2 = 29.02$ ,  $df = 3$ ,  $p = <0.001$ ). More herring gulls than expected were observed at rotor swept height during operational years one and two, whilst fewer herring gulls than expected were recorded at rotor swept height during operational years three and four.

**Table 2.126: Percentage of herring gulls recorded in different flight height bands across operational years one to four. Shaded column indicates percentage at rotor swept height (flight band 4).**

Operational year	Flight height band					
	1 (0–5 m)	2 (6–25 m)	3 (26–34 m)	4 (35–125 m)	5 (126–200 m)	6 (>200 m)
1	21.45	50.18	12.73	15.64	0.00	0.00
2	14.22	35.78	31.65	18.34	0.00	0.00
3	9.96	63.22	18.66	8.15	0.00	0.00
4	31.05	51.14	13.24	4.57	0.00	0.00

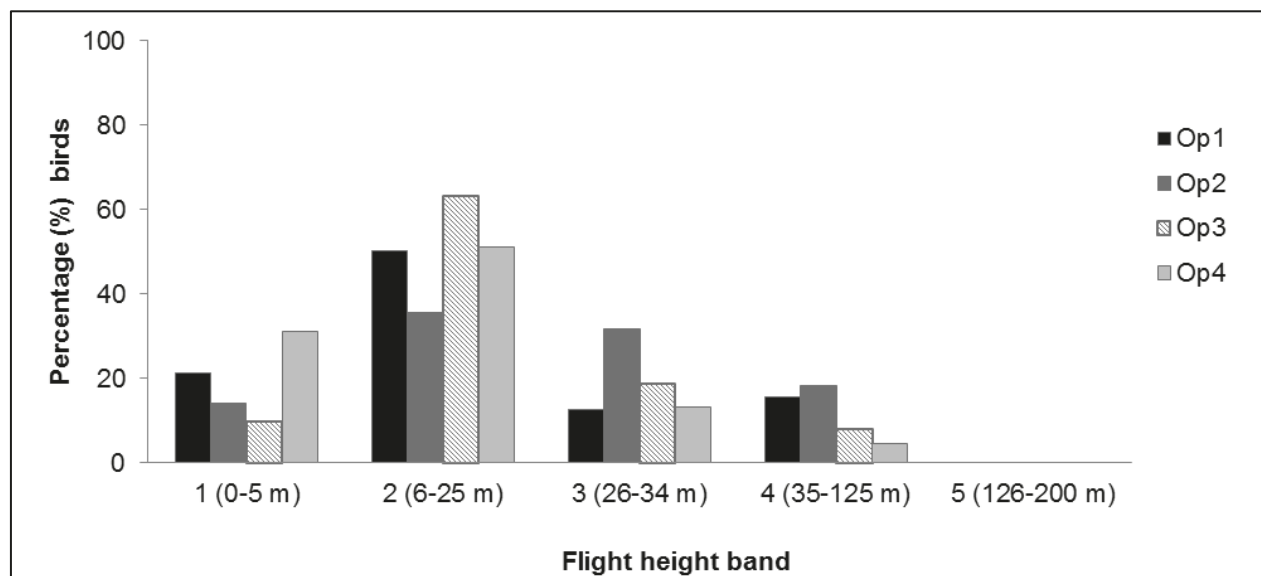


**Figure 2.207: Percentage of herring gulls recorded in different flight height bands across operational years one to four.**

## 2.4.12. Comparison of collection methods for birds in flight

A comparison of data recorded using best practice ESAS methodology versus the original methodology used to record birds in flight at Robin Rigg OWF, demonstrates that ESAS methodology results in many fewer observations being recorded as 'in transect' (Figure 2.208). This most likely represents the recording of the same birds multiple times as they fly in and out of the surveyed area using the original methodology. The ESAS 'snapshot' methodology has been designed to avoid this by effectively surveying fixed 'snapshots' in time equivalent to a series of point counts rather than a continuous line, as outlined in Section 2.3.2.

Since the Robin Rigg methodology has been used consistently across the entire period during which surveys have been carried out, it is still possible to make comparisons among phases (assuming that the rate of double counting remains more or less constant among phases). However, these results indicate that any estimates of abundance and density calculated from birds in flight in this study are likely to be over-estimates. In addition, these results demonstrate the need for consistent survey methodology throughout monitoring programs.

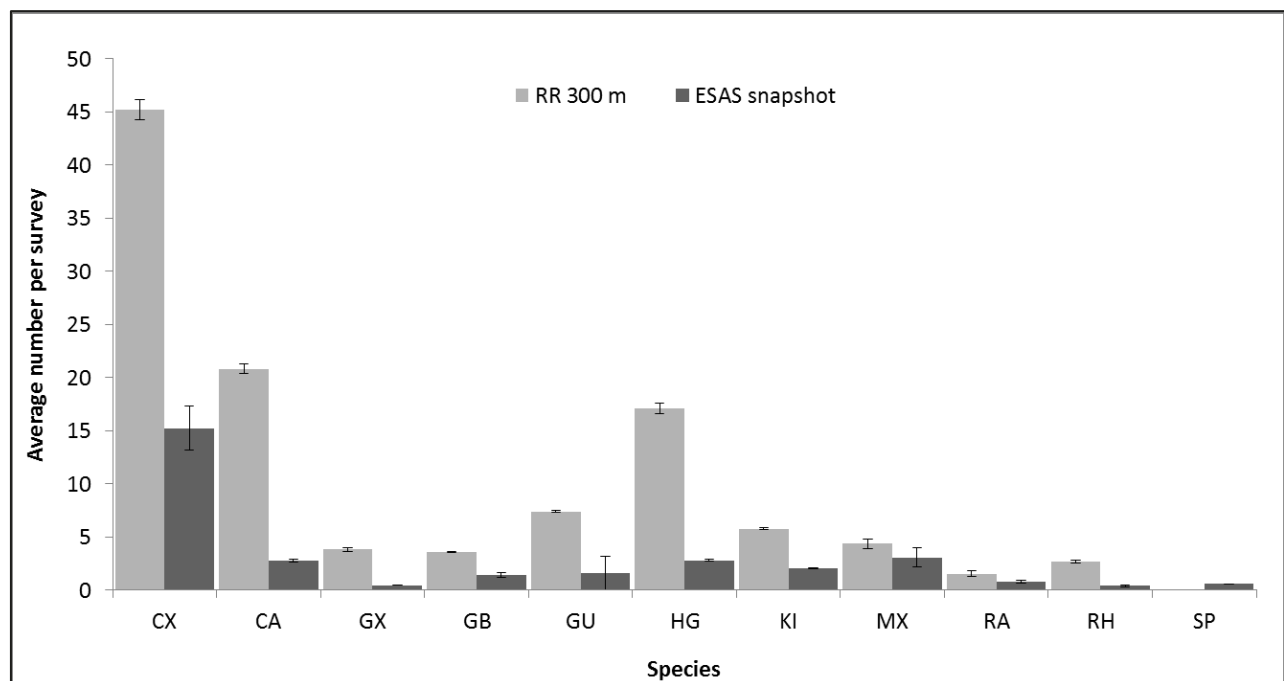


Figure 2.208: Average number of flying birds recorded using the two survey methods employed at Robin Rigg OWF ( $\pm$  standard error). BTO species codes are as follows: CX = common scoter, CA = cormorant, GX = gannet, GB = great black-backed gull, GU = guillemot, HG = herring gull, KI = kittiwake, MX = Manx shearwater, RA = razorbill, RH = red-throated diver and SP = scaup.



## 2.5. Discussion

This report assesses potential effects caused by the construction and operation of Robin Rigg OWF on birds, in accordance with the consent from Scottish Ministers under Section 36 of the Electricity Act 1989 and the Robin Rigg MEMP. Data for 11 key bird species was examined, up to and including the fourth year of operation at Robin Rigg OWF. Consistent with previous reports (Walls *et al.*, 2013a, 2013b and 2013c), evidence was found for few changes in bird abundance and distribution which were clearly attributable to Robin Rigg OWF.

### 2.5.1. Species accounts

As expected, scaup were only present within the Solway Firth during the winter (Wernham *et al.*, 2002; Musgrove *et al.*, 2011). Due to the small number of scaup observations within the survey area, abundance modelling could not be undertaken. However, there was an indication that the number of scaup, whilst still small, increased during the operational phase with numbers comparable across the four operational years. Although the significance of these results cannot be tested, this potential increase is in contrast to the most recent Wetland Bird Survey (WeBS) population estimate for scaup within the Solway Firth, which estimated a decline in numbers (Kershaw & Cranswick, 2003; Musgrove *et al.*, 2011). This is likely to be due to differences in survey methods or a consequence of spatial and/or temporal variation in scaup abundance rather than an effect of the OWF (Maclean *et al.*, 2012).

Whilst mean common scoter density remained similar across development phases, the number of common scoters recorded per kilometre (km) of survey effort was smaller during the construction phase. There was also evidence of a slight redistribution of birds during construction with a statistically significant decline in density to the north-east of the OWF. Common scoters are known to be highly sensitive to disturbance including from OWF construction and operation (Garthe & Hüppop, 2004; Schwemmer *et al.*, 2011; Furness *et al.*, 2013). However, there was evidence to suggest no avoidance of the OWF during operation as predicted abundance and distribution had recovered to pre-construction levels by operational year four. Mean densities indicated an increase of common scoters on the sea during successive operational years, although the significance of this increase could not be tested.

Due to the small number of red-throated diver observations, abundance modelling could not be undertaken across the three development phases. However, mean densities were similar across development phases. Since red-throated divers are thought to be highly sensitive to disturbance, a decrease during the construction phase might have been expected (Garthe & Hüppop, 2004; Schwemmer *et al.*, 2011; Furness *et al.*, 2013). Indeed, divers were displaced from the operational Horns Rev OWF and decreased by 96.2% at distances of 0-2 km from the site (Petersen, 2005). Despite the small numbers of red-throated divers encountered at Robin Rigg, it is clear that such a large displacement effect has not occurred at this site. Operational year did not have a statistically significant effect on red-throated diver abundance; small densities of red-throated divers were recorded throughout operation, mainly across the sandbanks in the north of the survey area.

Manx shearwaters were only recorded in the Solway Firth during the summer, which was as expected since birds breeding around the UK migrate to the southern Atlantic Ocean during the winter (Guilford *et al.*, 2009; Freeman *et al.*, 2013). Whilst numbers were small throughout, peaks occurred in July and August prior to birds departing for their wintering areas. There was a slight indication that larger numbers of Manx shearwaters were recorded on the sea during the construction phase. Density surface maps showed a statistically significant increase in Manx shearwater distribution to the south-east of the survey area between pre-construction and construction phases. While operational year did not have a statistically significant effect on flying Manx shearwater abundance on its own there was a statistically significant effect of the interaction of operational year and location. The pattern of spatial change of Manx shearwaters in flight across operational years was complex with statistically significant increases and decreases across the years. However, seabird numbers are known to fluctuate greatly at any given location (Maclean *et al.*, 2012) and because Manx shearwaters often occur in large flocks, this change can be large. Thus changes in Manx shearwater abundance and distribution were not clearly attributable to the presence of the OWF.

The development phase was predicted by the abundance model to have a statistically significant effect on the number of cormorants recorded in flight, and there was an indication that this was also the case for cormorants on the sea. Mean density showed an increase during the construction phase and abundance estimates also showed that the proportion of cormorants using the OWF site compared to the rest of the survey area was largest during

construction. Observations from surveyors show that cormorants rest on the handrails of the turbine transition pieces within Robin Rigg. It is likely that cormorants are exploiting the OWF for foraging, using the turbine transition pieces for maintenance behaviours. The presence of above-water structures is critical for the occurrence of cormorants in the area as they need to dry out their plumage after foraging, and similar behaviour at OWFs elsewhere in Europe has been recorded (Leopold *et al.*, 2011). However, predicted density of cormorants in flight both within the OWF and across the survey area declined after operational year one. Measures have recently been implemented by E.ON to try to discourage cormorants from using the turbines since fouling of the handrails poses a health and safety risk (Figure 2.209). Whilst evidence is limited, it may be that these measures have led to a decline in cormorant density within the OWF during operation.



**Figure 2.209: Wires deployed on handrails of the Robin Rigg transition pieces to discourage cormorant perching.**

Small numbers of gannets were observed throughout the monitoring programme. As such, there is a high degree of uncertainty in the conclusions drawn from these data. Mean density of gannets in flight showed a decrease across the survey area during successive development phases. Furthermore, the proportion of gannets utilising the OWF was smallest during the operational phase, with further declines in predicted gannet abundance across operational years. This is unlikely to reflect wider gannet population change as, unlike many other seabird species, there has been a consistent 2% per annum rise in the global population of gannets (Wanless *et al.*, 2005). Although the significance of these results cannot be tested, there is a suggestion of potential OWF avoidance during operation. A statistically significant decline in gannet densities to the south of Robin Rigg was predicted by the abundance model to occur between pre-construction and operation, with a small increase to the north-east during operation, suggesting that there may be some redistribution of birds. Significantly fewer gannets than expected were observed flying at rotor height during operation, again indicating a possible change in gannet behaviour during the post-construction phase.

Razorbill numbers within the Solway Firth dropped during the summer months of June to September as birds moved offshore to moult following breeding (Wernham *et al.*, 2002). The development phase was not predicted to have a statistically significant effect on razorbill abundance either for birds in flight or on the sea. However, although not significant, predicted razorbill distribution for birds in flight showed possible avoidance of the OWF during operation. Whilst confidence surrounding these density estimates was low (suggesting some uncertainty in predictions) it may be that Robin Rigg presents a barrier to flying razorbills. Across operation, the number of razorbills recorded per km of survey effort was similar across years and this was also reflected in the model outputs. Operational year was not predicted by the model to have a statistically significant effect on abundance.

In contrast to razorbills, development phase was predicted to have a statistically significant effect on guillemot abundance for birds on the sea. Mean densities of birds on the sea declined during the construction phase, before returning to pre-construction levels during operation. However, abundance estimates which were based on median bootstrap estimates indicated an increase in guillemot abundance across successive development phases, both within the OWF and across the wider survey area. This was also the case for birds in flight. There was some evidence for a shift in distribution across development phases, with the largest densities of guillemots on the sea concentrated in the west of the survey area during pre-construction, moving into deeper waters to the south during operation, suggesting that it is depth rather than the OWF driving their distribution. There was an indication of a slight decrease in guillemot abundance for birds on the sea across the four operational years, although this was not statistically significant. Furthermore, there were no significant changes in distribution during operation. Operational year was statistically significant for guillemots recorded in flight however, with significantly smaller numbers recorded in operational years two and four, when the density of birds predicted to occur in the far west of the survey area declined. It is likely that these differences are a result of normal annual and temporal variation in guillemot numbers in the wider area rather than being an effect of the OWF since the differences are not consistent across operational years (Maclean *et al.*, 2012).

Comparable numbers of kittiwakes were recorded in flight and on the sea during the three development phases. Kittiwake abundance across the survey area was slightly smaller during the construction phase although not significantly so, but the proportion of kittiwakes within the OWF itself was high during this phase. Indeed, development phase was not predicted to have a statistically significant effect on kittiwake abundance for either birds in flight or on the sea. However, operational year was predicted by the abundance model to have an effect on kittiwake abundance on the sea, with significantly smaller numbers recorded in operational year one in comparison to subsequent operational years. Statistically significant increases in density were predicted between operational year one and two, but no clear effect of the OWF on the abundance or spatial distribution of kittiwakes was detected.

Great black-backed gull density was small throughout the three development phases, with raw data indicating little change between phases for both birds on sea and in flight. However, due to the small numbers of observations, further modelling work could not be undertaken and the significance of these results could not be tested. Operational year had no effect on the predicted abundance of great black-backed gulls sitting on the water, with very small abundances predicted throughout operation. Whilst operational year did have a statistically significant effect on great black-backed gulls in flight, predicted densities were very small, likely causing the model to be over-sensitive to small changes in numbers. Fewer great black-backed gulls than expected were observed at rotor swept height during pre-construction surveys and larger numbers were present than expected during operational monitoring. This may be a result of great black-backed gull flight heights being underestimated during pre-construction surveys since there were no turbines present in the survey area to use as a reference. No clear effect, attraction or displacement, of the OWF was apparent from the raw data maps.

As for great black-backed gulls, mean densities of herring gulls on the sea showed little change throughout development. However, development phase was predicted to have a statistically significant effect on herring gull abundance for birds in flight. Mean density was smaller for herring gulls during operation, although predicted abundance based on median bootstrap estimates was smaller during construction, with a non-significant increase in density post-construction. However, the proportion of herring gulls in flight utilising the Robin Rigg OWF was similar across development phases. A statistically significant increase in herring gulls on the sea was predicted by the abundance model across operational years, although outliers within the data mean that confidence in these patterns is low. As with great black-backed gulls, larger numbers than expected were recorded at rotor swept height during operational monitoring. Again, this may reflect an increase in observer recording accuracy due to the presence of turbines rather than a change in behaviour. Indeed, large gulls are frequently recorded flying at rotor

height at OWFs across Europe (Cook *et al.*, 2012). There was no clear effect, displacement or attraction, of the OWF on the spatial distribution of herring gulls.

### 2.5.2. Modelling approach

Data analysis was undertaken using the R package 'MRSea' developed by CREEM in 2013 (Scott-Hayward *et al.*, 2013). This new analysis method was commissioned by Marine Scotland to facilitate the modelling of offshore line transect bird and marine mammal data. To our knowledge, this is the first time that this method has been employed outside of CREEM, largely due to the lack of long-term datasets available for modelling potential impacts caused by OWF construction and operation.

A total of 25 MRSea models were run out of a possible 44. Whilst for some species such as scaup, modelling could not be undertaken due to the small number of initial observations other models would not converge due to outliers in the data or zero-inflation. This was particularly true for species with few observations of large flocks, such as common scoter. Whilst modelling these species using a binomial distribution would allow estimation of predicted presence/absence within the survey area, the MRSea package was unable to accommodate distribution models other than Poisson at the time of analysis. However, following recent updates to the package (August 2014), binomial distributions can now be accommodated and should be explored in future.

The MRSea method offers a number of advantages which include: the implementation of Distance sampling to account for imperfect detection during surveys, flexible modelling of non-linear variables and the use of GEEs to account for spatio-temporal autocorrelation and over-dispersion. However, unlike previous analyses undertaken by Natural Power (Walls *et al.*, 2013a, 2013b and 2013c), the MRSea approach does not account for the underlying causes of zero-inflation within the data. One possibility for reducing zero-inflation would be to reduce the number of segments that each individual survey transect is divided into. Whilst the width of each block should remain at 600 m to account for transect width, segment length could be increased to capture a larger number of non-zero observations. However, square segments were deliberately chosen for this analysis to ensure that the resolution of spatial covariates was the same on both width and length axes. Further investigation into the effect of segment size on MRSea modelling is required to determine whether this can be reduced to overcome zero-inflation. In addition, a direct comparison between previous Natural Power analysis techniques and the MRSea method is needed to determine how comparable conclusions are between subsequent monitoring reports.



## 2.6. Conclusions

- The Robin Rigg dataset is a valuable resource providing an important contribution to our knowledge of the impacts of offshore wind developments on birds.
- Evidence was found for few changes in bird abundance and distribution which were directly attributable to Robin Rigg OWF. Seabird numbers at sea are subject to large fluctuations at any given location so the probability of detecting consistent directional change in abundance and distribution is low, unless the change is relatively large.
- There was limited evidence of avoidance of the OWF during the construction phase for common scoter, although predicted abundance and distribution returned to pre-construction levels during operation.
- Cormorants were attracted to the OWF, with birds using the turbine transition pieces for maintenance behaviour between foraging bouts. There was limited evidence of a decline in site usage during operation, which may be related to guano mitigation measures, implemented for health and safety reasons.
- The abundance model predicted that gannet abundance declined throughout development and operation, which is in contrast to national population trends.
- In the case of species such as red-throated diver, very small densities may have masked changes in abundance and distribution. However, when densities are very small the consequences of effects on populations are also likely to be very small.
- For several species, including razorbill and kittiwake, confidence intervals surrounding abundance and density estimates were relatively large resulting in a high degree of uncertainty in the predictions.
- Whilst for some species modelling was not attempted due to the small number of initial observations, other models would not converge due to outliers in the data or zero-inflation. Modelling binomial distributions and reducing the number of segments that each transect is divided into may overcome these difficulties in future.
- Few birds were recorded at rotor height, indicating that overall collision risk is small. Although great black-backed gulls and herring gulls appear to be flying more often at rotor height during operation, it is possible that this is an artefact of more accurate observer recording due to the presence of turbines which provide useful static height references. This highlights the importance of employing a consistent methodology throughout monitoring.

## 2.7. References

- Banks, A.N., Burton, N.H.K., Calladine, J.R. & Austin, G.E. (2007) *Winter gulls in the UK: population estimates from the 2003/04-2005/06 winter gull roost survey*. BTO Research Report No. 456.
- Bicknell, A.W.J., Oro, D., Camphuysen, C.J. & Votier, S.C. (2013) Potential consequences of discard reform for seabird communities. *Journal of Applied Ecology* 50: 649-658.
- BirdLife International (2014) <http://www.birdlife.org/datazone/speciesfactsheet.php?id=3220> [Accessed 14/07/2014]
- Bodey, T.W., Jessopp, M.J., Votier, S.C., Gerritsen, H.D., Cleasby, I.R., Hamer, K.C., Patrick, S.C., Wakefield, E.D. & Bearhop, S. (2014) Seabird movement reveals the ecological footprint of fishing vessels. *Current Biology* 24: <http://dx.doi.org/10.1016/j.cub.2014.04.041>
- Bogdanova, M.I., Daunt, F., Newell, M., Phillips, R.A., Harris, M.P. & Wanless, S. (2011) Seasonal interactions in the black-legged kittiwake, *Rissa tridactyla*: links between breeding performance and winter distribution. *Proceedings of the Royal Society B*. 278: 2412-2418.
- BOU (2013) The British List: a checklist of birds of Britain, 8<sup>th</sup> edition. *Ibis* 155, 635-676.
- Brown, A.F. & Grice, P.V. (2005) *Birds in England*. T & AD Poyser, London.
- Buckland, S.T., Anderson, D.R., Burnham, K.P., Laake, J.L., Borchers, D.L. & Thomas, L. (2001) *Introduction to Distance Sampling*. Oxford University Press, Oxford.
- Cabot, D. (2009) *Wildfowl*. Collins, London.
- Camphuysen, C. J. (1995) Herring gull *Larus argentatus* and lesser black-backed gull *L. fuscus* feeding at fishing vessels in the breeding season: competitive scavenging versus efficient flying. *Ardea* 83: 365–380.
- Chivers, L.S., Lundy, M.G., Colhoun, K., Newton, S.F., Houghton, J.D.R. & Reid, N. (2013) Identifying optimal feeding habitat and proposed Marine Protected Areas (pMPAs) for the black-legged kittiwake (*Rissa tridactyla*) suggests a need for complementary management approaches. *Biological Conservation* 164: 73-81.
- Cook, A.S.C.P., Johnston, A., Wright, L.J. & Burton, N.H.K. (2012) *A review of flight heights and avoidance rates of birds in relation to offshore wind farms*. British Trust for Ornithology report on behalf of The Crown Estate.
- Eaton, M.A., Brown, A.F., Noble, D.G., Musgrove, A.J., Hearn, R.H., Aebischer, N.J., Gibbons, D.W., Evans, A. & Gregory, R.D. (2009) Birds of Conservation Concern 3: the population status of birds in the United Kingdom, Channel Islands and the Isle of Man. *British Birds* 102: 296–341.
- Erikstad, K.E., Bustnes, J.O. & Jacobsen, O. (1988) Duration of ship-following by kittiwakes *Rissa tridactyla* in the Barents Sea. *Polar Research* 6: 191-194.
- Forrester, R.W., Andrews, I.J., McInerny, C.J., Murray, R.D., McGowan, R.Y., Zonfrillo, B., Betts, M.W., Jardine, D.C. & Grundy, D.S. (2007) *The Birds of Scotland*. Scottish Ornithologists' Club, Aberlady.
- Freeman, R., Dean, B., Kirk, H., Leonard, K., Phillips, R.A. Perrins, C.M. & Guilford, T. (2013) Predictive ethoinformatics reveals the complex migratory behaviour of a pelagic seabird, the Manx shearwater. *Journal of the Royal Society Interface* 84: 20130279.
- Furness, R.W., Wade, H.M. & Masden, E.A. (2013) Assessing vulnerability of marine bird populations to offshore wind farms. *Journal of Environmental Management* 119: 56-66.
- Garthe, S. & Hüppop, O. (2004) Scaling possible adverse effects of marine wind farms on seabirds: developing and applying a vulnerability index. *Journal of Applied Ecology* 41: 724–734.
- Garthe, S., Grémillet, D. & Furness, R.W. (1999) At-sea activity and foraging efficiency in chick-rearing northern gannet *Morus bassana*: a case study in Shetland. *Marine Ecology Progress Series* 185: 93-99.
- Grémillet, D. (1997) Catch per unit effort, foraging efficiency, and parental investment in breeding great cormorants (*Phalacrocorax carbo carbo*). *ICES Journal of Marine Science* 54: 635-644.
- Grémillet, D., Liu, H., Le Maho, Y. & Carss, D.N. (2003) Great cormorants and freshwater fish stocks: a pragmatic approach to an ecological issue. *Cormorant* 13: 131-136.

- Guilford, T., Meade, J., Willis, J., Phillips, R.A., Boyle, D., Roberts, S., Collett, M., Freeman, R. & Perrins, C.M. (2009) Migration and stopover in a small pelagic seabird, the Manx shearwater, *Puffinus puffinus*: insights from machine learning. *Proceedings of the Royal Society B* 276: 1215-1223.
- Guilford, T.C., Meade, J., Freeman, R., Birdo, D., Evans, T., Bonadonna, F., Boyle, D., Roberts, S. & Perrins, C.M. (2008) GPS Tracking of the foraging movements of Manx shearwaters *Puffinus puffinus* breeding on Skomer Island, Wales. *Ibis* 150: 462-473.
- Hamer, K.C., Humphreys, E.M., Garthe, S., Hennicke, J., Peters, G., Gremillet, D., Phillips, R.A., Harris, M.P. & Wanless, S. (2007) Annual variation in diets, feeding locations and foraging behaviour of gannets in the North Sea: flexibility, consistency and constraint. *Marine Ecology Progress Series* 338: 295-305.
- Hamer, K.C., Phillips, R.A., Wanless, S., Harris, M.P. & Wood, A.G. (2000) Foraging ranges, diets and feeding locations of gannets in the North Sea: evidence from satellite telemetry. *Marine Ecology Progress Series* 200: 257-264.
- Hardin, T.J. & Hilbe, J. (2002) *Generalised estimating equations*. Chapman & Hall/CRC.
- Harris, M.P. & Wanless, S. (1990) Moults and autumn colony attendance of auks. *British Birds* 83:55-66
- JNCC (2014) <http://jncc.defra.gov.uk/page-3201>. [Accessed 14/07/2014].
- Jones, J.J. & Drobney, R.D. (1986) Winter feeding ecology of scaup and common goldeneye in Michigan. *Journal of Wildlife Management* 50: 446-452.
- Kershaw, M. & Cranswick, P.A. (2003) Numbers of wintering waterbirds in Great Britain, 1994/95-1998/99: I. Wildfowl and selected waterbirds. *Biological Conservation* 111: 91-104.
- Kober, K., Webb, A., Win, I., Lewis, M., O'Brien, S., Wilson, L.J. & Reid, J.B. (2010) An analysis of the numbers and distribution of seabirds within the British Fishery Limit aimed at identifying areas that qualify as possible marine SPAs. JNCC Report 431.
- Kubetzki, U., Garthe, S., Fifield, D., Mendel, B. & Furness, R.W. (2009) Individual migratory schedules and wintering areas of northern gannets. *Marine Ecology Progress Series* 391: 257-265.
- Leopold, M.F., Van Damme, C.J.G. & Van der Weer, H.W. (1998) Diet of cormorants and the impact of cormorant predation on juvenile flatfish in the Dutch Wadden Sea. *Journal of Sea Research* 40: 93-107.
- Leopold, M.F., Dijkman, E.M., Teal, L. & the OWEZ-team (2011) Local Birds in and around the offshore wind farm Egmond aan Zee (T0 & T1, 2002-2010). Wageningen: IMARES.
- Macleane, I.M.D., Wright, L.J., Showler, D.A. & Rehfish, M.M. (2009) A review of assessment methodologies for offshore wind farms. Report commissioned by COWRIE Ltd.
- Macleane, I.M.D., Rehfish, M.M., Skov, H. & Thaxter, C.B. (2012) Evaluating the statistical power of detecting changes in the abundance of seabirds at sea. *Ibis* 155: 113-126.
- Mitchell, P.I., Newton, S.F., Ratcliffe, N. & Dunn, T.E. (2004) Seabird populations of Britain and Ireland. T & AD Poyser, London.
- Monaghan, P., Shedden, C.B., Ensor, K., Fricker, C.R. & Girdwood, R.W.A. (1985) Salmonella carriage by herring gulls in the Clyde area of Scotland in relation to their feeding ecology. *Journal of Applied Ecology* 22: 669-680
- Musgrove, A., Aebischer, N., Eaton, M., Hearn, R., Newson, S., Noble, D., Parsons, M., Risely, K. & Stroud, D. (2013) Population estimates of birds in Great Britain and the United Kingdom. *British Birds* 106: 64-100
- Musgrove, A.J., Austin, G.E., Hearn, R.D., Holt, C.A., Stroud, D.A. & Wotton, S.R. (2011) Overwinter population estimates of British waterbirds. *British Birds* 104: 364-397.
- Natural Power. (2002) Environmental Statement: supporting application for an offshore wind farm at Robin Rigg. Natural Power report to OERL and TXU.
- Newson, S.E., Marchant, J., Sellers, R., Ekins, G., Hearn, R. & Burton, N. (2013) Colonisation and range expansion of inland-breeding cormorants in England. *British Birds* 106: 737-743.
- Nilsson, L. (1970) Food-seeking activity of south Swedish diving ducks in the non-breeding season. *Oikos* 21: 145-154.

- O'Brien, S.H., Wilson, L.J., Webb, A. & Cranswick, P.A. (2008) Revised estimate of numbers of wintering red-throated divers *Gavia stellata* in Great Britain. *Bird Study* 55: 152-160.
- Parnell, M., Walls, R., Brown, M. D. & Brown, S. (2005) The remote monitoring of offshore avian movement using bird detection radar at Weybourne, North Norfolk. Central Science Laboratory, York, UK.
- Patrick, S.C., Bearhop, S., Grémillet, D., Lescroël, A., Grecian, W.J., Bodey, T.W., Hamer, K.C., Wakefield, E., Le Nuz, M. & Votier, S.C. (2013) Individual differences in searching behaviour and spatial foraging consistency in a central place marine predator. *Oikos* 123: 33-40.
- Pedersen, M.B. & Poulsen, E. (1991) Impact of a 90m/2MW wind turbine on birds: avian responses to the implementation of the Tjaereborg wind turbine at the Danish Wadden Sea. *Danske Vildtunders.* 47. 44 p. (Danish, Engl. summ.)
- Petersen, I.K. (2005) Bird numbers and distribution in the Horns Rev offshore wind farm area. Annual status report 2004. NERI report commissioned by Elsam Engineering A/S.
- Petersen, I.K., Christensen, T.K., Kahlert, J., Desholm, M. & Fox, A.D. (2006) Final results of bird studies at the offshore wind farms at Nysted and Horns Rev, Denmark. National Environmental Research Institute, Denmark.
- Platteeuw, M. & Beekman, J.H. (1994) Disturbance of waterbirds by ships on lakes Ketelmeer and IJsselmeer. *Limosa* 67: 27-33
- R Core Team (2014) R: A language and environment for statistical computing. R foundation for statistical computing, Vienna, Austria. URL <http://www.R-project.org/>.
- Schwemmer, P., Mendel, B., Sonntag, N., Dierschke, V. & Garthe, S. (2011) Effects of ship traffic on seabirds in offshore waters: implications for marine conservation and spatial planning. *Ecological Applications* 21: 1851–1860.
- Scott-Hayward, L., Mackenzie, M.L., Donovan, C.R., Walker, C.G. & Ashe, E. (2014) Complex region spatial smoother (CReSS). *Journal of Computational and Graphical Statistics* 23: 340-360.
- Scott-Hayward, L., Oedekoven, C.S., Mackenzie, M.L., Walker, C.G. & Rexstad, E. (2013) *User guide for the MRSea package: statistical modelling of bird and cetacean distributions in offshore renewables development area*. University of St. Andrews contract for Marine Scotland.
- Snow, D.W. & Perrins, C.M. (1998) The birds of the western Palearctic: concise edition. Oxford University Press.
- Stroud, D.A., Chambers, D., Cook, S., Buxton, N., Fraser, B., Clement, P., Lewis, P., McLean, I., Baker, H. & Whitehead, S. (eds). (2001) The UK SPA network: its scope and content. JNCC, Peterborough.
- Tasker M.L., Jones P.H., Dixon T.J. & Blake B.F. (1984) Counting seabirds at sea from ships: a review of methods employed and a suggestion for a standardized approach. *Auk* 101: 567-577.
- Thaxter, C.B., Lascelles, B., Sugar, K., Cook, A.S.C.P., Roos, S., Bolton, M., Langston, R.H.W. & Burton, N.H.K. (2012) Seabird foraging ranges as a preliminary tool for identifying candidate Marine Protected Areas. *Biological Conservation*. 156: 53-61.
- Thaxter, C.B., Wanless, S., Daunt, F., Harris, M.P., Benvenuti, S., Watanuki, Y., Grémillet, D. & Hamer, K.C. (2010) Influence of wing loading on the trade-off between pursuit diving and flight in common guillemots and razorbills. *Journal of Experimental Biology* 213: 1018-1025.
- Tu, W. (2002) Zero-inflated data. In: El-Shaarawi, A.H., Piegorisch, W.W. (eds) *Encyclopedia of Environmetrics*. John Wiley and Sons, Chichester, pp. 2387-2391.
- Votier, S.C., Bicknell, A., Cox, S.L., Scales, K.L. & Patrick, S.C. (2013) A bird's eye view of discard reforms: bird-borne cameras reveal bird/fishery interactions. *PLoS ONE* 8: e57376. doi:10.1371/journal.pone.0057376
- Wakefield, E.D., Bodey, T.W., Bearhop, S., Blackburn, J., Colhoun, K., Davies, R., Dwyer, R.G., Green, J.A., Grémillet, D., Jackson, A.L., Jessopp, M.J., Kane, A., Langston, R.H.W., Lescroël, A., Murray, S., Le Nuz, M., Patrick, S.C., Péron, C., Soanes, L.M., Wanless, S., Votier, S.C. & Hamer, K.C. (2013) Space partitioning without territoriality in gannets. *Science* 341: 68-70.
- Walker, C., Mackenzie, M., Donovan, C. & O'Sullivan, M. (2011) SALSA – a spatially adaptive local smoothing algorithm. *Journal of Statistical Computation and Simulation* 81: 179-191.



Walker, R. & Judd, A. (2010) Strategic Review of offshore wind farm monitoring data associated with FEPA licence conditions. CEFAS, SMRU Ltd, FERA on behalf of DEFRA & MMO.

Walls, R., Brown, M. B., Budgey, R., Parnell, M. & Thorpe, L. (2004) The remote monitoring of offshore avian movement using bird detection radar at Skegness, Lincolnshire. Central Science Laboratory, York, UK.

Walls, R., Canning, S., Lye, G., Givens, L., Garrett, C. & Lancaster, J. (2013a) Analysis of Marine Environmental Monitoring Plan Data from the Robin Rigg Offshore Wind Farm, Scotland (Operational Year 1). Natural Power report to E.ON Climate and Renewables.

Walls, R., Pendlebury, C., Lancaster, J., Lye, G., Canning, S., Malcom, F., Rutherford, V., Givens., L. & Walker, A. (2013b) Analysis of Marine Environmental Monitoring Plan Data from the Robin Rigg Offshore Wind Farm, Scotland (Operational Year 2). Natural Power report to E.ON Climate and Renewables.

Walls, R., Pendlebury, C., Lye, G., Canning, S., Kerr, D., Malcom, F. & Rutherford, V. (2013c) Analysis of Marine Environmental Monitoring Plan Data from the Robin Rigg Offshore Wind Farm, Scotland (Operational Year 3). Natural Power report to E.ON Climate and Renewables.

Wanless, S., Murray, S. and Harris, M.P. (2005) The status of northern gannet in Britain and Ireland in 2003/04. *British Birds* 98: 280-294

Wernham, C.V., Toms, M.P., Marchant, J.H., Clark, J.A., Siriwardena, G.M. & Baillie, S.R. (eds). (2002) The migration atlas: movements of the birds of Britain and Ireland. T & A.D. Poyser, London.

Zuur, A.F., Ieno, E.N., Walker, N.J., Saveliev, A.A., & Smith, G.M. (2009) *Mixed effects models and extensions in Ecology with R*. Springer, USA.

# Appendices

## A. Details of Survey regime

Table A.1: Schematic timetable of construction activities for the Robin Rigg Offshore Wind Farm (OWF).

	2001	2002	2003	2004	2005	2006	2007	2008	2009	2010	2011	2012	2013	2014
Jan		B		B	M			B M	B M	B M	B M	B M NM	B NM	B
Feb	Bth	B NM		B M				B M NM	B M EF NM	B M NM	B M	B M	B	B
Mar	Bth	B NM		B M				B Bth M EF NM	B M	B M	B M EF NM	B	B	
Apr		B NM	B	B				B M NM	B M	B M EF NM	B M Bth	B	B	
May	B	B NM	B	B M				B M Bth	B M	B M Bth	B M	B NM	B	
Jun	B	B NM		B				B M EF	B Bth M NM	B M	B M	B	B	
Jul	B	B NM		B M			B M Bth	B M NM	B M	B M EF NM	B M	B	B	
Aug	B	B NM		B M			EF	B M	B M NM	B M	B M	B	B	
Sep	B	B NM		B M				B M EF	B M	B M	B M	B	B	
Oct	B Bth	B		M				B M	B M	B M EF NM	B M	B	B	
Nov	B NM	B		M			Bth EF	B M NM Bth		B M	B M	B	B	
Dec	B Bth NM	B		M				B M	B M NM	B M	B M	B	B DDV	

	Baseline	B = Birds
	Pre-Construction	M = Mammals
	Construction	EF = Electro-sensitive fish
	Operation	Bth = Benthic
		NM = Non migratory Fish
		DDV = Drop Down Video

## B. Analytical Methods

The following sections provide full details of the analytical methods employed within the report.

### B.1. Data Manipulation

All data were collated and verified by Natural Power Ecology & Hydrology Department. Throughout this procedure, all data were visually inspected and any concerns referred back to the surveyors in order that any problems with the dataset could be resolved. All data were stored and managed using Microsoft Excel.

GPS tracks from each survey were obtained and input into ArcGIS v10. Each individual survey transect was divided into survey blocks (segments), 600 m square. The size was chosen to reflect the area (300 m) surveyed either side of the transect line. As it was intended to include a spatial component within the statistical models, segments were made square to ensure the coordinates represented the centre of the segment.

Observations were then assigned to segments and environmental data for each extracted. Sea depth (low water), sediment type at the midpoint of the block (data obtained from SeaZone Solutions Ltd) and distance of the block midpoint to the nearest coastline were estimated in GIS. Percentage gravel was subsequently calculated for each sediment class in order to allow analysis of sediment type as a continuous covariate. Tidal height was allocated using data supplied by the British Oceanographic Data Centre<sup>4</sup>. A third depth variable, sea depth adjusted for tide height, was calculated using this data. Sea state was also assigned to each survey block based on environmental data collected during surveys.

Data collected prior to October 2001 were removed from the dataset as records during this period were grouped in 10-minute blocks. Consequently, sufficiently accurate positions could not be extracted. Any segments for which tide height was not available were removed from the dataset. Finally, any surveys missing more than 2 transects following standardisation of the dataset were removed.

### B.2. Data Exploration

All data exploration and subsequent analysis was performed in R, version 3.0.3. Data exploration followed the protocol described by Zuur *et al.*, (2009). This involved answering the following questions:

1. *Are there outliers in the explanatory variables and is there even coverage?*

Cleveland dot plots for continuous variables (Figure B.1), bar plots of factor variables (Figure B.2) and X,Y-plots of spatial data (Figure B.3) were used to ensure even coverage of continuous variables for the duration of the study and no outlying values.

---

<sup>4</sup> Data collected in Workington harbour as part of the function of the National Tidal and Sea Level Facility, hosted by the Proudman Oceanographic Laboratory and funded by the Environmental Agency and the Natural Environmental Research Council.

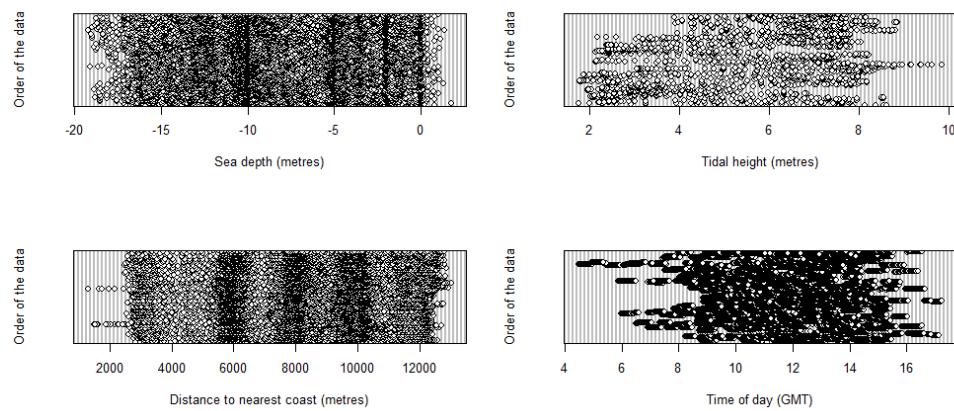


Figure B.1: Example of Cleveland dot plot of explanatory variables.

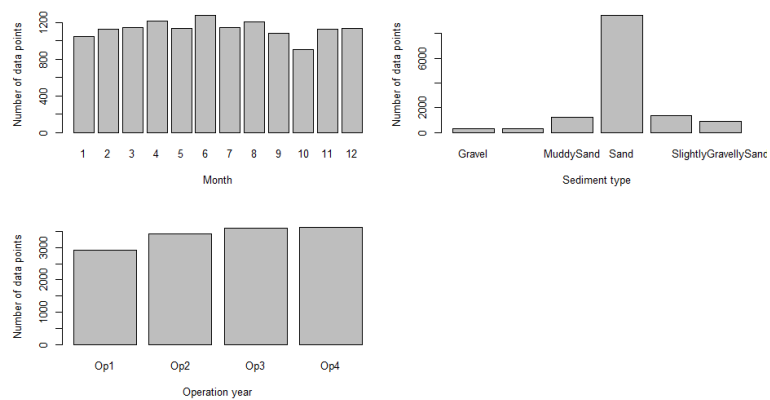


Figure B.2: Example bar plots of factor variables.

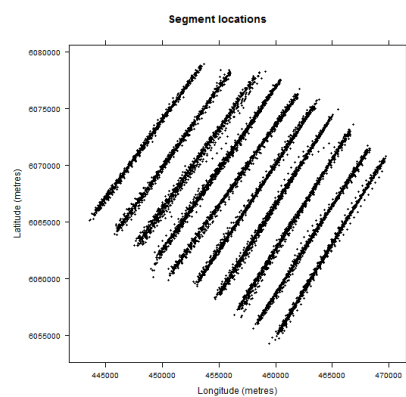
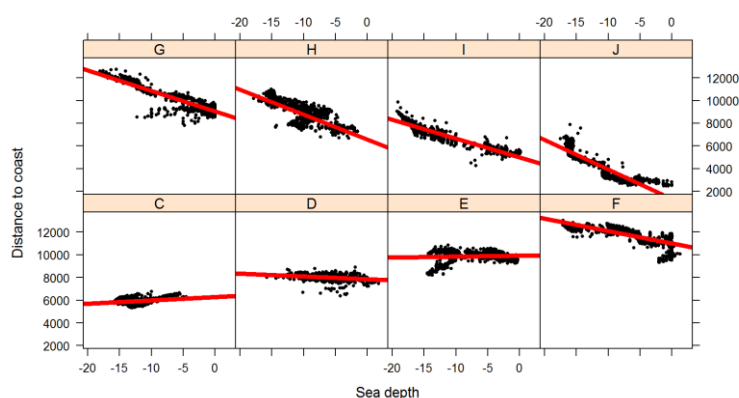


Figure B.3: X,Y-plot of spatial location data.

## II. Is there collinearity among explanatory variables?



Pearson's coefficients, variance inflation factors (VIF) and a range of plots were used to look for linear or non-linear relationships among continuous covariates (longitude, latitude, sea depth, tide height, distance to coast, distance to wind farm). Bivariate comparisons showed little evidence for collinearity; however, plotting relationships among covariates by transect revealed strong collinearity among all continuous covariates except tide height (Figure B.4). Since latitude and longitude are required to create the spatial smooth, neither sea depth, nor distance to coast were considered for inclusion in the final model. Time of day was also not considered since tidal height was expected to be more important in determining bird distribution, therefore this was the only covariate included in the models.



**Figure B.4:** Example of relationship between depth and distance to coast for each transect, illustrating strong collinearity.

Boxplots were used to investigate relationships between continuous and non-continuous covariates and tables were used to assess relationships among combinations of factor variables. No obvious collinearity was found among factor variables but sediment type was collinear with most of the continuous covariates (Figure B.5) and therefore not included in the models.

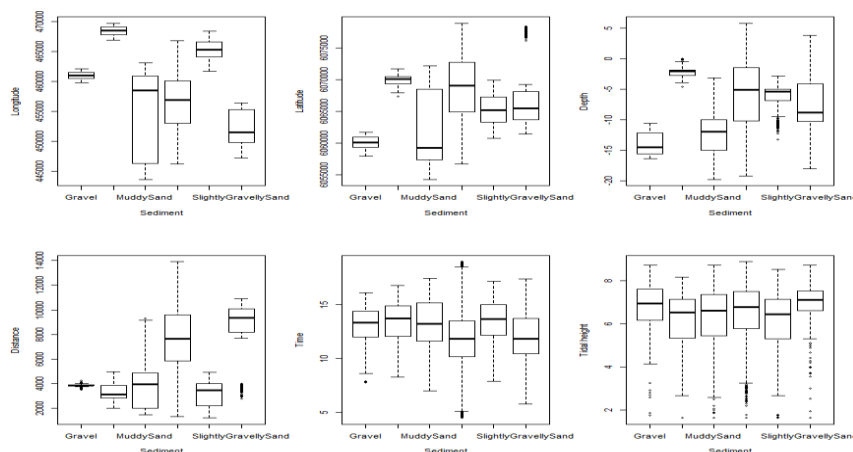


**Figure B.5:** Covariate boxplots of sediment types versus continuous covariates shows evidence of collinearity with longitude, latitude, depth and distance.

### III. Are there potential outliers in the response variable?

The response variable was visualised using dot plots and histograms for evidence of potential outliers that may influence the model (Figure B.6).

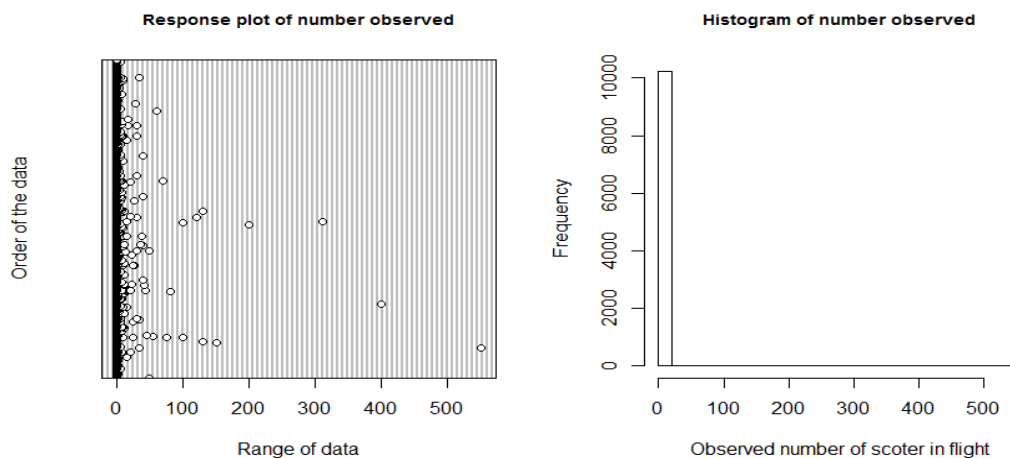


**Figure B.6:** Example response plot (left) and histogram (right) used to look for potential outlying observations that may influence model outputs.

#### IV. *Might the response variable be zero-inflated?*

The percentage of segments without any observations was calculated. Any datasets with fewer than 1% of segments with observations were not analysed.

Initial data exploration highlighted the following key issues:

- Uneven sampling among construction periods when the data were divided into three: pre-construction, construction and operation, the sampling regime (surveys per month) and area surveyed (number of transects and length of transects surveyed) differed among the phases. In order to standardise the dataset and allow like-for-like comparisons, data from a single randomly selected survey was used for any months where more than one survey was carried out. This was not required when comparing between operational years as only a single survey was conducted each month.
- In addition, for the three phase comparison analysis, the study area was cropped to remove an area to the north-east where shallow sea depth often prevented access, and the first two transects in the south-east which were under-surveyed during the pre-construction and construction phases. This was not required when comparing between operational years when surveying was much more consistent.
- Zero inflated data: calculating numbers of segments with zero observations as a proportion of the total number of segments suggested that zero-inflation could be a potential problem for all species datasets.
- Outliers in response variables: several species (specifically Manx shearwater and common scoter) can occur singly or as very large groups meaning that the data do not readily comply with distributions routinely used for analysis of these types of datasets.

If, for whatever reason, any survey effort was removed to allow analysis for a particular species, the data exploration step was repeated prior to analysis.

## B.3. Model Fitting

### B.3.1. Detection function fitting

A detection function was used to model the drop off in detectability as the distance from the observer increased. To obtain the most suitable model a comparison was made between functions (including half-normal and hazard rate) and then incorporating covariates that may affect detectability such as sea state and group size.

The most appropriate model for each species was selected based on minimising AIC, a relative measure that allows comparison of nested models based on a trade-off between the goodness-of-fit of the model to the data and the complexity of the model (e.g. Table B.1). The selected detection function for the guillemot operational year's comparison is presented in Figure B.7. Goodness of fit of the selected detection functions was assessed using QQ-plots (e.g. Figure B.8).

**Table B.1:** Detection functions trialled to model drop-off in detectability of guillemot with distance from the observer and their associated AIC values. The lowest AIC value (Model 8) is highlighted in bold.

Model	Detection function	Covariates	AIC
1	Half-normal	None	11019.31
2	Hazard rate	None	10933.45
3	Half-normal	Sea state	10928.14
4	Hazard rate	Sea state	10839.97
5	Half-normal	Cluster size	10948.25
6	Hazard rate	Cluster size	10891.09
7	Half-normal	Sea state and cluster size	10870.61
<b>8</b>	<b>Hazard rate</b>	<b>Sea state and cluster size</b>	<b>10806.76</b>

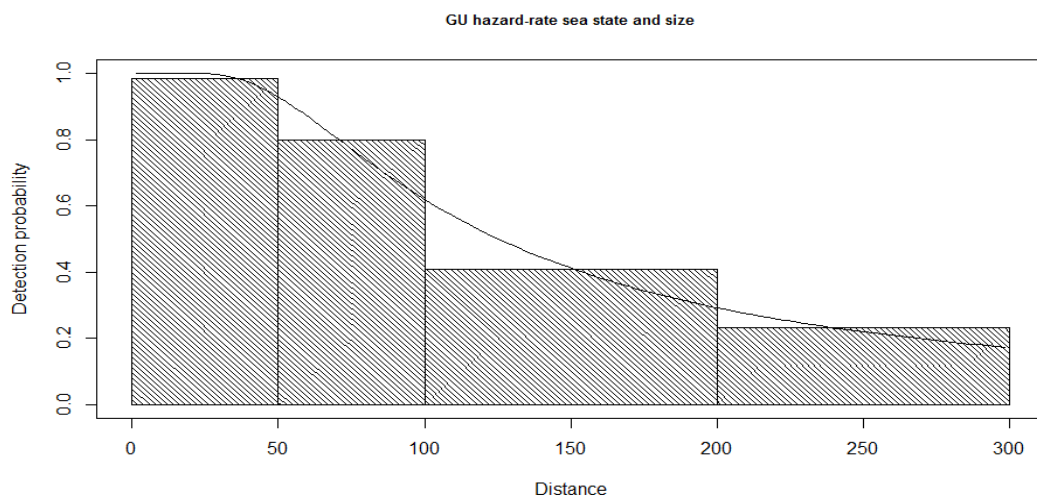


Figure B.7: Modelled drop-off in detectability of guillemot on sea with sea state and cluster size as covariates.

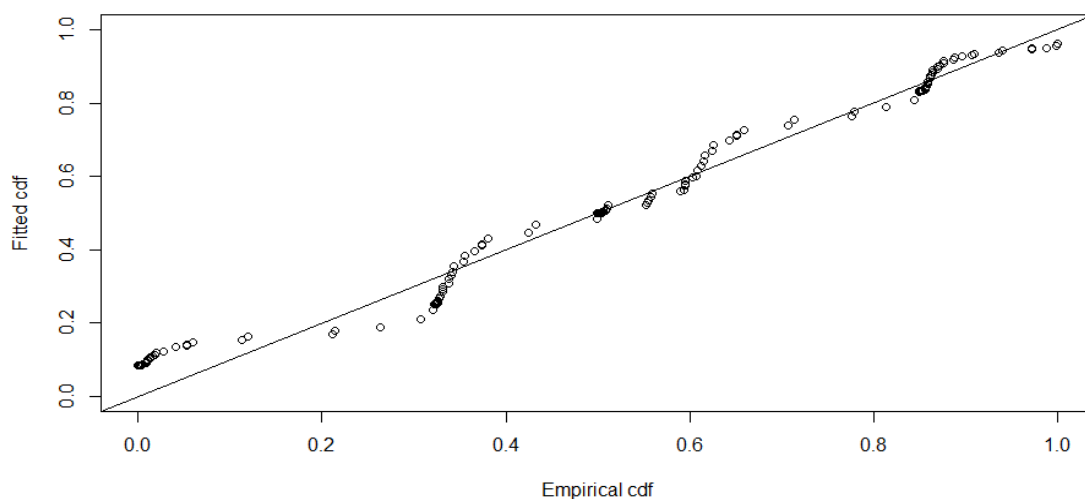


Figure B.8: QQ plot for selected detection function. The diagonal line represents the line along which points should fall if the model were a perfect fit to the data.

### B.3.2. Complex Region Spatial Smoother (CReSS)

Adjusted generalised variance inflation factors ( $\text{GVIF}_{\text{adj}}$ ; Table B.2) were used to confirm no issues with collinearity among any of the variables included in the model. Runs tests were used to demonstrate the presence of unmodelled correlation within the residuals which can be attributed to spatial and temporal dependency of the replicate segments. A blocking structure was selected to allow this correlation to be modelled within a Generalized Estimating Equation (GEE) framework. The blocking structure selected was unique transect-survey combinations, making the assumption that data collected along different transects are not correlated with one another and that data collected within the same transect but on different days are also not correlated with one another. An autocorrelation function plot demonstrates that correlation in all blocks declines to approximately zero demonstrating that this is an appropriate blocking structure (Figure B.9).



**Table B.2:** Example of adjusted generalised variance inflation factors ( $GVIF_{adj}$ ) used to assess collinearity among covariates retained in the modelling process.

Covariate	df	$GVIF_{adj}$
Month	11	1.00
Phase	3	1.00
Tide height	1	1.39
X location	1	1.21
Y location	1	1.30

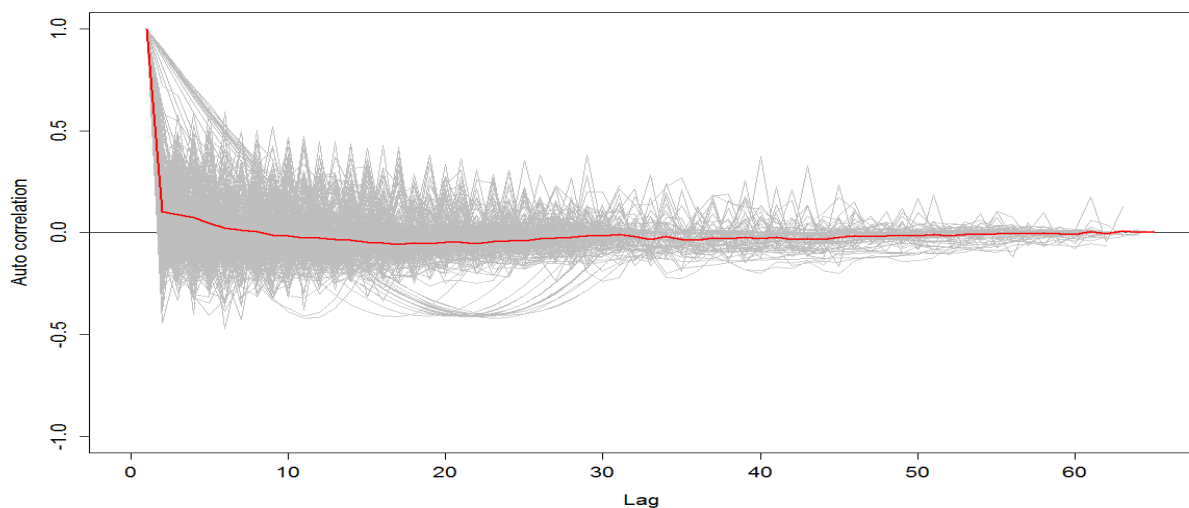


**Figure B.9:** Autocorrelation function plot demonstrating that correlation in all blocks declines to approximately zero indicating that use of transect-survey combinations is an appropriate blocking structure.

A two-dimensional CReSS-based smoother was fitted using the SALSA algorithm as a spatially variable relationship between x,y position and tidal height was expected. Knots were allocated evenly across the survey area (Figure B.10) A number of different starting knot numbers were assessed and the best model selected using k-fold Cross Validation (CV; see Table B.3 for example of output).

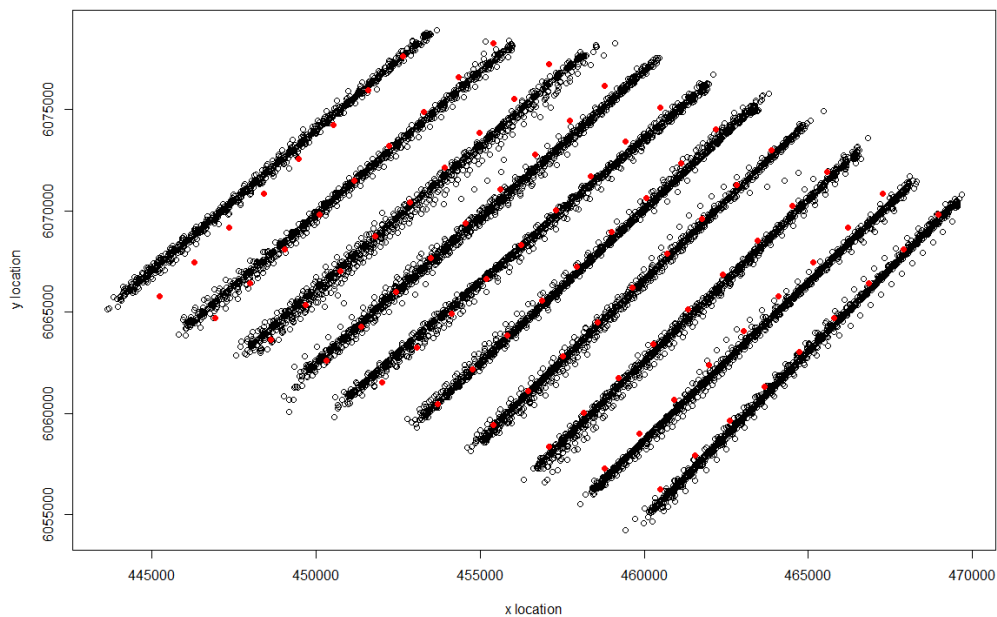


Figure B.10: Location of possible knots (red dots) in relation to data (black circles) that could be selected by 2-D SALSA for use in spatial smoother.

Table B.3: Example k-fold Cross Validation scores (CV) for a variety of knot numbers for the 2-D spatial smooth. Best fitting model (lowest CV score) is highlighted in bold.

Start knots	End knots	CV
5	5	4.239
<b>6</b>	<b>6</b>	<b>4.222</b>
7	7	4.229
9	7	4.232
19	11	4.251

## B.4. Model Validation

Models were fitted that allow non-linear covariate relationships and auto-correlated residuals. However, the following diagnostic tests were required to ensure that the model was appropriate.

### B.4.1. Observed vs. fitted

The agreement between observed and fitted data was quantified with Marginal R-squared and Concordance Correlation (Example output: Figure B.11). Concordance Correlations of 1 indicate a perfect fit between modelled and observed data. Figure B.11 indicates that the model is under-predicting high observed values, and over predicting observed zeros. However, this is common in noisy ecological data, particularly in over-dispersed count data, where concordance correlations of 0.25 are considered to be a good fit.

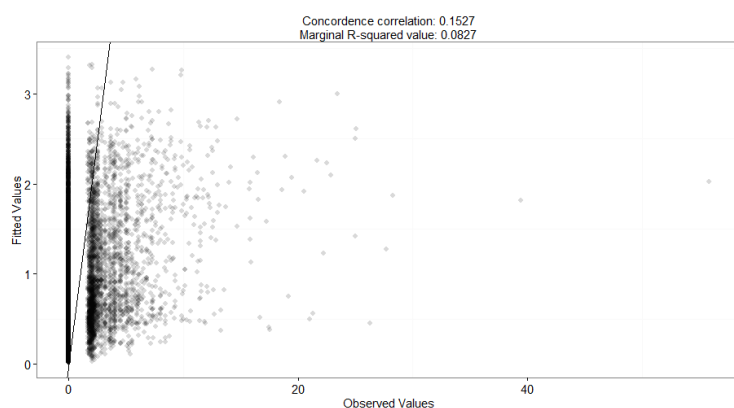


Figure B.11: Diagnostic plot of observed versus fitted data. The diagonal line indicates where data should lie.

### B.4.2. Fitted vs. residuals

Plots of fitted values versus scaled Pearson's residuals were examined for evidence of structure not accounted for by the model (Example output: Figure B.12). A locally weighted least squares regression remained close to zero, indicates there was no issue with mean-variance relationship (i.e. there were no patterns that may be hidden due to over-plotting).

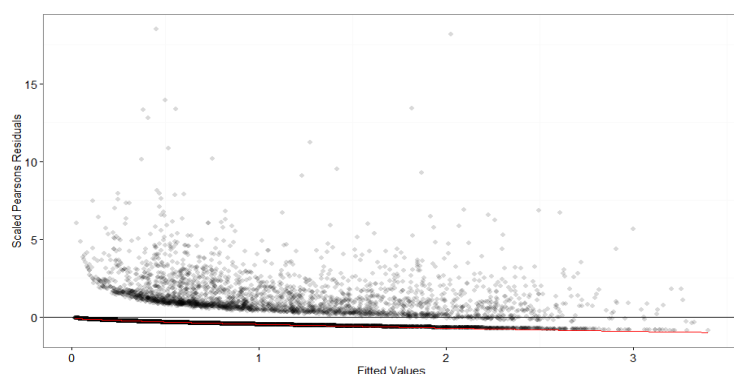
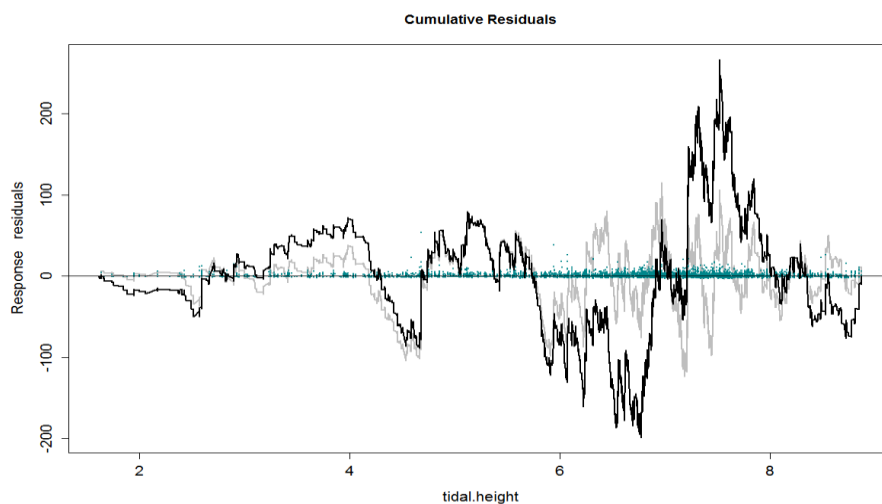


Figure B.12: Plot of fitted values versus scaled Pearson's residuals with a locally weighted least squares regression.

### B.4.3. Cumulative residuals

Systematic over- and under-prediction was assessed by plotting cumulative residuals. Example outputs:

- Figure B.13: Cumulative residuals indicate that tidal height was modelled appropriately as there is a reasonable amount of mixing between positive- and negative-correlation and substantial similarity to expected cumulative residuals.
- Figure B.14: When cumulative residuals were ordered by the predicted value there was evidence that very low values were over-predicted and mid-range to high values were under-predicted, which might be expected for over-dispersed count data.
- Figure B.15: Plots of cumulative residuals ordered temporally by observation indicated no systematic over- or under-prediction, with good mixing of high and low residual values through each of the four operational phases.



**Figure B.13:** Cumulative residuals plot for residuals ordered by tidal height as a smooth term in the GEE model. Residual values (blue points) and plotted against cumulative residuals (black line). The grey line represents how cumulative residuals would be expected to look if depth was modelled with greater flexibility.

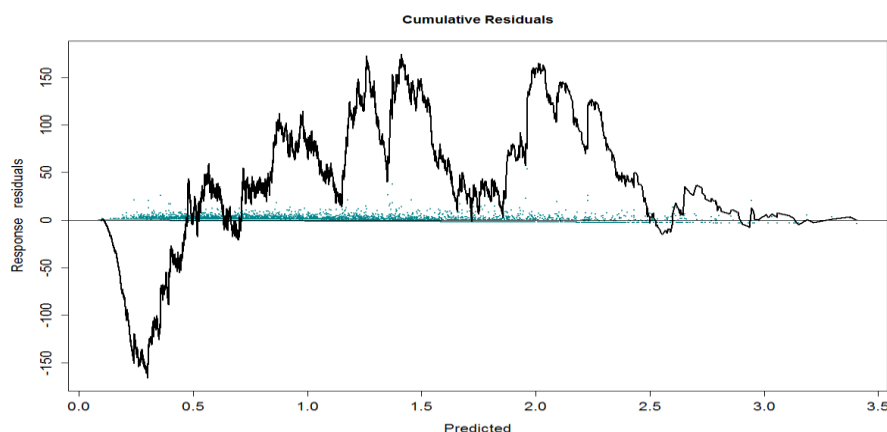


**Figure B.14:** Cumulative residuals plot for residuals ordered by predicted value. Residual values (blue points) and plotted against cumulative residuals (black line).



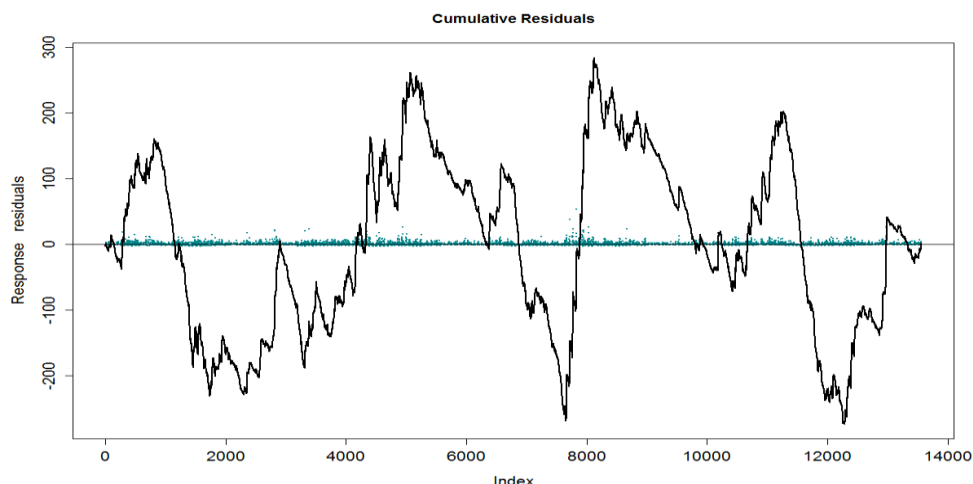


Figure B.15: Cumulative residuals plot for residuals ordered temporally by observation. Residual values (blue points) and plotted against cumulative residuals (black line).

#### B.4.4. Influential data

COVRATIO and PRESS statistics were used to evaluate how influential the removal of individual blocks would be to the model. COVRATIO statistics measure the change in precision of parameter estimates when individual blocks are removed, whereas PRESS statistics measure the sensitivity of model predictions to the removal of individual blocks. Example outputs:

- Figure B.16: COVRATIO statistics indicated that no blocks particularly increased or reduced parameter standard errors (by being extremely high or low, respectively), and therefore had little influence on model precision.
- Figure B.17: PRESS statistics indicated that one block (ID = 50) had potential to be of concern. Examination of the data revealed a Distance-adjusted observation of 55 birds which may inflate density surfaces a particular area. However, in this instance it was decided that the magnitude of the effect was not enough to be of any real concern.

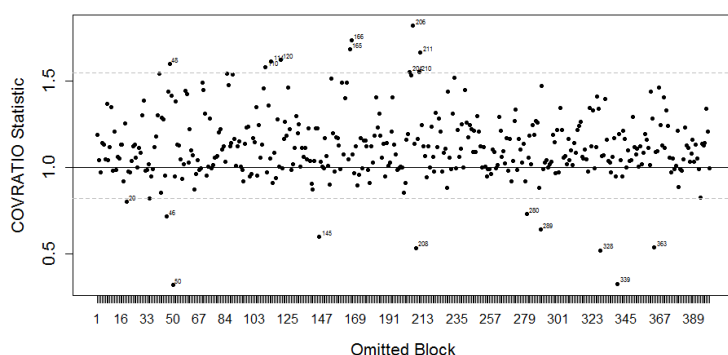


Figure B.16: Plot of COVRATIO statistics of the influence of individual blocks on estimated parameter precision. Lower 2.5 % and upper 97.5 % quantiles are indicated by dashed lines. Blocks that fall below the reference line at 1.0 indicated that precision decreases when the block is removed, and vice versa.

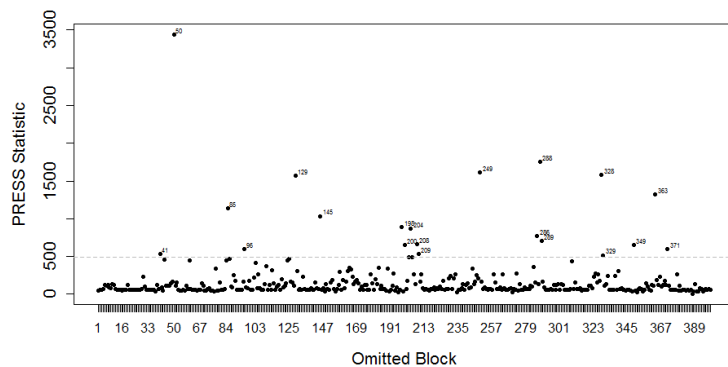


Figure B.17: Plot of PRESS statistics of model sensitivity to the removal of individual blocks. The most influential 5 % of block are shown above the dashed line.

#### B.4.5. Spatial patterns in raw residuals

The quality of spatial predictions was assessed by plotting model residuals spatially, which showed there were no spatial patterns in predictions (i.e. clumped over- or under-predictions. Example output: Figure B.18).

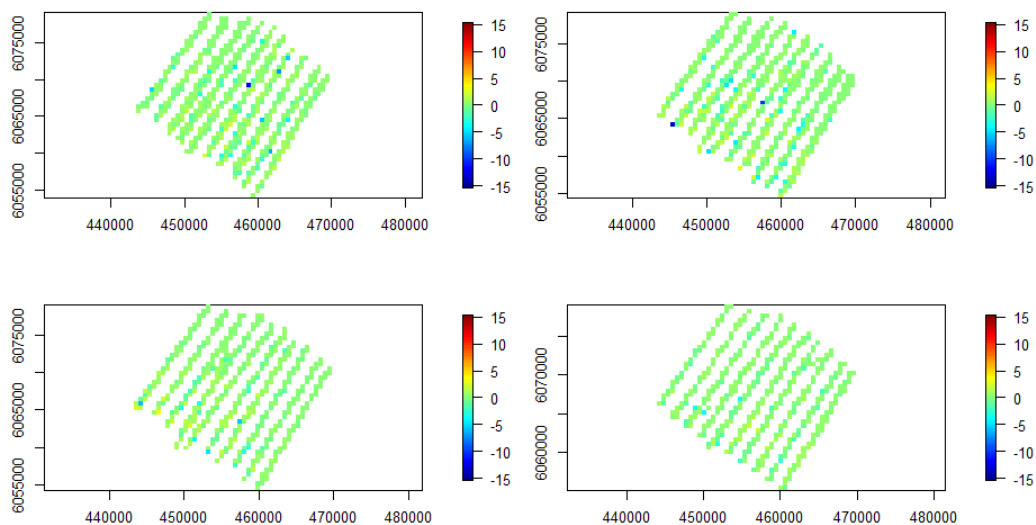


Figure B.18: Raw residuals (mean guillemots / km<sup>2</sup> per 600 (m)<sup>2</sup> grid cell) plotted by spatial location (x,y coordinates of grid centroid) within operational years 1 (top left), 2 (top right), 3, (bottom left), and 4 (bottom right).

# What We Do



Natural Power is a leading independent renewable energy consultancy and products provider. We offer proactive and integrated consultancy, management & due diligence services, backed by an innovative product range, across the onshore wind, offshore wind, wave, tidal, solar and bioenergy sectors, whilst maintaining a strong outlook on other new and emerging renewable energy sectors. Established in the mid-1990s, Natural Power has been at the heart of many ground-breaking projects, products and portfolios for close to two decades, assisting project developers, investors, manufacturers, finance houses and other consulting companies.

With its iconic Scottish headquarters, The Green House, Natural Power has expanded internationally employing 300 renewable energy experts across Europe and the Americas and operating globally. Providing Planning & Development, Ecology & Hydrology, Technical, Construction & Geotechnical, Asset Management and Due Diligence services, Natural Power is uniquely a full lifecycle consultancy – from feasibility to finance to repowering, and every project phase in between. We are a truly trailblazing consulting organisation; Natural Power has consistently invested in product development and technical research in order to progress certain key areas within the industry such as the operational management of wind farms, the design and assessment of wind farms in complex flow and the use of remote sensing for wind measurement. From award-winning consultancy and management services, through a string of technology world-firsts, Natural Power has a successful track record and the breadth of services and deep-rooted experience that provides a wealth of added value for our diverse client base.

**Natural Power – delivering your local renewable energy projects, globally.**

## Our Global Expertise

Natural Power delivers services and operates assets globally for our clients, with twelve offices across Europe and North America and agencies active in South America and AsiaPac.

### UK

#### Registered Office > Scotland

The Green House, Forrest Estate  
Dalry, Castle Douglas, DG7 3XS  
SCOTLAND, UK

#### Stirling > Scotland

Ochil House  
Springkerse Business Park  
Stirling, FK7 7XE  
SCOTLAND, UK

#### Inverness > Scotland

Suite 3, Spey House, Dochfour  
Business Centre, Dochgarroch  
Inverness, IV3 8GY  
SCOTLAND, UK

#### Dublin > Ireland

First Floor, Suite 6, The Mall,  
Beacon Court, Sandyford,  
Dublin 18  
IRELAND

#### Aberystwyth > Wales

Harbour House, Y Lanfa  
Aberystwyth, Ceredigion  
SY23 1AS  
WALES, UK

#### London > England

200 Aldersgate St  
City of London, EC1A 4HD  
ENGLAND, UK

#### Newcastle > England

Unit 5, Horsley Business Centre  
Horsley  
Northumberland, NE15 0NY  
ENGLAND, UK

#### Warrington > England

Suite 26, Genesis Centre,  
Birchwood, Warrington, WA3 7BH  
ENGLAND, UK

### EUROPE

#### Strasbourg > France

1, rue Goethe  
67000 Strasbourg  
FRANCE

#### Nantes > France

1 rue du Guesclin  
BP61905, 44019 Nantes  
FRANCE

#### Halmstad > Sweden

c/o The Green House,  
Forrest Estate  
Dalry, Castle Douglas, DG7 3XS  
SCOTLAND, UK

#### Ankara > Turkey

re-consult  
Bagi's Plaza  
- Muhsin Yazıcıoğlu Cad. 43/14  
TR / 06520 Balgat-Ankar  
TURKEY

### THE AMERICAS

#### New York > USA

63 Franklin St, Saratoga Springs,  
NY 12866, USA

#### Valparaiso > Chile

Latwind Energías Renovables  
Lautaro Rosas 366, Cerro  
Alegre Valparaiso, CHILE

**naturalpower.com**

**sayhello@naturalpower.com**

No part of this document or translations of it may be reproduced or transmitted in any form or by any means, electronic or mechanical including photocopying, recording or any other information storage and retrieval system, without prior permission in writing from Natural Power. All facts and figures correct at time of print. All rights reserved. © Copyright 2015

